UNIVERSIDAD DE OVIEDO

DEPARTAMENTO DE INGENIERÍA QUÍMICA Y TECNOLOGÍA DEL MEDIO AMBIENTE

PROGRAMA DE DOCTORADO EN INGENIERÍA QUÍMICA, AMBIENTAL Y BIOALIMENTARIA

SEPARACIÓN DE COMPUESTOS VALIOSOS A PARTIR DE LODOS DE EDAR Y CORRIENTES ACUOSAS COMPLEJAS

TESIS DOCTORAL

DANIEL NÚÑEZ DÍAZ

OVIEDO, 2024

UNIVERSITY OF OVIEDO

DEPARTMENT OF CHEMICAL AND ENVIRONMENTAL ENGINEERING

PHD PROGRAM IN CHEMICAL, ENVIRONMENTAL AND BIOFOOD ENGINEERING

SEPARATION OF ADDED-VALUE PRODUCTS FROM WASTE ACTIVATED SLUDGE AND COMPLEX AQUEOUS STREAMS

DOCTORAL THESIS

DANIEL NÚÑEZ DÍAZ

OVIEDO, 2024


Aun aprendo
54
71

Aún aprendo.

Francisco de Goya.

AGRADECIMIENTOS

Cuando era pequeño, veía la Universidad como un objetivo inalcanzable en el tiempo, un horizonte tan ilusionante como utópico, la meta máxima a la que aspirar. Cuando uno crece, gana perspectiva (no solo por el aumento en altura); hoy veo que esa meta no era sino un nuevo punto de partida. Debo mi más sincera gratitud a todos aquellos que me han permitido alcanzar exitosamente (cierto es que en más tiempo del originalmente planeado, si bien para nada perdido) este umbral que es a la vez fin y comienzo:

A Mario Díaz, por abrirme las puertas del grupo de investigación y haberme permitido recorrer este camino. Gracias por dirigirme y guiarme en mi camino académico ya desde antes de comenzar el doctorado.

A Paula Oulego, por su dedicadísima dirección y su infatigable ayuda a lo largo de todos estos años. Gracias por dar siempre el extra y por ese genuino amor por la docencia. Sin su pasión y su acertada guía, esta tesis no sería ni la sombra de lo que es. Siempre me enorgullecerá aparecer el primero en su (sin ninguna duda será así) extensísima lista de tesis dirigidas.

A Francisco Riera, por iniciarme de la mejor manera posible en el mundo de las membranas y por haberme acompañado como director estos últimos años.

To Jens Muff and Mahdi Nikbakht Fini from Aalborg University, as well as to the rest of the Esbjerg section of the Department of Chemistry and Bioscience, for all their help and support during my stay there. Thank you for making being in Denmark warm, despite the winter and the COVID.

A Adriana Laca, por su impecable tutela de la tesis, siempre dispuesta a ayudar con una sonrisa.

A Sergio Collado, por ser tan constante en su ayuda a lo largo de toda la tesis como en hacer la ronda para el café.

A Isma, por dejarse convencer de vez en cuando por Sergio para bajar y aderezar las charlas sobre *papers* con algo de política, filosofía, videojuegos o demás temas banales.

A todos los miembros pasados y presentes del grupo de Tecnología de Bioprocesos y Reactores, por toda la ayuda y la calidez humana a lo largo de los años. En especial, muchas gracias a todos mis compañeros de doctorado (no os nombro a todos porque capaz soy de dejarme a alguno). Gracias por las partidas de bolos, las cenas, las fiestas, los viajes, las chocolimpiadas, los maratones de ejercicio y Naruto durante el confinamiento, las conversaciones superficiales y las profundas, las catas de café, las noches europeas de los investigadores, los talleres de cocina de gyozas y las clases de chino, las sobremesas, las rutas, las pachangas de básquet… Y, sobre todo, por las muy buenas amistades que me llevo. Sois parte de las razones por las que esto se haya alargado tanto: cuando uno está a gusto, no se quiere ir.

Al resto del departamento de Ingeniería Química y Tecnología del Medio Ambiente que, de una forma u otra, me han ayudado a lo largo de esta tesis.

A mis amigos, no sé si por ayudarme a conseguir que mi director me diga "¿Y a dónde viajas ahora?", pero sí por todas las charlas y momentos que han servido de combustible para seguir esforzándome. En particular, gracias a Marcos por ser un espejo en el que mirarme y poder compartir nuestros avances.

A Kaldi, el legendario pastor abisinio que descubrió los efectos tonificantes del café.

A Laura, por haber hecho del mundo un lugar más bonito con tu sonrisa, incluyendo esta facultad, aunque a veces haya sido un infierno. Nunca sospeché que una conversación sobre pelos fuese a convertirse en algo tan importante. Gracias por todo, es un honor salir de esta etapa de la mano.

A mi familia, en especial a mis padres, por ser los gigantes sobre cuyos hombros he tenido el privilegio de poder subirme.

Gracias a todos.

ÍNDICE

RESUMEN

La presencia de moléculas orgánicas comercialmente valiosas es un factor común en efluentes de distintas actividades industriales o de gestión medioambiental. Sin embargo, a pesar de la creciente importancia de los sistemas circulares de gestión de residuos, la mayor parte del valor de las aguas residuales no se aprovecha, perdiendo la oportunidad de recuperar una gran cantidad de compuestos valiosos. La recuperación de estos compuestos podría generar un valor añadido durante el tratamiento de las corrientes que los contienen e incrementar la sostenibilidad del proceso. El problema que plantea la recuperación de estos compuestos es que están contenidos en matrices de gran complejidad, por lo que es preciso analizar diversos métodos de separación para optimizar su recuperación y purificación.

En esta tesis se han estudiado y optimizado diversos procesos de recuperación y purificación de varios compuestos de interés (ácidos orgánicos, lignina, ácidos húmicos, proteínas y carbohidratos) mediante tecnologías de membranas y extracción líquido-líquido a partir de varias biomasas residuales líquidas (lixiviado de vertedero, licor negro Kraft y lodos secundarios de depuradora). Asimismo, se ha estudiado la influencia de la matriz de la corriente en dichos procesos de recuperación y purificación y de la aplicación de un tratamiento hidrotérmico previo para la mejora de los rendimientos de extracción de estos compuestos de interés.

Por una parte, se ultrafiltraron lixiviados de vertedero y se estudió el efecto de su edad en términos de ensuciamiento y retención de ácidos húmicos y de varios parámetros fisicoquímicos. Se observó que la maduración del lixiviado tiene un efecto positivo en su ultrafiltración. La pérdida de permeabilidad de las membranas se debió principalmente al ensuciamiento reversible, causado por la formación de una torta de ensuciamiento en la superficie de la membrana. Además, la oxidación húmeda resultó ser una tecnología efectiva para la reducción del ensuciamiento en lixiviados estabilizados (maduro y tratado biológicamente), logrando incrementos de hasta el 66% en los flujos de permeado. El tratamiento combinado de oxidación húmeda seguido de ultrafiltración resultó adecuado para la recuperación de ácidos húmicos a partir de lixiviados estabilizados, así como para obtener un agua tratada que cumpla en su mayor parte los límites nacionales de descarga a sistemas de saneamiento público requeridos.

Con respecto al licor negro, se estudiaron distintas estrategias para la recuperación de ácidos orgánicos de cadena corta, consistentes en la aplicación de distintos pretratamientos (deslignificación y oxidación húmeda), filtración con membranas y extracción líquido-líquido. La deslignificación fue el pretratamiento más efectivo, consiguiéndose recuperar el 29.4% de los ácidos orgánicos totales utilizando trioctilamina al 30% en heptano (v/v) como extractante. Se observó que un aumento de temperatura hasta los 55 ºC tuvo un efecto positivo en la extracción.

Por último, en cuanto a los lodos secundarios de depuradora, se realizó una revisión bibliográfica sobre los distintos métodos de separación y purificación de biomoléculas de interés que puedan ser aplicados a los lodos, proponiéndose un proceso integrado para optimizar la recuperación de compuestos valiosos de los lodos. Se emplearon dos estrategias distintas de oxidación húmeda: una de condiciones más suaves para conseguir la solubilización de los lodos, y otra con condiciones más fuertes con el objetivo de oxidar parcialmente los lodos y producir ácidos orgánicos de cadena corta. En cuanto a la primera estrategia, tras la oxidación húmeda se fraccionó el lodo empleando membranas de distintos materiales y tamaños, llegando a conseguir una separación parcial entre proteínas y carbohidratos y ácidos húmicos tras filtrar sucesivamente con una membrana de polietersulfona de tamaño de corte de 50 kDa y otra del mismo material con tamaño de corte de 3 kDa. Se caracterizó en profundidad el ensuciamiento de las membranas, atendiendo a la reversibilidad del ensuciamiento y a la hidrofobicidad, la rugosidad y la morfología de la membrana. Se observó que las membranas de 50 kDa retenían altos porcentajes de metales pesados, y se determinó que el mecanismo por el cual ocurría esto era mediante la complejación con los ácidos húmicos y las proteínas presentes en el lodo.

En cuanto a la producción de ácidos orgánicos a través de la oxidación parcial de los lodos, se obtuvo una concentración máxima de 6.07 g/L de ácidos tras oxidar a 160 ºC durante 240 minutos. Posteriormente, se obtuvo una corriente pre-purificada de ácidos orgánicos mediante dos filtraciones sucesivas con membranas cerámicas de 50 y 1 kDa de tamaño de corte. Las mayores extracciones de ácidos orgánicos a temperatura ambiente se lograron con una mezcla de trioctilamina y tributilfosfato al 10% en octan-1-ol, extrayendo el 34% del total de los ácidos presentes en el permeado de 1 kDa. El aumento de la temperatura dentro del rango de 25 a 50 ºC tuvo un efecto favorable en la extracción. La matriz del lodo oxidado afectó de manera negativa al rendimiento de la extracción.

ABSTRACT

The presence of commercially valuable organic molecules is a common factor in effluents from different industrial or environmental management activities. However, despite the growing importance of circular waste management systems, most of the value of wastewater is not utilized, losing the opportunity to recover a large amount of valuable compounds. The recovery of these compounds could generate added value during the treatment of the streams that contain them and increase the sustainability of the process. The problem posed by the recovery of these materials is that they are contained in highly complex matrices, so it is necessary to analyse various separation methods to optimize their recovery and purification.

In this thesis, several recovery and purification processes of various compounds of interest (organic acids, lignin, humic acids, proteins and carbohydrates) have been studied and optimized using membrane technologies and liquid-liquid extraction from various liquid residual biomasses (landfill leachate, Kraft black liquor and waste activated sludge). Additionally, the influence of the current matrix on those recovery and purification processes and the application of a prior hydrothermal treatment to improve the extraction yields of these compounds of interest has been studied.

On the one hand, landfill leachates were ultrafiltered and the effect of their age was studied in terms of fouling and retention of humic acids and various physicochemical parameters. It was observed that the aging of the leachate had a positive effect on its ultrafiltration. The loss of permeability of the membranes was mainly due to reversible fouling, caused by the formation of cake fouling on the membrane surface. Furthermore, wet oxidation proved to be an effective technology for reducing fouling in stabilized leachates (mature and biologically treated), resulting in increases of up to 66% in permeate fluxes. The combined treatment of wet oxidation followed by ultrafiltration was suitable for humic acid recovery from stabilized leachates, as well as for obtaining treated water that meets required national discharge limits.

With respect to black liquor, different strategies were studied for the recovery of short-chain organic acids, consisting of the application of different pretreatments (delignification and wet oxidation), membrane filtration and liquid-liquid extraction. Delignification was the most effective pretreatment, recovering 29.4% of the total organic acids using 30% trioctylamide in heptane (v/v) as extractant. It was observed that an increase in temperature to 55 ºC had a positive effect on the extraction.

Finally, regarding waste activated sludge, a bibliographic review was carried out on the different methods of separation and purification of biomolecules of interest that can be applied to the sludge, proposing an integrated process to optimize the recovery of valuable compounds from the sludge. Two different wet oxidation strategies were used: one with milder conditions to achieve solubilization of the sludge, and another with more severe conditions with the aim of partially oxidizing the sludge and producing short-chain organic acids. Regarding the first strategy, the solubilised sludge was fractionated using membranes of different materials and sizes, achieving a partial separation between proteins and carbohydrates and humic acids after successively filtering with a polyethersulfone membrane with a cut-off size of 50 kDa and another of the same material with a cutoff size of 3 kDa. Membrane fouling was characterized in depth, taking into account the reversibility of the fouling and the hydrophobicity, surface roughness and morphology of the membrane. It was observed that the 50 kDa membranes retained high percentages of heavy metals, the mechanism by which this occurred being through complexation with humic acids and proteins present in the sludge.

Regarding the production of organic acids through the partial oxidation of the sludge, a maximum concentration of 6.07 g/L of acids was obtained after oxidizing at 160 ºC for 240 minutes. Subsequently, a prepurified stream of organic acids was obtained through two successive filtrations with ceramic membranes of 50 and 1 kDa cut-off size. The highest extractions of organic acids at room temperature were achieved with a mixture of trioctylamine and tributylphosphate at 10% in octan-1-ol, extracting 34% of the total acids present in the 1 kDa permeate. Increasing the temperature within the range of 25 to 50 °C had a favorable effect on the extraction. The oxidized sludge matrix negatively affected the extraction yields.

LISTA DE FIGURAS

LISTA DE TABLAS

LISTA DE ABREVIATURAS

ADH	Alcohol dehydrogenase
AFM	Atomic force microscopy
AOPs	Advanced oxidation processes
APTES	(3-aminopropyl)triethoxysilane
ATR	Attenuated total reflectance
BL	Kraft black liquor
BOD	Biological oxygen demand
BT	Stabilised leachate after biological treatment
BTX	Benceno, tolueno y xileno
CAGR	Compound annual growth rate
CF	Cake formation
CFV	Crossflow velocity
CN	Colour number
COD	Chemical oxygen demand
CPB	Complete pore blocking
DBO	Demanda biológica de oxígeno
DQO	Demanda química de oxígeno
EDAR	Estaciones depuradoras de aguas residuales
EDX	Energy dispersive X-ray analyzer
F	Fluorescence intensity in the presence of quencher
F_0	Fluorescence intensity in the absence of quencher
FTIR	Fourier-transformed infrared spectroscopy
HA	Humic acids
I_D	Total direct costs
I_F	Fixed-capital investment
I_I	Total indirect costs
I_L	Labour costs
I_M	Maintenance and repair costs
I_s	Operation supervision
I_W	Working capital
IPB	Internal pore blocking
J	Flujo de permeado / Permeate flux
J_0	Limiting flux
J_{CC}	Permeate flux achieved after chemical cleaning
J_{PC}	Permeate flux achieved after physical cleaning

J_S	Permeate flux achieved at the end of the ultrafiltration
K_b	Constant for CPB Hermia model
K_{BL}	Distribution constants for black liquor
K_c	Constant for CF Hermia model
K_D	Constante de distribución / Distribution constant
K_i	Constant for IPB Hermia model
K_{LRBL}	Distribution constants for black liquor after lignin recovery
K_p	Constant for PPB Hermia model
k_q	Bimolecular quenching constant
K_{WOBL}	Distribution constants for partially oxidised black liquor
LLE	Liquid-liquid extraction
LMH	L/m^{2}h
log P	Octanol-water partition coefficient
LR	Lignin recovery
LRBL	Black liquor after lignin recovery
μ	Viscosidad dinámica / Dynamic viscosity
M	Mature leachate
MBR	Membrane bioreactor
MT	Mature (leachate)
MF	Microfiltration
MWCO	Molecular weight cut-off
NF	Nanofiltration
NVAs	Non-volatile short-chain organic acids
OA	Organic acids
PAN	Poliacrionitrilo / Polyacrylonitrile
PAN50	PAN membrane, 50 kDa
PES	Polietersulfona / Polyethersulphone
PES10	PES membrane, 10 kDa
PES3	PES membrane, 3 kDa
PES50	PES membrane, 50 kDa
PES50-10	PES membrane of 10 kDa filtering the permeate from PES50 membrane
PES50-3	PES membrane of 3 kDa filtering the permeate from PES50 membrane
PESH	PES permanentemente hidrofílica / Permanently hydrophylic PES
PESH50	PESH membrane, 50 kDa
PPB	Partial pore blocking / Particle pore blocking
PS	Polysulphone

PVDF	Fluoruro de polivinilideno / Polyvinylidene fluoride
PVDF50	PVDF membrane, 50 kDa
PVP	Polyvinylpyrrolidone
PWO	Partial wet oxidation
Q	Concentration of quencher
R	Resistencia hidráulica / Hydraulic resistance
R	Rejection coefficient
R_a	Mean roughness
RC	Rejection coefficient
RC	Regenerated cellulose
$R_{irrecov}$	Hydraulic resistance caused by irrecoverable fouling
R_{irrev}	Hydraulic resistance caused by irreversible fouling
R_m	Hydraulic resistance caused by the membrane
R_{rev}	Hydraulic resistance caused by reversible fouling
R_T	Total hydraulic resistance
rms	Root mean square roughness
RO	Reverse osmosis
SAC	Spectral absorbance coefficient
SCFA	Short-chain organic acid / Short-chain fatty acid
SEM	Scanning electron microscopy
SSR	Sum of square residuals
TBP	Tributyl phosphate
TCOD	Total COD
TH	Thermal hydrolysis
TMP	Presión transmembrana / Transmembrane pressure
TOA	Trioctylamine
TOC	Total organic carbon
TOPO	Trioctylphosphine oxide
TPSA	Topological polar surface area
TR	Total recycle
UF	Ultrafiltration
VAs	Volatile short-chain organic acids
VC	Volume concentration
VCR	Ratio de concentración de volumen / Volume concentration ratio
VSS	Volatile suspended solids
WAS	Waste activated sludge

WO	Wet oxidation
WOBL	Partially oxidised black liquor
Y	Rendimiento de extracción / Extraction yield
Y	Young leachate
$\boldsymbol{\tau_0}$	Lifetime of the fluorophore in the absence of quencher

Capítulo 1.

INTRODUCCIÓN

1.1. Consideraciones previas

La correcta gestión de las aguas residuales, tanto urbanas como industriales, se ha convertido en un tema de gran relevancia debido al rápido aumento de la población y de la creciente concienciación ambiental tanto a nivel público como gubernamental. Las estrategias actuales de gestión buscan alejarse del modelo tradicional de economía lineal, centrado en la extracción de materias primas para fabricar productos que finalmente terminan como residuos y se desechan, en favor de modelos de economía circular. Dichos modelos circulares buscan crear un flujo de material de circuito cerrado, donde los subproductos de una operación se conviertan en materias primas para otra, conservando así el valor de todos los materiales del proceso. Con ello, se pretende que los modelos de producción y consumo sean más sostenibles al tratar de aprovechar al máximo las materias primas de las que se dispone alargando el ciclo de vida de los productos.

Sin embargo, las aguas residuales también presentan compuestos de interés que no se aprovechan en la mayoría de los casos, perdiendo así la oportunidad de recuperar una gran cantidad de productos de valor añadido. Cabe destacar que la presencia de biomoléculas comercialmente valiosas es un factor común en efluentes de distintas actividades tanto de tipo industrial como de gestión medioambiental. Así, por ejemplo, el licor negro de la industria papelera contiene ácidos orgánicos y lignina; los lixiviados de vertedero presentan ácidos húmicos; y los lodos de depuradora presentan en su composición proteínas, ácidos húmicos y carbohidratos, que además pueden ser oxidados a ácidos orgánicos). Todos estos compuestos pueden resultar de interés en sectores como el agroalimentario, la química fina o la cosmética. Asimismo, la recuperación de estos compuestos podría mejorar significativamente la gestión de este tipo corrientes e incrementar la sostenibilidad del proceso. Por tanto, la reutilización y valorización de estas aguas residuales urbanas e industriales se presenta como un área de trabajo fundamental para alcanzar una economía y una sociedad sostenibles. El problema que plantea la recuperación de estos compuestos es que están contenidos en matrices de gran complejidad, por lo que es preciso analizar diversos métodos de separación para optimizar su recuperación y purificación.

Por ello, en esta tesis se han estudiado y optimizado diferentes procesos de recuperación y purificación de estas biomoléculas (ácidos orgánicos, lignina, ácidos húmicos, proteínas y carbohidratos) mediante técnicas separativas de aplicación industrial, como son la tecnología de membranas y la extracción líquido-líquido. Además, se ha estudiado la influencia de la matriz de la corriente en dichos procesos de recuperación y purificación, así como la aplicación de un tratamiento hidrotérmico previo para la mejora de los rendimientos de extracción de estos compuestos de interés.

1.2. Objetivos de la tesis doctoral

Los objetivos generales de la tesis doctoral son los siguientes: i) el análisis del empleo de distintos tipos de procesos separativos para optimizar la recuperación y/o purificación de biomoléculas de interés, haciendo hincapié en el uso de la tecnología de membranas dado su elevado uso a nivel industrial, ii) el estudio de la influencia de la composición de la matriz en la eficacia del proceso de separación empleado y iii) el estudio del efecto de los tratamientos hidrotérmicos en el rendimiento de la obtención de biomoléculas.

Así, los objetivos específicos a cumplir son los siguientes:

- El análisis bibliográfico de las tecnologías de separación existentes para la revalorización de lodos secundarios de depuradora mediante la recuperación de biomoléculas de valor añadido, incluyendo el diseño de una estrategia de valorización del lodo por etapas.

- El estudio de la eficacia de recuperación de biomoléculas (proteínas, carbohidratos y ácidos húmicos) de lodos de depuradora tratados hidrotérmicamente mediante procesos de membrana centrándose en el contenido en materia orgánica (matriz) y el material y tamaño de corte de las membranas.

- El estudio de la retención de metales pesados presentes en lodos de depuradora mediante procesos de membrana centrándose en el contenido en materia orgánica (matriz) y en el material de las membranas, así como en la determinación del mecanismo por el que es posible esta retención.

- El estudio del efecto de un tratamiento hidrotérmico previo de tipo oxidativo del lodo secundario de depuradora en términos de generación de ácidos orgánicos de cadena corta y de la recuperación de estos ácidos mediante procesos de membrana y extracción líquido-líquido.
- La recuperación de ácidos orgánicos de cadena corta a partir de licor negro mediante procesos de membrana y extracción líquido-líquido atendiendo al contenido en lignina y a la influencia de un tratamiento hidrotérmico previo.
- El estudio de la eficacia de la recuperación de ácidos húmicos a partir de lixiviados de vertedero mediante filtración con membranas haciendo hincapié en la influencia del modo de operación, contenido en materia orgánica (matriz), edad de lixiviado y la existencia de un tratamiento biológico y/o hidrotérmico previo.
- El estudio del ensuciamiento de las membranas durante la operación con las diferentes corrientes estudiadas (lixiviado de vertedero, licor negro y lodos de depuradora) mediante análisis de estas con distintas técnicas de microscopía y modelización de los flujos obtenidos, a fin de optimizar los ciclos de operación y la vida útil de la membrana.

1.3. Estructura de la tesis doctoral

A lo largo de la presente tesis, el trabajo realizado a lo largo de la misma se ha ido recogiendo en artículos de investigación, la mayoría de los cuales han sido publicados en revistas incluidas en *Science Citation Index Expanded.* Por tanto, se ha decidido presentar esta tesis como un compendio de artículos.

El contenido de la tesis se ha dividido en cinco capítulos:

El **Capítulo 1** se corresponde con la introducción, donde se exponen las consideraciones previas al trabajo, se recogen los objetivos generales y específicos de la tesis y se justifica la estructura del documento.

En el **Capítulo 2** se desarrollan las consideraciones teóricas, donde se detallan los aspectos teóricos de los elementos presentes a lo largo de la tesis, incluyendo las corrientes tratadas, los tratamientos hidrotérmicos y los métodos de separación empleados.

En el **Capítulo 3** se recogen de forma general los materiales y métodos utilizados a lo largo de toda la tesis. Los detalles específicos de cada artículo pueden ser consultados en sus correspondientes secciones de *Materials and Methods*.

El **Capítulo 4** incluye todos los artículos de investigación escritos durante la presente tesis, que constituyen la sección de resultados y discusión. Al comienzo del capítulo se incluye una justificación de la organización de los artículos. Por otro lado, al final del mismo se desarrolla una discusión general y se proponen futuros trabajos para continuar con lo desarrollado en esta tesis.

Por último, en el **Capítulo 5** se exponen las principales conclusiones obtenidas tras la tesis.

Se incluye también un anexo donde se detalla la difusión de la tesis doctoral a través de publicaciones en revistas científicas y comunicaciones en congresos y seminarios.

La bibliografía de cada capítulo se incluye al final del mismo, salvo en el capítulo 4, donde se mantiene al final de cada subapartado, al tratarse de una compilación de artículos independientes.

Capítulo 2.

CONSIDERACIONES TEÓRICAS

2.1. Corrientes residuales en economía circular

En las últimas décadas, la creciente actividad económica y demográfica global ha traído consigo un aumento exponencial de la generación de residuos a nivel mundial poniendo de relieve la necesidad de desarrollar estrategias eficientes de gestión de residuos. A medida que han ido aumentando los esfuerzos para reducir el impacto causado por el ser humano en el medio ambiente [1,2], el concepto de economía circular se ha convertido en una estrategia prometedora para lograr alcanzar una economía sostenible. En este sentido, la Directiva Marco de residuos de la Unión Europea ha buscado desligar el crecimiento económico de la producción de residuos mediante el establecimiento del principio de jerarquía de los residuos [1]. Según dicho principio, las políticas de gestión de residuos deben priorizar la prevención, reutilización y reciclado de los residuos, así como otros tipos de valorización de los mismos, incluyendo la energética, antes que su eliminación. Esta estrategia de gestión busca transformar la Unión Europea en una “sociedad del reciclado” y circularizar su economía de manera eficaz. Siguiendo esta Directiva, en España se ha aprobado la Ley 7/2022, de 8 de abril, de residuos y suelos contaminados para una economía circular, que complementa la legislación anteriormente publicada en la que se introdujeron conceptos como subproducto (producto que se obtiene en un proceso industrial cuyo fin no es la producción del mismo, y que puede ser utilizado sin tener que someterse a ulteriores procesos de transformación) o fin de la condición de residuo (criterios específicos que determinados residuos deben seguir para dejar de ser considerados como tal, tras haber sido sometidos a alguna operación de valorización) y refuerza la legislación concerniente a la gestión circular de los residuos. Por estas razones, la economía circular, entendida como el aprovechamiento de subproductos derivados de la actividad industrial con el fin de revalorizar los residuos generados y reducir el consumo de materias primas [2,3], está cobrando cada vez más interés dentro del ámbito industrial y medioambiental.

A pesar de estas directrices comunitarias, se estima que el 60-70% del valor de las aguas residuales en la Unión Europea aún permanece desaprovechado, desperdiciando grandes cantidades de calor, energía, nutrientes, minerales, metales, químicos, etc. [4]; incluyendo el caso particular de España, en la que la gestión de residuos aún se basa mayoritariamente en la deposición en vertedero [1]. Por ello, el desarrollo en el campo de la valorización de las aguas residuales tales como los lodos secundarios de depuradora, el licor negro, o los lixiviados de vertedero es una gran oportunidad para poder seguir avanzando en materia de economía circular (Fig. 2.1).

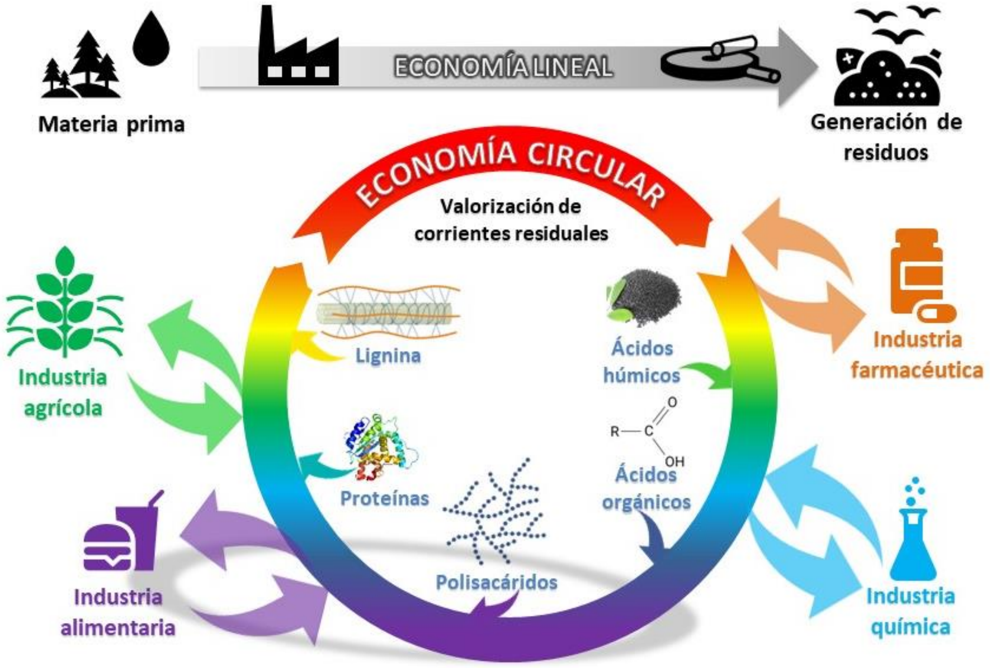

Figura 2.1. Gestión de residuos en modelos de economía lineal y circular.

2.1.1. Lodos de depuradora. Composición. Aprovechamiento actual

Los lodos secundarios de depuradora son residuos generados durante la decantación secundaria tras el tratamiento biológico de las aguas residuales en las Estaciones Depuradoras de Aguas Residuales (EDAR) (Fig. 2.2). Estos lodos son el resultado del crecimiento biológico de los microorganismos empleados para el tratamiento de las aguas residuales, y por tanto están compuestos principalmente por flóculos de células bacterianas, los cuales están formados por interacciones físico-químicas débiles con sustancias poliméricas extracelulares [5]. Dichas sustancias son una mezcla compleja de polímeros excretados por las bacterias, liberados tras la lisis de las bacterias o presentes en las aguas residuales a tratar [6]. La composición de los lodos es muy variable, dependiendo de las características del agua residual inicial y de los tratamientos realizados en la EDAR. Por lo general, es una corriente con un gran contenido acuoso (>95%), con materia suspendida o disuelta tanto con valor agronómico (materia orgánica, nitrógeno, fósforo y varios micronutrientes) como con potencial contaminante (metales pesados, patógenos y contaminantes orgánicos) [7].

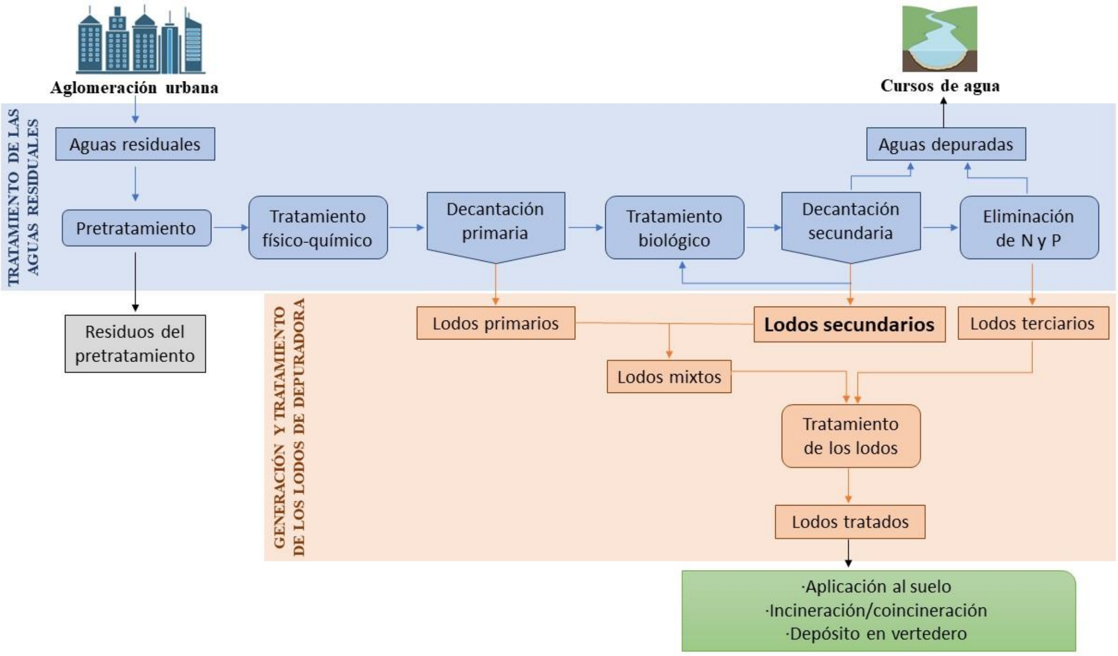

Figura 2.2. Generación y tratamiento de los lodos secundarios de depuradora. Adaptado de [7].

En Europa se producen anualmente unas 10 millones de toneladas en peso seco de lodos de depuradora [8], de los cuales 1.2 millones de toneladas son generadas en España. La gestión de estos lodos es uno de los aspectos más críticos de las EDAR, pudiendo llegar a suponer hasta el 65% de los costes de operación de las mismas [9]. Actualmente, el método principal de gestión de dichos lodos es la aplicación en suelo agrícola, siendo destinados a este fin aproximadamente el 80% de los lodos producidos en España. Le siguen el depósito en vertedero (8%) y la incineración (4%) [7], aunque también se han empleado en menor medida en suelos no agrícolas (reforestación, recuperación de suelos) y en co-compostaje [10,11]. Estos procesos de gestión presentan una serie de inconvenientes entre los que se incluyen poder causar emisiones de gases de efecto invernadero [12] y contaminación del aire [13]; acidificación y eutrofización terrestre

[14]; incremento de la presencia de genes de resistencia a antibióticos en la microbiota del suelo [15] y contaminación del suelo por patógenos [16], contaminantes orgánicos [17] o metales pesados [18]. Además, desperdician el gran potencial que tienen los lodos de depuradora como materia prima de biorrefinería, ya que son una fuente de distintas biomoléculas, como proteínas, lípidos, ácidos orgánicos, carbohidratos y ácidos húmicos; fósforo; bioplásticos; biopesticidas; y energía en forma de biodiésel o biogás [19–25]. La recuperación de las biomoléculas citadas es una vía novedosa para la valorización del lodo de depuradora y para conseguir su inclusión completa en un modelo económico circular.

El principal problema que se debe afrontar al intentar obtener dichas biomoléculas es el hecho de que se encuentran contenidas en las células que conforman los lodos y en sus estructuras poliméricas extracelulares. Esto hace que sea necesario un pretratamiento para la solubilización de los lodos, para lo cual se han estudiado varias técnicas, tales como la sonicación [26,27], cavitación [28], tratamiento alcalino [27,29], ozonólisis [30], oxidación húmeda e hidrólisis térmica [31]. La oxidación húmeda es una tecnología particularmente interesante, ya que la modificación de los parámetros de la operación permite variar la severidad del tratamiento, pudiendo tanto simplemente solubilizar el lodo rompiendo las estructuras poliméricas extracelulares y las paredes celulares, como convertir los biocompuestos más complejos y menos oxidados en otros compuestos de valor, como ácidos orgánicos de cadena corta.

Por último, hay que tener en cuenta que la solubilización de los lodos da lugar a una matriz compleja en la que están contenidas todas las biomoléculas de interés, por lo que son necesarios uno o varios procesos de separación para recuperar y purificar cada uno de los compuestos objetivo.

2.1.3. Lixiviados de vertedero

De acuerdo con la jerarquía actual de gestión de residuos a nivel comunitario, la deposición de residuos en vertedero es la opción menos preferible, y debería ser reducida al mínimo. El objetivo marcado por la Unión Europea es que menos de un 10% de los residuos urbanos generados sean depositados en vertederos para el 2035. Sin embargo, y a pesar de que en la última década se ha conseguido disminuir la tasa de vertido, la gestión de los residuos urbanos a través de la deposición en vertedero sigue suponiendo un 16% de media en la Unión Europea [32]. En España las cifras resultan muy superiores a la media, con un 52% de los residuos urbanos depositados en vertederos en 2020 [33]. Por otro lado, la composición de estos residuos es muy variable, pudiendo clasificarse como residuos biodegradables de comida y otros; papel y cartón; vidrios; plásticos y composites; domésticos peligrosos (medicamentos, bombillas, latas…); e inertes (de construcción, piedras…) [34].

Los lixiviados de vertedero son una corriente residual que se genera por la percolación del agua de lluvia a través de la capa de residuos del vertedero durante el proceso de descomposición de los residuos sólidos [35] (Fig. 2.3).

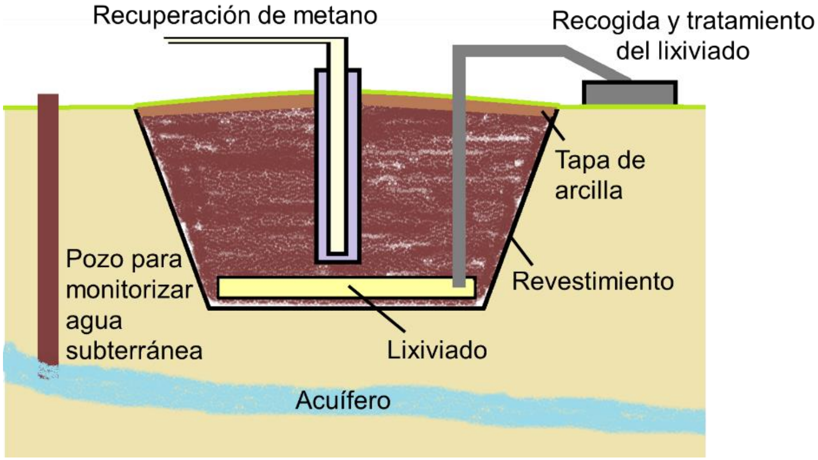

Figura 2.3. Esquema de un vertedero.

Estos lixiviados presentan una gran variabilidad en sus características, las cuales dependen de factores como el clima local, la estación del año, la profundidad del vertedero y, especialmente, la composición de los vertidos y la edad del lixiviado [36–38]. En función de su edad, los lixiviados son clasificados como jóvenes si proceden de un vertedero de menos de un año, y maduros si proceden de un vertedero de más de cinco años. Los lixiviados jóvenes poseen una elevada carga de materia orgánica (demanda química de oxígeno [DQO] >15 g/L O_2), proveniente de compuestos altamente biodegradables. En los vertederos jóvenes ocurre una primera fermentación anaerobia rápida (fase acidogénica), cuyo producto principal son los ácidos grasos volátiles. Durante esta fase, hasta el 95% de la materia orgánica es convertida en ácidos grasos volátiles libres. Posteriormente, durante la etapa metanogénica, estos ácidos grasos volátiles son transformados en biogás (CH_4 y CO_2) por organismos metanogénicos. Así, la fracción orgánica restante en el lixiviado maduro presenta valores de DQO que no superan los 3 g/L O_2, estando formada mayoritariamente por compuestos refractarios, principalmente sustancias húmicas [39,40]. Además, el tamaño medio de los biocompuestos y su biodegradabilidad (relación entre la demanda biológica y química de oxígeno: DBO/DQO), que suele presentar valores de 0.6-0.4 a 0.2-0.05 [41], también disminuye rápidamente durante el envejecimiento del vertedero.

Debido a esta alta variabilidad de los lixiviados, no es posible disponer de una metodología de tratamiento estándar, debiendo esta adecuarse a las características de cada corriente. Las técnicas de tratamiento convencionales de dichas corrientes residuales son la recirculación al vertedero y su tratamiento conjunto con las aguas residuales urbanas en las EDAR. Asimismo, los lixiviados también pueden ser tratados por diferentes métodos de tipo biológico, químico o fisicoquímico [41]. En la Tabla 2.1, se recoge una comparativa de dichos tratamientos.

Además de estos métodos de tratamiento, se ha propuesto valorizar el lixiviado por medio de diferentes vías, como la generación de energía [43]; la recuperación de sustancias húmicas para la elaboración de fertilizantes [44]; recuperación de nutrientes mediante operaciones como filtración con membranas, coagulación-floculación, precipitación, *stripping* o electrodiálisis [45]; co-compostaje [46]; o la obtención post-tratamiento de un subproducto semisólido que puede ser usado para la elaboración de productos cerámicos [47].

Tal y como se ha había indicado, debido a la alta variabilidad de los lixiviados no se puede elaborar una metodología de tratamiento o valorización general, debiendo atender a factores críticos como la edad del vertedero a la hora de decidir la mejor opción en cada caso.

Tabla 2.1. Comparativa de las técnicas para el tratamiento de lixiviados de vertedero [42].

Método		*Principio*	*Ventajas*	*Inconvenientes*
Tratamientos convencionales	Recirculación	Devolución del lixiviado de vertedero recogido al propio vertedero. El relleno del vertedero actúa como biofiltro.	Acelera la estabilización de los residuos del vertedero; aumenta la cantidad de residuos degradada; reduce el volumen de lixiviado.	Acumulación de materia orgánica disuelta, la cual es más difícil de tratar.
	Co-tratamiento	Tratamiento del lixiviado en una EDAR.	Conveniencia; bajo coste.	Hace inefectivo el proceso de desinfección.
Tratamientos biológicos		Degradación de contaminantes orgánicos en el lixiviado mediante reacciones aerobias o anaerobias.	Simplicidad; fiabilidad; buena relación coste-eficiencia.	No efectivo para eliminar la materia orgánica disuelta no biodegradable.
Tratamientos químicos	Precipitación química	Reacción entre químicos y sustancias solubles del lixiviado para formar precipitados.	Gran capacidad; simplicidad; bajos costes de operación.	Baja eficiencia en la eliminación de DQO; dependiente del pH; empleo de grandes cantidades de reactivos; elevada generación de lodos.
	Procesos avanzados de oxidación	Destrucción de la materia orgánica mediante radicales libres y degradación a moléculas más simples o mineralización a CO_2 y H_2O.	Fuerte poder oxidativo; alta eficiencia; condiciones suaves de operación; facilidad de operación y poca necesidad de mantenimiento; rápida velocidad de reacción.	Alto consumo de reactivos químicos; alto consumo de energía; no renovable
	Coagulación / floculación	Compresión de la doble capa, neutralización de cargas, adsorción y puente, y atrapamiento de partículas en un precipitado.	Bajo coste; alta eficiencia.	Elevada generación de lodos; contaminación secundaria; dependiente del pH.

Tabla 2.1. Comparativa de las técnicas para el tratamiento de lixiviados de vertedero [42] (continuación).

Tratamientos físicoquímicos	Adsorción	Los contaminantes son transferidos de la fase líquida a la superficie de un sólido mediante interacciones físicas y/o químicas.	Bajo coste; alta eficiencia.	Regeneración de los adsorbentes; alto consumo de adsorbentes.
	Desorción por aire	Transferencia del NH_3-N de la fase líquida a una corriente de aire o vapor pasada a través del lixiviado.	Simplicidad y estabilidad del proceso; gran adaptabilidad; bajos costes de inversión.	Fugas de NH_3; baja eficiencia en la eliminación de DQO, incrustaciones de carbonato de calcio de la torre de extracción.
	Tratamiento con membranas	Separación mediante tamaño e interacciones electroquímicas entre las membranas y las moléculas.	Alta efectividad; bajo coste; requisitos de equipamiento simples; condiciones suaves.	Ensuciamiento de las membranas y producción de lixiviado concentrado.

2.1.4. Licor negro de papelera

El consumo de madera en Europa por fábricas de pulpa de papel ascendió a cerca de 154.9 millones de toneladas en 2018 [48]. De entre los procesos de obtención de pulpa de celulosa, el método Kraft es el más utilizado, correspondiendo aproximadamente al 75% de la producción total [49].

El licor negro es un subproducto derivado de este proceso, y generado durante la etapa de cocción de la madera con licor blanco (una disolución formada principalmente por compuestos como NaOH y Na_2S) (Fig. 2.4). Esta corriente es resultado de la disolución de diversos compuestos orgánicos e inorgánicos presentes en la madera (tales como resinas, ligninas, hemicelulosas, carbohidratos, metanol, ácidos orgánicos y otros cientos de compuestos) en el licor blanco [50,51]. Por cada tonelada de pulpa producida mediante el proceso Kraft, se generan 7 toneladas de licor negro con aproximadamente un 15% de sólidos totales (10% compuestos orgánicos y 5% inorgánicos), elevados valores de DQO (>70 g/L), un pH altamente básico (>11) y un contenido calórico total de 13.5–14.5 MJ por kg de sólido [52].

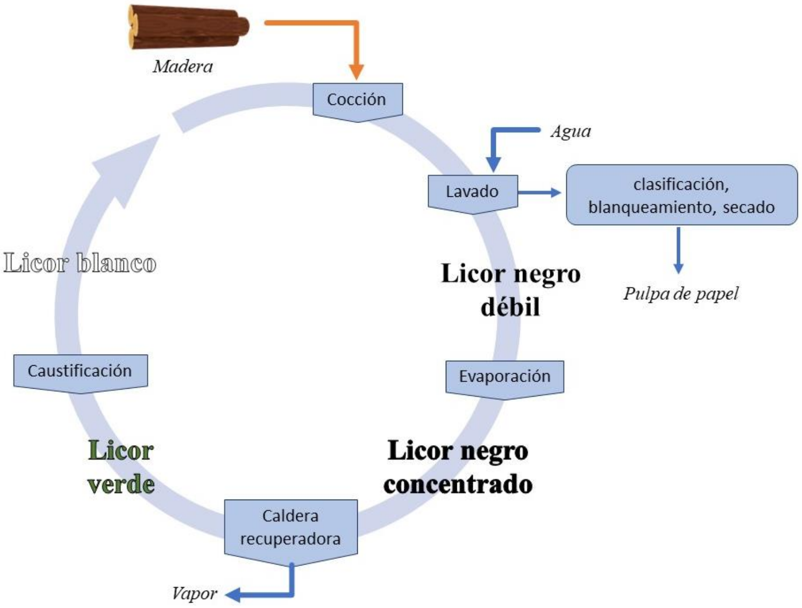

Figura 2.4. Esquema del proceso Kraft.

Actualmente, el licor negro se está aprovechando para la generación de vapor dentro de la misma planta mediante combustión, previa concentración por evaporación hasta un contenido en sólidos totales de 60-85%. Sin embargo, este método de gestión conlleva problemas como la liberación de malos olores durante la evaporación [53] y la generación de gases efecto invernadero, materia particulada, NO_X y SO_2 durante la combustión [54,55]. Además, este procedimiento se puede considerar subóptimo desde un punto de vista económico, ya que el valor específico de la lignina y de otros compuestos orgánicos de valor añadido empleados como combustible es menor que cuando actúan de materias primas para otros procesos o como precursores de otros compuestos valiosos [56].

Las estrategias más recientes de revalorización del licor negro incluyen la producción de polihidroxialcanoatos, biodiésel, hidrógeno, biogás o ácidos orgánicos mediante procesos biológicos, aunque la alta toxicidad del licor negro exige un tratamiento previo para poder usarlo como sustrato, *e.g.*, mediante otros organismos como *Pleurotus ostreatus* o *Pichia pastoris*, fotocatálisis con CuO/TiO_2, hidrólisis enzimática empleando lacasa, adsorción o sobreencalado. Asimismo, también se ha estudiado la generación de biocarbón, bioaceite, singás, metanol, dimetiléter, compuestos aromáticos (benceno, tolueno, furfural, fenol…), plásticos, poliuretanos, poliésteres, ácidos orgánicos, metano o hidrógeno mediante métodos químicos como pirólisis, tratamiento con BTX (benceno, tolueno y xileno), oxidación húmeda o gasificación [57].

2.2. Técnicas de aprovechamiento

En los últimos años, como se ha desarrollado en el apartado 2.1, se están realizando esfuerzos con el fin de cambiar la gestión de residuos desde una filosofía de eliminación a una de reciclaje y valorización, siguiendo los principios de la economía circular. Para ello, se pueden considerar varias estrategias, que pueden estar dirigidas a la valorización del residuo sin necesidad de pretratamiento, al tratamiento parcial de las corrientes para generar compuestos intermedios de valor añadido, o a una degradación más completa para la producción de biocombustibles.

Mediante una degradación parcial de las corrientes estudiadas, pueden obtenerse una gran variedad de compuestos biológicos de valor, como proteínas, enzimas, lípidos, ácidos húmicos, carbohidratos, o ácidos orgánicos. Sin embargo, las corrientes residuales suelen ser muy complejas, por lo que es necesario aplicar pasos de separación y purificación para recuperar los compuestos de interés.

2.2.1. Tratamientos hidrotérmicos

Los tratamientos hidrotérmicos se llevan a cabo a presión y temperatura elevadas empleando un medio acuoso de reacción [58], lo que los convierte en métodos adecuados para tratar corrientes residuales acuosas como las estudiadas en esta tesis. Esta tecnología ofrece varias ventajas, como poder emplear una alimentación mixta, no tener que secar el residuo a tratar o no generar apenas emisiones contaminantes gaseosas [59,60]. En función de los parámetros de presión y temperatura empleados, esta operación puede dirigirse a la obtención de corrientes acuosas susceptibles de ser valorizadas, ya sea en ausencia (hidrólisis térmica) o en presencia (oxidación húmeda) de oxígeno. Las condiciones típicas de estas operaciones son una temperatura de 150-350ºC para la oxidación húmeda [61], y una temperatura menor, ente 100 y 200ºC, para la hidrólisis térmica [58]. En cuanto a la presión, no se trata de un factor tan crítico como la temperatura, pudiendo ir desde los 3 a los 70 bar [62].

Los tratamientos hidrotérmicos degradan la materia orgánica mediante una serie de mecanismos [63]:

- *Formación de radicales libres*: tanto durante la hidrólisis térmica como durante la oxidación húmeda, se producen sendas reacciones en cadena propagada por radicales libres, siendo el mecanismo distinto en cada caso (Tabla 2.2). Se ha investigado el uso de catalizadores metálicos para reducir los altos requerimientos térmicos necesarios para iniciar dichas reacciones de formación de radicales libres [60].

Tabla 2.2. Mecanismos de degradación de la materia orgánica mediante la formación de radicales libres durante los tratamientos de hidrólisis térmica y oxidación húmeda.

Hidrólisis térmica [63]		*Oxidación húmeda* [60]	
$RH \overset{\Delta}{\rightarrow} R^{\bullet} + H^{\bullet}$	(1)	$RH + O_2 \overset{\Delta}{\rightarrow} R^{\bullet} + HO_2^{\bullet}$	(1)
$H^{\bullet} + H_2O \rightarrow HO^{\bullet} + H_2$	(2)	$O_2 + R^{\bullet} \rightarrow ROO^{\bullet}$	(2)
$RH + HO^{\bullet} \rightarrow R^{\bullet} + H_2O$	(3)	$RH + HO_2^{\bullet} \rightarrow R^{\bullet} + H_2O_2$	(3)
$R_2NH + HO^{\bullet} \rightarrow R_2N^{\bullet} + H_2O$	(4)	$H_2O_2 \rightarrow 2HO^{\bullet}$	(4)
		$ROO^{\bullet} + RH \rightarrow R^{\bullet} + ROOH$	(5)

- *Hidrólisis*: la temperatura aplicada durante los tratamientos hidrotérmicos aumenta la reactividad del agua, lo que la lleva a destruir enlaces de moléculas complejas para dar lugar a otras más simples, de acuerdo con la siguiente reacción [64,65]:

$$A - B + H_2O \overset{\Delta}{\rightarrow} A - H + B - OH$$

- *Reacción de Maillard*: a las temperaturas a las que se realizan los tratamientos hidrotérmicos, es posible que se formen polímeros refractarios por la reacción de Maillard, que es un conjunto de reacciones no enzimáticas entre grupos carbonilo y grupos amino presentes en las proteínas y carbohidratos [66]. Por debajo de los 140 ºC se pueden formar productos Amadori, con tamaños generalmente por debajo de los 70 kDa, fruto de la polimerización de aminoácidos de cadena corta y de carbohidratos. A partir de esta temperatura pueden formarse otros polímeros de mayor tamaño (>100 kDa), como las melanoidinas, que son el producto final de la reacción de Maillard [63].

Este tratamiento se ha empleado para obtener ácidos orgánicos a partir de licor negro [57], así como para valorizar la lignina proveniente del mismo [67]. En cuanto a los lodos de depuradora, se ha propuesto como pretratamiento para solubilizar los lodos para posteriormente producir biogás [63] o recuperar proteínas [31], lípidos, carbohidratos o ácidos grasos volátiles [68].

2.2.2. Métodos de separación

2.2.2.1. Separación por membranas

El concepto detrás de los procesos de separación por membranas es relativamente simple: las membranas pueden describirse como filtros convencionales, pero con un tamaño de malla o poro mucho más pequeño, lo que permite la separación de partículas del orden de micras o nanómetros [69]. Los procesos de membranas más estandarizados son aquellos que usan la presión como fuerza impulsora [70]. Así, dependiendo del peso molecular que permite rechazar el 90% del soluto macromolecular o lo que es lo mismo del tamaño de corte de la membrana, [71], esta tecnología puede clasificarse como microfiltración, ultrafiltración, nanofiltración u ósmosis inversa (Fig. 2.5). Por otro lado, las membranas se pueden producir en una amplia gama de materiales (cerámicos o poliméricos) y geometrías (planas, en espiral, tubulares o de fibra hueca [72]), los cuales determinan características operativas como el flujo, la vida útil o la selectividad de la membrana [73,74].

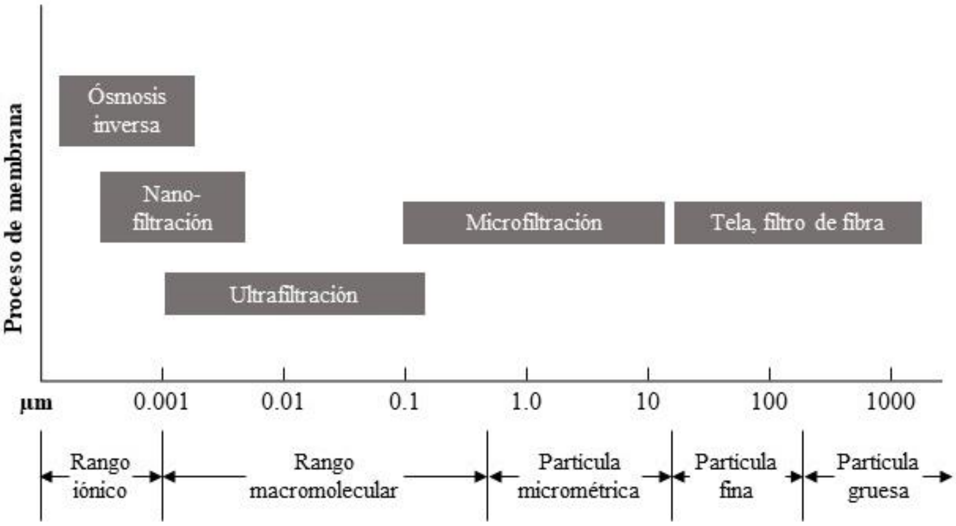

Figura 2.5. Rango de aplicación de distintos procesos de separación por membranas basado en tamaños de partícula [69].

Esta tecnología ha experimentado un significativo crecimiento en los últimos años debido a sus múltiples ventajas al tratarse de una tecnología flexible, limpia, con bajos costes energéticos, que permite sustituir a otros procesos convencionales y que puede acoplarse a otras tecnologías como un proceso híbrido [75].

El principal inconveniente de esta tecnología es la pérdida de flujo debida al ensuciamiento de membrana. Dicho ensuciamiento es causado por interacciones físicas, químicas o biológicas entre la membrana y los distintos solutos o materia suspendida de la corriente filtrada, lo que conduce a una pérdida de permeabilidad y/o selectividad de la membrana [76]. Comprender los mecanismos de ensuciamiento y la naturaleza de las partículas que causan el ensuciamiento es fundamental para abordar correctamente este importante problema [77]. Para este fin, pueden encontrarse varios modelos en la literatura, como los modelos de Hermia [78], el modelo de Mehta [79] o el modelo de resistencias en serie [80].

La tecnología de membranas se ha estudiado en lodos secundarios para obtener concentrados de ácidos húmicos mediante microfiltración o ultrafiltración [26,81–83]. En cuanto al licor negro, se ha estudiado la obtención de retenidos concentrados en lignina y hemicelulosas mediante microfiltración, ultrafiltración y nanofiltración, y la recuperación de ácidos orgánicos de cadena corta y sales inorgánicas mediante ósmosis inversa [84]. Por último, también se ha estudiado la recuperación de fósforo y nitrógeno de los lixiviados mediante nanofiltración y ósmosis inversa para elaborar fertilizantes [85].

En el contexto de esta tesis, la tecnología de membranas permite fraccionar una corriente empleando membranas de distinto tamaño de corte, pudiendo separar así los distintos compuestos presentes en el residuo a valorizar; o bien prepurificar dicha corriente con el fin de facilitar una etapa posterior de separación y mejorar su eficacia.

2.2.2.2. Extracción líquido-líquido

La extracción por disolventes consiste en el proceso de recuperación de un soluto contenido en una matriz mediante un disolvente. Cuando tanto la matriz como el disolvente son líquidos, el proceso se denomina extracción líquido-líquido, y el principio en que se basa es la diferencia entre las solubilidades de un soluto en dos disolventes inmiscibles o poco miscibles entre ellos. Al poner en contacto la matriz en la que está contenida el soluto con el disolvente adecuado, la mayor afinidad por este último hará que el soluto migre de la matriz al disolvente [86]. La extracción con disolventes presenta una serie de ventajas, tales como un mejor efecto de separación que la precipitación, una mayor selectividad y velocidad de transferencia de masa que el intercambio iónico, o un menor consumo de energía y una operación continua a gran escala más fácil que la destilación [87]. Una correcta elección del disolvente es crítica en la idoneidad de la operación y debe tener en cuenta factores como la selectividad y el coeficiente de distribución según el compuesto de interés, la inmiscibilidad con la fase líquida contraria, la facilidad de recuperación, la densidad, la tensión interfacial, la reactividad química, la viscosidad, la presión de vapor y el punto de congelación, y la disponibilidad y coste [88]. Los disolventes pueden ser físicos o reactivos. Estos últimos forman complejos con el soluto, y suelen ser compuestos, formados por un agente extractante que forma los complejos, y un diluyente que facilita el contacto entre el soluto y el extractante [88].

Esta tecnología se ha empleado en lodos de depuradora para la recuperación de lípidos [89–92] y biodiésel [93]; en licor negro para la recuperación de biocrudo, ácidos orgánicos, compuestos aromáticos y lignina [84]; y en lixiviados de vertedero para la recuperación de ácidos grasos volátiles [94,95].

Referencias

[1] Ley 7/2022, de 8 de abril, de residuos y suelos contaminados para una economía circular. Boletín Oficial del Estado, 85, de 9 de abril de 2022.

[2] Y. Geng, B. Doberstein, Developing the circular economy in China: Challenges and opportunities for achieving "leapfrog development," Https://Doi.Org/10.3843/SusDev.15.3:6. 15 (2010) 231–239. doi:10.3843/SUSDEV.15.3:6.

[3] K. Webster, The circular economy: A wealth of flows, Ellen MacArthur Foundation Publishing., 2016.

[4] Citation Water Europe, Water Europe Strategic Innovation and Research Agenda (Water Europe SIRA) 2030, Water Europe, Brussels.

[5] J.L. Urrea, S. Collado, P. Oulego, M. Díaz, Formation and Degradation of Soluble Biopolymers during Wet Oxidation of Sludge, ACS Sustain. Chem. Eng. 5 (2017) 3011–3018. doi:10.1021/ACSSUSCHEMENG.6B02664.

[6] G.P. Sheng, J. Xu, W.H. Li, H.Q. Yu, Quantification of the interactions between Ca2+, Hg2+ and extracellular polymeric substances (EPS) of sludge, Chemosphere. 93 (2013) 1436–1441. doi:10.1016/J.CHEMOSPHERE.2013.07.076.

[7] Ministerio para la Transición Ecológica y el Reto Demográfico, Lodos de depuración de aguas residuales, (2018). https://www.miteco.gob.es/es/calidad-y-evaluacion-ambiental/temas/prevencion-y-gestion-residuos/flujos/lodos-depuradora/ (accessed March 21, 2023).

[8] Eurostat, Sewage sludge production and disposal from urban wastewater (in dry substance (d.s)), 2022. (2022). https://ec.europa.eu/eurostat/databrowser/view/ten00030/default/table?lang=en (accessed January 24, 2022).

[9] J.A. Villamil, A.F. Mohedano, J. San Martín, J.J. Rodriguez, M.A. de la Rubia, Anaerobic co-digestion of the process water from waste activated sludge hydrothermally treated with primary sewage sludge. A new approach for sewage sludge management, Renew. Energy. 146 (2020) 435–443. doi:10.1016/j.renene.2019.06.138.

[10] J. Mateo-Sagasta, L. Raschid-Sally, A. Thebo, Global Wastewater and Sludge Production, Treatment and Use, in: Wastewater, Springer Netherlands, Dordrecht, 2015: pp. 15–38. doi:10.1007/978-94-017-9545-6_2.

[11] S. Shi, G. Xu, H. Yu, Z. Zhang, Strategies of valorization of sludge from wastewater treatment, J. Chem. Technol. Biotechnol. 93 (2018) 936–944. doi:10.1002/jctb.5548.

[12] M.K. Awasthi, Q. Wang, X. Ren, J. Zhao, H. Huang, S.K. Awasthi, A.H. Lahori, R. Li, L. Zhou, Z. Zhang, Role of biochar amendment in mitigation of nitrogen loss and greenhouse gas emission during sewage sludge composting, Bioresour. Technol. 219 (2016) 270–280. doi:10.1016/j.biortech.2016.07.128.

[13] J. Werther, T. Ogada, Sewage sludge combustion, Prog. Energy Combust. Sci. 25 (1999) 55–116. doi:10.1016/S0360-1285(98)00020-3.

[14] Y. Zhao, W. Lu, A. Damgaard, Y. Zhang, H. Wang, Assessment of co-composting of sludge and woodchips in the perspective of environmental impacts (EASETECH), Waste Manag. 42 (2015) 55–60. doi:10.1016/j.wasman.2015.04.021.

[15] Q. Chen, X. An, H. Li, J. Su, Y. Ma, Y.G. Zhu, Long-term field application of sewage sludge increases the abundance of antibiotic resistance genes in soil, Environ. Int. 92–93 (2016) 1–10. doi:10.1016/j.envint.2016.03.026.

[16] D.L. Lewis, D.K. Gattie, Pathogen risks from applying sewage sludge to land, Environ. Sci. Technol. 36 (2002). doi:10.1021/es0223426.

[17] J. Dai, M. Xu, J. Chen, X. Yang, Z. Ke, PCDD/F, PAH and heavy metals in the sewage sludge from six wastewater treatment plants in Beijing, China, Chemosphere. 66 (2007) 353–361. doi:10.1016/j.chemosphere.2006.04.072.

[18] P.C. Hsiau, S.L. Lo, Extractabilities of heavy metals in chemically-fixed sewage sludges, in: J. Hazard. Mater., 1998: pp. 73–82. doi:10.1016/S0304-3894(97)00121-0.

[19] A.P. Bora, D.P. Gupta, K.S. Durbha, Sewage sludge to bio-fuel: A review on the sustainable approach of transforming sewage waste to alternative fuel, Fuel. 259 (2020) 116262. doi:10.1016/j.fuel.2019.116262.

[20] A. Raheem, V.S. Sikarwar, J. He, W. Dastyar, D.D. Dionysiou, W. Wang, M. Zhao, Opportunities and challenges in sustainable treatment and resource reuse of sewage sludge: A review, Chem. Eng. J. 337 (2018) 616–641. doi:10.1016/j.cej.2017.12.149.

[21] B. Cieślik, P. Konieczka, A review of phosphorus recovery methods at various steps of wastewater treatment and sewage sludge management. The concept of “no solid waste generation” and analytical methods, J. Clean. Prod. 142 (2017) 1728–1740. doi:10.1016/j.jclepro.2016.11.116.

[22] W. Liu, H. Yang, J. Ye, J. Luo, Y.Y. Li, J. Liu, Short-chain fatty acids recovery from sewage sludge via acidogenic fermentation as a carbon source for denitrification: A review, Bioresour. Technol. 311 (2020) 123446. doi:10.1016/j.biortech.2020.123446.

[23] M.N. Siddiquee, S. Rohani, Lipid extraction and biodiesel production from municipal sewage sludges: A review, Renew. Sustain. Energy Rev. 15 (2011) 1067–1072. doi:10.1016/J.RSER.2010.11.029.

[24] K. Xiao, Y. Zhou, Protein recovery from sludge: A review, J. Clean. Prod. 249 (2020) 119373. doi:10.1016/j.jclepro.2019.119373.

[25] P. Supaporn, H.V. Ly, S.S. Kim, S.H. Yeom, Bio-oil production using residual sewage sludge after lipid and carbohydrate extraction, Environ. Eng. Res. 24 (2019) 202–210. doi:10.4491/eer.2017.178.

[26] L. Wei, K. Wang, X. Kong, G. Liu, S. Cui, Q. Zhao, F. Cui, Application of ultra-sonication, acid precipitation and membrane filtration for co-recovery of protein and humic acid from sewage sludge, Front. Environ. Sci. Eng. 10 (2016) 327–335. doi:10.1007/s11783-014-0763-9.

[27] J. Hwang, L. Zhang, S. Seo, Y.W. Lee, D. Jahng, Protein recovery from excess sludge for its use as animal feed, Bioresour. Technol. 99 (2008) 8949–8954. doi:10.1016/j.biortech.2008.05.001.

[28] A.P. Bhat, P.R. Gogate, Cavitation-based pre-treatment of wastewater and waste sludge for improvement in the performance of biological processes: A review, J. Environ. Chem. Eng. 9 (2021) 104743. doi:10.1016/J.JECE.2020.104743.

[29] M. Pervaiz, M. Sain, Protein extraction from secondary sludge of paper mill wastewater and its utilization as a wood adhesive, BioResources. 6 (2011) 961–970.

[30] B. Otieno, S. Apollo, J. Kabuba, B. Naidoo, G. Simate, A. Ochieng, Ozonolysis pre-treatment of waste activated sludge for solubilization and biodegradability enhancement, J. Environ. Chem. Eng. 7 (2019) 102945. doi:10.1016/J.JECE.2019.102945.

[31] M. García, J.L. Urrea, S. Collado, P. Oulego, M. Díaz, Protein recovery from solubilized sludge by hydrothermal treatments, Waste Manag. 67 (2017) 278–287. doi:10.1016/J.WASMAN.2017.05.051.

[32] European Environment Agency, Diversion of waste from landfill in Europe, (2022). https://www.eea.europa.eu/ims/diversion-of-waste-from-landfill (accessed March 22, 2023).

[33] European Environment Agency, Municipal waste landfill rates in Europe by country, (2023). https://www.eea.europa.eu/data-and-maps/figures/municipal-waste-landfill-rates-in-1 (accessed March 22, 2023).

[34] J.M. Díaz Fernández, Ingeniería de Bioprocesos, Madrid, 2012.

[35] T.A. Kurniawan, W. hung Lo, G.Y.S. Chan, Radicals-catalyzed oxidation reactions for degradation of recalcitrant compounds from landfill leachate, Chem. Eng. J. 125 (2006) 35–57. doi:10.1016/j.cej.2006.07.006.

[36] C.M. Moody, T.G. Townsend, A comparison of landfill leachates based on waste composition, Waste Manag. 63 (2017) 267–274. doi:10.1016/j.wasman.2016.09.020.

[37] L.M. Chu, K.C. Cheung, M.H. Wong, Variations in the chemical properties of landfill leachate, Environ. Manage. 18 (1994) 105–117. doi:10.1007/BF02393753.

[38] D. Kulikowska, E. Klimiuk, The effect of landfill age on municipal leachate composition, Bioresour. Technol. 99 (2008) 5981–5985. doi:10.1016/j.biortech.2007.10.015.

[39] S. Renou, J.G. Givaudan, S. Poulain, F. Dirassouyan, P. Moulin, Landfill leachate treatment: Review and opportunity, J. Hazard. Mater. 150 (2008) 468–493. doi:10.1016/j.jhazmat.2007.09.077.

[40] Y. Peng, Perspectives on technology for landfill leachate treatment, Arab. J. Chem. 10 (2017) S2567–S2574. doi:10.1016/j.arabjc.2013.09.031.

[41] R.C. Contrera, K.C. Da Cruz Silva, G.H. Ribeiro Silva, D.M. Morita, M. Zaiat, V. Schalch, The "chemical oxygen demand / total volatile acids" ratio as an anaerobic treatability indicator for landfill leachates, Brazilian J. Chem. Eng. 32 (2015) 73–86. doi:10.1590/0104-6632.20150321s00003024.

[42] C. Teng, K. Zhou, C. Peng, W. Chen, Characterization and treatment of landfill leachate: A review, Water Res. 203 (2021) 117525. doi:10.1016/J.WATRES.2021.117525.

[43] S.S. Kumar, A. Kumar, S.K. Malyan, P. Ghosh, M. Kumar, R. Kapoor, A.K. Agrawal, S. Kumar, V. Kumar, L. Singh, Landfill leachate valorization: A potential alternative to burden off resources and support energy systems, Fuel. 331 (2023) 125911. doi:10.1016/j.fuel.2022.125911.

[44] A. Tahiri, J. Destain, P. Thonart, P. Druart, Valorisation et propriétés des substances humiques des lixiviats de décharge, J. Mater. Environ. Sci. 5 (2014) 2495–2498.

[45] T.A. Kurniawan, D. Singh, R. Avtar, M.H.D. Othman, G.H. Hwang, A.B. Albadarin, M. Rezakazemi, T. Setiadi, S. Shirazian, Resource recovery from landfill leachate: An experimental investigation and perspectives, Chemosphere. 274 (2021) 129986. doi:10.1016/J.CHEMOSPHERE.2021.129986.

[46] H. Charkaoui, M. Benbouya, K. El Ass, S. Kitane, A. Bahloul, S. El Hajjaji, A. El Midaoui, Treatment and valorization of leachates from controlled landfills by composting the fermentable fraction of household and assimilated waste, Mediterr. J. Chem. 9 (2019) 12–23. doi:10.13171/mjc91190810100ab.

[47] Fundación CARTIF, National Technical University of Athens, Triton Water Technologies S.L., InfinitValuEngineering S.L., Low energy treatment technology for leachate valorisation, Eur. Comm. LIFE Public Database. (2023). https://webgate.ec.europa.eu/life/publicWebsite/project/details/4474 (accessed March 31, 2023).

[48] M.J. Quina, C.T. Pinheiro, Inorganic Waste Generated in Kraft Pulp Mills: The Transition from Landfill to Industrial Applications, Appl. Sci. 2020, Vol. 10, Page 2317. 10 (2020) 2317. doi:10.3390/APP10072317.

[49] D.G. Briggs, Forest products measurements and conversion factors : with special emphasis on the U.S. Pacific Northwest, 1994.

[50] P. Bajpai, Pulping Fundamentals, in: Biermann's Handb. Pulp Pap., 2018: pp. 295–351. doi:10.1016/b978-0-12-814240-0.00012-4.

[51] L. Pola, S. Collado, P. Oulego, M. Díaz, Production of carboxylic acids from the non-lignin residue of black liquor by hydrothermal treatments, Bioresour. Technol. 284 (2019) 105–114. doi:10.1016/j.biortech.2019.03.066.

[52] P. Bajpai, Pulping Fundamentals, in: Biermann's Handb. Pulp Pap., Elsevier, 2018: pp. 295–351. doi:10.1016/b978-0-12-814240-0.00012-4.

[53] E.R. Hendrickson, C.I. Harding, Black liquor oxidation as a method for reducing air pollution

from sulfate pulping, J. Air Pollut. Control Assoc. 14 (1964) 487–490. doi:10.1080/00022470.1964.10468320.

[54] D.M. Martin, E.W. Malcolm, M. Hupa, D.M. Martin, E.W. Malcolm, M. Hupa, The Effect of Fuel Composition on Nitrogen Release During Black Liquor Pyrolysis, n.d.

[55] E.K. Vakkilainen, M. Hamaguchi, D.C. Laux, Grouping Statistically Emissions from a Recovery Boiler, XXI Encontro Nac. Da Tec. / VI CIADICYP 2010, Lisboa, Port. (n.d.).

[56] I.F. Demuner, F.J. Borges Gomes, J.S. Gomes, M.R. Coura, F.P. Borges, A.M. Macedo Ladeira Carvalho, C.M. Silva, Improving kraft pulp mill sustainability by lignosulfonates production from processes residues, J. Clean. Prod. 317 (2021) 128286. doi:10.1016/j.jclepro.2021.128286.

[57] R. Morya, M. Kumar, I. Tyagi, A. Kumar Pandey, J. Park, T. Raj, R. Sirohi, V. Kumar, S.H. Kim, Recent advances in black liquor valorization, Bioresour. Technol. 350 (2022) 126916. doi:10.1016/j.biortech.2022.126916.

[58] K. Hii, S. Baroutian, R. Parthasarathy, D.J. Gapes, N. Eshtiaghi, A review of wet air oxidation and Thermal Hydrolysis technologies in sludge treatment, Bioresour. Technol. 155 (2014) 289–299. doi:10.1016/j.biortech.2013.12.066.

[59] K.Q. Tran, Process intensification and process integration for hydrothermal processing of forest residues and agricultural wastes, Waste Biorefinery Potential Perspect. (2018) 299–322. doi:10.1016/B978-0-444-63992-9.00010-0.

[60] H. Debellefontaine, J.N. Foussard, Wet air oxidation for the treatment of industrial wastes. Chemical aspects, reactor design and industrial applications in Europe, Waste Manag. 20 (2000) 15–25. doi:10.1016/S0956-053X(99)00306-2.

[61] C. Peral, Biomass Pretreatment Strategies (Technologies, Environmental Performance, Economic Considerations, Industrial Implementation), in: Biotransformation Agric. Waste By-Products Food, Feed. Fibre, Fuel Econ., Elsevier, 2016: pp. 125–160. doi:10.1016/B978-0-12-803622-8.00005-7.

[62] J. Zhang, H. Zhou, D. Liu, X. Zhao, Pretreatment of lignocellulosic biomass for efficient enzymatic saccharification of cellulose, in: Lignocellul. Biomass to Liq. Biofuels, Academic Press, 2019: pp. 17–65. doi:10.1016/B978-0-12-815936-1.00002-2.

[63] P.L. Ngo, I.A. Udugama, K. V. Gernaey, B.R. Young, S. Baroutian, Mechanisms, status, and challenges of thermal hydrolysis and advanced thermal hydrolysis processes in sewage sludge treatment, Chemosphere. 281 (2021). doi:10.1016/j.chemosphere.2021.130890.

[64] G. Brunner, Near critical and supercritical water. Part I. Hydrolytic and hydrothermal processes, J. Supercrit. Fluids. 47 (2009) 373–381. doi:10.1016/j.supflu.2008.09.002.

[65] S.S. Toor, L. Rosendahl, A. Rudolf, Hydrothermal liquefaction of biomass: A review of subcritical water technologies, Energy. 36 (2011) 2328–2342. doi:10.1016/j.energy.2011.03.013.

[66] A.D. Troise, Maillard Reaction and Food Safety, Encycl. Food Secur. Sustain. (2018) 364–369.

doi:10.1016/B978-0-08-100596-5.22146-X.

[67] A.G. Demesa, A. Laari, M. Sillanp, T. Koiranen, Valorization of lignin by partial wet oxidation using sustainable heteropoly acid catalysts, Molecules. 22 (2017). doi:10.3390/molecules22101625.

[68] O. Suárez-Iglesias, J.L. Urrea, P. Oulego, S. Collado, M. Díaz, Valuable compounds from sewage sludge by thermal hydrolysis and wet oxidation. A review, Sci. Total Environ. 584–585 (2017) 921–934. doi:10.1016/j.scitotenv.2017.01.140.

[69] Z.F. Cui, H.S. Muralidhara, Membrane Technology, Elsevier, 2010. doi:10.1016/C2009-0-19129-8.

[70] R.W. Baker, Overview of Membrane Science and Technology, in: Membr. Technol. Appl., John Wiley & Sons, Ltd, Chichester, UK, 2012: pp. 1–14. doi:10.1002/9781118359686.ch1.

[71] R. Singh, Membrane Technology and Engineering for Water Purification, Elsevier, 2015. doi:10.1016/C2013-0-15275-0.

[72] Z. Berk, Z. Berk, Chapter 10 – Membrane processes, Food Process Eng. Technol. (2009) 233–257. doi:10.1016/B978-0-12-373660-4.00010-7.

[73] D.M. Kanani, W.H. Fissell, S. Roy, A. Dubnisheva, A. Fleischman, A.L. Zydney, Permeability-selectivity analysis for ultrafiltration: Effect of pore geometry, J. Memb. Sci. 349 (2010) 405–410. doi:10.1016/j.memsci.2009.12.003.

[74] J.M. Gohil, R.R. Choudhury, Introduction to Nanostructured and Nano-enhanced Polymeric Membranes: Preparation, Function, and Application for Water Purification, in: Nanoscale Mater. Water Purif., Elsevier, 2018: pp. 25–57. doi:10.1016/B978-0-12-813926-4.00038-0.

[75] T.A. Saleh, V.K. Gupta, An Overview of Membrane Science and Technology, in: Nanomater. Polym. Membr., Elsevier, 2016: pp. 1–23. doi:10.1016/B978-0-12-804703-3.00001-2.

[76] H. Li, V. Chen, Membrane Fouling and Cleaning in Food and Bioprocessing, in: Membr. Technol., Elsevier Ltd, 2010: pp. 213–254. doi:10.1016/B978-1-85617-632-3.00010-0.

[77] W. Guo, H.H. Ngo, J. Li, A mini-review on membrane fouling, Bioresour. Technol. 122 (2012) 27–34. doi:10.1016/j.biortech.2012.04.089.

[78] J. Hermia, Constant Pressure Blocking Filtration Laws - Application Topower-Law Non-Newtonian Fluids., Trans Inst Chem Eng. V 60 (1982) 183–187.

[79] B. Mehta, Processing of model compositional whey solutions with pressure driven membranes, Ohio State University, 1973.

[80] G. Di Bella, D. Di Trapani, A brief review on the resistance-in-series model in membrane bioreactors (MBRs), Membranes (Basel). 9 (2019) 24. doi:10.3390/membranes9020024.

[81] H. Li, Y. Li, Y. Jin, S. Zou, C. Li, Recovery of sludge humic acids with alkaline pretreatment and its impact on subsequent anaerobic digestion, J. Chem. Technol. Biotechnol. 89 (2014) 707–713.

doi:10.1002/jctb.4173.

[82] H. Li, Y. Li, S. Zou, C. Li, Extracting humic acids from digested sludge by alkaline treatment and ultrafiltration, J. Mater. Cycles Waste Manag. 16 (2014) 93–100. doi:10.1007/s10163-013-0153-6.

[83] H. Li, Y. Jin, Y. Nie, Application of alkaline treatment for sludge decrement and humic acid recovery, Bioresour. Technol. 100 (2009) 6278–6283. doi:10.1016/j.biortech.2009.07.022.

[84] L. Pola, S. Collado, P. Oulego, M. Díaz, Kraft black liquor as a renewable source of value-added chemicals, Chem. Eng. J. 448 (2022) 137728. doi:10.1016/J.CEJ.2022.137728.

[85] T.A. Kurniawan, M.H.D. Othman, X. Liang, H.H. Goh, K.W. Chew, From liquid waste to mineral fertilizer: Recovery, recycle and reuse of high-value macro-nutrients from landfill leachate to contribute to circular economy, food security, and carbon neutrality, Process Saf. Environ. Prot. 170 (2023) 791–807. doi:10.1016/j.psep.2022.12.068.

[86] K.G. Clarke, Downstream processing, in: Bioprocess Eng., Elsevier, 2013: pp. 209–234. doi:10.1533/9781782421689.209.

[87] H. Chen, L. Wang, Posttreatment Strategies for Biomass Conversion, in: Technol. Biochem. Convers. Biomass, Metallurgical Industry Press, 2017: pp. 197–217. doi:10.1016/b978-0-12-802417-1.00008-9.

[88] L.M.J. Sprakel, B. Schuur, Solvent developments for liquid-liquid extraction of carboxylic acids in perspective, Sep. Purif. Technol. 211 (2019) 935–957. doi:10.1016/j.seppur.2018.10.023.

[89] M. Olkiewicz, M.P. Caporgno, A. Fortuny, F. Stüber, A. Fabregat, J. Font, C. Bengoa, Direct liquid-liquid extraction of lipid from municipal sewage sludge for biodiesel production, Fuel Process. Technol. 128 (2014) 331–338. doi:10.1016/j.fuproc.2014.07.041.

[90] L.H. Huynh, N.S. Kasim, Y.H. Ju, Extraction and analysis of neutral lipids from activated sludge with and without sub-critical water pre-treatment, Bioresour. Technol. 101 (2010) 8891–8896. doi:10.1016/j.biortech.2010.06.135.

[91] S. Dufreche, R. Hernandez, T. French, D. Sparks, M. Zappi, E. Alley, Extraction of lipids from municipal wastewater plant microorganisms for production of biodiesel, JAOCS, J. Am. Oil Chem. Soc. 84 (2007) 181–187. doi:10.1007/s11746-006-1022-4.

[92] J.A. Melero, R. Sánchez-Vázquez, I.A. Vasiliadou, F. Martínez Castillejo, L.F. Bautista, J. Iglesias, G. Morales, R. Molina, Municipal sewage sludge to biodiesel by simultaneous extraction and conversion of lipids, Energy Convers. Manag. 103 (2015) 111–118. doi:10.1016/j.enconman.2015.06.045.

[93] E. Revellame, R. Hernandez, W. French, W. Holmes, E. Alley, R. Callahan, Production of biodiesel from wet activated sludge, J. Chem. Technol. Biotechnol. 86 (2011) 61–68. doi:10.1002/jctb.2491.

[94] S. Begum, V. Arelli, G.R. Anupoju, S. S, S.K. Bhargava, N. Eshtiaghi, Optimization of feed and

extractant concentration for the liquid–liquid extraction of volatile fatty acids from synthetic solution and landfill leachate, J. Ind. Eng. Chem. 90 (2020) 190–202. doi:10.1016/j.jiec.2020.07.011.

[95] Y.S. Razali, H.A. Tajarudin, Z. Daud, Extraction of volatile fatty acids from leachate via liquid-liquid extraction and adsorption method, Int. J. Integr. Eng. 10 (2018) 79–84. doi:10.30880/ijie.2018.10.09.029.

Capítulo 3.
MATERIAL Y MÉTODOS

3.1. Corrientes residuales

Las corrientes residuales utilizadas durante esta tesis fueron lodos secundarios de depuradora, licor negro Kraft y lixiviados de vertedero. En este apartado se indican los intervalos de valores que presentan los distintos parámetros, ya que se utilizaron diferentes lotes de partida durante la experimentación. La caracterización concreta de cada corriente se encuentra en los subapartados correspondientes del Capítulo 4.

3.1.1. Lodos secundarios de depuradora

Los lodos secundarios de depuradora empleados se recogieron en la estación depuradora de aguas residuales situada en Baíña, (Asturias, España) una vez sometidos al tratamiento de espesamiento llevado a cabo por flotación con aire disuelto. Tras su recogida se almacenaron a 4 ºC hasta su tratamiento hidrotérmico, que en ningún caso superó más de tres días desde su recogida. En la Tabla 3.1, se indican los intervalos de valores de los principales parámetros fisicoquímicos de los lodos utilizados.

Tabla 3.1. Características fisicoquímicas de los lodos secundarios de depuradora.

Parámetro	Valor
pH	6.5 – 6.8
Demanda química de oxígeno total (mg O_2/L)	37121 – 37200
Demanda química de oxígeno soluble (mg O_2/L)	200 – 507
Carbono orgánico total (mg C/L)	373 – 484
Sólidos suspendidos totales (g/L)	32 – 33.5
Sólidos suspendidos volátiles (g/L)	26.5 – 27.2
Proteínas (mg/L) (1)	26 –181
Ácidos húmicos (mg/L) (1)	104 – 281
Carbohidratos (mg/L) (1)	17 –82

(1) Referido a la concentración soluble

3.1.2. Lixiviados

Los lixiviados estudiados durante esta tesis fueron obtenidos del vertedero de La Zoreda y proporcionados por el Consorcio para la Gestión de Residuos Sólidos de Asturias (COGERSA, S.A.U, Asturias, España). Durante la experimentación se emplearon diferentes lotes de tres tipos distintos de lixiviados: joven, maduro y tratado biológicamente. El lixiviado joven se obtuvo de una nueva área del vertedero que se encuentra en expansión, mientras que el lixiviado maduro procede de una zona del vertedero en la que no se depositan residuos desde 2010. El lixiviado tratado biológicamente procede del tratamiento combinado de tipo biológico y fisicoquímico de los lixiviados jóvenes y maduros, que está basado en la tecnología BIOMEMBRAT®. Así, estos efluentes son sometidos a procesos biológicos de nitrificación y desnitrificación para la eliminación de la materia orgánica y amonio, seguidos de un tratamiento con membranas de tamaño de poro 0.02 µm. Como efluentes se obtienen el lixiviado tratado y los lodos biológicos.

En la Tabla 3.2 se recogen los intervalos de valores de los principales parámetros fisicoquímicos de los lixiviados utilizados. Todos los lixiviados fueron prefiltrados con un filtro de malla metálica de 250 µm de tamaño de poro y 200 mm de diámetro para eliminar las partículas gruesas. Las muestras se almacenaron a 5ºC antes de ser utilizadas.

Tabla 3.2. Características fisicoquímicas de los lixiviados maduros, jóvenes y tratados biológicamente.

Parámetro	**Tipo de lixiviado**		
	Maduro	**Joven**	**Tratado biológicamente**
pH	7.8 – 8.6	8.6 – 9.0	6.7 – 6.9
Demanda química de oxígeno soluble (mg O_2/L)	3413 – 4597	5145 – 9973	1255 – 1271
Demanda biológica de oxígeno (mg O_2/L)	279 – 839	1461 – 3409	25 – 31
Sólidos suspendidos totales (mg/L)	5 – 53	27 – 157	6 – 7
Amonio (mg/L)	1832 – 2568	2532– 3386	18 – 24
Cloruros (mg/L)	1832 – 2568	2147 – 4511	n/a(1)
Nitratos (mg/L)	4 – 6	1 – 5	390 – 548
Nitritos (mg/L)	0.5 – 1.5	1 – 3	1 – 2
Alcalinidad (mg $CaCO_3$/L)	184 – 240	222 – 294	n/a(1)
Conductividad (μS/cm)	16532 – 25646	22414 – 29060	11270 – 12176

(1) n/a: datos no disponibles

3.1.3. Licor negro

El licor negro Kraft empleado en esta tesis procede de la cocción de madera de *Eucalyptus sp.*, y fue proporcionado por la empresa ENCE Energía y Celulosa S.A. (España). Tras su recogida, el licor negro fue almacenado a 4ºC hasta su uso posterior. Durante la experimentación, se emplearon diferentes lotes. Por ello, en la Tabla 3.3 se recogen los intervalos de valores de los principales parámetros fisicoquímicos del licor negro.

Tabla 3.3. Características fisicoquímicas del licor negro.

Parámetro	**Valor**
pH	12 – 13
Demanda química de oxígeno (g O_2/L)	110 – 150
Carbono orgánico total (g C/L)	40 – 60
Materia seca (%)	12 – 18
Número de color (cm^{-1})	140 – 160

3.2. Procedimientos experimentales

A lo largo de esta tesis, las corrientes a estudiar fueron tratadas mediante tratamientos hidrotérmicos (oxidación húmeda), procesos de membrana y extracción líquido-líquido.

3.2.1. Oxidación húmeda

Los experimentos de oxidación húmeda se realizaron en un reactor semicontinuo de acero inoxidable 316 (Parr Instrument Co., Moline, IL.) de 1 L de capacidad, equipado con controladores de presión, temperatura, agitación y caudal de oxígeno, sus correspondientes indicadores, un sistema de muestreo y una chaqueta calefactora. El contenido del reactor se mantuvo agitado durante todas las operaciones gracias a dos agitadores de turbina magnéticos de seis hojas. El oxígeno necesario para la oxidación húmeda fue aportado por una botella de oxígeno comprimido, el cual fue saturado de vapor de agua y calentado antes de su introducción en el reactor por medio de un humidificador de 2 L que precedía al mismo. Tanto el reactor como el humidificador fueron cargados hasta un máximo del 70% de su capacidad por motivos de seguridad. Además, el reactor contaba con sistemas de seguridad para evitar que la presión superara los 120 bares. En la Fig. 3.1 se muestra un esquema detallado del equipo.

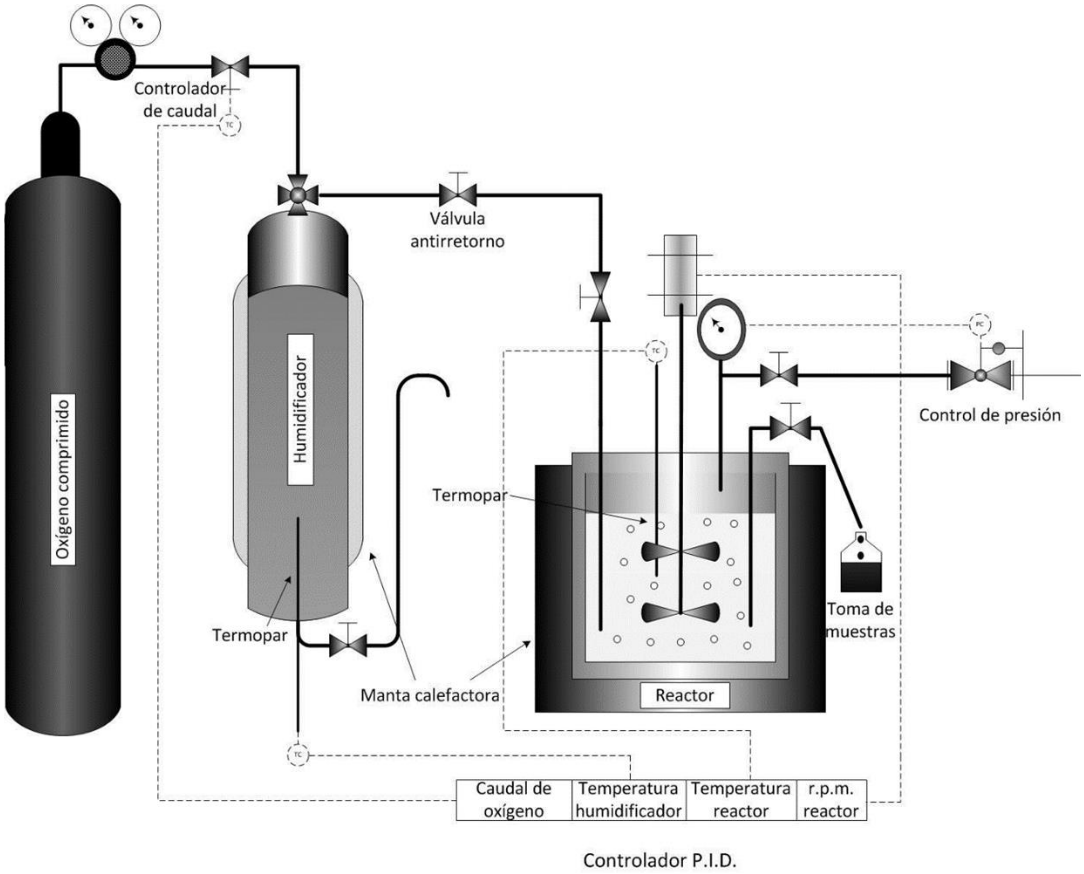

Figura 3.1. Esquema del equipo de oxidación húmeda. Adaptado de [1].

Las oxidaciones húmedas se realizaron a temperaturas entre 160 y 200 ºC, presiones entre 40 y 70 bar, flujos de oxígeno entre 1200 y 1800 mL O_2/min, velocidad de agitación de entre 150 y 500 rpm y tiempos de operación de hasta 300 minutos.

Todas las corrientes tratadas fueron centrifugadas tras la oxidación húmeda para trabajar con el sobrenadante y descartar la fracción sólida. Adicionalmente, se añadió azida de sodio 0.1% (p/v) al lodo de depuradora oxidado para prevenir el crecimiento microbiológico. Las corrientes oxidadas se conservaron a 4ºC hasta el momento de su uso.

3.2.2. Procesos de membrana

3.2.2.1. Membranas

Durante esta tesis se emplearon diferentes membranas cerámicas y poliméricas, que se recogen en la Tabla 3.4.

Tabla 3.4. Membranas utilizadas durante los procesos de filtración.

Marca	*Material*	*Geometría y dimensiones*	*Tamaño de corte*
Tami	ZrO_2-TiO_2	Tubular monocanal, 600 × 6 mm	150 kDa 50 kDa 1 kDa
Synder Filtration	Polietersulfona (PES)	Plana, 63.62 cm^2	50 kDa 3 kDa
Synder Filtration	Polietersulfona permanentemente hidrofílica (PESH)	Plana, 63.62 cm^2	50 kDa
Synder Filtration	Fluoruro de polivinilideno (PVDF)	Plana, 63.62 cm^2	50 kDa
Suez	Polietersulfona (PES)	Plana, 63.62 cm^2	10 kDa
Suez	Poliacrilonitrilo (PAN)	Plana, 63.62 cm^2	50 kDa

3.2.2.2. Equipos de filtración

Las filtraciones se llevaron a cabo en tres equipos de filtración distintos:

Los procesos de filtración de los lodos de depuradora tratados hidrotérmicamente relativos a la recuperación de biomoléculas y la retención de metales se llevaron a cabo en una unidad de filtración de escala de laboratorio de flujo cruzado FT17 (Armfield Ltd., Reino Unido), que permite realizar filtraciones con flujo tangencial en membranas planas. Este sistema comercial cuenta con un recipiente de alimentación de acero inoxidable 316 de 1 L de capacidad, con encamisado para permitir el enfriamiento de la alimentación. La alimentación se bombea mediante una bomba de pistón de triple émbolo construida con acero inoxidable 316, y controlada por variador de velocidad (inverter), que permite ajustar la velocidad del flujo cruzado sobre la superficie de la membrana. El flujo de permeado se midió mediante una balanza electrónica y los parámetros del proceso se registraron mediante software/registro de datos. Se muestra un diagrama del equipo en la Fig. 3.2.

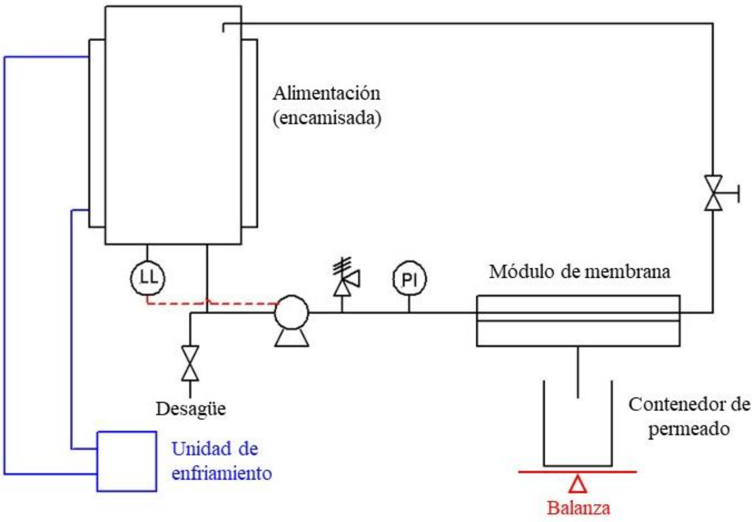

Figura 3.2. Esquema de la unidad de filtración Armfield FT17.

En dichas filtraciones se emplearon las membranas poliméricas de PES, PESH, PVDF y PAN con tamaños de corte entre 3 kDa y 50 kDa suministradas por Synder Filtration y Suez.

Los procesos de filtración de lixiviados de vertedero y de licor negro Kraft se realizaron en una unidad de filtración de laboratorio equipada con un vaso de vidrio de 3 L y una bomba peristáltica Masterflex I/P 7591-55 (Cole-Parmer, EEUU) acoplada a un cabezal Easyload Masterflex I/P 77601-10 (Cole-Parmer, EEUU). Dicha unidad contaba con indicadores y válvulas de presión en la línea de flujo colocadas antes y después del módulo de filtración para medir y controlar la presión transmembrana. En dichas filtraciones se emplearon membranas cerámicas con un tamaño de corte de 150 kDa sumistradas por Tami. Puede encontrarse un diagrama de este equipo en la Fig. 4.43.

Por otro lado, los procesos de filtración de los lodos de depuradora tratados hidrotérmicamente relativos a la recuperación ácidos orgánicos de cadena corta se realizaron con un equipo de filtración a escala de laboratorio fabricado por Addefi (España). El equipo, construido en acero inoxidable AISI316 e interconectado con racores de alta presión, constaba de un tanque de alimentación encamisado de 10 L provisto de una resistencia de calentamiento y conectado a una bomba trifásica IEC 60034 (AEG, Alemania). Asimismo, disponía de un controlador de temperatura y de manómetros antes y después del módulo de filtración, sensores de caudal y temperatura y una válvula de presión para ajustar la presión transmembrana.

Los caudales de permeado se determinaron gravimétricamente en todos los casos. El flujo de permeado se calculó mediante la siguiente ecuación:

$$\mathrm{J} = \frac{\mathrm{Q_P}}{\mathrm{A_M}}$$

Donde J es el flujo de permeado ($m \cdot s^{-1}$), Q_P es el caudal de permeado ($m^3 \cdot s^{-1}$), y A_M es el área superficial de la membrana (m^2).

Las filtraciones se realizaron en dos modos de operación distintos: por una parte, y con el fin de evaluar la evolución del ensuciamiento de la membrana con el tiempo, se trabajó en reciclo total, devolviendo el permeado al tanque de alimentación para mantener constante la composición de la misma. Por otro lado, se trabajó en concentración, retirando continuamente el permeado a fin de analizar el efecto de la concentración de la alimentación en la evolución del ensuciamiento de la membrana. En todos los casos, se recogieron muestras de permeado y retenido periódicamente para determinar las retenciones de los distintos compuestos y parámetros de interés mediante la siguiente fórmula:

$$R_i = 1 - \frac{C_{P_m,i}}{C_{R_t,i}}$$

Donde $C_{P_m,i}$ y $C_{R_t,i}$ son la concentración del compuesto “i” en el permeado y en el retenido, respectivamente.

Las filtraciones se realizaron con presiones transmembrana de 1.6 a 30 bar, de 50 a 70 ºC, de 3.0 a 3.2 m/s de velocidad de flujo cruzado. La duración de las filtraciones fue de hasta 300 minutos para el modo de operación de reciclo total o hasta alcanzar una ratio de concentración de volumen (VCR) de hasta 3.

Al finalizar cada filtración, la membrana se aclaró haciendo pasar agua destilada sin presión transmembrana hasta alcanzar un valor de flujo estable. Las membranas cerámicas también se limpiaron de forma química con una disolución acuosa al 0.5% de detergente básico (Divos 124 VM5, Diversey) a 70ºC hasta alcanzar un flujo de al menos el 90% del flujo de agua inicial.

Con el objetivo de modelizar el ensuciamiento en función de su reversibilidad y su mecanismo de formación, durante esta tesis se utilizaron los modelos de resistencias en serie, los modelos de Hermia y el modelo de Mehta.

La reversibilidad del ensuciamiento se estudió mediante el modelo de resistencias en serie, que descompone la resistencia hidráulica total de la membrana como la suma de diferentes resistencias causadas por los ensuciamientos reversible, irreversible o por la propia membrana. La resistencia hidráulica se puede calcular como se muestra en la siguiente ecuación:

$$\mathrm{R}=\frac{\mathrm{TMP}}{\mu \mathrm{J}}$$

Donde R es la resistencia hidráulica (m^{-1}), TMP es la presión transmembrana ($kg\cdot m^{-1}\cdot s^{-2}$), μ es la viscosidad dinámica de la corriente ($kg\cdot m\cdot s^{-1}$) y J es el flujo de permeado ($m\cdot s^{-1}$).

Los mecanismos de formación del ensuciamiento se estudiaron mediante los modelos de Hermia [2], que siguen el modelo general:

$$\frac{dJ}{dt} = -K \cdot (J - J_0) \cdot J^{2-n}$$

Donde t es el tiempo (min), K es una constante, J_0 es el flujo limitante ($m\cdot s^{-1}$), y n es una constante que toma diferentes valores para los cuatro mecanismos simples de ensuciamiento propuestos por Hermia: bloqueo completo de poros (n = 2, K = [min^{-1}]), donde los poros de la membrana se van cegando por la adsorción o deposición de partículas más pequeñas que el tamaño del poro; bloqueo estándar de poros (n = 1.5, K = [m^{-1}]), donde el área de la membrana activa queda bloqueada por partículas de tamaño similar al de los poros ; bloqueo intermedio de poros (n = 1, K = [m^{-1}]), donde las partículas pueden acabar taponando un poro con el tiempo, o formar un puente en su abertura y no bloquearlo por completo; y filtración de torta (n = 0, K =

[min·m^{-2}]), en el que las partículas tienen un tamaño mucho mayor que el de los poros, depositándose sobre la superficie de la misma y llegando a forma una torta. La elección del modelo que mejor se ajustó a los datos se basó en la suma de residuos al cuadrado, donde cada residuo es igual a la diferencia entre los datos experimentales y el valor predicho por el modelo.

El flujo también se modelizó utilizando el modelo de Mehta que tiene en cuenta los dos dominios de disminución del flujo que tienen lugar durante la filtración por membrana: el dominio 1, donde se produce una rápida disminución del flujo durante la etapa inicial de la filtración; y el dominio 2, donde el flujo disminuye más lentamente hasta alcanzar un valor casi estable (Fig. 3.3) [3]. El modelo se expresa mediante la siguiente ecuación:

$$J = J_0 - J_{\infty 1} \cdot \exp^{-\alpha t} + (J_{\infty 1} - J_{\infty 2}) \cdot \exp^{-\beta t} + J_{\infty 2}$$

Donde $J_{\infty 1}$ es el flujo al término del dominio 1 (m·s^{-1}); $J_{\infty 2}$ es el flujo al término del dominio 2 (*i.e.*, al final del experimento) (m·s^{-1}); y α (min^{-1}) y β (min^{-1}) son dos constantes determinadas experimentalmente que describen la tasa del decaimiento del flujo asociado con el ensuciamiento de membrana y con la polarización de concentración y la formación de la capa de gel, respectivamente.

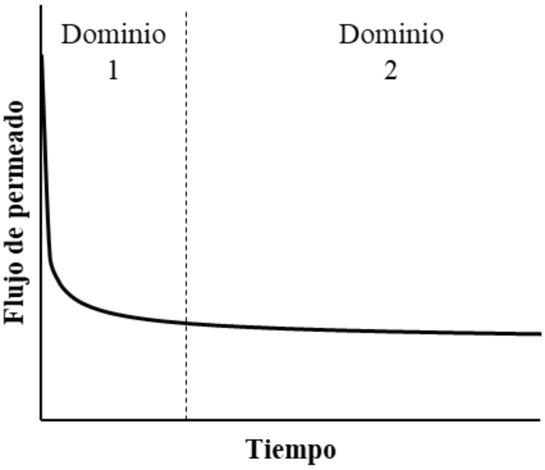

Figura 3.3. Curva típica de flujo de permeado vs tiempo durante la filtración con membranas. Adaptado de [3].

3.2.3. Extracción líquido-líquido

3.2.3.1. Extractantes y diluyentes usados

Las extracciones líquido-líquido realizadas durante esta tesis se llevaron a cabo empleando trioctilamina (97 %, Acros Organics), tributilfosfato (99.9 %, VWR) y óxido de trioctilfosfina (98 %, Alfa Aesar) como extractantes y n-hexano (grado HPLC, Merck), heptano (99.5%, Panreac) y octan-1-ol (99%, Sigma) como diluyentes. Las combinaciones específicas entre extractantes y diluyentes pueden consultarse en los capítulos 4.1.1 y 4.2.1.

Las extracciones fueron realizadas a temperaturas entre 25 y 55 ºC en proporción 1:1 (v/v) y agitadas a 250 rpm hasta alcanzar el equilibrio.

El rendimiento de la extracción (Y_i) se calculó de la siguiente forma:

$$Y_i(\%) = \left(1 - \frac{C_{R,i}}{C_{F,i}}\right) \cdot 100$$

Donde $C_{R,i}$ es la concentración del compuesto "i" en el refinado, y $C_{F,i}$ es la concentración del compuesto "i" en la alimentación.

Las constantes de distribución (K_D) se calcularon siguiendo la ecuación:

$$K_D = \frac{C_{i,org}}{C_{i,aq}}$$

Donde $C_{i,org}$ y $C_{i,aq}$ son las concentraciones del compuesto "i" en las fases orgánica y acuosa tras haber alcanzado el equilibrio, respectivamente.

3.2.4. Extracción de lignina

La lignina fue recuperada mediante precipitación ácida. Se agregó H_2SO_4 5M al licor negro mediante goteo hasta alcanzar un pH de 2.5. Dado que este tratamiento provoca la liberación de H_2S gaseoso, se realizó bajo una campana extractora usando una mascarilla con un filtro para gases y vapores inorgánicos. A continuación, el licor negro acidificado se centrifugó a 10000 g durante 30 minutos. Tras retirar el sobrenadante, la lignina precipitada se lavó con 3 volúmenes de agua acidificada para eliminar las sales residuales y se mantuvo a 110ºC durante 24 h para cuantificarla mediante gravimetría.

3.3. Métodos analíticos

Debido al elevado número de métodos analíticos empleados a lo largo de esta tesis, se han recopilado los métodos empleados en la Tabla 3.5, indicando en cada caso el parámetro junto con el método analítico o equipo empleado para su determinación. A lo largo del Capítulo 4, se pueden encontrar las descripciones detalladas y referenciadas de dichos métodos aplicadas a cada caso concreto.

Tabla 3.5. Parámetros medidos y método analíticos empleados en la tesis.

Parámetro	***Método analítico** / Equipo*
pH	pH-metro
Conductividad	Conductivímetro
Demanda química de oxígeno	Método estándar de oxidación con dicromato
Demanda biológica de oxígeno	Respirometría manométrica (método de Warburg)
Carbono orgánico e inorgánico total	Analizador TOC-V CSH
Sólidos totales	Método estándar de secado en estufa a 105 ºC
Sólidos volátiles	Método estándar de calcinado en mufla a 525-550 ºC
Carbohidratos totales	Método de Dubois
Número de color	Espectrofotometría
Proteínas	Método de Lowry modificado
Ácidos húmicos	Método de Thurman y Malcolm, método de Lowry modificado
Compuestos fenólicos totales	Método de Folin-Ciocalteu y fenol
Densidad	Picnometría
Viscosidad cinemática	Viscosímetro invertido Cannon-Fenske
Ácidos orgánicos	Cromatografía líquida de alta resolución
Iones inorgánicos	Cromatografía iónica
Rugosidad superficial (membranas)	Microscopía de fuerza atómica
Hidrofilicidad (membranas)	Medida de ángulo de contacto
Caracterización morfológica superficial y composición elemental semicuantitativa (membranas)	Microscopía electrónica de barrido
Concentración de metales y otros elementos	Espectrometría de masas con plasma acoplado inductivamente
Quenching de ácidos húmicos y proteínas con metales	Medidas de espectros de fotoluminiscencia
Toxicidad aguda	Ensayos de bioluminiscencia con *Vibrio fischeri*

Referencias

[1] J.L. Urrea, S. Collado, A. Laca, M. Díaz, Rheological behaviour of activated sludge treated by thermal hydrolysis, J. Water Process Eng. 5 (2015) 153–159. doi:10.1016/J.JWPE.2014.06.009.

[2] J. Hermia, Constant Pressure Blocking Filtration Laws - Application Topower-Law Non-Newtonian Fluids., Trans Inst Chem Eng. V 60 (1982) 183–187.

[3] M. Mondor, B. Girard, C. Moresoli, Modeling flux behavior for membrane filtration of apple juice, Food Res. Int. 33 (2000) 539–548. doi:10.1016/S0963-9969(00)00089-2.

Capítulo 4.

RESULTADOS Y DISCUSIÓN

4.0. Justificación de la organización

Para facilitar la lectura de los resultados, esta sección se ha dividido en tres apartados, atendiendo a la biomasa residual líquida tratada.

En el apartado 4.1 se recogen los trabajos relacionados con los lodos secundarios de depuradora. En el subapartado 4.1.1 se estudia la producción de ácidos orgánicos de cadena corta mediante la oxidación húmeda de lodos secundarios de depuradora y su recuperación mediante ultrafiltración y extracción líquido-líquido. En los subapartados 4.1.2 y 4.1.3 se presentan los resultados obtenidos durante la estancia en la Universidad de Aalborg, en la que se estudió el fraccionamiento de los lodos solubilizados mediante ultrafiltración con membranas poliméricas. Concretamente, el subapartado 4.1.2 consiste en un estudio sobre el efecto del material y el tamaño de corte de la membrana en la separación de biomoléculas de interés, mientras que en el subapartado 4.1.3 se analiza la capacidad de retención de metales pesados por estas membranas y el mecanismo de retención. Por último, el subapartado 4.1.4 recoge, a modo de perspectivas para futuros trabajos, el estado del arte de los métodos de separación y purificación de biomoléculas de interés aplicables a biomasas líquidas o acuosas, y en particular a los lodos.

En el apartado 4.2 se incluyen los trabajos relativos a las otras biomasas residuales líquidas tratadas, *i.e.*, lixiviados de vertedero y licor negro Kraft. En el subapartado 4.2.1, se recogen las distintas estrategias estudiadas para la recuperación de ácidos orgánicos de cadena corta a partir de licor negro Kraft, consistentes en la aplicación de distintos pretratamientos (deslignificación y oxidación húmeda), filtración con membranas y extracción líquido-líquido. En el subapartado 4.2.2, se detalla el efecto de la edad del lixiviado en su ultrafiltración, en términos de ensuciamiento de membrana y retención de ácidos húmicos y de varios parámetros fisicoquímicos. Por último, el subapartado 4.2.3 se centra en el tratamiento combinado de oxidación húmeda seguido de ultrafiltración para la recuperación de ácidos húmicos a partir de lixiviados estabilizados, y la obtención de un agua tratada que cumpla con los estándares requeridos para su liberación en el medio ambiente.

4. Resultados y discusión

Los resultados obtenidos durante esta tesis ya han sido parcialmente publicados, resultando en un total de cuatro artículos cuyas referencias se indican al comienzo de cada subapartado correspondiente.

4.1. Valorización de lodos secundarios de depuradora

4.1.1. Production and purification of organic acids from partially oxidised waste activated sludge

Daniel Núñez, Martina Zabatta, Paula Oulego, Francisco A. Riera, Mario Díaz*

Department of Chemical and Environmental Engineering, University of Oviedo, c/ Julián Clavería 8, 33006, Oviedo, Spain

*Corresponding author’s e-mail: mariodiaz@uniovi.es

Phone: +34 985 10 34 39, FAX: +34 985 10 34 40

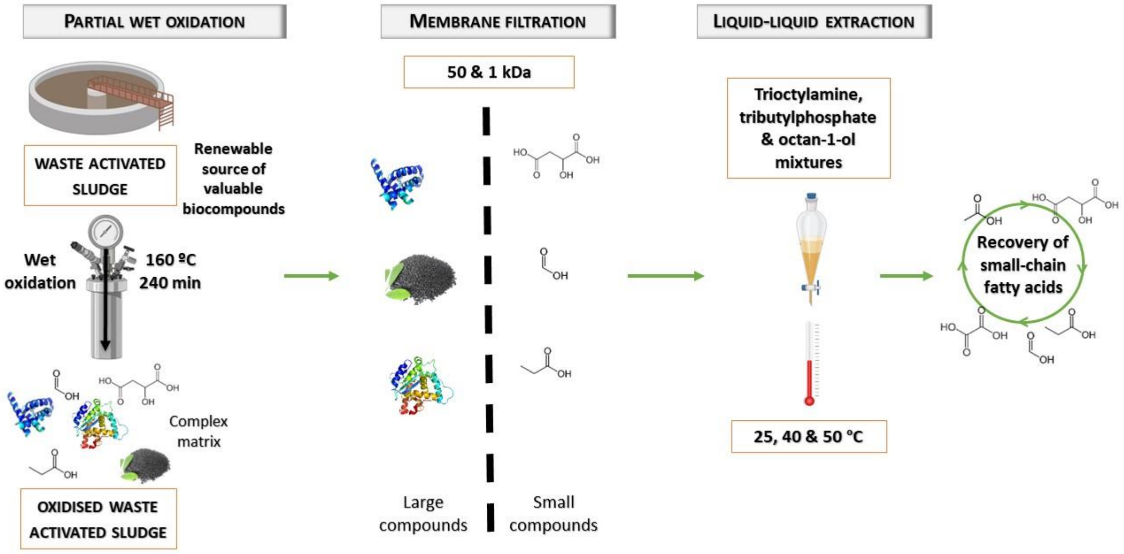

Figura 4.1. Resumen gráfico del artículo *Production and purification of organic acids from partially oxidised waste activated sludge*.

Artículo enviado a la revista **Separation and Purification Technology**

Cuartil: Q1 **Índice de impacto:** 8.6

Abstract

Short-chain organic acids (SCFAs) are widely used in the chemical and food industries. However, their conventional production relies heavily on fossil raw materials, necessitating sustainable alternatives. Waste activated sludge (WAS) can serve as a renewable feedstock for SCFA production through oxidative hydrothermal pretreatment. Thus, the aim of this work was to optimize the production and recovery of SCFAs from partially oxidised WAS. To achieve this, WAS was treated by wet oxidation (WO) at different temperatures (160-200ºC) and ultrafiltered using ceramic membranes (50 and 1 kDa) to pre-purify the SCFAs. Subsequently, these acids were extracted with different combinations of trioctylamine (TOA), tributylphosphate (TBP) and octan-1-ol in the temperature range 25-50ºC.

WO at 160ºC for 240 min maximized the SCFA production, obtaining a concentration of 6.07 g/L, with acetic acid as the main component (28.2%).

Membrane ultrafiltration operating in total recycle mode achieved rejections of 39% for TOC and 73% for colour, with a low SCFA rejection (4%) effectively pre-purifying the SCFAs present in the WAS. The main fouling mechanism was cake formation.

The highest extraction yields of SCFAs at room temperature were achieved with a mixture of TOA and TBP at 10% in octan-1-ol, extracting 34% of the total SCFAs present in the 1 kDa permeate. Lower extraction yields were obtained with the pre-purified WAS compared to synthetic solutions of SCFAs, showing the detrimental effect of the matrix in liquid-liquid extraction. Increasing the temperature within the range of 25 to 50 ºC generally had a favourable effect on the SCFA extraction.

Keywords: Hydrothermal treatments; liquid-liquid extraction; membrane filtration; fouling; waste valorisation.

1. Introduction

As global efforts to reduce the impact of human activity have gained importance over the years [1,2], the concept of circular economy has become a promising strategy to achieve a sustainable society. Circular economy can be defined as a closed-loop material flow within the entire economic system, where it is aimed to maintain all the materials at their highest utility value [3,4]. This stands in contrast to the traditional linear economy, where raw materials are transformed into products and eventually discarded as residues at the end of their lifespan.

The circularization of the economy involving urban wastewaters is of particular significance. The production volumes of these wastewaters and the restrictions on their discharge are increasing due to the global population growth and the rise on the environmental concerns [5,6]. Moreover, wastewater treatment plants themselves contribute to adverse environmental effects through material and energy consumption, as well as the release of various emissions into the environment. In this sense, significant amounts of waste activated sludge (WAS) are generated daily, necessitating subsequent treatment [7]. This sludge has been traditionally discarded in landfills or used as a low-value product, fuel or fertilizer [8]. However, this residue, mainly composed of microorganisms, their debris and extracellular polymeric substances, represents a promising source of valuable biological products like enzymes, proteins, humic acids, saccharides and lipids, along with short-chain fatty acids (SCFAs) [8,9]. This offers an interesting opportunity to valorise WAS and obtain high-value products through their recovery. In particular, SCFAs, due to their high industrial importance, are produced in large volumes and find wide-ranging applications across industries including food, chemical, biochemical, biofuel, textile, cosmetic, and pharmaceutical [10–12]. While SCFAs are not abundant in WAS, its organic matter can be transformed into organic acids through mild wet oxidation (WO), a hydrothermal technique that, in addition to SCFA production, also solubilises and sterilises the sludge [13]. The optimisation of the production of SCFAs using WO requires careful consideration of both operation time and temperature [14].

The treatment of the WAS by mild WO results in a complex matrix comprising a solid [15] and a liquid phase containing the solubilised organic and inorganic matter [16] as well as the SCFAs. As a result, separation and purification processes are necessary for their recovery. Membrane separation proves to be a very suitable technology for the pre-purification of these acids. It is considered a green technology since it can be continuously conducted under mild conditions without the need for additional chemicals, with high selectivity and low energy consumption, and it can be easily coupled with other operations [17]. In addition, affinity-based methods, such as resin adsorption or liquid-liquid extraction (LLE), are normally employed for the purification of SCFAs due to low energy and temperature requirements [9,11].

Both membrane filtration and LLE are conditioned by several factors. In the case of membrane filtration, factors such as geometry, material composition and, especially, molecular weight cut-off (MWCO), significantly impact selectivity and permeability [18,19]. On the other hand, the election of the solvent is critical for LLE, with the most suitable option depending on the nature of the desired compounds and the phase in which it is dissolved (the stationary phase). In particular, reactive extraction has gained relevance for the extraction of carboxylic acids, and has proven to be highly effective for their *in-situ* recovery [20,21]. A reactive solvent typically consists of a diluent, which is immiscible with the stationary phase, and acts as a transport phase; and an extractant, which forms a reversible complex with the carboxylic acid [22]. While both polar and non-polar diluents can be employed in reactive extraction, it has been reported that polar diluents are more effective, particularly for carboxylic acids [23]. In such cases, the optimal extraction yield of SCFAs is determined by the ratio between the diluent and the extractant. On one hand, the polar diluent provides additional solvating power to the relatively low polar extractants, allowing for higher levels of SCFA-extractant complexes to be formed in the transport phase. On the other hand, increasing the proportion of diluent reduces the number of extractant molecules available for forming complexes [24].

Works studying the production of SCFAs from WAS have mainly focused on bioproduction via fermentation [25]. Few of them studied physicochemical methods [26,27], and, to the best of our knowledge, none of them has focused on the recovery process of SCFAs.

Taking into account these considerations, this study was focused on evaluating the process for the production, separation and purification of SCFAs from WAS. To achieve this, the study aimed to: i) optimize the production of SCFAs through partial WO, ii) analyse the impact of the pre-purification by membrane filtration on partially oxidised WAS, and iii) assess the effect of LLE on the recovery of SCFAs.

2. Material and methods

2.1. Waste activated sludge

The thickened WAS was collected from a wastewater treatment plant in Baíña, Asturias, Spain, and then stored at 4 ºC until it underwent partial oxidation, a process that took place within no more than three days after collection. Its physical-chemical characteristics are shown in Table 4.1.

Table 4.1. Physical-chemical parameters of the thickened waste activated sludge.

Parameter	***Value***
pH	6.6 ± 0.2
Total chemical oxygen demand (mg O_2/L)	22030 ± 40
Soluble chemical oxygen demand (mg O_2/L)	350 ± 150
Total organic carbon (mg C/L)	6100 ± 800
Total suspended solids (g/L)	33 ± 1
Volatile suspended solids (g/L)	26.8 ± 0.4

2.2. Production of organic acids by partial wet oxidation

Different conditions of time and temperature were studied to optimize the production of SCFAs from WAS. Partial WO tests were performed in a 1 L 316 SS batch reactor (Parr Instrument Co., Moline, IL.) equipped with pressure and temperature controllers, indicators, a sampling system, and a heating jacket. The reactor content (loaded up to the 70% of its capacity for safety purposes) was stirred at 150 rpm by two six-bladed magnetically driven turbine agitators. A constant flow of 1600 mL/min of oxygen, previously saturated with water by a humidifier, was provided from a compressed bottle throughout the operation, and the pressure was set at 40 bar. A detailed scheme of the experimental setup can be found in [28]. The reaction was carried out without pH adjustment nor addition of catalyst. Temperatures of 160ºC, 180ºC and 200ºC were tested for a total reaction time of 5 h, taking samples at different intervals to analyse the evolution of SCFAs and their degradation throughout the partial oxidation.

After the partial WO, 0.1% (w/v) sodium azide was added to prevent microbiological growth. The oxidised sludge was then stored at 4 ºC for further usage.

2.3. Membrane filtration

In order to pre-purify the oxidised WAS prior to the LLE of SCFA, different filtration experiments were conducted. The filtrations were carried out with a laboratory-scale filtration device manufactured by Addefi (Spain). The equipment, built in AISI316 high-pressure stainless steel and connected with high-pressure fittings, consisted of a jacketed 10 L feed tank equipped with a heating resistance. From there, the feed was pumped into the gasketed membrane using an IEC 60034 three-phase pump (AEG, Germany). The equipment was equipped with a temperature controller, pressure gauges before and after the ultrafiltration module, as well as flow and temperature sensors. Transmembrane pressure (TMP) was regulated by a pressure valve located in the retentate line. The permeate line was built in rubber, and directed to a PS750R2 (Radwag, Poland) weighting scale for flux determination. A scheme of the device is shown in Fig. 4.2.

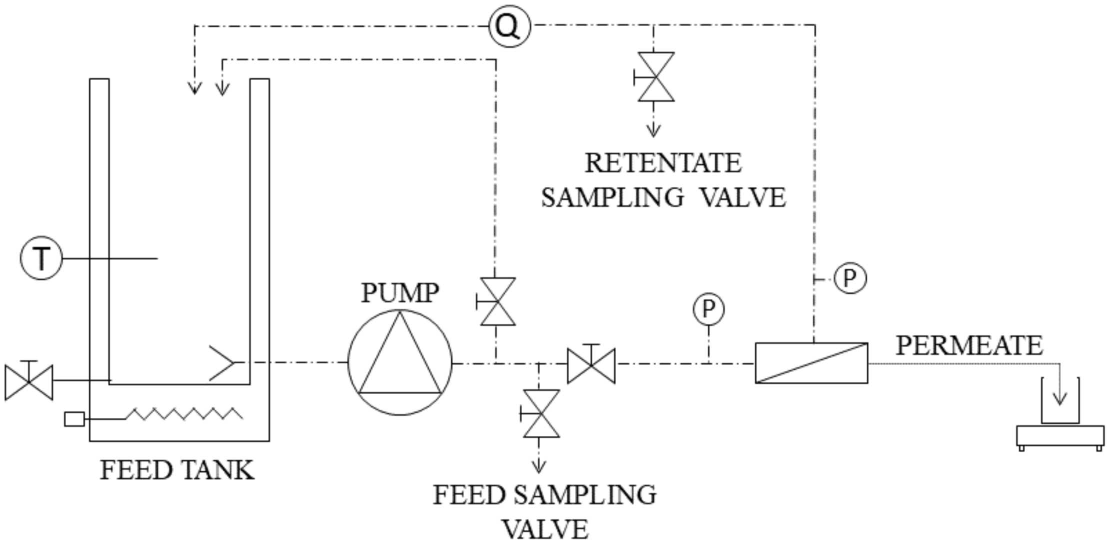

Figure 4.2. Filtration setup used in the pre-purification experiments of the oxidised WAS.

Tubular mono-channel ZrO_2-TiO_2 membranes of 50 and 1 kDa (TAMI Industries, France) were used for the experiments. The permeate obtained after the filtration with the 50 kDa membrane was used as the feed for the filtration with the 1 kDa membrane. The membranes had a length of 604 mm and an internal diameter of 6 mm. All filtration experiments were performed at 50ºC, with a TMP of 4 bar, and a cross-flow velocity 3.2 m/s.

Two modes of filtration were tested:

-Total recycle (TR) mode: the retentate and permeate were returned to the feed tank to maintain a constant feed composition. This mode allowed for the evaluation of membrane fouling evolution over time. TR experiments were conducted for a total of 300 min.

-Volume concentration (VC) mode: only the retentate was returned to the feed tank, concentrating the feed composition. This mode allowed for the assessment of the effect of concentration on fouling development. VC experiments were performed until a volume concentration ratio (VCR) of 3 was reached with the 50 kDa membranes; and of 1.5 with the 1 kDa membrane, due to the slow flux rate obtained. VCR is calculated as follows:

$$VCR = \frac{V_f}{V_r}$$

Where V_f is the initial feed volume, and V_r is the retentate volume.

In both modes, retentate and permeate samples were taken periodically and frozen until further use. Rejection coefficients (R_i) were determined using the following equation:

$$R_i = 1 - \frac{C_{P_m,i}}{C_{R_t,i}}$$

Where $C_{P_m,i}$ and $C_{R_t,i}$ represent the concentration of the compound "i" in the permeate and the retentate, respectively.

After each filtration, the membrane was rinsed with distilled water until attaining a stable flux value. Subsequently, it was cleaned at moderate temperature (70ºC) with a Diversey basic detergent (0.5% v/v). Cycles of chemical cleaning were performed as needed, until the final flux was over 90% of the initial water flux [29]. All experiments were performed in duplicate.

Membrane fouling was modelled with resistance-in-series and Hermia models, which are described elsewhere [30].

2.4. Liquid-liquid extraction

Tributyl phosphate (TBP) (99.9%, VWR) and trioctylamine (TOA) (97%, Acros Organics) were used as extractants, and octan-1-ol (99%, Sigma) as diluent. Octan-1-ol was selected due its polar character, which, as previously stated, favours the extraction of SCFAs. Additionally, it is totally immiscible with water; and presents a low latent heat of vaporization (65 kJ/mol). The tested solvents were prepared by dissolving TOA, TBP and a 50:50 (v/v) TOA/TBP mixture at concentrations of 10%, 25% and 40% (v/v) in octan-1-ol. They were designated based on the employed extractant and its concentration (e.g., TBP40 represents TBP at 40% in octan-1-ol).

Firstly, the extractions were performed at 25ºC by mixing the 1 kDa permeate with the solvent in a 1:1 (v/v) proportion and stirred overnight to ensure the equilibrium was reached. The aqueous phase was then analysed to determine the SCFA content.

After this initial screening, the effect of temperature on the extraction yields of SCFAs was also studied. The TOA, TBP and TOA/TBP mixtures that delivered the highest yields at room temperature were tested at 30, 40 and 50 ºC following the same procedure described above. Additionally, these extractions were performed using a synthetic solution prepared dissolving the studied SCFAs at the same concentrations present in the oxidised WAS, in order to study the effect of the WAS matrix on the LLE yield.

The extraction yield (Y_i) was determined as follows:

$$Y_i(\%) = \left(1 - \frac{C_{R,SCFA_i}}{C_{F,SCFA_i}}\right) \cdot 100$$

Where $C_{R,SCFA_i}$ represents the concentration of the SCFA “i” in the raffinate, and $C_{F,SCFA_i}$ the concentration of the SCFA “i” in the feed solution.

The distribution constants (K_D) were determined by the following equation:

$$K_D = \frac{C_{SCFA_i,org}}{C_{SCFA_i,aq}}$$

Where $C_{SCFA_i,org}$ and $C_{SCFA_i,aq}$ represent the concentrations of the SCFA “i” in the organic and aqueous phase respectively, after reaching the equilibrium.

2.5. Analytical methods

Density and kinematic viscosity were measured at 50ºC and room temperature with a pycnometer and a Cannon-Fenske inversed-flow viscometer (Proton, UK), respectively. pH was determined using a Basic 20 pH meter (Crison, Spain). Spectral absorbance coefficients (SAC) were measured at 436, 525 and 620 nm using a Helios Alpha UV-Vis spectrophotometer (Thermo Scientific, USA) to calculate the colour number (CN). Both SAC and CN have units of cm^{-1}. CN was calculated as follows:

$$CN = \frac{SAC_{436}^2 + SAC_{525}^2 + SAC_{620}^2}{SAC_{436} + SAC_{525} + SAC_{620}}$$

Total organic carbon (TOC) was determined using a TOC analyzer (Shimadzu TOC-V_{CSH}). The concentration of SCFAs were determined by HPLC Agilent Technologies 1200 Series, using an ICSep ICE-ION-300 column (Teknokroma, Spain) as the stationary phase and with H_2SO_4 0.45 mM (with pH adjusted to 3.2-3.3) as the mobile phase.

A refractive index detector was used to measure SCFAs. Standard curves of oxalic, maleic, pyruvic, lactobionic, malic, lactic, formic, acetic and propionic acids were elaborated to properly identify and quantify these SCFAs.

3. Results and discussion

3.1. Optimization of SCFAs production by partial WO

The production of SCFAs by partial oxidation of WAS is shown in Fig. 4.3.

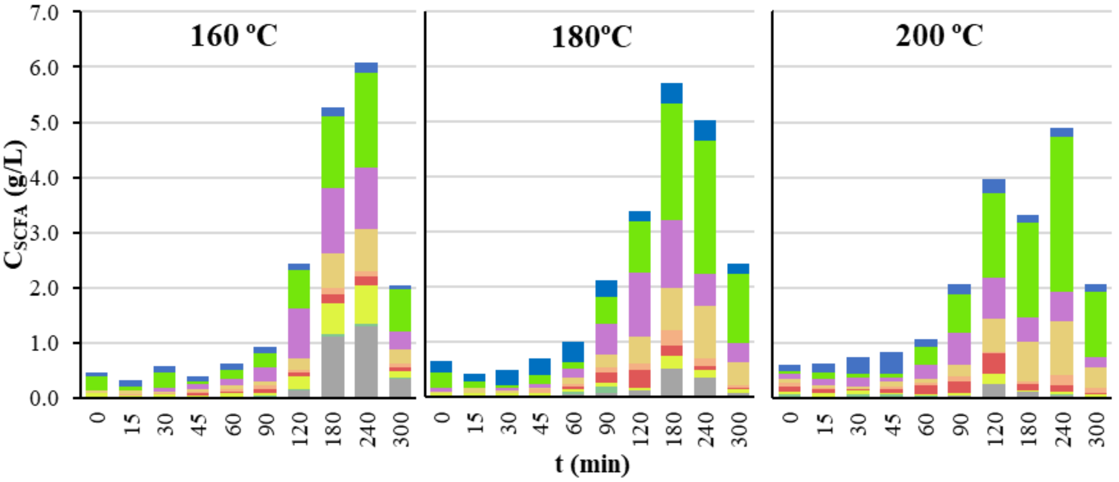

Figure 4.3. Evolution of the concentrations of oxalic (◼), maleic (🟩), pyruvic (🟨), lactobionic (🟥), malic (🟧), lactic (🟨), formic (🟪), acetic (🟩) and propionic (🟦) over time in the range 160-200ºC.

In all cases, the concentration of SCFAs presented a consistent pattern over time. Initially, the SCFA concentrations increased with time, as the sludge was solubilised, and the released biocompounds into the reaction media were oxidised into these acids. The concentration values eventually reached either a peak or a plateau, after which they began to decrease. This can be attributed to the SCFA degradation rate, which started to be faster than its production rate (Fig. 4.3). This behaviour was in accordance with other studies that have analysed the degradation pathways of organic matter. These studies indicated that the process involved the successive formation and degradation of peroxides, alcohols, ketones, and organic acids, consecutively, until their ultimate degradation to CO_2, H_2O and ash [31].

Volatile SFCAs (propionic, acetic, and formic acids) were produced in larger quantities than the non-volatile ones (oxalic, maleic, pyruvic, lactobionic, malic and lactic acids). This trend was more pronounced at higher temperatures (180ºC and 200ºC) and longer reaction times (from 180 min onwards), in which the average concentration of volatile SCFAs represented 70% of the total concentration of SCFAs. Among these, acetic acid showed at the highest concentration, reaching a maximum value of 2.83± 0.08 g/L at 200 ºC after 240 min of oxidation. Furthermore, it was observed that increasing the temperature favoured the formation of acetic acid. Specifically, a concentration of 1.28 ± 0.07 g/L was obtained at 160ºC for 180 min, while the value was 1.65 times higher at 180ºC for the same time. This finding is consistent with the studies of Chung et al. [29], who reported that acetic acid was the most produced SCFA due to its stability among the low molecular SCFAs obtained as intermediates.[32]. Moreover, the production of acetic acid as a final compound of the WO of sludge has been described by several other authors [32–35]. A similar behaviour was also observed for the non-volatile lactic, lactobionic and malic acids, which achieved maximum concentrations at 200ºC that were 1.3, 2.3 and 1.8 times higher than those obtained at 160 ºC (0.75 ± 0.02 g/L, 0.16 ± 0.05 mg/L; 0.11 ± 0.01 g/L, respectively). As for propionic acid, the increase in concentration with higher temperatures was more significant within 45 min of reaction. Specifically, the values were 3 times and 3.8 times higher at 180ºC and 200ºC for 45 min, compared to that of at 160ºC for the same reaction time (0.106 ± 0.003 g/L). Chung et al. [29] reported a similar increase in propionic acid concentration when oxidising sewage sludge at temperatures ranging from 200 to 240ºC.

However, the opposite behaviour was observed for oxalic, pyruvic, and formic acids, as their degradation rate accelerated with increasing temperature, although it was less pronounced for formic acid. Particularly, the maximum concentration of oxalic acid decreased from 1.3 ± 0.1 g/L at 160°C, to 0.243 ± 0.004 g/L at 200°C. For pyruvic acid, the concentration dropped from 0.700 ± 0.006 mg/L at 160°C to 0.20 ± 0.01 mg/L at 200°C, and for formic acid decreased from 1.19 ± 0.08 mg/L at 160°C to 0.7 ± 0.1 mg/L at 200°C.

Increasing the temperature resulted in a decrease in the maximum concentration of total SCFAs generated. Specifically, the concentrations were 6% and 18.3% lower at 180ºC and 200ºC compared to that of at 160ºC (6.07 g/L). This reduction can be attributed to a greater mineralization of the organic matter, where the oxidation routes leading to CO_2 formation are more favoured than those leading to acetic acid at higher temperatures (Fig. 4.4). This can be supported based on the data reported by Prince-Pike et al. [33] related to the oxidation of the "fast reacting" and "slow reacting" soluble organic matter to CO_2, acetic acid and other volatile fatty acids calculated from the. At low temperatures, "slow reacting" soluble organic matter was predominant, with higher kinetic constants for its oxidation to acetic acid (varied from $4.9\ 10^{-4}$ s^{-1} for 160ºC to $1.5{\cdot}10^{-3}$ s^{-1} for 200ºC) and other volatile fatty acids (varied from $3.7\ 10^{-4}$ s^{-1} for 160ºC to $8.9{\cdot}10^{-4}$ s^{-1} for 200ºC) compared to its oxidation to CO_2 (ranged from $4.8\ 10^{-8}$ s^{-1} for 160ºC to $6.0{\cdot}10^{-7}$ s^{-1} for 200ºC). However, at higher temperatures, "fast reacting" soluble organic matter is more favoured, resulting in higher kinetic constant for its oxidation to CO_2 (varied from $9.7\ 10^{-2}$ s^{-1} for 160ºC to $2.2{\cdot}10^{-1}$ s^{-1} for 200ºC) compared to that obtained for the oxidation to acetic acid (varied from 3.810^{-5} s^{-1} for 160ºC to $1.6{\cdot}10^{-4}$ s^{-1} for 200ºC) and other volatile fatty acids (ranged from $1.1{\cdot}10^{-22}$ s^{-1} for 160ºC to $8.0{\cdot}10^{-.21}$ s^{-1} for 200ºC).

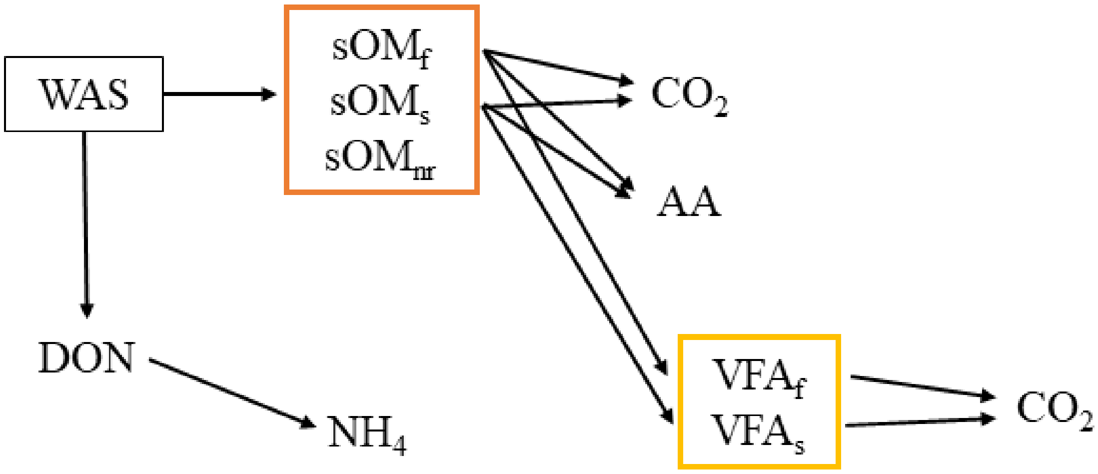

Figure 4.4. Proposed model for the oxidation of WAS adapted from [36]. sOM: soluble organic matter. DON: dissolved organic nitrogen. AA: acetic acid. VFA: volatile fatty acids without including AA. *f*, *s* and *nr* subscripts stand for fast reacting, slow reacting, and non-reacting, respectively.

These results followed the trend reported by other authors [32,36], who observed an increase in the concentration of SCFAs with reaction time. However, their experiments were only performed within 60-80 min, and stopped them while SCFAs were still being generated. Additionally, these studies did not analyse the concentration of non-volatile SCFAs. This is why they reported SCFA concentrations ranging from approximately 1 g/L to 4 g/L for the oxidation of sewage sludge at temperatures between 180ºC and 240ºC, and pressures from 20 bar to 60 bar.

The highest concentration of total SCFAs (6.07 g/L) was reached at 160 ºC after 240 min. Therefore, the subsequent experiments were performed with the WAS partially oxidised at these conditions.

3.2. Membrane filtration

3.2.1. Flux

The obtained fluxes for all filtration experiments are shown in Fig. 4.5.

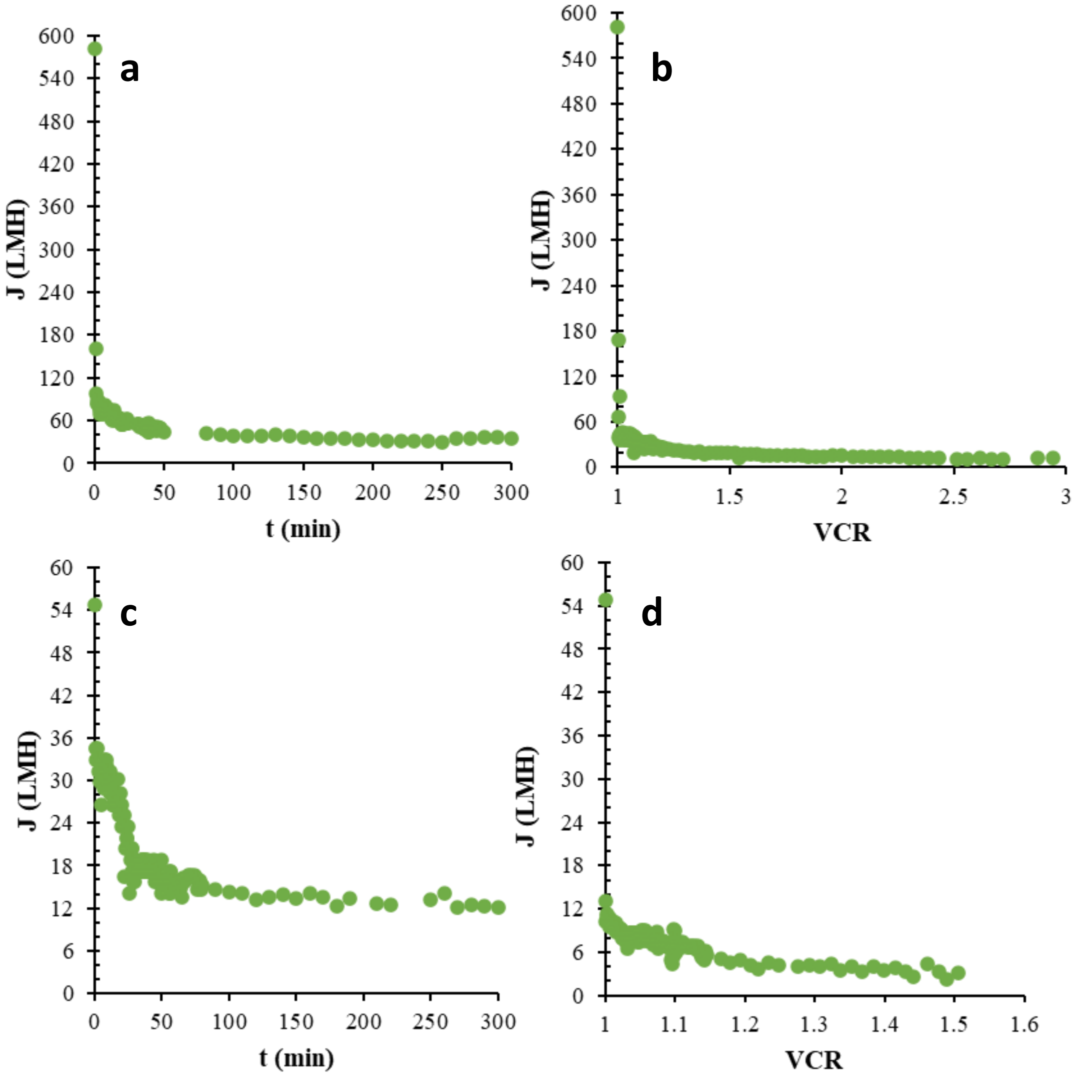

Figure 4.5. Flux evolution during the filtration of the oxidised WAS with the 50 kDa membrane in TR (a) and VC (b) mode; and with the 1 kDa membrane in TR (c) and VC (d) mode.

The permeability of the clean 50 kDa membrane (581 ± 1 LMH) was over 10 times higher than that of the clean 1 kDa membrane (54.8 ± 0.1 LMH). It should be noted that the oxidised WAS filtered with the 1 kDa membrane was previously pre-filtered with the 50 kDa membrane, thus showing the importance of a pre-filtration stage. The concentration of the feed also significantly influenced the resulting flux, this effect being more pronounced with the 1 kDa membrane. Thus, the mean fluxes in VC mode with 50 kDa and 1 kDa membranes (excluding the clean fluxes) were approximately 1.85 times and 2 times lower, respectively, than those obtained in the TR mode (60 ± 40 LMH and 14 ± 5 LMH, respectively) in both cases.

In terms of flux loss during filtration, higher relative losses (compared to the initial flux) were measured during the filtration with the 50 kDa membrane in both TR and VC modes (93.9 % and 98.5%, respectively) than those achieved with the 1 kDa membrane (78% and 94.3%, respectively). This can be explained by considering that the stream filtered with the 1 kDa membrane had already undergone pre-filtration with the 50 kDa membrane.

The measured fluxes were generally lower compared to those obtained in ultrafiltration and nanofiltration studies with different polymeric and ceramic membranes, which reported values from 300 to 30 LMH (50 kDa) and from 40 to 20 LMH (1 kDa) [37,38,47,48,39–46]. This difference can be attributed to the high complexity of the solubilised WAS. For instance, Cassini et al. [48] achieved fluxes of around 300 LMH with a 50 kDa ceramic membrane, which approximately 5 times higher than the fluxes obtained in this study with the 50 kDa membrane under similar operation conditions when treating soy protein wastewaters.

Fluxes obtained in TR mode were also modelled with Hermia models in order to determine the main fouling mechanism (Fig. 4.6). Knowing this can facilitate the optimization of the cleaning cycles of the membrane, improving its performance and expanding its lifespan. Hermia models contemplate four different fouling mechanisms: complete pore blocking (CPB), where particles are larger than the pore size and reduce the active membrane area; internal pore blocking (IPB), where the particles are smaller than the pore and reduce the pore size itself; partial pore blocking (PPB), where particles may bridge pores without completely seal them, resulting in similar effects to CPB but less severe; and cake formation (CF), where fouling particles form a layer on the top of the membrane without entering the pores. The main fouling mechanism of both 50 and 1 kDa membranes was CF, which is primarily reversible, and can be removed by physical methods [49].

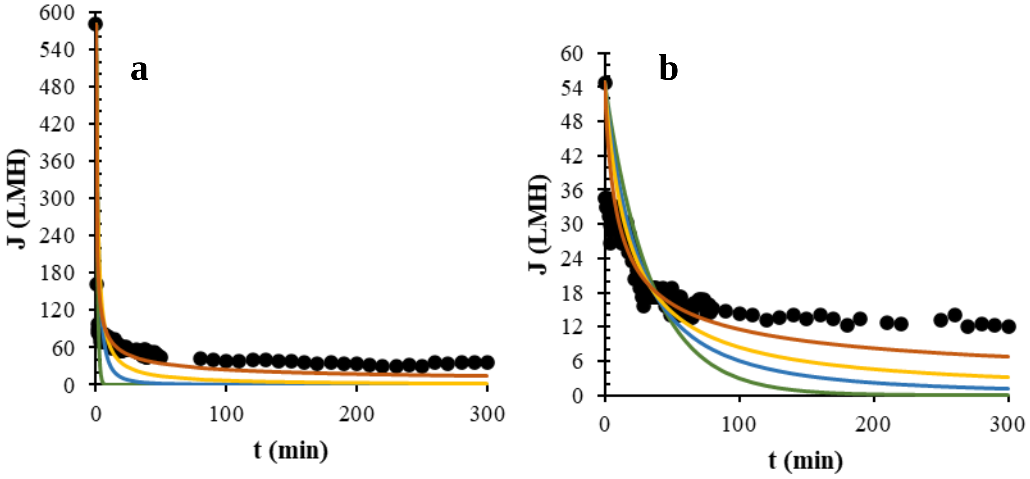

Figure 4.6. CPB [—], IPB [—], PPB [—] and CF [—] flux models, and experimental fluxes (●) for 50 kDa (a) and 1 kDa (b) membranes.

As shown in Table 4.2, hardly any retention of SCFAs was observed with the 50 kDa membrane operating in TR mode, and even negative retentions occurred for some SCFAs. These negative retentions can be attributed to the Donnan effect: CN in organic matter (NOM) is produced by compounds rich in aromatic C=C bonds [50], such as humic acids (the main biopolymer found in the studied WAS) or melanoidin, which are a group of large, negatively charged, coloured, refractory, nitrogenous molecules produced by Maillard reaction from the heating of amino acids and carbohydrates [51], and thus generated during the WO of the WAS. Humic acids and melanoidin are strongly negatively charge at the operational pH [52]. With the high rejection values for CN, it is likely that these negatively charged molecules were concentrated in the retentate side. Consequently, SCFAs were compelled to pass through the membranes to reach charge equilibrium [53]. Furthermore, negative charges would be attracted to the solution-membrane surface interface, as ZrO_2-TiO_2 has been reported to be positively charged at pH levels below ~6.5 [54], which facilitated the permeation of the SCFAs through the membrane. Negative retentions of SCFAs have already been reported by several authors [55,56].

In contrast with the SCFAs rejections, TOC rejection of around 50% was obtained with the 50 kDa membrane in TR mode, indicating that a partial purification of the SCFAs was achieved after membrane filtration. However, a slightly lower TOC rejection (39 ± 3%) was observed during the filtration with the 1 kDa membrane in TR mode. This can be due to the removal of a significant portion of larger molecules by the 50 kDa filtration. The high TOC rejections obtained are consistent with the considerable CN rejections achieved in all cases, ranging from 53 to 73%. Operating in VC mode significantly increased the CN rejections when filtering with the 50 kDa membrane, but made no significant difference filtering with the 1 kDa membrane.

Table 4.2. Average rejection coefficients with 50 kDa and 1 kDa membranes during the operation in TR and VC modes.

R	**TR 50 kDa**	**VC 50 kDa**	**TR 1 kDa**	**VC 1 kDa**
CN	0.53 ± 0.09	0.73 ± 0.07	0.86 ± 0.06	0.73 ± 0.06
Total SCFAs	-0.08 ± 0.2	0.1 ± 0.3	0.04 ± 0.1	0.2 ± 0.2
Oxalic	0.03 ± 0.2	0.3 ± 0.2	0.3 ± 0.3	0.47 ± 0.09
Maleic	0.002 ± 0.191	0.2 ± 0.5	0.2 ± 0.2	0.42 ± 0.06
Pyruvic	0.07 ± 0.44	0.4 ± 0.5	-0.3 ± 1	0.45 ± 0.09
Lactobionic	-0.2 ± 0.3	0.3 ± 0.4	0.4 ± 0.4	0.4 ± 0.1
Malic	-0.010 ± 0.285	0.2 ± 0.3	0.002 ± 0.4	0.05 ± 0.2
Lactic	-0.03 ± 0.2	-0.2 ± 0.7	-0.1 ± 0.3	0.05 ± 0.4
Formic	-0.03 ± 0.3	0.1 ± 0.3	0.2 ± 0.2	0.3 ± 0.4
Acetic	-0.2 ± 0.3	-0.01 ± 0.5	-0.04 ± 0.1	0.2 ± 0.2
Propionic	-2 ± 4	-0.5 ± 1	-0.2 ± 0.7	0.3 ± 0.2
Total TOC	0.48 ± 0.07	0.61 ± 0.06	0.39 ± 0.03	0.469 ± 0.005
Theoretical COD from SCFAs	-0.18 ± 0.05	0.0280 ± 0.0003	-0.01 ± 0.02	0.20 ± 0.20

Based on the flux loss and the increase in SCFA rejections observed in VC mode, this operating mode can be considered inadequate for the treatment of oxidised WAS.

3.3. Liquid-liquid extraction

3.3.1. Solvent Screening

Initial concentrations in the permeate before the LLE are shown in Table 4.3.

Table 4.3. SCFA concentrations in the raffinate before extraction.

SCFA	Concentration (g/L)
Oxalic	0.68 ± 0.02
Maleic	0.020 ± 0.002
Pyruvic	0.51 ± 0.07
Lactobionic	0.08 ± 0.01
Malic	0.120 ± 0.001
Lactic	0.91 ± 0.02
Formic	0.54 ± 0.02
Acetic	1.89 ± 0.07
Propionic	0.23 ± 0.06

Extraction yields and distribution constants obtained during the solvent screening are displayed in Tables 4.4, 4.5, 4.6 and 4.7. To ensure clarity, the SCFAs were divided into non-volatile SCFAs (NVAs) (oxalic, maleic, pyruvic, lactobionic, malic and lactic acids) and volatile SCFAs (VAs) (formic, acetic and propionic acids).

Table 4.4. Extraction yields (Y) of NVAs.

	Extraction Yield (%) - NVAs								
	TOA10	***TOA25***	***TOA40***	***TBP10***	***TBP25***	***TBP40***	***T/T 10***	***T/T 25***	***T/T 40***
Oxalic	12.0 ± 0.9	11.9 ± 0.2	15 ± 1	**n.d.**[1]	0.63 ± 0.07	21 ± 2	26 ± 4	31 ± 4	2.7 ± 0.4
Maleic	38.0	29.2	24.7	16.5	19.3	0	1.0	11.8	79.8
Pyruvic	38 ± 5	29 ± 6	25 ± 3	17 ± 1	19.3 ± 0.3	**n.d.**[1]	5.1 ± 0.2	10 ± 10	80 ± 80
Lactobionic	8.2	100.0	10.5	32.9	27.6	28.8	42.2	29.1	31.9
Malic	**n.d.**[1]	9.7 ± 0.9	18.0 ± 0.4	**n.d.**[1]	6.2 ± 0.3	11 ± 1	**n.d.**[1]	**n.d.**[1]	50 ± 50
Lactic	25.7	35.5	29.7	9.2	90.8	2.6	88.9	42.3	90.6

*Large: SCFA not detected in the raffinate.

(1)n.d.: not detected.

Table 4.5. Extraction yields (Y) of VAs.

	Extraction Yield (%) - VAs								
	TOA10	***TOA25***	***TOA40***	***TBP10***	***TBP25***	***TBP40***	***T/T 10***	***T/T 25***	***T/T 40***
Formic	60 ± 20	30 ± 9	28 ± 8	29.522 ± 0.003	23 ± 1	9.215 ± 0.001	80 ± 10	23.3 ± 0.3	64 ± 7
Acetic	19.7	27.6	20.8	12.7	16.4	6.4	89.2	19.1	80.0
Propionic	20 ± 2	28 ± 2	21 ± 1	12.7 ± 0.3	16.4 ± 0.4	6.4 ± 0.4	19.1 ± 0.2	22.3 ± 0.9	16.0 ± 0.9

Table 4.6. Distribution constants (K_D) of NVAs.

	Distribution Constants - NVAs								
	TOA10	***TOA25***	***TOA40***	***TBP10***	***TBP25***	***TBP40***	***T/T 10***	***T/T 25***	***T/T 40***
Oxalic	0.14 ± 0.01	0.14 ± 0.05	0.18 ± 0.02	**n.d.**⁽¹⁾	0.006 ± 0.001	0.27 ± 0.03	0.36 ± 0.06	0.45 ± 0.07	0.015 ± 0.002
Maleic	0.61	0.41	0.33	0.20	0.24	/	0.01	0.13	3.94
Pyruvic	0.6 ± 0.1	0.4 ± 0.1	0.32 ± 0.04	0.20 ± 0.02	0.24 ± 0.01	**n.d.**⁽¹⁾	0.054 ± 0.004	0.1 ± 0.1	4 ± 4
Lactobionic	**n.d.**⁽¹⁾	0.10 ± 0.01	0.22 ± 0.02	**n.d.**⁽¹⁾	0.067 ± 0.007	0.12 ± 0.02	**n.d.**⁽¹⁾	**n.d.**⁽¹⁾	1 ± 1
Malic	0.09 ± 0.01	**n.d.**⁽¹⁾	0.12 ± 0.01	0.49 ± 0.04	0.38 ± 0.03	0.40 ± 0.06	0.7 ± 0.8	0.4 ± 0.4	0.47 ± 0.06
Lactic	4.7 ± 0.4	3.80 ± 0.06	2.2 ± 0.1	3.8 ± 0.4	11 ± 11	3 ± 3	**n.d.**⁽¹⁾	**n.d.**⁽¹⁾	**n.d.**⁽¹⁾

(1) n.d.: not detected.

Table 4.7. Distribution constants (K_D) of VAs.

	Distribution Constants - VAs								
	TOA10	***TOA25***	***TOA40***	***TBP10***	***TBP25***	***TBP40***	***T/T 10***	***T/T 25***	***T/T 40***
Formic	1 ± 1	0.4 ± 0.3	0.4 ± 0.3	0.4 ± 0.2	0.3 ± 0.1	0.10 ± 0.04	5 ± 3	0.3 ± 0.1	1.8 ± 0.9
Acetic	0.25 ± 0.05	0.38 ± 0.07	0.26 ± 0.04	0.15 ± 0.02	0.20 ± 0.03	0.07 ± 0.01	0.24± 0.03	0.29 ± 0.04	0.19 ± 0.03
Propionic	1.1 ± 0.4	1.15 ± 0.09	1.2 ± 0.2	1.1 ± 0.2	1.07 ± 0.07	0.9 ± 0.2	1.1 ± 0.1	1.0 ± 0.2	0.9 ± 0.2

The effect of the extractant on the yield obtained for the different SCFAs varies depending on the nature of the extractant. In the case of TBP, which is a phosphorous-based extractant, its complexation mechanism with SCFAs primarily relies on the hydrophobicity of SCFAs due to hydrogen bond formation [57]. As a result, the complexation is more pronounced when the SCFA is less hydrophobic. The octanol-water partition coefficient (log P) is the parameter commonly employed to quantify hydrophobicity. The lower the log P value, the lower the hydrophobicity of the SCFA [57]. In this context, polar and hydrophilic compounds may even exhibit negative log P values. As for the complexation with amines like TOA, the mechanism is more intricated, involving different factors such as acid concentration, the nature of the diluent and the number of carboxyl groups [58]. However, the pKa value can serve as an indicator for monocarboxylic acids: pyruvic, lactobionic, lactic, formic, acetic and propionic acids. In this sense, the strongest acids (i.e., those with lower pKa values) are more strongly complexed and, consequently, more efficiently extracted.

The values of LogPs and pKas of the studied SCFAs are shown in Table 4.8.

Table 4.8. Values of the pKa and LogP of the studied SCFAs.

SCFAs	pKa	ref	Log P	ref
Oxalic$^{(1)}$	pKa_1 = 1.46; pKa_2 = 4.40	[59]	-0.688	[60]
Maleic$^{(1)}$	pKa_1 = 1.90; pKa_2 = 6.07	[61]	-0.650	[62]
Pyruvic	2.39	[63]	-0.38	[64,65]
Lactobionic	3.28 ± 0.35 $^{(2)}$	[66]	-4.847	[67]
Malic$^{(1)}$	pKa_1 = 3.51; pKa_2 = 5.03	[68]	-1.474	[69]
Lactic	3.86	[24]	-0.413	[24]
Formic	3.75	[24]	-0.538	[24]
Acetic	4.75	[24]	-0.313	[24]
Propionic	4.87	[24]	0.290	[24]

$^{(1)}$ Dicarboxylic acid; $^{(2)}$ Predicted value

Some deviations from the theoretically expected extraction order were observed. After the extraction with TOA, all monocarboxylic acids were recovered in the expected order except for pyruvic and propionic. In this sense, pyruvic acid exhibited the lowest extraction efficiency, with a maximum value of 12.9%, whereas it was anticipated to be the most efficiently extracted monocarboxylic SCFA. Conversely, propionic acid presented an average yield of 53.4%, despite being expected to be the least efficiently extracted acid. Lactobionic acid was also less extracted than expected when using TOA10 and TOA40 as solvents, although it could not be detected in the raffinate after extracting with TOA25. Regarding the extractions with TBP, slight deviations from the expected order were observed for most of the acids, with significant deviations noted for propionic, lactobionic and pyruvic acids. Consequently, propionic acid, which was expected to be the least extracted acid, yielded an average of 50.3%. On the other hand, lactobionic acid, which was expected to be the acid extracted more efficiently, exhibited an average yield of 29.8%, while malic acid obtained the highest average value at 82.1%. In the case of pyruvic acid, higher values were expected, but the maximum observed was 5.2%. This behaviour can be attributed to differences between the concentrations of the different acids or to interferences between the SCFAs or with other elements of the matrix. Similar results were obtained by Morales et al. when they studied the extraction of butyric, propionic, formic, acetic and lactic acids with TBP in dodecane and with TOA in decane-1-ol and dodecane [23]. They reported extraction yields that differed from what was expected. Thus, propionic and butyric acids, which were expected to be the least complexed, turned out to be the most extracted SCFAs with both TOA and TBP. Similarly, formic acid, with the lowest pKa among the extracted SCFAs, was the least extracted with TOA, contrary to expectations [23]. These deviations from the theoretical extractions were also observed in other studies [70], although some authors have been able to observe a rough correlation between log K and log P [58].

The effect of extractant concentration also varied between SCFAs. As explained before, the optimization of the solvent composition while using a polar diluent relies on a compromise between the concentration of diluent and of extractant. On viewing the results, no clear trends were observed, and the optimal choice of extractant and the ideal diluent:extractant ratio differed for nearly every acid. The combination of TOA and TBP seemed to enhance the extraction in most cases, except for malic acid. Similar synergistic effects between TBP and TOA have been reported by other authors [58,71]. Matsumoto et al., in particular, observed an enhancement in the extraction efficiency for all acids, thus showing that the complex matrix of the oxidised WAS can alter the extraction equilibria.

Regarding K_D values, high values indicate that the extraction process was efficient. In the case of pyruvic acid, low K_D values were obtained with TOA extractant, ranging from 0.1 ± 0.01 to 0.22 ± 0.02. These values are in line with those reported Marti et al. (2011) [72], who obtained a K_D value of 0.10, when they extracted pure pyruvic acid using concentrations of TOA ranging from 0.1 M to 0.4 M in 1-octanol at pH 4. For oxalic acid, a significant increase (25%) in K_D value was observed when TOA concentration increased from 25% to 40%. Qin et al. (2001) [73] also reported that an increase in TOA from 10% to 50% resulted in an increase in K_D values when pure oxalic acid was extracted in TOA:n-octanol mixtures. In the case of TBP:1-octanol mixtures, K_D values (varied from 0.006 ± 0.001 to 0.27 ± 0.03) were lower than that reported by

Barnes et al. (1999) [74] for the extraction of aqueous solutions of oxalic acid with pure TBP (1.275). In the case of malic acid, the values obtained for TOA25 (3.80 ± 0.06) and TOA40 (2.2 ± 0.1) were 4 and 1.5 times higher than those reported by Uslu and Kırbaşlar [75]. This difference can be due to the effect of the matrix and the initial acid concentration, as pure malic acid with a concentration of approximately 107 g/L was used, while in this study the concentration was 0.12 g/L. For lactic acid, K_D values ranging from 0.027 ± 0.003 to 0.10 ± 0.01 were achieved with TBP:1-octanol mixtures. Labbaci et al. (2010) [76] also obtained similar K_D values, varying between 0.03 and 0.08, when extracting pure lactic acid using TBP:dodecane mixtures at similar concentrations.

Considering VAs, when TOA:1-octanol mixtures were used, the K_D values for formic acid ranged from 0.4 ± 0.3 to 1 ± 1, for acetic acid from 0.25 ± 0.05 to 0.38 ± 0.07, and for propionic acid from 1.1 ± 0.4 to 1.2 ± 0.2. These values were higher compared to those obtained with TBP:1-octanol mixtures, which varied from 0.10 ± 0.04 to 0.4 ± 0.2 for formic acid, from 0.07 ± 0.01 to 0.20 ± 0.03 for acetic acid, and from 0.9 ± 0.2 to 1.1 ± 0.2 for propionic acid. This difference may be attributed to 1-octanol exhibiting an acid interaction functional group, resulting in higher specific and general solvation to the acid-TOA complexes, leading to a greater distribution than the TBP mixtures (Keshav et al., 2008) [77].

By comparing the extraction yields obtained for each SCFA using different combinations of extractant-diluent, the most effective process was found to be the one involving n-octanol as diluent and a combination of TOA and TBP at 10% (v/v) as extractant. Both extractants synergised when combined, as indicated in the previous section. Under these conditions, the total extracted SCFAs consisted mainly of formic (14 ± 2% of total SCFAs weight in feed) and acetic (10.4 ± 0.1% of total SCFAs weight in feed) acids, followed by propionic and lactic acids (4.0 ± 0.2% and 3.77 ± 0.01% of total SCFAs weight in feed each). Altogether, a maximum of 34% of total SCFAs weight in feed was extracted under these conditions.

3.3.2. Effect of temperature on organic acid extraction

Based on the results obtained, TOA25, TBP25 and T/T10 were the chosen solvents for the temperature study. Additionally, synthetic solutions containing the same quantities of SCFAs as those found in the pre-purified WAS were prepared and subjected to extraction to evaluate the effect of the matrix. The extraction yields obtained for total, NVAs and VAs are shown in Fig. 4.7.

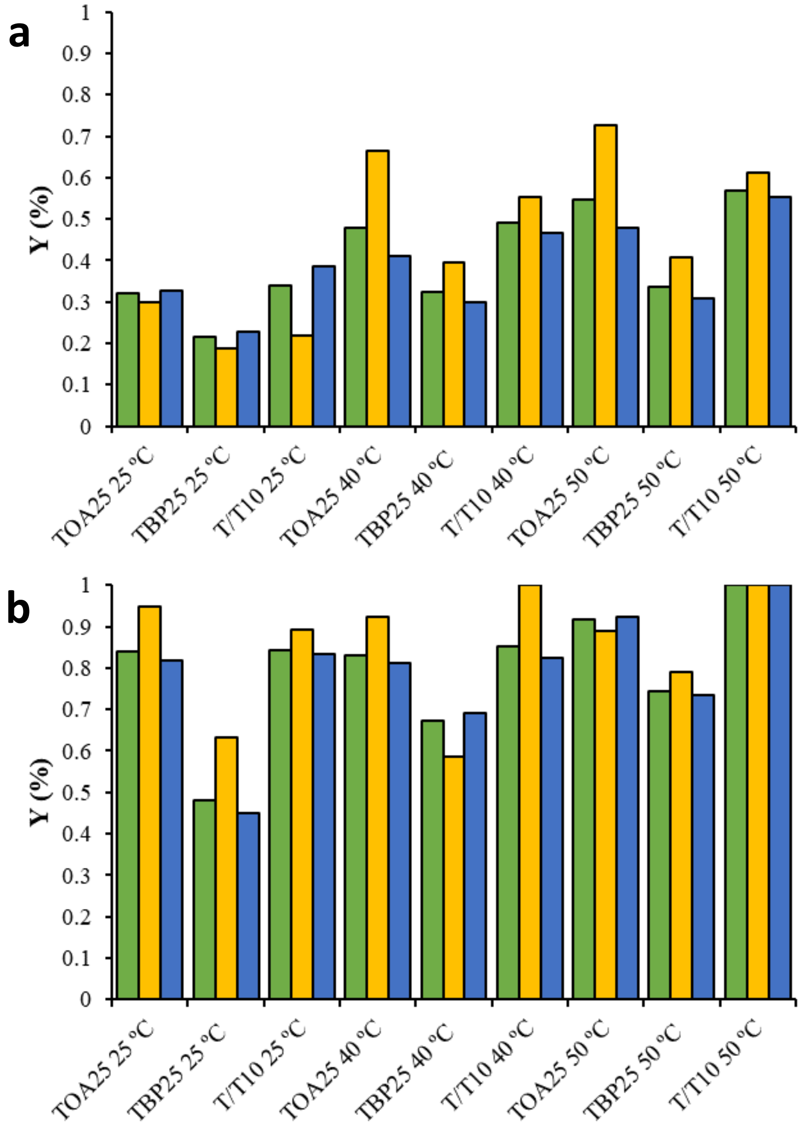

Figure 4.7. Effect of temperature in extraction yields of total (🟩), non-volatile OA (🟨) and volatile OA (🟦) from WAS (above) and synthetic SCFAs solution (below).

As it can be seen in Fig. 4.7, temperature had a generally positive effect on the extraction of both NVAs and VAs from pre-purified WAS in the range 25ºC-50ºC. It is important to note that a further increase in temperature could lead to a loss of extractables caused by thermal degradation [70,78]. Higher yields were observed for total NVAs, ranging from 18.8% to 72.6%, compared to total VAs, in which the values varied from 22.7% to 46.1%. These results are in agreement with those reported by other authors when SCFAs from oxidised Kraft black liquor was extracted with 30% TOA in heptane in the range 25-55ºC, who obtained extraction yields for NVAs and VAs, which varied from 28% to 72%, and from 15% to 45%, respectively [56]. Additionally, the influence of temperature was more pronounced for TOA25 and T/T10 in comparison to TBP25. Thus, in the temperature range of 25ºC-50ºC, the extraction yields for NVAs and VAs with TOA25 and T/T10 were notably higher, showing increases of 2.4 times and 1.5 times, respectively, at 50ºC compared to 25ºC forTOA25, and of 2.8 and 1.4 times, respectively, in the case of T/T10. T/T10 was the most efficient solvent for total SCFAs at all temperatures, with slightly higher yields than TOA25. The extraction yields for NVAs were higher with TOA25, while they were higher for VAs using T/T10.

The extraction of SCFAs from the synthetic solution showed that the components present in the sludge matrix hindered the LLE. As a result, the extraction yields of NVAs and VAs were significantly higher than those of WAS for every solvent and temperature. Besides, the synergistic effect of both extractants was more significant in synthetic solution for both NVAs and VAs, achieving complete separation with T/T10 at 50ºC. Additionally, the theoretical extraction order was neither observed in the synthetic solution. Therefore, it can be concluded that the presence of multiple SCFAs can also alter the theoretical distribution constants, presumably due to competition influenced by the different concentrations in which the SCFAs are present [79].

In this case, a positive effect of temperature was also observed for the extraction of VAs from synthetic solution when temperature increased from 25ºC to 50ºC. The most marked influence was obtained with TBP25 in which the yield increased 1.6 times at 50ºC compared to 25ºC

(44.9%). However, in the case of TOA25, a slight detrimental effect of temperature was observed for NVAs, where the yield decreased from 94.8% at 25ºC to 89.1% at 50ºC.

Besides, the highest extraction yields were obtained with the T/T10 solvent at all temperatures. This showed the beneficial synergistic effect of TOA and TBP for both real and synthetic solutions. TBP25 exhibited the lowest extraction efficiency for WAS at 40 and 50ºC, although it yielded slightly better results than TOA25 at 25ºC. In the case of synthetic solutions, TBP25 consistently produced the lowest yields across all temperatures.

The values of K_D for the extraction from pre-purified WAS and synthetic solutions are shown in Table 4.9.

Table 4.9. K_D values for non-volatile and volatile SCFAs using TOA25, TBP25 and T/T10 as solvent mixtures in the temperature range 25ºC-50ºC.

WAS									
	Oxalic			**Maleic**			**Pyruvic**		
T (ºC)	TOA25	TBP25	T/T10	TOA 25	TBP25	T/T10	TOA 25	TBP25	T/T10
25	0.14 ± 0.05	0.006 ± 0.001	0.36 ± 0.06	0.4 ± 0.1	0.24 ± 0.01	0.054 ± 0.004	0.10 ± 0.01	0.067 ± 0.007	n.d.(1)
40	1.8 ± 0.3	0.32 ± 0.9	1.1 ± 0.3	2.4 ± 0.3	0.64 ± 0.09	1.0 ± 0.4	2.2 ± 0.3	0.4 ± 0.2	1.0 ± 0.3
50	2.4 ± 0.9	0.6 ± 0.4	1.8 ± 0.9	4.8 ± 0.3	0.8 ± 0.5	3.0 ± 0.4	2.6 ± 0.3	0.4 ± 0.3	1.1 ± 0.3
	Lactobionic			**Malic**			**Lactic**		
T (ºC)	TOA25	TBP25	T/T10	TOA 25	TBP25	T/T10	TOA 25	TBP25	T/T10
25	n.d.(1)	0.38 ± 0.03	0.7 ± 0.8	3.80 ± 0.06	11 ± 11	n.d.(1)	0.55 ± 0.09	0.09 ± 0.01	8 ± 1
40	*	*	*	1.9 ± 0.3	1.1 ± 0.2	1.6 ± 0.1	0.8 ± 0.4	0.8 ± 0.3	1.0 ± 0.4
50	*	*	*	2.8 ± 0.8	0.9 ± 0.2	2.2± 0.5	1.2 ± 0.1	0.5 ± 0.3	1.0 ± 0.4
	Formic			**Acetic**			**Propionic**		
T (ºC)	TOA25	TBP25	T/T10	TOA 25	TBP25	T/T10	TOA 25	TBP25	T/T10
25	0.4 ± 0.3	0.3 ± 0.1	5 ± 3	0.38 ± 0.07	0.20 ± 0.03	0.24± 0.03	1.15 ± 0.09	1.07 ± 0.07	1.1 ± 0.1
40	1.2 ± 0.1	0.46 ± 0.08	2.2 ± 0.2	0.5 ± 0.1	0.35 ± 0.04	0.45 ± 0.08	1.0 ± 0.5	1.1 ± 0.6	1.9 ± 0.9
50	1.5 ± 0.3	0.6 ± 0.3	5.6 ± 0.4	0.6 ± 0.1	0.30 ± 0.02	0.6 ± 0.1	2 ± 1	1.4 ± 0.5	2.1 ± 0.8
Synthetic solution									
	Oxalic			**Maleic**			**Pyruvic**		
T (ºC)	TOA25	TBP25	T/T10	TOA 25	TBP25	T/T10	TOA 25	TBP25	T/T10
25	*	0.3 ± 0.1	*	11.2 ± 0.7	0.524 ± 0.009	5 ± 1	*	*	*
40	*	0	*	*	0.4 ± 0.1	*	*	*	*
50	*	*	*	4.7 ± 0.3	1.2 ± 0.2	*	*	*	*
	Lactobionic			**Malic**			**Lactic**		
T (ºC)	TOA25	TBP25	T/T10	TOA 25	TBP25	T/T10	TOA 25	TBP25	T/T10
25	2.4 ± 0.3	2.3 ± 0.2	2.0 ± 0.2	*	2.2 ± 0.2	*	*	*	7 ± 3
40	2.0 ± 0.2	0.2 ± 0.1	*	*	*	*	5 ± 2	*	*
50	0.58 ± 0.04	1.8 ± 0.2	*	*	2.1 ± 0.9	*	*	*	*
	Formic			**Acetic**			**Propionic**		
T (ºC)	TOA25	TBP25	T/T10	TOA 25	TBP25	T/T10	TOA 25	TBP25	T/T10
25	5.2 ± 0.3	0.69 ± 0.07	16 ± 1	7 ± 1	1.1 ± 0.2	4.4 ± 0.8	n.d.	n.d.	n.d.
40	5.2 ± 0.5	*	19.8 ± 0.8	6.0 ± 0.8	0.91 ± 0.05	3.5 ± 0.9	n.d.	n.d.	n.d.
50	*	7.1 ± 0.9	*	7.9 ± 0.6	1.6 ± 0.1	*	1.0 ± 0.4	1.5 ± 0.3	*

*Large: SCFA not detected in aqueous phase.

(1)n.d.: not detected.

The K_Ds observed were in line with those reported by other authors [23,80]. Türk et al. [81] obtained K_Ds in the range of 0.638-1.609 for acetic acid and of 0.496-1.502 for formic acid extracting with TBP diluted in cyclopentyl methyl ether and 2-methyltetrahydrofuran at similar extractant concentrations. Nonetheless, the K_Ds for oxalic, pyruvic, and propionic acids were lower than those found in the literature [24,72,82,83]. For instance, Keshav et al. [84] achieved K_Ds in the range of 5.72–10.11 for propionic acid while extracting TOA 30% in oleyl alcohol, while in our case it could only be extracted at 50 ºC with a K_D of 1.0 ± 0.4. It should be noted than these studies analysed the extraction of the pure acid, without the hindering effects of a complex matrix or the competition with other SCFAs for the formation of complexes with the solvent.

4. Conclusions

WO proved to be an efficient treatment for the valorisation of WAS, converting a significant portion of the natural organic matter into value-added SCFAs, such as acetic, lactic, and lactobionic acids. However, the combination of higher reaction temperatures and longer reaction times favoured the oxidation of the organic matter to CO_2, leading to a reduction in the maximum concentration of SCFAs obtained. Thus, the most suitable conditions were achieved at lower temperature and longer reaction time (160 ºC, 240 min), allowing for the achievement of a maximum concentration of total SCFAs of 6.07 g/L.

Membrane filtration effectively pre-purified the SCFAs present in the oxidised WAS, facilitating the subsequent extraction. Operating in TR mode with the 50 kDa ZrO_2-TiO_2 membrane resulted in average rejections of 53% of CN and 48% of TOC and also negative rejections of the SCFAs (-15%) due to the Donnan effect. Concentrating the oxidised WAS positively influenced CN and TOC retentions, increasing to 73% and 61%, respectively; but also increased the retention of SCFAs to a 4%. Despite the effectiveness in terms of rejections, the substantial flux loss (94.29% in VC mode compared to 78.00% in TR mode) indicated that concentrating the oxidized WAS was impractical. Subsequent filtration of the 50 kDa permeate with the 1 kDa membrane in TR mode further purified the SCFAs, achieving rejections of 73% for CN and 39% for TOC, with a low SCFAs rejection of 4%. Concentrating the oxidised WAS was considered unsuitable for SCFAs recovery, given their high retention (23%). In all cases, the main fouling mechanism was cake formation, indicating that non-aggressive cleaning protocols can be applied to maintain membrane efficiency.

LLE extraction with a mixture of TOA and TBP at 10% in octan-1-ol was found to be the most suitable for the recovery of both NVAs and VAs, obtaining a total yield of 34%. This proved the synergistic effect of the two extractants during the extraction of SCFAs. Lower extraction yields were obtained with the pre-purified WAS compared to synthetic solutions of SCFAs, thus showing the detrimental effect of the matrix in LLE. Increasing the temperature within the range of 20 to 50 ºC generally had a favourable effect on the extraction of SCFAs.

Declaration of Competing Interest

The authors declare that they have no known competing financial interests or personal relationships that could have appeared to influence the work reported in this paper.

Acknowledgements

The authors are grateful for the financial support from the Spanish Ministry of Science and Innovation through the projects MCIU-19-RTI2018-094218-B-I00 and MCIU-22-PID2021-125942OB-I00. Authors also want to acknowledge the Employment, Industry and Tourism Office of the Principality of Asturias, Spain, for their financial support through the project AYUD/2021/51041. The author Daniel Núñez thanks the Principality of Asturias, Spain, for their financial support through the Severo Ochoa scholarship nº BP19-093.

References

[1] S. Beck, S. Jasanoff, A. Stirling, C. Polzin, The governance of sociotechnical transformations to sustainability, Curr. Opin. Environ. Sustain. 49 (2021) 143–152. doi:10.1016/j.cosust.2021.04.010.

[2] J. Markard, R. Raven, B. Truffer, Sustainability transitions: An emerging field of research and its prospects, Res. Policy. 41 (2012) 955–967. doi:10.1016/j.respol.2012.02.013.

[3] Y. Geng, B. Doberstein, Developing the circular economy in China: Challenges and opportunities for achieving "leapfrog development," Https://Doi.Org/10.3843/SusDev.15.3:6. 15 (2010) 231–239. doi:10.3843/SUSDEV.15.3:6.

[4] K. Webster, The circular economy: A wealth of flows, Ellen MacArthur Foundation Publishing., 2016.

[5] D. Fytili, A. Zabaniotou, Utilization of sewage sludge in EU application of old and new methods-A review, Renew. Sustain. Energy Rev. 12 (2008) 116–140. doi:10.1016/j.rser.2006.05.014.

[6] Q.H. Zhang, W.N. Yang, H.H. Ngo, W.S. Guo, P.K. Jin, M. Dzakpasu, S.J. Yang, Q. Wang, X.C. Wang, D. Ao, Current status of urban wastewater treatment plants in China, Environ. Int. 92–93 (2016) 11–22. doi:10.1016/j.envint.2016.03.024.

[7] Y. Zang, Y. Li, C. Wang, W. Zhang, W. Xiong, Towards more accurate life cycle assessment of biological wastewater treatment plants: A review, J. Clean. Prod. 107 (2015) 676–692. doi:10.1016/j.jclepro.2015.05.060.

[8] S. Shi, G. Xu, H. Yu, Z. Zhang, Strategies of valorization of sludge from wastewater treatment, J. Chem. Technol. Biotechnol. 93 (2018) 936–944. doi:10.1002/jctb.5548.

[9] D. Núñez, P. Oulego, S. Collado, F.A. Riera, M. Díaz, Separation and purification techniques for the recovery of added-value biocompounds from waste activated sludge. A review, Resour. Conserv. Recycl. 182 (2022) 106327. doi:10.1016/j.resconrec.2022.106327.

[10] S.K. Panda, L. Sahu, S.K. Behera, R.C. Ray, Research and Production of Organic Acids and Industrial Potential, in: Bioprocess. Biomol. Prod., John Wiley & Sons, Ltd, 2019: pp. 195–209. doi:10.1002/9781119434436.ch9.

[11] L.M.J. Sprakel, B. Schuur, Solvent developments for liquid-liquid extraction of carboxylic acids in perspective, Sep. Purif. Technol. 211 (2019) 935–957. doi:10.1016/j.seppur.2018.10.023.

[12] K. Jawed, A.J. Mattam, Z. Fatma, S. Wajid, M.Z. Abdin, S.S. Yazdani, Engineered production of short chain fatty acid in Escherichia coli using fatty acid synthesis pathway, PLoS One. 11 (2016) 160035. doi:10.1371/journal.pone.0160035.

[13] M.T. Munir, B. Li, I. Mardon, B.R. Young, S. Baroutian, Integrating wet oxidation and struvite precipitation for sewage sludge treatment and phosphorus recovery, J. Clean. Prod. 232 (2019) 1043–1052. doi:10.1016/j.jclepro.2019.06.007.

[14] S. Baroutian, D.J. Gapes, A.K. Sarmah, M.M. Farid, B.R. Young, Formation and degradation of valuable intermediate products during wet oxidation of municipal sludge, Bioresour. Technol. 205 (2016) 280–285. doi:10.1016/J.BIORTECH.2016.01.039.

[15] T.R. Bridle, D. Pritchard, Energy and nutrient recovery from sewage sludge via pyrolysis, Water Sci. Technol. 50 (2004) 169–175. doi:10.2166/wst.2004.0562.

[16] A. Raheem, V.S. Sikarwar, J. He, W. Dastyar, D.D. Dionysiou, W. Wang, M. Zhao, Opportunities and challenges in sustainable treatment and resource reuse of sewage sludge: A review, Chem. Eng. J. 337 (2018) 616–641. doi:10.1016/j.cej.2017.12.149.

[17] T.A. Saleh, V.K. Gupta, An Overview of Membrane Science and Technology, in: Nanomater. Polym. Membr., Elsevier, 2016: pp. 1–23. doi:10.1016/B978-0-12-804703-3.00001-2.

[18] J.M. Gohil, R.R. Choudhury, Introduction to Nanostructured and Nano-enhanced Polymeric Membranes: Preparation, Function, and Application for Water Purification, in: Nanoscale Mater. Water Purif., Elsevier, 2018: pp. 25–57. doi:10.1016/B978-0-12-813926-4.00038-0.

[19] D.M. Kanani, W.H. Fissell, S. Roy, A. Dubnisheva, A. Fleischman, A.L. Zydney, Permeability-selectivity analysis for ultrafiltration: Effect of pore geometry, J. Memb. Sci. 349 (2010) 405–410. doi:10.1016/j.memsci.2009.12.003.

[20] M. Djas, M. Henczka, Reactive extraction of carboxylic acids using organic solvents and supercritical fluids: A review, Sep. Purif. Technol. 201 (2018) 106–119. doi:10.1016/j.seppur.2018.02.010.

[21] F. Chemarin, M. Moussa, M. Chadni, B. Pollet, P. Lieben, F. Allais, I.C. Trelea, V. Athès, New insights in reactive extraction mechanisms of organic acids: An experimental approach for 3-hydroxypropionic acid extraction with tri-n-octylamine, Sep. Purif. Technol. 179 (2017) 523–532. doi:10.1016/j.seppur.2017.02.018.

[22] J.A. Tamada, A.S. Kertes, C.J. King, Extraction of Carboxylic Acids with Amine Extractants. 1. Equilibria and Law of Mass Action Modeling, Ind. Eng. Chem. Res. 29 (1990) 1319–1326. doi:10.1021/ie00103a035.

[23] A.F. Morales, J. Albet, G. Kyuchoukov, G. Malmary, J. Molinier, Influence of extractant (TBP and TOA), diluent, and modifier on extraction equilibrium of monocarboxylic acids, in: J. Chem. Eng. Data, 2003: pp. 874–886. doi:10.1021/je020179o.

[24] W. Qin, Z. Li, Y. Dai, Extraction of Monocarboxylic Acids with Trioctylamine: Equilibria and Correlation of Apparent Reactive Equilibrium Constant, Ind. Eng. Chem. Res. 42 (2003) 6196–6204. doi:10.1021/ie021049b.

[25] X. Li, W. Liu, W. Zhang, A. Zhou, Q. Xu, Z. He, C. Yang, A. Wang, Short-chain fatty acid production from waste activated sludge and in situ use in wastewater treatment plants with life cycle assessment, Resour. Conserv. Recycl. 198 (2023) 107186. doi:10.1016/j.resconrec.2023.107186.

[26] F. laqa Kakar, S.N. Liss, E. Elbeshbishy, Effect of Hydrothermal Pretreatment on Resource Recovery from Thickened Waste Activated Sludge, in: 95th Water Environ. Fed. Tech. Exhib. Conf. WEFTEC 2022, Springer, 2022: pp. 2774–2779. doi:10.1007/S12155-019-10056-Z/METRICS.

[27] R. Babu, G. Capannelli, M. Bernardini, M. Pagliero, A. Comite, Effect of varying hydrothermal temperature, time, and sludge pH on sludge solubilisation, Carbon Resour. Convers. 6 (2023) 142–149. doi:10.1016/j.crcon.2022.12.001.

[28] L. Pola, S. Collado, P. Oulego, P. Calvo, M. Díaz, Characterisation of the wet oxidation of black liquor for its integration in Kraft paper mills, Chem. Eng. J. 405 (2021) 126610. doi:10.1016/j.cej.2020.126610.

[29] I. Sutzkover-Gutman, D. Hasson, R. Semiat, Humic substances fouling in ultrafiltration processes, Desalination. 261 (2010) 218–231. doi:10.1016/j.desal.2010.05.008.

[30] S. Collado, D. Núñez, P. Oulego, F.A. Riera, M. Díaz, Effect of landfill leachate ageing on ultrafiltration performance and membrane fouling behaviour, J. Water Process Eng. 36 (2020). doi:10.1016/j.jwpe.2020.101291.

[31] S. Baroutian, A.M. Smit, J. Andrews, B. Young, D. Gapes, Hydrothermal degradation of organic matter in municipal sludge using non-catalytic wet oxidation, Chem. Eng. J. 260 (2015) 846–854. doi:10.1016/j.cej.2014.09.063.

[32] J. Chung, M. Lee, J. Ahn, W. Bae, Y.W. Lee, H. Shim, Effects of operational conditions on sludge degradation and organic acids formation in low-critical wet air oxidation, J. Hazard. Mater. 162 (2009) 10–16. doi:10.1016/j.jhazmat.2008.05.038.

[33] J.L. Urrea, S. Collado, A. Laca, M. Díaz, Wet oxidation of activated sludge: Transformations and mechanisms, J. Environ. Manage. 146 (2014) 251–259. doi:10.1016/J.JENVMAN.2014.07.043.

[34] A. Shanableh, Production of useful organic matter from sludge using hydrothermal treatment, Water Res. 34 (2000) 945–951. doi:10.1016/S0043-1354(99)00222-5.

[35] P.J. Strong, D.J. Gapes, Thermal and thermo-chemical pre-treatment of four waste residues and the effect on acetic acid production and methane synthesis, Waste Manag. 32 (2012) 1669–1677. doi:10.1016/J.WASMAN.2012.04.004.

[36] A. Prince-Pike, D.I. Wilson, S. Baroutian, J. Andrews, D.J. Gapes, A kinetic model of municipal sludge degradation during non-catalytic wet oxidation, Water Res. 87 (2015) 225–236. doi:10.1016/j.watres.2015.09.009.

[37] O. Al-Akoum, L.H. Ding, M.Y. Jaffrin, Microfiltration and ultrafiltration of UHT skim milk with a vibrating membrane module, Sep. Purif. Technol. 28 (2002) 219–234. doi:10.1016/S1383-5866(02)00076-X.

[38] L.E. Fratila-Apachitei, M.D. Kennedy, J.D. Linton, I. Blume, J.C. Schippers, Influence of membrane morphology on the flux decline during dead-end ultrafiltration of refinery and

petrochemical waste water, J. Memb. Sci. 182 (2001) 151–159. doi:10.1016/S0376-7388(00)00557-3.

[39] L. Li, L. Ding, Z. Tu, Y. Wan, D. Clausse, J.L. Lanoisellé, Recovery of linseed oil dispersed within an oil-in-water emulsion using hydrophilic membrane by rotating disk filtration system, J. Memb. Sci. 342 (2009) 70–79. doi:10.1016/J.MEMSCI.2009.06.023.

[40] M. Al-Maas, A. Hussain, J. Minier Matar, D. Ponnamma, M.K. Hassan, M. Al Ali Al-Maadeed, K. Alamgir, S. Adham, Validation and application of a membrane filtration evaluation protocol for oil-water separation, J. Water Process Eng. 43 (2021) 102185. doi:10.1016/J.JWPE.2021.102185.

[41] S.F.E. Boerlage, M.D. Kennedy, M.R. Dickson, D.E.Y. El-Hodali, J.C. Schippers, The modified fouling index using ultrafiltration membranes (MFI-UF): characterisation, filtration mechanisms and proposed reference membrane, J. Memb. Sci. 197 (2002) 1–21. doi:10.1016/S0376-7388(01)00618-4.

[42] Q. Yang, J. Luo, S. Guo, X. Hang, X. Chen, Y. Wan, Threshold flux in concentration mode: Fouling control during clarification of molasses by ultrafiltration, J. Memb. Sci. 586 (2019) 130–139. doi:10.1016/J.MEMSCI.2019.05.063.

[43] M. Cifuentes-Cabezas, C. Carbonell-Alcaina, M.C. Vincent-Vela, J.A. Mendoza-Roca, S. Álvarez-Blanco, Comparison of different ultrafiltration membranes as first step for the recovery of phenolic compounds from olive-oil washing wastewater, Process Saf. Environ. Prot. 149 (2021) 724–734. doi:10.1016/J.PSEP.2021.03.035.

[44] A. Arkell, J. Olsson, O. Wallberg, Process performance in lignin separation from softwood black liquor by membrane filtration, Chem. Eng. Res. Des. 92 (2014) 1792–1800. doi:10.1016/j.cherd.2013.12.018.

[45] A. Urbanowska, M. Kabsch-Korbutowicz, The Use of Flat Ceramic Membranes for Purification of the Liquid Fraction of the Digestate from Municipal Waste Biogas Plants, Energies 2021, Vol. 14, Page 3947. 14 (2021) 3947. doi:10.3390/EN14133947.

[46] L. De Angelis, M.M.F. De Cortalezzi, Ceramic membrane filtration of organic compounds: Effect of concentration, pH, and mixtures interactions on fouling, Sep. Purif. Technol. 118 (2013) 762–775. doi:10.1016/J.SEPPUR.2013.08.016.

[47] M. Dilaver, S.M. Hocaoğlu, G. Soydemir, M. Dursun, B. Keskinler, İ. Koyuncu, M. Ağtaş, Hot wastewater recovery by using ceramic membrane ultrafiltration and its reusability in textile industry, J. Clean. Prod. 171 (2018) 220–233. doi:10.1016/J.JCLEPRO.2017.10.015.

[48] A.S. Cassini, I.C. Tessaro, L.D.F. Marczak, C. Pertile, Ultrafiltration of wastewater from isolated soy protein production: A comparison of three UF membranes, J. Clean. Prod. 18 (2010) 260–265. doi:10.1016/j.jclepro.2009.10.016.

[49] G. Di Bella, D. Di Trapani, A brief review on the resistance-in-series model in membrane bioreactors (MBRs), Membranes (Basel). 9 (2019) 24. doi:10.3390/membranes9020024.

[50] J. Chen, B. Gu, E.J. LeBoeuf, H. Pan, S. Dai, Spectroscopic characterization of the structural and functional properties of natural organic matter fractions, Chemosphere. 48 (2002) 59–68. doi:10.1016/S0045-6535(02)00041-3.

[51] J. Dwyer, L. Kavanagh, P. Lant, The degradation of dissolved organic nitrogen associated with melanoidin using a UV/H2O2 AOP, Chemosphere. 71 (2008) 1745–1753. doi:10.1016/j.chemosphere.2007.11.027.

[52] J. Shao, L. Zhao, X. Chen, Y. He, Humic acid rejection and flux decline with negatively charged membranes of different spacer arm lengths and charge groups, J. Memb. Sci. 435 (2013) 38–45. doi:10.1016/j.memsci.2013.01.063.

[53] P. Fievet, Donnan Effect, Encycl. Membr. (2014) 1–3. doi:10.1007/978-3-642-40872-4_1714-1.

[54] M. Williams, C.A. Pineda-Vargas, E. V. Khataibe, B.J. Bladergroen, A.N. Nechaev, V.M. Linkov, Surface functionalization of porous ZrO2–TiO2 membranes using γ-aminopropyltriethoxysilane in palladium electroless deposition, Appl. Surf. Sci. 254 (2008) 3211–3219. doi:10.1016/J.APSUSC.2007.10.100.

[55] S. Hellstén, J. Lahti, J. Heinonen, M. Kallioinen, M. Mänttäri, T. Sainio, Purification process for recovering hydroxy acids from soda black liquor, Chem. Eng. Res. Des. 91 (2013) 2765–2774. doi:10.1016/J.CHERD.2013.06.001.

[56] M. Mänttäri, M. Nyström, Negative retention of organic compounds in nanofiltration, Desalination. 199 (2006) 41–42. doi:10.1016/J.DESAL.2006.03.015.

[57] C. Scheler, M. Popovic, E. Iannotti, R. Mueller, R. Bajpai, Chemical interactions between aqueous and organic phases in a reactive extraction process, Appl. Biochem. Biotechnol. - Part A Enzym. Eng. Biotechnol. 57–58 (1996) 29–38. doi:10.1007/BF02941685.

[58] M. Matsumoto, T. Otono, K. Kondo, Synergistic extraction of organic acids with tri-n-octylamine and tri-n-butylphosphate, Sep. Purif. Technol. 24 (2001) 337–342. doi:10.1016/S1383-5866(01)00137-X.

[59] National Center for Biotechnology Information, Oxalic acid | HOOCCOOH - PubChem, Oxalic Acid. (2004). https://pubchem-ncbi-nlm-nih-gov.ezproxy.umng.edu.co/compound/971#section=Top (accessed April 9, 2021).

[60] Royal Society of Chemistry, Oxalic acid | C2H2O4 | ChemSpider, 2021. (n.d.). http://www.chemspider.com/Chemical-Structure.946.html (accessed April 9, 2021).

[61] A.S. Amarasekara, B. Wiredu, Y.M. Lawrence, Hydrolysis and interactions of d-cellobiose with polycarboxylic acids, Carbohydr. Res. 475 (2019) 34–38. doi:10.1016/J.CARRES.2019.02.002.

[62] D. Klimoszek, A. Pyka-Pająk, Lipophilicity Study of Fumaric and Maleic Acids, Processes. 11 (2023) 1–13. doi:10.3390/pr11040993.

[63] A.J. Eugene, E.A. Pillar-Little, A.J. Colussi, M.I. Guzman, Enhanced Acidity of Acetic and Pyruvic Acids on the Surface of Water, (2018). doi:10.1021/acs.langmuir.8b01606.

[64] I. V. Tetko, J. Gasteiger, R. Todeschini, A. Mauri, D. Livingstone, P. Ertl, V.A. Palyulin, E. V. Radchenko, N.S. Zefirov, A.S. Makarenko, V.Y. Tanchuk, V. V. Prokopenko, Virtual computational chemistry laboratory--design and description, J. Comput. Aided. Mol. Des. 19 (2005) 453–463. doi:10.1007/S10822-005-8694-Y.

[65] VCCLAB, Virtual Computational Chemistry Laboratory, 2005. (n.d.). https://vcclab.org/lab (accessed November 29, 2023).

[66] Chemical Book, Lactobionic acid | 96-82-2, 2017. (n.d.). https://www.chemicalbook.com/ChemicalProductProperty_EN_CB8713997.htm (accessed April 9, 2021).

[67] Royal Society of Chemistry, Lactobionic acid | C12H22O12 | ChemSpider, 2021. (n.d.). http://www.chemspider.com/Chemical-Structure.7040.html (accessed April 12, 2021).

[68] U.S. National Library of Medicine, Malic acid | C4H6O5 - PubChem, PubChem. (2019). https://pubchem.ncbi.nlm.nih.gov/compound/Malic-acid#section=Viscosity%0Ahttps://pubchem.ncbi.nlm.nih.gov/compound/Malic-acid#section=Names-and-Identifiers (accessed April 9, 2021).

[69] Royal Society of Chemistry, (±)-Malic Acid | C4H6O5 | ChemSpider, 2021. (n.d.). http://www.chemspider.com/Chemical-Structure.510.html (accessed April 9, 2021).

[70] D. Núñez, P. Oulego, S. Collado, F.A. Riera, M. Díaz, Recovery of organic acids from pre-treated Kraft black liquor using ultrafiltration and liquid-liquid extraction, Sep. Purif. Technol. 284 (2022) 120274. doi:10.1016/j.seppur.2021.120274.

[71] D. Pal, N. Thakre, A. Kumar, A. Keshav, Reactive extraction of pyruvic acid using mixed extractants, Http://Dx.Doi.Org/10.1080/01496395.2016.1143508. 51 (2016) 1141–1150. doi:10.1080/01496395.2016.1143508.

[72] M.E. Marti, T. Gurkan, L.K. Doraiswamy, Equilibrium and Kinetic Studies on Reactive Extraction of Pyruvic Acid with Trioctylamine in 1-Octanol, Ind. Eng. Chem. Res. 50 (2011) 13518–13525. doi:10.1021/IE200625Q.

[73] W. Qin, Y. Cao, X. Luo, G. Liu, Y. Dai, Extraction mechanism and behavior of oxalic acid by trioctylamine, Sep. Purif. Technol. 24 (2001) 419–426. doi:10.1016/S1383-5866(01)00141-1.

[74] N.G. Barnes, M.B. Gramajo De Doz, H.N. Sólimo, Liquid-liquid extraction of oxalic acid from aqueous solutions with tributyl phosphate and a mixed solvent at 303.15 K, J. Chem. Eng. Data. 44 (1999) 430–434. doi:10.1021/je980198r.

[75] H. Uslu, Ş.I. Kirbaşlar, Extraction of aqueous of malic acid by trioctylamine extractant in various diluents, Fluid Phase Equilib. 287 (2010) 134–140. doi:10.1016/j.fluid.2009.09.022.

[76] A. Labbaci, G. Kyuchoukov, J. Albet, J. Molinier, Detailed Investigation of Lactic Acid Extraction with Tributylphosphate Dissolved in Dodecane, J. Chem. Eng. Data. 55 (2009) 228–233. doi:10.1021/JE900315R.

[77] A. Keshav, K.L. Wasewar, S. Chand, Extraction of propionic acid using different extractants (tri-n-butylphosphate, tri-n-octylamine, and Aliquat 336), Ind. Eng. Chem. Res. 47 (2008) 6192–6196. doi:10.1021/ie800006r.

[78] I.S. Che Sulaiman, M. Basri, H.R. Fard Masoumi, W.J. Chee, S.E. Ashari, M. Ismail, Effects of temperature, time, and solvent ratio on the extraction of phenolic compounds and the anti-radical activity of Clinacanthus nutans Lindau leaves by response surface methodology, Chem. Cent. J. 11 (2017) 54. doi:10.1186/s13065-017-0285-1.

[79] G. Maurer, Modeling the liquid-liquid equilibrium for the recovery of carboxylic acids from aqueous solutions, Fluid Phase Equilib. 241 (2006) 86–95. doi:10.1016/j.fluid.2005.11.005.

[80] E. Hasret, Ş.I. Klrbaşlar, H. Uslu, Extraction of Citric Acid and Maleic Acid from Their Aqueous Solutions Using a Phosphorus-Bonded Extractant, Tri-n-octylphosphineoxide, and a Secondary Amine, Dioctylamine, J. Chem. Eng. Data. 63 (2018) 39–48. doi:10.1021/ACS.JCED.7B00562/ASSET/IMAGES/MEDIUM/JE-2017-00562D_0005.GIF.

[81] F.N. Türk, S. Çehreli, N. Baylan, Reactive Extraction of Monocarboxylic Acids (Formic, Acetic, and Propionic) Using Tributyl Phosphate in Green Solvents (Cyclopentyl Methyl Ether and 2-Methyltetrahydrofuran), J. Chem. Eng. Data. 66 (2021) 130–137. doi:10.1021/acs.jced.0c00486.

[82] V.H. Shah, V. Pham, P. Larsen, S. Biswas, T. Frank, Liquid-Liquid Extraction for Recovering Low Margin Chemicals: Thinking beyond the Partition Ratio, Ind. Eng. Chem. Res. 55 (2016) 1731–1739. doi:10.1021/ACS.IECR.5B03914/SUPPL_FILE/IE5B03914_SI_001.PDF.

[83] D. Pal, N. Thakre, A. Keshav, A. Kumar, D. Singh, N. Kumari, Liquid-liquid extraction equilibrium for pyruvic acid recovery: experimental data and modeling, Brazilian J. Chem. Eng. 34 (2017) 919–925. doi:10.1590/0104-6632.20170343S20150276.

[84] A. Keshav, K.L. Wasewar, S. Chand, Extraction of propionic acid with tri-n-octyl amine in different diluents, Sep. Purif. Technol. 63 (2008) 179–183. doi:10.1016/j.seppur.2008.04.012.

4.1.2. Membrane fractioning of pre-treated waste activated sludge for the recovery of valuable biocompounds

Daniel Núñez[1], Paula Oulego[1], Mahdi Nikbakht Fini[2], Jens Muff[2], Sergio Collado[1], Francisco A. Riera[1], Mario Díaz[1]*

[1]Department of Chemical and Environmental Engineering, University of Oviedo.

c/ Julián Clavería 8, 33006, Oviedo, Spain

[2]Department of Chemistry and Bioscience, Aalborg University Esbjerg, Niels Bohrs Vej

8, Esbjerg, 6700, Denmark

*Corresponding author's e-mail: mariodiaz@uniovi.es

Phone: +34 985 10 34 39, FAX: +34 985 10 34 40

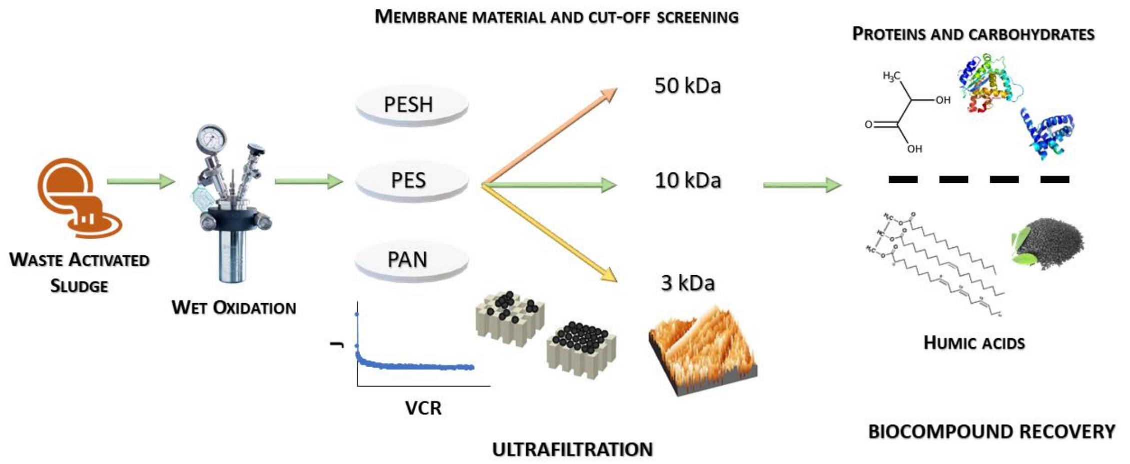

Figura 4.8. Resumen gráfico del artículo *Separation and purification techniques for the recovery of added-value biocompounds from waste activated sludge. A review*.

Artículo publicado en la revista **Journal of Water Process Engineering**

Cuartil: Q1 **Índice de impacto:** 7.53

Referencia: Daniel Núñez, Paula Oulego, Mahdi Nikbakht Fini, Jens Muff, Sergio Collado, Francisco A. Riera, Mario Díaz, Membrane fractioning of pre-treated waste activated sludge for the recovery of valuable biocompounds, Journal of Water Process Engineering, Volume 55, 2023, 104086.

Abstract

The recovery of added-value biocompounds from waste activated sludge (WAS) is a promising alternative to its current management. In this study, WAS was partially wet oxidised producing a highly complex stream mainly composed of humic acids, proteins and carbohydrates. This stream was ultrafiltered to assess the influence of membrane material and molecular weight cut-off (MWCO) on its fractioning based on the different sizes of the biomolecules contained in the oxidised WAS.

Flat-sheet polyethersulfone (PES), permanently hydrophilic polyethersulfone (PESH), and polyacrylonitrile (PAN) membranes with a MWCO of 50 KDa were evaluated. The best performance was obtained with PES membrane, achieving high retention values (around 70% for proteins and carbohydrates, and 47% for humic acids) and high differences in selectivity between proteins and carbohydrates with humic acids (around 23%). For the size fractioning experiments, PES membranes of 10 and 3 kDa (PES10 and PES3) were used, obtaining the best results when filtering the PES50 membrane permeate with the PES3 membrane, retaining 83% of carbohydrates, 87% of proteins and 69% of humic acids. These results open the possibility of separating carbohydrates, proteins and humic acids through an integrated membrane process.

Besides, membranes were characterized by atomic force microscopy, infrared spectroscopy, and contact angle measurements.

Multiple fouling models were assessed, and the main fouling in PAN membrane, and to a lesser extent in PES, was reversible. Conversely, PESH membrane fouling had a strongly irreversible character. Cake filtration can be considered the main fouling mechanism in all experiments.

Keywords: Biomolecules; modelisation; ultrafiltration; waste valorisation; wet oxidation.

1. Introduction

The biorefining of biowastes has been proposed as a sustainable means of waste valorisation, obtaining energy and biochemical resources while the volume of final waste is reduced [1]. Although it is yet at its conceptual phase [2], the steady rising trend of the biorefinery market value, expected to show an annual growth of 2.2% until reaching a total value of USD 52680 million by 2027 [3], is a reliable marker for its potential. Waste activated sludge (WAS) is a promising raw matter for biorefinery, as it is a source of biomolecules (proteins, lipids, carbohydrates, humic acids and enzymes), phosphorus, bio-plastics, bio-pesticides and also energy [4–10]. The current global market size of just the biomolecules present in WAS is of almost USD 200 billion, turning its recovery economically appealing [11].

WAS mainly consists of flocs of bacterial cells, which are formed by weak physical chemical interactions with extracellular polymeric substances [12] (a complex mixture of polymers generated by bacterial excretion, released after cell lysis or present in the incoming wastewater [13]). Thus, in order to recover the above-mentioned biocompounds, a prior solubilisation of the sludge is needed in order to break both the structure formed by the extracellular polymeric substances and the cell walls, thus releasing their intracellular content to the liquid medium. Several solubilisation methods have been tested for WAS, including ultra-sonication [14,15], cavitation [16], alkali treatment [15,17], ozonolysis [18], wet oxidation (WO) and thermal hydrolysis [19]. Among these techniques, WO is particularly interesting, due to its feasibility to be used at an industrial scale for sludge stabilisation [20].

It should be noted that this solubilisation results in a complex matrix, where interactions between the different released biomolecules can difficult their purification. For instance, electrostatic interactions between proteins and humic acids occur while binding to heavy metals such as Cu^{2+}, Zn^{2+}, and Cd^{2+} [21]; and even aggregates are formed when complexed with Cu^{2+} [22], hindering a suitable separation of these molecules by immobilised metal affinity chromatography. Besides, a selective precipitation is also not possible from this complex matrix, as proteins, carbohydrates and humic acids co-precipitate with several precipitation methods [19]. These molecules have important industrial applications separately: proteins are used in cosmetics, food industry, pharmaceuticals and animal feed; humic acids can be applied in agriculture, pharmaceuticals or ecological remediation, among other uses; and carbohydrates are often used in the food industry [11]. Thus, their separation is of great interest for the incorporation of WAS as a valuable raw material in a context of circular economy. Besides, lipid recovery for its use as biofuel from WAS faces difficulties during its purification with solvent extraction, as other lipidic contaminants such as wax esters, terpenoids and polycyclic aromatic hydrocarbons are extracted together with the desired lipids [4].

For these reasons, fractioning the solubilised WAS would improve the efficiency of further separation and purification steps. To that end, membrane filtration is a suitable technology for this purpose due to its advantages, such as high selectivity, low energy consumption, low cost, and mild operating conditions [23]. Nevertheless, the performance of the membrane filtration is affected by several factors, especially the choice of membrane material and its molecular weight cut-off (MWCO) [24–26]. Most membranes are polymeric, and the choice of this polymer is critical for the efficiency of the operation, since it affects the permeability rate, the separation ability or the fouling process, key parameters in the filtration process [23].

Despite their utter importance, polymeric materials have not yet been studied for the filtration of solubilised WAS, and the effect of MWCO has been scarcely studied. Hence, only Li et al. have tested the use of 1, 10, 30, and 50 kDa polysulphone membranes to concentrate humic acids [27,28]. Therefore, the objective of this work was to study the influence of the membrane material and MWCO on the fractionation of hydrothermally solubilised WAS in order to separate carbohydrates, proteins, and humic acids based on their size differences aiming to obtain partially purified streams of these compounds. In this sense, 3 different polymeric materials: polyethersulphone, hydrophylic polyethersulphone and polyacrylonitrile, with a MWCO from 3 KDa to 50 KDa, were evaluated, paying special attention to fouling modelling. Hydrophilic polyethersulfone and polyacrylonitrile have a hydrophilic character, unlike polyethersulfone, which is a hydrophobic material. Besides, an integrated membrane process for the recovery of biomolecules from WAS was also proposed.

2. Experimental

2.1. Oxidised waste activated sludge

Waste activated sludge was collected from the thickening unit of a wastewater treatment plant located in northern Spain (Baíña, Asturias). The collection was performed by trained plant personnel to ensure the representativeness of the samples. WAS was immediately solubilised by a partial WO at 160 ºC and 40 bar for 80 minutes. These oxidation conditions were selected to maximise the production of the target molecules: if the intensity of the treatment is too high, the target molecules get oxidised or mineralised; if the intensity is too low, the sludge does not completely solubilise [29]. Additionally, as the oxidation intensity increases, the particle size decreases, reducing the retention capabilities of the membranes. A constant flow of 1200 mL/min of O_2 saturated with steam was maintained during the entire reaction. The content of the reactor was kept stirring at 150 rpm. A more detailed description of the reactor can be found in [30]. After the reaction, the oxidised WAS was centrifuged in order to work with the liquid phase. Sodium azide 0.1% (w/v) was added to the oxidised WAS in order to prevent microbiological growth. The oxidised sludge was stored at 4 ºC for 15 days and then replaced with fresh oxidised sludge.

2.2. Membrane filtration

2.2.1. Membranes

MQ (Synder Filtration) polyethersulfone (PES), UH050 (Microdyn Nadir) hydrophylic polyethersulfone (PESH), and MW (Suez) polyacrylonitrile (PAN) flat-sheet membranes with MWCO of 50 kDa (named as PES50, PESH50, and PAN50, respectively) were employed to perform the material screening experiments. Additionally, ST (Synder Filtration) and VT

(Synder Filtration) PES flat-sheet membranes with MWCO of 3 and 10 kDa, respectively (named as PES3 and PES10), were used for the cut-off size screening experiments. All membranes were cut to a circular shape of 9 cm of diameter, and a filtration area of 63.62 cm^2.

Membrane hydrophilicity was characterized by contact angle measurements. The images were obtained with a CAM 200 optical contact angle meter (KSV Instruments Ltd., Finland). Sessile water droplets were dropped on the clean and fouled membrane surfaces using a syringe and let to spread freely. Images of the droplets were taken by a high-resolution CCD camera at 40 ms intervals for the first 0.36 s, and at 1 s intervals for the subsequent 19 s. Equilibrium sessile drop contact angles were determined from the steady-state angles using the KSV CAM 200 software by measuring the angle between the baseline of a liquid drop and the tangent at the solid–liquid boundary. All contact angle measurements were performed in triplicate using three different membrane samples.

2.2.2. Equipment and filtration conditions

Filtration experiments were carried out in duplicate using an FT17 Cross-flow Filtration Unit (Armfield Ltd., United Kingdom), which allows to perform tangential flow filtrations with flat sheet membranes. Prior to conducting the experiments, all polymeric membranes were pre-conditioned by running the equipment with no pressure for 30 minutes using distilled water. Subsequently, water was filtered under the operational conditions (indicated below) for an additional 30 minutes. The flux obtained in this sted was considered as the flux at t=0. The permeate flux of the clean membranes was measured during this step for further fouling modelling. All the material screening filtration experiments were performed under the following conditions: temperature of 50.0 ± 0.4 ºC, transmembrane pressure (TMP) of 4.0 ± 0.2 bar and crossflow velocity (CFV) of 3.00 m/s. The oxidised WAS was filtrated without permeate recirculation until a volume concentration rate (VCR) of 2.5 was reached.

During the MWCO screening experiments, the oxidised WAS was filtered with the PES50, PES10 and PES3 membranes. Besides, in order to assess the viability of the fractioning of the oxidised WAS, the permeate obtained after the filtration with PES50 was subsequently filtered with the PES10 or with the PES3 membranes, naming these permeates as PES50-10 and PES50-3, respectively. The experiments were performed under the same conditions than those used in the material screening ones. Only for obtaining the PES50-3 permeate, pressure was set at 30 bar and a VCR value of 1.25 was achieved.

Permeate flow was determined by gravimetric measurements of the permeate, which were collected automatically by the FT17 Cross-flow Filtration Unit software. Flux was calculated by the following equation (Eq. 1):

$$J = \frac{Q_P}{A_M} \qquad (1)$$

Where J is the permeate flux ($m \cdot s^{-1}$), Q_P is the permeate flow ($m^3 \cdot s^{-1}$), and A_M is the membrane surface area (m^2).

In addition, samples of the permeate and retentate were collected periodically and kept at 4 ºC for further analysis.

After the filtrations, the fouled membrane was rinsed with distilled water until a constant flux was obtained, and its permeability was measured for further fouling modelling.

2.2.3. Fouling modelling

Resistance-in-series, Hermia's, and Mentha's fouling models were employed to characterise both the reversibility and main mechanism of membrane fouling occurred during the different filtration experiments.

Resistance-in-series model expresses the total hydraulic resistance of the membrane (R_T, m^{-1}) as the sum of different resistances caused by reversible fouling (R_{rev}, m^{-1}), irreversible fouling (R_{irrev}, m^{-1}), or by the membrane itself (R_m, m^{-1}) (Eq. 2). Hydraulic resistance can be calculated as shown in Eq. 3:

$$R_T=R_m+R_{rev}+R_{irrev} \qquad (2)$$

$$R=\frac{TMP}{\mu J} \tag{3}$$

Where μ is the dynamic viscosity of the WAS at 50 ºC (kg·m·s^{-1}). By adding or subtracting the resistances obtained with the clean, fouled, or rinsed membrane fluxes, R_m, R_{rev}, and R_{irrev} can be easily calculated. A more detailed explanation of these calculations can be found in the Appendix of [31]).

The main fouling mechanism occurred on each membrane during ultrafiltration was determined through Hermia's model [32] (Eq. 4):

$$\frac{dJ}{dt}=-K_j\cdot(J-J_0)\cdot J^{2-n} \tag{4}$$

Where t is time (min), K_j is the model constant that depends on the fouling phenomenon, J_0 is the limiting flux (m·s^{-1}), and n is a constant that varies for the fouling mechanism: complete pore blocking (CPB) (n=2, K_b in min^{-1}), where the active membrane area is blocked by particles larger than the pore size; internal pore blocking (IPB) (n=1.5, K_i in m^{-1}), where membrane pores are blinded by either adsorption or deposition of particles smaller than the pore size; particle pore blocking (PPB) (n=1, K_p in m^{-1}), where particles might seal a pore over time, or bridge it and not block it completely; and cake filtration (CF) (n=0, K_c in min·m^{-2}), where a cake of particles that does not enter the pores is formed on the membrane surface [33].

The K_j for the four models were calculated by minimizing the difference between the predicted values and the experimental data, calculated as the sum of squared residuals (SSR). The model with the lowest SSR was chosen as the most suitable one for each set of experimental data.

In addition, flux was also modelled using the Mehta's model [34], which takes into account the two flux decline domains that take place during membrane filtration: domain 1, where a rapid flux decline occurs during the early stage of filtration; and domain 2, where the flux decline decreases until the flux remains quasi-stable [35]. It can be expressed as follows (Eq. 5):

$$J = J_0 - J_{\infty 1} \cdot \exp^{-\alpha t} + (J_{\infty 1} - J_{\infty 2}) \cdot \exp^{-\beta t} + J_{\infty 2} \qquad (5)$$

Where $J_{\infty 1}$ is the flux at the end of domain 1 ($m \cdot s^{-1}$); $J_{\infty 2}$ is the flux at the end of domain 2 (i.e., at the end of the experiment) ($m \cdot s^{-1}$); and α (min^{-1}) and β (min^{-1}) are two constants determined experimentally that describe the rate of flux decline associated with the membrane fouling and the concentration polarization and gel layer formation, respectively.

2.3. Atomic force microscopy

The roughness of the fouled and clean membranes was analysed by atomic force microscopy (AFM). All AFM measurements were performed at room temperature (20ºC) using a Nanoscale scanning tunnelling microscope (Nanotec Cervantes FullMode SPM), working in contact mode in air medium with gold coated silicon nitride tips. Membrane samples were fixed to the sample holder of the microscope with high-vacuum silicone grease. Roughness parameters were determined from the collected data using the WSxM 5.0 software [36]. Membrane roughness was compared in terms of mean roughness (R_a [nm/µm]), root mean square roughness (rms), peak-to-peak distance (nm/µm), and surface skewness and kurtosis. R_a is the mean value of the surface relative to the centre plane; rms is the standard deviation of the heights for all the pixels in the image from the arithmetic mean [37]; and skewness and kurtosis describe the shape of a probability distribution, reflecting the obliquity and the flatness of the curve, respectively [38].

2.4. Infrared spectroscopy

Infrared spectra (FTIR) of the clean and fouled membranes were taken in the range from 600 to 4000 cm^{-1} using Varian 670-IR FTIR spectrometer equipped with a Golden Gate horizontal attenuated total reflectance (ATR) accessory. Experimental conditions were 32 scans, 4 cm^{-1} resolution and aperture open.

2.5. Analytical methods

Proteins, humic acids, carbohydrates, colour number (CN) and chemical oxygen demand (COD) were measured by colorimetric methods. Proteins and humic acids were measured following the modified Lowry method described by Frølund et al. [39], using bovine serum albumin and commercial humic acid as standards. Carbohydrates were measured according to the Dubois method [40] using D-glucose as standard. Spectral absorbance coefficients (SAC [cm^{-1}]) were measured at 436, 525 and 620 nm and used to calculate the CN value (cm^{-1}) according to Eq. 6:

$$CN = \frac{SAC_{436}^2+SAC_{525}^2+SAC_{620}^2}{SAC_{436}+SAC_{525}+SAC_{620}} \qquad (6)$$

The absorbances of proteins, humic acids, carbohydrates and SAC were measured with a Helios Alpha UV-Vis spectrophotometer (Thermo Scientific, USA).

Density was measured at 50 ºC and 1 atm with a pycnometer. Kinematic viscosity was measured at 50 ºC and 1 atm with a Cannon-Fenske inversed-flow viscometer (Proton, UK). Dynamic viscosity was calculated by multiplying the kinematic viscosity by the density. pH was measured with a Basic 20 pH meter (Crison, Spain). COD values were determined by the potassium dichromate method [41], and the absorbance at 600 nm was measured with a HACH DR/2500 spectrophotometer (Hach Company, USA). Total organic carbon (TOC) was determined with a Shimadzu TOC-V_{CSH} TOC analyser (Shimadzu, Japan).

Rejection coefficients (RC_i) were calculated according to the Eq. 7:

$$RC_i=1-\frac{C_{P_m,i}}{C_{R_t,i}} \qquad (7)$$

Where $C_{P_m,i}$ and $C_{R_t,i}$ the concentration of the compound “i” in the permeate and the retentate ($g \cdot L^{-1}$), respectively. All analytical measurements were conducted at least three times.

3. Results and discussion

3.1. Oxidised waste activated sludge

The oxidised WAS was slightly acid and presented a deep brown colour. Its main physical-chemical characteristics are shown in Table 4.10.

Table 4.10. Main physical-chemical characteristics of the oxidised waste activated sludge.

Parameter	*Value*
pH	5.04 ± 0.03
COD* (g O_2 L^{-1})	20.5 ± 0.5
TOC* (g L^{-1})	8.00 ± 0.01
CN* (cm^{-1})	3.9 ± 0.2
Proteins (g L^{-1})	3.4 ± 0.3
Humic acids (g L^{-1})	8.4 ± 0.2
Carbohydrates (g L^{-1})	2.75 ± 0.03

*COD: chemical oxygen demand; TOC: total organic carbon; CN: colour number.

3.2. Membrane material screening

3.2.1. Contact angle measurements

Measured contact angles of water on the polymeric membranes used in the ultrafiltration of the oxidised WAS are shown in Table 4.11. A selection of the pictures of the sessile drops, from which the contact angles were calculated, can be found in Fig. A.4.1.

Table 4.11. Water surface contact angles on the studied membranes.

Membrane size	*Membrane material*	*Membrane state*	*Contact angle*
50 kDa	**PES**	**Clean**	90 ± 3
		Fouled	70 ± 2
	PESH	**Clean**	72 ± 1
		Fouled	54 ± 11
	PAN	**Clean**	39 ± 4
		Fouled	57 ± 10

A surface is considered hydrophilic if the contact angle is lower than 90º [42]. Thus, PES50 could be considered hydrophobic, while PESH50 and PAN50 were found to be hydrophilic. This was in accordance with the results obtained by other authors related to fouling resistance of ultrafiltration membranes [43]. After filtering the oxidised WAS, the fouled PES50 and PESH50 turned more hydrophilic than the pristine ones, while PAN50 became less hydrophilic after being fouled, which showed the different nature of the foulant-membrane interactions depending on the membrane material: it seems that PES50 and PESH50 were coated with more hydrophilic foulants, while PAN50 interacted with foulants less hydrophilic than itself.

3.2.2. Permeability tests

The fluxes obtained with PES50, PESH50 and PAN50 are shown in Fig. 4.9.

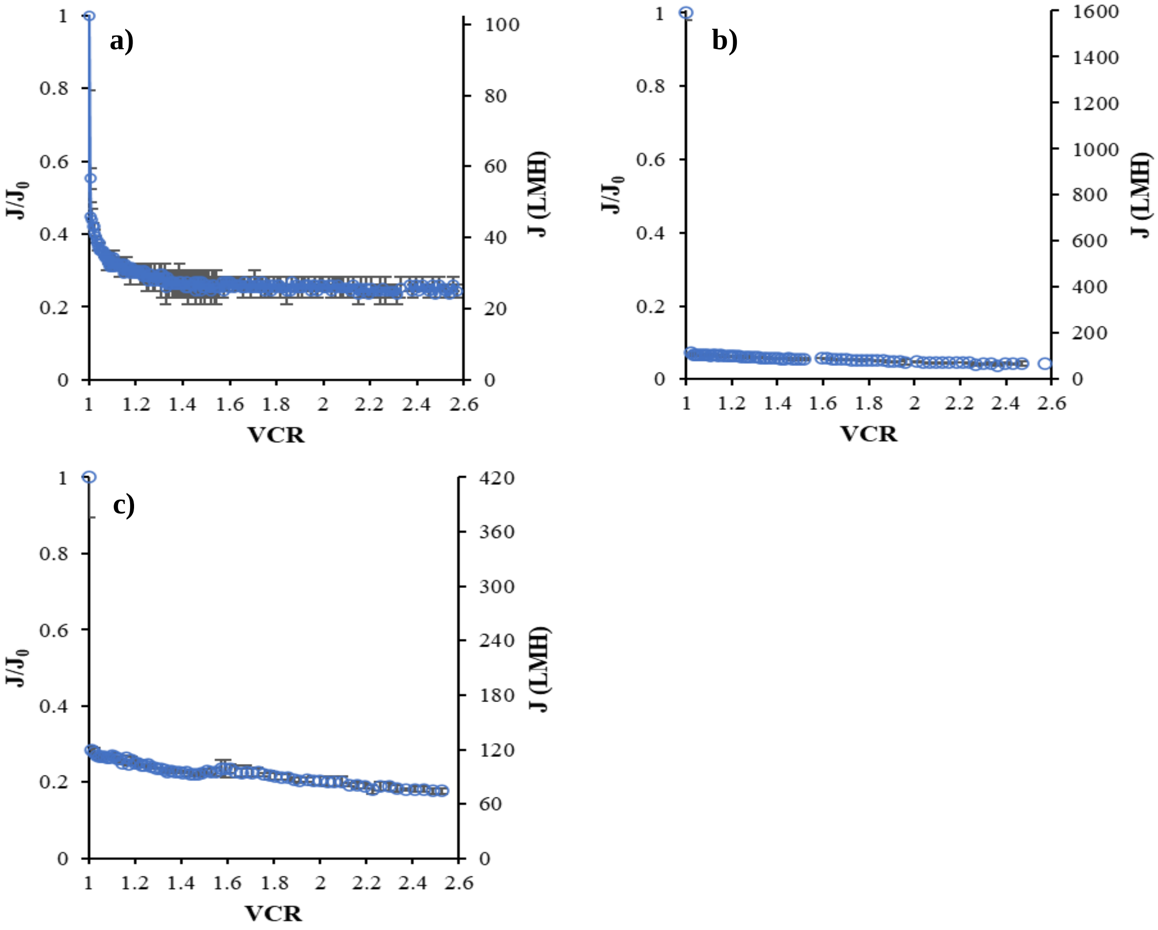

Figure 4.9. Normalised flux variation over VCR for the oxidised WAS filtration with (a) PES50 (J_0=102.4 ± 0.2 L/m^{2}h), (b) PESH50 (J_0=1590 ± 40 L/m^{2}h) and (c) PAN50 (J_0=420 ± 40 L/m^{2}h).

Final fluxes approximately 3 times higher were obtained with PESH50 (67.2 ± 0.9 LMH) and PAN50 (74 ± 3 LMH) compared to the one achieved by PES50 (25 ± 2 LMH), due to their hydrophilic character. In this sense, membrane hydrophilicity prevented fouling, in accordance to what was reported by other authors [44,45]. The resistance-in-series models (Fig. 4.10) confirmed the aforementioned about hydrophobicity and its higher tendency to fouling. In this sense, all the resistances (membrane, reversible and irreversible) measured for PES50, which added up a total hydraulic resistance of $1.07 \cdot 10^{14}$ m^{-1}, were higher than those of PESH50 (13.3, 2.5 and 1.1 times higher, respectively) and PAN50 (3.4, 2.4 and 6.3 times higher, respectively). On the other hand, the different behaviour between fluxes in PESH50 and PAN50 can be explained based on the values of irreversible fouling for each membrane. Thus, the resistance-in-series modelling showed that the higher tendency to fouling observed in PESH50 is due to irreversible fouling, since its R_{irrev} accounted for the 49.6% of its total hydraulic resistance, while R_{irrev} observed in PAN50 only represented 12.4% of the total hydraulic resistance. The total R_{irrev} also seemed to be correlated with the hydrophobicity of the membrane, as PES50 showed the highest R_{irrev} ($[2.8 \pm 0.4] \cdot 10^{13}$ m^{-1}), followed by PESH50 ($[2.45 \pm 0.01] \cdot 10^{13}$ m^{-1}) and PAN50 ($[4.3 \pm 0.6] \cdot 10^{12}$ m^{-1}).

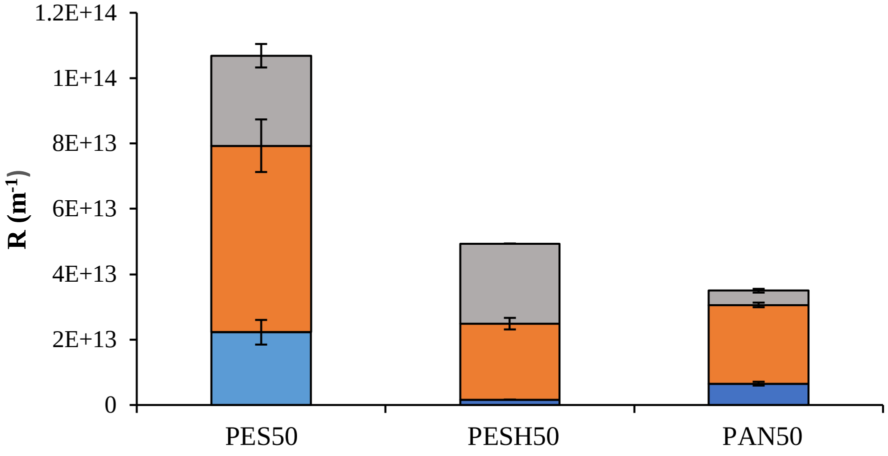

Figure 4.10. R_m (🟦), R_{rev} (🟧) and R_{irrev} (⬜) after filtration with PES50, PESH50 and PAN50.

Besides, reversible fouling was found to be the main fouling in PES50 and PAN50 membranes, corresponding to a 53.4% and to a 68.9% of the total fouling for PES50 and PAN50, respectively.

The fluxes obtained in this study were in the same order of magnitude than those obtained by other authors when PES membranes were used during the filtration of milk [46], refinery and petrochemical wastewater [47] and oil-in-water emulsion [48,49]; and with PAN membranes when tap water [50] and oil-in-water emulsion [49] were filtered. Besides, lower initial fluxes were obtained when PESH membranes were employed for the filtration of molasses [51], while similar fluxes were attained for olive oil washing wastewater [52].

It should be noted that the higher fluxes obtained with PESH50 and PAN50 come along with lower rejection coefficients and lower selectivities between proteins and humic acids (Table 4.12). In particular, the lowest rejection coefficients for CN, TOC, and the three measured biocompounds were those corresponding to PESH50. On the other hand, the highest rejections were obtained with PES50, also achieving the highest rejection differences between proteins and humic acids (22% difference vs 7% difference obtained with PAN50, and 10% difference obtained with PESH50); and between carbohydrates and humic acids (23% difference vs 13% obtained with PAN50 and 17% difference obtained with PESH50).

Table 4.12. Rejection coefficients (RC) obtained with the 50 kDa polymeric membranes.

	PES50*	**PESH50***	**PAN50***
RC_{CN*}	0.80 ± 0.02	0.69 ± 0.03	0.73 ± 0.04
RC_{TOC*}	0.47 ± 0.03	0.34 ± 0.04	0.38 ± 0.05
RC_{COD*}	0.48 ± 0.08	0.41 ± 0.03	0.4 ± 0.1
RC_{CH*}	0.70 ± 0.02	0.57 ± 0.07	0.60 ± 0.06
RC_{PROT*}	0.69 ± 0.06	0.50 ± 0.05	0.54 ± 0.09
RC_{HA*}	0.47 ± 0.04	0.40 ± 0.03	0.47 ± 0.03

*CN: colour number; TOC: total organic carbon; COD: chemical oxygen demand; CH: carbohydrates; PROT: proteins; HA: humic acids; PES50: polyethersulphone, 50 kDa; PESH50: permanently hydrophilic polyethersulphone, 50 kDa; PAN: polyacrylonitrile, 50 kDa.

These higher retentions may be due to the formation of a thicker cake layer on top of the membrane, which would act as a secondary filtration mesh, increasing the selectivity of the membrane [53]. The formation of this thicker fouling cake could be observed through the resistance-in-series model (Fig. 4.10), where the R_{rev}, mainly associated with the formation of the fouling cake [54], was more than two-fold higher after filtering with PES50 ($[5.7 \pm 0.8] \cdot 10^{13}$ m^{-1}) than with PESH50 ($[2.3 \pm 0.2] \cdot 10^{13}$ m^{-1}) or PAN50 ($[2.41 \pm 0.07] \cdot 10^{13}$ m^{-1}). Rejection differences between PESH50 and PAN50 are coherent with this explanation, as the R_{rev} of PESH50 is slightly lower than that of PAN50.

As both higher rejection coefficients and higher rejection differences between humic acids and the other biomolecules (proteins and carbohydrates) were achieved with PES50, the fractionation tests with membranes of different MWCO (MWCO screening experiments) was carried out with PES membranes.

3.2.3. Flux modelling

As it can be seen in Fig. 4.11 and Table 4.13 (SSR), CF was the best-fitting Hermia’s model in all three cases, although the fittings indicated that none of the Hermia’s models fully explain the fouling mechanism, thus indicating several fouling mechanisms may have occurred throughout the filtration. Indeed, the fact that different fouling mechanisms occur at different stages of the filtration is well documented in the literature [55,56] and it was taken into account by Mehta’s model [34]. Thus, CF was the main fouling mechanism overall, although irreversible pore blocking also occurred; especially during the filtration with PESH50, where the IPB model showed better fitting than in the filtrations with PES50 and PAN50, reflecting the above-mentioned more irreversible nature of the PESH50 fouling. Besides, CF has also been described by other authors as the main fouling mechanism of natural organic matter during ultrafiltration with PES membranes [57,58].

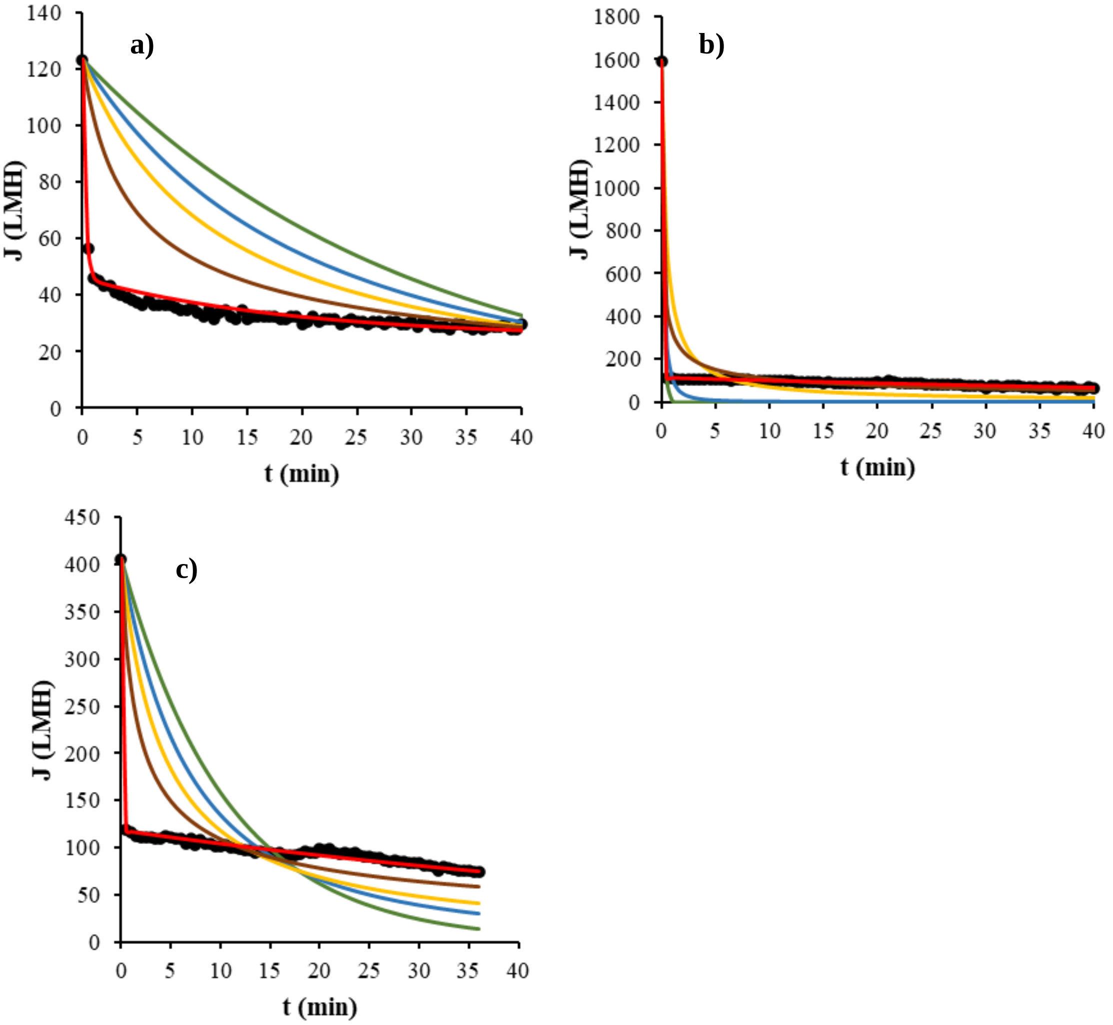

Figure 4.11. Hermia's (complete pore blocking [—], intermediate pore blocking [—], partial pore blocking [—] and cake formation [—]) and Mehta's (—) flux models for PES50 (a), PESH50 (b) and PAN50 (c) experimental fluxes (●).

However, it should be noted that the best fitting of the experimental data was achieved with Mehta's model, which provides information about the effect of membrane fouling (parameter α) and concentration polarization and gel layer formation (parameter β) on the flux decline. The optimised values for these two constants are shown in Table 4.13. Higher α and β values represent faster initial membrane fouling and faster stabilisation of the flux by the establishment of the concentration polarization gradient and gel layer formation, respectively. The α values obtained for the filtrations with PESH50 and PAN50 were 10-fold higher than those of PES50

(3.88), while the β values were 4-fold lower than those obtained for PES50 ($5.20 \cdot 10^{-2}$). This indicates that a strong initial membrane fouling occurred after starting the filtration of the oxidised WAS with PESH50 and PAN50, causing a rapid decrease in the flux. After this initial drop, the stabilisation of the flux by concentration polarization occurred more slowly. Regarding the behaviour during the filtration with PES50, it was opposite to that of the other polymeric membranes: the initial drop caused by membrane fouling was less drastic, and the equilibrium in concentration polarization was reached faster.

This result is in accordance with the literature, and can be explained considering the polarization sieving model [59], based on the differences of hydrophilicity between the membranes:

Thus, in hydrophilic membranes, an initial irreversible adsorption layer is formed, regardless of the solute concentration, and subsequent fouling will appear in the form of a gel-polarization layer. On the other hand, in hydrophobic membranes, the size of the irreversible adsorption layer increases until its thickness protects the hydrophobic surface from the adsorbed molecules, which generates higher values of irreversible fouling than in hydrophilic surfaces, and only after this limit is reached, the gel-polarization layer starts to form [59]. According to this, the behaviour of PES50 can be explained by its hydrophobic character, since more time was required for the initial membrane fouling to be fully occur, and the final concentration polarization layer needed less time to stabilise, thus starting to form at higher feed concentrations.

Table 4.13. Fitting parameters for the adjusted models.

		PES50	**PESH50**	**PAN50**
Hermia's models				
CPB	**K_b (min^{-1})**	$3.31 \cdot 10^{-2}$	5.29	$9.43 \cdot 10^{-2}$
	SSR	172041.83	617253.55	628747.63
IPB	**K_i (m^{-1})**	$4.58 \cdot 10^{-3}$	$1.37 \cdot 10^{-1}$	$7.31 \cdot 10^{-3}$
	SSR	116241.52	590551.29	431129.86
PPB	**K_p (m^{-1})**	$6.54 \cdot 10^{-4}$	$1.40 \cdot 10^{-3}$	$5.97 \cdot 10^{-4}$
	SSR	77545.23	852391.39	286513.46
CF	**K_c (min·m^{-2})**	$1.45 \cdot 10^{-5}$	$4.42 \cdot 10^{-6}$	$3.86 \cdot 10^{-6}$
	SSR	32776.51	255336.20	129005.00
Mehta's model				
$J_{\infty 1}$ (LMH)		46.05	114.16	116.08
α (min^{-1})		3.88	30.70	30.70
β (min^{-1})		$5.20 \cdot 10^{-2}$	$1.33 \cdot 10^{-2}$	$1.26 \cdot 10^{-2}$
SSR		700.38	1401.89	783.73

3.2.4. Atomic force microscopy

AFM images were taken from clean and fouled membranes in order to analyse the surface morphology (Fig. 4.12). The vertical profile of the membrane surface was represented by the colour intensity, with lighter colours indicating higher regions, and darker colours indicating depressions.

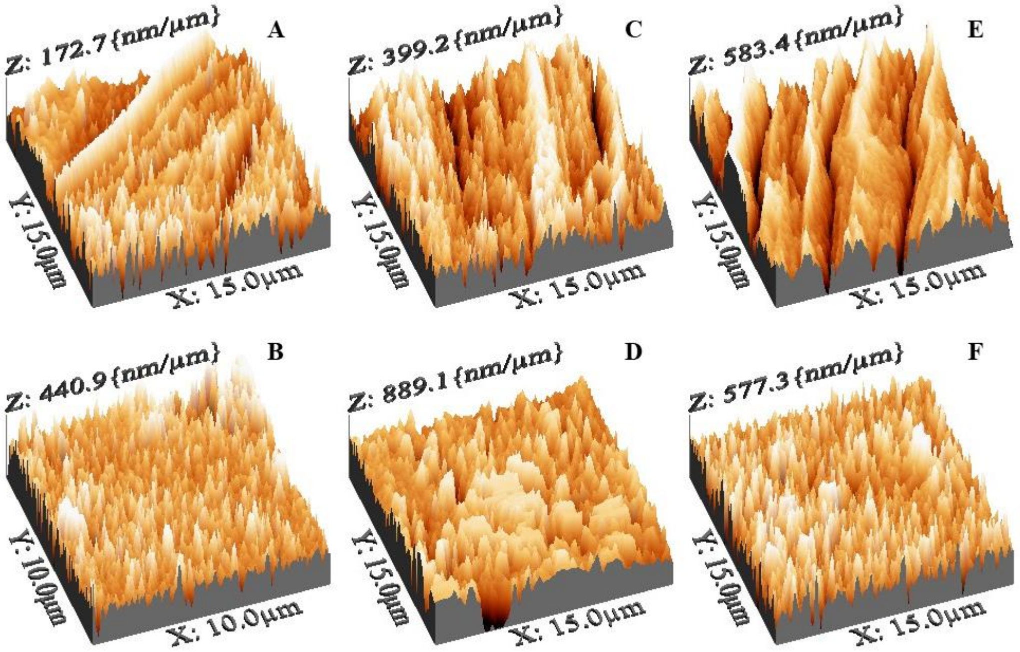

Figure 4.12. AFM images of clean and fouled PES50 (A and B), PESH50 (C and D) and PAN50 (E and F) for membrane surface morphology analysis.

The surface of all the three clean membranes was clearly arranged in a “crest and valley” or “nodule and valley” pattern, originated by the random orientation and overlapping of the fibre structure [60]. This surface arrangement has also been observed by other authors when PES, PAN and polyamide membranes with flat-sheet, tubular and hollow-fibre geometries were used in ultrafiltration and nanofiltration processes [60–63]. The presence of valley-like formations is highly related to fouling, as foulant particles tend to deposit in these formations [64]. This fact was supported by the images of fouled membranes, where crest-like formations could no longer be seen, indicating that the valley-like regions had been clogged by foulants.

In addition to AFM imaging, membrane roughness was compared in terms of mean roughness (R_a [nm/µm]), root mean square roughness (rms), peak-to-peak distance (nm/µm), and surface skewness and kurtosis in order to analyse its relationship with fouling (Table 4.14).

Table 4.14. Membrane surface roughness parameters.

	Clean			*Fouled*		
	PES50	**PESH50**	**PAN50**	**PES50**	**PESH50**	**PAN50**
R_a [nm/µm]	23.0±0.6	74±5	67±8	56±15	164±37	92±6
rms	30.4±0.9	94±7	89±5	41±12	212±47	119±7
Peak-to-peak distance [nm/µm]	142±5	391±32	365±16	255±59	918±208	487±26
Skewness	-0.23±0.04	-	-0.08±0.03	-	-	-0.05±0.03
Kurtosis	3.35±0.03	2.72±0.05	2.8±0.3	3.4±0.4	2.89±0.01	2.7±0.1

The loss of normalised flux was inversely related to R_a and rms values. In this sense, PES50, whose normalised flux decreased the least (77%) during the ultrafiltration of the oxidised WAS, also showed the lowest R_a, rms and peak-to-peak distance values. Furthermore, the highest values were obtained with PESH50, which lost the highest proportion of normalised flux (96%). The difference between normalised fluxes of PES50 and PAN50 was less marked than the roughness values may suggest, which could be explained based on their different hydrophilic properties (fouling allegedly increases with hydrophobicity [61]). The relationship between loss of normalised flux and R_a and rms values is in accordance with the existing literature, indicating that surface roughness plays a key role in flux loss [61,64–66]. As it was previously commented, in the initial stages of filtration, the particles tend to deposit in the “valley-like” formations of the membranes, clogging these depressed regions. Membranes with lower surface roughness present fewer "valley-like" formations on their surface, so the attachment of solute molecules is restricted [64]. The effect of this fewer presence of valley-like regions can be attended contrasting the roughness values from Table 4.14 with the images in Fig. 4:12. Valley formations were more evident in PAN50 and PESH50 than in PES50, and the depth of the valleys was lower in the latter membrane, as it can be confirmed by the peak-to-peak distance.

As proved by the permeability tests and the AFM measurements, flux loss is a complex phenomenon, which depends on several factors, among which, the nature of the membrane surface (hydrophilic surfaces prevent fouling) and its rugosity (the higher the rugosity, the more space the solute molecules have for depositing) can be considered determinant.

3.3. Membrane molecular weight cut-off screening

3.3.1. Permeability tests

As PES was selected as the most suitable material for WAS fractioning (section 3.2.2), the MWCO screening experiments were carried out with membranes made of this polymeric material (PES10 and PES3). The flux obtained with PES3 was extremely low (around 0.5 LMH on average), making this filtration unfeasible, and thus no data from this experiment are depicted. The fluxes obtained with PES10, PES50-10 and PES50-3 are shown in Fig. 4.13.

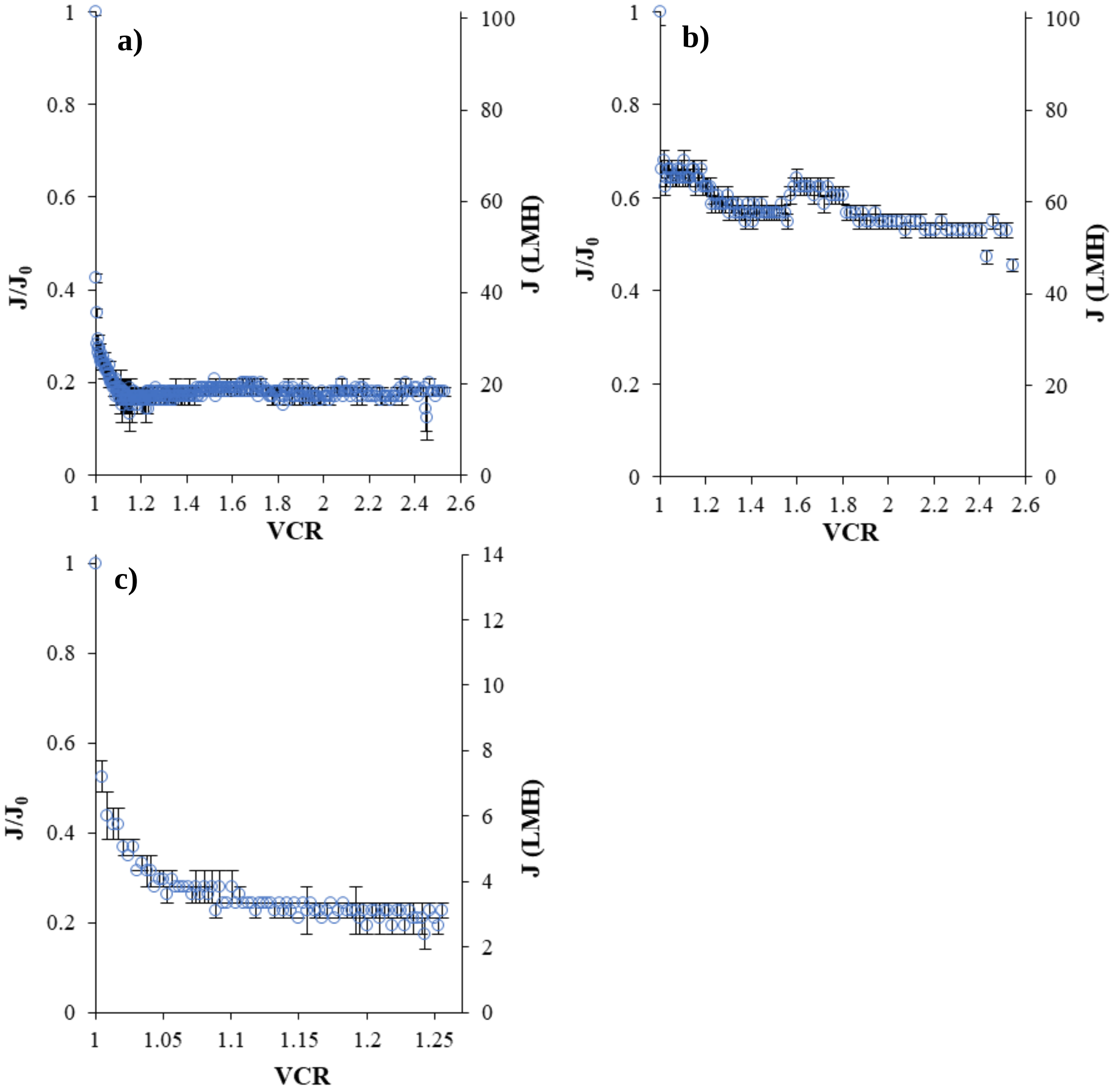

Figure 4.13. Flux variation over VCR for the oxidised WAS filtration with PES10 (a) (J_0=101.5 ± 0.9 L/m^{2}h), PES50-10 (b) (J_0=102 ± 3 L/m^{2}h) and PES50-3 (c) (J_0=13.72 ± 0.01 L/m^{2}h).

The highest flux obtained during the MWCO screening was achieved with PES50-10. However, the low rejection coefficients observed made this option unfeasible (Table 4.15). The highest rejections in terms of CN, TOC and COD were achieved with PES50-3. Nevertheless, in the case of the biomolecules, slightly differences were observed in rejections and rejection differences between PES10 and PES50-3.

Table 4.15. Rejection coefficients obtained with PES10, PES50-10 and PES50-3.

	PES10	**PES50-10**	**PES50-3**
RC_{CN}	0.90 ± 0.01	0.35 ± 0.01	0.9942 ± 0.0009
RC_{TOC}	0.70 ± 0.16	0.17 ± 0.09	0.88 ± 0.01
RC_{COD}	0.60 ± 0.04	0.09 ± 0.04	0.66 ± 0.04
RC_{CH*}	0.79 ± 0.05	0.14 ± 0.05	0.83 ± 0.05
RC_{PROT*}	0.84 ± 0.09	0.21 ± 0.08	0.87 ± 0.06
RC_{HA*}	0.63 ± 0.05	0.15 ± 0.06	0.67 ± 0.06

*CH: carbohydrates; PROT: proteins; HA: humic acids.

Based on the rejection coefficients and the observed decrease in flux during the ultrafiltration of the oxidised WAS using PES10, as well as the permeates obtained from PES50 with PES10 and PES3, it can be concluded that the majority of molecules retained by the PES10 membrane can also be retained by the PES50 membrane. Therefore, coupling these two membranes would be redundant and unnecessary. This behaviour was in accordance with the work by Urrea et al. [67], where the effect of WO on the different molecular weight fractions of WAS was studied. They reported that, after a WO treatment at 190 ºC and 90 min, the molecular weight of the majority of the present molecules was comprised in the ranges between 0-35 kDa (referred by Urrea et al. as low molecular weight molecules) and 35-150 kDa (medium molecular weight molecules). Moreover, hydrophobic molecules were also present due to the interactions with size-exclusion column. According to the results attained in this study, the sizes of the majority of the low molecular weight molecules were comprised between 0-10 kDa, and the ones of the medium molecular weight molecules were above 50 kDa.

The resistance-in-series model (Fig. 4.14) showed that approximately half of the membrane fouling during the filtration with both PES10 and PES50-3 was irreversible, which contrast to the results obtained with PES50, where only 33% of the fouling resistance was attributable to irreversible fouling. Moreover, a comparison between the values of the R_{rev} and the R_{irrev}

obtained when filtering with PES50 and PES10 shows that no significant differences could be found between the values of reversible fouling, whereas the irreversible one of the PES10 membrane was around 2.5 times higher than that of the PES50 membrane. Thus, the additional flux decay observed between the filtration with PES10 and PES50 was exclusively due to an increase in irreversible fouling. It has been reported that irreversible fouling during the filtration of natural organic matter is primarily caused by the hydrophilic fraction of this organic matter [68–70]. Therefore, the additional irreversible fouling observed in this study is likely attributed to hydrophilic substances, presumably oxidised HA, since their rejection coefficients were lower than those of the other biomolecules, which suggests a lower average size. In this sense, several authors have reported that the oxidation of HA increased their hydrophilicity [71–74] by oxidizing benzene groups into different aldehydes and carboxylic acids [72,74]. After a subsequent reduction of the membrane MWCO to 3 kDa, the fouling profile remained similar (slightly more irreversible than reversible fouling), proving that the molecules retained by the PES50 membrane mainly caused reversible fouling. In this sense, Taniguchi et al. [57] compared the fouling of PES membranes with MWCOs from 10 to 1000 kDa during the UF of natural organic matter, and reported that membranes with lower MWCO (10 and 30 kDa) showed higher irreversible fouling, although fouling was mostly reversible in all cases.

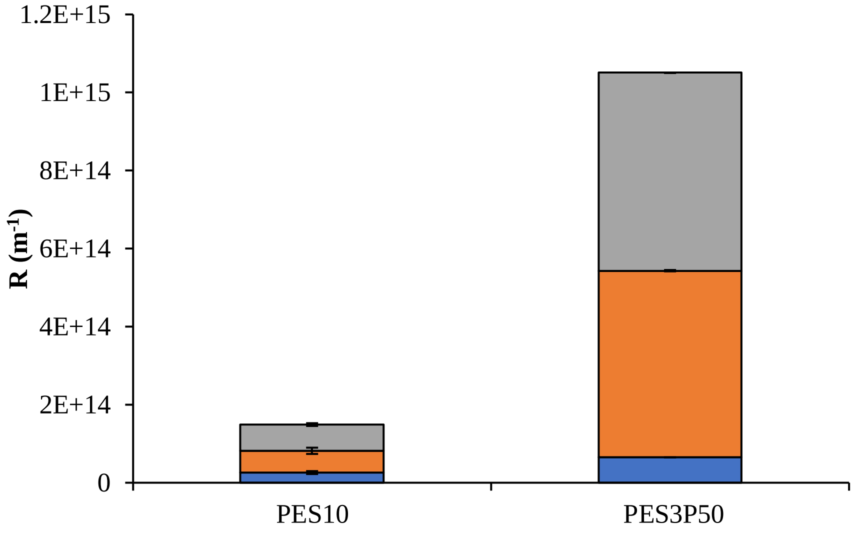

Figure 4.14. R_m (🟦), R_{rev} (🟧) and R_{irrev} (⬜) after filtration with PES10 and PES50-3 membranes.

3.3.2. Fouling modelling

The fitting of the studied fouling models to the experimental data corresponding to the filtrations with PES10, PES50-10 and PES50-3 is shown in Fig. 4.15.

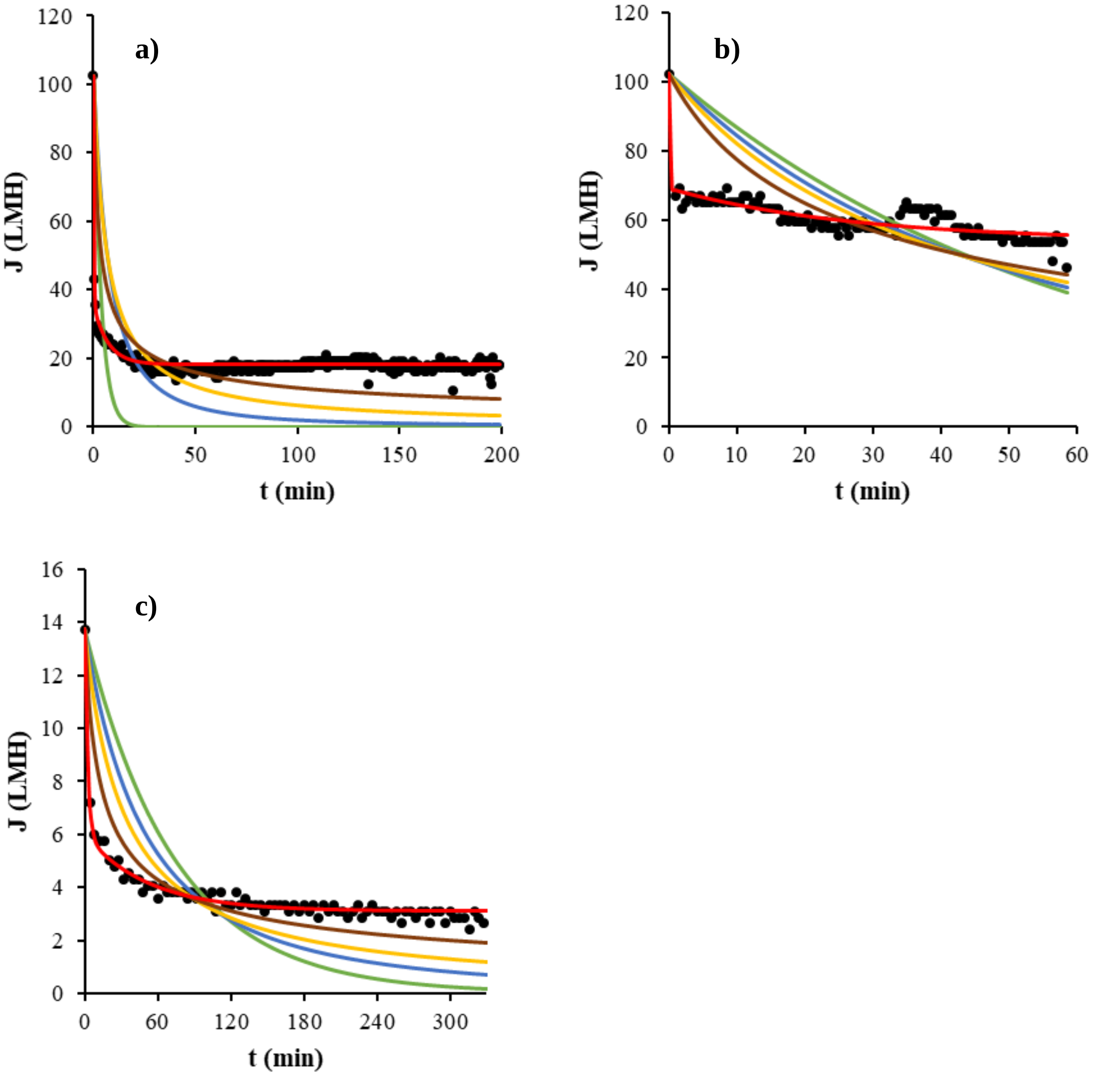

Figure 4.15. Hermia's (complete pore blocking [—], intermediate pore blocking [—], partial pore blocking [—] and cake formation [—]) and Mehta's (—) flux models for PES10 (a), PES50-10 (b) and PES50-3 (c) experimental fluxes (●).

Similarly to the filtration with the 50 kDa membranes, the best fitting Hermia's model was CF in the three filtrations. This results were in accordance to those reported by Peeva et al. [75] related to the ultrafiltration of humic acid solutions with PES membranes. However, as it was discussed in the previous section, the fitting showed that this model alone could not adequately explain the observed fouling tendency. In this case, the ultrafiltration of both the oxidised WAS with PES10 and the permeates obtained from PES50 with PES10 and PES3 suffered a proportionately higher irreversible fouling compared with the ultrafiltration of oxidised WAS with the PES50 membrane, which in all cases could be mainly attributed to PPB, as it was the second-best fitting Hermia's model (Table 4.16). The fact that PPB remained the main irreversible fouling mechanism in membranes with lower MWCO is in accordance with the literature. Thus, it has been reported that, when filtering humic acids with PES membranes, a bigger pore size implied a greater fouling tendency towards pore narrowing instead of pore blocking [75]. This may indicate that the modification of the PES membrane to convert it into PESH enlarged its pores, which led to pore narrowing due to internal pore blocking as the major cause of its irreversible fouling.

Mehta's model fitted the data of the three filtrations perfectly. The high α value obtained for PES50-10 (Table 4.16) highlights the drastic initial membrane fouling. This may have occurred due to a fast pore clogging caused by the removal of molecules of higher molecular weight. These molecules, bigger than the pores, would have partially obstructed the access to the pores, thus starting to form the cake layer. Without the presence of the molecules higher than 50 kDa to favour the formation of this second barrier, smaller molecules would have entered the pores with much more ease at the beginning of the operation, clogging the pores in a faster way. This theory is supported by the fact that the β value obtained for PES50-10 was almost an order of magnitude smaller than that obtained for PES10, which indicates that the concentration polarization gradient and gel layer formation took more time to stabilise.

Table 4.16. Fitting parameters for the adjusted models.

		PES10	**PES50-10**	**PES50-3**
Hermia's models				
CPB	**K_b (min^{-1})**	$2.68\cdot10^{-1}$	$1.65\cdot10^{-2}$	$1.36\cdot10^{-2}$
	SSR	129413.22	37272.70	596.61
IPB	**K_i (m^{-1})**	$1.26\cdot10^{-2}$	$1.99\cdot10^{-3}$	$5.52\cdot10^{-3}$
	SSR	108753.21	33256.49	372.75
PPB	**K_p (m^{-1})**	$1.51\cdot10^{-3}$	$2.41\cdot10^{-4}$	$2.32\cdot10^{-3}$
	SSR	73673.60	29768.57	227.88
CF	**K_c (min·m^{-2})**	$3.92\cdot10^{-5}$	$3.54\cdot10^{-6}$	$4.12\cdot10^{-4}$
	SSR	30830.14	24176.71	78.10
Mehta's model				
	$J_{\infty 1}$ (LMH)	35.50	69.07	6.00
	α (min^{-1})	4.03	36.27	$4.09\cdot10^{-1}$
	β (min^{-1})	$1.40\cdot10^{-1}$	$3.69\cdot10^{-2}$	$1.92\cdot10^{-2}$
	SSR	701.32	5599.28	3.95

3.4. Infrared spectroscopy

In order to better understand the nature of the membrane materials used, as well as the interactions between the WAS and membranes of different materials and MWCOs, FTIR measurements were conducted on both the clean and fouled membranes.

All PES membranes and the PESH membrane exhibited the same FTIR profile (Figs. 4.16, A.4.2 & A.4.3), characterized by small bands at 3096 and 3068 cm^{-1}, corresponding to aromatic CH vibration; a small band at around 2964 cm^{-1}, caused by γ_a CH_3 asymmetric aliphatic stretching; two aromatic peaks at 1576 and 1484 cm^{-1} [76]; and peaks at 1409, 1296 and 1147 cm^{-1} indicating the presence of -S=O residues corresponding to the polysulfone material [77,78]. The band appearing at 1666 cm^{-1} could possibly be attributed to the presence of a preservative agent in the membrane [76].

The clean PAN membrane exhibited peaks at 2935 cm^{-1}, corresponding to alkane stretching, and at 2242 cm^{-1}, resulting from C≡N stretching. Additionally, it showed peaks in the 1500-1000 cm^{-1} region, indicative of alkanes. Furthermore, peaks at 1735 and 1661 cm^{-1} (Fig. A.4.3) may be attributed to the C=C stretching of residual acrylonitrile monomers present in the membrane [78].

After filtration, a peak appeared in the fouled PES membranes at 1735-1712 cm^{-1} (Figs. 4.16 & A.4.2), which is associated with C=O bonds [77,79]. The stretching at 1735 cm^{-1} corresponds to an aldehyde (which may originate from the alcohols present in carbohydrates, proteins and humic acids), while the peak at 1714 cm^{-1} to carboxylic acids (which are part of proteins, humic acids and fatty acids generated during the oxidation of organic matter [80]). Additionally, the spectra of all the fouled PES membranes showed a band at 1373 cm^{-1}, corresponding to phenolic -OH groups [81], which are highly prevalent in humic substances [82]. These two signals were relatively weak in the PES50-10 spectrum, indicating lighter fouling of the membrane due to low retentions.

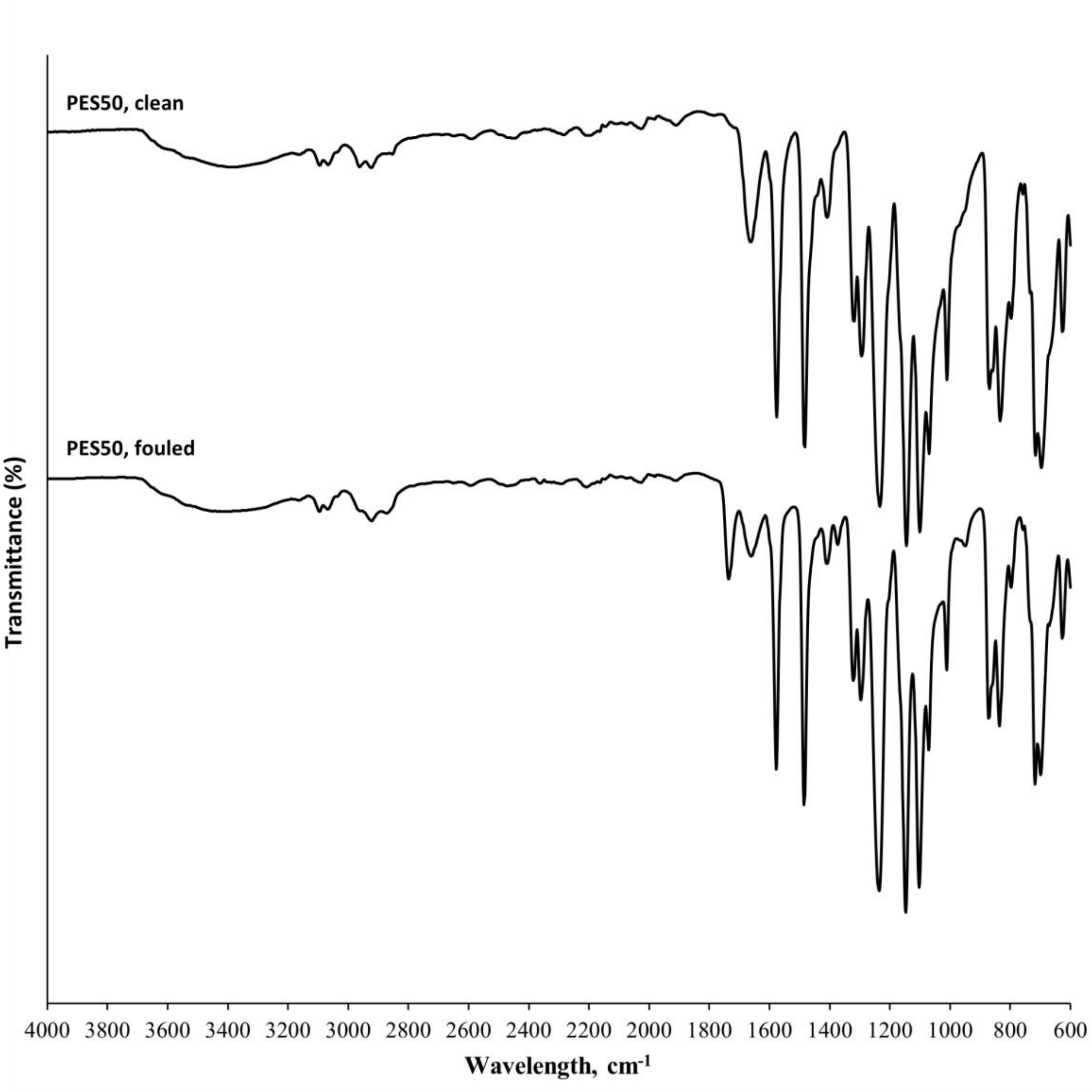

Figure 4.16. FTIR spectra of PES50 membranes from 600 to 4000 cm^{-1}.

In addition to this, a band at 950 cm^{-1}, caused by alkene flexing, appeared only in the PES-based membranes that directly filtered the WAS (PES50, PESH50 and PES10), but not in the membranes that filtered WAS permeate (PES 50-10 and PES 50-3). This indicates that the molecule containing alkenes that interacted with the membrane surface was totally retained by the PES50 membrane.

PES50-3 exhibited the highest level of surface interactions after filtering, which is consistent with its predominant irreversible fouling. The aromatic bands at 3095 and 3068 cm^{-1} completely disappeared, while the aromatic peaks at 1578 and 1486 cm^{-1} nearly vanished. Similarly, the peaks at 1296, 1147 and 1071 cm^{-1}, corresponding to the sulfone group of the membrane, were significantly diminished. Furthermore, peaks associated to C-H bonds (at 830, 699 and 626 cm^{-1}) were no longer observable. This indicates that chemical (irreversible) interactions occurred between the foulants and both the aril and sulfone groups of the membrane.

The protein surface interaction with PESH50 membrane was confirmed by the presence of a peak at 1651 cm^{-1}, corresponding to Amine I [78], and a poorly resolved shoulder at 1550 cm^{-1} attributed to Amide II [76]. There is also a potential Amide I peak at 1640 cm^{-1} [75] that overlaps with the Amine I peak. [76].

The spectrum of the PAN membrane showed only minor changes after filtering the WAS, indicating that most of its fouling was reversible. However, there were noticeable increases in the intensity of certain peaks after filtration. Thus, the peak at 1661 cm^{-1}, as well as the peaks at 1040 and 1069 cm^{-1} showed an increased intensity, which are often correlated with carbohydrates [83]. Some bands corresponding to C-H bonds disappeared, indicating that foulant-membrane interactions occurred primarily in the alkane section of the polymer rather than the nitrile radical.

3.5. Proposal of an integrated membrane process for biomolecule fractioning

The results here obtained were used as a basis to propose an integrated membrane process to recover valuable biocompounds from WAS in order to valorise it in the context of circular economy. This process is based on size fractioning of oxidised WAS, thus obtaining two purified streams, one containing carbohydrates and proteins and the other one containing humic acids (Fig. 4.17).

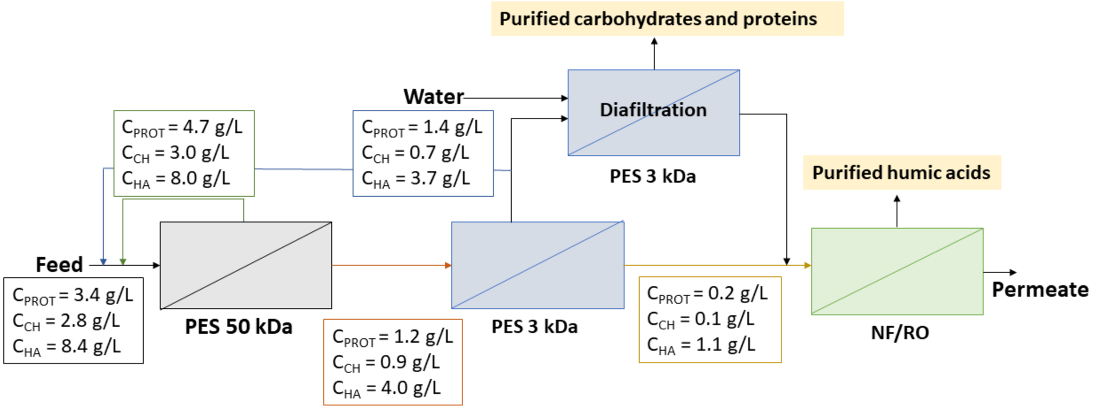

Figure 4.17. Size fractioning results and proposal for carbohydrates (CH) and proteins (P), and humic acids (HA) purification.

PES membranes were found to be the suitable material for the ultrafiltration steps of the oxidised WAS due to their higher rejection coefficients and higher rejection differences between humic acids and the other biomolecules (proteins and carbohydrates). In this sense, a prefiltration with PES50 would be needed prior to the filtration with PES3 to prevent excessive fouling and the retentate of this prefiltration would be recirculated to the feed in order to keep the target biomolecules within the process. Then, the permeate of the PES50 prefiltration would be filtered with PES3. The concentration of the biomolecules at each ultrafiltration step was determined based on the rejection coefficients obtained in this study. Afterwards, a diafiltration step of the retentate of PES3 filtration would take place. The high rejection coefficients of proteins and carbohydrates (nearly 1), and the significant difference with the rejection coefficient of humic acid would allow a concentration and purification of carbohydrates and proteins thanks to this diafiltration, while humic acid would be washed in the permeate. Proteins and carbohydrates could then be separated by a chromatographic technique, such as expanded bed chromatography with an ion exchange resin [84] or immobilised metal affinity chromatography [85]. The permeate of PES3 filtrations, mainly consisting of a humic acid solution, could be concentrated by nanofiltration or reverse osmosis to obtain humic fertilizer, as reported by Li et al. [27,28,86]. It is important to note that the high proportion of irreversible fouling observed during the filtration with the PES3 membrane (51.5% of total fouling) would pose challenges to the viability of the process. Therefore, future studies should focus on optimizing the filtration conditions, such as investigation the critical flux [87] or employing techniques like backwashing, air scouring [88], membrane patterning [87], and surface coating [89], among others.

4. Conclusions

The screening tests of membrane material showed that PES was found to be the best material for the fractionation of humic acids and proteins from oxidised WAS, since higher rejection coefficients and differences between these biomolecules were achieved after filtering with PES50, although lower fluxes were obtained compared to PESH50 and PAN50 membranes. In particular, the rejection coefficients attained with the PES50 membrane were 0.70 ± 0.02 for carbohydrates, 0.69 ± 0.06 for proteins and 0.47 ± 0.04 for humic acids (with a difference of 23% and 22% comparing carbohydrates and proteins selectivities with humic acids, respectively).

The main fouling mechanism can be considered CF in all cases, but with an important irreversible component in PES50 and especially in PESH50, as shown by the resistance-in-series model. Thanks to AFM imaging, the key role of the arrangement of the surface of the membranes and their mean roughness in flux loss was proven in all cases. The screening tests of membrane MWCO showed that both the 50 kDa and 10 kDa PES membranes exhibited high biomolecule retentions, reaching rates of up to 84%. However, when the permeate from the PES50 filtration was subsequently filtered using the PES10 membrane, lower retentions (up to 21%) were observed. Therefore, in order to fractionate the oxidised WAS, the use of PES50 and PES3 membranes would be more adequate, the filtration with the PES50 one being necessary to attain acceptable fluxes with the PES3 membrane. Excellent retentions of 0.83 ± 0.05 and 0.87 ± 0.06 for carbohydrates and proteins, respectively, as well as a difference of 20% in selectivity between proteins and humic acids, were obtained with the PES3 membranes, although its efficiency was affected by a significant irreversible fouling (51.5% of total fouling). Although

CF was still the main fouling mechanism, a reduction of the membrane MWCO derived in a more irreversible fouling, presumably due to particle pore blocking.

Based on the results here obtained, an integrated process of membrane filtration was proposed in order to obtain purified streams of humic acids, carbohydrates and proteins. Future works should indicate the efficiency of the suggested steps of diafiltration and nanofiltration/reverse osmosis, and evaluate how affects the higher concentration of humic acids in the WAS in comparison with proteins and carbohydrates on the effective separation of these biomolecules.

Declaration of Competing Interest

The authors declare that they have no known competing financial interests or personal relationships that could have appeared to influence the work reported in this paper.

Acknowledgements

The authors are grateful for the financial support from the Spanish Ministry of Science, Innovation and Universities through the projects MCIU-19-RTI2018-094218-B-I00 and MCIU-22-PID2021-125942OB-I00. Authors also want to acknowledge the Employment, Industry and Tourism Office of the Principality of Asturias, Spain, for their financial support through the project AYUD/2021/51041. The author Daniel Núñez thanks the Principality of Asturias, Spain, for their financial support through the Severo Ochoa scholarship nº BP19-093.

References

[1] S. Venkata Mohan, G.N. Nikhil, P. Chiranjeevi, C. Nagendranatha Reddy, M. V. Rohit, A.N. Kumar, O. Sarkar, Waste biorefinery models towards sustainable circular bioeconomy: Critical review and future perspectives, Bioresour. Technol. 215 (2016) 2–12. doi:10.1016/j.biortech.2016.03.130.

[2] V. De Buck, M. Polanska, J. Van Impe, Modeling Biowaste Biorefineries: A Review, Front. Sustain. Food Syst. 4 (2020) 11. doi:10.3389/fsufs.2020.00011.

[3] Market Study Report, Global biorefinery market value to surpass USD 52680, 2021.

[4] A.P. Bora, D.P. Gupta, K.S. Durbha, Sewage sludge to bio-fuel: A review on the sustainable approach of transforming sewage waste to alternative fuel, Fuel. 259 (2020) 116262. doi:10.1016/j.fuel.2019.116262.

[5] A. Raheem, V.S. Sikarwar, J. He, W. Dastyar, D.D. Dionysiou, W. Wang, M. Zhao, Opportunities and challenges in sustainable treatment and resource reuse of sewage sludge: A review, Chem. Eng. J. 337 (2018) 616–641. doi:10.1016/j.cej.2017.12.149.

[6] B. Cieślik, P. Konieczka, A review of phosphorus recovery methods at various steps of wastewater treatment and sewage sludge management. The concept of “no solid waste generation” and analytical methods, J. Clean. Prod. 142 (2017) 1728–1740. doi:10.1016/j.jclepro.2016.11.116.

[7] W. Liu, H. Yang, J. Ye, J. Luo, Y.Y. Li, J. Liu, Short-chain fatty acids recovery from sewage sludge via acidogenic fermentation as a carbon source for denitrification: A review, Bioresour. Technol. 311 (2020) 123446. doi:10.1016/j.biortech.2020.123446.

[8] M.N. Siddiquee, S. Rohani, Lipid extraction and biodiesel production from municipal sewage sludges: A review, Renew. Sustain. Energy Rev. 15 (2011) 1067–1072. doi:10.1016/J.RSER.2010.11.029.

[9] K. Xiao, Y. Zhou, Protein recovery from sludge: A review, J. Clean. Prod. 249 (2020) 119373. doi:10.1016/j.jclepro.2019.119373.

[10] P. Supaporn, H.V. Ly, S.S. Kim, S.H. Yeom, Bio-oil production using residual sewage sludge after lipid and carbohydrate extraction, Environ. Eng. Res. 24 (2019) 202–210. doi:10.4491/eer.2017.178.

[11] D. Núñez, P. Oulego, S. Collado, F.A. Riera, M. Díaz, Separation and purification techniques for the recovery of added-value biocompounds from waste activated sludge. A review, Resour. Conserv. Recycl. 182 (2022) 106327. doi:10.1016/j.resconrec.2022.106327.

[12] J.L. Urrea, S. Collado, P. Oulego, M. Díaz, Formation and Degradation of Soluble Biopolymers during Wet Oxidation of Sludge, ACS Sustain. Chem. Eng. 5 (2017) 3011–3018. doi:10.1021/ACSSUSCHEMENG.6B02664.

[13] G.P. Sheng, J. Xu, W.H. Li, H.Q. Yu, Quantification of the interactions between Ca2+, Hg2+ and extracellular polymeric substances (EPS) of sludge, Chemosphere. 93 (2013) 1436–1441. doi:10.1016/J.CHEMOSPHERE.2013.07.076.

[14] L. Wei, K. Wang, X. Kong, G. Liu, S. Cui, Q. Zhao, F. Cui, Application of ultra-sonication, acid precipitation and membrane filtration for co-recovery of protein and humic acid from sewage sludge, Front. Environ. Sci. Eng. 10 (2016) 327–335. doi:10.1007/s11783-014-0763-9.

[15] J. Hwang, L. Zhang, S. Seo, Y.W. Lee, D. Jahng, Protein recovery from excess sludge for its use as animal feed, Bioresour. Technol. 99 (2008) 8949–8954. doi:10.1016/j.biortech.2008.05.001.

[16] A.P. Bhat, P.R. Gogate, Cavitation-based pre-treatment of wastewater and waste sludge for improvement in the performance of biological processes: A review, J. Environ. Chem. Eng. 9 (2021) 104743. doi:10.1016/J.JECE.2020.104743.

[17] M. Pervaiz, M. Sain, Protein extraction from secondary sludge of paper mill wastewater and its utilization as a wood adhesive, BioResources. 6 (2011) 961–970.

[18] B. Otieno, S. Apollo, J. Kabuba, B. Naidoo, G. Simate, A. Ochieng, Ozonolysis pre-treatment of waste activated sludge for solubilization and biodegradability enhancement, J. Environ. Chem. Eng. 7 (2019) 102945. doi:10.1016/J.JECE.2019.102945.

[19] M. García, J.L. Urrea, S. Collado, P. Oulego, M. Díaz, Protein recovery from solubilized sludge by hydrothermal treatments, Waste Manag. 67 (2017) 278–287. doi:10.1016/J.WASMAN.2017.05.051.

[20] E. Slavik, R. Galessi, A. Rapisardi, R. Salvetti, P. Bonzagni, G. Bertanza, L. Menoni, D. Orhon, S. Sözen, Wet Oxidation as an Advanced and Sustainable Technology for Sludge Treatment and Management: Results from Research Activities and Industrial-Scale Experiences, Dry. Technol. 33 (2015) 1309–1317. doi:10.1080/07373937.2015.1036282.

[21] L. Wei, J. Li, M. Xue, S. Wang, Q. Li, K. Qin, J. Jiang, J. Ding, Q. Zhao, Adsorption behaviors of Cu2+, Zn2+ and Cd2+ onto proteins, humic acid, and polysaccharides extracted from sludge EPS: Sorption properties and mechanisms, Bioresour. Technol. 291 (2019) 121868. doi:10.1016/j.biortech.2019.121868.

[22] I. Sargin, G. Arslan, M. Erzengin, Interactions of bovine serum albumin with humic acid-Cu(II) aggregates in poly(hydroxyethylmethacrylate) cryogel column, J. Taiwan Inst. Chem. Eng. 63 (2016) 101–106. doi:10.1016/j.jtice.2016.03.032.

[23] T.A. Saleh, V.K. Gupta, An Overview of Membrane Science and Technology, in: Nanomater. Polym. Membr., Elsevier, 2016: pp. 1–23. doi:10.1016/B978-0-12-804703-3.00001-2.

[24] D.M. Kanani, W.H. Fissell, S. Roy, A. Dubnisheva, A. Fleischman, A.L. Zydney, Permeability-selectivity analysis for ultrafiltration: Effect of pore geometry, J. Memb. Sci. 349 (2010) 405–410. doi:10.1016/j.memsci.2009.12.003.

[25] A. Behboudi, Y. Jafarzadeh, R. Yegani, Enhancement of antifouling and antibacterial properties of

PVC hollow fiber ultrafiltration membranes using pristine and modified silver nanoparticles, J. Environ. Chem. Eng. 6 (2018) 1764–1773. doi:10.1016/J.JECE.2018.02.031.

[26] H.J. Tanudjaja, A. Anantharaman, A.Q.Q. Ng, Y. Ma, M.B. Tanis-Kanbur, A.L. Zydney, J.W. Chew, A review of membrane fouling by proteins in ultrafiltration and microfiltration, J. Water Process Eng. 50 (2022) 103294. doi:10.1016/j.jwpe.2022.103294.

[27] H. Li, Y. Li, S. Zou, C. Li, Extracting humic acids from digested sludge by alkaline treatment and ultrafiltration, J. Mater. Cycles Waste Manag. 16 (2014) 93–100. doi:10.1007/s10163-013-0153-6.

[28] H. Li, Y. Li, Y. Jin, S. Zou, C. Li, Recovery of sludge humic acids with alkaline pretreatment and its impact on subsequent anaerobic digestion, J. Chem. Technol. Biotechnol. 89 (2014) 707–713. doi:10.1002/jctb.4173.

[29] L. Pola, L. Fernández-García, S. Collado, P. Oulego, M. Díaz, Macronutrient solubilisation during hydrothermal treatment of sewage sludge, J. Water Process Eng. 43 (2021) 102270. doi:10.1016/J.JWPE.2021.102270.

[30] L. Pola, S. Collado, P. Oulego, M. Díaz, Production of carboxylic acids from the non-lignin residue of black liquor by hydrothermal treatments, Bioresour. Technol. 284 (2019) 105–114. doi:10.1016/j.biortech.2019.03.066.

[31] S. Collado, D. Núñez, P. Oulego, F.A. Riera, M. Díaz, Effect of landfill leachate ageing on ultrafiltration performance and membrane fouling behaviour, J. Water Process Eng. 36 (2020). doi:10.1016/j.jwpe.2020.101291.

[32] J. Hermia, Constant Pressure Blocking Filtration Laws - Application Topower-Law Non-Newtonian Fluids., Trans Inst Chem Eng. V 60 (1982) 183–187.

[33] Z.F. Cui, H.S. Muralidhara, Membrane Technology, Elsevier, 2010. doi:10.1016/C2009-0-19129-8.

[34] B. Mehta, Processing of model compositional whey solutions with pressure driven membranes, Ohio State University, 1973.

[35] M. Mondor, B. Girard, C. Moresoli, Modeling flux behavior for membrane filtration of apple juice, Food Res. Int. 33 (2000) 539–548. doi:10.1016/S0963-9969(00)00089-2.

[36] I. Horcas, R. Fernández, J.M. Gómez-Rodríguez, J. Colchero, J. Gómez-Herrero, A.M. Baro, WSxM: A software for scanning probe microscopy and a tool for nanotechnology, Rev. Sci. Instrum. 78 (2007) 013705. doi:10.1063/1.2432410.

[37] A.W. Mohammad, N. Hilal, L.Y. Pei, I.N.H. Mohd Amin, R. Raslan, Atomic force microscopy as a tool for asymmetric polymeric membrane characterization, Sains Malaysiana. 40 (2011) 237–244.

[38] R. Sudha, Measures of Skewness and Kurtosis, Res. Biostat. Nurses. 200 (2017) 412–412. doi:10.5005/jp/books/13016_16.

[39] B. Frølund, R. Palmgren, K. Keiding, P.H. Nielsen, Extraction of extracellular polymers from activated sludge using a cation exchange resin, Water Res. 30 (1996) 1749–1758. doi:10.1016/0043-1354(95)00323-1.

[40] M. Dubois, K.A. Gilles, J.K. Hamilton, P.A. Rebers, F. Smith, Colorimetric Method for Determination of Sugars and Related Substances, Anal. Chem. 28 (1956) 350–356. doi:10.1021/ac60111a017.

[41] APHA, AWWA, WEF, APHA, AWWA, WEF. "Standard Methods for examination of water and wastewater.," An. Hidrol. Médica. 5 (2012) 185–186. doi:10.5209/rev_ANHM.2012.v5.n2.40440.

[42] K.Y. Law, Definitions for hydrophilicity, hydrophobicity, and superhydrophobicity: Getting the basics right, J. Phys. Chem. Lett. 5 (2014) 686–688. doi:10.1021/jz402762h.

[43] A.V.R. Reddy, H.R. Patel, Chemically treated polyethersulfone/polyacrylonitrile blend ultrafiltration membranes for better fouling resistance, Desalination. 221 (2008) 318–323. doi:10.1016/j.desal.2007.01.089.

[44] C. Zhao, J. Xue, F. Ran, S. Sun, Modification of polyethersulfone membranes - A review of methods, Prog. Mater. Sci. 58 (2013) 76–150. doi:10.1016/j.pmatsci.2012.07.002.

[45] V. Vatanpour, M. Mehrabi, M. Masteri-Farahani, A.H. Behroozi, M. Niakan, I. Koyuncu, Sulfonic acid functionalized dendrimer-grafted cellulose as a charge and hydrophilic modifier of cellulose acetate membranes in removal of inorganic and organic pollutants, J. Water Process Eng. 50 (2022) 103307. doi:10.1016/j.jwpe.2022.103307.

[46] O. Al-Akoum, L.H. Ding, M.Y. Jaffrin, Microfiltration and ultrafiltration of UHT skim milk with a vibrating membrane module, Sep. Purif. Technol. 28 (2002) 219–234. doi:10.1016/S1383-5866(02)00076-X.

[47] L.E. Fratila-Apachitei, M.D. Kennedy, J.D. Linton, I. Blume, J.C. Schippers, Influence of membrane morphology on the flux decline during dead-end ultrafiltration of refinery and petrochemical waste water, J. Memb. Sci. 182 (2001) 151–159. doi:10.1016/S0376-7388(00)00557-3.

[48] L. Li, L. Ding, Z. Tu, Y. Wan, D. Clausse, J.L. Lanoisellé, Recovery of linseed oil dispersed within an oil-in-water emulsion using hydrophilic membrane by rotating disk filtration system, J. Memb. Sci. 342 (2009) 70–79. doi:10.1016/J.MEMSCI.2009.06.023.

[49] M. Al-Maas, A. Hussain, J. Minier Matar, D. Ponnamma, M.K. Hassan, M. Al Ali Al-Maadeed, K. Alamgir, S. Adham, Validation and application of a membrane filtration evaluation protocol for oil-water separation, J. Water Process Eng. 43 (2021) 102185. doi:10.1016/J.JWPE.2021.102185.

[50] S.F.E. Boerlage, M.D. Kennedy, M.R. Dickson, D.E.Y. El-Hodali, J.C. Schippers, The modified fouling index using ultrafiltration membranes (MFI-UF): characterisation, filtration mechanisms and proposed reference membrane, J. Memb. Sci. 197 (2002) 1–21. doi:10.1016/S0376-7388(01)00618-4.

[51] Q. Yang, J. Luo, S. Guo, X. Hang, X. Chen, Y. Wan, Threshold flux in concentration mode: Fouling control during clarification of molasses by ultrafiltration, J. Memb. Sci. 586 (2019) 130–139. doi:10.1016/J.MEMSCI.2019.05.063.

[52] M. Cifuentes-Cabezas, C. Carbonell-Alcaina, M.C. Vincent-Vela, J.A. Mendoza-Roca, S. Álvarez-Blanco, Comparison of different ultrafiltration membranes as first step for the recovery of phenolic compounds from olive-oil washing wastewater, Process Saf. Environ. Prot. 149 (2021) 724–734. doi:10.1016/J.PSEP.2021.03.035.

[53] I.S. Chang, S.O. Bag, C.H. Lee, Effects of membrane fouling on solute rejection during membrane filtration of activated sludge, Process Biochem. 36 (2001) 855–860. doi:10.1016/S0032-9592(00)00284-3.

[54] G. Di Bella, D. Di Trapani, A brief review on the resistance-in-series model in membrane bioreactors (MBRs), Membranes (Basel). 9 (2019) 24. doi:10.3390/membranes9020024.

[55] A.R. Costa, M.N. de Pinho, M. Elimelech, Mechanisms of colloidal natural organic matter fouling in ultrafiltration, J. Memb. Sci. 281 (2006) 716–725. doi:10.1016/J.MEMSCI.2006.04.044.

[56] W. Guo, H.H. Ngo, J. Li, A mini-review on membrane fouling, Bioresour. Technol. 122 (2012) 27–34. doi:10.1016/j.biortech.2012.04.089.

[57] M. Taniguchi, J.E. Kilduff, G. Belfort, Modes of natural organic matter fouling during ultrafiltration, Environ. Sci. Technol. 37 (2003) 1676–1683. doi:10.1021/es020555p.

[58] L. Bai, H. Wu, J. Ding, A. Ding, X. Zhang, N. Ren, G. Li, H. Liang, Cellulose nanocrystal-blended polyethersulfone membranes for enhanced removal of natural organic matter and alleviation of membrane fouling, Chem. Eng. J. 382 (2020) 122919. doi:10.1016/J.CEJ.2019.122919.

[59] A.N. Cherkasov, S. V. Tsareva, A.E. Polotsky, Selective properties of ultrafiltration membranes from the standpoint of concentration polarization and adsorption phenomena, J. Memb. Sci. 104 (1995) 157–164. doi:10.1016/0376-7388(95)00022-5.

[60] S. Rajesh, Y. Zhao, H. Fong, T.J. Menkhaus, Polyacrylonitrile nanofiber membranes modified with ionically crosslinked polyelectrolyte multilayers for the separation of ionic impurities, Nanoscale. 8 (2016) 18376–18389. doi:10.1039/C6NR06295D.

[61] N. Hilal, H. Al-Zoubi, N.A. Darwish, A.W. Mohammad, Characterisation of nanofiltration membranes using atomic force microscopy, Desalination. 177 (2005) 187–199. doi:10.1016/j.desal.2004.12.008.

[62] H.R. Lohokare, M.R. Muthu, G.P. Agarwal, U.K. Kharul, Effective arsenic removal using polyacrylonitrile-based ultrafiltration (UF) membrane, J. Memb. Sci. 320 (2008) 159–166. doi:10.1016/J.MEMSCI.2008.03.068.

[63] M.S. Muhamad, M.R. Salim, W.-J. Lau, Surface modification of SiO2 nanoparticles and its

impact on the properties of PES-based hollow fiber membrane, RSC Adv. 5 (2015) 58644–58654. doi:10.1039/C5RA07527K.

[64] K. Boussu, B. Van Der Bruggen, A. Volodin, J. Snauwaert, C. Van Haesendonck, C. Vandecasteele, Roughness and hydrophobicity studies of nanofiltration membranes using different modes of AFM, J. Colloid Interface Sci. 286 (2005) 632–638. doi:10.1016/J.JCIS.2005.01.095.

[65] G. Makdissy, J.P. Croué, H. Buisson, G. Amy, B. Legube, Organic matter fouling of ultrafiltration membranes, Water Supply. 3 (2003) 175–182. doi:10.2166/WS.2003.0164.

[66] Y.L. Thuyavan, N. Anantharaman, G. Arthanareeswaran, A.F. Ismail, Impact of solvents and process conditions on the formation of polyethersulfone membranes and its fouling behavior in lake water filtration, J. Chem. Technol. Biotechnol. 91 (2016) 2568–2581. doi:10.1002/JCTB.4846.

[67] J.L. Urrea, S. Collado, P. Oulego, M. Díaz, Effect of wet oxidation on the fingerprints of polymeric substances from an activated sludge, Water Res. 105 (2016) 282–290. doi:10.1016/J.WATRES.2016.09.004.

[68] H. Yamamura, K. Okimoto, K. Kimura, Y. Watanabe, Hydrophilic fraction of natural organic matter causing irreversible fouling of microfiltration and ultrafiltration membranes, Water Res. 54 (2014) 123–136. doi:10.1016/j.watres.2014.01.024.

[69] K. Kimura, H. Yamamura, Y. Watanabe, Irreversible fouling in MF/UF membranes caused by Natural Organic Matters (NOMs) isolated from different origins, Sep. Sci. Technol. 41 (2006) 1331–1344. doi:10.1080/01496390600634665.

[70] Y. Bessiere, B. Jefferson, E. Goslan, P. Bacchin, Effect of hydrophilic/hydrophobic fractions of natural organic matter on irreversible fouling of membranes, Desalination. 249 (2009) 182–187. doi:10.1016/j.desal.2008.12.047.

[71] L. Doskočil, L. Grasset, D. Válková, M. Pekař, Hydrogen peroxide oxidation of humic acids and lignite, Fuel. 134 (2014) 406–413. doi:10.1016/J.FUEL.2014.06.011.

[72] L. Zhou, L. Yuan, B. Zhao Id, Y. Li, Z. Lin, Structural characteristics of humic acids derived from Chinese weathered coal under different oxidizing conditions, (2019). doi:10.1371/journal.pone.0217469.

[73] R. Zhu, A.J. Diaz, Y. Shen, F. Qi, X. Chang, D.P. Durkin, Y. Sun, S.D. Solares, D. Shuai, Mechanism of humic acid fouling in a photocatalytic membrane system, J. Memb. Sci. 563 (2018) 531–540. doi:10.1016/j.memsci.2018.06.017.

[74] T. Zeng, C.J. Wilson, W.A. Mitch, Effect of chemical oxidation on the sorption tendency of dissolved organic matter to a model hydrophobic surface, Environ. Sci. Technol. 48 (2014) 5118–5126. doi:10.1021/es405257b.

[75] P.D. Peeva, A.E. Palupi, M. Ulbricht, Ultrafiltration of humic acid solutions through unmodified

and surface functionalized low-fouling polyethersulfone membranes – Effects of feed properties, molecular weight cut-off and membrane chemistry on fouling behavior and cleanability, Sep. Purif. Technol. 81 (2011) 124–133. doi:10.1016/J.SEPPUR.2011.07.005.

[76] S. Belfer, R. Fainchtain, Y. Purinson, O. Kedem, Surface characterization by FTIR-ATR spectroscopy of polyethersulfone membranes-unmodified, modified and protein fouled, J. Memb. Sci. 172 (2000) 113–124.

[77] S. Acarer, İ. Pir, M. Tüfekci, G. Türkoğlu Demirkol, N. Tüfekci, Manufacturing and Characterisation of Polymeric Membranes for Water Treatment and Numerical Investigation of Mechanics of Nanocomposite Membranes, Polym. 2021, Vol. 13, Page 1661. 13 (2021) 1661. doi:10.3390/POLYM13101661.

[78] Merck KGaA, IR Spectrum Table, (2023). https://www.sigmaaldrich.com/ES/en/technical-documents/technical-article/analytical-chemistry/photometry-and-reflectometry/ir-spectrum-table (accessed June 5, 2023).

[79] R.E. Farsani, S. Raissi, A. Shokuhfar, A. Sedghi, FT-IR study of stabilized pan fibers for fabrication of carbon fibers, World Acad. Sci. Eng. Technol. 38 (2009) 434–437.

[80] S. Baroutian, A.M. Smit, J. Andrews, B. Young, D. Gapes, Hydrothermal degradation of organic matter in municipal sludge using non-catalytic wet oxidation, Chem. Eng. J. 260 (2015) 846–854. doi:10.1016/j.cej.2014.09.063.

[81] C.M. Popescu, C. Vasile, M.C. Popescu, G. Singurel, V.I. Popa, B.S. Munteanu, Analytical methods for lignin characterization. II. Spectroscopic studies, Cellul. Chem. Technol. 40 (2006) 597–621.

[82] M. Banach-Szott, B. Debska, Content of phenolic compounds in fulvic and humic acid fractions of forest soils, Polish J. Environ. Stud. 17 (2008) 463–472.

[83] L. Zhu, H. ying Qi, M. Le Lv, Y. Kong, Y.W. Yu, X.Y. Xu, Component analysis of extracellular polymeric substances (EPS) during aerobic sludge granulation using FTIR and 3D-EEM technologies, Bioresour. Technol. 124 (2012) 455–459. doi:10.1016/j.biortech.2012.08.059.

[84] A. -K Barnfield Frej, R. Hjorth, Å. Hammarström, Pilot scale recovery of recombinant annexin V from unclarified escherichia coli homogenate using expanded bed adsorption, Biotechnol. Bioeng. 44 (1994) 922–929. doi:10.1002/bit.260440808.

[85] H. Block, B. Maertens, A. Spriestersbach, N. Brinker, J. Kubicek, R. Fabis, J. Labahn, F. Schäfer, Chapter 27 Immobilized-Metal Affinity Chromatography (IMAC). A Review, in: Methods Enzymol., 2009: pp. 439–473. doi:10.1016/S0076-6879(09)63027-5.

[86] H. Li, Y. Jin, Y. Nie, Application of alkaline treatment for sludge decrement and humic acid recovery, Bioresour. Technol. 100 (2009) 6278–6283. doi:10.1016/j.biortech.2009.07.022.

[87] S.H. Maruf, A.R. Greenberg, J. Pellegrino, Y. Ding, Critical flux of surface-patterned ultrafiltration membranes during cross-flow filtration of colloidal particles, (2014).

doi:10.1016/j.memsci.2014.07.071.

[88] X. Tang, T. Guo, H. Chang, X. Yue, J. Wang, H. Yu, B. Xie, X. Zhu, G. Li, H. Liang, Membrane Fouling Alleviation by Chemically Enhanced Backwashing in Treating Algae-Containing Surface Water: From Bench-Scale to Full-Scale Application, (n.d.). doi:10.1016/j.eng.2021.01.013.

[89] Y. Bhoj, M. Tharmavaram, D. Rawtani, A comprehensive approach to antifouling strategies in desalination, marine environment, and wastewater treatment, Chem. Phys. Impact. 2 (2021) 100008. doi:10.1016/j.chphi.2020.100008.

Supplementary Information to

‘Membrane fractioning of pre-treated waste activated sludge for the recovery of valuable biocompounds’

Daniel Núñez[1], Paula Oulego[1], Mahdi Nikbakht Fini[2], Jens Muff[2], Sergio Collado[1], Francisco A. Riera[1], Mario Díaz[1]*

[1]Department of Chemical and Environmental Engineering, University of Oviedo.

c/ Julián Clavería 8, 33006, Oviedo, Spain

[2]Department of Chemistry and Bioscience, Aalborg University Esbjerg, Niels Bohrs Vej 8,

Esbjerg, 6700, Denmark

*Corresponding author’s e-mail: mariodiaz@uniovi.es

Phone: +34 985 10 34 39, FAX: +34 985 10 34 40

(4 Pages, 3 Figures)

Table of contents

1. Contact angle measurements

Representative obtained pictures of the sessile water droplets, from which the contact angles were measured, are shown in Fig. A.4.1.

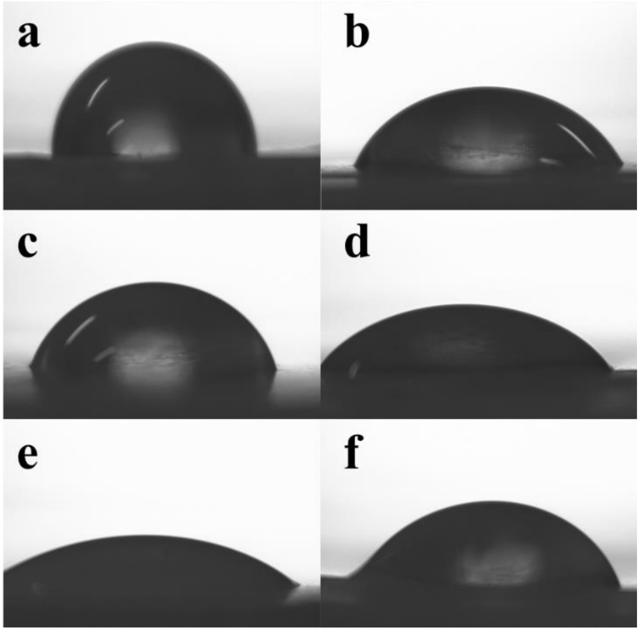

Figure A.4.1. Pictures of sessile droplets on a) PES50, clean; b) PES50, fouled; c) PESH50, clean; d) PESH50, fouled; e) PAN50, clean; f) PAN50, fouled.

2. Infrared spectroscopy

The Fourier transform infrared spectroscopy (FTIR) spectra of the clean and fouled membranes employed in this study are shown in Figs. A.4.2 and A.4.3. Note that "PES3, clean" and "PES10, clean" spectra are the clean counterpart of both PES3 and PES50-3, and of PES10 and PES50-10, respectively.

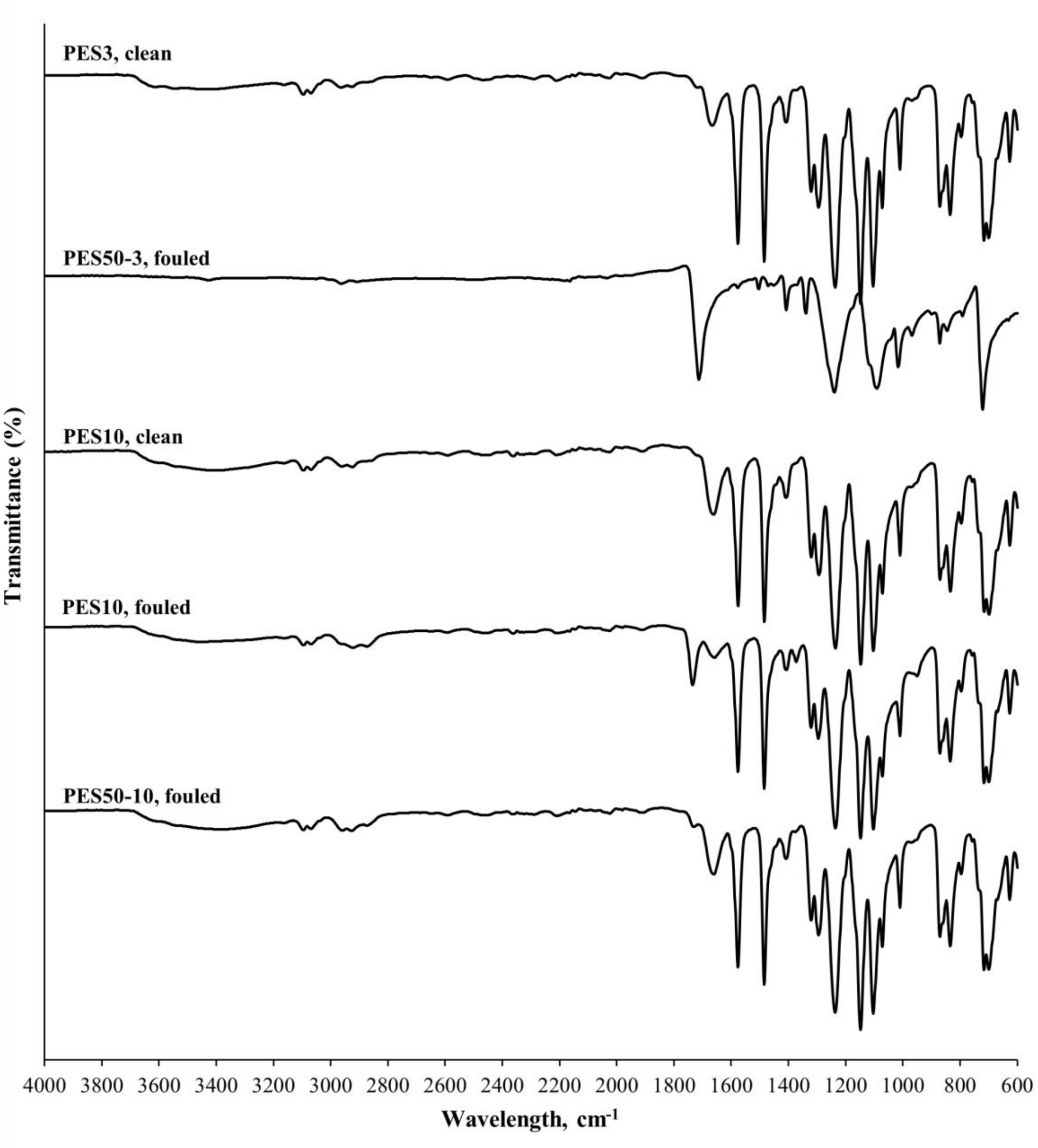

Figure A.4.2. FTIR spectra of PES10, PES3, PES50-10 and PES50-3 membranes.

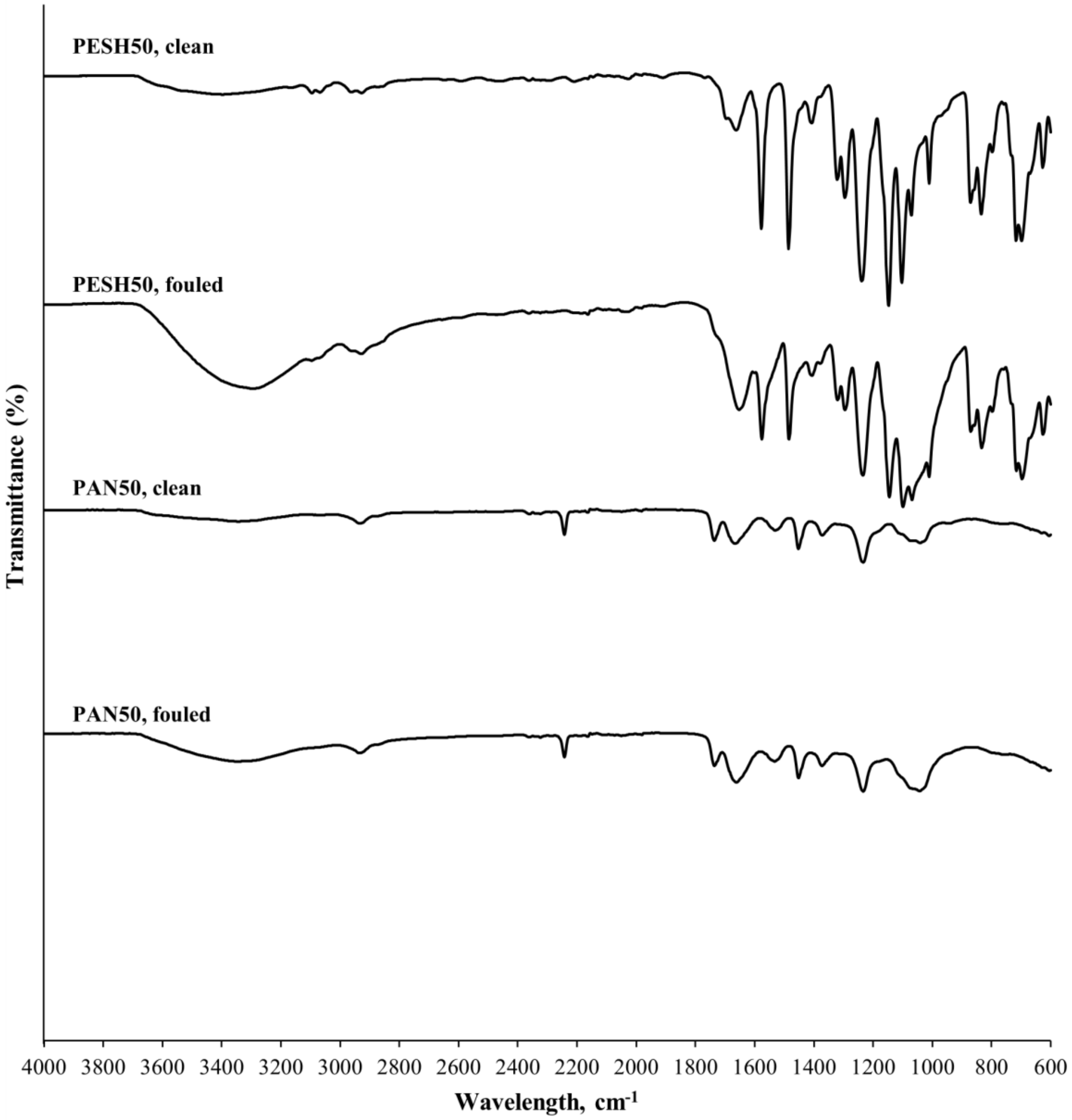

Figure A.4.3. FTIR spectra of PESH50 and PAN50 membranes.

4.1.3. Heavy metal removal from hydrothermally treated waste activated sludge by ultrafiltration with polymeric membranes

Daniel Núñez[1], Paula Oulego[1], Mahdi Nikbakht Fini[2], Jorge Espina-Casado[3], Jens Muff[2], Sergio Collado[1], Francisco A. Riera[1], Mario Díaz[1]*

[1]Department of Chemical and Environmental Engineering, University of Oviedo, c/ Julián Clavería 8, 33006, Oviedo, Spain

[2]Department of Chemistry and Bioscience, Aalborg University Esbjerg, Niels Bohrs Vej 8, Esbjerg, 6700, Denmark

[3]Department of Physical and Analytical Chemistry, University of Oviedo, c/ Julián Clavería 8, 33006, Oviedo, Spain

*Corresponding author's e-mail: mariodiaz@uniovi.es

Phone: +34 985 10 34 39, FAX: +34 985 10 34 40

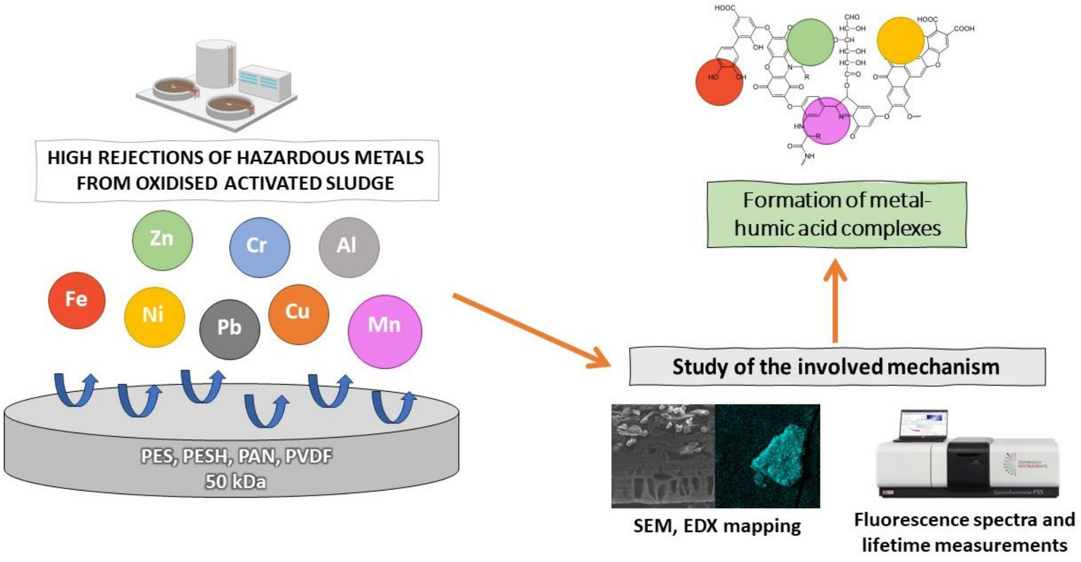

Figura 4.18. Resumen gráfico del artículo *Heavy metal removal from hydrothermally treated waste activated sludge by ultrafiltration with polymeric membranes*.

Abstract

This study assessed the capability of various polymeric membranes to retain hazardous metals form hydrothermally treated waste activated sludge (WAS). After the ultrafiltration of the treated WAS with flat sheet membranes of 50 kDa composed of polyethersulphone (PES), permanently hydrophylic polyethersulphone (PESH), polyacrylonitrile (PAN) and polyvinylidene fluoride (PVDF), it was found that the PES membrane exhibited the highest retentions for all of the main metals (Fe, Zn, Mn, Al, Ni, Cu and Cr) with values varying from 41% to 96%, except for Pb, in which the higher value (79%) was achieved with the PAN membrane. Foulants, including hazardous metals, were present on the surface of the membranes, but not within the pores, thus suggesting that fouling comprised cake layer formation. Additionally, crystal structures composed of sulphate or silicates of heavy or alkali metals were also identified on the membrane surfaces.

Photoluminescence and absorption spectra measurements revealed that interaction of the studied metals (Fe, Zn, Mn, Al, Ni, Cu, Cr and Pb) and humic acid can be explained considering static quenching, implying the formation of ground-state complexes with humic acid. Formation constants were also determined, with Cu^{2+}, Ni^{2+} and Cr^{3+} being the metal ions which formed the strongest complex. Other mechanisms, including complexation with proteins and precipitation may also contribute to metal retention.

Keywords: Formation constants; membrane fouling; metal complexes; photoluminescence; sewage sludge; ultrafiltration.

1. Introduction

Waste activated sludge (WAS) is a hazardous residue generated during the secondary treatment of urban wastewaters. Its management, which can take up to 65% of the wastewater treatment plant's operation costs of wastewater treatment plants [1], has arisen great concern due to the large amounts of WAS generated, reaching around 10 million tons (dry weight) in Europe in 2019 [2]; and the increasing legal regulations [3,4] imposed because of the toxic nature of the WAS. Currently, the standard methods for its management, including agricultural use, land reclamation, incineration or landfill disposal [5,6], can cause environmental and health problems such as greenhouse gas emissions [7], air pollution [8], terrestrial acidification and eutrophication [9], increment of the presence of antibiotic resistance genes in the soil microbiota [10], and contamination of soil by pathogens [11], organic pollutants [12] or heavy metals [13]. Additionally, biogas production is also gaining attention to valorise sewage sludge because of its high organic content [14]. Nevertheless, anaerobic digestion requires extended processing times and a strict control of conditions [15].

Heavy metals are defined as naturally occurring metal/metalloids having an atomic number greater than 20 and elemental density greater than 5 $g \cdot cm^{-3}$, and include iron (Fe), zinc (Zn), manganese (Mn), nickel (Ni), copper (Cu), chromium (Cr) or lead (Pb) [16,17]. These elements, which have been reported to account for 0.5-2% of the total solids in WAS [18], are hazardous contaminants due to their drastic effects on health and their non-degradability and high abundance in the environment [16]. Furthermore, they are bioaccumulated and biomagnified throughout the whole trophic chain, , with dietary exposure being the major pathway for human exposure to heavy metals [16,19], primarily via food crops [19], fish [20,21] and seafood [22,23]. Overexposure to these elements has carcinogenic, genotoxic, teratogenic and mutagenic effects [24,25] and may cause endocrine disruption and various neurological and neurobehavioral disorders even at low concentrations of exposure [16,25–27]. Additionally, overexposure to other metals like aluminium (Al) may also trigger neurological disorders such as cognitive impairment or dementia [28].

Alternative WAS management methods, such as hydrothermal treatments [29], fermentation [30], ozonation [31], activated sludge process [32], ultrasonication [33] or worms' predation technology [34] do not solve the heavy metal problem, requiring another treatment specifically for the removal of heavy metals.

To this end, membrane filtration is an interesting separation technology as it is considered a green technology with low energy requirements. Besides, it can be easily coupled with other processes, and is technically mature [35,36]. However, due to the molecular weight of heavy metals, membranes with a small pore size or molecular weight cut-off (MWCO), in the range of nanofiltration or reverse osmosis, are required in order to retain these compounds, leading to higher equipment and operations costs [37,38]. While ultrafiltration (UF) membranes have been studied for heavy metal removal, their large pore size have led to the use of additives to form complexes with the heavy metals [39,40], thus increasing operation costs. Nevertheless, with a proper solubilisation step, the use of additives may become unnecessary thanks to the composition of WAS. In this sense, the interaction between heavy metals and proteins, the main biocompound in WAS [41], through chelation or complex formation is well-documented [42,43]. Moreover, humic acids are also present in significant quantities in WAS composition [44]. These compounds, with sizes between 2 and 1300 kDa, are characterized by being amphiphilic weak acidic electrolytes with carboxylic, phenolic or quinone groups [45,46], and their interaction with metals has also been reported [47,48]. As previously mentioned, it is necessary to release these biocompounds into the liquid media through a solubilisation process. In this sense, partial wet oxidation (WO) can be considered an interesting methodology due to its ability to both solubilise and sterilise WAS. Besides, its feasibility at an industrial scale has also been reported [49]. Furthermore, proteins could be recovered after filtration by precipitation [50], and concentrated humic acids could be used as fertilizer [51]. Additionally, membrane performance is significantly determined by their material [52]. Therefore, it is necessary to analyse the effect of the membrane material in heavy metal separation. To the best of our knowledge, there is no studies related to the assessment of heavy metal retention from

WAS treated by partial WO with UF membranes. Thus, the effect of the membrane material on the separation performance, along with the mechanism involved in retention, was carefully studied.

2. Materials and methods

2.1. Waste activated sludge

Thickened WAS was collected from a wastewater treatment plant in northern Spain (Baíña, Asturias). WAS solubilization was achieved by a partial WO at 160 ºC and 40 bar for 80 min. These mild conditions were chosen to solubilise WAS and avoid the oxidation or mineralisation of the biomolecules released into the reaction medium [53]. A constant flow of 1200 mL/min of O_2 saturated with steam and a stirring speed of 150 rpm were employed. A more detailed description of the reactor can be found in [54]. To prevent microbial growth, sodium azide 0.1% (w/v) was added to the oxidised WAS and stored at 4 ºC for further usage. The main physico-chemical characteristics of the oxidised WAS can be found in Table 4.17.

Table 4.17. Main physical-chemical characteristics of oxidised waste activated sludge.

Parameter	**Value**
pH	5.02 ± 0.02
Colour number (cm^{-1})	3.8 ± 0.1
Chemical oxygen demand (mg O_2/L)	20500 ± 510
Total organic carbon (mg C/L)	8000 ± 10
Proteins (mg/L)	3400 ± 300
Humic acids (mg/L)	8400 ± 200
Carbohydrates (mg/L)	2750 ± 30

2.2. Membrane filtration

All membrane filtration experiments were performed using an FT17 Cross-flow Filtration Unit (Armfield Ltd., United Kingdom), which allows to carry out tangential filtrations with flat-sheet membranes. Different polymeric flat-sheet membranes were used for the filtration of the oxidised sludge: MQ (Synder Filtration), made of polyethersulphone (PES); UH050 (Synder Filtration), made of hydrophylic polyethersulphone (PESH); MW (Suez), made of hydrophilic polyacrylonitrile (PAN); and BN (Synder Filtration), made of polyvinylidene fluoride (PVDF). All membranes had a MWCO of 50 kDa. All membranes were shaped into circles with a diameter of 9 cm , providing a filtration area of 63.62 cm2.

The conditions for the filtration experiments were set as follows: temperature of 50.0 ± 0.4 ºC, transmembrane pressure (TMP) of 4.0 ± 0.2 bar, and crossflow velocity (CFV) of 3.00 m/s. Membranes were conditioned before every experiment by running the equipment for 30 min with distilled water without pressure, and at the operation conditions for another 30 min. Subsequently, WAS was ultrafiltered without recirculation of the permeate until a volume concentration rate (VCR) of 2.5 was reached. Permeate and retentate samples were taken periodically and stored at 4ºC for further usage. All filtration experiments were performed in duplicate.

2.3. Scanning electron microscopy

In order to assess membrane-heavy metals interactions, the surface morphology of the fouled membranes was examined by scanning electron microscopy (SEM). Additionally, compositional analysis of deposits and elemental mapping of membrane surface were conducted. A scanning electron microscope (JEOL JMS-6610LV) coupled with energy dispersive X-ray analyser (EDX) at 20 kV was used. The membrane samples were coated with a thin layer of gold to make them conductive before the SEM analysis.

2.4. Measurement of metal concentrations

A semi-quantitative analysis was performed with an Agilent 7500ce Inductively Coupled Plasma Mass Spectrometer (Agilent Technologies, CA, USA) to measure the concentrations of 75 metals. The eight most prevalent hazardous metals (Al, Cu, Fe, Mn, Ni and Zn) were quantitatively determined in both the permeate and retentate using the same apparatus. Their rejection coefficients (R) were calculated according to Eq. 1:

$$R_i=1-\frac{C_{P,i}}{C_{R,i}} \qquad (1)$$

Where $C_{P,i}$ and $C_{R,i}$ are the concentration of the metal “i” in the permeate and the retentate, respectively.

The internal standards used were ^{45}Sc for Al, and ^{103}Rh for Cu, Fe, Mn and Ni.

2.5. Photoluminiscence and absorption spectra measurements

Photoluminiscence spectra measurements were conducted to measure the quenching of humic acids and proteins with metals. In addition, absorption spectra measurements were made to determine the characteristics of the interaction between humic acids and proteins with metals.

2.5.1. Instruments

The Edinburgh Instruments FS5 assembled with a 150W continuous and pulsed Xe-lamp was used to record fluorescence spectra and lifetime measurements (405 nm ps laser). Determination of lifetime can be obtained from Eq. 2:

$$I(t)=\sum_i I_i exp(-t/\tau_i) \qquad (2)$$

Where I_i refers to intensity at different times and τ_i represents the decay time.

2.5.2. Experimental

Aliquots of each metal solution (1000 ppm in water) were individually added to a series of 10 mL volumetric flasks. Subsequently, 1 mL of phosphate buffer solution (pH 5.05; 0.1 M), 0.1 mL of humic acid solution (1000 ppm in water), and Milli-Q water were added to reach a final volume of 10 mL.

To measure the fluorescence spectra for each solution, the excitation wavelength was fixed at 297 nm and was used to record the emission spectra. For lifetime measurements, samples were irradiated with a 405 nm laser, and fluorescence decay was recorded at 513 nm.

To investigate the formation of metal ion complexes, fluorescence quenching was measured. In this sense, fluorescence quenching usually refers to nonradiative energy transfer from an excited species to other molecules [55] and it has been used as a basis for determination of analytes using the spectrofluorimetric technique.

Fluorescence quenching can be static (complex formation) or dynamic (collisional) quenching [56,57]. Collisional quenching of fluorescence is described by Stern-Volmer equation (Eq. 3) [58].

$$\frac{F_0}{F} = 1 + k_q \tau_0 [Q] = 1 + K_D [Q] \qquad (3)$$

Where F_0 and F are the fluorescence intensities in the absence and presence of quencher, respectively; k_q is the bimolecular quenching constant; τ_0 is the lifetime of the fluorophore in the absence of quencher and Q is the concentration of quencher. The Stern-Volmer equation can be derived by considering fluorescence intensities observed in the absence and presence of quencher and the Eq. 4 can be obtained:

$$\frac{\tau_0}{\tau} = 1 + k_q \tau_0 [Q] \qquad (4)$$

This equation illustrates an equivalent decrease in fluorescence intensity and lifetime for collisional quenching (Eq. 5):

$$\frac{F_0}{F} = \frac{\tau_0}{\tau} \qquad (5)$$

In static quenching, nonfluorescent ground-state complex are formed between the fluorophore and quencher. The dependence of the fluorescence intensity on quencher concentration is derived by association constant for complex formation (Eq. 6):

$$K_s = \frac{[F-Q]}{[F][Q]} \tag{6}$$

Where [F-Q] is the concentration of the complex, [F] is the concentration of uncomplexed fluorophore and [Q] is the concentration of quencher. The total concentration of fluorophore $[F]_0$ is given by Eq. 7:

$$[F]_0 = [F] + [F-Q] \tag{7}$$

Substituting Eq. 7 into Eq. 6 results in:

$$K_s = \frac{[F]_0 - [F]}{[F][Q]} = \frac{[F]_0}{[F][Q]} - \frac{1}{[Q]} \tag{8}$$

$$\frac{F_0}{F} = 1 + K_s[Q] \tag{9}$$

In static quenching the complexed fluorophores are nonfluorescent, and the only observed fluorescence is from uncomplexed fluorophores. Therefore, for static quenching $\tau_0/\tau=1$ in contrast to dynamic quenching (Eq. 5). In this sense, measuring fluorescence lifetime is the most definitive method to distinguish static and dynamic quenching.

3. Results

3.1. Scanning electron microscopy

The morphology of the membrane surfaces was analysed by SEM. Imaging at x15000 augments (Fig. 4.19) highlighted the differences between membrane morphologies: PES and PESH membranes displayed a highly cracked surface, PVDF had a slightly cracked surface, and PAN surface was smooth. These differences on the membrane surface can be due to the different manufacturing methods, and could imply differences between the selective and support layers of the different membranes [59], which can be related to their different permeabilities and selectivities.

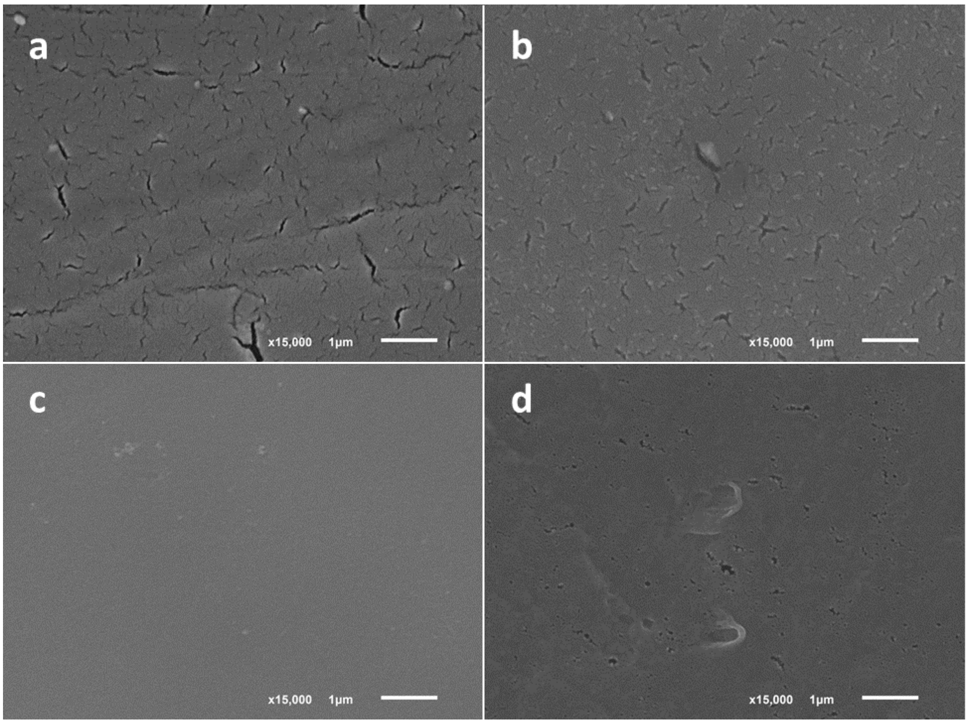

Figure 4.19. SEM images of pristine membrane surfaces of PES (a), PESH (b), PAN (c), and PVDF (d).

After filtration, a crust was formed on top of the membrane surface, indicating the formation of the fouling cake (Fig. 4.20). Additionally, deposits with crystal structures of various morphologies were also identified on the fouled membrane surfaces.

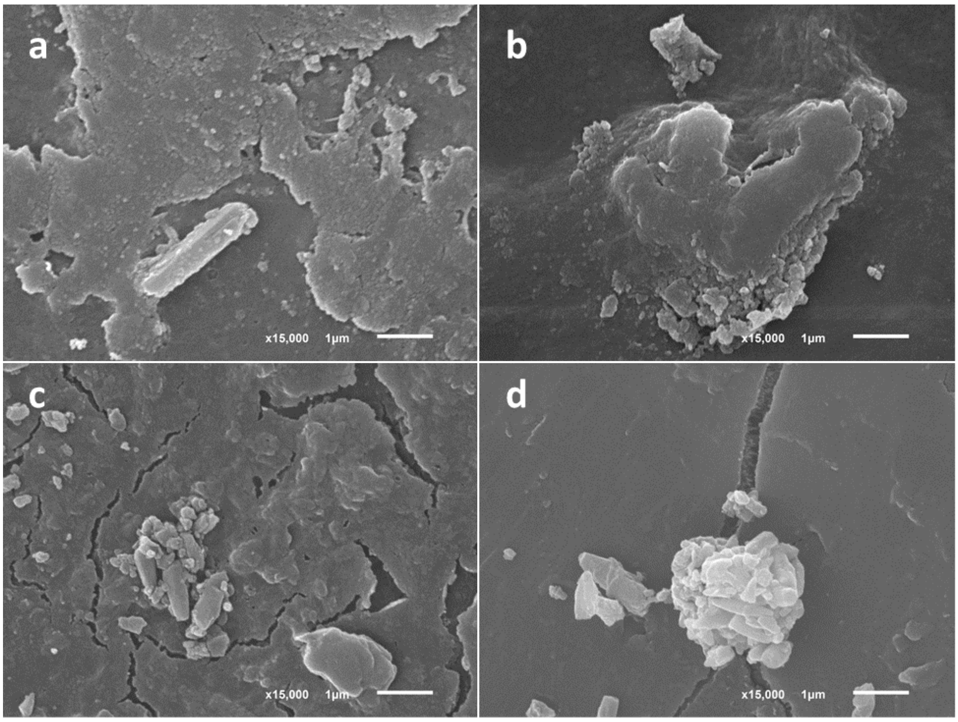

Figure 4.20. SEM images of fouled membrane surfaces of PES (a), PESH (b), PAN (c), and PVDF (d).

EDX analysis allowed us to determine the average elemental composition of both the clean and fouled membranes, as well as the specific composition of different parts/points. In this sense, C, N and S were identified in PES and PESH clean membranes, with average concentrations (% wt.) of 60 ± 2%, 26 ± 3% and 12 ± 2% for PES and 50.5 ± 0.6%, 33 ± 1 % and 14.7 ± 0.3% for PESH, respectively. For PAN clean membranes, the identified elements were C (67 ± 2%), N (26 ± 3%), and O (7 ± 1%). In the case of PVDF clean membranes, the elements were C (36 ± 1%) and F (61 ± 1%). Additionally, Na (found in both PES and PESH) and Cl (found in PES) were detected in very low concentrations (from 0.48 ± 0.01% to 1.2 ± 0.3%) in the clean membranes. This can be explained by considering slight surface contamination during handling or storage.

Regarding the fouled membranes, EDX analyses highlighted the significant changes in the elemental composition of the membrane surfaces, providing insights into the nature of the deposited fouling on the membranes. After the filtration of WAS, nitrogen (N) was detected in various deposits across all fouled membranes, i.e. PES, PESH, PVDF and PAN, obtaining concentrations between 2.75 to 35.01 %wt. This indicates the retention of nitrogenated compounds like proteins and humic acids (Fig. 4.21, Fig. 4.22 and Table A.4.1). Besides, sulphur (S) was also identified in the fouled membranes of PES, PESH and PAN, with values up to 9.8 %wt, which also suggested the retention of sulphur-based compounds like proteins. Additionally, the EDX results of the crystal structures observed in Fig. 4.20 suggested the presence of Ca-containing precipitates, although other metals, such as Si and Al, as well as heavy metals (Fe and Cu), were also observed in PAN fouled membrane surface (Fig. 4.21A).

In order to delve into the nature of this superficial fouling, a long-term filtration experiment was made with the PES membrane (Fig. 4.21B). EDX analysis of this highly fouled membrane showed the presence of metals (Al and Si), heavy metals (Fe) and nutrients (P, Cl, K and Ca), indicating effective retention of at least these elements during the filtration with the 50 kDa membrane.

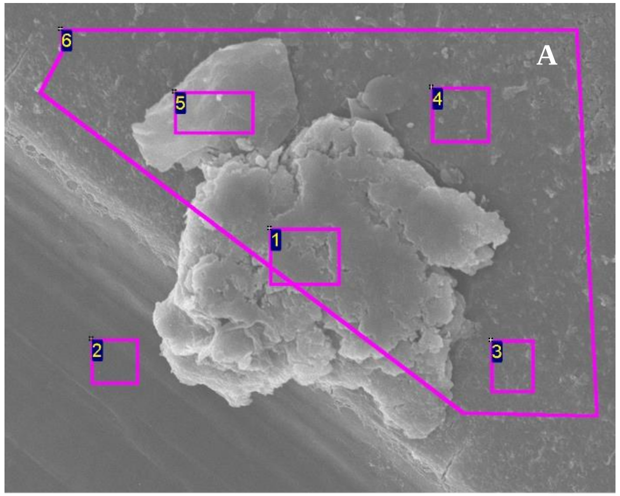

Spectrum	*C*	*N*	*O*	*Al*	*Si*	*S*	*Cl*	*Ca*	*Fe*	*Cu*
1	47.53	5.91	19.75	0.24	5.28	9.80	0.08	0.28	0.74	10.40
2	57.56	35.01	6.58	0.07	0.12	0.29	0.13	0.06	0.08	0.11
3	45.72	23.55	28.75	0.33	0.29	0.20	n.d.*	0.10	0.86	0.20
4	51.52	24.26	22.18	0.25	0.21	0.18	0.13	0.09	0.84	0.34
5	49.42	23.69	25.70	0.14	0.11	0.22	0.13	0.15	0.36	0.08
6	54.93	17.10	18.68	0.22	0.99	3.37	0.07	0.25	0.60	3.80

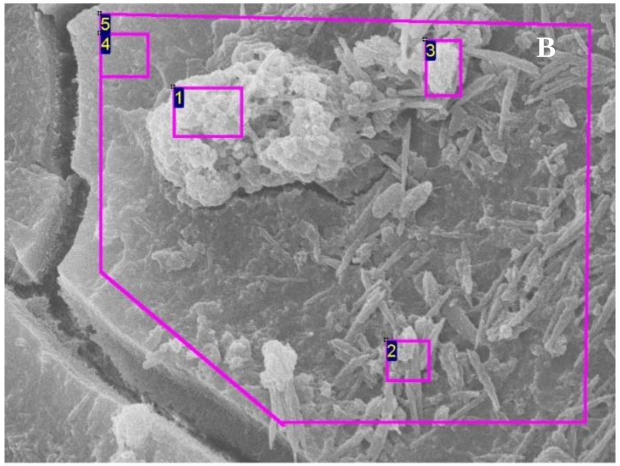

Spectrum	*C*	*N*	*O*	*Na*	*Al*	*Si*	*P*	*S*	*K*	*Ca*	*Fe*
1	33.32	6.66	45.72	0.98	0.68	0.16	2.42	0.66	0.54	7.06	1.80
2	45.57	n.d.*	38.72	1.32	0.64	0.60	2.70	4.04	0.54	3.45	2.43
3	40.98	n.d.*	42.47	1.27	1.02	0.70	3.50	1.59	0.55	4.84	3.07
4	53.80	4.00	31.88	0.59	0.63	0.45	1.78	4.42	0.29	0.52	1.65
5	41.73	2.75	38.66	0.99	0.92	0.88	3.45	3.63	0.56	2.74	3.68

n.d.*: not detected

Figure 4.21. EDX analysis of the fouled PAN (A) and the highly fouled PES (B) membranes (all results in %wt).

EDX analysis of the inner structures of the fouled membranes did not reveal the presence of metals, unlike the membrane surfaces, as illustrated by the example of PESH (Fig. 4.22). This suggested that at least a significant amount of the metals and heavy metals was retained either on the membrane surface or embedded in the cake layer atop of the membrane, not being present in the pores. This observation may also imply that the structures in which the metals were complexed were larger than the pore size of the 50 kDa membranes. The retention of the Pb, Cu and Cd through the cake layer during the ultrafiltration of extracellular polymer substances (EPS) from excess sludge was also reported by Cao et al. [60] using a membrane with a MWCO of 10 kDa.

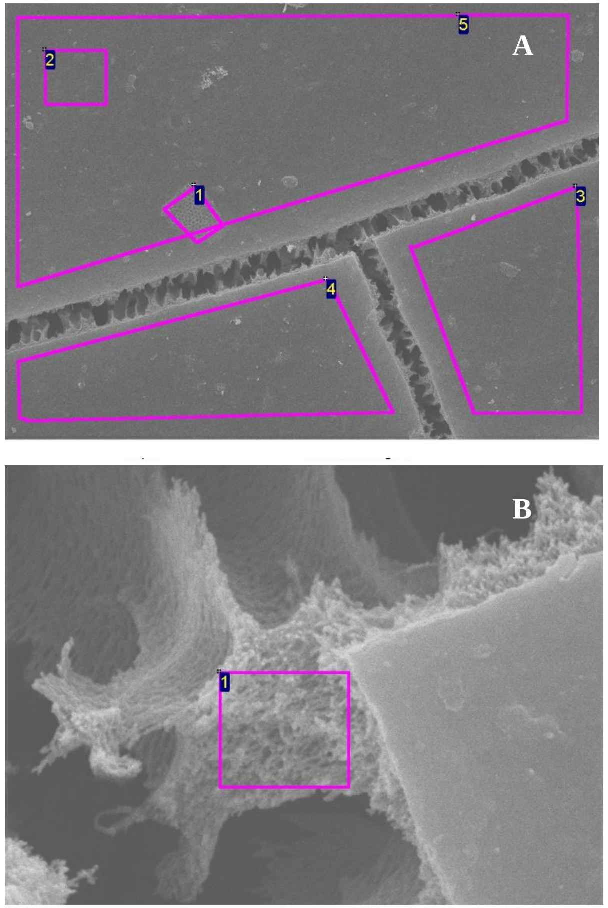

Spectrum	*C*	*N*	*O*	*Si*	*S*	*Ca*	*Fe*
1	39.38	14.20	34.32	0.67	8.62	0.62	2.18
2	44.83	12.31	28.65	0.75	11.07	0.26	2.14
3	47.20	13.25	24.67	0.57	12.58	0.47	1.26
4	59.67	n.d.*	24.47	0.65	13.30	0.28	1.62
5	43.25	14.67	24.27	1.12	14.31	0.07	2.31

n.d.*: not detected

Spectrum	*C*	*N*	*O*	*S*
1	57.40	9.81	23.06	9.72

Figure 4.22. EDX analysis of the superficial (A) and inner (B) fouled PESH membrane (all results in %wt).

Elemental mapping of the cross-sectional SEM images of the fouled membranes confirmed the absence of metals inside the membranes, indicating that metal retention occurred exclusively at the membrane surface level (Fig. 4.24). Differences were observed not only on the membrane surface but also in the inner membrane morphology, depending on the material (Fig. 4.23). All membranes consisted of a selective layer, comprised a thin, dense top layer and a porous sub-layer, along with a supporting fibre layer. The PVDF membrane also featured an outer sponge layer, with the porous layer positioned between the sponge and the support layer. This structural configuration resulted from the use of more concentrated polymer [61], as reported in other PVDF membrane studies [62]. The aim was to reduce pore wetting while reducing membrane tortuosity and, consequently, increasing water flux [63,64]. PAN and PESH membranes exhibited a thinner porous layer and thicker fibres in the support layer, potentially contributing to their higher permeability and lower selectivity.

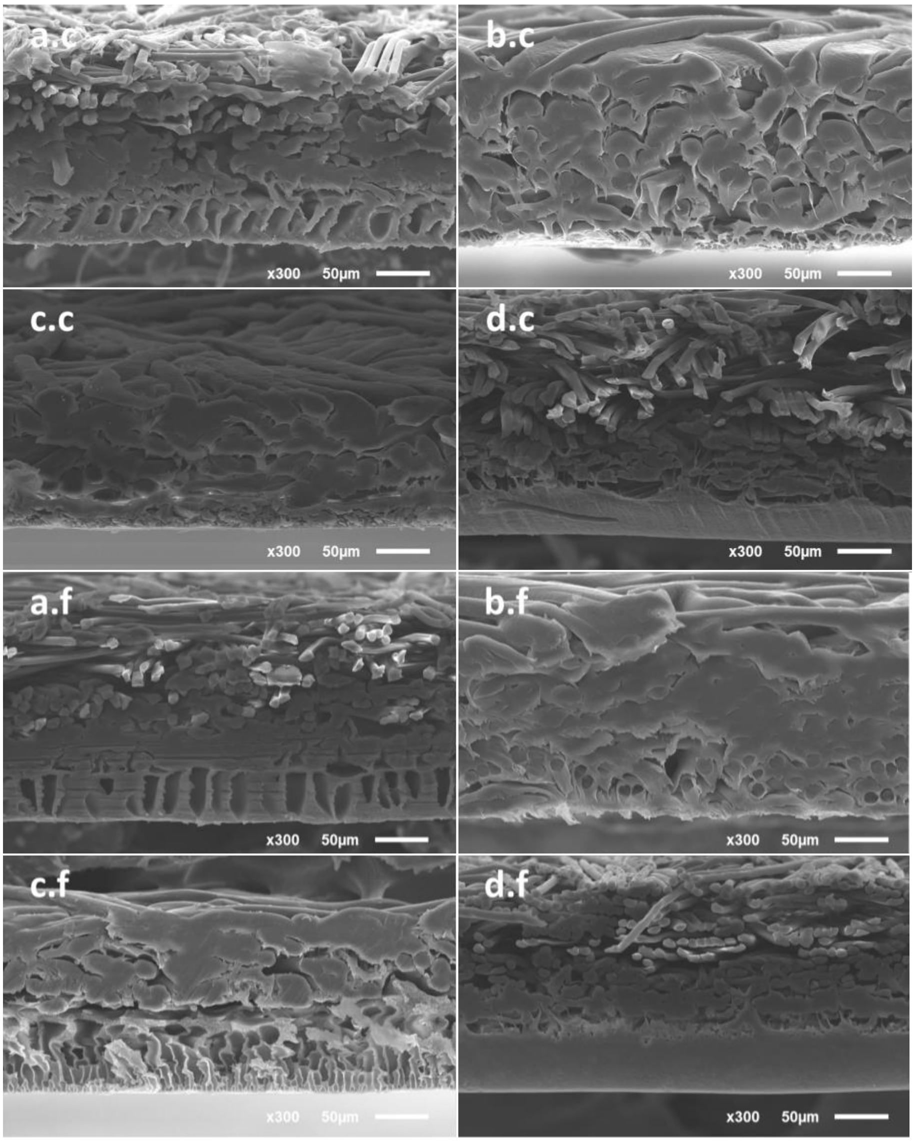

Figure 4.23. Cross-sectional SEM images of clean (.c) and fouled (.f) membranes for PES (a), PESH (b), PAN (c), and PVDF (d).

The distribution of the selective and support layers could be better appreciated with the EDX mapping (Fig. 4.24). A dense layer of sulphur in the porous layer of the PES membrane, fluorine in the porous layer of the PVDF membrane, and more subtly, nitrogen in the porous layer of the PAN membrane (indicating a higher presence of their corresponding monomers on those areas) revealed that the selective layer was concentrated at the contact surface of the membrane, forming part only of the porous or macro void structures. This observation is particularly significant for the PVDF membrane. The absence of fluorine in the outer sponge layer highlighted that the selective layer is sandwiched between the sponge and the fibre layers. In contrast, a network of sulphur can be identified throughout the entire support layer of the PESH membrane, in addition to the sulphur present in the porous layer.

After membrane filtration, changes in the morphology of the membranes were identified. In this sense, a compaction of the support fibres and/or of the selective layer was observed at different levels in PES, PESH and PVDF membranes. Membrane compaction can lead to an irreversible flux loss and affect separation efficiency [65], even when it occurs in the support layer [66]. Strikingly, the PAN membrane suffered a decompaction after filtration, resulting in an increased size of its finger-like macro void sub-layer. This might be indicative of a manufacturing defect, or more severe damage of the membrane.

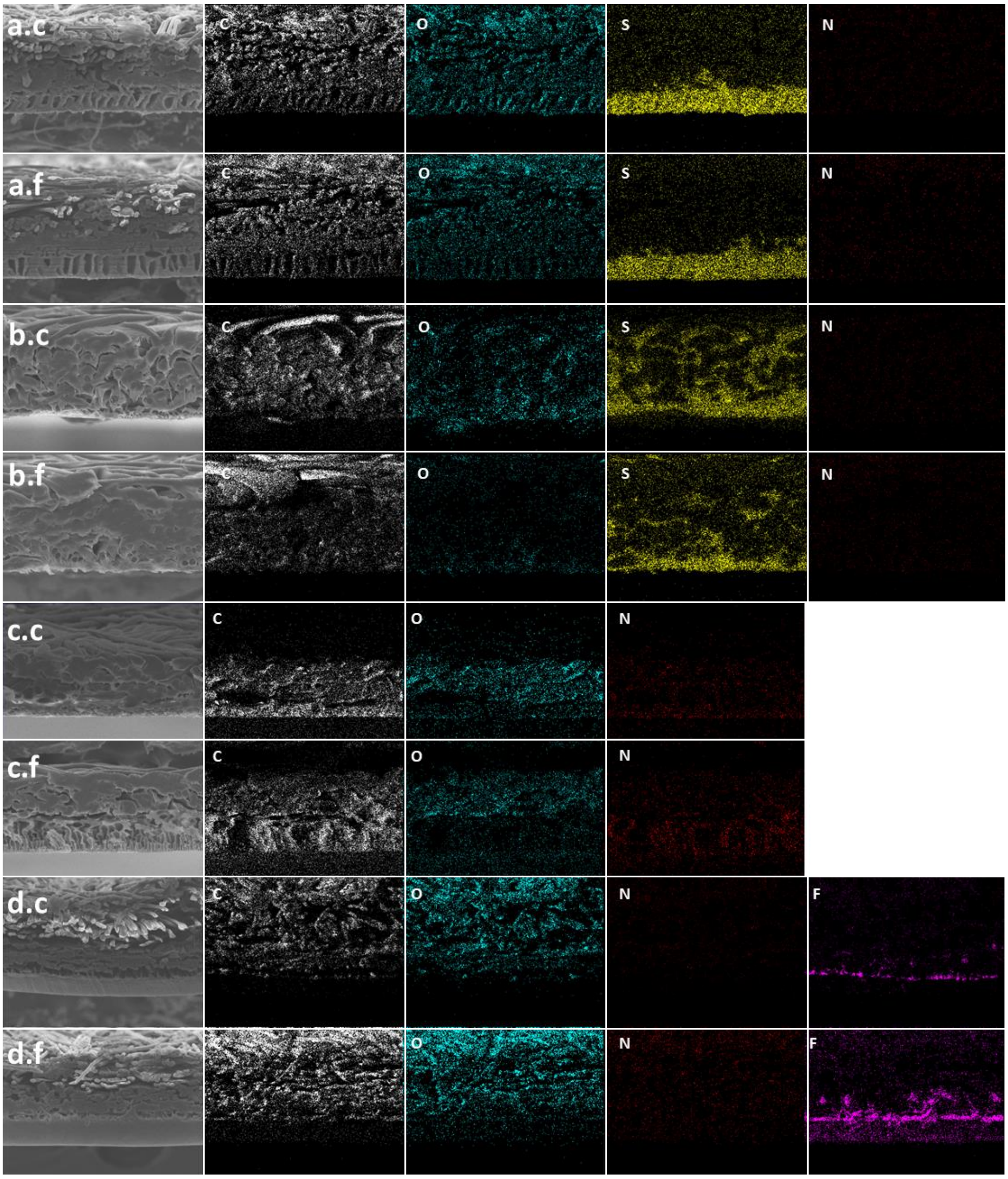

Figure 4.24. EDX elemental mapping of the cross-sectional SEM images of clean (.c) and fouled (.f) membranes for PES (a), PESH (b), PAN (c), and PVDF (d).

Apart from morphology changes, no new elements were detected in the cross-sectional mappings, indicating that fouling did not occur at a pore level. On the contrary, as observed during the EDX analysis, various foulants were present on the surface of all the membranes (Fig. 4.25). Structures of calcium, copper and zinc sulphates, magnesium silicate, phosphates, as well as calcium, magnesium, aluminium and iron oxides were identified on the different membrane surfaces (Fig. 4.25, Figs. A.4.4-6). Furthermore, elements like Fe and N were evenly distributed on the fouled surfaces PES, PESH and PAN membranes. Besides, even distributions were also observed in the foulants (Al, Si, Fe, Ca, K, Mg, N and P) of the highly fouled PES membrane. This is indicative of reversible fouling since they did not form part of any recognizable particle [67].

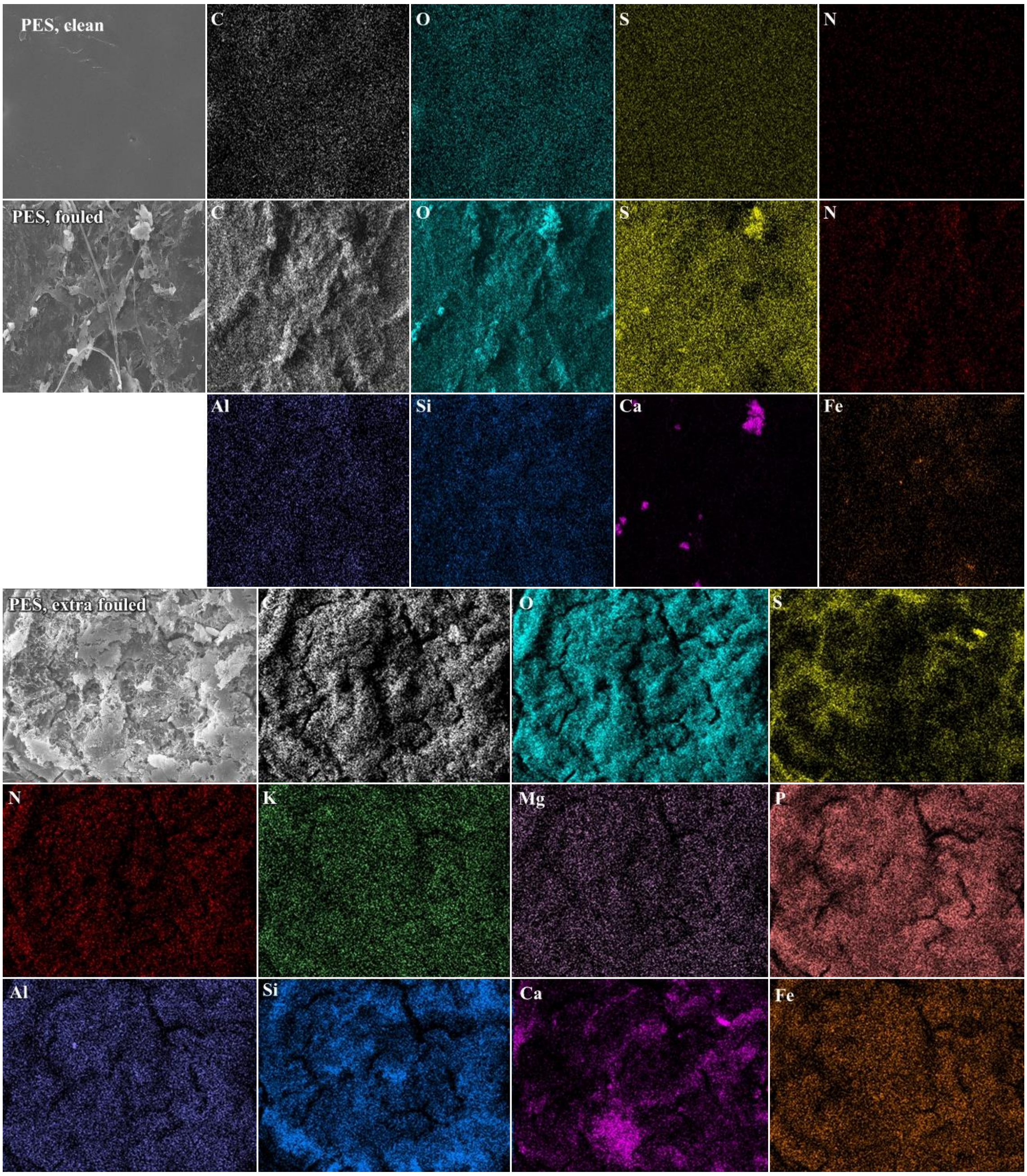

Figure 4.25. EDX elemental mapping of clean, fouled and highly fouled PES membranes.

3.2. Membrane retention

As previously indicated, the semi-quantitative metal analysis showed that the hazardous metals in present in higher concentrations in WAS were Fe, Zn, Mn, Al, Ni, Cu, Cr and Pb, in that order. A quantitative analysis of these 8 metals provided their initial concentrations, which are shown in Fig. 4.26.

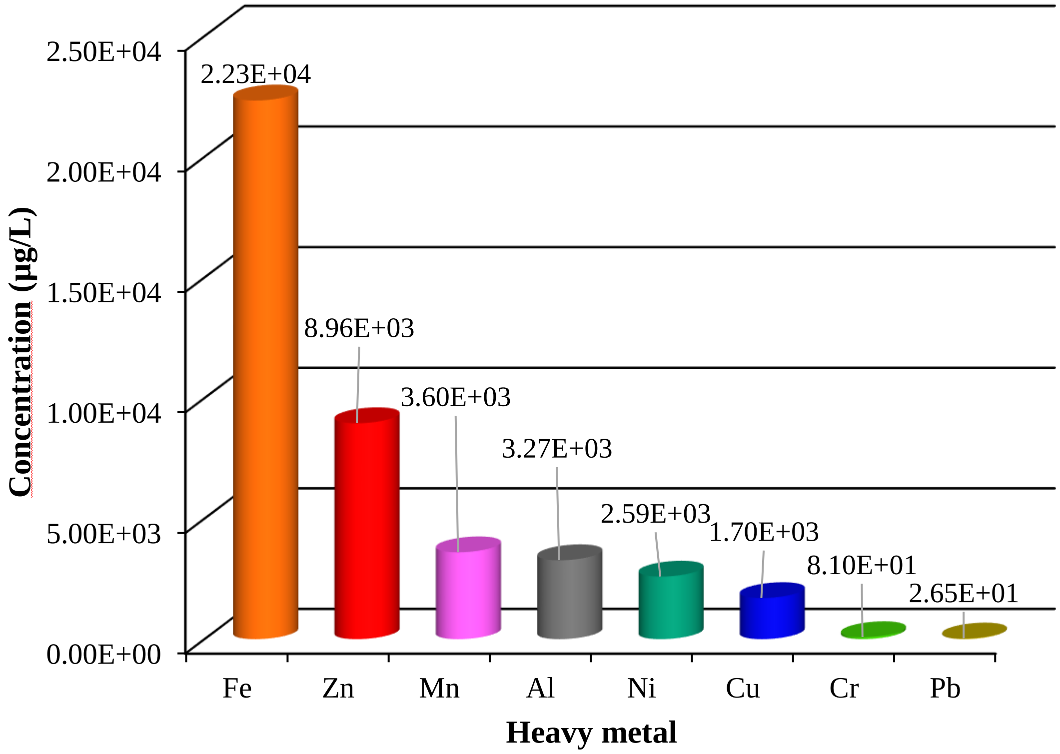

Figure 4.26. Concentrations of the eight most present heavy metals in the oxidised waste activated sludge.

Contrary to expectations based on the cut-off size of the membranes and in line with the findings from the EDX analysis, all metals were significantly retained by the four 50 kDa membranes (Fig. 4.27). The highest retentions were achieved with the PES membrane for all metals, except for Pb, which exhibited the highest value in the PAN membrane. Remarkably high retentions, reaching up to 96% (Al retention with the PES membrane) were obtained. Even the least retained metal, Mn, showed acceptable mean retentions (41% with the PES membrane).

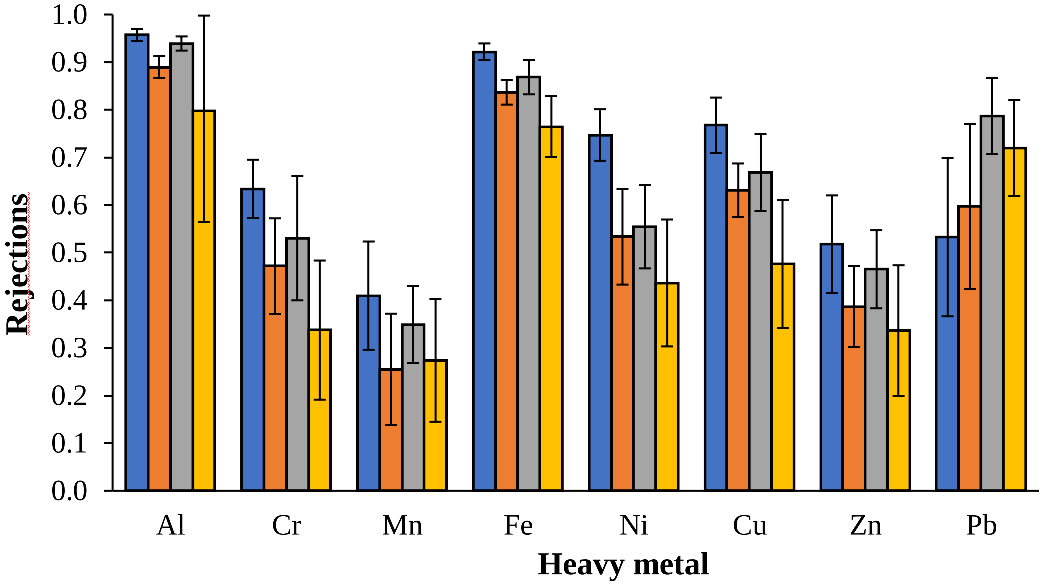

Figure 4.27. Mean heavy metal retentions with PES (🟦), PESH (🟧), PAN (■) and PVDF (🟨) membranes.

The metal retention by the 50 kDa membranes could be explained by various mechanisms, including metal precipitation or complexation with macromolecules present in the WAS, such as proteins, carbohydrates or humic acids. In this sense, Juang et al. [68] observed increased retention of Cu(II), Co(II), Ni(II) and Zn(II) retention with membranes of 10 and 30 kDa, achieved through complexation with chitosan (a high molecular weight carbohydrate) and precipitation induced by pH shifting. Thus, the effect of pH proved to be crucial, as retentions increased from below 0.2 to almost 1 after shifting the pH to values over 6, due to the formation of crystal precipitates. To investigate whether complexation with metals occurred, photolumiscence and absorption spectra measurements were carried out. As the protein-metal interaction has been thoroughly studied [42,69–71], and given the prevalence of humic acids in the oxidised WAS, these measurements aimed to determine the formation of metal-humic acid complexes, and their formation constants.

3.3. Analysis of the formation of metal-humic acid complexes: photolumiscence and absorption spectra measurements

Firstly, fluorescence lifetime was measured to assess whether the quenching between every metal and humic acid was static or dynamic quenching; i.e., if the formation of metal-humic acid complexes was taking place in the oxidised WAS.

Table 4.18 confirms that for every metal the quenching effect is due to static quenching, thereby proving that these metals can form ground-state complexes with humic acid.

Table 4.18. Lifetime measured for 10 ppm humic acid water solution and humic acid water solution with 20 ppm for each metal element.

Lifetimes (ns)

	τ_1	τ_2	τ_3	X_2
Humic acid	0.8	3.5	7.6	1.2
	τ_1/τ	τ_2/τ	τ_3/τ	
Fe	1	1.03	1	
Cu	1	1	1	
Ni	0.9	1	0.99	
Cr	1.15	0.95	1.03	
Zn	1.15	1	1	
Pb	1	1.07	0.97	
Al	1.15	0.95	0.97	
Mn	0.9	1	1.04	

The formation constant for the reaction can be calculated using Eq. 9. Stern-Volmer plot for fluorescence quenching at 513 nm between F_0/F and [Q] were found linear and the slop gives the formation constant between humic acid and metal (Fe is depicted in Fig. 4.28 as an example). Table 4.19 shows the calculated formation constant for each metal ion.

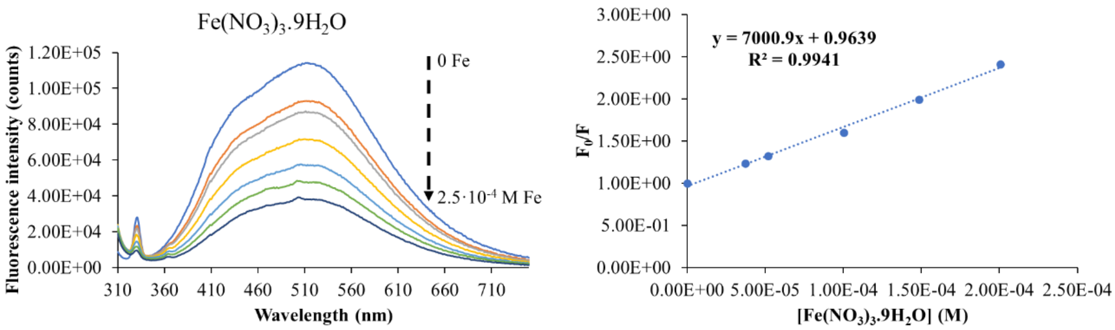

Figure 4.28. Left: Effect of concentration of $Fe(NO_3)_3.9H_2O$ (0, 0.37, 0.52, 1, 1.49, 2, $2.52 \cdot 10^{-4}$ mol/L) on fluorescence intensity of humic acid. Right: Stern-Volmer calibration curve of $Fe(NO_3)_3.9H_2O$.

Table 4.19. Calculated formation constant between humic acid and each metal ion.

	Ks (M^{-1})
Fe^{3+}	7000 ± 417
Cu^{2+}	60053 ± 3220
Ni^{2+}	18676 ± 965
Cr^{3+}	11639 ± 379
Zn^{2+}	4350 ± 152
Pb^{2+}	738± 96
Al^{3+}	822 ± 40
Mn^{3+}	1573 ± 116

The observed formation constants indicated strong complex formation between Cu^{2+}, Ni^{2+} and Cr^{3+} with the measured humic acid, suggesting a significant role of complexation in the retention of these three metal species.

Despite its notable affinity for humic acid, Cu^{2+} is well-known for forming stable complex with proteins [72–74]. However, Al^{3+} and Fe^{3+} exhibited higher retention than this metal.

Even though Al^{3+} displayed a low formation constant, the observed retentions were the highest. The formation of precipitates can explain this phenomenon, as evidenced in the mapping (Fig. 4.25, Figs. A.4.4-6). These precipitates may have formed during the oxidation process. For instance, the hydrolysis of Al^{3+} into boehmite have been reported under conditions of high pressure and temperature in aqueous solutions [75].

Fe^{3+} was the second most retained metal, although its measured formation constant not reflecting such a high affinity for humic acid. The prevalence of iron as a common metal cofactor [76] suggests that its complexation may primarily occur with proteins. Additionally, the low solubility of Fe^{3+} and the oxidation of the WAS may lead to precipitation in the form of ferric oxides, as can be observed in the EDX surface mapping (Fig. 4.25, Fig. A.4.4, Fig. A.4.5). It should be noted that, in bacteria, Fe^{3+} strongly binds to siderophores, small peptidic compounds with formation constants often greater than 1030. However, due to their low molecular weight (600-1500 Da), they would not be retained by the 50 kDa membranes [77].

Ni^{2+} and Cr^{3+} also exhibited significant formation constants with several aminoacids [72,73,78]. However, low formation constants (of log Ks≈2) have been reported for complexes of Ni^{2+} with bean protein extracts [79], and log K values ranging from 2 to 9 with different Hpn-like bacterial proteins [80].

Protein can also serve as major ligands for Pb^{2+}, Zn^{2+} and Mn^{3+} [81–83], and some precipitation was observed for Zn^{2+} with the EDX mapping (Fig. A.4.6). Pb^{2+} has the capability to displace relative metal ions, such as calcium and zinc, in proteins, with oxygen atoms acting as their primary ligand [82]. The high retentions observed for Pb^{2+}, not reflected by its measured formation constant with humic acid, may be explained by a displacement of the complex formation equilibrium caused by the ample excess of humic acid and the low concentration of Pb^{2+} ions.

Additionally, although no Pb precipitates could be observed in the EDX mapping, the high value at lower wavelengths of Pb + humic acids (Fig. A.4.7) implies that precipitation of the aggregates may occur.

4. Conclusions

The main hazardous metals present in the oxidised WAS were Fe, Zn, Mn, Al, Ni, Cu, Cr and Pb, in that order, with concentrations that ranged from 22.3 ± 0.3 ppm to 2.65 ± 0.01 ppb. The PES membrane exhibited higher retentions up to 96%, except for Pb, where the highest ones were achieved with the PAN membrane. The least retained metal was found to be Mn, with mean retentions around 41% with PES membrane.

Photolumiscence and absorption spectra measurements confirmed that all the studied metals formed ground-state complexes with humic acids, Cu^{2+}, Ni^{2+} and Cr^{3+} being the metal ions which formed the strongest complexes. Other mechanisms, such as complexation with proteins and precipitation, may also contributed to metal retention.

SEM-EDX analysis of the fouled membranes of PES, PESH, PAN and PVDF revealed that fouling comprised cake layer formation, mainly due to the retention of proteins and humic acids, and crystal structures composed of calcium, copper and zinc sulphates or magnesium silicate, among others. Additionally, no foulants were detected within the pores of the membranes according to SEM-EDX cross-sectional analysis, indicating that fouling was predominantly superficial, and metal retention occurred in the membrane surface. A noticeable compression of the membranes was also observed after filtration, which can be attributed to the applied pressure.

Declaration of Competing Interest

The authors declare that they have no known competing financial interests or personal relationships that could have appeared to influence the work reported in this paper.

Acknowledgements

The authors are grateful for the financial support from the Spanish Ministry of Science and Innovation through the projects MCIU-19-RTI2018-094218-B-I00 and MCIU-22-PID2021-

125942OB-I00.. Authors also want to acknowledge the Employment, Industry and Tourism Office of the Principality of Asturias, Spain, for their financial support through the project AYUD/2021/51041. The author Daniel Núñez thanks the Principality of Asturias, Spain, for their financial support through the Severo Ochoa scholarship no BP19-093.

References

[1] J.A. Villamil, A.F. Mohedano, J. San Martín, J.J. Rodriguez, M.A. de la Rubia, Anaerobic co-digestion of the process water from waste activated sludge hydrothermally treated with primary sewage sludge. A new approach for sewage sludge management, Renew. Energy. 146 (2020) 435–443. doi:10.1016/j.renene.2019.06.138.

[2] Eurostat, Sewage sludge production and disposal from urban wastewater (in dry substance (d.s)), 2022. (2022). https://ec.europa.eu/eurostat/databrowser/view/ten00030/default/table?lang=en (accessed January 24, 2022).

[3] W.Q. Guo, S.S. Yang, W.S. Xiang, X.J. Wang, N.Q. Ren, Minimization of excess sludge production by in-situ activated sludge treatment processes - A comprehensive review, Biotechnol. Adv. 31 (2013) 1386–1396. doi:10.1016/j.biotechadv.2013.06.003.

[4] D. Fytili, A. Zabaniotou, Utilization of sewage sludge in EU application of old and new methods-A review, Renew. Sustain. Energy Rev. 12 (2008) 116–140. doi:10.1016/j.rser.2006.05.014.

[5] J. Mateo-Sagasta, L. Raschid-Sally, A. Thebo, Global Wastewater and Sludge Production, Treatment and Use, in: Wastewater, Springer Netherlands, Dordrecht, 2015: pp. 15–38. doi:10.1007/978-94-017-9545-6_2.

[6] S. Shi, G. Xu, H. Yu, Z. Zhang, Strategies of valorization of sludge from wastewater treatment, J. Chem. Technol. Biotechnol. 93 (2018) 936–944. doi:10.1002/jctb.5548.

[7] M.K. Awasthi, Q. Wang, X. Ren, J. Zhao, H. Huang, S.K. Awasthi, A.H. Lahori, R. Li, L. Zhou, Z. Zhang, Role of biochar amendment in mitigation of nitrogen loss and greenhouse gas emission during sewage sludge composting, Bioresour. Technol. 219 (2016) 270–280. doi:10.1016/j.biortech.2016.07.128.

[8] J. Werther, T. Ogada, Sewage sludge combustion, Prog. Energy Combust. Sci. 25 (1999) 55–116. doi:10.1016/S0360-1285(98)00020-3.

[9] Y. Zhao, W. Lu, A. Damgaard, Y. Zhang, H. Wang, Assessment of co-composting of sludge and woodchips in the perspective of environmental impacts (EASETECH), Waste Manag. 42 (2015) 55–60. doi:10.1016/j.wasman.2015.04.021.

[10] Q. Chen, X. An, H. Li, J. Su, Y. Ma, Y.G. Zhu, Long-term field application of sewage sludge increases the abundance of antibiotic resistance genes in soil, Environ. Int. 92–93 (2016) 1–10. doi:10.1016/j.envint.2016.03.026.

[11] D.L. Lewis, D.K. Gattie, Pathogen risks from applying sewage sludge to land, Environ. Sci. Technol. 36 (2002). doi:10.1021/es0223426.

[12] J. Dai, M. Xu, J. Chen, X. Yang, Z. Ke, PCDD/F, PAH and heavy metals in the sewage sludge from six wastewater treatment plants in Beijing, China, Chemosphere. 66 (2007) 353–361. doi:10.1016/j.chemosphere.2006.04.072.

[13] P.C. Hsiau, S.L. Lo, Extractabilities of heavy metals in chemically-fixed sewage sludges, in: J. Hazard. Mater., 1998: pp. 73–82. doi:10.1016/S0304-3894(97)00121-0.

[14] D. Elalami, H. Carrere, F. Monlau, K. Abdelouahdi, A. Oukarroum, A. Barakat, Pretreatment and co-digestion of wastewater sludge for biogas production: Recent research advances and trends, Renew. Sustain. Energy Rev. 114 (2019) 109287. doi:10.1016/j.rser.2019.109287.

[15] J. Gao, W. Weng, Y. Yan, Y. Wang, Q. Wang, Comparison of protein extraction methods from excess activated sludge, Chemosphere. 249 (2020). doi:10.1016/j.chemosphere.2020.126107.

[16] G. Saxena, D. Purchase, S.I. Mulla, G.D. Saratale, R.N. Bharagava, Phytoremediation of heavy metal-contaminated sites: Eco-environmental concerns, field studies, sustainability issues, and future prospects, Rev. Environ. Contam. Toxicol. 249 (2020) 71–131. doi:10.1007/398_2019_24.

[17] J.W. Lee, C.K. Lee, C.S. Moon, I.J. Choi, K.J. Lee, S.M. Yi, B.K. Jang, B. jun Yoon, D.S. Kim, D. Peak, D. Sul, E. Oh, H. Im, H.S. Kang, J.H. Kim, J.T. Lee, K. Kim, K.L. Park, R. Ahn, S.H. Park, S.C. Kim, C.H. Park, J.H. Lee, Korea National Survey for Environmental Pollutants in the Human Body 2008: Heavy metals in the blood or urine of the Korean population, Int. J. Hyg. Environ. Health. 215 (2012) 449–457. doi:10.1016/j.ijheh.2012.01.002.

[18] A. Pathak, M.G. Dastidar, T.R. Sreekrishnan, Bioleaching of heavy metals from sewage sludge: A review, J. Environ. Manage. 90 (2009) 2343–2353. doi:10.1016/j.jenvman.2008.11.005.

[19] J.E. Emurotu, P.C. Onianwa, Bioaccumulation of heavy metals in soil and selected food crops cultivated in Kogi State, north central Nigeria, Environ. Syst. Res. 6 (2017) 21. doi:10.1186/s40068-017-0098-1.

[20] A.S. Shafiuddin Ahmed, S. Sultana, A. Habib, H. Ullah, N. Musa, M. Belal Hossain, M. Mahfujur Rahman, M. Shafiqul Islam Sarker, Bioaccumulation of heavy metals in some commercially important fishes from a tropical river estuary suggests higher potential health risk in children than adults, PLoS One. 14 (2019). doi:10.1371/journal.pone.0219336.

[21] P. Li, J. Zhang, H. Xie, C. Liu, S. Liang, Y. Ren, W. Wang, Heavy metal bioaccumulation and health hazard assessment for three fish species from Nansi Lake, China, Bull. Environ. Contam. Toxicol. 94 (2015) 431–436. doi:10.1007/s00128-015-1475-y.

[22] M.I. Khan, M. Khisroon, A. Khan, N. Gulfam, M. Siraj, F. Zaidi, Ahmadullah, Abidullah, S.H. Fatima, S. Noreen, Hamidullah, Z.A. Shah, F. Qadir, Bioaccumulation of heavy metals in water, sediments, and tissues and their histopathological effects on anodonta cygnea (Linea, 1876) in Kabul River, Khyber Pakhtunkhwa, Pakistan, Biomed Res. Int. 2018 (2018). doi:10.1155/2018/1910274.

[23] C. Di Bella, A. Traina, C. Giosuè, D. Carpintieri, G.M. Lo Dico, A. Bellante, M. Del Core, F. Falco, S. Gherardi, M.M. Uccello, V. Ferrantelli, Heavy Metals and PAHs in Meat, Milk, and Seafood From Augusta Area (Southern Italy): Contamination Levels, Dietary Intake, and Human Exposure Assessment, Front. Public Heal. 8 (2020) 273. doi:10.3389/fpubh.2020.00273.

[24] N. Sarwar, M. Imran, M.R. Shaheen, W. Ishaque, M.A. Kamran, A. Matloob, A. Rehim, S. Hussain, Phytoremediation strategies for soils contaminated with heavy metals: Modifications and future perspectives, Chemosphere. 171 (2017) 710–721. doi:10.1016/j.chemosphere.2016.12.116.

[25] H. Hu, Q. Jin, P. Kavan, A study of heavy metal pollution in China: Current status, pollution-control policies and countermeasures, Sustain. 6 (2014) 5820–5838. doi:10.3390/su6095820.

[26] P.B. Tchounwou, C.G. Yedjou, A.K. Patlolla, D.J. Sutton, Heavy metal toxicity and the environment, EXS. 101 (2012) 133–164. doi:10.1007/978-3-7643-8340-4_6.

[27] S.L. O'Neal, W. Zheng, Manganese Toxicity Upon Overexposure: a Decade in Review, Curr. Environ. Heal. Reports. 2 (2015) 315–328. doi:10.1007/s40572-015-0056-x.

[28] D. Krewski, R.A. Yokel, E. Nieboer, D. Borchelt, J. Cohen, J. Harry, S. Kacew, J. Lindsay, A.M. Mahfouz, V. Rondeau, Human health risk assessment for aluminium, aluminium oxide, and aluminium hydroxide, J. Toxicol. Environ. Heal. - Part B Crit. Rev. 10 (2007) 1–269. doi:10.1080/10937400701597766.

[29] M. Park, N. Kim, S. Lee, S. Yeon, J.H. Seo, D. Park, A study of solubilization of sewage sludge by hydrothermal treatment, J. Environ. Manage. 250 (2019) 109490. doi:10.1016/J.JENVMAN.2019.109490.

[30] J. Luo, Q. Zhang, J. Zhao, Y. Wu, L. Wu, H. Li, M. Tang, Y. Sun, W. Guo, Q. Feng, J. Cao, D. Wang, Potential influences of exogenous pollutants occurred in waste activated sludge on anaerobic digestion: A review, J. Hazard. Mater. 383 (2020) 121176. doi:10.1016/J.JHAZMAT.2019.121176.

[31] C. Qiu, Y. Bi, J. Zheng, D. Wang, C. Wang, N. Liu, S. Wang, L. Sun, Effect of ozonation treatment on the chemical speciation distributions of heavy metals in sewage sludge and subsequent bioleaching process, Environ. Sci. Pollut. Res. 27 (2020) 19946–19954. doi:10.1007/s11356-020-08539-0.

[32] T.A. Özbelge, H.Ö. Özbelge, P. Altinten, Effect of acclimatization of microorganisms to heavy metals on the performance of activated sludge process, J. Hazard. Mater. 142 (2007) 332–339. doi:10.1016/J.JHAZMAT.2006.08.031.

[33] J. Deng, X. Feng, X. Qiu, Extraction of heavy metal from sewage sludge using ultrasound-assisted nitric acid, Chem. Eng. J. 152 (2009) 177–182. doi:10.1016/J.CEJ.2009.04.031.

[34] X. Zhang, Y. Tian, Q. Wang, L. Chen, X. Wang, Heavy metal distribution and speciation during sludge reduction using aquatic worms, Bioresour. Technol. 126 (2012) 41–47. doi:10.1016/J.BIORTECH.2012.09.015.

[35] T.A. Saleh, V.K. Gupta, An Overview of Membrane Science and Technology, in: Nanomater. Polym. Membr., Elsevier, 2016: pp. 1–23. doi:10.1016/B978-0-12-804703-3.00001-2.

[36] N.A.A. Qasem, R.H. Mohammed, D.U. Lawal, Removal of heavy metal ions from wastewater: a comprehensive and critical review, Npj Clean Water. 4 (2021). doi:10.1038/s41545-021-00127-0.

[37] SAMCO, How Much Do Microfiltration and Ultrafiltration Membrane Systems Cost?, (2017). https://www.samcotech.com/how-much-do-microfiltration-and-ultrafiltration-membrane-systems-cost/ (accessed January 25, 2022).

[38] SAMCO, How Much Do Reverse Osmosis and Nanofiltration Systems Cost?, (2017). https://www.samcotech.com/much-reverse-osmosis-nanofiltration-membrane-systems-cost/ (accessed January 25, 2022).

[39] N.H. Baharuddin, N.M.N. Sulaiman, M.K. Aroua, Removal of heavy metal ions from mixed solutions via polymer-enhanced ultrafiltration using starch as a water-soluble biopolymer, Environ. Prog. Sustain. Energy. 34 (2015) 359–367. doi:10.1002/EP.11995.

[40] J. Huang, F. Qi, G. Zeng, L. Shi, X. Li, Y. Gu, Y. Shi, Repeating recovery and reuse of SDS micelles from MEUF retentate containing Cd2+ by acidification UF, Colloids Surfaces A Physicochem. Eng. Asp. 520 (2017) 361–368. doi:10.1016/J.COLSURFA.2017.02.001.

[41] K. Xiao, Y. Chen, X. Jiang, W.Y. Seow, C. He, Y. Yin, Y. Zhou, Comparison of different treatment methods for protein solubilisation from waste activated sludge, Water Res. 122 (2017) 492–502. doi:10.1016/J.WATRES.2017.06.024.

[42] M.J. Tamás, S.K. Sharma, S. Ibstedt, T. Jacobson, P. Christen, Heavy Metals and Metalloids As a Cause for Protein Misfolding and Aggregation, Biomolecules. 4 (2014) 252. doi:10.3390/BIOM4010252.

[43] J.D. García-García, R. Sánchez-Thomas, R. Moreno-Sánchez, Bio-recovery of non-essential heavy metals by intra- and extracellular mechanisms in free-living microorganisms, Biotechnol. Adv. 34 (2016) 859–873. doi:10.1016/J.BIOTECHADV.2016.05.003.

[44] J.L. Urrea, S. Collado, P. Oulego, M. Díaz, Formation and Degradation of Soluble Biopolymers during Wet Oxidation of Sludge, ACS Sustain. Chem. Eng. 5 (2017) 3011–3018. doi:10.1021/acssuschemeng.6b02664.

[45] W. Bleam, Natural Organic Matter, (2017). doi:10.1016/B978-0-12-804178-9.00007-0.

[46] B.A.G. De Melo, F.L. Motta, M.H.A. Santana, Humic acids: Structural properties and multiple functionalities for novel technological developments, Mater. Sci. Eng. C. 62 (2016) 967–974. doi:10.1016/J.MSEC.2015.12.001.

[47] P. Boguta, Z. Sokołowska, Interactions of humic acids with metals, Acta Agrophysica Monogr. (2013) 1–113.

[48] S. Wu, R. Li, S. Peng, Q. Liu, X. Zhu, Effect of humic acid on transformation of soil heavy metals, in: IOP Conf. Ser. Mater. Sci. Eng., 2017. doi:10.1088/1757-899X/207/1/012089.

[49] E. Slavik, R. Galessi, A. Rapisardi, R. Salvetti, P. Bonzagni, G. Bertanza, L. Menoni, D. Orhon, S. Sözen, Wet Oxidation as an Advanced and Sustainable Technology for Sludge Treatment and Management: Results from Research Activities and Industrial-Scale Experiences, Dry. Technol. 33 (2015) 1309–1317. doi:10.1080/07373937.2015.1036282.

[50] J. Hwang, L. Zhang, S. Seo, Y.W. Lee, D. Jahng, Protein recovery from excess sludge for its use as animal feed, Bioresour. Technol. 99 (2008) 8949–8954. doi:10.1016/j.biortech.2008.05.001.

[51] H. Li, Y. Jin, Y. Nie, Application of alkaline treatment for sludge decrement and humic acid recovery, Bioresour. Technol. 100 (2009) 6278–6283. doi:10.1016/j.biortech.2009.07.022.

[52] J.M. Gohil, R.R. Choudhury, Introduction to Nanostructured and Nano-enhanced Polymeric Membranes: Preparation, Function, and Application for Water Purification, in: Nanoscale Mater. Water Purif., Elsevier, 2018: pp. 25–57. doi:10.1016/B978-0-12-813926-4.00038-0.

[53] L. Pola, L. Fernández-García, S. Collado, P. Oulego, M. Díaz, Macronutrient solubilisation during hydrothermal treatment of sewage sludge, J. Water Process Eng. 43 (2021) 102270. doi:10.1016/J.JWPE.2021.102270.

[54] L. Pola, S. Collado, P. Oulego, M. Díaz, Production of carboxylic acids from the non-lignin residue of black liquor by hydrothermal treatments, Bioresour. Technol. 284 (2019) 105–114. doi:10.1016/j.biortech.2019.03.066.

[55] D.A. Skoog, F.J. Holler, S.R. Crouch, Principles of Instrumental Analysis, Seventh Ed, Cengage Learning, Boston, 2017.

[56] J. Yan, Y. Yu, B. Kong, S. Zhao, Highly sensitive detection of sulfasalazine based on the fluorescence quenching of a terbium complex probe, Microchem. J. 154 (2020) 104553. doi:10.1016/J.MICROC.2019.104553.

[57] Q. Wu, C. Li, Y. Hu, Y. Liu, Study of caffeine binding to human serum albumin using optical spectroscopic methods, Sci. China Ser. B Chem. 2009 5212. 52 (2009) 2205–2212. doi:10.1007/S11426-009-0114-Z.

[58] J.R. Lakowicz, Principles of fluorescence spectroscopy, Springer, 2006. doi:10.1007/978-0-387-46312-4.

[59] A. Kowalik-Klimczak, A. Bednarska, M. Grądkowski, Scanning Electron Microscopy (Sem) in the Analysis of the Structure, Probl. Eksploat. – Maint. Probl. 1 (2016) 119–128.

[60] D.Q. Cao, X. Wang, Q.H. Wang, X.M. Fang, J.Y. Jin, X. Di Hao, E. Iritani, N. Katagiri, Removal of heavy metal ions by ultrafiltration with recovery of extracellular polymer substances from excess sludge, J. Memb. Sci. 606 (2020) 118103. doi:10.1016/j.memsci.2020.118103.

[61] S. Hamzah, N. Ali, M.M. Ariffin, A. Ali, A.W. Mohammad, High performance of polysulfone ultrafiltration membrane: Effect of polymer concentration, ARPN J. Eng. Appl. Sci. 9 (2014) 2543–2550.

[62] F.Y.C. Huang, C. Medin, A. Arning, Mechanical Vibration for the Control of Membrane Fouling in Direct Contact Membrane Distillation, Symmetry 2019, Vol. 11, Page 126. 11 (2019) 126. doi:10.3390/SYM11020126.

[63] D. Li, T.S. Chung, R. Wang, Morphological aspects and structure control of dual-layer asymmetric hollow fiber membranes formed by a simultaneous co-extrusion approach, J. Memb. Sci. 243 (2004) 155–175. doi:10.1016/j.memsci.2004.06.014.

[64] D. Li, T.S. Chung, R. Wang, Y. Liu, Fabrication of fluoropolyimide/polyethersulfone (PES) dual-layer asymmetric hollow fiber membranes for gas separation, J. Memb. Sci. 198 (2002) 211–223. doi:10.1016/S0376-7388(01)00658-5.

[65] S. Stade, M. Kallioinen, A. Mikkola, T. Tuuva, M. Mänttäri, Reversible and irreversible compaction of ultrafiltration membranes, Sep. Purif. Technol. 118 (2013) 127–134. doi:10.1016/j.seppur.2013.06.039.

[66] D.M. Davenport, C.L. Ritt, R. Verbeke, M. Dickmann, W. Egger, I.F.J. Vankelecom, M. Elimelech, Thin film composite membrane compaction in high-pressure reverse osmosis, J. Memb. Sci. 610 (2020) 118268. doi:10.1016/j.memsci.2020.118268.

[67] A. Basile, A. Cassano, N.K. Rastogi, Advances in Membrane Technologies for Water Treatment: Materials, Processes and Applications, 2015. doi:10.1016/C2013-0-16469-0.

[68] R.S. Juang, R.C. Shiau, Metal removal from aqueous solutions using chitosan-enhanced membrane filtration, J. Memb. Sci. 165 (2000) 159–167. doi:10.1016/S0376-7388(99)00235-5.

[69] A. Rodzik, P. Pomastowski, G.N. Sagandykova, B. Buszewski, Interactions of whey proteins with metal ions, Int. J. Mol. Sci. 21 (2020) 1–26. doi:10.3390/ijms21062156.

[70] J. Steinhardt, J.A. Reynolds, Metal-Ion Binding, Mult. Equilibria Proteins. (1969) 214–233. doi:10.1016/B978-0-12-665450-9.50010-4.

[71] C. Guo, M. Cheng, M.L. Gross, Protein-Metal-Ion Interactions Studied by Mass Spectrometry-Based Footprinting with Isotope-Encoded Benzhydrazide, Anal. Chem. 91 (2019) 1416–1423. doi:10.1021/acs.analchem.8b04088.

[72] C. Conato, H. Kozlowski, P. Mlynarz, F. Pulidori, M. Remelli, Copper and nickel complex-formation equilibria with Lys–Gly–His–Lys, a fragment of the matricellular protein SPARC, Polyhedron. 21 (2002) 1469–1474. doi:10.1016/S0277-5387(02)00952-X.

[73] Y. Sugiura, Y. Hirayama, Cu(II) and Ni(II) Complexes of Sulfhydryl Peptides Contribution from the Faculty of Pharmaceutical Structural and Electronic Effects on Complex Formation of Copper(II) and Nickel(II) with Sulfhydryl-Containing Peptides, Inorg. Chem. 15 (1976) 679.

[74] P.G. Daniele, E. Prenesti, R. Aigotti, G. Ostacoli, Complex formation between copper(II) and hippuryl-L-histidyl-L-leucine in aqueous solution: A model for coordination properties of internal chains of proteins, J. Inorg. Biochem. 58 (1995) 139–146. doi:10.1016/0162-0134(94)00049-G.

[75] D.D. Macdonald, P. Butler, D. Owen, Hydrothermal Hydrolysis of Al3+ and the Precipitation of Boehmite from Aqueous Solution, (n.d.).

[76] I. Sepúlveda Cisternas, J.C. Salazar, V.A. García-Angulo, Overview on the Bacterial Iron-Riboflavin Metabolic Axis, Front. Microbiol. 0 (2018) 1478. doi:10.3389/FMICB.2018.01478.

[77] S.M. Glasauer, E.P. Burford, G.M. Gadd, Transformation of metals and metalloids by microorganisms, Ref. Modul. Earth Syst. Environ. Sci. (2022). doi:10.1016/B978-0-12-822974-3.00011-2.

[78] E.G. Vinokurov, V. V. Bondar’, Prediction of Stability Constants for Cr(III) and Cr(II) Complexes, Russ. J. Coord. Chem. Khimiya. 29 (2003) 66–72. doi:10.1023/A:1021851219309.

[79] K. Lange-Hesse, L. Dunemann, G. Schwedt, Properties and binding forms of cadmium and nickel in protein extracts from bean seeds (Phaseolus vulgaris L.), Fresenius’ J. Anal. Chem. 1994 3496. 349 (1994) 460–464. doi:10.1007/BF00322934.

[80] D. Witkowska, A. Szebesczyk, J. Wątły, M. Braczkowski, M. Rowińska-żyrek, A Comparative Study on Nickel Binding to Hpn-like Polypeptides from Two Helicobacter pylori Strains, Int. J. Mol. Sci. 22 (2021). doi:10.3390/IJMS222413210.

[81] A. Krężel, W. Maret, The biological inorganic chemistry of zinc ions, Arch. Biochem. Biophys. 611 (2016) 3–19. doi:10.1016/j.abb.2016.04.010.

[82] H.C. Gonick, Lead-binding proteins: A review, J. Toxicol. 2011 (2011). doi:10.1155/2011/686050.

[83] S. Udayalaxmi, M.R. Gangula, K. Ravikiran, P. Ettaiah, Investigation of manganese metal coordination in proteins: a comprehensive PDB analysis and quantum mechanical study, Struct. Chem. 31 (2020) 1057–1064. doi:10.1007/S11224-020-01488-X/FIGURES/6.

Supplementary Information to

'Heavy metal removal from hydrothermally treated waste activated sludge by ultrafiltration with polymeric membranes'

Daniel Núñez[1], Paula Oulego[1], Mahdi Nikbakht Fini[2], Jorge Espina-Casado[3], Jens Muff[2], Sergio Collado[1], Francisco A. Riera[1], Mario Díaz[1]*

[1]Department of Chemical and Environmental Engineering, University of Oviedo.

c/ Julián Clavería 8, 33006, Oviedo, Spain

[2]Department of Chemistry and Bioscience, Aalborg University Esbjerg, Niels Bohrs Vej 8,

Esbjerg, 6700, Denmark

[3]Department of Physical and Analytical Chemistry, University of Oviedo, c/ Julián

Clavería 8, 33006, Oviedo, Spain

*Corresponding author's e-mail: mariodiaz@uniovi.es

Phone: +34 985 10 34 39, FAX: +34 985 10 34 40

(3 Pages, 4 Figures, 1 Table)

Table of contents

1. EDX analysis

Table A.4.1. EDX analysis of the fouled PES and PVDF membranes (all results in %wt).

PES, fouled					*PVDF, fouled*					
Spectrum	***C***	***N***	***O***	***S***	**Spectrum**	***C***	***N***	***O***	***F***	***Ca***
1	60.72	7.43	15.66	16.19	**1**	30.00	3.34	26.18	32.28	8.19
2	59.39	12.28	19.81	8.52	**2**	43.19	3.78	2.02	51.01	n.d.*
3	54.87	10.69	18.63	15.81	**3**	30.84	4.28	23.05	34.99	6.83
4	60.84	0.68	19.49	18.99	**4**	41.27	4.21	5.90	47.49	1.14
5	58.09	8.84	15.86	17.21						
6	50.59	12.15	21.76	15.50						

n.d.*: not detected.

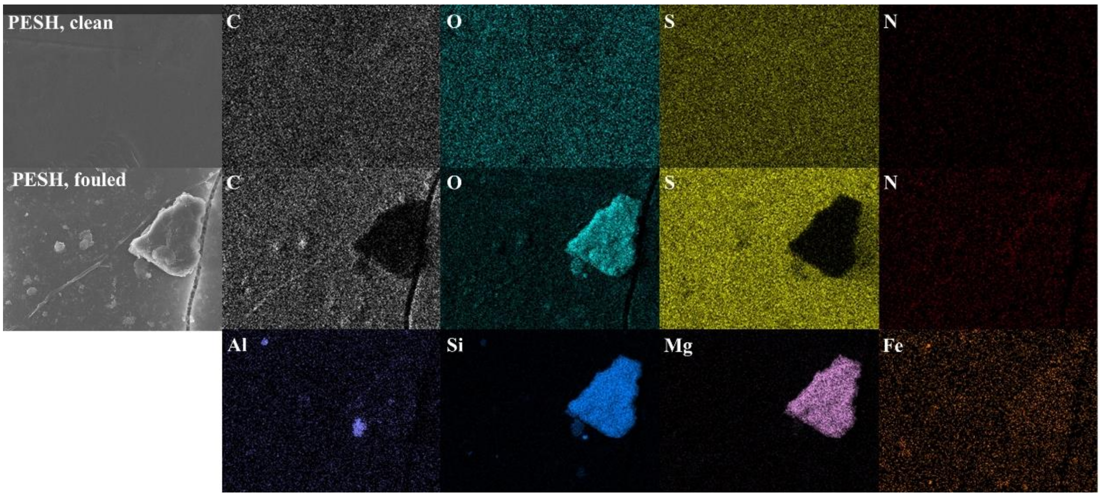

Figure A.4.4. EDX elemental mapping of the surface of clean and fouled PESH membranes.

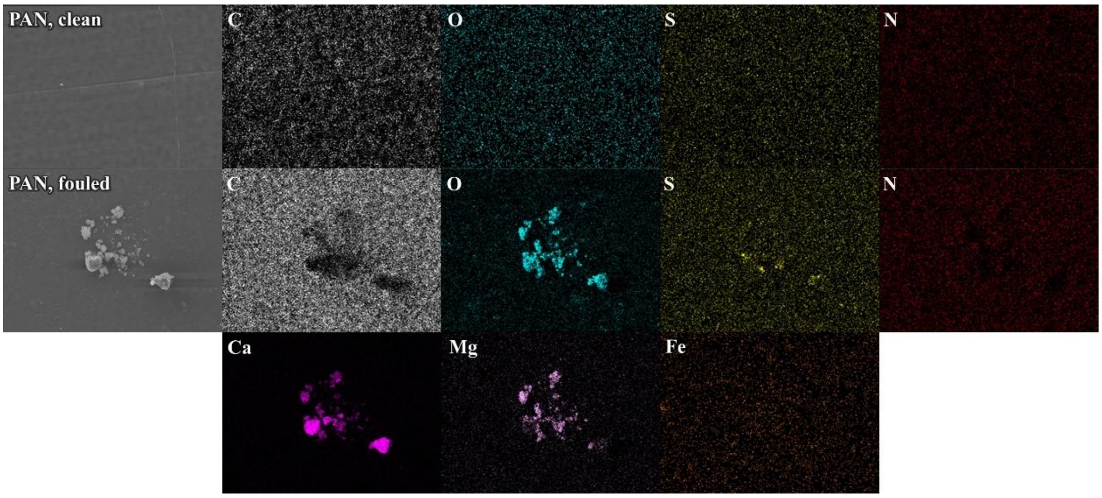

Figure A.4.5. EDX elemental mapping of the surface of clean and fouled PAN membranes.

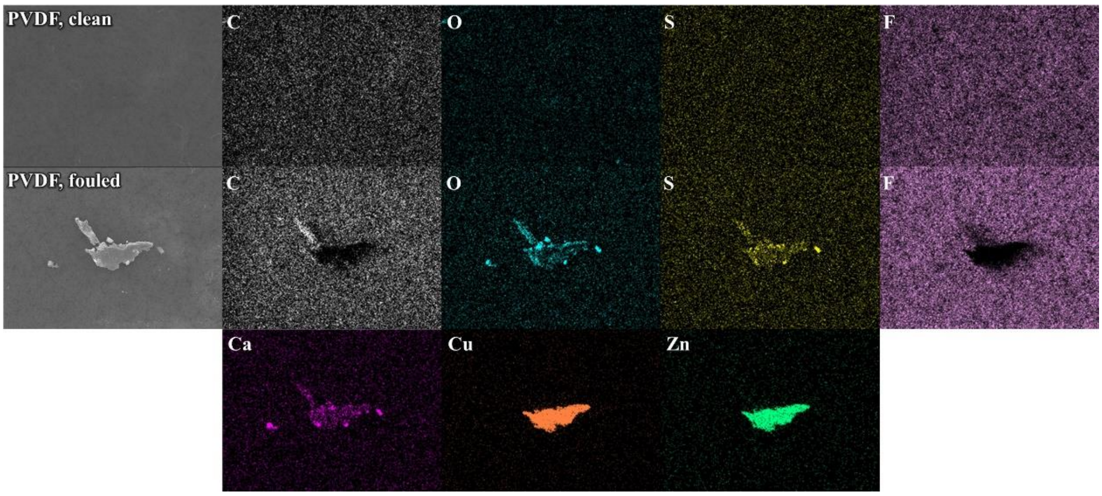

Figure A.4.6. EDX elemental mapping of the surface of clean and fouled PVDF membranes.

2. Photolumiscence and absorption spectra measurements

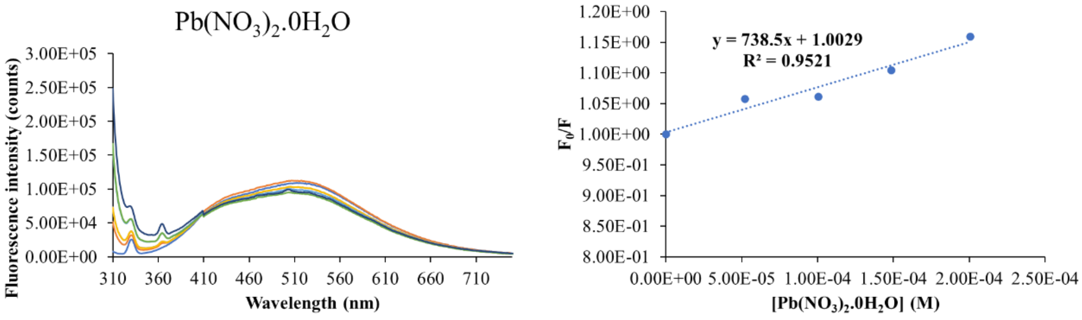

Figure A.4.7. Left: Effect of concentration of Pb(NO$_3$)$_2$.0H$_2$O (0, 0.52, 1.00, 1.49 and 2·10^{-4} mol/L) on fluorescence intensity of humic acid. Right: Stern-Volmer calibration curve of Pb(NO$_3$)$_2$.0H$_2$O.

4.1.4. Separation and purification techniques for the recovery of added-value biocompounds from waste activated sludge. A review

Daniel Núñez, Paula Oulego, Sergio Collado, Francisco A. Riera, Mario Díaz*

Department of Chemical and Environmental Engineering, University of Oviedo.

c/ Julián Clavería 8, 33006, Oviedo, Spain

*Corresponding author’s e-mail: mariodiaz@uniovi.es

Phone: +34 985 10 34 39, FAX: +34 985 10 34 40

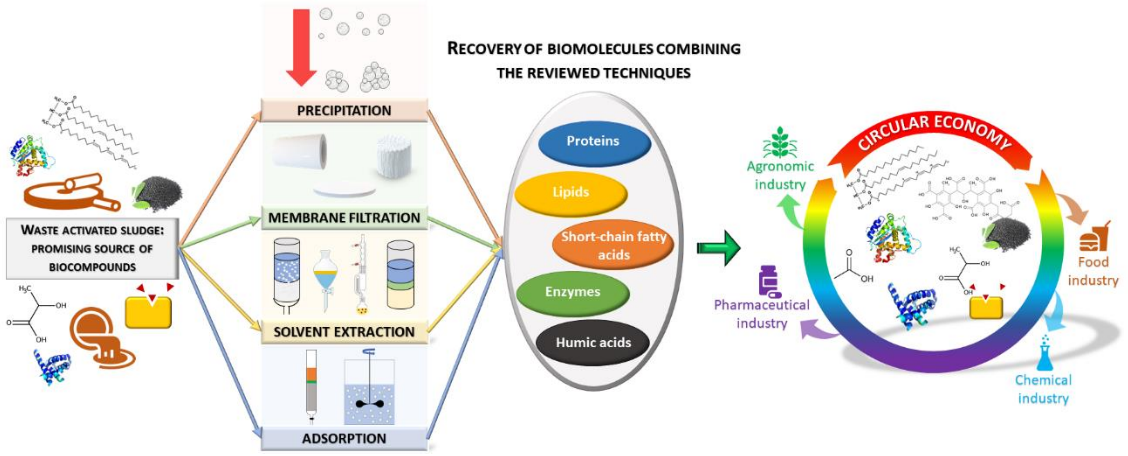

Figura 4.29. Resumen gráfico del artículo *Separation and purification techniques for the recovery of added-value biocompounds from waste activated sludge. A review*.

Artículo publicado en la revista **Conservation, Resources and Recycling**

Cuartil: Q1 **Índice de impacto:** 13.22

Referencia: Daniel Núñez, Paula Oulego, Sergio Collado, Francisco A. Riera, Mario Díaz, Separation and purification techniques for the recovery of added-value biocompounds from waste activated sludge. A review, Resources, Conservation and Recycling, Volume 182, 2022, 106327.

Abstract

The need of developing a new growth model based on circular economy has led to an increasing interest in the revalorization of urban and industrial wastewaters in order to use the resources efficiently. The most stablished way of valorising these residues implies the energy production in the form of biomethane. However, urban and industrial wastewaters can also be considered promising raw sources for the recovery of valuable chemical compounds. Especially, waste activated sludge from water treatment plants is a fantastic source of biomolecules such as lipids (triglycerides or fatty acids), proteins and enzymes, carbohydrates, and humic and fulvic acids. However, prior to the recovery of these biocompounds, sludge solubilization processes (thermal hydrolysis, sonication and acidification, among others) must be conducted, in order to break the cell walls and release the protoplasmic content into the liquid media, thus obtaining a matrix of high complexity, which condition the possible strategies to be applied.

This review gathered and discussed in-depth the studies that deal with the recovery of valuable biocompounds from secondary waste activated sludge. Furthermore, other types of sludge comparable to the activated one, such as cell cultures and food-related sources, have been also discussed here, in order to be used as a starting point for further research on the valorisation of waste activated sludge.

Keywords: Adsorption; biorefinery; circular economy; membrane filtration; precipitation; solvent extraction.

Abbreviations

Abbreviation	Meaning
ADH	Alcohol dehydrogenase
APTES	(3-aminopropyl)triethoxysilane
CAGR	Compound annual growth rate
CFV	Crossflow velocity
MF	Microfiltration
MWCO	Molecular weight cut-off
NF	Nanofiltration
PES	Polyethersulphone
PS	Polysulphone
RC	Regenerated cellulose
RO	Reverse osmosis
SCFAs	Short-chain fatty acids
TCOD	Total COD
TH	Thermal hydrolysis
TMP	Tansmembranar pressure
UF	Ultrafiltration
VCR	Volume concentration ratio
VSS	Volatile suspended solids
WAS	Waste activated sludge
WO	Wet oxidation
PVP	Polyvinylpyrrolidone

1. Introduction

Efficient wastewater management has become a topic of prime concern, due to increasing pressure derived from rapid population growth and increasing public and governmental environmental awareness. One of the main wastewater management challenges is related to waste activated sludge (WAS), which is generated during the secondary treatment stage in the water treatment process. Indeed, around 10 million tons (dry weight basis) of sewage sludge were generated in Europe in 2019 (Eurostat, 2022), and WAS disposal volume is intended to be reduced by 50% by 2050 (as compared with the production rates recorded in 2000) (Fytili and Zabaniotou, 2008). Hence, the development and application of optimized procedures for WAS management will turn even more critical in the upcoming years. Standard methods for WAS management include agricultural use, forestry and land reclamation, incineration, carbonization, co-composting or landfill disposal (Mateo-Sagasta et al., 2015; Shi et al., 2018). All of these treatments pose important health and environmental hazards, such as heavy metals (Hsiau and Lo, 1998), organic pollutants (Dai et al., 2007) or pathogens (Lewis and Gattie, 2002) contamination of soil; increase of antibiotic resistance genes in soil (Chen et al., 2016); greenhouse gas emissions (Awasthi et al., 2016) and air pollution (Werther and Ogada, 1999); or terrestrial acidification and eutrophication (Zhao et al., 2015).

In the latter years, tendencies in environmental management have evolved from eliminating wastes to recycling and valorising them, within the context of circular economy (Geissdoerfer et al., 2017). Many processes for WAS valorisation have focused on total oxidation of sludge, mainly producing biofuels (Bharathiraja et al., 2014; Manara and Zabaniotou, 2012; Rulkens, 2008; Zhao et al., 2014). Nevertheless, this approach leads to the loss of added-value products present in the sludge, since it is mainly composed of bacteria and other microorganisms (Urbain et al., 1993). Therefore, WAS is considered a fantastic source of biorefinery products (Raheem et al., 2018). Its main constituents are summarized in Table 4.20 (Chen et al., 2007; Contreras et al., 2002; García et al., 2017; Gascó and Lobo, 2007; H. Li et al., 2013; Suárez-Iglesias et al., 2017). To that end, it is required a controlled breaking of the biological structures to generate these bio-based products. Less aggressive solubilization processes enable the release of enzymes (Karn and Kumar, 2019; Nabarlatz et al., 2011, 2010; Ni et al., 2017; Yu et al., 2009), bioplastics (Chen, 2017; Liu et al., 2019; Morgan-Sagastume et al., 2010; Pittmann and Steinmetz, 2014), proteins (Hwang et al., 2008; Jimenez et al., 2013; Pervaiz and Sain, 2011; Wei et al., 2016), humic acids (Li et al., 2014a, 2009; Motojima et al., 2012; Wei et al., 2016) and lipids (Dong et al., 2019; Olkiewicz et al., 2014; Revellame et al., 2012; Siddiquee and Rohani, 2011) to the liquid media. The market size of all these biocompounds is forecasted to increase in the following years due to their numerous industrial applications, as it is indicated below. Therefore, WAS valorisation through the recovery of biocompounds such as proteins, enzymes, humic acids, lipids or short-chain fatty acids (SCFAs) appears to be an interesting economic opportunity.

Proteins are biological heteropolymers, composed by subunits of peptides linked by peptide bonds. They have a massive number of sequential and structural arrangements, greatly varying in size (the majority of the proteins are comprised between 20 and 100 kDa (Sokatch, 1969)) and structure (Nussinovitch, 2013; Pollock, 2007). Bulk proteins have several market applications, including food and beverages, personal care and cosmetics, pharmaceuticals, and animal feed, this last application being the most common one for the proteins from microbial sources (Ritala et al., 2017). Protein market size was valued in USD 33.9 billion in 2020, and is expected to grow up to USD 48.1 billion by 2026 (Expert Market Research, 2020a).

Regarding enzymes (a subtype of proteins characterised for catalysing chemical reactions), (Litalien and Beaulieu, 2011), hydrolytic enzymes (proteases, lipases, amylases and cellulases) are the most commercially used ones in the field of cleaning product, food and beverage, biofuel production, and animal feed, among others. Besides, other enzymes, such as dehydrogenases, galactosidases, other glucosidases, and phosphatases, can also be produced and recovered from WAS (Liu and Smith, 2019; Nabarlatz et al., 2010). In this sense, enzymes are considered a valuable product, with a market price near USD 10 billion in 2020 and expected to grow at a compound annual growth rate (CAGR) of 7.5% for the next five years (Expert Market Research, 2020b).

Humic acids are a loosely defined group of molecules, consisting of the fraction of precipitated compounds after the acidification of strong-base extracted natural organic matter (the fraction of organic matter that remains dissolved corresponds to the fulvic acids) (Bleam, 2017). Chemically, they have an undefined composition, varying both in chemical composition and size (comprised between 2.0 and 1300 kDa), but essentially they are amphiphilic weak acidic electrolytes with carboxylic, phenolic or quinone groups, which give them their useful properties, such as being anti-inflammatory, antioxidant, fungicide and bactericide (De Melo et al., 2016). From an economic point of view, they are applied in agriculture, animal feed, ecological remediation, and in more innovative fields promoted by the growing awareness of the health benefits of humic acids, like dietary supplements or pharmaceuticals. However, its commercial use is somehow hindered by the inconsistent efficacy of humic acid products (Market Research Future, 2019). Humic acids market is more restrained, this being valued at USD 503million in 2020 and expected to grow at CAGR of 11.2% during the forecast period 2020-2026 (Mordor Intelligence, 2021).

Lipids are a heterogeneous group of biomolecules with the common property of being soluble in non-polar solvents (IUPAC, 2014a). The most relevant lipids are glycerides (esters of glycerol and fatty acids [aliphatic carboxylic acids] (IUPAC, 2008)), phospholipids (lipids with phosphoric acids as mono- or di-esters (IUPAC, 2014b)) or non-saponifiable lipids like steroids (IUPAC, 2014c). Lipids have a wide range of industrial applications, such as personal care, cosmetics, agrochemicals, animal feed, and biodiesel. Among them, SCFAs (carboxylic acids with an aliphatic chain length of up to six carbon atoms (Silva et al., 2020)) have been widely applied in food, chemical, biochemical, textile, cosmetic or pharmaceutical industries (Panda et al., 2019). The global market for lipids was estimated at USD 6.4 billion in 2020, and it is forecasted to grow at a CAGR of 5.2% to reach USD 9.4 billion by 2027 (MarketWatch, 2022).

As for fatty acids, their global market value was USD 134.2 billion in 2020, and it is expected to grow at a CAGR of 4% to reach USD 148.2 billion by 2023 (Research and Markets, 2021).

Saccharides are polymers of highly variable length and with linear or ramified structures, composed of monosaccharides and that respond to the general formula of $(CH_2O)_n$, (Castro-Puyana et al., 2013). Bacteria are the main source for saccharides in the industry, where are used in the areas of beverages, savoury and snacks or animal feed, among others. Saccharides had a USD 13.5 billion market value in 2020, and are expected to grow at a CAGR of over 5% in the period between 2020 and 2030 (Fact.MR, 2020).

To sum up, the bioproducts that can be obtained from WAS have a current global market size of almost USD 200 billion, proving that its revalorization is economically interesting, and essential to make more sustainable WAS management.

Table 4.20. Biocompounds content in WAS.

Parameter	**Units**	**Value**
pH		6.5-8.0
TSS	g/L	8.3-33
VSS	%TSS	59-88
COD	gO_2/L	5.88-43.82
Carbohydrates	mg/L	506.3-3234
Proteins	mg/L	2656-13530
Lipids	mg/L	166-3960
Humic acids	mg/L	196.71-5849
SCFAs	mg/L as acetic acid	16-1700

After solubilization, a complex stream is obtained, consisting of a solid fraction, which can also be valorised (Bridle and Pritchard, 2004); and a liquid fraction containing a mixture of the above-mentioned biorefinery products, in addition to inorganic N, P, K, Ca, S and Mg, heavy metals, dioxins, furans and other organic and inorganic matter (Raheem et al., 2018). P and N can be simultaneously recovered through the struvite precipitation method (Tong and Chen, 2009), while larger biocompounds can be purified by a variety of techniques. This last purification step, however, has been scarcely studied for WAS, and only a few papers focused on WAS valorisation discuss this topic. Thus, it is difficult to accurately assess the best recovery strategy based on the existing literature, when WAS is revalorized through the purification of biocompounds. Nonetheless, the separation of biorefinery products is more common in other industries, including water management (Chishti et al., 1992; Olkiewicz et al., 2015; Talebi et al., 2020; Zhou et al., 2018); and farming (Wilken et al., 2016; Wu et al., 2007; Zhang et al., 2015), biotechnology (Boychyn et al., 2000; Costa et al., 2018; Hansson et al., 1994; Johansson et al., 1996), food (Abejón et al., 2016; Białas et al., 2015; Tahergorabi et al., 2011; Xu et al., 2001), alcohol (Hegazi et al., 1973; Li et al., 2018) or textile (Capar et al., 2008; Feairheller et al., 1972; Li et al., 2015) industries; those techniques being applicable in WAS treatment. Classic separation methods, such as extraction (Li et al., 2018; Tabtabaei and Diosady, 2013), adsorption (Wang et al., 2009), precipitation (Li et al., 2019; Motojima et al., 2012; Tahergorabi et al., 2011), membrane separation (Li et al., 2009; Nguyen et al., 2016; Wu et al., 2007) or chromatography (Dong et al., 2019) have been used for this purpose, along with more specific techniques. These technologies are readily available for WAS revalorization, so the reported results in these analogous streams can serve as a starting point for further research into the recovery of biocompounds from WAS.

In order to gather all the knowledge applicable to WAS revalorization through the recovery of biocompounds, and to facilitate further investigation into this matter, the current efforts in separation and purification of these valuable products by the most established techniques, either from WAS or from other comparable sources, such as primary sludge (Melero et al., 2015; Olkiewicz et al., 2015, 2014), landfill leachate (Iskander et al., 2019; Talebi et al., 2020; Zhou et al., 2018), cell cultures (Djamai et al., 2019; Lorenzo-Hernando et al., 2019; Richardson et al., 1990; Ward et al., 2016), or complex aqueous streams from animal or vegetal sources (Li et al., 2013; Saidi et al., 2013; Strætkvern and Schwarz, 2012; Taskila et al., 2017), have been thoroughly reviewed in this work.

2. Precipitation

Precipitation is a well-known separation method in the municipal wastewater treatment (Wang et al., 2005), pharmaceutical (Linn, 2009; Martinez et al., 2019) and food (Hoare and Dunnill, 1984) industries. This technique relies on the separation of a component of a solution either by changing the solubility of the molecule (converting the compound to an insoluble form) or the nature of the solvent. It is mainly used for the precipitation of metallic ions (Wang et al., 2005), but also for biological molecules, such as phenols, oily emulsions (Wang et al., 2005), proteins (Burgess, 2009), or humic substances (Chen et al., 2021). There are different strategies to achieve this, such as changing pH; salting-out by the addition of certain salts that interact with the compound of interest and increase its hydrophobicity, which eventually makes it insoluble; heating; or phase partitioning with organic polymers or solvents (Burgess, 2009; Ojovan et al., 2019; Waglay et al., 2014). The advantages of precipitation over other methods lie in the fact that it is relatively simple, effective, selective and easily implemented. However, it usually presents higher costs, and may require further purification steps (Linn, 2009). Precipitation studies have been conducted for the recovery of biorefinery products (mainly bulk proteins, but also for enzymes and humic acids) in a broad range of sources, namely from WAS and other urban residues; from cell cultures, culture broths and synthetic solutions; and from food and other animal-related industries (Fig. 4.30).

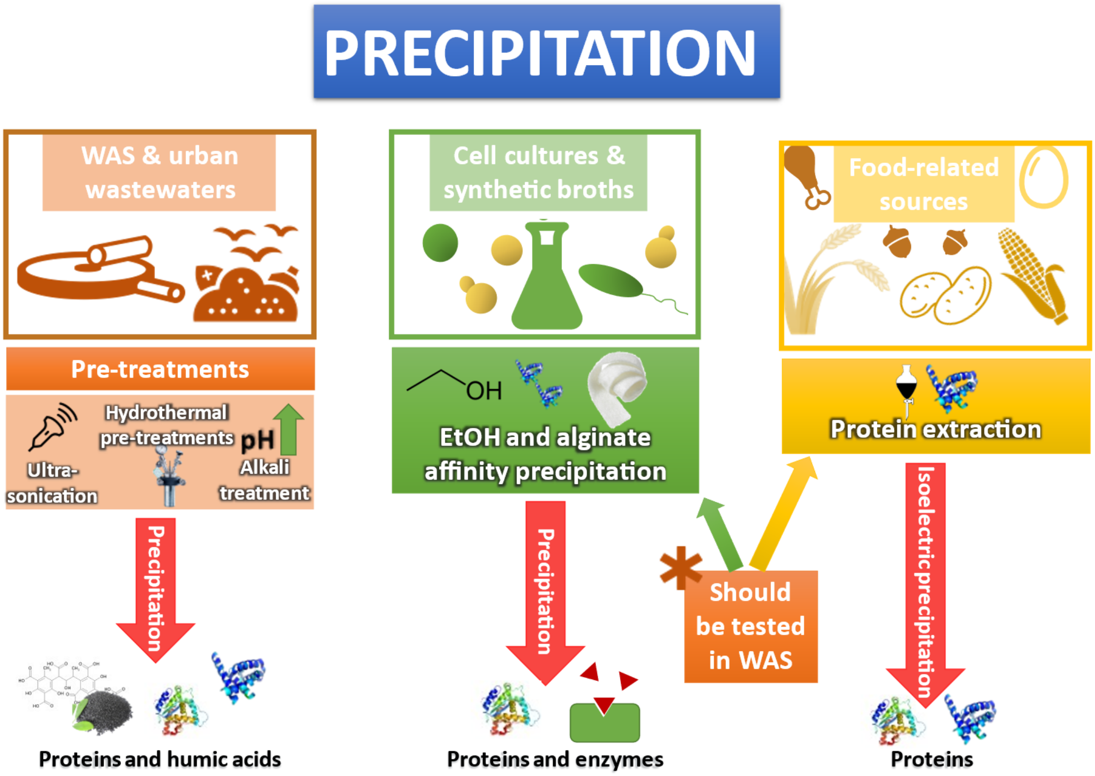

Figure 4.30. Uses of precipitation technology for the recovery of added-value biomolecules.

2.1. Precipitation in urban wastewater

Regarding the use of precipitation techniques for the revalorization of WAS, the use of precipitation is mainly focused on the recovery of phosphate and ammonium as struvite (Akmehmet Balcioglu et al., 2017; Mazlum and İkizoğlu, 2018), and only a few papers dealing with the recovery of biological biorefinery products can be found. All four papers consulted (García et al., 2017; Hwang et al., 2008; Pervaiz and Sain, 2011; Wei et al., 2016) recovered soluble proteins, while (Wei et al., 2016) also recovered humic acids from the supernatant through membrane filtration.

Both solubilization and precipitation methods were found to affect the final recovery yield. García et al. (García et al., 2017) studied two hydrothermal pre-treatments (wet oxidation [WO] and thermal hydrolysis [TH]) and four precipitation methods (ammonium sulphate precipitation, acetone precipitation, trichloroacetic acid precipitation and pH adjustment to values of 2.0, 3.0, 4.5, 5.5 and 9.0), and concluded that TH followed by ammonium sulphate precipitation attained the best purification result, yielding 87% protein recovery. Furthermore, pH adjustment was found to be the worst precipitation strategy, with yields lower than 35% in all cases. Recovery yields obtained with this strategy greatly differ between those reported by García et al. and the rest of the studies: Wei et al. obtained 78.3% separation yield at pH 2.0 (Wei et al., 2016), Pervaiz and Sain reported that 92% of soluble protein precipitated at pH 3 (Pervaiz and Sain, 2011), and Hwang et al. measured a maximum precipitation of 80.5% of soluble protein at pH 3.3 (Hwang et al., 2008). In all of these studies, 2 M H_2SO_4 was used for the acid pH adjustment and short times of precipitation (15 min) were selected. Therefore, the extraction yields were not affected by these parameters. Nevertheless, García et al. considered the interference of humic acid when measuring proteins. The methods used by the other authors overestimate the presence of proteins: Foulin-Ciocalteu reagents employed in the Lowry method can react with the phenolic groups of humic acids (Vakondios et al., 2014), resulting in overestimations of protein concentration by approximately 40% (Frølund et al., 1995). Kjeldahl method measures total N content, and protein content is then calculated by a conversion factor of 6.25 (average N presence in protein is 16% w/w, so 1 g of N would be equivalent to 6.25g of protein (Mæhre et al., 2018)). N content in humic acids ranges between 1.7 and 5.6% (Kumada, 1955; Piper and Posner, 1972), so its presence would lead to an overestimation of protein content. García et al. measured humic acids and proteins with a modification of the Lowry method proposed by Frølund et al. (Frølund et al., 1995), which helped correct this overestimation. These significant differences between the extraction yields can also be explained taking into account the pre-treatment methods employed for the WAS solubilisation, which conditioned the efficiency obtained. In this sense, Hwang et al. compared the effects of alkali treatment, ultra-sonication and alkali treatment followed by ultra-sonication as pre-treatments on protein extraction performance (Hwang et al., 2008). The highest solubilisation rate was achieved after alkali treatment and ultra-sonication (2626 mg/L), followed by ultra-sonication (1818 mg/L) and alkali treatment (932 mg/L). Precipitation yields greatly changed as a function of the solubilization method: only 41.7% of soluble protein obtained after alkali treatment precipitated at pH 3.3, while the values was 80.5% when alkali treatment and ultra-sonication were used at the same pH. García et al. also found differences between the yields achieved after WO and TH. For a given treatment time, the presence of an oxidising atmosphere fastened protein solubilisation, reaching a concentration of 7700 mg/L of soluble protein after WO versus 7200 mg/L after TH. Depending on the precipitation technique, protein precipitation was favoured by one treatment or the other: ammonium sulphate precipitation was slightly more effective after TH (87% TH, 80% WO), and acetone precipitation after WO (77% WO, 70%TH). Trichloroacetic acid precipitation was favoured by TH, and the difference between the recovery yields was higher than in other cases (53% TH, 40% WO). Precipitation through pH adjustment was higher after TH at pH values of 2.0, 3.0 and 4.5; similar at pH 5.5; and higher after WO at pH 9.0. These variations can be explained by: i) variations in protein soluble concentration due to distinct degrees of solubilisation achieved by different treatments, and ii) possible changes in protein structure or chemical characteristics (e.g., oxidation degree, geometry and conformation, size, surface functional groups…) that can alter the protein proneness to precipitation.

It should be noted that most of these methods: pH adjustment, acetone, trichloroacetic acid and ammonium sulphate precipitations, led to the precipitation humic acids together with the proteins. Therefore, it is also interesting to determine the selectivity factor for proteins against humic acids for each of the pre-treatments and precipitation methods evaluated. This was only reported by García et al. 2017, who found that the use of ammonium sulphate, TCA and pH 9 had better performance for TH, whereas the precipitation at pH 3, 4 and 5.5 worked greater on WO. Besides, only short precipitation times were analysed for acid precipitation once the desired pH value was reached. Moreover, it could be convenient to study longer times in order to analyse its influence on protein extraction.

Based on the existing literature, it is difficult to determine which pre-treatment, sonication or alkali treatment, is considered the best one, as Hwang et al. (Hwang et al., 2008) observed that sonication better solubilised sludge than alkali treatment, but did not study their effect on protein precipitation yield (only compared alkali treatment vs sonication and alkali treatment combined). On the other hand, Pervaiz and Sain (Pervaiz and Sain, 2011) achieved a higher protein recovery yield using alkali treatment as a pre-treatment than Wei et al. (Wei et al., 2016) with sonication.

As for the feasibility of the application of the different pre-treatments, sonication is the most used mechanical method for WAS disruption, as it does not require highly costly equipment (Des Soye et al., 2018; Kim et al., 2003; Shrestha et al., 2012). Conversely, hydrothermal and alkali treatments face higher costs, this being their main drawback. It should be noted that hydrothermal treatments can achieve similar effects with lower temperatures by increasing the contact time. Alkali treatments, apart from the higher cost associated with chemical treatments compared to mechanical or biological ones (Kim et al., 2009), have other drawbacks, including corrosion, odours and the need to neutralize the treated stream (Ruiz-Hernando et al., 2013).

Landfill leachate is also a stream with high COD and humic substances content. Two different strategies for humic acid precipitation have been reported: classic acidic precipitation (Iskander et al., 2019) achieved recoveries of 1.86 g per L of raw leachate, while a maximum recovery yield of 95.5% was obtained after coagulation by (3-aminopropyl)triethoxysilane. Unfortunately, initial concentration of landfill leachate in (Zhou et al., 2018) is not clearly stated, so no comparisons in terms of precipitation yields can be made. Protein recovery has also been studied for primary sewage sludge: Chishti et al. studied the use of several precipitating agents for protein recovery, ammonium sulphate being the most effective one (Chishti et al., 1992). This conclusion agrees with that of García et al.

A summary of the studies consulted for this section, including source, precipitated compound(s), pre-treatment(s), precipitation method(s), and main results, is displayed on Table 4.21.

One of the main applications of proteins obtained by this kind of bulk extraction is animal feed. However, due to the presence of toxic components in sewage sludge, toxicity tests must be conducted to certify that this separation method generates edible, non-toxic proteins. Amongst the consulted works, only Hwang et al. studied the possibility of using precipitated protein for this purpose without further purification steps, thereby concluding that its use as animal feed would be “technically feasible” (Hwang et al., 2008).

Table 4.21. Consulted studies about precipitation in urban wastewater.

Source	Compounds	Content	Pre-treatment	Precipitation method	Main results	ref
WAS	Proteins	181 mg/L	TH or WO	(a) pH precipitation (2.0, 3.0, 4.5, 5.5 and 9.0,) (b) acetone precipitation, (c) trichloroacetic acid (TCA) precipitation, (d) ammonium sulphate precipitation	Recoveries: Ammonium sulphate 87% (TH), 86% (WO) Acetone 75% (TH), 77% (WO) TCA 53% (TH), 43% (WO) pH adjustment <35% (WO and TH)	(García et al., 2017)
WAS	Proteins, humic acids	1345.4-1633.7 mg/L (proteins) 1199.1-1456.05 mg/L (humic acids)	Sonication, ultrafiltration (UF) (for humic acid recovery)	pH precipitation (1.0, 2.0, 3.0, 4.0 and 5.0)	Recoveries of 78.3% for protein and 88.6% for humic acid	(Wei et al., 2016)
WAS	Proteins	800 mg/L	Alkali treatment	pH precipitation (1.5, 3.0, 4.5 and 5.5)	Recovery of 92% at pH 3.0	(Pervaiz and Sain, 2011)

Table 4.21. Consulted studies about precipitation in urban wastewater (continued).

WAS	Proteins	932.3 mg/L	Alkali treatment, ultra-sonication and alkali treatment followed by ultra-sonication	pH precipitation (1.0, 3.3 and 5.0)	80.5% recovery at pH 3.3 after alkali treatment and ultra-sonication	(Hwang et al., 2008)
Landfill leachate and synthetic humic acid solutions	Humic acids	50-1000 mg/L	-	Coagulation by (3-aminopropyl)triethoxysilane (APTES)	Maximum humic acid separation efficiency at pH 3.0-5.0 Maximum recovery yield of 95.5% at 35°C, 4.0 mL/L of APTES, contact time of 60 min and HA concentration of 250 mg/L.	(Zhou et al., 2018)
Landfill leachate	Humic acids	763 mg/L	Concentration by forward osmosis	Acidic precipitation (pH 1.5 or 2).	No recovery differences due to pH. 2.45 g/L raw leachate recovered.	(Iskander et al., 2019)
Primary sewage sludge	Proteins	3.2-21.3 g/L	Alkaline solubilisation (NaOH, pH 12.5)	Hydrochloric acid, sodium lignosulphonate, sulphuric acid, acetic acid and ammonium sulphate precipitations	Maximum protein recovery of 91%, obtained with ammonium sulphate (40%).	(Chishti et al., 1992)

2.2. Precipitation in cell cultures and synthetic broths

Single-cell cultures are more easily comparable with WAS than the mixed-cell or pluricellular ones. Solubilisation of *Saccharomyces cerevisiae* and microalgae generate analogous biomolecules solutions. Protein recoveries reported by Boychyn et al. (Boychyn et al., 2000) after ammonium sulphate and by Lorenzo-Hernando et al. (Lorenzo-Hernando et al., 2019) after acidic precipitation are quite low (27.5% and 16.9% respectively). Besides, Boychyn et al. (Boychyn et al., 2000) also achieved poor alcohol dehydrogenase (ADH) recoveries of 7.7% (see Table 4.22). However, these low yields could be attributed to unoptimized extraction methods (indeed, Lorenzo-Hernando et al. (Lorenzo-Hernando et al., 2019) acknowledge that their study is still at a preliminary stage). For instance, Richardson et al. (Richardson et al., 1990) achieved maximum 100% ADH precipitation yield and near 80% of total protein precipitation yield from *S. cerevisiae* adding ammonium sulphate at 60% of saturation.

Pluricellular cultures were also tested for proteins or enzyme recovery, all of them consisting of *Aspergillus* sp. cultures (Costa et al., 2018; Nakkeeran et al., 2010; Netsopa et al., 2019). Two methods previously untested in WAS were employed (ethanol precipitation and alginate affinity precipitation), achieving protein recoveries over 86% with ethanol precipitation. The high yields obtained with this method makes it appealing for application on WAS. As a starting point, it could be used ethanol concentrations from 78% to 92% (added dropwise), since they were reported as the most suitable ones, and it would be necessary the adjustment of the pH of WAS to obtain a slightly acidic one (5.5). The precipitation should be performed at low temperature (10-15ºC) and for at least 3h.

Table 4.22. Consulted studies about precipitation in cell cultures and synthetic broths.

Source	Compounds	Content	Pre-treatment	Precipitation method	Main results	ref
S. cerevisiae	Enzymes (ADH)	444 U/mL	High-pressure homogenization	Ammonium sulphate precipitation	Maximum ADH precipitation yield of 100% (Ammonium sulphate 60%sat).	(Richardson et al., 1990)
S. cerevisiae	Proteins, enzymes (ADH)	17300 U/mL (ADH), 1270 g/L (proteins)	High-pressure homogenization	Ammonium sulphate precipitation	Protein recovery yield of 27.53%. ADH recovery yield of 7.7%	(Boychyn et al., 2000)
Microalgae	Proteins	46.7% (dry-weight ash-free basis)	Alkaline hydrolysis	Acidic precipitation (HCl, pH 2.5)	Maximum protein extraction yield of 16.9%.	(Lorenzo-Hernando et al., 2019)
***Aspergillus niger* submerged fermentation broths**	Proteins, enzymes (xylanases)	7.68 U/mL (xylanases), 120 mg/L (proteins)	Filtration and centrifugation	Ethanol precipitation	Maximum recoveries 85.3% of protein and of 68.7% of xylanase activity	(Costa et al., 2018)
***Aspergillus allahabadii* X26 culture supernatant**	Proteins, enzymes (dextranase)	110.0 U/mL (dextranase), 641 mg/L (proteins)	Filtration and centrifugation	Ammonium sulphate precipitation	Protein recovery yield of 57.6%, total activity recovery yield of 82.0%.	(Netsopa et al., 2019)

2.3. Precipitation in farming and food-related sources

Information about biomolecules precipitation from several other sources is presented in Table 4.23. Previous extraction is conducted in most of the studies to ameliorate protein purification. This strategy could be applied in WAS to solve the problem of protein-humic acid separation reported by García et al (García et al., 2017). Extraction methods used for this purpose were isoelectric (alkaline and acidic) solubilisation, sodium acetate buffer solution, water extraction and urea extraction.

As for the precipitation method, isoelectric precipitation was by far the most widely used. Other precipitation agents were ethanol, carboxymethylcellulose (CMC), ferric chloride, alginate, distilled water, polyacrylic acid, ammonium sulphate, manganese (II) chloride, carrageenan, a set of non-ionic and ionic surfactants, glacial acetic acid, lignosulfonate and bentonite. As seen in WAS, ammonium sulphate achieves high yields of protein recovery in all the analysed sources. Polyacrylic acid, sodium alginate and isoelectric precipitation also showed especially high yields of protein recovery (96%, 95.3% and up to 90%, respectively). Precipitating agents reported in those works should be studied for WAS to determine their eligibility in terms of cost and purification yield, taking as a starting extraction conditions the optimum ones used in them.

Protein extraction from dried WAS with hot alkaline water should be studied, since it is a simple way of separating protein from the matrix prior to its precipitation according to Wilken et al. (Wilken et al., 2016). The extraction yields obtained by these authors were not as high as it would be desirable (from 27.3 to 53.7% protein recovered, depending on the sample). However, this technique has been studied with a simpler substrate (defatted corn flour), therefore, the achievable extraction yield and purity of the protein obtained from WAS may be different.

Few studies have obtained protein recovery yields higher than those reported by Pervaiz and Sain, 2011, in which 92% recovery was attained by alkali treatment and acidic precipitation at pH 3.0, and García et al. 2017, who achieved 87% recovery after TH pre-treatment and ammonium sulphate precipitation. Therefore, without considering the difficulties of the co-precipitation of proteins and humic acids, it seems that the matrix of WAS has not a remarkable effect on the protein extraction yield.

Table 4.23. Consulted studies about precipitation in farming and food-related sources.

Source	Compounds	Content	Pre-treatment	Precipitation method	Main results	ref
Potato fruit juice	Proteins	n/a	-	Thermal/acidic, acidic, $FeCl_3$, $MnCl_2$, ethanol, or $(NH_4)_2SO_4$ precipitation; and CMC complexation	Maximum recovery yields (%) by precipitation agent: Thermal/acidic, 90.2 acidic, 64.7 $FeCl_3$, 75.2 $MnCl_2$, 16.8 Ethanol, 55.2 $(NH_4)_2SO_4$, 98.8 CMC, 75.3	(Waglay et al., 2014)
Dry-milled corn germ	Proteins	17.6-31.3% (% dry basis)	Wet milling, defatting, protein extraction in alkali water	Acid precipitation	Protein recoveries from 27.3% to 41.6%, depending on the source of origin.	(Wilken et al., 2016)
Sorghum distillers grains	Proteins	n/a	Solubilisation in urea (8 M, 1:7.5 ratio), alkali treatment	Isoelectric precipitation (pH 4.5, addition of HCl 7M + Na_2SO_4 2wt%)	Maximum protein extraction yield of 70%.	(Li et al., 2018)
Milled rice bran	Proteins	n/a	Soxhlet extraction with water	Sodium alginate and carrageenan precipitation	Maximum recovery yields of 95.3% of protein recovered with carrageenan and of 87.5% using alginate were obtained at 20°C.	(Fabian et al., 2010)

Table 4.23. Consulted studies about precipitation in farming and food-related sources (continued).

Dehulled soybean flour	Proteins	24.18-24.95% (dry-weight basis)	Oleosome supernatant preparation in lab and pilot-plant scale	Distilled water and ethanol precipitation	Protein recovery yields: In lab scale, 48.4% (water) and 62.3% (ethanol). In pilot-plant scale, 49.6% (water) and 75.4% (ethanol).	(Kapchie et al., 2012)
***Jatropha curcas* kernel and seed press cake**	Proteins	23% (dry-weight basis)	Extraction with water; NaCl (0.1, 0.55 and 1.0 M); or NaOH (0.01, 0.055 and 0.1 M).	Acid precipitation	Better extraction and recovery yields with NaOH 0.055 M extraction. Maximum recovery yields of 69.6% (kernel) and 64.9% (seed press cake).	(Lestari et al., 2010)
***Lupinus angustifolius* seeds**	Proteins	34.8% (w/w)	Dehulling, NaCl extraction, filtration, pH adjustment	Precipitation with cold demineralised water	34.7% extraction yield	(Sussmann et al., 2013)
Chicken drumsticks (skin-on bone-in)	Proteins	n/a	Homogenization, isoelectric solubilization	Isoelectric precipitation, pH 5.5, 10 min, 32-34°C or 4°C	51.9% extraction yield at 32-34°C; 29.7% at 4°C.	(Tahergorabi et al., 2011)
Bovine and porcine lung	Proteins	323-649 g/kg lung	Mincing, alkali extraction	Isoelectric precipitation	Protein recoveries of 62.03% from bovine lung and 63.01% from porcine lung.	(Lynch et al., 2018)
Egg white	Lysozyme	n/a	Dilution in buffer	Polyacrylic acid precipitation	Maximum recovery of 96%	(Fisher and Glatz, 1988)

Table 4.23. Consulted studies about precipitation in farming and food-related sources (continued).

Egg processing plant wastewater	Proteins, fats	1280-4313 mg/L (proteins), 1132-3892 mg/L (fats)	-	Lignosulfonate, CMC, bentonite, and $FeCl_3$ precipitation	Maximum recovery yields by precipitation agent: lignosulfonate, 90-95% (proteins), 92% (fats); CMC, 81-95% (proteins), 82-96% (fats); Bentonite, 90-95% (proteins), 90-96% (fats); Ferric chloride, 81-92% (proteins), 82-92% (fats).	(Xu et al., 2001)
Mackerel whole fish	Proteins	14-16 % w/w	Homogenization, ultrasound assisted extraction	Isoelectric precipitation	Maximum protein recovery yield of 74.3%	(Álvarez et al., 2018)
Rainbow trout (*Oncorhynchus mykiss*) processing byproducts	Proteins	71.5% (dry-weight basis)	Trout mincing and homogenization with water, acidic (pH 2.5, 3.0) or alkaline (pH 12.0, 12.5, 13.0) solubilisation (aqueous phase)	Isoelectric precipitation (pH 5.5 for 10 min+ 1% beef plasma protein)	Maximum recovery yield of 90%	(Chen and Jaczynski, 2007)

Table 4.23. Consulted studies about precipitation in farming and food-related sources (continued).

Atlantic croaker (*Micropogonias undulates*)	Proteins	16.2% w/w	Blending, homogenization with water 1:9, protein solubilisation from pH 1.5 (acid-aided process) to pH 12.0 (alkali-aided process) in intervals of 0.5, centrifugation	Isoelectric precipitation (pH 5.5)	Maximum protein recovery yield of 78.7% after acid-aided process (pH 1.5).	(Kristinsson and Liang, 2006)
Channel catfish (*Ictalurus punctatus*)	Proteins	n/a	Grinding, homogenization with deionized water 1:9, protein solubilisation from pH 2.5 (acid-aided process) to pH 11 (alkali-aided process), centrifugation	Isoelectric precipitation (pH 5.5)	71.5% protein recovery after acid-aided process, 70.3% protein recovery after alkali-aided process.	(Kristinsson et al., 2006)

3. Membrane filtration

The use of membranes allows for the selective separation of stream components. Depending on the membrane characteristics, this separation may be driven by the molecular size, charge, concentration, chemical-physical properties, etc. (Saleh and Gupta, 2016). The most standardised membrane technologies are pressure-driven processes (Baker, 2012). Depending on the molecular weight cut-off (MWCO), i.e., the molecular weight at which 90% of the macromolecular solute is rejected by the membrane (Singh, 2014), this technology is denominated microfiltration (MF), UF, nanofiltration (NF) or reverse osmosis (RO) filtration (Fig. 4.31).

Membranes can be produced in a broad range of materials (ceramic, polymeric) and geometries (commonly flat, spiral wound, tubular or hollow fiber (Berk and Berk, 2009)) which determine operational characteristics, such as flux, lifespan, or selectivity (Gohil and Choudhury, 2018; Kanani et al., 2010).

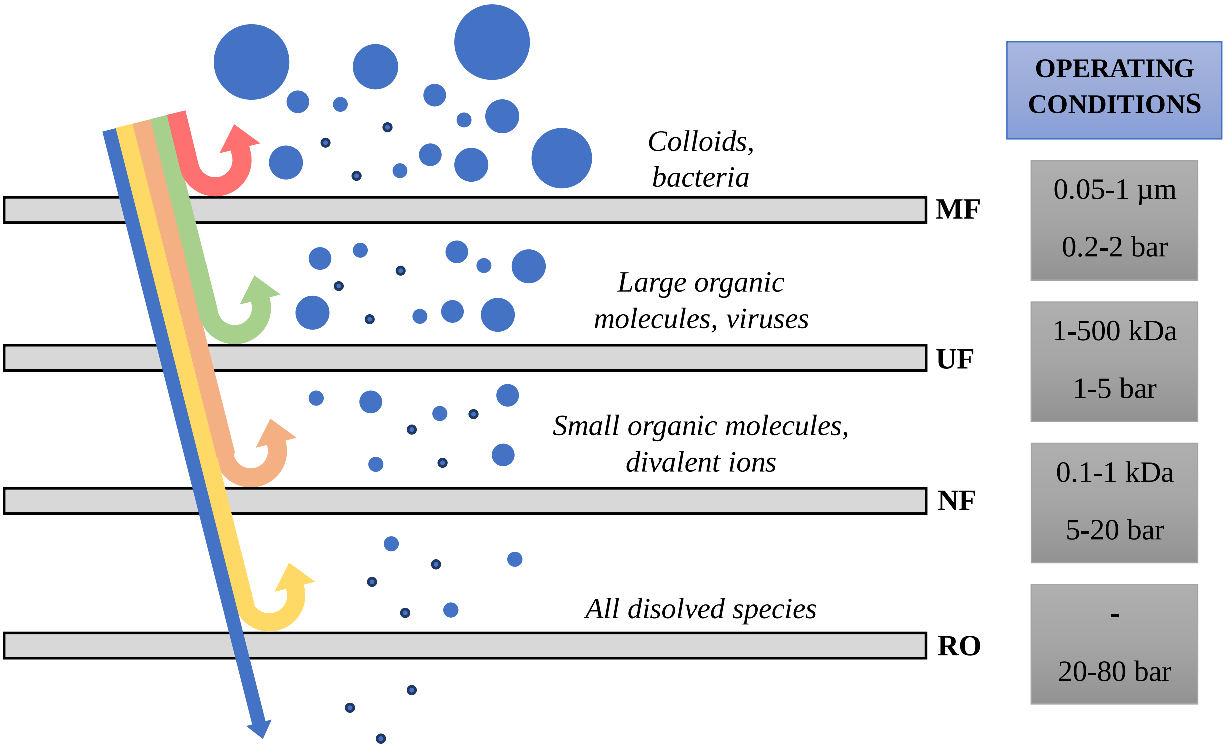

Figure 4.31. Membrane pressure-driven processes (Cui and Muralidhara, 2010).

The fact that it is a clean technology with low energy costs, able to replace other conventional processes and couple it with other technologies as a hybrid process, has aroused great interest, finding application in a broad range of industries, such as food, agriculture, medicine, pharmacy, energetics, soil, or water technologies, among others (Saleh and Gupta, 2016).

The main drawback of this technology is membrane fouling. Membrane fouling is caused by physical, chemical or biological interactions between the foulants and the membrane, which eventually leads to a loss in membrane permeability and/or selectivity (Li and Chen, 2010). Understanding fouling mechanisms and foulants nature is critical to correctly deal with this major issue (Guo et al., 2012). This phenomenon occurs differently depending on the technology used. NF and RO have smaller pores, so the fouling will be more severe and they will normally require some sort of pre-treatment before operation, especially if working with highly contaminated streams (SAMCO, 2019), thus increasing the operating cost. These membranes with smaller pores demand higher pressures to filter the target stream while delivering lower fluxes of permeate, which results in a higher operating cost per litre of permeate obtained (SAMCO, 2017a, 2017b). In turn, these technologies allow to retain and concentrate molecules (or even ions) with smaller MWCO. Thus, a decrease in pore size is only justified when aiming to concentrate smaller biocompounds.

The use of membrane technology for the recovery of added-value biomolecules has been mainly studied as a means of concentration of a broad range of compounds from primary and secondary sludges, cell cultures, synthetic broths and food-related sources (Fig. 4.32).

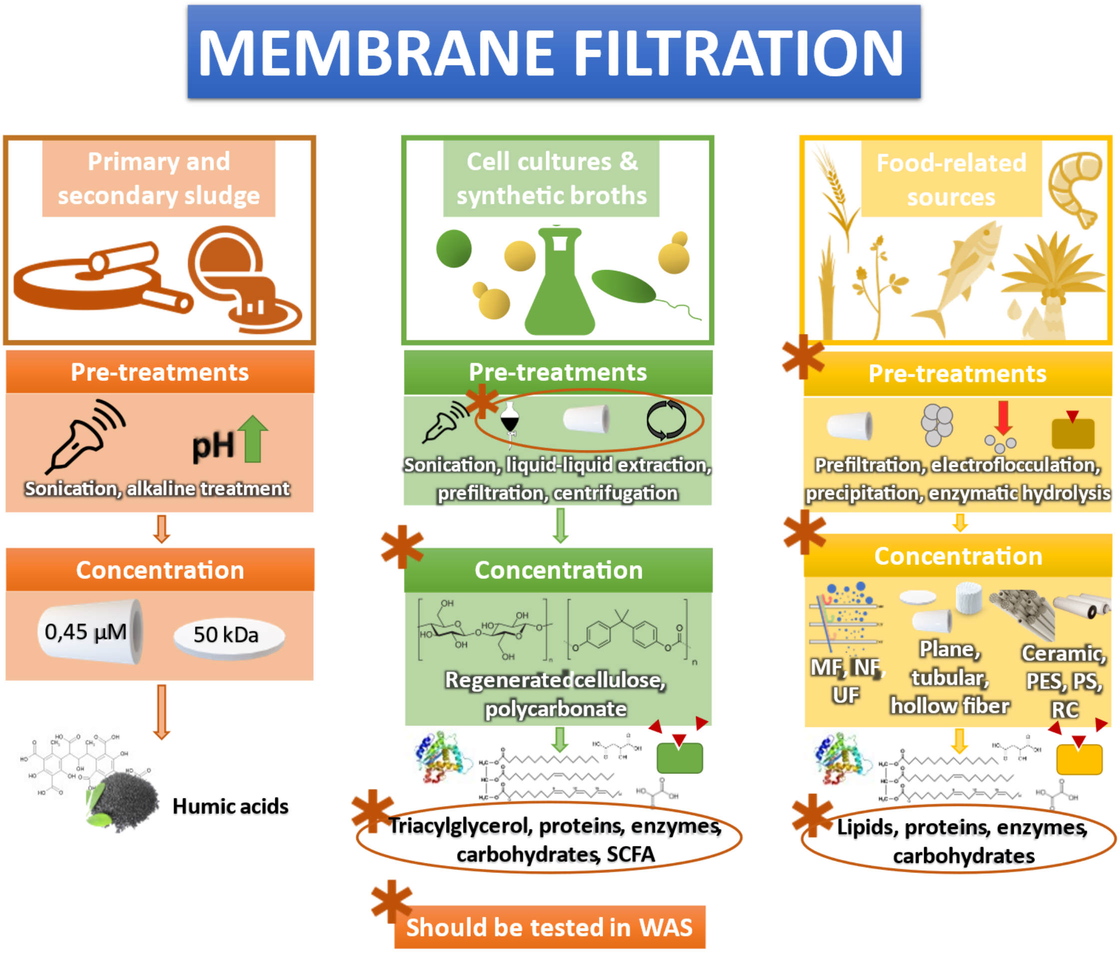

Figure 4.32. Uses of membrane technology for the recovery of added-value biomolecules.

3.1. Membrane separation in WAS, cell cultures and synthetic broths

Revalorization of WAS is mainly focused on the recovery of nutrients as ammonia or struvite through dialysis, NF or RO (Xie et al., 2016). Few works are focused on humic and fulvic acids, which are the only larger biomolecules whose recovery by membrane filtration has been studied (Table 4.24). The aim was not to purify the humic acids, but to concentrate them in order to obtain a fertilizer. Only four papers have focused on humic acid recovery from secondary sludge employing membrane separation, three of them being from the same first author. These three similar works aim to dewater sludge via alkaline treatment and concentrate humic acids by means of membrane filtration. To this end, Li et al. concentrated humic acid by 20-fold with a UF membrane (MWCO is not specified in the study), obtaining a more nutritional sludge humic fertilizer than other sludge fertilizers, and with a lower content of heavy metals (Li et al., 2009). However, Li et al. achieved a humic acid concentration far from the standard set by the Chinese Ministry of Agriculture (4.9 g/L vs 30 g/L required by the standard) (Li et al., 2014b), so further treatment steps are needed to increase it by seven-fold. In this study, retentions of 96% for proteins, 63% for polysaccharides, 48% for nucleic acids, and 21% for fats were obtained. Nevertheless, the separation of these compounds was of secondary importance, for their concentrations (213.5, 760.7, 330.0, and 415.0 mg/L for protein, polysaccharide, fat, and nucleic acids, respectively), which were significantly lower than that of humic acids, were considered as an add-on to humic acid fertilizer composition. These results were validated by the same authors in another study (Li et al., 2014a).

On the other hand, Wei et al. designed an integrated process to recover proteins and humic acids from sewage sludge, which has already been partially discussed in the precipitation section. They studied recoveries at different pH values ranging from 1.0 to 4.0. pH values higher than 2.0 greatly hampered humic acids recovery, so this value was chosen as the most suitable in terms of yield and cost. They reported a humic acid recovery of 124.4 mg/g volatile suspended solids (VSS).

With regards to filtration characteristics, the studies reported by Li et al. (Li et al., 2009)and Wei et al. (Wei et al., 2016) on the one hand, and Li et al. (Li et al., 2014b) and Li et al. (Li et al., 2014a) on the other hand, used the same type of membranes. In both the first two studies, a tubular ceramic membrane with a mesh size of 0.45 μm, which falls more in the range of MF, was used, although both authors claim that they ultrafiltered the sludge. Otherwise, polysulphone (PS) flat sheet membranes were tested more thoroughly in Li et al. (Li et al., 2014b, 2014a) works, where MWCO of 1, 10, 30, and 50 kDa were tested. The 50 kDa membrane proved to be the most suitable regarding balance between dissolved organic carbon ratio of the retentate solution and the membrane flux.

Based on these studies, the use of UF with low MWCO, between 1 and 10 kDa, has the advantage of obtaining slightly higher retentions (up to 79%) than those attained with higher MWCO, from 30-50 kDa (~70%). This indicates that humic acids mainly present a MW higher than 50 kDa. Thus, the assessment of NF and RO for the recovery of this macromolecular compound is considered not necessary. Besides, the membrane fluxes decrease significantly when MWCO of 1 and 10 kDa were used, the values being from 3 to 4 times lower than those obtained with MWCO of 30 and 50 kDa. Therefore, low MWCO has the disadvantage of operational efficiencies, since the increase in the humic acid retention does not justify the significant decrease in membrane flux. Recovery of triacylglycerol, proteins and carbohydrates from a similar source (microalgae) was reported by Djamai et al. (Djamai et al., 2019). In their study, several membranes were tested, and it was disclosed that regenerated cellulose (RC) membrane (30 kDa) was less prone to fouling. Dumay et al. (Dumay et al., 2008), who studied the concentration of lipids and peptides from surimi manufacturing washing waters, also concluded that recovered cellulose (10 kDa) was the best performing membrane among those studied, due to its higher efficiency and regenerability. Isa et al. (Isa et al., 2008) also found that polycarbonate membrane was easier to clean compared to polyethersulphone (PES) membrane when purifying surfactin from fermentation broth, although it showed lower recoveries.

Taking into account these studies, UF can be considered the suitable membrane technology for the recovery of proteins, carbohydrates and lipids since yields between 70% and 98% were obtained. Polymeric membranes were found to be more adequate than ceramic ones since they allowed to obtain higher biocompound yields. Besides, membrane fouling can also be controlled as function of the membrane material selected. In this sense, the use of regenerated cellulose showed the advantage of the better regenerability and less susceptibility to fouling than other polymeric materials tested, including PES, polyacrylonitrile and polyvinylidene fluoride. Regarding MWCO, the most appropriate varied from10 to 40 kDa in order to reach a compromise between recovery yields and flux decrease. It should be noted that with a MWCO of 3 kDa, the flux was half the one obtained with 10 kDa and the improvement in recovery was minimum. For this reason, the analysis of NF and RO is considered not needed since the increase in the recovery would not justify the greater fouling and the corresponding decrease in flux.

Although the literature about solubilised/liquefied WAS is very limited, its high content in natural organic matter is expected to cause difficulties in membrane operation, in terms of flux performance and fouling, since it is reported as the main foulant in surface waters (Fane et al., 2006). Therefore, it will be necessary to establish a cleaning strategy to lessen the organic matter effect and enhance productivity. To that end, physical cleaning should be used to reduce membrane fouling and the frequency of chemical cleaning, which extends membrane lifetime and decreases operating costs. Backwashing, backpulsing, crossflushing, sponge ball cleaning and air sparging are the most widely employed methods of physical cleaning (Gao et al., 2019). It was reported that backpulsing cause the detaching of the trapped foulants and backwashing remove them from membrane surface and pores (Fraga et al., 2017). Thus, the combination of backpulsing and backwashing can provide a synergistic effect on membrane cleaning (Fraga et al., 2017; Hau and Leung, 2016).

Table 4.24. Consulted studies about membrane separation in WAS.

Source	Compounds	Content	Pre-treatment	Filtration conditions	Main results	Ref
Thickened activated sludge	Humic acids	24% w/w organic matter	Alkaline treatment, dewatering, pre-filtering with membrane with mesh size of 0.45 µm.	Porous tubular membrane Membrane area: 0.35 m^2 Transmembrane pressure (TMP): 1.0 MPa	20-fold concentration of humic acid.	(Li et al., 2009)
Activated sludge	Humic acids	1199.1-1456.1 mg/L	Ultrasonication, protein precipitation	Porous tubular ceramic membrane TMP: 1.0 MPa. Mesh size: 0.45 µm	Maximum recovery rate of humic acid during the co-recovery of 154.1 mg/gVSS at pH 1.	(Wei et al., 2016)
Activated sludge	Humic acids	1467.3 mg/L	Alkaline treatment, centrifugation	Flat sheet membranes MWCO: 1, 10, and 50 kDa TMP: 0.2 MPa.	3 to 3.5-fold concentration of humic acid (4239 mg/L).	(Li et al., 2014b)
Mixed primary and secondary sludge	Humic and fulvic acids	1913.8-2535.1 mg/L (humic acids), 238.8-316.3 g/L (fulvic acids)	Alkaline treatment, centrifugation	Flat sheet membranes MWCO: 1, 10, 30 and 50 kDa TMP: 0.2 MPa. Volume concentration ratio (VCR): 5.	Membranes with MWCO of 30-50 kDa are more appropriate than those with lower MWCO for the recovery of macromolecular organic substances.	(Li et al., 2014a)

Table 4.24. Consulted studies about membrane separation in WAS (continued).

Microalgae	Triacylglycerol, proteins and carbohydrates	251 mg/g dry cells (triacylglycerols), 302 mg/g dry cells (proteins), 83 mg/g dry cells (carbohydrates).	Cell disruption by ultrasonication, pigment and triacylglycerol extraction in organic solvent	Membranes: Al_2O_3, 600 kDa, tubular; TiO_2, 60 kDa, tubular (ceramic); PS, 600 kDa, plane; RC, 100 kDa, plane; RC, 30 kDa, plane (polymeric) plane membrane filtration area 12.56 cm^2, tubular membrane: filtration area 18.68 cm^2 TMP: 0.4 bar T: 25°C VCR: 2	Membrane used for fractionation was RC, 30 kDa, plane. Recovery of carbohydrates (88%) and proteins (68%) in the retentate. Recovery of triacylglycerol in the permeate (recovery factor of 60%, purity of ~70%).	(Djamai et al., 2019)

Table 4.24. Consulted studies about membrane separation in WAS (continued).

Solid-state cultures of *Aspergillus carbonarius*	Enzymes (polygalacturonase)	2450 U/mg	Extraction, alginate affinity precipitation	Integrated membrane processing 3 membranes studied: MF: Hydrophilic amphoteric nylon membrane, pore size 450 nm UF: Hydrophilic plane membranes with PS (MWCO of 50 kDa) and PES (MWCO of 10 kDa) as active layer/coating and polypropylene as support layer, effective area of 15 cm^2 TMP: 0.1 MPa (MF); 0.5 MPa (UF) T=25 °C VCR: 10	80% cumulative recovery of polygalacturonase after integrated process, 72% of protein, 99% of carbohydrates	(Nakkeeran et al., 2010)

Table 4.24. Consulted studies about membrane separation in WAS (continued).

Fermentation broth	Enzymes (surfactin)	596 mg/L	Centrifugation	Two-step UF, with (1st mode) and without (2nd mode) cleaning the membrane between UF steps. Membranes tested: RC, 10 kDa, effective area 50 cm^2 PES, 10 kDa, effective area 50 cm^2 TMP: 1.5, 2.0 and 2.5 bar (1st mode), 2.0 bar (2nd mode) Room temperature	Total recoveries of 94% for PES 10 kDa and 92% for RC 10kDa after UF-2. Applied TMP or mode of filtration had no significant effect in the selectivity of filtration. PES membrane showed higher recovery and similar purity compared to RC.	(Isa et al., 2008)
Fermentation broth	Succinic acid	n/a	UF preclarification Ion exchange	NF Polyamide (active layer) and PS flat sheet membrane, 150-300 Da, effective area 155 cm^2 TMP: 1.6 MPa T: 25°C ± 2°C. Flow rate: 160 L/h	Retention of succinic acid of 92%	(Antczak et al., 2018)

Table 4.24. Consulted studies about membrane separation in WAS (continued).

Fermentation broths	Lactic acid	84.30-86.40 g/L	Precipitation, centrifugation	Protein removal from the cell-free broth by sequential UFs (30 kDa, 5 kDa, and 1 kDa). Lactic acid separation and concentration by in-series RO.	Recovery of 100% of lactic acid with 97% purity.	(Phanthumchinda et al., 2018)
Humic acid solutions	Humic acids	n/a	-	Polymeric membranes tested: YM2 (flat hydrophilic, 1 kDa, 45 cm2), PM10 (flat, lipophilic, 10 kDa, 45 cm^2), YM100 (flat, hydrophilic, 100 kDa, 45 cm^2), H10P3-20 (hollow fiber, PS, 3 kDa, $9·10^3$ cm^2).	Retentions of 80-90% for humic acid, 60-70% for fulvic acid and 40-70% for calcein.	(Küchler and Miekeley, 1994)

3.2. Membrane filtration in other industries

Although the studies conducted on WAS only contemplated the recovery of humic acids through UF, the works which employed other source streams report a broader range of potential target biomolecules. Proteins, enzymes, fats and carbohydrates (apart from humic acids) have been successfully recovered from different vegetal and animal wastewaters (Table 4.25).

Carbohydrates, proteins and humic acids were all recovered in the retentate. The role of membrane filtration in the recovery of these molecules from WAS could be to concentrate them prior to a subsequent purification step, or the fractionation of the stream using membranes of different MWCO to obtain solutions concentrated in the different species.

Due to the particular characteristics of the streams reviewed in this sub-section, some of the pre-treatments used may not be applicable to WAS filtration (e.g., as Dumay et al. work with a sludge consisting mostly of proteins generated during surimi manufacturing, they perform a hydrolysis with proteases prior to a subsequent UF). On the other hand, several pre-treatments here reviewed may serve as a pre-treatment for reducing membrane fouling and improving the efficiency of this operation, namely centrifugation, prefiltration, protein extraction or electroflocculation.

As the industrial application of centrifugation is hindered by its high cost (Najjar and Abu-Shamleh, 2020), its use as a pre-treatment stage before WAS filtration would not be competitive against prefiltration. Prefiltrations, either surface or depth filtrations (with sand and stone beds), as tested by Wu et al. (Wu et al., 2007) or Mohammad et al. (Mohammad et al., 2009), are aimed to remove larger suspended residues, so membranes with lower cut-off would be more adequate as those tested by Li et al. (Li et al., 2009). Since only one mesh size has been evaluated in WAS, the cut-off size of the pre-filtration membrane could be optimised. This pre-filtration is not considered a high energy-consuming stage, as the temperature and pressure set for it can be maintained during subsequent filtrations.

As discussed in the previous section, an aqueous protein extraction from dried WAS together with its concentration by membrane filtration could be a feasible way of fractionating the sludge. Thus, proteins would be recovered before concentrating them through membrane filtration and then subsequent precipitation could be applied.

Electroflocculation can also be used as a low-cost pre-treatment prior to sludge filtration, with the aim of reducing membrane fouling. It has yet to be tested in WAS to determine if this treatment is more cost-effective than prefiltration or centrifugation (Gringer et al., 2015).

In-depth studies on membrane performance should be conducted to test different materials (only PS membranes have been tested within the UF range) and geometries (hollow fiber, tubular…), as well as to characterize and model fouling and to optimize the operating conditions in order to maximize permeate fluxes. The suitability of other pre-treatments, such as the WO discussed in section 2, should also be evaluated.

Table 4.25. Consulted studies about membrane separation in other industries.

Source	Compounds	Content	Pre-treatment	Filtration conditions	Main results	Ref.
Barley (*Hordeum vulgare*)	Enzymes (β-glycosidases)	82.23 U/mL (β-galactosidase), 40.64 U/mL (β-glucosidase)	Preparation of enzyme extract through extraction in 0.1 M, pH 6.0 ammonium acetate buffer.	Plane PES membrane, 100 kDa, effective filtration area of 50 cm^2. 2 modes of operation: 1) Concentration followed by diafiltration, 2) diafiltration followed by concentration TMP: 0.6 bar T: 25 ± 2°C VCR: 3	Best results: Mode 1) β-glucosidase was purified 4.38-fold and concentrated from 40.64 to 111.87 U/mL. Mode 2) β-galactosidase was purified by 4.56-fold and concentrated from 82.23 to 236.03 U/mL.	(Hemavathi and Raghavarao, 2011)
Palm oil mill effluent	Proteins, carbohydrates	12.9 g/L (proteins), 28.9 g/L (carbohydrates)	Prefiltration through stones and sand filter beds, and surface filtration with paper of 8 µm pore size.	PS plane membrane, 20 kDa, effective membrane area15.2 cm^2 TMP: 0.8MPa T: 25 ºC (±2 ºC).	Recovery of protein and carbohydrate up to 61.4% and 76.4%, respectively	(Wu et al., 2007)

Table 4.25. Consulted studies about membrane separation in other industries (continued).

Palm mill oil effluent	Proteins	91.4 g/L	Physical pre-treatment processes (depth and surface filtrations) and MF process.	3 membranes tested: PS UF membrane, 20 kDa PES membranes, 10 and 2 kDa TMP: 1-10 bar. T: 25 ºC (±2 ºC).	Best performance at highest MWCO and TMP (20 kDa, 10 bar) Maximum reduction of total suspended solids, turbidity, chemical oxygen demand, total dissolved solids of 98.3%, 96.2%, 82.0%, 41.2%, respectively. Maximum protein recovery of 98.3%, 96.2%, 82.0%, 41.2% and 78.0%, respectively.	(Mohammad et al., 2009)
Isolated soy protein production wastewater	Proteins	1870 mg/L		3 monotubular ceramic membranes: 5, 20 and 50 kDa; membrane area of 0.0047 m^2. TMP: 1-8 bar Crossflow velocity (CFV): 2.4 m/s T: 25ºC	Best results with 5-kDa membrane, showing the least reduction in permeate flux over time and the highest retention percentages of protein (52%).	(Cassini et al., 2010)

Table 4.25. Consulted studies about membrane separation in other industries (continued).

Poultry processing wastewaters	Proteins	20.15 g/L	MF	2 membranes used: RC, spiral-wound membranes, 3 and 30 kDa, area of 0.92 m^2. TMP: 200 ± 15 kPa CFV: 2.5 ± 0.2 m/s. T: 20ºC	Total recovery of soluble proteins as well as the average degree of concentration amounted to 84 % and 9.3, respectively using crossflow filtration.	(Białas et al., 2015)
Marinated herring (*Clupea harengus*) brine	Proteins and fatty acids	6.99% w/w (proteins), 0.96% w/w (fatty acids)	Electroflocculation, prefiltration	Tubular SiC membrane, pore size 0.040 µm, filtration area 0.09 m^2 TMP: 2-2.6 bar T: from 5-7 °C to 24-26 °C CFV: 2 m/s	75-82% (<62.7 mg/mL) of the protein and 75-100% of the fatty acids retained	(Gringer et al., 2015)
Fish meal effluent	Proteins and oil	1.2-8.1 g/L (proteins), 0.39-20.5 g/L (oil)	MF	Mono-tubular mineral (thin deposit of ZrO-TiO, on a carbon support) membrane, 15 kDa,. Surface area 0.0226 m^2. TMP: 4 bar CFV: 4 m/s T: 20°C	Maximum retentions of 40.0% and 26.0% for oils and proteins, respectively. Lower protein rejections after concentration to VCR=17 (11.5%).	(Afonso and Bórquez, 2002)

Table 4.25. Consulted studies about membrane separation in other industries (continued).

Washing water from surimi manufacturing	Proteins and lipids	26.5 g/L (proteins), 1.8 g/L (lipids)	Centrifugation, enzymatic hydrolysis	Polymeric plane membranes tested, membrane surface 100 cm^2. Materials: PES, polyacrylonitrile, polyvinylidene fluoride and RC. MWCO: 3, 10, 40, 50, and 100 kDa. TMP: 0-3 bar T: 15°C CFV: 1.7 m/s	10 kDa RC membrane had the highest performance and was further evaluated. COD reduced by 75%. Recovery rates of 98.0% for lipids and 79.9% for proteins with RC membrane (10 kDa). VCR of 3.8	(Dumay et al., 2008)

4. Solvent extraction

Solvent extraction mechanism relies on the difference of solubility of a solute between two immiscible or lowly miscible solvents. During this operation, a solvent with higher solubility is put in contact with the phase where the solute is initially present, and so the solute migrates to the solvent with higher solubility (Clarke, 2013). Depending on the state of aggregation of the two phases, the solvent extraction is named solid-liquid extraction if the solute is contained in a solid matrix and extracted with a liquid solvent, or liquid-liquid extraction if both the matrix and the solvent are in liquid state. Solvent extraction presents advantages, such as better separation effect than precipitation, higher selectivity and mass transfer velocity than ion exchange, or lower energy consumption and easier large continuous operation than distillation (Chen and Wang, 2017). A correct choice of the solvent is critical in the suitability of the operation and must take into account factors, such as the distribution coefficient, the immiscibility with the contrary liquid phase, the ease of recovery and cost (Sprakel and Schuur, 2019).

Besides the conventional methods of liquid-liquid extraction, new methods combining solvent extraction with other technologies have been developed (Chen and Wang, 2017), mainly liquid biphasic flotation systems, a bubble-assisted, gentler and greener L-L extraction technique (Khoo et al., 2020; Leong et al., 2019). These technologies have not yet been studied on WAS, but only on other cell cultures (Fig. 4.33).

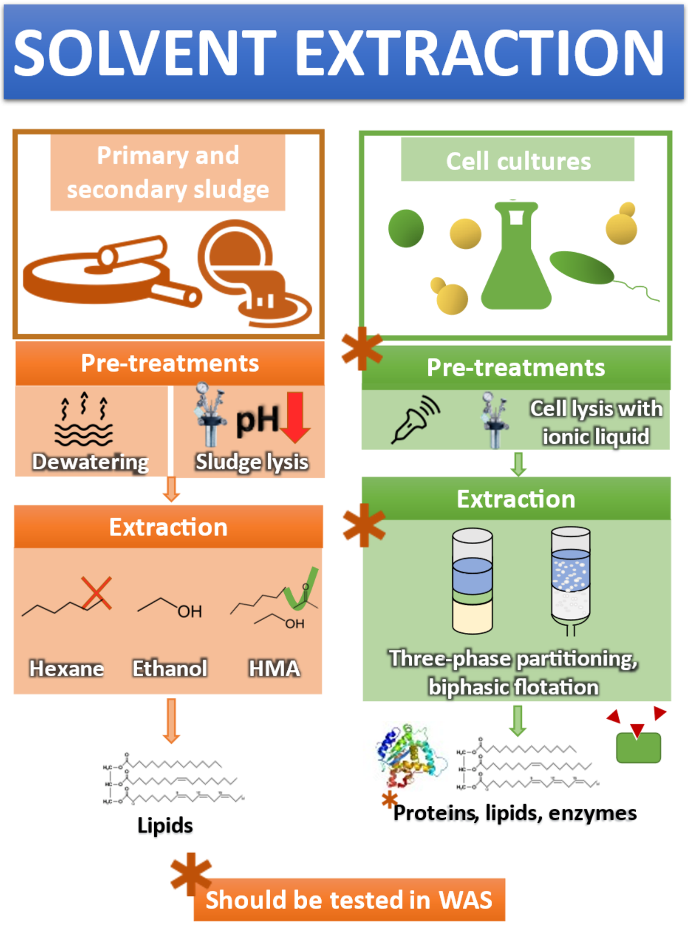

Figure 4.33. Uses of solvent extraction technology for the recovery of added-value biomolecules.

4.1. Solvent extraction on WAS

Solvent extraction on WAS has been studied exclusively for the recovery of lipids (Table 4.26). In all the consulted literature, pre-treatments, such as centrifugation, sun drying, oven drying, or pressure filtration were conducted in order to dewater the WAS to some extent prior to the extraction. Besides these pre-treatments, the influence of acidification or sub-critical water pre-treatments was also studied. The work of Olkiewicz et al. (Olkiewicz et al., 2014) analysed the influence of the drying method and acidification in lipid extraction efficiencies from primary, secondary and blended sludges. $MgSO_4{\cdot}H_2O$ drying, oven drying at 105 and 70°C, freeze-dryer drying, fume hood drying and sun drying methods were tested, the $MgSO_4{\cdot}H_2O$ being the method that achieved the best moisture removal and lipid yield, thereby disclosing that moisture levels directly affect the extractability of the lipids. As for the acidification pre-treatment, it increased lipid extractability in all cases, although in WAS the resulting improvement was low (from 5.1% to 6.3% of lipid yield). Huynh et al. (Huynh et al., 2010) studied the effect of sub-critical water pre-treatment of powdered and oven dried WAS (which was also mixed with diatomaceous earth to improve the solvent flow through the sample) on lipid extraction efficiency, using hexane as the solvent. Sub-critical water pre-treatment increased four times the amount of extractable neutral lipids.

Hexane, methanol and acetone were employed as solvents for lipid extraction. The more exhaustive comparison between these three solvents was carried out by Dufreche et al. (Dufreche et al., 2007). In this study, hexane, methanol, and a 60% hexane/20% methanol/20% acetone mixture (HMA) were tested as solvents at 10.3 MPa and 100 °C for 1 h. The extraction yields achieved with pure hexane were really small (1.94%), and 10 times lower than those achieved with pure methanol (19.39%) and HMA (21.96%). Such low yields were reported by all the authors that worked with hexane: Olkiewicz et al. (Olkiewicz et al., 2014) obtained a maximum yield of 6.3% after 9 extraction stages at room temperature, with 1:1 ratio and for 20 min; Huynh et al. (Huynh et al., 2010) achieved a maximum yield of 7.87% with a Soxhlet extraction; Melero et al. (Melero et al., 2015) reported negligible yields (less than 1%) at ~65°C during 2.5 h. Methanol gave better results as reported by Dufreche et al (Dufreche et al., 2007) (19.39%, as mentioned above), but gave lower yields based on the studies by Melero et al. (Melero et al., 2015), with only 2.1% at ~65°C during 2.5 h; and by Revellame et al. (Revellame et al., 2011), with a maximum yield of 3.93% at 75°C, using a solvent ratio of 30mL methanol:g sludge and 10% (volume) of catalyst concentration.

Apart from the abovementioned chemical or hydrothermal pre-treatments, WAS dewatering has been studied by several authors before solvent extraction. Sludge dewatering is the bottleneck of WAS management, and many efforts have been made towards developing cost-effective methods that significantly reduce the amount of water on WAS. Due to its particular structure, it is estimated that only 15-30% of WAS water content can be removed with mechanical methods, such as decantation (Wang et al., 2009). Direct thermal drying of sludge has been implemented at industrial level, although the very high energy demand of this technology has restricted its use (Wang et al., 2009). Nonetheless, new drying methods, such as microwave drying (Kocbek et al., 2020), have been promisingly researched.

4.2. Solvent extraction on cell cultures

The study of solvent extraction of biomolecules from microorganisms is better developed for microalgae (*Arthrospira platensis*, *Chlorella vulgaris*, *Chlorella pyrenoidosa*, *Chlorella sorokiniana* and *Nannochloropsis gaditana*) and bacteria (*Burkholderia cepacian*) than for WAS. Most of the reviewed papers focused on the recovery of proteins (9 to 6 that study the recovery of lipids), although two thirds of these works reported on liquid biphasic flotation (Table 4.27). For the extraction of lipids, n-hexane was used after cellular lysis with ionic liquid (Lu et al., 2019) or steam explosion (Lorente et al., 2017). Ionic liquids ([C_4mim][$MeSO_4$] and [$P(CH_2OH)_4$]Cl) were scarcely used as extractants, as only (Olkiewicz et al., 2015) employed them for the recovery of proteins and lipids from primary sludge (as mentioned above, (Lu et al., 2019) used [BMIM]Cl to lysate the cell prior to extraction with n-hexane). This technique has not been tested as a lysis pre-treatment for WAS; nonetheless, ionic liquids are from 2 to 8-fold more expensive than regular organic solvents, and some of them are toxic, preventing the recovered biocompounds from being subsequently used for nutritional purposes or as animal feed.

Regarding more novel techniques, one study (Chew et al., 2019) dealt with a microwave-assisted three-phase partitioning, employing t-butanol as solvent and completing the three-phase system with ammonium sulphate. As for biphasic flotation extractions, several combinations of solvents were assayed, all of them obtaining high yields except for Sankaran et al. (Sankaran et al., 2018b), which only achieved 23% protein recovery yield.

In the light of these data, it can be deduced that hexane is not a suitable extractant for lipids from secondary sludge, whereas methanol provides higher rates only under harsh conditions

(~100 bar and 100°C). The efficiency of other solvents should be tested, whether they are traditional ones, such as chloroform; or novel ones, such as ionic liquids. An optimization of the extraction conditions should be conducted in addition to a hydrolytic pre-treatment that unbinds fats from protein, carbohydrate and/or minerals, since it has been reported that these bindings prevent solvent alone to fully recover lipids from WAS (Luthria and Anderson, 2004). Other hydrolytic or disruptive pre-treatments should also be studied, such as steam explosion, lysis with ionic liquid, sonication, TH, or WO. Also, the extraction of other biomolecules, such as proteins or humic acids, should be explored, as well as the application of newer technologies, such as biphasic flotation to reduce costs and energy expenditures.

Results reported by Huynh et al. (Huynh et al., 2010) showed that the physicochemical characteristics of WAS hindered the lipid extractability during a S-L extraction, as the lipids are mainly embedded in the membrane cell. Accordingly, a previous cell lysis pre-treatment (as sub-critical water treatment in the case of Huynh et al.) can significantly improve the extraction yield. It can also be seen that neither proteins (in algae) nor humic acids (in landfill leachate) affect the extractability of oils and lipids during a L-L extraction, so this technique is also expected to be efficiently applicable in lipid extraction from WAS. It remains uncertain if humic acids could interfere with proteins during three-phase partitioning or other extraction methods, and research is needed at this point to clarify the feasibility of protein extraction from WAS in an efficient and selective way.

4.3. Solvent extraction from animal and vegetal sources

Recent research in solvent extraction from vegetal sources has paid more attention to protein recovery (Table 4.28). In this sense, ethanol and alkaline solutions were studied as solvents. As the yields obtained highly differ depending on the source, aqueous protein solution should be tested in WAS to determine its feasibility. However, in the study by Uddin et al. (Uddin et al., 2018), in which different aqueous solvents for protein extraction were evaluated, the highest recovery yield (85.2%) was achieved with NaOH solution, this being in accordance with the results obtained by Álvarez et al. (Álvarez et al., 2018).

On the other hand, extraction with liquefied gas has been recently tested as a green extraction method (Chemat et al., 2020). However, the application of this technology in an integrated process may be hindered by the need of pressurizing, which can increase the total cost of the operation.

Research on solvent extraction from animal sources is scarce, and the literature is focused, as with vegetal sources, on S-L extraction. Thus, those procedures would only be applicable to dried sludge. Aqueous alkaline protein extractions have been tested with high yields, reaching a 94.71% recovery with NaOH 0.1 M and ultrasound assistance (Álvarez et al., 2018). Alternatively, lipid recovery from egg yolk by subcritical fluid-propane extraction has been studied, although the high cost and complexity of the operation is not presumably competitive against more standarised extraction methods.

Table 4.26. Consulted studies about solvent extraction on WAS.

Source	Compounds	Content	Pre-treatment	Extraction conditions	Main results	Ref.
Primary, thickened secondary and blended sludges	Lipids	26.3% dry-weight basis (primary sludge), 7.7% dry-weight basis (WAS), 21.1% dry-weight basis (blended sludge)	Acidification and drying or acidification.	Solvent: hexane. 2 methods: a) Soxhlet extraction of dried sludges. b) Sequential 9-stage liquid-liquid extraction with mechanical agitation at room temperature.	Primary sludge: a) 26.3% recovery yield. b) Maximum recovery yield of 29.6% (dry weight basis) with sludge to hexane ratio 1:2. Secondary and blended sludges: Absolute yields of 19.1% for blended sludge and of 6.3% for secondary sludge after 9 extraction stages (conditions: 1:1 sludge to hexane volume ratio, each stage extraction time — 20 min.)	(Olkiewicz et al., 2014)
Dewatered activated sludge	Lipids	2.10-7.87% (w/w)	Sub-critical water pre-treatment.	Soxhlet extraction. Solvent: hexane.	Oil recoveries of 2.10% and 7.87% (dry weight basis) without and with sub-critical water pre-treatment, respectively.	(Huynh et al., 2010)

Table 4.26. Consulted studies about solvent extraction on WAS (continued).

Secondary sewage sludge	Lipids	n/a	Dewatering by centrifugation or pressure filtration and posterior Hydromatrix addition.	Extraction at 10.3 MPa and 100 °C for 1 h. Different solvents used: 1. 60% hexane/20% methanol/20% acetone (HMA) (same mixture three times); 2. Pure methanol followed by pure hexane (MH); 3. Pure hexane (single extraction); 4. Pure methanol (single extraction). Solvent to solid ratio 40:1 g/g	Gravimetric yields of oil in grams of oil per gram of dry sludge: 1. HMA extraction 1 yield=21.20%, total yield (27.43 ± 0.98) %. 2. Pure methanol extraction yield: 19.39%, total yield (21.96 ± 2.28)% 3. Pure hexane extraction yield: 1.94%. 4. Pure methanol extraction yield: (19.39 ± 3.20)%.	(Dufreche et al., 2007)

Table 4.26. Consulted studies about solvent extraction on WAS (continued).

Primary and secondary sewage sludge	Lipids	n/a	Dewatering by settling and centrifugation, oven drying and milling into powder	Tested solvents: n-hexane, methanol. Extraction time: 2.5 or 4 h. Sewage sludge to solvent ratio: 10 g:100 mL or 10 g:150 mL. T~65°C	No substantial differences at different extraction conditions of time and sewage sludge to solvent ratio. Lipid extraction yields (based on the starting dry sludge): Primary sludge, n-hexane: 7.4 wt% Primary sludge, methanol: 13.6wt% Secondary sludge, methanol: 2.1wt%	(Melero et al., 2015)
Activated sludge	Biodiesel (in-situ transesterification)	n/a	Gravity-settling overnight, followed by centrifugation	Optimization of conditions: T from 45 to 75 ºC; methanol to sludge (solids) ratios from 5 to 30 mL/g; catalyst concentrations from 1 to 10% (based on volume of methanol).	Maximum yield of 3.93 ± 0.15 wt% at 75◦C, 30 mL/g methanol:sludge ratio and 10% volume of catalyst concentration.	(Revellame et al., 2011)

Table 4.26. Consulted studies about solvent extraction on WAS (continued).

Primary sludge	Lipids, proteins	n/a	Oven drying	Solvents: $[C_4mim][MeSO_4]$ and $[P(CH_2OH)_4]Cl$. Conditions: 1 g TS equivalent to 10 cm^3 ionic liquid ratio, 100 °C, 24 h, with stirring.	Higher yields obtained with raw sludge. Extraction yield of 26.9 ± 1.0 (g/100g dry sludge) obtained with $[C_4mim][MeSO_4]$ and 27.6 ± 0.6 with $[P(CH_2OH)_4]Cl$ vs 27.2 ± 0.4 obtained with standard Soxhlet method. Protein extraction of 16.6 ± 1.2 g/100g dry sludge) with $[P(CH_2OH)_4]Cl$.	(Olkiewicz et al., 2015)

Table 4.27. Consulted studies about solvent extraction on cell cultures.

Source	Compounds	Content	Pre-treatment	Extraction conditions	Main results	Ref.
***A. platensis* (spirulina)**	Proteins	n/a	Sonication, manothermosonication	Solvent: sodium phosphate buffer (0.1 M; pH 7.0). Ratio biomass/solvent 1:20 (g/g), pressure 1 or 3 bar, T 10 or 30 °C, ultrasonic intensity 20 or 60 W/cm^2	Maximum protein recovery yield of 28.42 ± 1.15 g/100 g DW achieved with 2 bar, 24 °C and ultrasound intensity of 55 W/cm^2.	(Vernès et al., 2019)

Table 4.27. Consulted studies about solvent extraction on cell cultures (continued).

C. vulgaris	Proteins	n/a	-	Microwave-assisted three phase partitioning (MWTPP): ammonium sulphate-t-butanol (solvent)-protein solution Conditions for MWTPP (optimized): 30 %w/w ammonium sulphate; 0.5 %w/w microalgae solution; 1:1 vol ratio; 120 s microwave time, 80% duty cycle; 100W	Yield of protein: 63.2%. Separation efficiency: 67.2%	(Chew et al., 2019)
***C. pyrenoidosa* sludge**	Lipids	10.3 % (dry-weight basis)	Lysis with [BMIM]Cl.	2-step extraction: n-hexane in 2:1 ratio for 30 minutes; ethyl alcohol 2:1 ratio.	The average lipid yield of 89.3% using the recycled [BMIM]Cl.	(Lu et al., 2019)
***N. gaditana* microalgae**	Lipids	22.2% (dry ash free-weight basis)	Steam explosion (150 °C, 5% sulfuric acid), optional prefiltration with 5000 Da membrane	Solvent: n-hexane, ratio 1:1. Experimental conditions; 60°C, 2h, with stirring.	Pre-treatment with prefiltration was preferred. 17.6% lipid recovery (w/w, DAF of untreated microalgae basis, 79% of the total lipid).	(Lorente et al., 2017)

Table 4.27. Consulted studies about solvent extraction on cell cultures (continued).

***C. vulgaris* FSP-E strain**	Proteins	n/a	Sugaring out, sonication	Liquid-liquid flotation using glucose and acetonitrile	Lab scale: 86.38% efficiency and 93.33% yield at 0.6% biomass concentration, 200 g/L of glucose concentration, 100% acetonitrile concentration with 5 min of 5s ON/10s OFF pulse mode and at a flow rate of 100 cc/min. Large scale: 85.25% efficiency and 92.24% yield.	(Sankaran et al., 2018a)
B. cepacia	Enzyme (lipase)	n/a	-	Liquid-liquid flotation using Triton X-100 and xylitol	Average lipase separation efficiency and yield of 86.46 and 87.49% with 25% w/w of xylitol concentration, 15% (w/w) Triton X-100, 80% w/w of crude lipase, 4 mL of top phase, 35 mL of bottom phase, pH 7 and 15 min of flotation time.	(Sankaran et al., 2018c)

Table 4.27. Consulted studies about solvent extraction on cell cultures (continued).

***C. sorokiniana* CY-1 strain**	Proteins	57% (dry-weight basis)	-	Liquid-liquid electric flotation using 1-propanol and dipotassium hydrogen phosphate	23.41% recovery and 173.08% separation efficiency with 60% (v/v) of 1-propanol as top phase, 250 g/L of dipotassium hydrogen phosphate as bottom phase, crude microalgae loading of 0.1 g, air flowrate of 150 cm^3/min, flotation time of 10 min, voltage of 20 V and electrode's tip touching the top phase of LBEF.	(Sankaran et al., 2018b)
***C. sorokiniana* CY 1**	Proteins	n/a	-	Liquid-liquid flotation using glucose and acetonitrile assisted by ultrasonication	81% yield with 200 g/L glucose as bottom phase with volume ratio of 1:1.25, 10 s of resting time for ultrasonication, 5 s of ultrasonication in pulse mode and 0.25 g of biomass (dry weight basis).	(Chia et al., 2019)

Table 4.27. Consulted studies about solvent extraction on cell cultures (continued).

***C. vulgaris* FSP-E**	Proteins	>70%	-	Sugaring-out assisted liquid biphasic electric flotation using sugar and acetonytrile	Separation efficiency of 73.999% separation efficiency and 69.665% yield with 0.05 g of microalgae biomass, 15 V of DC current supply with tip of the electrode at the bottom phase, 300 g/L glucose and CAN concentration of 100%, air flowrate of 150 cm^3/min, flotation time of 15 min.	(Koyande et al., 2019)
***C. sorokiniana* CY-1**	Proteins	33.70% w/w	-	Liquid biphasic flotation with the aid of ultrasonication using ammonium sulphate and propanol	97.44% separation efficiency and 88.86% yield with 250 g/L ammonium sulphate, 60% (v/v) 2-propanol, 1.0 VR, initial, 20 g/L crude biomass load, 4 mm^3/min air flowrate and 10 min of flotation time.	(Phong et al., 2017)

Table 4.28. Consulted studies about solvent extraction on animal and vegetal sources.

Source	Compounds	Content	Pre-treatment	Extraction conditions	Main results	Ref.
***Moringa oleifera* seeds**	Proteins, lipids	n/a	Drying, hulling and grinding	Aqueous extraction at 30ºC for 2 h with ethanol and petroleum ether (sample to solvent ratio 8:10).	33% protein recovery, 22.3% lipid recovery	(Chen et al., 2019)
***Acacia tortilis* seeds**	Proteins	37.5%	Grinding, defatting	2 extractions: 95% ethanol extraction and 1 M NaOH extraction with sample to solvent ratio 1:20 (w/v), room temperature, 1 h (EtOH) or 2 h (NaOH) at pH 11.	Yield of protein: 63.2%. Separation efficiency: 67.2%	(Embaby et al., 2018)
Grass pea flour	Protein	26.16 %	Defatting, sieving	Extraction with 1 M NaOH with sample to solvent ratio of 1:15 (w/v) at room temperature and pH 9.96	14.25% recovery	(Feyzi et al., 2018)

Table 4.28. Consulted studies about solvent extraction on animal and vegetal sources (continued).

Mung bean	Proteins	23.73% (dry-weight basis)	Hulling, grinding, sieving	Extraction with KOH with sample to solvent ratio of 20 mL/g at 40 ºC and pH 9.1	77.32% yield	(Du et al., 2018)
Defatted peanut meal	Proteins	53.02%		Extraction with deionized water, 0.2 M KOH, NaOH, 0.2 M NaCl or $NaHCO_3$, with sample to solvent ratio of 1:20 (w/v) for 1 h at 52ºC and pH 9-10	85.2% protein yield obtained using 0.2 M NaOH	(Uddin et al., 2018)
Defatted rice bran	Protein	16.75% (dry-weight base)	-	Extraction with 1 M NaOH with sample to solvent ratio 6:34 (w/v) for 300 min at 52ºC and pH of 10	34.51% recovery	(Bernardi et al., 2018)
***Perilla frutescens* flour**	Lipids	40.06%	-	Extraction with liquefied n-propane at 40°C and 8 MPa for 80 min	34.78% yield	(Da Silva et al., 2015)
Sesame seed	Lipids	52.6% (w/w)	Drying, milling	Extraction with liquefied n-propane at 60°C and 12 MPa for 55 min	34.1% yield	(Corso et al., 2010)

Table 4.28. Consulted studies about solvent extraction on animal and vegetal sources (continued).

Sunflower seeds	Fatty acids	53.4% (w/w)	Grinding	n-Butane at 40°C and 370 kPa	36.9% yield, solvent-free and food grade	(Rapinel et al., 2017)
Chicken liver	Proteins	-	Blending, degreasing, drying	Alkaline (0.80% NaOH, sample to solvent ratio 1:70 [w/v], 50ºC, 5h) and ultrasound-assisted alkaline (0.80% NaOH, 40ºC, on-time 2s, off-time 3s pulses, 24 kHz, 300W) extractions	67.6% and 43.5% yield for ultrasound-assisted and alkaline extractions, respectively.	(Zou et al., 2017)
Mackerel fish	Proteins	14-16% (w/w)	Blending	Acidic, alkaline (HCl or NaOH 0.1-0.4 M, sample to solvent ratio 1:10, 4ºC, 10 min) and ultrasound-assisted (HCl or NaOH 0.1 M, sample to solvent ratio 1:10, 4ºC, 750W, 20 kHz [5s on-5s off], 60% amplitude, 10 min) extractions	94.71% yield with ultrasound assisted NaOH 0.1 M extraction, vs 74.25% recovery with NaOH 0.4 M	(Álvarez et al., 2018)

Table 4.28. Consulted studies about solvent extraction on animal and vegetal sources (continued).

Egg yolk	Lipids	58.26% (w/w)	Spray-drying	Subcritical fluid-propane extraction (solid-liquid ratio of 1:9 (g/mL), 40ºC, 120 min)	63.88% extraction yield	(Su et al., 2020)

5. Adsorption

Adsorption is a separation method where a solid or liquid surface is used to retain specific components from a feed solution, which can be later recovered by desorption (Hu and Xu, 2019). The adsorption forces can be either physical or chemical, their respective characteristics being presented in Table 4.29.

Table 4.29. Main characteristics of physical and chemical adsorption. Adapted from (Hu and Xu, 2019).

	Adsorption categories	
	Physical adsorption	*Chemical adsorption*
Adsorption force	Van der Waals forces	Chemical bond force
Selectivity	Non-selective adsorption	Selective adsorption
Adsorption layer	Single or multiple layers	Single layer
Adsorption heat	Low	High
Adsorption rate	Fast	Slow
Stability	Unstable	Stable

The nature of the adsorbent can be very varied. Activated carbons, which can be produced from any carbonaceous material (Saleem et al., 2019), are the most widely used adsorbents in wastewater treatment (Hu and Xu, 2019), along with other adsorbents, such as inorganic materials (activated alumina, silica gel…) or ion-exchange resins (Crini et al., 2019).

Adsorption can be performed in different configurations, namely in batch (Eregowda et al., 2020; Reyhanitash et al., 2017) or by chromatography, either in an expanded bed (Hansson et al., 1994; Johansson et al., 1996; Strætkvern and Schwarz, 2012) or in a packed column (Li et al., 2013).

Adsorption technology can specifically recover different compounds of interest by applying different adsorbents and elution conditions, being a valuable method in purification processes.

Drawbacks of this technique include the high cost of the adsorbent and the lack of research in complex wastewaters (Hu and Xu, 2019).

Adsorption technology as a means of waste valorization has been studied in a broad range of both synthetic and real sources, but not yet in WAS (Fig. 4.34).

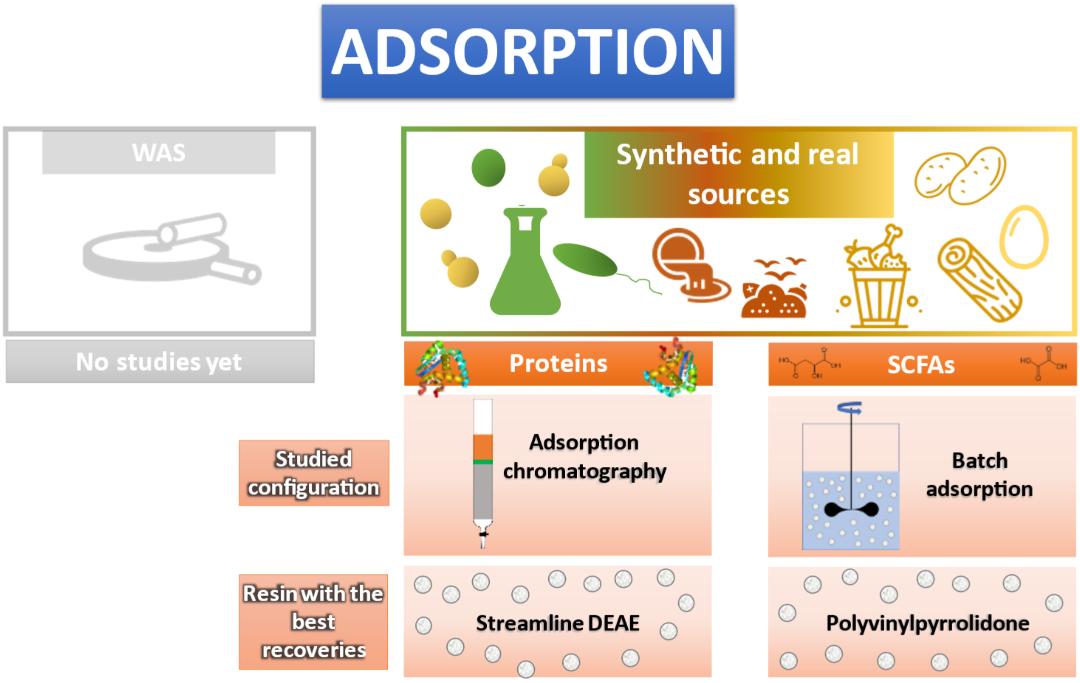

Figure 4.34. Uses of adsorption technology for the recovery of added-value biomolecules.

5.1. Adsorption on WAS

As far as we know, no literature about recovery of biomolecules from WAS hydrolysates by adsorption has been published. SCFAs, carbohydrates and proteins could be recovered by this technique, although it has been seen that protein and humic acid are difficult to separate due to their similar adsorption affinities.

Regarding the application of adsorption chromatography, expanded bed adsorption is the most suitable for WAS, as it allows to work with unclarified streams, in opposition to packed columns (Barnfield Frej et al., 1994).

The adsorption step usually goes with the chromatography step to achieve valuable protein recovery. As future steps in WAS research, it would be necessary to characterise the proteins present in the hydrolysate and study if there are any valuable ones that justify their purification by means of this high-performance, more expensive separation and purification method.

5.2. Adsorption in other industries

Works regarding the recovery of proteins and SCFAs are prevalent in the existing literature, while only one study regarding the recovery of carbohydrates via adsorption techniques (Westerberg et al., 2012) has been found, and none recovering humic acids. Depending on the biomolecules to be recovered, the nature of the source varies: protein recovery has only been studied from real sources, namely microorganisms (Barnfield Frej et al., 1994; Bierau et al., 2001; Hansson et al., 1994; Johansson et al., 1996) and food-related sources (Li et al., 2013; Strætkvern and Schwarz, 2012); whereas SCFAs were almost evenly extracted from synthetic (Eregowda et al., 2020; López-Velandia et al., 2014; Reyhanitash et al., 2017; Suescún-Mathieu et al., 2014; Yousuf et al., 2016) and from real sources (Da Silva and Miranda, 2013; Karp et al., 2018; Talebi et al., 2020) (Table 4.30).

Protein recovery has been studied exclusively by adsorption chromatography, mainly of the expanded bed type, which, as stated above, would be the most recommendable configuration dealing with a complex matrix as solubilised WAS. The literature focus on the recovery of single specific valuable proteins rather than on separating the bulk protein present on the feed. The highest protein recoveries (95%), both at lab and pilot scale, were achieved with the ion exchange resin STREAMLINE DEAE as stationary phase (Barnfield Frej et al., 1994). However, it is important to note, that these recovery yields vary depending on the target protein. For instance, while using the same resin (STREAMLINE DEAE) and starting from the same source (*E.coli* culture), the extraction yields of recombinant ZZ-M5 (Hansson et al., 1994) and modified *Pseudomonas aeruginosa* exotoxin A (Johansson et al., 1996) proteins differed from 93% to 79%, respectively. Resins are the most widely used stationary phase. Furthermore, the only adsorbent which is not a resin (i.e., collagen fibre) is used in packed bed adsorption chromatography to separate lysozyme from a much simpler source (egg white), so towards the use of this adsorbent with solubilised WAS, a prior separation/clarification step should be regarded.

In respect of the adsorption of SCFAs, all the consulted studies but one performed batch adsorptions as the preferred configuration for the separation of the target compounds. The most studied species of SCFAs were propionic, acetic and butyric acids. In this case, the adsorbent aimed to capture all the SCFAs present in the feed and not just one specific species, like in protein adsorption. Thus, batch adsorption can be used as a straightforward means to extract SCFAs from solubilised WAS. Furthermore, as these batch adsorptions have been tested, it is reasonable to think that no major difficulties should be encountered. Nevertheless, studies on the adsorption of SCFAs from WAS should be performed before implementing this technique in a functioning process.

Several adsorbents have been tested, mainly activated carbons and different resins. In both papers where weak base resin and activated carbon were compared, the first adsorbent showed higher affinity for all SCFAs (propionic, acetic, butyric and lactic), although desorption was not studied. Polyvinylpyrrolidone (PVP) was the resin that achieved the highest recoveries, fully adsorbing and desorbing propionic and succinic acids under adequate conditions (using enough adsorbent/ bed volumes of elution solution).

Cell lysis by osmotic shock or wet bead milling appear to be applicable pre-treatments for WAS solubilisation reviewed in this section. Cell lysis can be achieved by osmotic shock by suddenly reducing the osmotic pressure around the cell, i.e., changing the cells from a highly saline medium to a low saline one (Johansson et al., 1996). This pre-treatment has not yet been tested on WAS; however, due to the great dewaterability difficulties that this sludge poses, it is reasonable to think that other methods, such as sonication or hydrothermal treatments may be more efficient in breaking the floc structures of the sludge.

(Bierau et al., 2001) tested wet bead milling (mechanical disruption of the cell suspension by fine particles) as a pre-treatment for cell liquefaction, although the degree of solubilisation was not indicated in the article. Milling as a pre-treatment on WAS has not been thoroughly studied, and never towards the recovery of biocompounds. Its main drawbacks include lower solubilisation rates compared to the other reviewed pre-treatments and high energy consumption rates (Khanh Nguyen et al., 2021).

Table 4.30. Consulted studies about adsorption.

Source	Compounds	Content	Pre-treatment	Extraction conditions	Main results	Ref.
***Escherichia coli* culture**	Protein (recombinant protein ZZ-M5)	550 mg/L fermentation broth	-	Expanded bed adsorption chromatography with ion exchange resin (STREAMLINE DEAE) Online 1:1 mixing with loading buffer. pH adjusted to 5.5 to adsorb target protein. Elution with 0.5 M NaCl.	16-fold size reduction 93% protein recovery 99.6% OD reduction	(Hansson et al., 1994)
***E. coli* culture**	Protein (modified *Pseudomonas aeruginosa* exotoxin A)	1.95 g/L	Cell disruption by osmotic shock	Expanded bed adsorption chromatography with ion exchange resin (STREAMLINE DEAE) Column washing with 50 mM Tris buffer pH 7.4. Elution with 20 mM Tris buffer, pH 7.4 containing 0.5 M NaCl.	79% protein recovery, 92.5% volume reduction	(Johansson et al., 1996)

Table 4.30. Consulted studies about adsorption (continued).

Potato juice	Protein	10.1 g/L	Homogeneization, centrifugation to remove starch	Expanded bed adsorption chromatography with resin modified with a mixed mode ligand. Column washing with 10 mM citric acid/citrate pH 4.5; elution with 20 mM sodium hydroxide, pH 12.	Total protein yield: 54.0±9.8% Esterase yield: 80.5±11.4%	(Strætkvern and Schwarz, 2012)
Chicken egg white powder	Enzyme (lysozyme)	n/a	-	Packed bed adsorption chromatography with collagen fiber adsorbent Elution with pH 7.5 buffer and pH 7.5 buffer containing 0.6 M NaCl subsequently	93.6% purity obtained with a mass recovery of 86.7%	(Li et al., 2013)
***E. coli* homogenate**	Protein (annexin V)	n/a		Expanded bed adsorption chromatography with ion exchange resin (STREAMLINE DEAE) Washing with 30 mM ammonium acetate, pH 5.5, 3 mS/cm; Elution with 30 mM ammonium acetate containing 250 mM NaCl, pH 5.5, 28 mS/cm	Recovery of approximately 95% at both lab scale and pilot scale	(Barnfield Frej et al., 1994)

Table 4.30. Consulted studies about adsorption (continued).

Waste brewers' yeast	Enzyme (glyceraldehyde 3-phophate dehydrogenase)	5.9 U/mL	Wet-milling, filtering	Expanded bed adsorption dye-ligand affinity chromatography (Cibacron Blue 3GA immobilised as a pseudo-affinity ligand upon Macrosorb K6AX)	Purification factor of 3.9	(Bierau et al., 2001)
Fermentation broths	Propionic acid	0.5-50.0 g/L		Batch adsorption with weak base resin (Purolite A133S) and activated carbon (Carbomafra 119) tested as adsorbents Water, ethanol and n-propanol tested as eluents	64% recovery with resin and n-propanol	(Da Silva and Miranda, 2013)
Synthetic carboxylic acid solutions	Acetic, propionic and butyric acids	acetic acid 16% v/v, propionic acid 2% v/v, butyric acid 2% v/v	-	Batch adsorption with activated carbon and modified activated carbon from watermelon shells tested as adsorbents.	Adsorption efficiencies of 71%, 70% and 63% for acetic acid, propionic acid and butyric acid with modified activated carbon; and of 32%, 30% and 27% for the respective acids with activated carbon.	(López-Velandia et al., 2014)

Table 4.30. Consulted studies about adsorption (continued).

Fermentation broths	Succinic and propionic acids	38.7 g/L (succinic acid), 35.6 g/L (propionic acid)	Pre-filtering, chromatography with cation exchange resin (DOWEX G-26 resin) to remove cations, activated carbon treatment	Packed bed adsorption chromatography with PVP resin (Reillex 425) Elution with methanol for succinic acid and acetone for propionic acid.	Loading capacity of 106 mg of succinic acid/g dry PVP. 4 BV of methanol needed to completely desorb succinic acid. Loading capacity of 85 mg of propionic acid/g dry PVP. 2.5 BV of acetone required to fully desorb propionic acid.	(Karp et al., 2018)
Synthetic carboxylic acid solutions	Acetic, propionic and butyric acid	acetic acid 16% v/v, propionic acid 2% v/v and butyric acid 2% v/v		Batch adsorption with activated carbon from sugarcane bagasse. Desorption tested by sonication, heating, sonication followed by heating and heating followed by sonication.	Highest individual VCA adsorption percentages of 60, 48 and 21%. Highest VCA desorption percentage obtained by sonication (38.02%), then by heating (34.68%)	(Suescún-Mathieu et al., 2014)
Dark fermented synthetic food waste	Lactic, acetic and butyric acids	11.6 g/L (lactic acid), 6.6 g/L (butyric acid), 2.8 g/L (acetic acid)		Batch adsorption with weakly basic anion exchange resin (Amberlite® IRA-67) and activated carbon (Norit® type Darco®)	Adsorption of 73% and 63% of carboxylic acids by resin and activated carbon, respectively. Desorption was not studied.	(Yousuf et al., 2016)

Table 4.30. Consulted studies about adsorption (continued).

Synthetic fermented wastewater	Lactic, acetic, propionic and butyric acids	All acids at 0.25% wt		Batch adsorption with four types of polystyrene-divinylbenzene-based resins (Lewatit VP OC 1065 [primary amine], Amberlite IRA96 RF [secondary amine], Amberlite IRA96 SB [tertiary amine], and Lewatit VP OC1064 MD PH [nonfunctionalized]). Desorption by a temperature-profiles evaporation and stripping with N2.	Batch capacity of 9.7 g of lactic acid, 12.5 g of acetic acid, 26.5 g of propionic acid and 65.2 g of butyric acid per kg of nonfunctionalized adsorbent. After desorption, butyric acid was obtained with purities of up to 91 wt %. The other VFA could not be effectively concentrated.	(Reyhanitash et al., 2017)
Synthetic carboxylic acid solution	Acetic, propionic, isobutyric, butyric, isovaleric and valeric acids	n/a		Batch adsorption with two anion exchange resins (Amberlite IRA-67 and Dowex optipore L-493). Desorption with NaOH solution.	Selective recoveries of > 85% for acetic acid and of ~ 75% for propionic acid.	(Eregowda et al., 2020)

Table 4.30. Consulted studies about adsorption (continued).

Fermented landfill leachate	Acetic and butyric acids	3.28 g/L (acetic acid), 1.12 g/L (butyric acid)		Batch adsorption with activated carbon (Bendosen C1570-5330341) Vortex, water bath sonicator, probe sonicator, and shaker studied as desorption methods. Deionized water, isopropyl alcohol and ethanol studied as desorbents.	Adsorptions of acetic and butyric acid of 88.94% and 98.53% respectively, with activated carbon and shaker. Selective recovery of 89.1% (2.54 g/L) of acetic acid with deionized water; 67.8% (0.71 g/L) of butyric acid recovery by ethanol.	(Talebi et al., 2020)
Hot-water-extracted spruce wood	Saccharides (galactoglucomannans)	79%	Filtration, fixed-bed adsorption chromatography with hydrophobic polymeric resin (Amberlite XAD-16).	Fixed-bed adsorption chromatography with a phenylic reversed-phase analytical chromatographic column (XBridge Phenyl 5 µm). Elution with acetonitrile.	The upgraded GGM fraction contained about 1.5% aromatics. Polymeric xylan was accumulated in the GGM fraction. As products, 88% of upgraded hemicelluloses recovered.	(Westerberg et al., 2012)

6. Conclusions and knowledge gaps

The revalorization of WAS through the recovery of added value biocompounds has been unevenly studied, depending on the target biomolecule and the technology employed for its obtention. In this sense, besides the recovery of inorganic compounds, such as phosphorus or nitrogen, the main biocompounds recovered were: i) lipids by solvent extraction to obtain biofuel, ii) humic substances using membrane filtration to produce also fertilizers, and iii) proteins, although at lesser extent, through precipitation to use as animal feed or wood adhesive.

Considering the revalorization studies of other wastes with similar characteristics to that of WAS reviewed in this work, several research lines towards optimizing the process of WAS revalorization can be opened, including: i) the use of ethanol or alginate as precipitation agents for proteins; ii) the application of membrane technology for the concentration and further recovery of enzymes, proteins, lipids, carbohydrates and SCFAs; iii) the use of state-of-the-art solvent extraction techniques (biphasic flotation or three-phase partitioning), to extract more efficiently not only lipids, but also proteins; iv) the application of adsorption technology, either through adsorption chromatography to recover high-value target proteins, or batch adsorption to recover SCFAs. It should be noted that, prior to the use of adsorption chromatography to recover proteins, it is necessary to perform a proteomic characterization of WAS to determine the presence of the high-value ones, otherwise the use of this technology would not be justified, since it is a highly selective technique. Besides, specific protocols should be developed based on the physical-chemical properties of the target proteins.

The results gathered in this review show that the revalorization of WAS through an integrated process involving the recovery of bulk and specific proteins, lipids, SCFAs, and humic acids can be feasible, although more investigation is required to prove the extent of its effectiveness.

The effective recovery of carbohydrates has yet to be investigated, as reviewed studies tackling this matter were only focused on their concentration by membrane technology.

Two different integrated methods for the recovery of lipids, proteins and humic acids from WAS are proposed below based on the different reported technologies (Fig. 4.35):

A) First, WAS would be dewatered. Dewatering WAS would both allow to extract lipids by a S-L extraction and concentrate the sludge for next purification steps. WAS would then be solubilised (the optimal solubilisation method among those reviewed in this paper should be determined in further studies). Bulk proteins would then be recovered by precipitation methods. After precipitation, high-value proteins, as well as SCFAs, would be recovered by either adsorption chromatography or batch adsorption. Finally, a concentrated humic acid fertilizer would be obtained by membrane filtration.

B) WAS would be solubilised in the first place and concentrated and fractionated afterwards by membrane filtration. Lipids would then be recovered by either three-phase partitioning or by liquid biphasic flotation. Proteins and enzymes could also be recovered by this technique. From this point, the rest of the purification steps would be as detailed above (precipitation, adsorption and membrane filtration).

Regarding the preference of integrated method A or B, it should be noted that it is needed to perform a sub-critical water pre-treatment before S-L extraction in method A in order to improve the recovery of neutral lipids significantly. This pre-treatment is carried out at similar operating conditions (temperatures and pressures) than those used in WAS solubilisation stage by means of hydrothermal treatments (TH or WO). Therefore, the proposed method B could be preferable since WAS solubilisation stage is applied first, thus avoiding the sub-critical water pre-treatment. Besides, membrane filtration is employed for fractioning and concentration of biocompounds in method B. The use of this technique is highly convenient for three reasons: i) the production of two valuable streams that can be purified: retentate and permeate, ii) the improvement of the subsequent purification steps due to the high proportion of the biocompounds in each of these streams and iii) its low energy consumption.

The main difference between the recovery efficiencies of the two proposed methods would lay on the solvent extraction step for the recovery of lipids: higher yields have been reported with L-L extraction, with recoveries between 6.3 and 7.87 g of lipids per 100 g of dry sludge (Huynh et al., 2010; Olkiewicz et al., 2014), while recoveries of only 2 to 4 g per 100 g of dry sludge were reported after S-L extraction (Melero et al., 2015; Revellame et al., 2011). As for the rest of the process, recoveries are expected to be similar: up to 92% of protein can be recovered by precipitation ((Pervaiz and Sain, 2011), and SCFAs are expected to be fully recovered by batch adsorption with PVP or with polystyrene-divinylbenzene-based resins applying optimised WAS:resin ratio and bed volumes of recovery solution. Finally, humic acids could be concentrated up to 20-fold by membrane filtration, with a recovery yield of 88.6% according to (Wei et al., 2016).

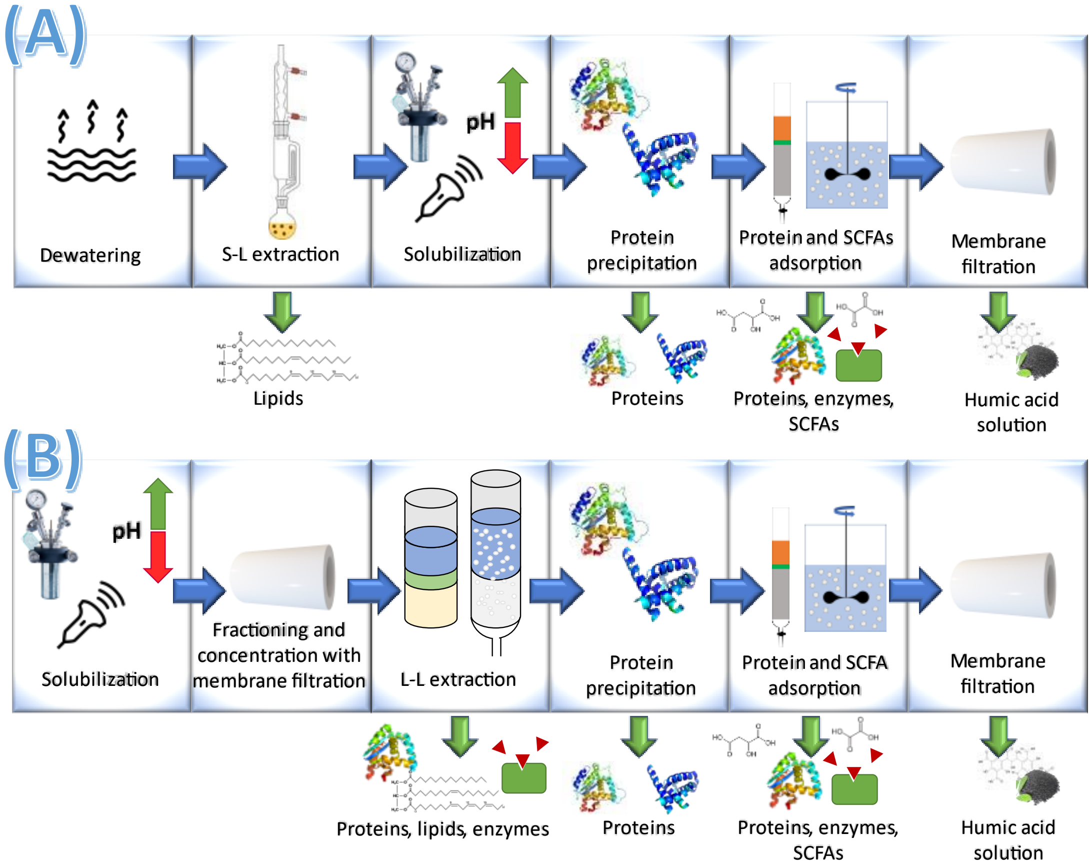

Figure 4.35. Proposed integrated methods for WAS revalorization.

More investigation has yet to be conducted before this integrated process can be effectively implemented, this being essential to turn the WAS residue into a renewable source in the context of circular economy.

The application of the proposed integrated methods to other waste streams will imply a thorough evaluation of the characteristics and composition of those streams in order to determine which steps/stages will be required.

Declaration of Competing Interest

The authors declare that they have no known competing financial interests or personal relationships that could have appeared to influence the work reported in this paper.

Acknowledgements

The authors are grateful for the financial support from the Spanish Ministry of Science, Innovation and Universities (MCIU) through the project RTI2018-094218-B-I00 and FEDER funds from European Union. The author Daniel Núñez thanks the Principality of Asturias, Spain, for their financial support through the Severo Ochoa scholarship no BP19-093.

References

Abejón, R., Abejón, A., Belleville, M.-P., Garea, A., Irabien, A., Sanchez-Marcano, J., 2016. Water recovery and reuse in the fractionation of protein hydrolysate by ultrafiltration and nanofiltration membranes. Chem. Eng. Trans. 52, 283–288. https://doi.org/10.3303/CET1652048

Afonso, M.D., Bórquez, R., 2002. Review of the treatment of seafood processing wastewaters and recovery of proteins therein by membrane separation processes - Prospects of the ultrafiltration of wastewaters from the fish meal industry. Desalination 142, 29–45. https://doi.org/10.1016/S0011-9164(01)00423-4

Akmehmet Balcioglu, I., Bilgin Oncu, N., Mercan, N., 2017. Beneficial effects of treating waste secondary sludge with thermally activated persulfate. J. Chem. Technol. Biotechnol. 92, 1192–1202. https://doi.org/10.1002/jctb.5108

Álvarez, C., Lélu, P., Lynch, S.A., Tiwari, B.K., 2018. Optimised protein recovery from mackerel whole fish by using sequential acid/alkaline isoelectric solubilization precipitation (ISP) extraction assisted by ultrasound. LWT - Food Sci. Technol. 88, 210–216. https://doi.org/10.1016/j.lwt.2017.09.045

Antczak, J., Szczygiełda, M., Prochaska, K., 2018. An environment-friendly multi-step membrane-based system for succinic acid recovery from the fermentation broth. Desalin. Water Treat. 128, 51–60. https://doi.org/10.5004/dwt.2018.22575

Awasthi, M.K., Wang, Q., Ren, X., Zhao, J., Huang, H., Awasthi, S.K., Lahori, A.H., Li, R., Zhou, L., Zhang, Z., 2016. Role of biochar amendment in mitigation of nitrogen loss and greenhouse gas emission during sewage sludge composting. Bioresour. Technol. 219, 270–280. https://doi.org/10.1016/j.biortech.2016.07.128

Baker, R.W., 2012. Overview of Membrane Science and Technology, in: Membrane Technology and Applications. pp. 1–14. https://doi.org/10.1002/9781118359686.ch1

Barnfield Frej, A. -K, Hjorth, R., Hammarström, Å., 1994. Pilot scale recovery of recombinant annexin V from unclarified escherichia coli homogenate using expanded bed adsorption. Biotechnol. Bioeng. 44, 922–929. https://doi.org/10.1002/bit.260440808

Berk, Z., Berk, Z., 2009. Chapter 10 – Membrane processes. Food Process Eng. Technol. 233–257. https://doi.org/10.1016/B978-0-12-373660-4.00010-7

Bernardi, S., Corso, M.P., Baraldi, I.J., Colla, E., Canan, C., 2018. Obtaining concentrated rice bran protein by alkaline extraction and stirring - Optimization of conditions. Int. Food Res. J. 25, 1133–1139.

Bharathiraja, B., Yogendran, D., Ranjith Kumar, R., Chakravarthy, M., Palani, S., 2014. Biofuels from sewage sludge- A review. Int. J. ChemTech Res. 6, 4417–4427.

Białas, W., Stangierski, J., Konieczny, P., 2015. Protein and water recovery from poultry processing wastewater integrating microfiltration, ultrafiltration and vacuum membrane distillation. Int. J. Environ. Sci. Technol. 12, 1875–1888. https://doi.org/10.1007/s13762-014-0557-4

Bierau, H., Hinton, R.J., Lyddiatt, A., 2001. Direct process integration of cell disruption and fluidised bed adsorption in the recovery of labile microbial enzymes. Bioseparation 10, 73–85. https://doi.org/10.1023/A:1012054622066

Bleam, W., 2017. Natural Organic Matter. https://doi.org/10.1016/B978-0-12-804178-9.00007-0

Boychyn, M., Doyle, W., Bulmer, M., More, J., Hoare, M., 2000. Laboratory scaledown of protein purification processes involving fractional precipitation and centrifugal recovery. Biotechnol. Bioeng. 69, 1–10. https://doi.org/10.1002/(SICI)1097-0290(20000705)69:1<1::AID-BIT1>3.0.CO;2-4

Bridle, T.R., Pritchard, D., 2004. Energy and nutrient recovery from sewage sludge via pyrolysis. Water Sci. Technol. 50, 169–175. https://doi.org/10.2166/wst.2004.0562

Burgess, R.R., 2009. Chapter 20 Protein Precipitation Techniques, in: Methods in Enzymology. pp. 331–342. https://doi.org/10.1016/S0076-6879(09)63020-2

Capar, G., Aygun, S.S., Gecit, M.R., 2008. Treatment of silk production wastewaters by membrane processes for sericin recovery. J. Memb. Sci. 325, 920–931. https://doi.org/10.1016/j.memsci.2008.09.020

Cassini, A.S., Tessaro, I.C., Marczak, L.D.F., Pertile, C., 2010. Ultrafiltration of wastewater from isolated soy protein production: A comparison of three UF membranes. J. Clean. Prod. 18, 260–265. https://doi.org/10.1016/j.jclepro.2009.10.016

Castro-Puyana, M., Herrero, M., Mendiola, J.A., Ibáñez, E., 2013. Subcritical water extraction of bioactive components from algae. Funct. Ingredients from Algae Foods Nutraceuticals 534–560. https://doi.org/10.1533/9780857098689.3.534

Chemat, F., Abert Vian, M., Fabiano-Tixier, A.S., Nutrizio, M., Režek Jambrak, A., Munekata, P.E.S., Lorenzo, J.M., Barba, F.J., Binello, A., Cravotto, G., 2020. A review of sustainable and intensified techniques for extraction of food and natural products. Green Chem. 22, 2325–2353. https://doi.org/10.1039/C9GC03878G

Chen, C.Y., Li, W.T., Pan, S.Y., 2021. Performance Evaluation of Cascade Separation for a Humic Substance and Nutrient Recovery from Piggery Wastewater toward a Circular Bioeconomy. ACS Sustain. Chem. Eng. 9, 8115–8124. https://doi.org/10.1021/acssuschemeng.1c01106

Chen, H., Wang, L., 2017. Posttreatment Strategies for Biomass Conversion, in: Technologies for Biochemical Conversion of Biomass. Metallurgical Industry Press, pp. 197–217. https://doi.org/10.1016/b978-0-12-802417-1.00008-9

Chen, J., 2017. From waste to treasure: turning activated sludge into bioplastic poly-3-hydroxybutyrate. Shengwu Gongcheng Xuebao/Chinese J. Biotechnol. 33, 1934–1944.

https://doi.org/10.13345/j.cjb.170391

Chen, Q., An, X., Li, H., Su, J., Ma, Y., Zhu, Y.G., 2016. Long-term field application of sewage sludge increases the abundance of antibiotic resistance genes in soil. Environ. Int. 92–93, 1–10. https://doi.org/10.1016/j.envint.2016.03.026

Chen, R., Wang, X.J., Zhang, Y.Y., Xing, Y., Yang, L., Ni, H., Li, H.H., 2019. Simultaneous extraction and separation of oil, proteins, and glucosinolates from Moringa oleifera seeds. Food Chem. 300, 125162. https://doi.org/10.1016/J.FOODCHEM.2019.125162

Chen, Y., Jiang, S., Yuan, H., Zhou, Q., Gu, G., 2007. Hydrolysis and acidification of waste activated sludge at different pHs. Water Res. 41, 683–689. https://doi.org/10.1016/j.watres.2006.07.030

Chen, Y.C., Jaczynski, J., 2007. Protein recovery from rainbow trout (Oncorhynchus mykiss) processing byproducts via isoelectric solubilization/precipitation and its gelation properties as affected by functional additives. J. Agric. Food Chem. 55, 9079–9088. https://doi.org/10.1021/jf071992w

Chew, K.W., Chia, S.R., Lee, S.Y., Zhu, L., Show, P.L., 2019. Enhanced microalgal protein extraction and purification using sustainable microwave-assisted multiphase partitioning technique. Chem. Eng. J. 367, 1–8. https://doi.org/10.1016/j.cej.2019.02.131

Chia, S.R., Chew, K.W., Show, P.L., Sivakumar, M., Ling, T.C., Tao, Y., 2019. Isolation of protein from Chlorella sorokiniana CY1 using liquid biphasic flotation assisted with sonication through sugaring-out effect. J. Oceanol. Limnol. 37, 898–908. https://doi.org/10.1007/s00343-019-8246-2

Chishti, S.S., Nazrul Hasnain, S., Altaf Khan, M., 1992. Studies on the recovery of sludge protein. Water Res. 26, 241–248. https://doi.org/10.1016/0043-1354(92)90224-R

Clarke, K.G., 2013. Downstream processing, in: Bioprocess Engineering. pp. 209–234. https://doi.org/10.1533/9781782421689.209

Contreras, E.M., Bertola, N.C., Giannuzzi, L., Zaritzky, N.E., 2002. A modified method to determine biomass concentration as COD in pure cultures and in activated sludge systems. Water SA 28, 463–467. https://doi.org/10.4314/wsa.v28i4.4920

Corso, M.P., Fagundes-Klen, M.R., Silva, E.A., Cardozo Filho, L., Santos, J.N., Freitas, L.S., Dariva, C., 2010. Extraction of sesame seed (Sesamun indicum L.) oil using compressed propane and supercritical carbon dioxide. J. Supercrit. Fluids 52, 56–61. https://doi.org/10.1016/J.SUPFLU.2009.11.012

Costa, M.A.L., Farinas, C.S., Miranda, E.A., 2018. Ethanol precipitation as a downstream processing step for concentration of xylanases produced by submerged and solid-state fermentation. Brazilian J. Chem. Eng. 35, 477–488. https://doi.org/10.1590/0104-6632.20180352s20160502

Crini, G., Lichtfouse, E., Wilson, L.D., Morin-Crini, N., 2019. Conventional and non-conventional adsorbents for wastewater treatment. Environ. Chem. Lett. 17, 195–213. https://doi.org/10.1007/s10311-018-0786-8

Cui, Z.F., Muralidhara, H.S., 2010. Membrane Technology. Membr. Technol. https://doi.org/10.1016/C2009-0-19129-8

Da Silva, A.H., Miranda, E.A., 2013. Adsorption/desorption of organic acids onto different adsorbents for their recovery from fermentation broths. J. Chem. Eng. Data 58, 1454–1463. https://doi.org/10.1021/je3008759

Da Silva, C.M., Zanqui, A.B., Gohara, A.K., De Souza, A.H.P., Cardozo-Filho, L., Visentainer, J.V., Rovigatti Chiavelli, L.U., Bittencourt, P.R.S., Da Silva, E.A., Matsushita, M., 2015. Compressed n-propane extraction of lipids and bioactive compounds from Perilla (Perilla frutescens). J. Supercrit. Fluids 102, 1–8. https://doi.org/10.1016/J.SUPFLU.2015.03.016

Dai, J., Xu, M., Chen, J., Yang, X., Ke, Z., 2007. PCDD/F, PAH and heavy metals in the sewage sludge from six wastewater treatment plants in Beijing, China. Chemosphere 66, 353–361. https://doi.org/10.1016/j.chemosphere.2006.04.072

De Melo, B.A.G., Motta, F.L., Santana, M.H.A., 2016. Humic acids: Structural properties and multiple functionalities for novel technological developments. Mater. Sci. Eng. C 62, 967–974. https://doi.org/10.1016/J.MSEC.2015.12.001

Des Soye, B.J., Davidson, S.R., Weinstock, M.T., Gibson, D.G., Jewett, M.C., 2018. Establishing a High-Yielding Cell-Free Protein Synthesis Platform Derived from Vibrio natriegens. https://doi.org/10.1021/acssynbio.8b00252

Djamai, W., Mazzei, R., Bazzarelli, F., Dahmani, B., Giorno, L., 2019. Membrane-assisted biorefinery of microalgae to obtain enriched fractions of bioderived molecules. Biofuels, Bioprod. Biorefining 1–11. https://doi.org/10.1002/bbb.2006

Dong, Y., Zhu, F.F., Zhang, R.Y., Wang, P., Chen, B.L., Zhang, D.R., 2019. Preliminary study on extraction and purification of ceramide in sewage sludge. Zhongguo Huanjing Kexue/China Environ. Sci. 39, 2063–2070.

Du, M., Xie, J., Gong, B., Xu, X., Tang, W., Li, X., Li, C., Xie, M., 2018. Extraction, physicochemical characteristics and functional properties of Mung bean protein. Food Hydrocoll. 76, 131–140. https://doi.org/10.1016/J.FOODHYD.2017.01.003

Dufreche, S., Hernandez, R., French, T., Sparks, D., Zappi, M., Alley, E., 2007. Extraction of lipids from municipal wastewater plant microorganisms for production of biodiesel. JAOCS, J. Am. Oil Chem. Soc. 84, 181–187. https://doi.org/10.1007/s11746-006-1022-4

Dumay, J., Radier, S., Barnathan, G., Bergé, J.P., Jaouen, P., 2008. Recovery of valuable soluble compounds from washing waters generated during small fatty pelagic surimi processing by membrane processes. Environ. Technol. 29, 451–461. https://doi.org/10.1080/09593330801983912

Embaby, H.E., Swailam, H.M., Rayan, A.M., 2018. Preparation and physicochemical properties of protein concentrate and isolate produced from Acacia tortilis (Forssk.) Hayne ssp. raddiana. J. Food Sci.

Technol. 55, 489–495. https://doi.org/10.1007/S13197-017-2957-1

Eregowda, T., Rene, E.R., Rintala, J., Lens, P.N.L., 2020. Volatile fatty acid adsorption on anion exchange resins: kinetics and selective recovery of acetic acid. Sep. Sci. Technol. 55, 1449–1461. https://doi.org/10.1080/01496395.2019.1600553

Eurostat, 2022. Sewage sludge production and disposal from urban wastewater (in dry substance (d.s)) [WWW Document]. URL https://ec.europa.eu/eurostat/databrowser/view/ten00030/default/table?lang=en (accessed 1.24.22).

Expert Market Research, 2020a. Protein Ingredients Market Size, Share, Analysis, Report 2022-2027 [WWW Document]. URL https://www.expertmarketresearch.com/reports/protein-ingredients-market (accessed 1.18.22).

Expert Market Research, 2020b. Enzymes Market Report Size, Share, Growth, Price Trends 2022-2027 [WWW Document]. URL https://www.expertmarketresearch.com/reports/enzymes-market (accessed 1.18.22).

Fabian, C.B., Huynh, L.H., Ju, Y.H., 2010. Precipitation of rice bran protein using carrageenan and alginate. LWT - Food Sci. Technol. 43, 375–379. https://doi.org/10.1016/j.lwt.2009.08.005

Fact.MR, 2020. Polysaccharides and Oligosaccharides Market Forecast, Trend Analysis & Competition Tracking - Global Market Insights 2020 to 2030 [WWW Document]. URL https://www.factmr.com/report/427/polysaccharides-oligosaccharides-market (accessed 1.26.22).

Feairheller, S.H., Taylor, M.M., Windus, W., Filachione, E.M., Naghski, J., 1972. Recovery and Analyses of Hair Proteins from Tannery Unhairing Wastes. J. Agric. Food Chem. 20, 668–670. https://doi.org/10.1021/jf60181a033

Feyzi, S., Milani, E., Golimovahhed, Q.A., 2018. Grass Pea (Lathyrus sativus L.) Protein Isolate: The Effect of Extraction Optimization and Drying Methods on the Structure and Functional Properties. Food Hydrocoll. 74, 187–196. https://doi.org/10.1016/J.FOODHYD.2017.07.031

Fisher, R.R., Glatz, C.E., 1988. Polyelectrolyte precipitation of proteins: I. The effect of reactor conditions. Biotechnol. Bioeng. 32, 777–785. https://doi.org/10.1002/bit.260320609

Fraga, M.C., Sanches, S., Crespo, J.G., Pereira, V.J., 2017. Assessment of a new silicon carbide tubular honeycomb membrane for treatment of olive mill wastewaters. Membranes (Basel). 7. https://doi.org/10.3390/membranes7010012

Frølund, B., Griebe, T., Nielsen, P.H., 1995. Enzymatic activity in the activated-sludge floc matrix. Appl. Microbiol. Biotechnol. 43, 755–761. https://doi.org/10.1007/s002530050481

Fytili, D., Zabaniotou, A., 2008. Utilization of sewage sludge in EU application of old and new methods-A review. Renew. Sustain. Energy Rev. 12, 116–140. https://doi.org/10.1016/j.rser.2006.05.014

Gao, Y., Qin, J., Wang, Z., Østerhus, S.W., 2019. Backpulsing technology applied in MF and UF processes for membrane fouling mitigation: A review. J. Memb. Sci. 587, 117136. https://doi.org/10.1016/J.MEMSCI.2019.05.060

García, M., Urrea, J.L., Collado, S., Oulego, P., Díaz, M., 2017. Protein recovery from solubilized sludge by hydrothermal treatments. Waste Manag. 67, 278–287. https://doi.org/10.1016/J.WASMAN.2017.05.051

Gascó, G., Lobo, M.C., 2007. Composition of a Spanish sewage sludge and effects on treated soil and olive trees. Waste Manag. 27, 1494–1500. https://doi.org/10.1016/J.WASMAN.2006.08.007

Geissdoerfer, M., Savaget, P., Bocken, N.M.P., Hultink, E.J., 2017. The Circular Economy – A new sustainability paradigm? J. Clean. Prod. 143, 757–768. https://doi.org/10.1016/j.jclepro.2016.12.048

Gohil, J.M., Choudhury, R.R., 2018. Introduction to Nanostructured and Nano-enhanced Polymeric Membranes: Preparation, Function, and Application for Water Purification, in: Nanoscale Materials in Water Purification. Elsevier, pp. 25–57. https://doi.org/10.1016/B978-0-12-813926-4.00038-0

Gringer, N., Hosseini, S.V., Svendsen, T., Undeland, I., Christensen, M.L., Baron, C.P., 2015. Recovery of biomolecules from marinated herring (Clupea harengus) brine using ultrafiltration through ceramic membranes. LWT - Food Sci. Technol. 63, 423–429. https://doi.org/10.1016/j.lwt.2015.03.001

Guo, W., Ngo, H.H., Li, J., 2012. A mini-review on membrane fouling. Bioresour. Technol. 122, 27–34. https://doi.org/10.1016/j.biortech.2012.04.089

Hansson, M., Ståhl, S., Hjorth, R., Uhlén, M., Moks, T., 1994. Single-step recovery of a secreted recombinant protein by expanded bed adsorption. Bio/Technology 12, 285–288. https://doi.org/10.1038/nbt0394-285

Hau, C.W.Y., Leung, W.W.F., 2016. Experimental investigation of backpulse and backblow cleaning of nanofiber filter loaded with nano-aerosols. Sep. Purif. Technol. 163, 30–38. https://doi.org/10.1016/j.seppur.2016.02.041

Hegazi, S.M., Foda, M.S., Salem, S.A., Eldin, S.M.B., 1973. Recovery and Amino Acid Composition of Protein Precipitates Isolated from Rice Starch Processing Liquors. Starch - Stärke 25, 92–94. https://doi.org/10.1002/star.19730250306

Hemavathi, A.B., Raghavarao, K.S.M.S., 2011. Membrane processing for purification and concentration of β-glycosidases from barley (Hordeum vulgare). Biotechnol. Bioprocess Eng. 16, 282–290. https://doi.org/10.1007/s12257-010-0368-5

Hoare, M., Dunnill, P., 1984. Precipitation of Food Proteins and Their Recovery By Centrifuging and Ultrafiltration. J. Chem. Technol. Biotechnol. Biotechnol. 34 B, 199–205. https://doi.org/10.1002/jctb.280340309

Hsiau, P.C., Lo, S.L., 1998. Extractabilities of heavy metals in chemically-fixed sewage sludges, in: Journal of Hazardous Materials. pp. 73–82. https://doi.org/10.1016/S0304-3894(97)00121-0

Hu, H., Xu, K., 2019. Physicochemical technologies for HRPs and risk control, High-Risk Pollutants in Wastewater. https://doi.org/10.1016/B978-0-12-816448-8.00008-3

Huynh, L.H., Kasim, N.S., Ju, Y.H., 2010. Extraction and analysis of neutral lipids from activated sludge with and without sub-critical water pre-treatment. Bioresour. Technol. 101, 8891–8896. https://doi.org/10.1016/j.biortech.2010.06.135

Hwang, J., Zhang, L., Seo, S., Lee, Y.W., Jahng, D., 2008. Protein recovery from excess sludge for its use as animal feed. Bioresour. Technol. 99, 8949–8954. https://doi.org/10.1016/j.biortech.2008.05.001

Isa, M.H.M., Frazier, R.A., Jauregi, P., 2008. A further study of the recovery and purification of surfactin from fermentation broth by membrane filtration. Sep. Purif. Technol. 64, 176–182. https://doi.org/10.1016/j.seppur.2008.09.008

Iskander, S.M., Novak, J.T., He, Z., 2019. Reduction of reagent requirements and sludge generation in Fenton’s oxidation of landfill leachate by synergistically incorporating forward osmosis and humic acid recovery. Water Res. 151, 310–317. https://doi.org/10.1016/j.watres.2018.11.089

IUPAC, 2014a. Lipids. IUPAC Compend. Chem. Terminol. https://doi.org/10.1351/GOLDBOOK.L03571

IUPAC, 2014b. Phospholipids. IUPAC Compend. Chem. Terminol. https://doi.org/10.1351/GOLDBOOK.P04559

IUPAC, 2014c. Steroids. IUPAC Compend. Chem. Terminol. https://doi.org/10.1351/GOLDBOOK.S06005

IUPAC, 2008. Glycerides. IUPAC Compend. Chem. Terminol. https://doi.org/10.1351/GOLDBOOK.G02647

Jimenez, J., Vedrenne, F., Denis, C., Mottet, A., Déléris, S., Steyer, J.P., Cacho Rivero, J.A., 2013. A statistical comparison of protein and carbohydrate characterisation methodology applied on sewage sludge samples. Water Res. 47, 1751–1762. https://doi.org/10.1016/j.watres.2012.11.052

Johansson, H.J., Jägersten, C., Shiloach, J., 1996. Large scale recovery and purification of periplasmic recombinant protein from E. coli using expanded bed adsorption chromatography followed by new ion exchange media. J. Biotechnol. 48, 9–14. https://doi.org/10.1016/0168-1656(96)01390-9

Kanani, D.M., Fissell, W.H., Roy, S., Dubnisheva, A., Fleischman, A., Zydney, A.L., 2010. Permeability-selectivity analysis for ultrafiltration: Effect of pore geometry. J. Memb. Sci. 349, 405–410. https://doi.org/10.1016/j.memsci.2009.12.003

Kapchie, V.N., Towa, L.T., Hauck, C.C., Murphy, P.A., 2012. Recovery and functional properties of soy storage proteins from lab- and pilot-plant scale oleosome production. JAOCS, J. Am. Oil Chem. Soc. 89, 947–956. https://doi.org/10.1007/s11746-011-1976-8

Karn, S., Kumar, A., 2019. Protease, lipase and amylase extraction and optimization from activated sludge of pulp and paper industry. Indian J. Exp. Biol. 57, 201–205.

Karp, E.M., Cywar, R.M., Manker, L.P., Saboe, P.O., Nimlos, C.T., Salvachúa, D., Wang, X., Black, B.A., Reed, M.L., Michener, W.E., Rorrer, N.A., Beckham, G.T., 2018. Post-Fermentation Recovery of Biobased Carboxylic Acids. ACS Sustain. Chem. Eng. 6, 15273–15283. https://doi.org/10.1021/acssuschemeng.8b03703

Khanh Nguyen, V., Kumar Chaudhary, D., Hari Dahal, R., Hoang Trinh, N., Kim, J., Chang, S.W., Hong, Y., Duc La, D., Nguyen, X.C., Hao Ngo, H., Chung, W.J., Nguyen, D.D., 2021. Review on pretreatment techniques to improve anaerobic digestion of sewage sludge. Fuel 285, 119105. https://doi.org/10.1016/J.FUEL.2020.119105

Khoo, K.S., Leong, H.Y., Chew, K.W., Lim, J.W., Ling, T.C., Show, P.L., Yen, H.W., 2020. Liquid biphasic system: A recent bioseparation technology. Processes 8, 149. https://doi.org/10.3390/pr8020149

Kim, J., Park, C., Kim, T.-H., Lee, M., Kim, S., Kim, S.-W., Lee, J., 2003. Effects of various pretreatments for enhanced anaerobic digestion with waste activated sludge. J. Biosci. Bioeng. 95, 271–275. https://doi.org/10.1016/S1389-1723(03)80028-2

Kim, T.H., Lee, S.R., Nam, Y.K., Yang, J., Park, C., Lee, M., 2009. Disintegration of excess activated sludge by hydrogen peroxide oxidation. Desalination 246, 275–284. https://doi.org/10.1016/J.DESAL.2008.06.023

Kocbek, E., Garcia, H.A., Hooijmans, C.M., Mijatović, I., Lah, B., Brdjanovic, D., 2020. Microwave treatment of municipal sewage sludge: Evaluation of the drying performance and energy demand of a pilot-scale microwave drying system. Sci. Total Environ. 742, 140541. https://doi.org/10.1016/J.SCITOTENV.2020.140541

Koyande, A.K., Chew, K.W., Lim, J.W., Lee, S.Y., Lam, M.K., Show, P.L., 2019. Optimization of protein extraction from Chlorella Vulgaris via novel sugaring-out assisted liquid biphasic electric flotation system. Eng. Life Sci. 19, 968–977. https://doi.org/10.1002/elsc.201900068

Kristinsson, H.G., Liang, Y., 2006. Effect of pH-shift processing and surimi processing on atlantic croaker (micropogonias undulates) muscle proteins. J. Food Sci. 71. https://doi.org/10.1111/j.1750-3841.2006.00046.x

Kristinsson, H.G., Theodore, A.E., Demir, N., Ingadottir, B., 2006. A Comparative Study between Acid- and Alkali-aided Processing and Surimi Processing for the Recovery of Proteins from Channel Catfish Muscle. J. Food Sci. 70, C298–C306. https://doi.org/10.1111/j.1365-2621.2005.tb07177.x

Küchler, I.L., Miekeley, N., 1994. Ultrafiltration of humic compounds through low molecular mass cut-off level membranes. Sci. Total Environ. 154, 23–28. https://doi.org/10.1016/0048-9697(94)90610-6

Kumada, K., 1955. Elementary composition of humic acids. Soil Sci. Plant Nutr. 1, 75–76. https://doi.org/10.1080/00380768.1955.10434379

Leong, H.Y., Chang, C.K., Lim, J.W., Show, P.L., Lin, D.Q., Chang, J.S., 2019. Liquid biphasic systems for oil-rich algae bioproducts processing. Sustainability 11, 4682. https://doi.org/10.3390/su11174682

Lestari, D., Mulder, W., Sanders, J., 2010. Improving Jatropha curcas seed protein recovery by using counter current multistage extraction. Biochem. Eng. J. 50, 16–23. https://doi.org/10.1016/j.bej.2010.02.011

Lewis, D.L., Gattie, D.K., 2002. Pathogen risks from applying sewage sludge to land. Environ. Sci. Technol. https://doi.org/10.1021/es0223426

Li, H., Chen, V., 2010. Membrane Fouling and Cleaning in Food and Bioprocessing, in: Membrane Technology. Elsevier Ltd, pp. 213–254. https://doi.org/10.1016/B978-1-85617-632-3.00010-0

Li, H., Jin, Y., Nie, Y., 2009. Application of alkaline treatment for sludge decrement and humic acid recovery. Bioresour. Technol. 100, 6278–6283. https://doi.org/10.1016/j.biortech.2009.07.022

Li, H., Li, Y., Jin, Y., Zou, S., Li, C., 2014a. Recovery of sludge humic acids with alkaline pretreatment and its impact on subsequent anaerobic digestion. J. Chem. Technol. Biotechnol. 89, 707–713. https://doi.org/10.1002/jctb.4173

Li, H., Li, Y., Li, C., 2013. Characterization of humic acids and fulvic acids derived from sewage sludge. Asian J. Chem. 25, 10087–10091. https://doi.org/10.14233/ajchem.2013.15162

Li, H., Li, Y., Zou, S., Li, C., 2014b. Extracting humic acids from digested sludge by alkaline treatment and ultrafiltration. J. Mater. Cycles Waste Manag. 16, 93–100. https://doi.org/10.1007/s10163-013-0153-6

Li, H., Shi, W., Wang, W., Zhu, H., 2015. The extraction of sericin protein from silk reeling wastewater by hollow fiber nanofiltration membrane integrated process. Sep. Purif. Technol. 146, 342–350. https://doi.org/10.1016/j.seppur.2015.04.004

Li, J., Liao, X. pin, Zhang, Q. xian, Shi, B., 2013. Adsorption and separation of proteins by collagen fiber adsorbent. J. Chromatogr. B Anal. Technol. Biomed. Life Sci. 928, 131–138. https://doi.org/10.1016/j.jchromb.2013.03.031

Li, W., Mu, B., Xu, H., Xu, L., Yang, Y., 2018. Urea-cysteine based extraction of densely crosslinked proteins from sorghum distillers grains with high yield and quality. Ind. Crops Prod. 121, 360–371. https://doi.org/10.1016/j.indcrop.2018.05.035

Li, Z., Yan, L., Zhou, J., Wang, X., Sun, Y., Xiu, Z.L., 2019. Two-step salting-out extraction of 1,3-propanediol, butyric acid and acetic acid from fermentation broths. Sep. Purif. Technol. 209, 246–253. https://doi.org/10.1016/j.seppur.2018.07.021

Linn, S., 2009. Chapter 2 Strategies and Considerations for Protein Purifications, in: Methods in Enzymology. pp. 9–19. https://doi.org/10.1016/S0076-6879(09)63002-0

Litalien, C., Beaulieu, P., 2011. Molecular Mechanisms of Drug Actions: From Receptors to Effectors. Pediatr. Crit. Care 1553–1568. https://doi.org/10.1016/B978-0-323-07307-3.10117-X

Liu, F., Li, J., Zhang, X.L., 2019. Bioplastic production from wastewater sludge and application, in: IOP Conference Series: Earth and Environmental Science. https://doi.org/10.1088/1755-1315/344/1/012071

Liu, Z., Smith, S.R., 2019. Enzyme activity of waste activated sludge extracts. Water Sci. Technol. 80, 1861–1869. https://doi.org/10.2166/WST.2020.002

López-Velandia, C., Moreno-Barbosa, J., Sierra-Ramirez, R., Giraldo, L., Moreno-Piraján, J., 2014. Adsorption of volatile carboxylic acids on activated carbon synthesized from watermelon shells. Adsorpt. Sci. Technol. 32, 227–242. https://doi.org/10.1260/0263-6174.32.2-3.227

Lorente, E., Hapońska, M., Clavero, E., Torras, C., Salvadó, J., 2017. Microalgae fractionation using steam explosion, dynamic and tangential cross-flow membrane filtration. Bioresour. Technol. 237, 3–10. https://doi.org/10.1016/j.biortech.2017.03.129

Lorenzo-Hernando, A., Ruiz-Vegas, J., Vega-Alegre, M., Bolado-Rodríguez, S., 2019. Recovery of proteins from biomass grown in pig manure microalgae-based treatment plants by alkaline hydrolysis and acidic precipitation. Bioresour. Technol. 273, 599–607. https://doi.org/10.1016/j.biortech.2018.11.068

Lu, H., Yu, X., Li, H., Tu, S.T., Sebastian, S., 2019. Lipids extraction from wet Chlorella pyrenoidosa sludge using recycled [BMIM]Cl. Bioresour. Technol. 291. https://doi.org/10.1016/j.biortech.2019.121819

Luthria, D., Anderson, S., 2004. Soxtec: Its principles and applications. Oil Extr. Anal. 1, 10–24. https://doi.org/10.1201/9781439822340.ch2

Lynch, S.A., Álvarez, C., O'Neill, E.E., Keenan, D.F., Mullen, A.M., 2018. Optimization of protein recovery from bovine lung by pH shift process using response surface methodology. J. Sci. Food Agric. 98, 1951–1960. https://doi.org/10.1002/jsfa.8678

Mæhre, H.K., Dalheim, L., Edvinsen, G.K., Elvevoll, E.O., Jensen, I.J., 2018. Protein determination—method matters. Foods 7. https://doi.org/10.3390/foods7010005

Manara, P., Zabaniotou, A., 2012. Towards sewage sludge based biofuels via thermochemical conversion - A review. Renew. Sustain. Energy Rev. https://doi.org/10.1016/j.rser.2012.01.074

Market Research Future, 2019. Humic Acid Market Size, Share, Growth, Trends, Industry Research Report 2030 | MRFR [WWW Document]. URL https://www.marketresearchfuture.com/reports/humic-acid-market-5708 (accessed 1.19.22).

MarketWatch, 2022. Lipid Market In 2022 : 5.2% CAGR with Top Countries Data, Which aspirants are pulling the development of the Lipid Industry? [WWW Document]. URL https://www.marketwatch.com/press-release/lipid-market-in-2022-52-cagr-with-top-countries-data-which-aspirants-are-pulling-the-development-of-the-lipid-industry-latest-94-pages-report-2022-01-26 (accessed 2.17.22).

Martinez, M., Spitali, M., Norrant, E.L., Bracewell, D.G., 2019. Precipitation as an Enabling Technology for the Intensification of Biopharmaceutical Manufacture. Trends Biotechnol. https://doi.org/10.1016/j.tibtech.2018.09.001

Mateo-Sagasta, J., Raschid-Sally, L., Thebo, A., 2015. Global wastewater and sludge production, treatment and use, in: Wastewater: Economic Asset in an Urbanizing World. pp. 15–38. https://doi.org/10.1007/978-94-017-9545-6_2

Mazlum, N., İkizoğlu, B., 2018. Nutrient removal by chemical post treatment with lime following the biological stage. Polish J. Environ. Stud. 27, 1187–1195. https://doi.org/10.15244/pjoes/76178

Melero, J.A., Sánchez-Vázquez, R., Vasiliadou, I.A., Martínez Castillejo, F., Bautista, L.F., Iglesias, J., Morales, G., Molina, R., 2015. Municipal sewage sludge to biodiesel by simultaneous extraction and conversion of lipids. Energy Convers. Manag. 103, 111–118. https://doi.org/10.1016/j.enconman.2015.06.045

Mohammad, A.W., Yap, P.T., Wu, T.Y., 2009. Performance of hydrophobic ultrafiltration membranes in the treatment and protein recovery from palm oil mill effluent (POME). Desalin. Water Treat. 10, 332–338. https://doi.org/10.5004/dwt.2009.932

Mordor Intelligence, 2021. Humic Acid Market | 2022 - 27 | Industry Share, Size, Growth [WWW Document]. URL https://www.mordorintelligence.com/industry-reports/humic-acid-market (accessed 2.17.22).

Morgan-Sagastume, F., Karlsson, A., Johansson, P., Pratt, S., Boon, N., Lant, P., Werker, A., 2010. Production of polyhydroxyalkanoates in open, mixed cultures from a waste sludge stream containing high levels of soluble organics, nitrogen and phosphorus. Water Res. 44, 5196–5211. https://doi.org/10.1016/j.watres.2010.06.043

Motojima, H., Yamada, P., Irie, M., Ozaki, M., Shigemori, H., Isoda, H., 2012. Amelioration effect of humic acid extracted from solubilized excess sludge on saline-alkali soil. J. Mater. Cycles Waste Manag. 14, 169–180. https://doi.org/10.1007/s10163-012-0056-y

Nabarlatz, D., Stüber, F., Font, J., Fortuny, A., Fabregat, A., Bengoa, C., 2011. Activated sludge characterization: Extraction and identification of hydrolytic enzymes, in: Water Production and Wastewater Treatment. pp. 11–26.

Nabarlatz, D., Vondrysova, J., Jenicek, P., Stüber, F., Font, J., Fortuny, A., Fabregat, A., Bengoa, C., 2010. Hydrolytic enzymes in activated sludge: Extraction of protease and lipase by stirring and ultrasonication. Ultrason. Sonochem. 17, 923–931. https://doi.org/10.1016/j.ultsonch.2010.02.006

Najjar, Y.S.H., Abu-Shamleh, A., 2020. Harvesting of microalgae by centrifugation for biodiesel production: A review. Algal Res. 51, 102046. https://doi.org/10.1016/J.ALGAL.2020.102046

Nakkeeran, E., Subramanian, R., Umesh-Kumar, S., 2010. Purification of polygalacturonase from solid-state cultures of Aspergillus carbonarius. J. Biosci. Bioeng. 109, 101–106. https://doi.org/10.1016/j.jbiosc.2009.08.005

Netsopa, S., Niamsanit, S., Araki, T., Kongkeitkajorn, M.B., Milintawisamai, N., 2019. Purification and Characterization Including Dextran Hydrolysis of Dextranase from Aspergillus allahabadii X26. Sugar Tech 21, 329–340. https://doi.org/10.1007/s12355-018-0652-9

Nguyen, L.Q.T., Engelhart, M., Wagner, M., Cornel, P., 2016. Protein recovery by selective separation using ceramic membranes. Water Pract. Technol. 11, 384–395. https://doi.org/10.2166/wpt.2016.047

Ni, H., Fan, X.M., Guo, H.N., Liang, J.H., Li, Q.R., Yang, L., Li, H., Li, H.H., 2017. Comprehensive utilization of activated sludge for the preparation of hydrolytic enzymes, polyhydroxyalkanoates, and water-retaining organic fertilizer. Prep. Biochem. Biotechnol. 47, 611–618. https://doi.org/10.1080/10826068.2017.1286599

Nussinovitch, A., 2013. Biopolymer Films and Composite Coatings. Handb. Biopolym. Biodegrad. Plast. Prop. Process. Appl. 295–327. https://doi.org/10.1016/B978-1-4557-2834-3.00013-6

Ojovan, M.I., Lee, W.E., Kalmykov, S.N., 2019. An introduction to nuclear waste immobilisation, An Introduction to Nuclear Waste Immobilisation. https://doi.org/10.1016/C2017-0-03752-7

Olkiewicz, M., Caporgno, M.P., Fortuny, A., Stüber, F., Fabregat, A., Font, J., Bengoa, C., 2014. Direct liquid-liquid extraction of lipid from municipal sewage sludge for biodiesel production. Fuel Process. Technol. 128, 331–338. https://doi.org/10.1016/j.fuproc.2014.07.041

Olkiewicz, M., Plechkova, N. V., Fabregat, A., Stüber, F., Fortuny, A., Font, J., Bengoa, C., 2015. Efficient extraction of lipids from primary sewage sludge using ionic liquids for biodiesel production. Sep. Purif. Technol. 153, 118–125. https://doi.org/10.1016/j.seppur.2015.08.038

Panda, S.K., Sahu, L., Behera, S.K., Ray, R.C., 2019. Research and Production of Organic Acids and Industrial Potential, in: Bioprocessing for Biomolecules Production. John Wiley & Sons, Ltd, pp. 195–209. https://doi.org/10.1002/9781119434436.ch9

Pervaiz, M., Sain, M., 2011. Protein extraction from secondary sludge of paper mill wastewater and its utilization as a wood adhesive. BioResources 6, 961–970.

Phanthumchinda, N., Thitiprasert, S., Tanasupawat, S., Assabumrungrat, S., Thongchul, N., 2018. Process and cost modeling of lactic acid recovery from fermentation broths by membrane-based process. Process Biochem. 68, 205–213. https://doi.org/10.1016/j.procbio.2018.02.013

Phong, W.N., Show, P.L., Teh, W.H., Teh, T.X., Lim, H.M.Y., Nazri, N.S. binti, Tan, C.H., Chang, J.S., Ling, T.C., 2017. Proteins recovery from wet microalgae using liquid biphasic flotation (LBF). Bioresour. Technol. 244, 1329–1336. https://doi.org/10.1016/j.biortech.2017.05.165

Piper, T.J., Posner, A.M., 1972. Humic acid nitrogen. Plant Soil 36, 595–598.

https://doi.org/10.1007/BF01373509

Pittmann, T., Steinmetz, H., 2014. Polyhydroxyalkanoate production as a side stream process on a municipal waste water treatment plant. Bioresour. Technol. 167, 297–302. https://doi.org/10.1016/j.biortech.2014.06.037

Pollock, V., 2007. Proteins. xPharm Compr. Pharmacol. Ref. 1–11. https://doi.org/10.1016/B978-008055232-3.60055-8

Raheem, A., Sikarwar, V.S., He, J., Dastyar, W., Dionysiou, D.D., Wang, W., Zhao, M., 2018. Opportunities and challenges in sustainable treatment and resource reuse of sewage sludge: A review. Chem. Eng. J. https://doi.org/10.1016/j.cej.2017.12.149

Rapinel, V., Rombaut, N., Rakotomanomana, N., Vallageas, A., Cravotto, G., Chemat, F., 2017. An original approach for lipophilic natural products extraction: Use of liquefied n-butane as alternative solvent to n-hexane. LWT - Food Sci. Technol. 85, 524–533. https://doi.org/10.1016/J.LWT.2016.10.003

Research and Markets, 2021. 2020 Fatty Acids Market Study: Key Insights Through [WWW Document]. URL https://www.globenewswire.com/news-release/2020/02/24/1989024/0/en/2020-Fatty-Acids-Market-Study-Key-Insights-Through-2015-2030.html (accessed 2.17.22).

Revellame, E., Hernandez, R., French, W., Holmes, W., Alley, E., Callahan, R., 2011. Production of biodiesel from wet activated sludge. J. Chem. Technol. Biotechnol. 86, 61–68. https://doi.org/10.1002/jctb.2491

Revellame, E.D., Hernandez, R., French, W., Holmes, W.E., Benson, T.J., Pham, P.J., Forks, A., Callahan, R., 2012. Lipid storage compounds in raw activated sludge microorganisms for biofuels and oleochemicals production. RSC Adv. 2, 2015–2031. https://doi.org/10.1039/c2ra01078j

Reyhanitash, E., Kersten, S.R.A., Schuur, B., 2017. Recovery of Volatile Fatty Acids from Fermented Wastewater by Adsorption. ACS Sustain. Chem. Eng. 5, 9176–9184. https://doi.org/10.1021/acssuschemeng.7b02095

Richardson, P., Hoare, M., Dunnill, P., 1990. A new biochemical engineering approach to the fractional precipitation of proteins. Biotechnol. Bioeng. 36, 354–366. https://doi.org/10.1002/bit.260360406

Ritala, A., Häkkinen, S.T., Toivari, M., Wiebe, M.G., 2017. Single cell protein-state-of-the-art, industrial landscape and patents 2001-2016. Front. Microbiol. 8, 2009. https://doi.org/10.3389/FMICB.2017.02009/BIBTEX

Ruiz-Hernando, M., Martinez-Elorza, G., Labanda, J., Llorens, J., 2013. Dewaterability of sewage sludge by ultrasonic, thermal and chemical treatments. Chem. Eng. J. 230, 102–110. https://doi.org/10.1016/J.CEJ.2013.06.046

Rulkens, W., 2008. Sewage sludge as a biomass resource for the production of energy: Overview and assessment of the various options. Energy and Fuels 22, 9–15. https://doi.org/10.1021/ef700267m

Saidi, S., Deratani, A., Ben Amar, R., Belleville, M.P., 2013. Fractionation of a tuna dark muscle hydrolysate by a two-step membrane process. Sep. Purif. Technol. 108, 28–36. https://doi.org/10.1016/j.seppur.2013.01.048

Saleem, J., Shahid, U. Bin, Hijab, M., Mackey, H., McKay, G., 2019. Production and applications of activated carbons as adsorbents from olive stones. Biomass Convers. Biorefinery 9, 775–802. https://doi.org/10.1007/s13399-019-00473-7

Saleh, T.A., Gupta, V.K., 2016. An Overview of Membrane Science and Technology, in: Nanomaterial and Polymer Membranes. pp. 1–23. https://doi.org/10.1016/b978-0-12-804703-3.00001-2

SAMCO, 2019. How Much Does It Cost to Properly Maintain Membrane Filtration Systems vs. Treat Fouled Membranes? [WWW Document]. URL https://www.samcotech.com/cost-to-properly-maintain-membrane-filtration-systems/ (accessed 1.25.22).

SAMCO, 2017a. How Much Do Reverse Osmosis and Nanofiltration Systems Cost? [WWW Document]. URL https://www.samcotech.com/much-reverse-osmosis-nanofiltration-membrane-systems-cost/ (accessed 1.25.22).

SAMCO, 2017b. How Much Do Microfiltration and Ultrafiltration Membrane Systems Cost? [WWW Document]. URL https://www.samcotech.com/how-much-do-microfiltration-and-ultrafiltration-membrane-systems-cost/ (accessed 1.25.22).

Sankaran, R., Manickam, S., Yap, Y.J., Ling, T.C., Chang, J.S., Show, P.L., 2018a. Extraction of proteins from microalgae using integrated method of sugaring-out assisted liquid biphasic flotation (LBF) and ultrasound. Ultrason. Sonochem. 48, 231–239. https://doi.org/10.1016/j.ultsonch.2018.06.002

Sankaran, R., Show, P.L., Cheng, Y.S., Tao, Y., Ao, X., Nguyen, T.D.P., Van Quyen, D., 2018b. Integration Process for Protein Extraction from Microalgae Using Liquid Biphasic Electric Flotation (LBEF) System. Mol. Biotechnol. 60, 749–761. https://doi.org/10.1007/s12033-018-0111-6

Sankaran, R., Show, P.L., Yap, Y.J., Tao, Y., Ling, T.C., Tomohisa, K., 2018c. Green technology of liquid biphasic flotation for enzyme recovery utilizing recycling surfactant and sorbitol. Clean Technol. Environ. Policy 20, 2001–2012. https://doi.org/10.1007/s10098-018-1523-5

Shi, S., Xu, G., Yu, H., Zhang, Z., 2018. Strategies of valorization of sludge from wastewater treatment. J. Chem. Technol. Biotechnol. https://doi.org/10.1002/jctb.5548

Shrestha, P., Holland, T.M., Bundy, B.C., 2012. Streamlined extract preparation for Escherichia coli-based cell-free protein synthesis by sonication or bead vortex mixing. Biotechniques 53, 163–174. https://doi.org/10.2144/0000113924/ASSET/IMAGES/LARGE/FIGURE3.JPEG

Siddiquee, M.N., Rohani, S., 2011. Experimental analysis of lipid extraction and biodiesel production from wastewater sludge. Fuel Process. Technol. 92, 2241–2251. https://doi.org/10.1016/j.fuproc.2011.07.018

Silva, Y.P., Bernardi, A., Frozza, R.L., 2020. The Role of Short-Chain Fatty Acids From Gut Microbiota in Gut-Brain Communication. Front. Endocrinol. (Lausanne). 11, 25. https://doi.org/10.3389/FENDO.2020.00025/BIBTEX

Singh, R., 2014. Membrane Technology and Engineering for Water Purification: Application, Systems Design and Operation: Second Edition, Membrane Technology and Engineering for Water Purification: Application, Systems Design and Operation: Second Edition. https://doi.org/10.1016/C2013-0-15275-0

Sokatch, J.R., 1969. Chemical composition of bacteria, in: Bacterial Physiology and Metabolism. Academic Press, pp. 25–51. https://doi.org/10.1016/b978-1-4832-3137-2.50007-4

Sprakel, L.M.J., Schuur, B., 2019. Solvent developments for liquid-liquid extraction of carboxylic acids in perspective. Sep. Purif. Technol. https://doi.org/10.1016/j.seppur.2018.10.023

Strætkvern, K.O., Schwarz, J.G., 2012. Recovery of Native Potato Protein Comparing Expanded Bed Adsorption and Ultrafiltration. Food Bioprocess Technol. 5, 1939–1949. https://doi.org/10.1007/s11947-010-0494-2

Su, Y., Ji, M., Li, J., Chang, C., Dong, S., Deng, Y., Yang, Y., Gu, L., 2020. Subcritical fluid extraction treatment on egg yolk: Product characterization. J. Food Eng. 274, 109805. https://doi.org/10.1016/J.JFOODENG.2019.109805

Suárez-Iglesias, O., Urrea, J.L., Oulego, P., Collado, S., Díaz, M., 2017. Valuable compounds from sewage sludge by thermal hydrolysis and wet oxidation. A review. Sci. Total Environ. 584–585, 921–934. https://doi.org/10.1016/j.scitotenv.2017.01.140

Suescún-Mathieu, E., Bautista-Carrizosa, A., Sierra, R., Giraldo, L., Moreno-Piraján, J.C., 2014. Carboxylic acid recovery from aqueous solutions by activated carbon produced from sugarcane bagasse. Adsorption 20, 935–943. https://doi.org/10.1007/s10450-014-9638-4

Sussmann, D., Pickardt, C., Schweiggert, U., Eisner, P., 2013. Influence of different processing parameters on the isolation of Lupin (Lupinus Angustifolius L.) protein isolates: A preliminary study. J. Food Process Eng. 36, 18–28. https://doi.org/10.1111/j.1745-4530.2011.00647.x

Tabtabaei, S., Diosady, L.L., 2013. Aqueous and enzymatic extraction processes for the production of food-grade proteins and industrial oil from dehulled yellow mustard flour. Food Res. Int. 52, 547–556. https://doi.org/10.1016/j.foodres.2013.03.005

Tahergorabi, R., Beamer, S.K., Matak, K.E., Jaczynski, J., 2011. Effect of isoelectric solubilization/precipitation and titanium dioxide on whitening and texture of proteins recovered from dark chicken-meat processing by-products. LWT - Food Sci. Technol. 44, 896–903. https://doi.org/10.1016/j.lwt.2010.10.018

Talebi, A., Razali, Y.S., Ismail, N., Rafatullah, M., Azan Tajarudin, H., 2020. Selective adsorption and recovery of volatile fatty acids from fermented landfill leachate by activated carbon process. Sci. Total Environ. 707, 134533. https://doi.org/10.1016/j.scitotenv.2019.134533

Taskila, S., Ahokas, M., Järvinen, J., Toivanen, J., Tanskanen, J.P., 2017. Concentration and Separation of Active Proteins from Potato Industry Waste Based on Low-Temperature Evaporation and Ethanol Precipitation. Scientifica (Cairo). 2017, 1–6. https://doi.org/10.1155/2017/5120947

Tong, J., Chen, Y., 2009. Recovery of nitrogen and phosphorus from alkaline fermentation liquid of waste activated sludge and application of the fermentation liquid to promote biological municipal wastewater treatment. Water Res. 43, 2969–2976. https://doi.org/10.1016/j.watres.2009.04.015

Uddin, S., Islam, A., Rahman, M.M., Uddin, M.B., Mazumder, A.R., 2018. Isolation of Protein from Defatted Peanut Meal and Characterize their Nutritional Profile. Chem. Res. J. 3, 187–196.

Urbain, V., Block, J.C., Manem, J., 1993. Bioflocculation in activated sludge: an analytic approach. Water Res. 27, 829–838. https://doi.org/10.1016/0043-1354(93)90147-A

Vakondios, N., Koukouraki, E.E., Diamadopoulos, E., 2014. Effluent organic matter (EfOM) characterization by simultaneous measurement of proteins and humic matter. Water Res. 63, 62–70. https://doi.org/10.1016/j.watres.2014.06.011

Vernès, L., Abert-Vian, M., El Maâtaoui, M., Tao, Y., Bornard, I., Chemat, F., 2019. Application of ultrasound for green extraction of proteins from spirulina. Mechanism, optimization, modeling, and industrial prospects. Ultrason. Sonochem. 54, 48–60. https://doi.org/10.1016/j.ultsonch.2019.02.016

Waglay, A., Karboune, S., Alli, I., 2014. Potato protein isolates: Recovery and characterization of their properties. Food Chem. 142, 373–382. https://doi.org/10.1016/j.foodchem.2013.07.060

Wang, L.K., Vaccari, D.A., Li, Y., Shammas, N.K., 2005. Chemical Precipitation, in: Physicochemical Treatment Processes. pp. 141–197. https://doi.org/10.1385/1-59259-820-x:141

Wang, S., Ma, Q., Zhu, Z.H., 2009. Characteristics of unburned carbons and their application for humic acid removal from water. Fuel Process. Technol. 90, 375–380. https://doi.org/10.1016/j.fuproc.2008.10.010

Wang, W., Luo, Y., Qiao, W., 2009. Possible solutions for sludge dewatering in China. Front. Environ. Sci. Eng. China 2010 41 4, 102–107. https://doi.org/10.1007/S11783-010-0001-Z

Ward, K., Cheng, S.I., Stuckey, D.C., 2016. Protein separation using non-ionic and cationic surfactant precipitation. J. Chem. Technol. Biotechnol. 91, 2563–2567. https://doi.org/10.1002/jctb.4942

Wei, L., Wang, K., Kong, X., Liu, G., Cui, S., Zhao, Q., Cui, F., 2016. Application of ultra-sonication, acid precipitation and membrane filtration for co-recovery of protein and humic acid from sewage sludge. Front. Environ. Sci. Eng. 10, 327–335. https://doi.org/10.1007/s11783-014-0763-9

Werther, J., Ogada, T., 1999. Sewage sludge combustion. Prog. Energy Combust. Sci. https://doi.org/10.1016/S0360-1285(98)00020-3

Westerberg, N., Sunner, H., Helander, M., Henriksson, G., Lawoko, M., Rasmuson, A., 2012. Separation of galactoglucomannans, lignin, and lignin-carbohydrate complexes from hot-water-extracted norway spruce by cross-flow filtration and adsorption chromatography. BioResources 7, 4501–4516. https://doi.org/10.15376/biores.7.4.4501-4516

Wilken, L.R., Ogle, E.T., Lohrmann, T., Nikolov, Z.L., 2016. Impact of Dry-milled Germ Processing on Aqueous Protein and Oil Extraction. Food Bioprocess Technol. 9, 612–620. https://doi.org/10.1007/s11947-015-1650-5

Wu, T.Y., Mohammad, A.W., Md. Jahim, J., Anuar, N., 2007. Palm oil mill effluent (POME) treatment and bioresources recovery using ultrafiltration membrane: Effect of pressure on membrane fouling. Biochem. Eng. J. 35, 309–317. https://doi.org/10.1016/j.bej.2007.01.029

Xie, M., Shon, H.K., Gray, S.R., Elimelech, M., 2016. Membrane-based processes for wastewater nutrient recovery: Technology, challenges, and future direction. Water Res. https://doi.org/10.1016/j.watres.2015.11.045

Xu, L.J., Sheldon, B.W., Carawan, R.E., Larick, D.K., Chao, A.C., 2001. Recovery and characterization of by-products from egg processing plant wastewater using coagulants. Poult. Sci. 80, 57–65. https://doi.org/10.1093/ps/80.1.57

Yousuf, A., Bonk, F., Bastidas-Oyanedel, J.R., Schmidt, J.E., 2016. Recovery of carboxylic acids produced during dark fermentation of food waste by adsorption on Amberlite IRA-67 and activated carbon. Bioresour. Technol. 217, 137–140. https://doi.org/10.1016/j.biortech.2016.02.035

Yu, G., He, P., Shao, L., Zhu, Y., 2009. Enzyme extraction by ultrasound from sludge flocs. J. Environ. Sci. 21, 204–210. https://doi.org/10.1016/S1001-0742(08)62252-4

Zhang, W., Grimi, N., Jaffrin, M.Y., Ding, L., 2015. Leaf protein concentration of alfalfa juice by membrane technology. J. Memb. Sci. 489, 183–193. https://doi.org/10.1016/j.memsci.2015.03.092

Zhao, P., Shen, Y., Ge, S., Yoshikawa, K., 2014. Energy recycling from sewage sludge by producing solid biofuel with hydrothermal carbonization. Energy Convers. Manag. 78, 815–821. https://doi.org/10.1016/j.enconman.2013.11.026

Zhao, Y., Lu, W., Damgaard, A., Zhang, Y., Wang, H., 2015. Assessment of co-composting of sludge and woodchips in the perspective of environmental impacts (EASETECH). Waste Manag. 42, 55–60. https://doi.org/10.1016/j.wasman.2015.04.021

Zhou, T., Huang, S., Niu, D., Su, L., Zhen, G., Zhao, Y., 2018. Efficient Separation of Water-Soluble Humic Acid Using (3-Aminopropyl)triethoxysilane (APTES) for Carbon Resource Recovery from Wastewater. ACS Sustain. Chem. Eng. 6, 5981–5989. https://doi.org/10.1021/acssuschemeng.7b04507

Zou, Y., Li, P.P., Zhang, K., Wang, L., Zhang, M.H., Sun, Z.L., Sun, C., Geng, Z.M., Xu, W.M., Wang, D.Y., 2017. Effects of ultrasound-assisted alkaline extraction on the physiochemical and functional characteristics of chicken liver protein isolate. Poult. Sci. 96, 2975–2985. https://doi.org/10.3382/PS/PEX049

Supplementary Material to

‘Separation and purification techniques for the recovery of added-value biocompounds from waste activated sludge. A review’

Daniel Núñez[a], *Paula Oulego*[a], *Sergio Collado*[a], *Francisco A. Riera* [a] *and Mario Díaz*[a,*]

[a]Department of Chemical and Environmental Engineering, University of Oviedo.
c/Julián Clavería 8, 33006, Oviedo, Spain

(21 Pages, 3 Tables)

Table of contents

*Corresponding author’s e-mail: mariodiaz@uniovi.es (M. Díaz)
Phone: +34 985 10 34 39, Fax: +34 985 10 34 40

1. Precipitation

Additional studies on the precipitation of biomolecules from cell cultures and synthetic broths (Table A.4.2) and from farming and food-related sources (Table A.4.3) are here included.

Table A.4.2. Additional consulted studies about precipitation in cell cultures and synthetic broths.

Source	Compounds	Content	Pre-treatment	Precipitation method	Main results	ref
***A. niger* solid-state fermentation broths**	Proteins, enzymes (xylanases)	4.15 UI/mL (xylanases), 230 mg/L (proteins)	Enzyme extraction by sodium acetate buffer solution (pH 4.5), subsequent filtration and centrifugation	Ethanol precipitation	Maximum recoveries of 86.2% of protein and of 64.4% of xylanase activity	(Costa et al., 2018)
Solid-state cultures of *Aspergillus carbonarius*	Enzymes (polygalacturonase)	80 U/mL	Extraction in acetate buffer	Alginate affinity precipitation	-	(Nakkeeran et al., 2010)
Bovine serum albumin, lysozyme and trypsin inhibitor solutions	Proteins, enzyme (lysozyme)	n/a	-	Non-ionic (Triton X-100, Tween 85 and Brij 30) and ionic (TOMAC and DODMAC solutions) surfactant precipitation	No precipitation observed for lysozyme. A maximum of 94.2% of bovine serum albumin precipitated with TOMAC at pH 9.0. A maximum of 58% of trypsin inhibitor precipitated with TOMAC at pH 6.2.	(Ward et al., 2016)

Table A.4.3. Additional consulted studies about precipitation in farming and food-related sources.

Source	Compounds	Content	Pre-treatment	Precipitation method	Main results	ref
Potato fruit juice	Proteins	13 g/L	Concentration by low-temperature evaporation	Ethanol precipitation	62% of protein precipitated. 12% of the total protein recovered by resolubilization from the precipitate.	(Taskila et al., 2017)
Simulated potato processing plant waste effluent	Proteins	24 g/L	-	Precipitation by CMC complexation (tested conditions: pH 1.0-6.0; T=25°C; NaCl 0.05, 0.1, 0.2 and 0.3 N; 0.05, 0.1, 0.2 and 0.3 CMC/protein ratio)	pH 2.5-3.5, CMC/protein ratio from 0.05:1 to 0.1:1. Optimal results were obtained using CMC with a degree of substitution of 0.85-0.95, CMC: protein ratio of 0.05, NaCl from 0.0 to 1.0%, and pH 1.5-4.0. The complex obtained, which was easily separated, contained 76.6% protein and 17.6% CMC.	(Gonzalez et al., 1991)

Table A.4.3. Additional consulted studies about precipitation in farming and food-related sources (continued).

Rice processing liquors	Proteins	7.7-13.0 g/L	-	Acid precipitation	Protein recovery yields of 47.7% and 30.5% for rice starch steep and sorter liquors, respectively.	(Hegazi et al., 1973)
Coriander fruit (defatted whole fruit, dehulled seed, press cake from dehulled seed, steam-distilled dehulled seed, and press cake from steam-distilled dehulled seed meal)	Proteins	13.0 % (dry-weight basis)	Defatting, dehulling	Alkali solubilization-acid precipitation	Proteins recoveries of 41.9 ± 4.6 (defatted whole fruit), 39.6 ± 0.1 (dehulled seed), 38.1 ± 0.0 (press cake from dehulled seed), 26.2 ± 0.2 (steam-distilled dehulled seed) and 29.3 ± 0.9 (press cake from steam-distilled dehulled seed meal).	(Hojilla-Evangelista and Evangelista, 2017)
Dissolved hair	Proteins	n/a	-	Glacial acetic acid precipitation	Maximum protein recovery yield of 68%.	(Feairheller et al., 1972)
Antarctic krill (*Euphasia superba*)	Proteins	76.54% (dry-weight basis)	Homogenization with deionized water 1:3 (1-4 °C), isoelectric solubilisation (pH 2.0, 2.50, 3.0, 12.0, 12.50 and 13.0), centrifugation	Isoelectric precipitation (pH 5.5)	Maximum protein recovery yield of 50 % after solubilisation at pH 2.	(Chen et al., 2009)

Table A.4.3. Additional consulted studies about precipitation in farming and food-related sources (continued).

Silver carp (*Hypophthalmichthys molitrix*)	Proteins	52.4% w/w	Grinding, homogenization with water 1:6, isoelectric solubilisation (acidic (2.0 and 3.0) and basic (11.5 and 12.5) pH), centrifugation.	Isoelectric precipitation (pH 5.5, 10 min)	Maximum protein recovery yield of 660 g/kg after solubilisation at pH 12.5.	(Taskaya et al., 2009)

2. Membrane filtration

Additional studies on the recovery of biomolecules by membrane filtration are shown in Table A.4.4.

Table A.4.4. Additional consulted studies about membrane separation.

Source	Compounds	Content	Pre-treatment	Filtration conditions	Main results	Ref.
Alfalfa juice	Proteins	21 g/L	Prefiltration	MF (0.2 μm) and UF (20 kDa) with three different membranes Filtration modules: Dead-end filtration using amicon cell (DA) effective membrane area 31.7 cm^2, Dynamic cross filtration using disk module (CRDM) effective area 176 cm^2, Dead end filtration using rotating disk module (DRDM) TMP: 0.5-3 bar T: 35°C Full recycling and concentration (VCR = 6) tests.	Productivities (L/m^2 h bar) MF DA 0.48 DRDM 4.73 CRDM 6.06 UF DA 0.43 DRDM 1.42 CRDM 1.70	(Zhang et al., 2015)

Table A.4.4. Additional consulted studies about membrane separation (continued).

Skim milk	Carbohydrates (lactose)	46 g/L	MF	UF (concentration step) PS membranes, 10 kDa, membrane area 0.47 m^2. TMP: 1 bar T: 25°C NF Spiral wound thin film composite polyamide Membrane, 180 Da, membrane surface 1.5 m^2 TMP: 8 bar T: 25°C ± 1 °C VCR = 4.	UF Concentrated feed solution contained 4.6 ± 0.3 % lactose, negligible amounts of proteins and a relatively high content of mineral salts. NF Lactose rejection = 92 % Ash content in the feed reduced from 0.36 ± 0.04 (%w/v) to 0.108 ± 0.02, purity higher than 90 %.	(Rinaldoni et al., 2009)
Tuna protein hydrolysate	Proteins in the range of 1-4 kDa	72 g/L		Six-stage (3 UF and 3 NF) cascade Membranes tested: UF 3 channel tubular ceramic membrane, 8 kDa, surface area 155 cm^2 NF PES membrane, 1 kDa TMP: 2 bar (UF), 10 bar (NF). CFV: 3 m/s (UF), 1.25 m/s (NF) T: 25 °C	Product purity of 49.3 % with a process yield of 62.6 %	(Abejón et al., 2016; Saidi et al., 2013)

Table A.4.4. Additional consulted studies about membrane separation (continued).

Herring marinade	fats, proteins, amino acids, salt, acetic acid and water	10.6 wt% dry matter, 3.9 wt% protein, 0.22 wt% fat, 9.0 wt% NaCl, 2.0 wt% acetic acid.	Mechanical fat removal, sieving	Sequential filtration, employed membranes, MWCO, CFV (in kg/min) and TMP (in bar) (all experiments conducted at room temperature): Fluoro polymer, 0.2 µm, 5 CFV, 0.9 TMP. PS, 50 kDa, 5 CFV, 7.8 TMP. Fluoro polymer, 20 kDa, 5.5-6-6 CFV, 5.9-6.0 TMP. Composite fluoro polymer, 10 kDa, 6.5 CFV, 5.4-6.3 TMP. Fluoro polymer, 1 kDa, 6.5 CFV, 4.2-6.7 TMP. Polyamide on polyester, reject >98% $MgSO_4$ (2000 ppm, 9 bar, 25°C), 6.5 CFV, 26.4-29.1 TMP.	The 50 kDa stage produces a protein concentrate (>17 kDa). NF produces a retentate containing sugars, amino acids and smaller peptides and a NF permeate containing salt and acetic acid ready for reuse. Proteins are concentrated 30-fold, while amino acids and smaller peptides are concentrated 11-fold.	(Søtoft et al., 2015)
Shrimp waste	Protein (chitin)	60 g/L		3 tubular membranes tested: MF membrane, 0.1 µm 2 NF membranes, 450 and 300 Da, filtration surface area 1.68 m^2 and 1.75 m^2, respectively. TMP: 1.5 bar (MF), 3 bar, (NF 450), 5 bar (NF <300). CFV: 3.5 m-s, T: 70 °C	Increase of recovered proteins in the concentrate between 7 and 16%, can be achieved in the concentrate stream by reducing the chosen MWCOs. Concentration from 60 g/L to 156 g/L with NF membrane	(Nguyen et al., 2016)

Table A.4.4. Additional consulted studies about membrane separation (continued).

Cocoon cooking wastewater, refining wastewater and mixed wastewater from silk reeling	Protein (sericin)	n/a	-	4 hollow fiber PSF membranes tested MWCO: 6, 20 and 100 kDa for UF, and of 95.00% $MgSO_4$ rejection for NF. TMP: 0.7 MPa T: 20-60°C	Higher retentions of 97.1%, 97.2% and 98.1% for cocoon cooking wastewater, refining wastewater and mixed wastewater, respectively. More than 86% sericin protein recycled after the treatment by optimized UF–NF combination process.	(Li et al., 2015)
Cocoon cooking wastewater	Protein (sericin)	5510-9883 mg/L	Precipitation, MF	Polymeric membranes tested: MF: cellulose, 20-25 µm; cellulose, 8 µm; glass fiber, 1.6 µm; glass fiber, 1 µm. All membranes effective area 10 cm^2 UF: PES, 20 kDa; PES, 5 kDa; Thin film, 1 kDa. All membranes effective area 44 cm2 NF: Thin film, 190 Da, effective area 44-36 cm^2; thin film, 100 Da, effective area 44-72 cm^2. TMP: 200 kPa (UF), 500 kPa (NF). Flow rate: 0.03 m^3/h T: 18-25°C	UF: partial recovery from 37 to 60% of sericin polypeptides. NF: maximum sericin recovery of 94–95%, containing all molecular weight fractions.	(Capar et al., 2008)

References

Abejón, R., Abejón, A., Belleville, M.-P., Garea, A., Irabien, A., Sanchez-Marcano, J., 2016. Water recovery and reuse in the fractionation of protein hydrolysate by ultrafiltration and nanofiltration membranes. Chem. Eng. Trans. 52, 283–288. https://doi.org/10.3303/CET1652048

Capar, G., Aygun, S.S., Gecit, M.R., 2008. Treatment of silk production wastewaters by membrane processes for sericin recovery. J. Memb. Sci. 325, 920–931. https://doi.org/10.1016/j.memsci.2008.09.020

Chen, Y.C., Tou, J.C., Jaczynski, J., 2009. Amino acid and mineral composition of protein and other components and their recovery yields from whole antarctic krill (Euphausia superba) using isoelectric solubilization/precipitation. J. Food Sci. 74. https://doi.org/10.1111/j.1750-3841.2008.01026.x

Costa, M.A.L., Farinas, C.S., Miranda, E.A., 2018. Ethanol precipitation as a downstream processing step for concentration of xylanases produced by submerged and solid-state fermentation. Brazilian J. Chem. Eng. 35, 477–488. https://doi.org/10.1590/0104-6632.20180352s20160502

Feairheller, S.H., Taylor, M.M., Windus, W., Filachione, E.M., Naghski, J., 1972. Recovery and Analyses of Hair Proteins from Tannery Unhairing Wastes. J. Agric. Food Chem. 20, 668–670. https://doi.org/10.1021/jf60181a033

Gonzalez, J.M., Lindamood, J.B., Desai, N., 1991. Recovery of protein from potato plant waste effluents by complexation with carboxymethylcellulose. Top. Catal. 4, 355–363. https://doi.org/10.1016/S0268-005X(09)80131-8

Hegazi, S.M., Foda, M.S., Salem, S.A., Eldin, S.M.B., 1973. Recovery and Amino Acid Composition of Protein Precipitates Isolated from Rice Starch Processing Liquors. Starch - Stärke 25, 92–94. https://doi.org/10.1002/star.19730250306

Hojilla-Evangelista, M.P., Evangelista, R.L., 2017. Effects of Steam Distillation and Screw-Pressing on Extraction, Composition and Functional Properties of Protein in Dehulled Coriander (Coriandrum sativum L.). JAOCS, J. Am. Oil Chem. Soc. 94, 315–324. https://doi.org/10.1007/s11746-017-2948-4

Li, H., Shi, W., Wang, W., Zhu, H., 2015. The extraction of sericin protein from silk reeling wastewater by hollow fiber nanofiltration membrane integrated process. Sep. Purif. Technol. 146, 342–350. https://doi.org/10.1016/j.seppur.2015.04.004

Nakkeeran, E., Subramanian, R., Umesh-Kumar, S., 2010. Purification of polygalacturonase from solid-state cultures of Aspergillus carbonarius. J. Biosci. Bioeng. 109, 101–106. https://doi.org/10.1016/j.jbiosc.2009.08.005

Nguyen, L.Q.T., Engelhart, M., Wagner, M., Cornel, P., 2016. Protein recovery by selective separation using ceramic membranes. Water Pract. Technol. 11, 384–395.

https://doi.org/10.2166/wpt.2016.047

Rinaldoni, A.N., Campderros, M., Menendez, C.J., Prez Padilla, A., 2009. Fractionation of skim milk by an integrated membrane process for yoghurt elaboration and lactose recuperation. Int. J. Food Eng. 5. https://doi.org/10.2202/1556-3758.1531

Saidi, S., Deratani, A., Ben Amar, R., Belleville, M.P., 2013. Fractionation of a tuna dark muscle hydrolysate by a two-step membrane process. Sep. Purif. Technol. 108, 28–36. https://doi.org/10.1016/j.seppur.2013.01.048

Søtoft, L.F., Lizarazu, J.M., Parjikolaei, B.R., Karring, H., Christensen, K. V., 2015. Membrane fractionation of herring marinade for separation and recovery of fats, proteins, amino acids, salt, acetic acid and water. J. Food Eng. 158, 39–47. https://doi.org/10.1016/j.jfoodeng.2015.02.020

Taskaya, L., Chen, Y.C., Beamer, S., Jaczynski, J., 2009. Texture and colour properties of proteins recovered from whole gutted silver carp (Hypophthalmichthys molitrix) using isoelectric solubilisation/ precipitation. J. Sci. Food Agric. 89, 349–358. https://doi.org/10.1002/jsfa.3461

Taskila, S., Ahokas, M., Järvinen, J., Toivanen, J., Tanskanen, J.P., 2017. Concentration and Separation of Active Proteins from Potato Industry Waste Based on Low-Temperature Evaporation and Ethanol Precipitation. Scientifica (Cairo). 2017, 1–6. https://doi.org/10.1155/2017/5120947

Ward, K., Cheng, S.I., Stuckey, D.C., 2016. Protein separation using non-ionic and cationic surfactant precipitation. J. Chem. Technol. Biotechnol. 91, 2563–2567. https://doi.org/10.1002/jctb.4942

Zhang, W., Grimi, N., Jaffrin, M.Y., Ding, L., 2015. Leaf protein concentration of alfalfa juice by membrane technology. J. Memb. Sci. 489, 183–193. https://doi.org/10.1016/j.memsci.2015.03.092

4.2. Valorización de otras biomasas residuales líquidas

4.2.1. Recovery of organic acids from pre-treated Kraft black liquor using ultrafiltration and liquid-liquid extraction

Daniel Núñez, Paula Oulego, Sergio Collado, Francisco A. Riera, Mario Díaz*

Department of Chemical and Environmental Engineering, University of Oviedo.

c/ Julián Clavería 8, 33006, Oviedo, Spain

*Corresponding author's e-mail: mariodiaz@uniovi.es

Phone: +34 985 10 34 39, FAX: +34 985 10 34 40

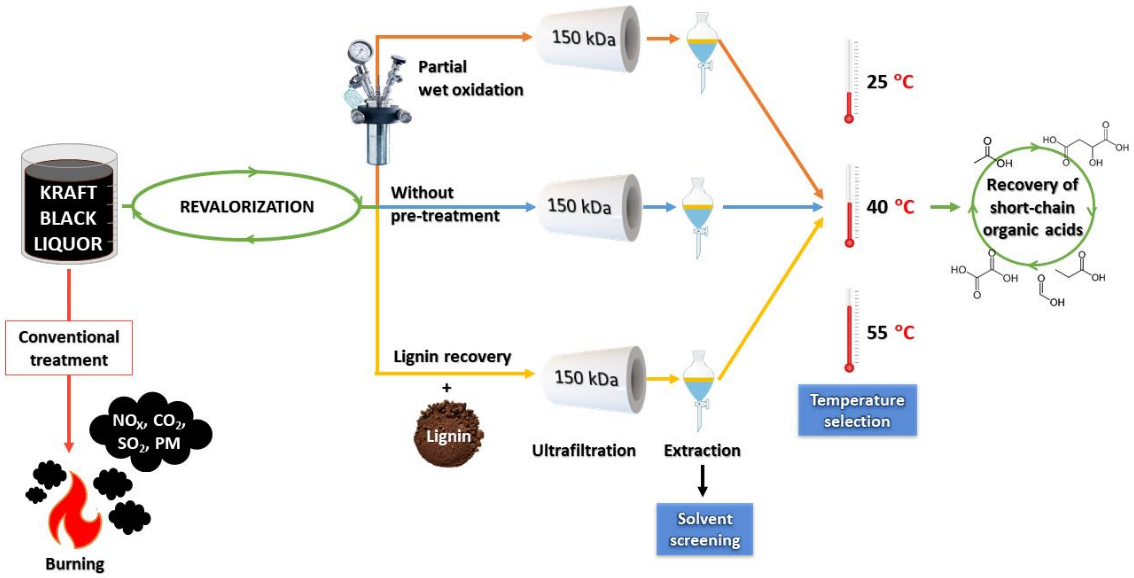

Figura 4.36. Resumen gráfico del artículo *Recovery of organic acids from pre-treated Kraft black liquor using ultrafiltration and liquid-liquid extraction*.

Artículo publicado en la revista **Separation and Purification Technology**

Cuartil: Q1 **Índice de impacto:** 9.14

Referencia: Daniel Núñez, Paula Oulego, Sergio Collado, Francisco A. Riera, Mario Díaz, Recovery of organic acids from pre-treated Kraft black liquor using ultrafiltration and liquid-liquid extraction, Separation and Purification Technology, Volume 284, 2022, 120274.

Abstract

Kraft black liquor (BL) is a toxic residue from paper manufacture that can be revalorized to obtain high value-added products. In this study, different integrated processes, consisting of a pre-treatment (lignin recovery [LR] or partial wet oxidation [PWO]) followed by ultrafiltration (UF) and liquid-liquid extraction (LLE), have been evaluated in order to recover short-chain organic acids (OA) from BL.

After the UF step, a partial purification of OA was observed. Thus, the COD fraction attributable to OA increase 26.0%, 36.6% and 11.3% for untreated BL, BL after lignin recovery (LRBL) and partially oxidised BL (WOBL), respectively.

The final LLE step was optimised analysing different combinations of extractants (trioctylamine, trioctylphosphine oxide and tributylphosphate), diluents (n-hexane and heptane) and temperatures (25, 40 and 55ºC), concluding that the most suitable solvent was 30% trioctylamine in heptane (v/v) at 40ºC, in which 76% of the OA mass was recovered in LRBL, 72% in BL and 68% in WOBL.

The pre-treatment of BL improved the final recovery yield of OAs, increasing from 24.7% to 28.1% and 29.4% through PWO and LR, respectively. Therefore, LR was considered the most suitable pre-treatment due to its lower operating cost, widespread use, and greater recovery of OA.

Keywords: circular economy; lignin recovery; membrane filtration; partial wet oxidation; short-chain fatty acids.

1. Introduction

Kraft black liquor (BL) is a by-product derived from paper milling, which is formed during the cooking of wood with white liquor (fresh pulping liquor mainly consisting of active pulping species, such as NaOH and Na_2S) to disrupt its structure and separate the cellulose fibres from the other compounds that conform the wood matrix [1]. BL is composed of the inorganic and organic compounds from the original wood cooking, mainly lignin, hemicellulose, carbohydrates and organic acids (OA) [1]. This results in a stream with values of chemical oxygen demand (COD) over 70 g/L and pH above 11 [2].

Over 26 million tonnes of sulphate paper pulp were produced in 2018 in Europe [3], which implies the generation of about 42 million tonnes of BL in dry weight basis [4]. Although several strategies have been evaluated for BL treatment, including coagulation and acid precipitation [5], electrocoagulation [6], biological treatment [7–9], electrodialysis [10–12], membrane filtration [13–17], Fenton oxidation [18,19], gasification or wet air oxidation [20], the standard treatment of BL still consists in its concentration by means of evaporation until a solid concentration of 65-73% is reached, and subsequent burning in boilers for white liquor regeneration and energy production [21].

However, this treatment possesses several drawbacks, such as the generation of greenhouse gases, NO_X, particulate matter and SO_2 emissions [22,23], as well as the loss of potential added value products present in the BL, such as lignin and OA [8]. Regarding lignin, its recovery from BL has already been carried out at commercial scale, and the industrial conversion of lignin into high-value products, such as vanillin, dimethyl sulfoxide and lignin-based polyols for the synthesis of polymers has also been analysed [24,25]. In this sense, the global market size of Kraft lignin is expected to exceed $15 million by 2025 [26].

Furthermore, OA, including oxalic, acetic, lactic, propionic or succinic acids are widely employed in food, chemical, biochemical, textile, cosmetic or pharmaceutical industries [27]. The global OA market size was valued at $16,837 million in 2016, and is expected to reach $29,197 million by 2023 [28]. However, despite this great economic potential, the recovery of OA from BL has been scarcely studied [29,30]. Besides, these works only employed raw BL and failed to analyse the effect of BL pre-treatment on the improvement of the OA extraction and the reduction of its environmental hazards. In this sense, a three-step process is here proposed to recover green valuable products such as OA and lignin from BL, consisting of pre-treatment, ultrafiltration and liquid-liquid extraction (LLE). For the pre-treatment step, two different operations were analysed:

Partial wet oxidation (PWO): This technique, performed under controlled oxidizing conditions to avoid total oxidation of the treated stream, was selected since its use was reported to increase the concentration of OA in black liquor by the cleavage of lignin into shorter chain molecules [31].

Lignin recovery (LR): By so doing, most COD of BL can be recovered in the form of lignin, which results in the reduction of the solid content and viscosity, thus facilitating the handling of the resulting stream. Through this strategy, both lignin and OA can be recovered.

Besides, the direct use of BL without PWO or LR pre-treatment was also considered.

An ultrafiltration (UF) step was performed after the pre-treatments in order to remove the bulk of higher molecular size remnants, such as cellulose, hemicellulose or lignin. This treatment is employed to purify OA partially, since the acids easily pass through the UF membrane due to their lower molecular size.

The last step of the proposed process was a LLE to purify the OA from the UF permeate. Although LLE of OA is mainly based on the complexation with trioctylamine (TOA) or alamine 336 (a commercially available equivalent consisting of a mixture with C_8-C_{10} alkyl chains), other extracting agents including trioctylphosphine oxide (TOPO), tributylphosphate (TBP) or ionic liquids are also used [32]. The nature of the diluent is also important for an efficient LLE, affecting properties of the solvent, such as viscosity, density or solvation degree of the acid-extractant complex [32].

In this sense, the aim of this work was to recover OA from untreated BL or pre-treated by PWO or for LR, by means of a pre-purification step using UF and a subsequent LLE. Besides, LLE was thoroughly analysed, paying special attention to the combinations of different extracting agents, diluents, extracting agent-diluent ratios, and extraction temperature.

2. Material and methods

2.1. Kraft black liquor

Kraft BL of *Eucalyptus* wood was provided by a paper mill located in Asturias (Spain). After its recollection, the BL was stored at 4 °C until further usage.

2.2. Black liquor pre-treatments

2.2.1. Partial wet oxidation

The BL was partially wet oxidized in order to generate OA through the partial degradation of larger compounds, as well as to treat the BL itself, thereby reducing the COD and the viscosity of the stream. The PWO reaction was carried out in a 1 L 316 SS batch reactor (Parr Instrument Co., Moline, IL.). More specific details of the reactor setup are provided in [2]. According to previous experiments, the optimal conditions for the maximization of OA were 190 ºC, 70 bar and 120 minutes without pH adjustment nor catalyst. The content of the reactor was stirred at 150 rpm. O_2 flow, which was provided by a compressed bottle and saturated with humidity before entering the reactor, was maintained at 1800 mL/min during the entire reaction. For safety purposes, the reactor was loaded up to 70% of its capacity. After the reaction, the liquid fraction was stored at 4 °C until further usage for no longer than a week.

2.2.2. Lignin recovery

Lignin is one of the main organic components found in BL [33]. Thus, partial purification of the OA present in the BL can be achieved via LR. Lignin was recovered by acid precipitation. H_2SO_4 5M was added dropwise to the BL until a pH value of 2.5 was reached. Since this treatment causes the release of gaseous H_2S from the BL, it was performed under an extractor hood wearing a mask fitted with a polyfilter. Afterwards, the sample was centrifuged at 10000 g for 30 minutes, and the supernatant was collected as the feed for the subsequent UF step. Lignin was then washed with 3 volumes of acidified water to remove residual salts and kept at 110ºC for 24 h to measure the dry weight.

2.3. Membrane filtration

The streams of untreated BL and pre-treated by PWO or for LR were filtered with a tubular monochannel ZrO_2-TiO_2 membrane (600 × 6 mm) (TAMI Industries) with a molecular weight cut-off (MWCO) of 150 kDa and an effective area of $1.14\ 10^{-2}\ m^2$. A more thorough description of the ultrafiltration device can be found in [34]. A ceramic membrane was chosen due to its higher resistance to temperature and pH compared with polymeric membranes [35], which allows it to withstand the elevated temperatures and pH values (up to 70ºC and 12.4, respectively) that occurred during the filtration of BL.

All filtrations were performed at 70 ºC, a transmembrane pressure (TMP) of 1.5 bar and at a cross-flow velocity (CFV) of 0.81 ± 0.06 m/s. Temperature was selected in accordance to the existing literature [36–38], since it reduces the high viscosity of the BL, easing its pumping.

Permeate flux was determined by weighing of the permeate. Besides, permeate and retentate samples were collected on a periodical basis for further analysis.

After the filtration, membrane was rinsed with tap water until a constant flux value was reached and cleaned afterwards at 70ºC with 0.5% aqueous solution of basic detergent (Divos 124 VM5 provided by Diversey). The cleaning cycles were repeated if necessary, until a final flux of at least 90% of the initial permeate flux was reached.

All experiments were performed at least in duplicate, and in all cases the experimental error was below 5%.

2.4. Organic acid extraction

2.4.1. Materials

TOA (97%, Acros Organics), TBP (99.9%, VWR) and TOPO (98%, Alfa Aesar) were used as extractants in a first screening to determine an optimum solvent for LLE. These extractants were selected because of their wide use in the state-of-the-art extraction processes, their high extraction efficiency and selectivity towards carboxylic acids and their excellent chemical stability [32,39,40]. Their chemical structure is shown in Fig. 4.37.

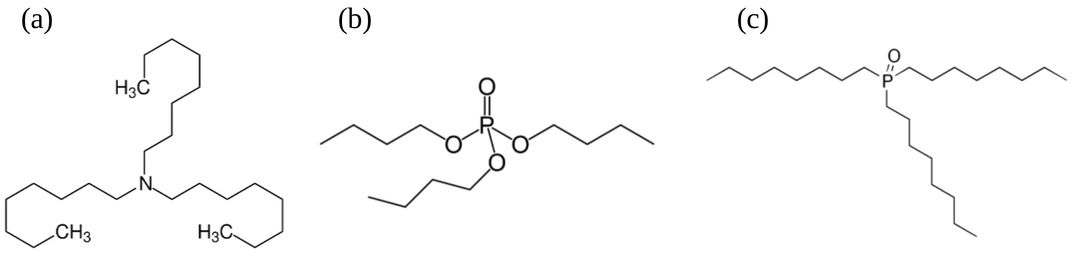

Figure 4.37. Molecular structures of a) TOA, b) TBP, and c) TOPO.

TOA and TBP are liquids at room temperature, whereas TOPO is a solid powder. Moreover, TBP is the most polar extractant according to its value of topological polar surface area (TPSA): 44.8 Å^2, followed by TOPO (TPSA = 17.1 Å^2). TOA is the least polar extractant (TPSA =3.2

Å^2). TPSA indicates the polar part of the molecule and it is evaluated by summation of the participation of its polar substituents or fragments [41].

These extractants are considered reactive extractants, as they interact with weak acids in the liquid-liquid interface, forming weak complexes that are insoluble in water, and therefore being extracted into the organic phase ([42,43]). Amine (TOA) and organophosphorus-based (TBP and TOPO) extractants interact with the OA as shown in the following reactive extraction mechanism [44,45]:

$$m\ R\text{—}COOH_{aq} + n\ NR_{3(org)} = R\text{—}COOH_mNR_{3n(org)}$$

$$m\ R\text{—}COO^-_{aq} + H^+_{aq} + n\ NR_{3(org)} = (R\text{—}COO^-H^+)_mNR_{3n(org)}$$

$$m\ R\text{—}COOH_{aq} + n\ P_{(org)} = R\text{—}COOH_mP_{n(org)}$$

Where R—COOH is the organic acid, NR_3 is the amine-based extractant, P is the organophosphorus-based extractant, and n and m are stoichiometric coefficients.

The phosphorous-based extractants interact with the OA through hydrogen bonding with the undissociated acid molecule; while the amine-based ones form complexes both with the undissociated OA through hydrogen bonding, and with the dissociated OA through ion pair formation [45].

n-Hexane (liquid chromatography grade, Merk) and heptane (99.5%, Panreac) were selected as diluents since they are totally immiscible in water, and have a low latent heat of vaporization. Besides, they are commonly employed in carboxylic acid extractions. These diluents are considered inactive since they do not participate in the mechanism of the acid complexation [32].

The screening was carried out employing several combinations of TOA, TOPO and TBP diluted in n-hexane or heptane as solvents for the LLE of OA from the UF permeates. The different solvents used are referred to under consideration of the extractant and the diluent, e.g., TOA30hep is a mixture of 30% TOA and 70% heptane (v/v), and TOPO10hex is a mixture of 10% TOPO and 90% n-hexane (wt/v).

2.4.2. Methodology

Extractions were carried out at room temperature after mixing the feed and the solvent (mixture of extractant and diluent or only extractant) in a proportion 1:1 (v/v for TOA and TBP, and wt/v for TOPO) until equilibrium was reached (OA concentration in the aqueous phase remained stable). The aqueous phase was then kept at 4ºC for further OA content analysis.

After this initial screening, the effect of temperature during the LLE was also studied to determine the optimal operating conditions. Extractions with the selected solvent from the previous step were carried out at 25ºC, 40ºC and 55ºC in the same feed:solvent proportion. In all cases, equilibrium was reached after 30 min of extraction (after this time OA concentrations in the aqueous phase remained constant). The aqueous phase was kept at 4ºC for further OA content analysis.

The extraction yield (Y_i) was calculated by the following equation (Eq. 1):

$$Y_i(\%) = \left(1 - \frac{C_{R,i}}{C_{F,i}}\right) \cdot 100 \qquad (1)$$

Being $C_{R,i}$ the concentration of the compound “i” in the raffinate, and $C_{F,i}$ the concentration of the compound “i” in the feed solution.

The distribution constants (K_D) for BL (K_{BL}), BL after lignin recovery (K_{LRBL}) and wet oxidised BL (K_{WOBL}) were calculated as follows (Eq. 2):

$$K_D = \frac{C_{i,org}}{C_{i,aq}} \qquad (2)$$

Being $C_{i,org}$ and $C_{i,aq}$ the concentrations of the compound “i” in the organic and aqueous phase respectively, after the equilibrium was reached.

2.5. Analytical methods

Density was measured with a pycnometer and was measured at room temperature and pressure. Kinematic viscosity was measured with a Cannon-Fenske inversed-flow viscometer (Proton, UK) at room temperature and pressure. pH was determined using a Basic 20 pH meter (Crison, Spain). In order to calculate the colour number (CN), which is defined in Eq. 3, spectral absorbance coefficients (SAC) were measured at 436, 525 and 620 nm using a Helios Alpha UV-Vis spectrophotometer (Thermo Scientific, USA). Both CN and SAC have units of cm^{-1}.

$$CN = \frac{SAC_{436}^2 + SAC_{525}^2 + SAC_{620}^2}{SAC_{436} + SAC_{525} + SAC_{620}} \quad (3)$$

COD was determined by the potassium dichromate method [46] using a HACH DR/2500 spectrophotometer (Hach Company, USA). OA concentrations were measured by HPLC Agilent Technologies 1200 Series, employing an ICSep ICE-ION-300 column (Teknokroma, Spain) as the stationary phase and H_2SO_4 0.45 mM as the mobile phase. Mobile phase pH was adjusted to 3.2-3.3 before running the HPLC. A refractive index detector was used to measure OA. Standard curves of oxalic, maleic, pyruvic, lactobionic, malic, lactic, formic, acetic and propionic acids were used for the proper identification and quantification of these acids. In order to correct the interferences caused by the inorganic anions in the signal produced by the oxalate, the peak signals corresponding to chloride, nitrate and sulphate were subtracted to the oxalate peak signal. The concentrations of these inorganic anions in the BL were measured by ion chromatography using a Dionex DX-120 ion chromatograph (Thermo Scientific, USA). The eluent used was mixture of Na_2CO_3 (4.5 mM) and $NaHCO_3$ (0.8 mm) at a flow rate of 1 mL/min. The precolumn and column used were IonPac AG23 (4 × 50 mm) and IonPac AS23 (4 × 250 mm).

Rejection coefficients (R) were defined as follows (Eq. 4):

$$R_i = 1 - \frac{C_{P_m,i}}{C_{R_t,i}} \quad (4)$$

Where $C_{P_m,i}$ and $C_{R_t,i}$ the concentration of the compound “i” in the permeate and the retentate, respectively.

3. Results and discussion

3.1. Black liquor pre-treatments

BL is a highly alkaline residue, which presents an elevate concentration of COD (>110 g O_2 /L) and dark colouration. The main physical-chemical characteristics of BL, BL after lignin recovery (LRBL) and partially wet oxidised BL (WOBL) are shown in Table 4.31.

Table 4.31. Physical-chemical characteristics of BL, LRBL and WOBL.

		BL	***LRBL***	***WOBL***
pH		12.4 ± 0.1	3.0 ± 0.1*	8.3 ± 0.1
Density (kg/m^3)		1074 ± 6	1068 ± 2	1064.8 ± 0.1
Kinematic viscosity (m^2/s)		$(1.94 \pm 0.01) \times 10^{-6}$	$(6.38 \pm 0.04) \times 10^{-7}$	$(1.22 \pm 0.01) \times 10^{-6}$
COD (g O_2/L)		113 ± 9	55.0 ± 0.9	60 ± 5
CN (cm^{-1})		150 ± 10	26 ± 2	30 ± 3
COD as OA (g O_2/L)		38.4 ± 0.6	29 ± 1	38 ± 4
OA (g/L)	*Oxalic acid*	89 ± 1	84 ± 2	64 ± 4
	Lactobionic acid	0.96 ± 0.01	0.42 ± 0.05	0.5 ± 0.1
	Malic acid	1.44 ± 0.02	0.81 ± 0.02	0.33 ± 0.01
	Lactic acid	8.0 ± 0.2	4.3 ± 0.3	10.2 ± 0.8
	Formic acid	2.51 ± 0.07	1.4 ± 0.1	1.6 ± 0.1
	Acetic acid	6.6 ± 0.2	5.8 ± 0.3	10 ± 2
	Propionic acid	4.20 ±0.02	2.2 ± 0.3	4.1 ± 0.6

*pH was set to 3.0 by adding H_2SO_4 to precipitate lignin.

Both LR and PWO lowered the density and viscosity of the BL. LR was more effective in reducing viscosity than PWO (64% of viscosity reduction after LR [$(6.38 \pm 0.04) \times 10^{-7}$ m^2/s] vs 31% of viscosity reduction after PWO [$(1.22 \pm 0.01) \times 10^{-6}$ m^2/s]). A moderate reduction of COD was achieved after both pre-treatments, the drop being around 50% of the initial COD. This reduction was higher than those obtained in other studies with BL that used PWO catalysed by Fe_2O_3, CuO, CeO_2 or Fe supported on activated carbon, in which the values varied from 13.95% to 16.88% [47]. In the case of CN, its decrease was very significant, attaining reductions of 83% and 80% after LR and PWO, respectively.

As for OA, although both pre-treatments cause a similar loss in OA concentration, the COD attributable to the OA increases from 34% to 52% after LR and to 63% after PWO, thus achieving a partial purification of the OA. Regarding the concentration of specific acids, such as acetic and lactic acids, their values increased importantly after PWO, the rise being 46.7% and 27.8%, respectively. The results obtained by Muddassar et al. [31] showed that the increase in acetic and lactic acid concentrations (8.45% and 11.61%) was lower when BL was treated by PWO at softer conditions (170ºC and 60 bar for 30 min) than those used in this work (190ºC and 70 bar for 120 min).

3.2. Membrane filtration

After UF, a partial purification of the OA was achieved in all cases, which was the main purpose of this step. In this sense, 42.9% (26.0% increase) of the BL's COD, a 71.2% (36.6% increase) of the LRBL's COD and a 69.9% (11.3% increase) of the WOBL's COD were attributable to the OA (see Table 4.32).

The other objective pursued by this treatment was the reduction of COD and CN in the permeate stream. It should be noted that higher retentions of COD (26%) and CN (33%) were obtained in the untreated BL in comparison to the ones attained in LRBL (19% for COD and 23% for CN) and WOBL (17% for COD and 19% for CN). This reduction can be explained by the transformations occurred during the LR and PWO pre-treatments: lignin is one of the components with high molecular weight in the BL, so its removal will lessen the amount of retained compounds. On the other hand, PWO degrades the BL, causing the cleavage of its larger molecules into smaller compounds, which can pass through the membrane more easily. Nevertheless, the retention of COD and CN did barely changed when pre-treatments were compared (2% for COD and 4% for CN), so, they had a minimum effect on this parameter.

Considering both the pre-treatment (LR or PWO) and UF step, the total reduction of COD and CN was slightly higher in the case of LRBL (after UF) than in WOBL (after UF), the values being 60% and 87% in the former and 57% and 84% in the latter, respectively.

Both LR and PWO pre-treatments showed a positive impact on UF performance, increasing the mean flux with respect to the untreated BL (24 ± 2 L/m^{2}h) by 13.7% and 17.9% after LR and PWO, respectively.

The results related to membrane fouling and its modelization can be found in the Supplementary Material.

Table 4.32. Physical-chemical characteristics of BL, LRBL and WOBL after UF.

		BL	*LRBL*	*WOBL*
COD (g O_2/L)		81 ± 4	40 ± 5	50 ± 3
CN (cm^{-1})		50 ± 5	43 ± 2	9 ± 3
COD as OA (g O_2/L)		35 ± 2	29 ± 1	35 ± 2
OA (g/L)	*Oxalic acid*	69 ± 4	85 ± 2	48 ± 1
	Lactobionic acid	1.04 ± 0.06	0.43 ± 0.01	0.53 ± 0.03
	Malic acid	1.32 ± 0.03	0.91 ± 0.04	0.31 ± 0.02
	Lactic acid	7.7 ± 0.8	4.3 ± 0.3	10.2 ± 0.3
	Formic acid	2.4 ± 0.2	1.4 ± 0.1	1.6 ± 0.4
	Acetic acid	6.2 ± 0.6	5.6 ± 0.3	9.7 ± 0.7
	Propionic acid	4.51 ± 0.07	2.0 ± 0.1	4.1 ± 0.4

3.3. Extraction

3.3.1. Solvent screening

For the sake of clarity, the yield results have been divided into non-volatile OA (NVA) (oxalic, lactobionic, malic and lactic acids) and volatile OA (VA) (formic, acetic and propionic acids). Yields obtained during solvent screening are presented in Tables 4.33 and 4.34.

Table 4.33. Yields (%) for NVA obtained during solvent screening.

	Oxalic acid			Lactobionic acid			Lactic acid			Malic acid		
Solvent	Y_{BL}^*	Y_{LRBL}^*	Y_{WOBL}^*	Y_{BL}	Y_{LRBL}	Y_{WOBL}	Y_{BL}	Y_{LRBL}	Y_{WOBL}	Y_{BL}	Y_{LRBL}	Y_{WOBL}
30TOAhex	84.5±0.1	18.2±0.4	0	74.3±0.0	37±2	23±1	14±3	19±3	0	41.60±0.01	46.6±3.7	0
20TOAhex	80.8±0.3	18±1	2.0±0.9	73.2±0.9	39±3	39±2	9±4	14±3	0	41.73±0.04	32.3±3.5	0
10TOAhex	70.71±0.01	24±1	0	73.3±0.8	38±1	29±1	4±1	15±5	0	60.04±0.02	27.5±5.1	0
30TBPhex	78.7±0.2	13±2	0	75.3±0.5	36±1	38.5±0.8	7.1±0.8	12±2	0	44.4±0.1	36.1±11.3	0
20TBPhex	81.1±0.1	21.0±0.6	0	72.5±1.8	41.7±0.1	30.9±0.9	9.0±0.6	16±4	0	35.70±0.01	10.4±1.7	0
10TBPhex	70.9±0.1	19±1	0	73.7±1.2	38±2	15±2	0	11.7±0.7	0	28.73±0.01	13.9±6.5	0
30TOPOhex	71.82±0.03	7.5±0.9	6.4±0.5	73.8±1.1	36±3	43±2	2±1	0	0	53.61±0.03	1.8±0.3	0
20TOPOhex	65.1±0.1	23±2	2±1	75.8±0.2	42.03±0.04	34.3±0.1	0	17±2	0	25.30±0.02	11.3±3.0	0
10TOPOhex	76.2±0.1	15±3	0	74.4±0.9	33±4	30±3	3±2	10.5±0.8	0	31.58±0.03	3.6±6.1	0
30TOAhep	66.40±0.02	29±7	28±4	74.0±0.4	30±3	43±2	9±2	45±6	10±4	63.01±0.03	7.6±7.0	17.1±3.5
20TOAhep	80.6±0.1	16±8	7±4	69.3±2.7	32.0±0.8	22±2	9±2	17±4	0	56.14±0.04	27.3±8.7	6.8±4.4
10TOAhep	82.8±0.2	19.9±2.1	0	73.4±1.9	39±3	41±2	13±3	16.4±0.1	0	54.38±0.06	15.6±2.7	23.2±1.4
30TBPhep	78.9±0.3	9.5±0.5	34.0±0.4	72.9±2.0	37±3	43±3	0	8±3	0	64.2±0.1	3.1±8.4	0
20TBPhep	78.3±0.1	12±3	14±2	71.1±1.9	41.3±0.1	47±1	6±3	13.6±0.8	0	45.59±0.05	4.8±5.4	0
10TBPhep	74.92±0.02	5.7±1.7	33.8±0.9	65.8±7.2	41.1±0.5	41±4	0	2.3±0.8	0	41.94±0.02	0	0
30TOPOhep	75.1±0.1	7.9±0.6	35.9±0.3	75.2±0.2	31±5	35±3	0	0	1.1±0.4	15.20±0.07	0	0
20TOPOhep	67.1±0.4	13±4	18±3	74.7±1.3	36±4	14±2	0	5±2	0	30.42±0.01	0	0
10TOPOhep	73.7±0.2	19.9±0.3	8.2±0.3	71.7±2.8	41.7±0.1	46±2	0	0	0	16.03±0.04	0	0
TOA	55.8±0.1	31±2	26.8±1.0	72.7±1.5	39±2	42±2	0	0	0	0	0	0
TBP	77.3±0.2	5.2±0.6	0	76.0±0.6	37±1	31.1±0.9	0	0	0	27.9±1.0	0	0

*Y_{BL} is Y_i for BL; Y_{LRBL} is Y_i for LRBL; Y_{WOBL} is Y_i for WOBL.

Table 4.34. Yields (%) for VA obtained during solvent screening.

	Formic acid			Acetic acid			Propionic acid		
Solvent	Y_{BL}	Y_{LRBL}	Y_{WOBL}	Y_{BL}	Y_{LRBL}	Y_{WOBL}	Y_{BL}	Y_{LRBL}	Y_{WOBL}
30TOAhex	51.4±0.4	16.6±0.2	21.0±0.3	15±2	14.2±0.5	0	84.1±0.3	42±11	45±6
20TOAhex	46±1	26±7	22±4	0	9.04±0.05	0	84.1±0.1	34±3	20±1
10TOAhex	39.5±0.9	26.6±0.5	22.5±0.7	0	18±1	0	83.8±0.3	44.60±0.06	35.5±0.2
30TBPhex	43.7±0.1	12±4	15±2	3.87±0.04	6±4	0	84±1	45±4	28±3
20TBPhex	52.4±0.3	17±6	17±6	11±3	11±5	0	81.9±0.0	48±6	43±3
10TBPhex	45.6±0.5	11±4	22±2	4±1	11±2	0	81.0±0.9	41±2	27±1
30TOPOhex	36.1±0.5	5±2	37±2	0	0	0	83.0±0.3	54±5	30±3
20TOPOhex	38.2±0.2	20±7	13±4	0	18±5	0	81±1	62±2	26±2
10TOPOhex	47.32±0.07	11±2	12.6±0.9	5±2	8.1±0.6	0	79.8±0.6	44±5	20±3
30TOAhep	40.2±0.3	31±6	40±3	0	23±9	10±4	78.1±0.0	18±5	26±3
20TOAhep	41.6±0.5	30±4	25±2	8±2	22±2	0	78.3±0.3	13±5	0
10TOAhep	47.4±0.5	16±4	27±2	16±7	19±1	8±3	78.6±0.3	13±6	26±3
30TBPhep	41.5±0.6	8±2	38±2	0	6.3±0.1	8±3	71.8±0.1	38.1±0.7	32.7±0.4
20TBPhep	44.4±0.2	17±2	35.5±0.9	12±4	11±1	4±2	76.6±0.4	27±1	35.1±0.9
10TBPhep	42.4±0.2	0	38.4±0.6	0	0	5±2	73±1	32±2	31±2
30TOPOhep	47.5±0.1	0	37±2	5.1±0.2	0	11±1	86.4±0.1	38.8±0.7	29.1±0.4
20TOPOhep	38.9±0.1	4±1	20.3±0.7	0	0	0	83±2	43.7±0.2	26.0±0.9
10TOPOhep	45.6±0.2	17±1	16.6±0.8	6.5±0.1	12±3	2±1	80.5±0.6	39±4	47±2
TOA	44.1±0.3	0	26.0±0.2	17±2	0	11±2	84.8±0.2	24.8±0.3	24.5±0.3
TBP	40.9±0.4	8±3	24.3±0.8	0	0	0	81±3	48.6±0.7	37.1±0.3

The influence of the extractant on the yield for different OA can be explained by their chemical properties. It was reported that the OA complexation with phosphorous based extractants (i.e., TBP and TOPO) is mainly dependent on the hydrophobicity of the OA, as its complexation mechanism is based on the formation of hydrogen bonds [39,40,48]. The less hydrophobic the OA is, the better it is complexed with the TBP or the TOPO. The hydrophobicities are generally expressed as log P or octanol-water partition coefficient. Polar and hydrophilic compounds present low values of log P (even negative), while non-polar and hydrophobic compounds exhibit higher values. So, the higher the log P value, the higher the hydrophobic character of the OA. On the other hand, the complexation mechanism when an amine as TOA is used as the extractant is more difficult to predict, as it depends on the acid concentration, the number of carboxyl groups in the OA, and the nature of the diluent [32]. For monocarboxylic acids (formic, acetic, propionic, lactic and lactobionic acids), the strength of the acid also affects the extraction yields. In this sense, the lower the pK_a value, the higher the extraction yields [49,50]. The hydrophobicities and the pK_as of the studied OA are shown in Table 4.35.

Table 4.35. Hydrophobicities (expressed as log P) and acidities of the studied OA.

	pK_a	**ref**	**Log P**	**ref**
Oxalic acid[a]	pK_{a1}=1.46; pK_{a2}=4.40	[51]	-0.688	[52]
Lactobionic acid	3.28±0.35[b]	[53]	-4.847	[54]
Malic acid[a]	pK_{a1}=3.51; pK_{a2}=5.03	[55]	-1.474	[56]
Lactic acid	3.86	[57]	-0.413	[57]
Formic acid	3.75	[57]	-0.538	[57]
Acetic acid	4.75	[57]	-0.313	[57]
Propionic acid	4.87	[57]	0.290	[57]

[a]Dicarboxylic acid; [b]predicted value

Based on the pK_a and Log P values, lactobionic acid should have been the OA with the highest yield. However, propionic acid was the most extracted OA in BL, regardless of the extractant used, with yields varied from 71.8±0.1% to 86.4±0.1%. Besides, an increase in the extractant concentration should lead to a higher extraction yield, as the interfacial amount of TOA, TBP or TOPO would increment, thus forming more OA-extractant complexes and extracting more OA into the organic phase. However, this trend was not observed in most of the extractions of NVA or VA in BL. In this way, the extraction yield of lactobionic acid was very similar (varied from 73.8±1.1% to 75.8±0.2%) regardless of the concentration of TOPO used diluted in n-hexane. For formic acid, the extraction yield (47.4±0.5%) was higher when 10TOAhep was used than in the case of 30TOAhep (40.2±0.3%). These facts indicate that some intricate complexation mechanisms must be occurring during LLE, fostered by the complexity of the BL matrix, which can alter extraction equilibria. These phenomena were also observed for LRBL and WOBL. In this sense, the extraction yields of lactobionic acid (41.7±0.1% in LRBL and 46±2% in WOBL) were higher when 10TOPOhep was employed than in the case of 30TOPOhep (31±5% in LRBL and 35±3% in WOBL). Therefore, it can be deduced that BL matrix significantly affects the OA complexation mechanisms, and that these interactions cannot be exclusively attributed to lignin and lignin derivatives.

It should be noted that the effect of the diluent was more noticeable than that of the extractant. Thus, higher extraction yields for oxalic, formic, and acetic acids were observed when heptane was used. Besides, heptane also favoured the extraction of oxalic and acetic acids from BL (and malic acid, with the exception of TOPO as extractant). On the contrary, n-hexane improved the extraction yields of malic, oxalic, formic, lactic, and propionic acids from LRBL. On the other hand, the effect of extractant on the improvement of the extraction yield in WOBL was only observed for formic acid, where TBP was found to be the best extractant regardless of the diluent employed, with yields ranging from 35.5±0.9% to 38.4±0.6%.

In the case of BL and LRBL, clearer tendencies were observed: TOPO was an unsuitable extractant, achieving the lowest extraction yields for malic, oxalic, lactic and acetic acids, whereas TOA was the most suitable one for these same acids.

The extractabilities of malic acid in both LRBL and WOBL were generally lower than expected considering its pKa and hydrophobicity values, thus being even non-extractable with TOPO diluted in heptane, with 10TBPhep and with undiluted extractants in LRBL; and with any solvent in WOBL, with the exception of TOA diluted in heptane. This fact may indicate that non-oxidised lignin plays a role in malic acid stabilization in the organic phase.

3.3.1.1. Non-volatile organic acids

The means of the yields obtained for NVA are shown in Fig. 4.38.

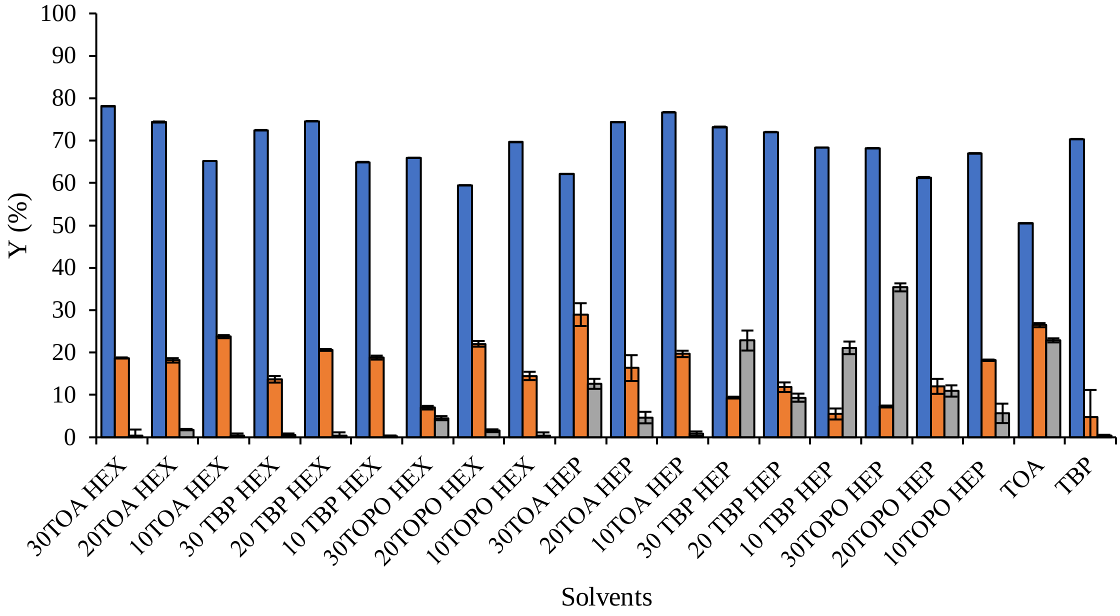

Figure 4.38. Extraction yields for NVA in BL (🟦), LRBL (🟧) and WOBL (⬜).

On viewing the results, both LR and PWO caused a significant reduction in the extraction yields of NVA. The mechanisms that underlie these reductions may vary for each pre-treatment. The decrease in extraction efficiency after PWO may be due to an increase in the amount of competing molecules: acid molecules are generated after the cleavage of lignin [31,58], as it is reflected by the decrease in the pH value after PWO (Table 4.31). These new-formed acids would compete with the target OA in forming acid-extractant complexes [43], reducing the amount of available interfacial extractant, and, consequently, the extraction yield. As for LR, the addition of H_2SO_4 could explain the yield reduction using TOA as the extractant, as they can form complexes by ion pairing [45]. This competing mechanism, however, is not appliable to TBP and TOPO, as they only form complexes with undissociated acids, so the lignin may play a role in reactive extraction, fostering the formation of OA-extractant complexes in untreated BL.

The use of TOA as extractant delivered the highest extraction yields in LRBL, both with n-hexane and heptane as diluents, while TOPO in heptane was the most suitable for WOBL.

The extraction yield of the oxalic acid greatly depended on the matrix: it was the most extracted one from BL, achieving a higher extraction value (84.5±0.1%) than lactobionic acid (76.0±0.6%). However, both pre-treatments affected its extractability more severely, thus being less extractable than lactobionic acid in LRBL, and lactobionic and formic acids in WOBL.

Lactobionic acid presented a mean extraction yield of 73±2% in BL, showing no great differences between values when different extractants were tested. After both LR and PWO, the mean extraction yield decreased to 37±3% and 33±9%, respectively.

Malic and lactic acids could not be extracted from WOBL with almost any of the tested solvents. In this sense, malic acid could only be extracted with TOA in heptane, obtaining the highest extraction yield (23±1%) with 10TOAhep. Lactic acid could only be extracted with 30TOAhep, achieving an extraction yield of 10±3%; and with 30TOPOhep, with a poor extraction yield of 1.1±0.4%.

Malic acid maximum extraction yields also decreased after both pre-treatments, from 64.2±0.1% in BL to 47±4% in LRBL and to 23±1% in WOBL (see Table 4.33). In this case, the obtained extraction yield values were dissimilar and highly dependent on the extractant used: TOA mixtures delivered the highest yields in BL and LRBL, with heptane being a better diluent in BL and hexane in LRBL.

Lactic acid extraction from BL and LRBL was also very dependent on the solvent used. Regarding TOPO as extractant, almost no extraction could be achieved in BL, while decent extraction yields were obtained only with 20TOPOhex and 10TOPOhex in LRBL. Maximum extraction yields of 14±3% and 45±6% were obtained with 30TOAhex and 30TOAhep for BL and LRBL, respectively (see Table 4.33).

3.3.2.2. Volatile organic acids

As for the impact of the treatments on the extraction of the VA, the yields presented in Fig. 4.39 showed the same tendency as for the NVA, being lowered after both treatments, especially after PWO. Also, the election of the solvent was found to be more determinant after any of the two pre-treatments (10.1% variation in BL and 44.4% and 51.4% for LRBL and WOBL, respectively). As with NVA, TOA proved to be the best extractant.

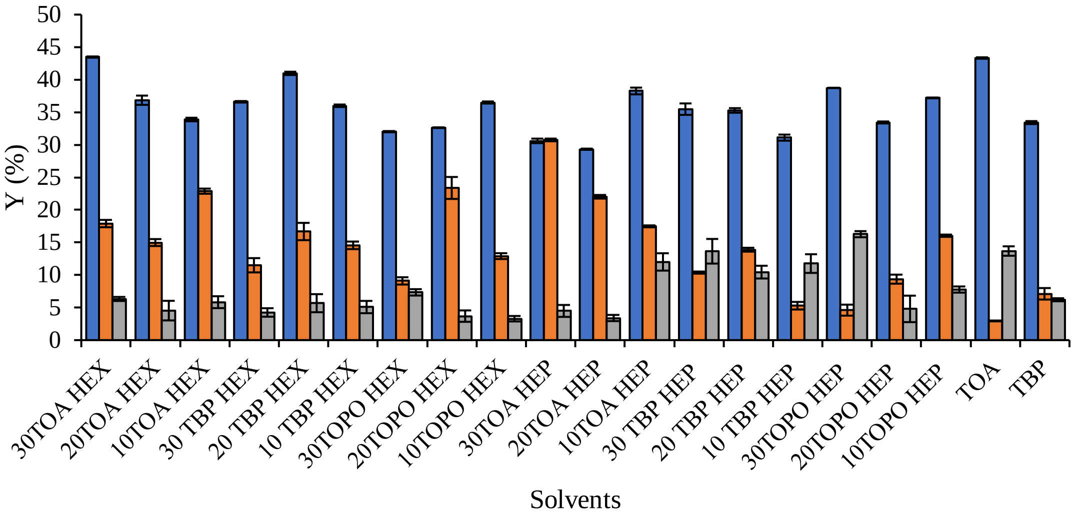

Figure 4.39. Extraction yields for VA in BL (🟦), LRBL (🟧) and WOBL (⬜).

Yields obtained for VA were higher than those obtained for NVA both in LRBL and WOBL. This has also been observed by other authors [59,60] using ionic liquids or TBP as extractant agents.

Propionic acid was the most extracted VA, with a mean extraction yield of 77±8% in BL, of 39±12% in LRBL, and of 28±12% in WOBL. Maximum yields of 86.4±0.1% with 30TOPOhep, 62±2% with 20TOPOhex and 47±2% with 10TOPOhep were obtained for BL, LRBL and WOBL, respectively.

Regarding formic acid, maximum extraction yields of 52.4±0.3% with 20TBPhex, 31±6% with 30TOAhep and 40±3% with 30TOAhep were obtained for BL, LRBL and WOBL, respectively.

Finally, acetic acid was the least extracted VA, and the extraction yields for this acid were highly dependent on the solvent in all cases. It was only extracted from WOBL when heptane was used as diluent. Maximum yields of 17±2% with TOA, 23±9% with 30TOAhep and 11±1% with 30TOPOhep were obtained for BL, LRBL and WOBL, respectively.

3.3.2. Election of the extraction conditions

The election of the best extractant was made based on the economic value of the extracted acids, taking into account the concentration of each acid present in the UF permeate, the economic value of each acid, and its extraction yield. In this sense, the value of the different OA was estimated after searching in the online catalogues of the main chemical suppliers (Sigma Aldrich and VWR). The estimated prices for the different OAs are shown in Table 4.36.

Table 4.36. Estimated prices for the evaluated OAs.

	OA	**Estimated price (€/kg)**
NVA	Oxalic	40.80
	Malic	33.26
	Lactobionic	257.76
	Lactic	74.49
VA	Formic	41.30
	Acetic	39.44
	Propionic	28.08

Based on these estimated prices, the studied OA can be classified into three value categories: i) oxalic, malic, formic, acetic and propionic acids are considered acids with moderate value; ii) lactic acid is considered a high-value acid; and finally, lactobionic acid is the one with the highest value. According to this classification, the most suitable extractant was found to be different for each of the liquors: 30TOAhex for BL, 30TOAhep for LRBL and 30TOPOhep for WOBL. It should be noted that TOA at 30% (v/v) was the proper extractant in two of the three black liquors (BL and LRBL) and heptane was the most adequate diluent in also two of the three black liquors (LRBL and WOBL). Since 30TOAhep was the best solvent for LRBL and considering that the OA extraction was more effective in LRBL than in WOBL, this solvent was selected for the analysis of the effect of temperature on the OA extraction. Besides, the use of heptane is more desirable than that of n-hexane due to its lower toxicity and higher flash point [61].

3.3.3. Effect of temperature on organic acid extraction

After selecting the most suitable extractant, several extraction temperatures (25, 40 and 55 ºC) were tested to assess the best temperature conditions for the LLE. The extraction yields, considering total NVA and total VA and each of the OA individually, are shown in Fig. 4.40.

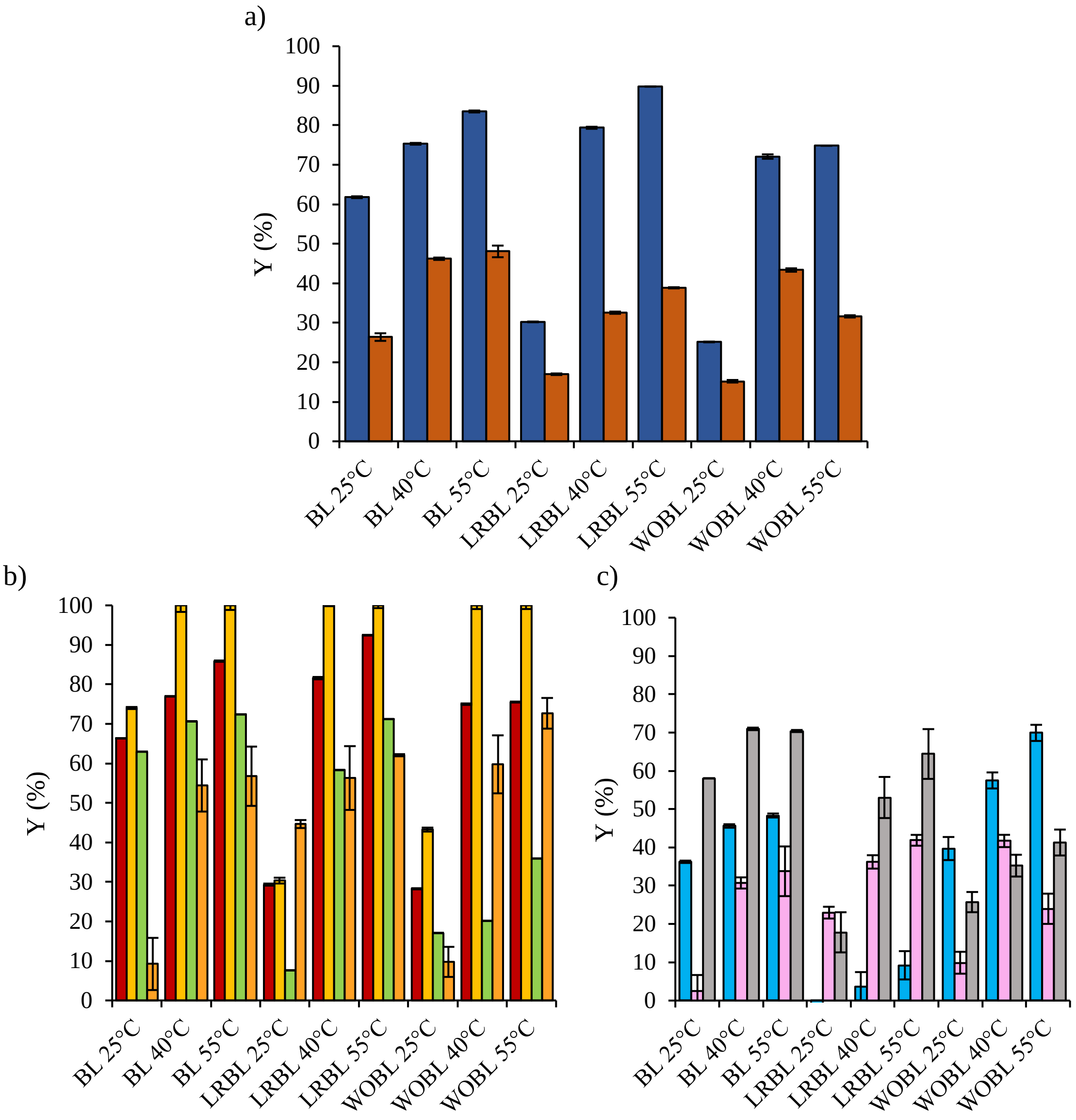

Figure 4.40. Effect of temperature in extraction yields in BL, DBL and WOBL of (a) total volatile OA (🟧) and non-volatile OA (🟦); (b) OA individually: oxalic (🟥), lactobionic (🟨), malic (🟩) and lactic (🟧) acids; and (c) formic (🟦), acetic (🟪) and propionic (⬜) acids.

As it can be seen in Fig. 4.40, higher yields were obtained after increasing the temperature. This increase in the extraction yield can be explained by a higher extractant-OA interaction: it has been reported that, when extracting OA with inert diluents, strong dimerization of the acids occurs by doble hydrogen bonding, impeding the extractant-OA interaction; and that this dimerization decreases with increasing temperature due to the increasing entropy, especially in diluents with low dielectric constants such as n-hexane and heptane [32]. So, the increase in the temperature up to 55ºC had a positive effect on the OA extraction. This improvement was particularly significant for NVA in LRBL and WOBL when temperature rose from 25ºC to 40ºC, in which the yield increased from 30.2% and 25.1% to 79.4% and 72.1%, respectively. However, setting temperatures above 55ºC could have a detrimental effect in the LLE, as it has been reported that higher yields could be eclipsed by the loss of the extractables due to thermal degradation [62]. Moreover, the increase in the yields was generally higher from 25ºC to 40ºC than from 40ºC to 55ºC. Thus, the maximum rise for VA in BL and LRBL was 19.8% and 15.6%, when the temperature increased from 25ºC to 40ºC, whereas it was 1.8% and 6.3%, respectively, when the increase varied between 40ºC and 55ºC. This, added to the fact that the latter temperature rise implies a higher energy cost, causes that extraction temperatures higher than 40ºC may not be justified from a profitability standpoint.

The K_D values obtained during the optimization step were also determined for comparison with the data reported by other authors. Their values are presented in Table 4.37. It should be noted that high values of K_D means that the extraction was effective. Matsumoto et al. [59] reported a K_D value of 1.34 for the extraction of pure malic acid employing pure TOA as extractant (extraction conditions: temperature = 30ºC and ratio sample:extractant = 1:1). In this study, the K_D value of malic acid at similar conditions (temperature = 25ºC and ratio sample:extractant = 1:1) was higher (1.70) when using 30TOAhep in BL, although it was much lower in LRBL (0.15) and in WOBL (0.21). This difference reflects both the positive effect of the diluent in OA extraction also reported by other authors [32] and the great effect that the BL matrix exerted on the LLE performance. This influence of the matrix was also observed in the LLE performance for propionic acid. Thus, the K_D values reported for Keshav et al. [63] for the extraction at 40ºC for 2 h of pure propionic acid with concentrations between 3.7 g/L and 29.6 g/L, varied from 0.42 to 0.62 using 30%TOA as extractant and heptane as diluent, this values being lower than those obtained for the extraction of this acid in BL (1.38), LRBL (4.30), but slightly higher than those obtained for WOBL (0.35) after 30 min at the same temperature.

TOA effectiveness as extractants for OA was further studied by Morales et al. [60]. These authors used mixtures of TOA as extractant, dodecane as inactive diluent and decane-1-ol as modifier (active diluent), and determined the extraction equilibrium of pure formic, lactic, and acetic acids at room temperature (20±1 ºC) and for 30 min. They reported that the K_D values ranged from 1.57 to 1.41, from 1.42 to 1.08 and from 2.29 to 1.84 for formic, acetic and lactic acids when their concentrations varied between 0.07 and 0.24 mol/L using TOA and decane-1-ol in dodecane (20:20:60% in v/v). In this study, only the extraction of formic and lactic acids in WOBL at 55ºC presented K_D values (2.32 and 2.66, respectively) higher than that reported by Morales et al. [48], the others being much lower in all the liquors. Based on these results, the K_D values are highly dependent on the matrix where the OAs are present, the effect of the diluent being generally positive.

Table 4.37. K_D values for NVA and VA using 30TOAhep as solvent.

NVA												
	Oxalic acid			Lactobionic acid			Lactic acid			Malic acid		
T (ºC)	K_{BL}	K_{LRBL}	K_{WOBL}	K_{BL}	K_{LRBL}	K_{WOBL}	K_{BL}	K_{LRBL}	K_{WOBL}	K_{BL}	K_{LRBL}	K_{WOBL}
25	1.97±0.04	0.460±0.005	0.394±0.004	2.85±0.06	2.5±0.3	0.762±0.006	0.102±0.001	0.93±0.01	0.108±0.002	1.70±0.03	0.153±0.003	0.206±0.003
40	3.4±0.1	4.60±0.02	3.00±0.04	n.a.*	n.a.*	n.a.*	1.19±0.03	1.45±0.02	1.49±0.03	2.41±0.03	0.75±0.04	0.25±0.01
55	6.1±0.3	12.7±0.1	3.09±0.05	n.a.*	n.a.*	n.a.*	1.31±0.03	1.82±0.03	2.66±0.05	2.63±0.03	1.5±0.1	0.561±0.005

*n.a.: not detected

VA									
	Formic acid			Acetic acid			Propionic acid		
T (ºC)	K_{BL}	K_{LRBL}	K_{WOBL}	K_{BL}	K_{LRBL}	K_{WOBL}	K_{BL}	K_{LRBL}	K_{WOBL}
25	0.57±0.01	0.64±0.01	0.66±0.01	$(2.56\pm0.03)\cdot10^{-2}$	0.491±0.005	0.110±0.001	1.384±0.006	4.30±0.04	0.35±0.03
40	0.84±0.02	0.84±0.01	1.35±0.02	$(44.32\pm0.04)\cdot10^{-2}$	0.800±0.009	0.715±0.008	2.44±0.02	8.3±0.1	0.54±0.01
55	0.94±0.02	0.95±0.02	2.32±0.05	$(50.97\pm0.05)\cdot10^{-2}$	0.98±0.01	0.315±0.003	2.38±0.02	11.2±0.3	0.70±0.01

3.3. Process diagram

In order to evaluate the best process for recovering OA from BL, the schematic shown in Fig. 4.41 has been made to allow for a clear comparison between the three proposed integrated processes. Starting from a common BL composition, the OA concentrations at each step of the process were calculated taking into account the retentions and extraction yields obtained in the experiments reported in this study. To determine which the most profitable process is, an economic evaluation of the final extract was made in the same manner than in the solvent screening.

Both pre-treatments implied similar losses in OA concentration, namely 15.3% loss after LR and 16.7% after PWO. However, LR proved to be helpful in reducing the OA retentions during the UF. In fact, most retentions were slightly negative, probably due to the Gibbs-Donnan effect [64,65]. On the other hand, all the OA except propionic acid were retained to some extent during BL UF: although almost every OA showed small retentions (from 4 to 9%), oxalic acid was significantly retained (22%), and, as it was the main OA in weight (72% of the OA mass), this higher retention implied a 17% loss of the OA mass. A similar behaviour was observed with WOBL, where only oxalic acid was retained, but its 25% retention led to a loss of 15% of the OA mass.

LLE temperature was set to 40ºC. After this step, 76% of the OA mass was recovered in LRBL, 72% in BL, and 68% in WOBL.

Taking into account the three factors previously considered for the election of the extraction conditions (section 3.3.2.): OA concentration, OA extraction yield and OA estimated market price), a total revenue of 3300 and 2200 €/m^3 of BL could be obtained through the LR and the PWO integrated processes, respectively, the value being 3000 €/m^3 of BL for the integrated process without pre-treatment. Thus, LR integrated process was considered to be the most advantageous in terms of OA recovery. Besides, after LR, 33 g/L of lignin could be recovered. Although raw Kraft lignin is not as valuable as the OA (Kraft lignin market value falls in the range of 230-450 €/tonne [66]), an average revenue of 11 €/m^3 of BL can be obtained. It is also worthy to note that lignin value could be multiplied if treated to obtain modified products [66,67]. Furthermore, LR is a well-established and cheap technology, since it has been estimated that lignin can be recovered from BL at 33-60 € per tonne [68]. Therefore, the average cost of attributed to lignin recovery is approximately 1.5 €/m^3. Regarding PWO process, it was estimated that the cost of treating BL is 667.4 €/m^3, this being around 14 times higher than the average cost of LR. This is mainly due to the high total capital investment (~35.4 M€) and the significant cost of the maintenance (~1.8 M€) and auxiliary services (~1.5 M€). This was also reported for other authors as one of the main drawbacks of wet oxidation [69,70]. The estimate of the total cost of this operation was performed based on the study of Chatzisymeon et al. [71] and it is explained in detail in section 3 of the Supplementary Material. Besides, the readiness level of this technology is low [72], thus hindering its implementation at a commercial scale. Therefore, LR can be considered the most suitable pre-treatment for the OA recovery from BL.

Due to the wide casuistry in BL treatment and disposal methods, the applicability of these strategies should be analysed based on each case and depending on the characteristics of the paper mill and discharge requirements. Implementing any of these strategies would imply added operational costs, which could be compensated by both the recovery of the OA and the reduction in discharge treatment costs, as the employed pre-treatments greatly reduced COD and CN values.

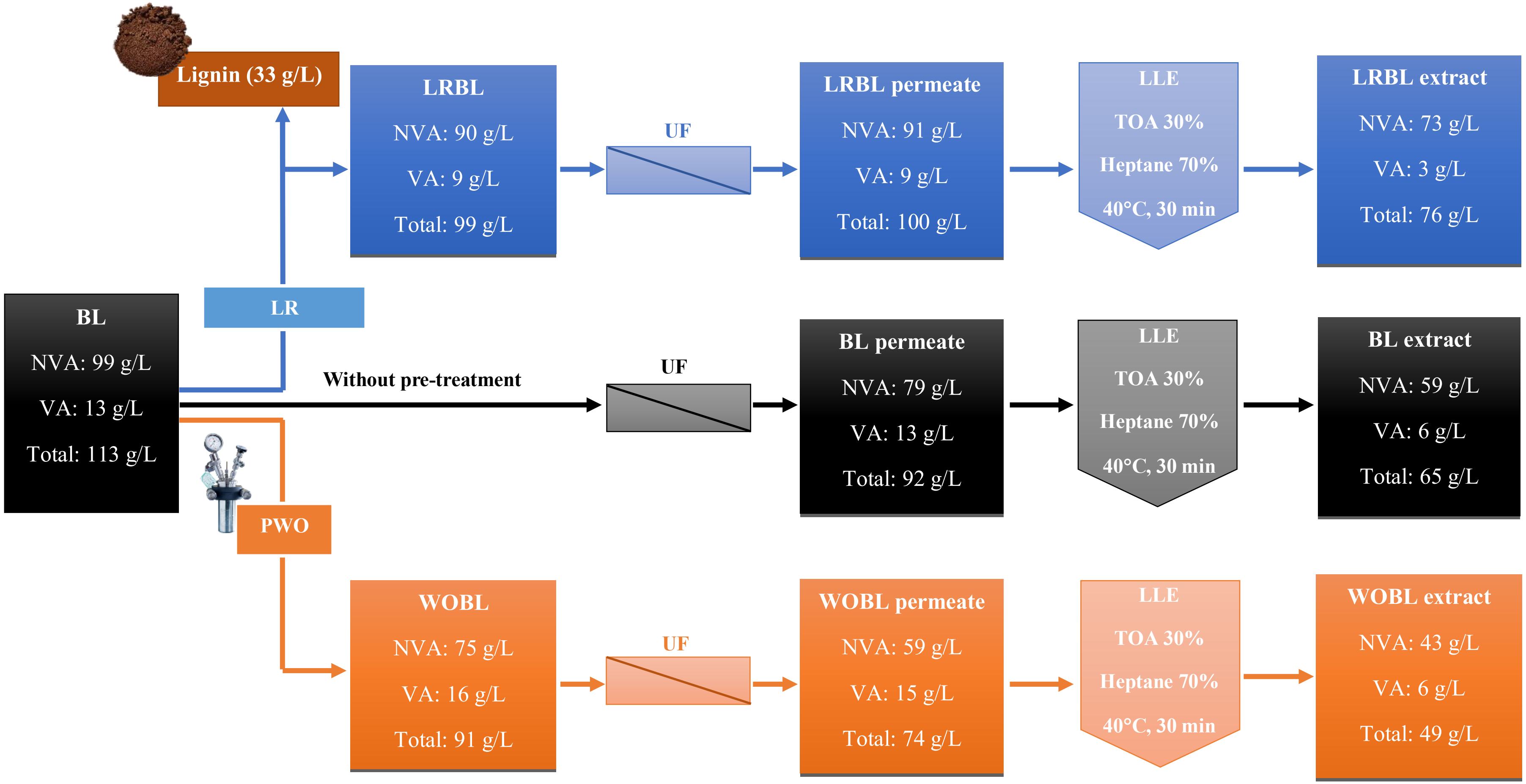

Figure 4.41. Overview of the integrated process for OA recovery from BL.

4. Conclusions

The combination of UF and LLE on pre-treated BL produced a recovery of OA of 28.1% and 29.4% for WOBL and LRBL, respectively, the value being 24.7% without pre-treatment. Therefore, LR proved to be more suitable as pre-treatment than PWO since it is a cheaper, much more widely implemented technique, and the OA recovery was higher.

Pre-treating the BL, either by LR or by PWO, caused a loss in the total OA mass. Nevertheless, the reduction in the organic content of the BL (as demonstrated by the reduction in COD and CN values), can achieve some reduction in the BL discharge treatment costs and partially mitigated membrane fouling during the UF step, thereby reducing the operational costs by increasing the lifespan of the membranes and reducing the membrane area needed to obtain a certain flux. In BL and WOBL, oxalic acid, which presented the highest concentration in the raw BL, was significantly retained, meaning a loss of 10-14 g/L of OA concentration after UF. Recovering the lignin of the BL avoided such a loss.

LLE is a complex operation, and variations in the feed composition greatly affected the efficiency of each solvent. Basing on the economic value of the extracted NVA and VA, 30% TOA in heptane (v/v) was selected as the suitable solvent.

Increasing the temperature had a positive effect on OA extraction. The increase in LLE yields was more significant between 25ºC and 40ºC than from 40ºC to 55ºC. Therefore, balance between OA recoveries and heating costs should be targeted before setting the optimal conditions for LLE.

Declaration of Competing Interest

The authors declare that they have no known competing financial interests or personal relationships that could have appeared to influence the work reported in this paper.

Acknowledgements

The authors are grateful for the financial support from the Spanish Ministry of Economy and Competitiveness (MINECO) through the project CTM2015-63864-R, the Spanish Ministry of Science, Innovation and Universities (MCIU) through the project RTI2018-094218-B-I00 and FEDER funds from European Union. Authors also acknowledge the financial support from the Employment, Industry and Tourism Office of the Principality of Asturias, Spain, through the project GRUPIN IDI/2018/000127. The author Daniel Núñez thanks the Principality of Asturias, Spain, for their financial support through the Severo Ochoa scholarship nº BP19-093.

References

[1] P. Bajpai, Pulping Fundamentals, in: Biermann’s Handb. Pulp Pap., 2018: pp. 295–351. doi:10.1016/b978-0-12-814240-0.00012-4.

[2] L. Pola, S. Collado, P. Oulego, M. Díaz, Production of carboxylic acids from the non-lignin residue of black liquor by hydrothermal treatments, Bioresour. Technol. 284 (2019) 105–114. doi:10.1016/j.biortech.2019.03.066.

[3] CEPI Confederation Of European Paper Industries, KEY STATISTICS 2018: European pulp & paper industry, (2019) 32.

[4] IEA Bioenergy, Black liquor gasification. Summary and Conclusions from the IEA Bioenergy ExCo54 Workshop, n.d.

[5] A. Garg, I.M. Mishra, S. Chand, Effectiveness of coagulation and acid precipitation processes for the pre-treatment of diluted black liquor, J. Hazard. Mater. 180 (2010) 158–164. doi:10.1016/j.jhazmat.2010.04.008.

[6] M. Zaied, N. Bellakhal, Electrocoagulation treatment of black liquor from paper industry, J. Hazard. Mater. 163 (2009) 995–1000. doi:10.1016/j.jhazmat.2008.07.115.

[7] S. Kortekaas, G. Vidal, H. Yan-Ling, G. Lettinga, J.A. Field, Anaerobic-aerobic treatment of toxic pulping black liquor with upfront effluent recirculation, J. Ferment. Bioeng. 86 (1998) 97–110. doi:10.1016/S0922-338X(98)80041-X.

[8] M.A. Lara, A.J. Rodríguez-Malaver, O.J. Rojas, O. Holmquist, A.M. González, J. Bullón, N. Peñaloza, E. Araujoa, Black liquor lignin biodegradation by Trametes elegans, Int. Biodeterior. Biodegrad. 52 (2003) 167–173. doi:10.1016/S0964-8305(03)00055-6.

[9] X. An, B. Zhong, G. Chen, W. An, X. Xia, H. Li, F. Lai, Q. Zhang, Evaluation of bioremediation and detoxification potentiality for papermaking black liquor by a new isolated thermophilic and alkali-tolerant Serratia sp. AXJ-M, J. Hazard. Mater. 406 (2021) 124285. doi:10.1016/j.jhazmat.2020.124285.

[10] H. Kumar, R. Alén, Partial recovery of aliphatic carboxylic acids and sodium hydroxide from hardwood black liquor by electrodialysis, Ind. Eng. Chem. Res. 53 (2014) 9464–9470. doi:10.1021/ie5006004.

[11] A.K. Mishra, P.K. Bhattacharya, Alkaline black liquor treatment by batch electrodialysis, Can. J. Chem. Eng. 62 (1984) 723–727. doi:10.1002/cjce.5450620520.

[12] A.K. Mishra, P.K. Bhattacharya, Alkaline black liquor treatment by continuous electrodialysis, J. Memb. Sci. 33 (1987) 83–95. doi:10.1016/S0376-7388(00)80053-8.

[13] A. Arkell, J. Olsson, O. Wallberg, Process performance in lignin separation from softwood black liquor by membrane filtration, Chem. Eng. Res. Des. 92 (2014) 1792–1800.

doi:10.1016/j.cherd.2013.12.018.

[14] O. Wallberg, A.S. Jönsson, R. Wimmerstedt, Ultrafiltration of kraft black liquor with a ceramic membrane, Desalination. 156 (2003) 145–153. doi:10.1016/S0011-9164(03)00337-0.

[15] N.S. Kevlich, M.L. Shofner, S. Nair, Membranes for Kraft black liquor concentration and chemical recovery: Current progress, challenges, and opportunities, Sep. Sci. Technol. 52 (2017) 1070–1094. doi:10.1080/01496395.2017.1279180.

[16] O. Wallberg, A.S. Jönsson, R. Wimmerstedt, Fractionation and concentration of kraft black liquor lignin with ultrafiltration, Desalination. 154 (2003) 187–199. doi:10.1016/S0011-9164(03)80019-X.

[17] O. Rojas, J. Song, D.S. Argyropoulos, Lignin separation from Kraft black liquors by tangential ultrafiltration, La Chim. e l’Industria. 1 (2006) 88–95. doi:10,1016/S0011-9164(03)00337-0.

[18] E. Araujo, A.J. Rodríguez-Malaver, A.M. González, O.J. Rojas, N. Peñaloza, J. Bullón, M.A. Lara, N. Dmitrieva, Fenton’s reagent-mediated degradation of residual Kraft black liquor, Appl. Biochem. Biotechnol. - Part A Enzym. Eng. Biotechnol. 97 (2002) 91–103. doi:10.1385/ABAB:97:2:091.

[19] M. Escalante, A.J. Rodríguez-Malaver, E. Araujo, A.M. González, O.J. Rojas, N. Peñaloza, J. Bullón, M.A. Lara, N. Dmitrieva, E. Pérez-Pérez, Effect of surfactants on Fenton’s reagent-mediated degradation of Kraft black liquor, J. Environ. Biol. 26 (2005) 709–718.

[20] H. Debellefontaine, J.N. Foussard, Wet air oxidation for the treatment of industrial wastes. Chemical aspects, reactor design and industrial applications in Europe, Waste Manag. 20 (2000) 15–25. doi:10.1016/S0956-053X(99)00306-2.

[21] P. Bajpai, Kraft Spent Liquor Recovery, in: Biermann’s Handb. Pulp Pap., 2018: pp. 425–451. doi:10.1016/b978-0-12-814240-0.00017-3.

[22] D.M. Martin, E.W. Malcolm, M. Hupa, D.M. Martin, E.W. Malcolm, M. Hupa, The Effect of Fuel Composition on Nitrogen Release During Black Liquor Pyrolysis, n.d.

[23] E.K. Vakkilainen, M. Hamaguchi, D.C. Laux, Grouping Statistically Emissions from a Recovery Boiler, XXI Encontro Nac. Da Tec. / VI CIADICYP 2010, Lisboa, Port. (n.d.).

[24] M. Benali, O. Ajao, J. Jeaidi, B. Gilani, B. Mansoornejad, Integrated Lignin-Kraft Pulp Biorefinery for the Production of Lignin and Its Derivatives: Economic Assessment and LCA-Based Environmental Footprint, in: 2016: pp. 379–418. doi:10.1007/978-981-10-1965-4_13.

[25] S. Laurichesse, L. Avérous, Chemical modification of lignins: Towards biobased polymers, Prog. Polym. Sci. 39 (2014) 1266–1290. doi:10.1016/j.progpolymsci.2013.11.004.

[26] K.M. Kunal Ahuja, Lignin Market Growth Statistics | 2019-2025 Industry Share Projections, Glob. Mark. Insights. (n.d.). https://www.gminsights.com/industry-analysis/lignin-market

(accessed May 19, 2020).

[27] S.K. Panda, L. Sahu, S.K. Behera, R.C. Ray, Research and Production of Organic Acids and Industrial Potential, in: Bioprocess. Biomol. Prod., John Wiley & Sons, Ltd, 2019: pp. 195–209. doi:10.1002/9781119434436.ch9.

[28] Y. Sahu, Organic Acids Market Size, Share and Trends | Industry Growth, 2023, 2017.

[29] H.S. Kwon, B.H. Um, Optimization and Evaluation of Organic Acid Recovery from Kraft Black Liquor Using Liquid-Liquid Extraction, Korean Chem. Eng. Res. 54 (2017) 753–761. doi:10.9713/kcer.2016.54.6.753.

[30] S. Hellstén, J. Lahti, J. Heinonen, M. Kallioinen, M. Mänttäri, T. Sainio, Purification process for recovering hydroxy acids from soda black liquor, Chem. Eng. Res. Des. 91 (2013) 2765–2774. doi:10.1016/J.CHERD.2013.06.001.

[31] H.R. Muddassar, K. Melin, D. De Villalba Kokkonen, G.V. Riera, S. Golam, J. Koskinen, Green chemicals from pulp production black liquor by partial wet oxidation, Waste Manag. Res. 33 (2015) 1015–1021. doi:10.1177/0734242X15602807.

[32] L.M.J. Sprakel, B. Schuur, Solvent developments for liquid-liquid extraction of carboxylic acids in perspective, Sep. Purif. Technol. 211 (2019) 935–957. doi:10.1016/j.seppur.2018.10.023.

[33] P. Bajpai, Pulping Fundamentals, in: Biermann's Handb. Pulp Pap., Elsevier, 2018: pp. 295–351. doi:10.1016/b978-0-12-814240-0.00012-4.

[34] S. Collado, D. Núñez, P. Oulego, F.A. Riera, M. Díaz, Effect of landfill leachate ageing on ultrafiltration performance and membrane fouling behaviour, J. Water Process Eng. 36 (2020). doi:10.1016/j.jwpe.2020.101291.

[35] Z. Yang, C.Y. Tang, Novel membranes and membrane materials, in: Membr. Salin. Gradient Process. Water Treat. Power Gener., Elsevier, 2018: pp. 201–221. doi:10.1016/B978-0-444-63961-5.00007-9.

[36] M. Ebrahimi, N. Busse, S. Kerker, O. Schmitz, M. Hilpert, P. Czermak, Treatment of the bleaching effluent from sulfite pulp production by ceramic membrane filtration, Membranes (Basel). 6 (2015) 1–15. doi:10.3390/membranes6010007.

[37] M.K. Hill, D.A. Violette, D.L. Woerner, Lowering kraft black liquor viscosity by ultrafiltration, Sep. Sci. Technol. 23 (1988) 1789–1798. doi:10.1080/01496398808075663.

[38] A. Keyoumu, R. Sjödahl, G. Henriksson, M. Ek, G. Gellerstedt, M.E. Lindström, Continuous nano- and ultra-filtration of kraft pulping black liquor with ceramic filters: A method for lowering the load on the recovery boiler while generating valuable side-products, in: Ind. Crops Prod., 2004: pp. 143–150. doi:10.1016/j.indcrop.2004.04.017.

[39] T. Hano, M. Matsumoto, T. Ohtake, K. Sasaki, F. Hori, Y. Kawano, Extraction equilibria of

organic acids with tri-n-octylphosphineoxide, J. Chem. Eng. Japan. 23 (1990) 734–738. doi:10.1252/jcej.23.734.

[40] M. Matsumoto, T. Otono, K. Kondo, Synergistic extraction of organic acids with tri-n-octylamine and tri-n-butylphosphate, Sep. Purif. Technol. 24 (2001) 337–342. doi:10.1016/S1383-5866(01)00137-X.

[41] R. Barret, Importance and Evaluation of the Polar Surface Area (PSA and TPSA), Ther. Chem. (2018) 89–95. doi:10.1016/b978-1-78548-288-5.50005-6.

[42] D. Caşcaval, L. Kloetzer, A.I. Galaction, Influence of organic phase polarity on interfacial mechanism and efficiency of reactive extraction of acetic acid with tri-n-octylamine, J. Chem. Eng. Data. 56 (2011) 2521–2526. doi:10.1021/je200044y.

[43] G. Maurer, Modeling the liquid-liquid equilibrium for the recovery of carboxylic acids from aqueous solutions, Fluid Phase Equilib. 241 (2006) 86–95. doi:10.1016/j.fluid.2005.11.005.

[44] S. Şahin, Ş.S. Bayazit, M. Bilgin, I. Inci, Investigation of Formic Acid Separation from Aqueous Solution by Reactive Extraction: Effects of Extractant and Diluent, J. Chem. Eng. Data. 55 (2009) 1519–1522. doi:10.1021/JE9006635.

[45] D. Datta, S. Kumar, H. Uslu, Status of the reactive extraction as a method of separation, J. Chem. 2015 (2015). doi:10.1155/2015/853789.

[46] APHA, AWWA, WEF, APHA, AWWA, WEF. “Standard Methods for examination of water and wastewater.,” An. Hidrol. Médica. 5 (2012) 185–186. doi:10.5209/rev_ANHM.2012.v5.n2.40440.

[47] G. Viader Riera, Catalytic wet oxidation of black liquor, (2012).

[48] C. Scheler, M. Popovic, E. Iannotti, R. Mueller, R. Bajpai, Chemical interactions between aqueous and organic phases in a reactive extraction process, Appl. Biochem. Biotechnol. - Part A Enzym. Eng. Biotechnol. 57–58 (1996) 29–38. doi:10.1007/BF02941685.

[49] J.A. Tamada, C.J. King, Extraction of Carboxylic Acids with Amine Extractants. 2. Chemical Interactions and Interpretation of Data, Ind. Eng. Chem. Res. 29 (1990) 1327–1333. doi:10.1021/ie00103a036.

[50] G.M. Barrow, E.A. Yerger, Acid-Base Reactions in Non-dissociating Solvents. Acetic Acid and Triethylamine in Carbon Tetrachloride and Chloroform, J. Am. Chem. Soc. 76 (1954) 5211–5216. doi:10.1021/ja01649a080.

[51] National Center for Biotechnology Information, Oxalic acid | HOOCCOOH - PubChem, Oxalic Acid. (2004). https://pubchem-ncbi-nlm-nih-gov.ezproxy.umng.edu.co/compound/971#section=Top (accessed April 9, 2021).

[52] Royal Society of Chemistry, Oxalic acid | C2H2O4 | ChemSpider, 2021. (n.d.). http://www.chemspider.com/Chemical-Structure.946.html (accessed April 9, 2021).

[53] Chemical Book, Lactobionic acid | 96-82-2, 2017. (n.d.). https://www.chemicalbook.com/ChemicalProductProperty_EN_CB8713997.htm (accessed April 9, 2021).

[54] Royal Society of Chemistry, Lactobionic acid | C12H22O12 | ChemSpider, 2021. (n.d.). http://www.chemspider.com/Chemical-Structure.7040.html (accessed April 12, 2021).

[55] U.S. National Library of Medicine, Malic acid | C4H6O5 - PubChem, PubChem. (2019). https://pubchem.ncbi.nlm.nih.gov/compound/Malic-acid#section=Viscosity%0Ahttps://pubchem.ncbi.nlm.nih.gov/compound/Malic-acid#section=Names-and-Identifiers (accessed April 9, 2021).

[56] Royal Society of Chemistry, (±)-Malic Acid | C4H6O5 | ChemSpider, 2021. (n.d.). http://www.chemspider.com/Chemical-Structure.510.html (accessed April 9, 2021).

[57] W. Qin, Z. Li, Y. Dai, Extraction of Monocarboxylic Acids with Trioctylamine: Equilibria and Correlation of Apparent Reactive Equilibrium Constant, Ind. Eng. Chem. Res. 42 (2003) 6196–6204. doi:10.1021/ie021049b.

[58] F.M. Casimiro, C.A.E. Costa, C.M. Botelho, M.F. Barreiro, A.E. Rodrigues, Kinetics of Oxidative Degradation of Lignin-Based Phenolic Compounds in Batch Reactor, Ind. Eng. Chem. Res. 58 (2019) 16442–16449. doi:10.1021/acs.iecr.9b02818.

[59] M. Matsumoto, K. Mochiduki, K. Fukunishi, K. Kondo, Extraction of organic acids using imidazolium-based ionic liquids and their toxicity to Lactobacillus rhamnosus, Sep. Purif. Technol. 40 (2004) 97–101. doi:10.1016/j.seppur.2004.01.009.

[60] A.F. Morales, J. Albet, G. Kyuchoukov, G. Malmary, J. Molinier, Influence of extractant (TBP and TOA), diluent, and modifier on extraction equilibrium of monocarboxylic acids, in: J. Chem. Eng. Data, 2003: pp. 874–886. doi:10.1021/je020179o.

[61] D.R. Joshi, N. Adhikari, An Overview on Common Organic Solvents and Their Toxicity, J. Pharm. Res. Int. 28 (2019) 1–18. doi:10.9734/JPRI/2019/V28I330203.

[62] I.S. Che Sulaiman, M. Basri, H.R. Fard Masoumi, W.J. Chee, S.E. Ashari, M. Ismail, Effects of temperature, time, and solvent ratio on the extraction of phenolic compounds and the anti-radical activity of Clinacanthus nutans Lindau leaves by response surface methodology, Chem. Cent. J. 11 (2017) 54. doi:10.1186/s13065-017-0285-1.

[63] A. Keshav, K.L. Wasewar, S. Chand, Extraction of propionic acid with tri-n-octyl amine in different diluents, Sep. Purif. Technol. 63 (2008) 179–183. doi:10.1016/j.seppur.2008.04.012.

[64] T.T. Van Tran, S.R. Kumar, S.J. Lue, Separation mechanisms of binary dye mixtures using a PVDF ultrafiltration membrane: Donnan effect and intermolecular interaction, J. Memb. Sci. 575 (2019) 38–49. doi:10.1016/j.memsci.2018.12.070.

[65] F. Zhou, C. Wang, J. Wei, Separation of acetic acid from monosaccharides by NF and RO

membranes: Performance comparison, J. Memb. Sci. 429 (2013) 243–251. doi:10.1016/j.memsci.2012.11.043.

[66] H. Ludmila, J. Michal, Š. Andrea, H. Aleš, Lignin, potential products and their market value, Wood Res. 60 (2015) 973–986.

[67] P. Varanasi, P. Singh, M. Auer, P.D. Adams, B.A. Simmons, S. Singh, Survey of renewable chemicals produced from lignocellulosic biomass during ionic liquid pretreatment, Biotechnol. Biofuels. 6 (2013) 1–9. doi:10.1186/1754-6834-6-14.

[68] A.S. Jönsson, O. Wallberg, Cost estimates of kraft lignin recovery by ultrafiltration, Desalination. 237 (2009) 254–267. doi:10.1016/j.desal.2007.11.061.

[69] S.K. Bhargava, J. Tardio, J. Prasad, K. Föger, D.B. Akolekar, S.C. Grocott, Wet oxidation and catalytic wet oxidation, Ind. Eng. Chem. Res. 45 (2006) 1221–1258. doi:10.1021/ie051059n.

[70] G. Bertanza, M. Canato, S. Heimersson, G. Laera, R. Salvetti, E. Slavik, M. Svanström, Techno-economic and environmental assessment of sewage sludge wet oxidation, Environ. Sci. Pollut. Res. 22 (2015) 7327–7338. doi:10.1007/s11356-014-3378-6.

[71] E. Chatzisymeon, S. Foteinis, D. Mantzavinos, T. Tsoutsos, Life cycle assessment of advanced oxidation processes for olive mill wastewater treatment, J. Clean. Prod. 54 (2013) 229–234. doi:10.1016/j.jclepro.2013.05.013.

[72] M.T. Munir, S.S. Mansouri, I.A. Udugama, S. Baroutian, K. V. Gernaey, B.R. Young, Resource recovery from organic solid waste using hydrothermal processing: Opportunities and challenges, Renew. Sustain. Energy Rev. 96 (2018) 64–75. doi:10.1016/j.rser.2018.07.039.

Supplementary Material to

‘Recovery of organic acids from pre-treated Kraft black liquor using ultrafiltration and liquid-liquid extraction’

Daniel Núñez[a], *Paula Oulego*[a], *Sergio Collado*[a], *Francisco A. Riera* [a] *and Mario Díaz*[a,*]

[a]Department of Chemical and Environmental Engineering, University of Oviedo.

c/Julián Clavería, s/n, 33071, Oviedo, Spain

(13 Pages, 2 Figures, 4 Tables)

Table of contents

*Corresponding author’s e-mail: mariodiaz@uniovi.es (M. Díaz)
Phone: +34 985 10 34 39, Fax: +34 985 10 34 40

1. Membrane fouling

Flux evolution over time was studied in order to evaluate fouling tendencies and discuss the maximization of membrane performance. Normalised fluxes of BL, LRBL and WOBL for 1 h of operation are shown in Fig. A.4.8.

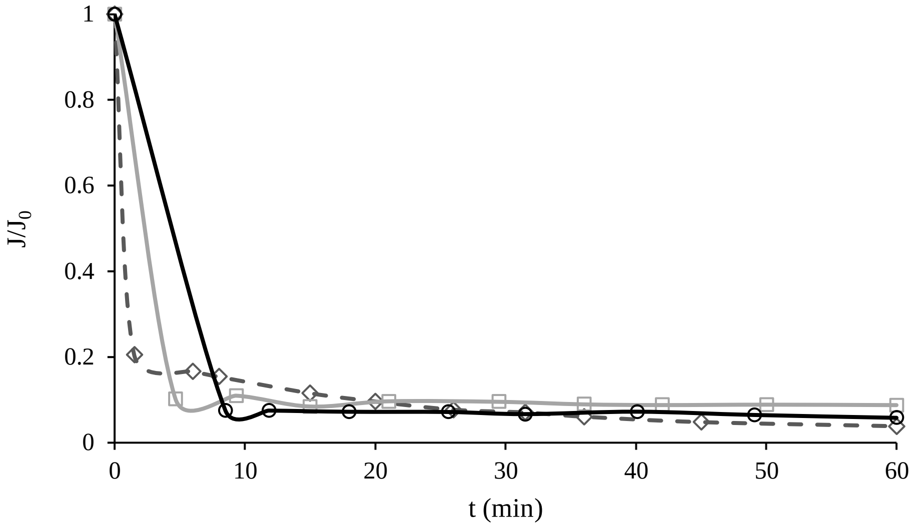

Figure A.4.8. Normalised fluxes of BL (○), DBL (□) and WOBL (◇).

In the case of WOBL filtration, the flux reduction during the first 15 minutes of the filtration was smaller compared to the BL and LRBL. From this time one, however, flux rate continued to drop, while BL and LRBL fluxes plateaued. This difference between trends can be explained by the effect of foulant-membrane and foulant-foulant interactions. Greater fouling occurrence in ceramic membranes during the separation of lignin oxidation products was reported by Abdelaziz et al. [1] when compared to the separation of lignin derivatives. According to this, despite the average molecule size reduction due to the hydrothermal treatment, and although WOBL presented lower COD values than BL, the nature of the foulants makes membrane permeability lower in the long term. The pH drop could also be responsible for this lessening in filtration performance, as numerous colloidal materials present in BL, such as phenolic compounds, see their solubility decreased at less basic pHs [2].

Comparison between fluxes from the literature is difficult, as many factors such as temperature, MWCO, TMP or CFV directly affect the flux. For instance, fluxes of 10-15 L/m^{2}h (LMH) and 20 LMH were reported by Ren [3] and Arkell et al. [4], respectively, while filtering BL with membranes of 10, 5, 3 kDa [3] and 1 kDa [4] of MWCO at low TMPs and CFVs, like in the filtrations described in this study; nevertheless, increasing these parameters can result in fluxes up to [4] and over 200 LMH [5].

Delignification of the BL alleviated membrane fouling, but it failed to avoid the drastic initial flux decay. This implies that, although lignin and lignoid components have been reported to be the main foulant agents present in the BL [4,6], their contribution alone is not enough to explain flux decline, which may also be due to a synergistic combination of the organic and inorganic components present in the BL.

Nevertheless, both pre-treatments show a positive impact on UF performance, increasing the mean flux with respect to the untreated BL by 13.7% and 17.9% after delignification and PWO, respectively.

Considering that the fouling rate is important in the different BLs, a cleaning strategy should be stablished in order to maximize productivity. In this sense, physical cleaning can be used to mitigate membrane fouling and decrease the frequency of chemical cleaning, thus prolonging membrane lifetime and reducing operational costs. The common physical cleaning methods include backwashing/backflusing, backpulsing, crossflushing, sponge ball cleaning, air sparging, etc [7]. Among them, backpulsing seems to be the most proper technology in this case, since, according to the literature, it is usually employed for water and wastewater treatment, for ceramic membranes and tubular configuration [7,8].

2. Fouling modeling

To delve deeper into the subject of membrane cleaning, it is important to evaluate the reversibility or irreversibility of membrane fouling. Fouling nature was determined following the Hermia's model [9], which enable to determine the main fouling mechanisms for all filtrations (Eq. A1):

$$\frac{dJ}{dt} = -K \cdot (J - J_0) \cdot J^{2-n} \qquad \text{(A1)}$$

Where J is the permeate flux ($m \cdot s^{-1}$), K is a constant, J_0 is the limiting flux ($m \cdot s^{-1}$), and n is a constant that varies for the complete blocking (n=2, K in min^{-1}), standard blocking (n=1.5, K in m^{-1}) intermediate pore blocking (n=1, K in m^{-1}) and cake filtration (n=0, K in $min \cdot m^{-2}$) mechanisms [10]. The best model was chosen based on the difference between the predicted values and the experimental data, calculated as the sum of squared residuals (SSR).

The experimental fluxes and the adjusted four studied Hermia models: i) complete pore blocking (CPB), ii) standard pore blocking (SPB), iii) intermediate pore blocking (IPB) and iv) cake formation (CF), are shown in Fig. A.4.9 and Table A.4.5.

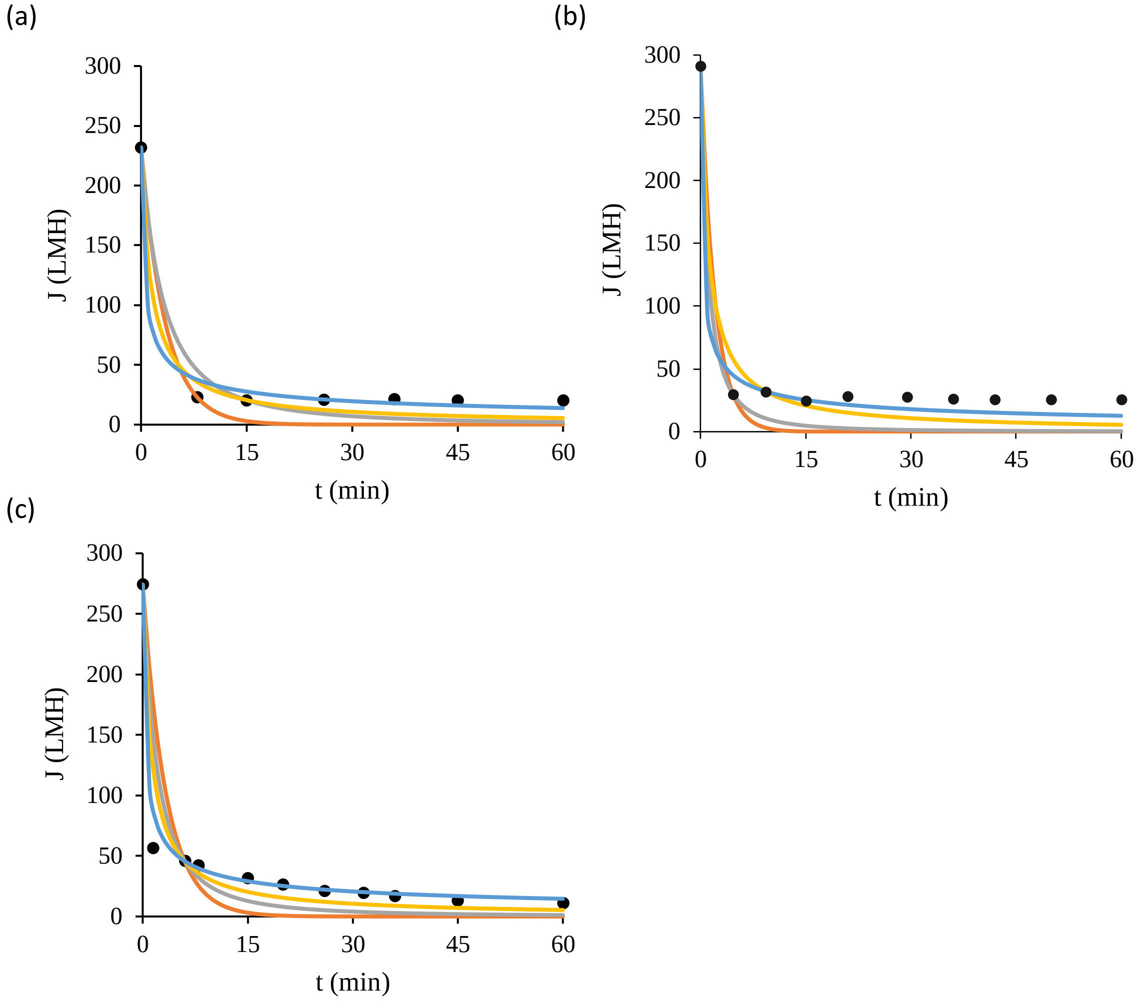

Figure A.4.9. Experimental data (●) and adjusted CPB (—), SPB (—), IPB (—) and CF (—) models for (a) BL, (b) DBL, and (c) WOBL.

Table A.4.5. Minimized sum of squares due to regression (SSR) for the adjusted models.

	SSR			
	CPB	PPB	IPB	CF
BL	178.53	142.65	102.26	52.35
DBL	212.47	193.79	135.80	77.30
WOBL	110.75	104.60	89.02	40.38

On viewing the results, CF is the main fouling mechanism in all cases. This mechanism was also reported by Wallberg et al. [5] as the main cause of flux reduction when filtrating Kraft BL with an Al_2O_3-TiO_2 ceramic membrane with a MWCO of 15kDa at 60ºC, 2 bar of TMP and 4.5 m/s of CFV. However, this behaviour was not observed by Wallberg et al. [12] when filtrating the BL at 70 and 90ºC under the same conditions, as no stationary flux rate was achieved. The lower proneness to CF when compared to our results can be explained by the differences in CFV, as a higher flow velocity reduces the deposition rate of foulants on the membrane surface [11,12]. This has also been reported to be the main cause of flux decline while operating with polymeric membranes, such as cellulose-based membranes [13]. CF is mostly reversible fouling [14], and therefore can be removed by physical cleaning, which is cheaper and less complex than chemical cleaning, and does not reduce the lifespan of the membrane [15].

3. Total cost estimation of PWO

The estimate of the total cost of PWO was performed based on the study of Chatzisymeon *et al*. [16]. The capital cost was determined according to a study estimate (factored estimate) considering the knowledge of major equipments, the accuracy of estimate being up to ± 30% [17].

In order to determine the cost of each piece of equipment, the Cost Estimator tool provided by Peters et al. [17] was used. This program calculates the estimated prices for 2002, therefore, it is necessary to update them. Besides, it is also necessary to correct these estimated prices based on construction materials and operating conditions. Additionally, the change from US dollars to euros was also considered. Thus, the equation used was the following [17]:

$$\mathrm{C_E} = \mathrm{C_B}\left(\frac{\mathrm{Q_E}}{\mathrm{Q_B}}\right)^{0.6} \mathrm{f_M f_P f_T}\left(\frac{\mathrm{I_{2021}}}{\mathrm{I_{2002}}}\right) ER \tag{A2}$$

Where: C_E is the cost of the equipment in 2021, C_B is the cost of the reference equipment in 2002, Q_E is the capacity of the equipment, Q_B is the capacity of the reference equipment obtained using Cost Estimator tool, f_M is the material factor, f_p is the pressure factor, f_T is the temperature factor, I_{2021} is the last Plant Cost Index (September 2021): 750.0 [18], I_{2002} is the last Plant Cost Index (September 2002): 390.4 [19], ER is the currency exchange rate from dollars to euros:0.89 €/$ [20].

The equipments required in the PWO process were a pump, a heat exchanger and a continuous oxidation reactor. It was taken as calculation basis of 1000 m^3/day (typical flow rate of design according to Chatzisymeon *et al.* [16]).

Regarding the cost of the pump, a centrifugal pump of stainless steel 316 (f_M =3.4) was selected because it is the most suitable for pumping liquids with suspended solids at alkaline pH. The temperature in the stream was 90ºC (f_T =1) and the pressure 70 bar (f_p =1.9). In the case of the heat exchanger, it was selected a shell and tube heat exchanger of stainless steel 316 (f_M =3.4) with an area of 2308 m^2. The maximum temperature allowed was 190ºC (f_T =1.6) since it is the temperature in the outlet stream of the reactor. Considering the oxidation reactor, it was selected a continuous stirred tank reactor of stainless steel 316 (f_M =3.4) with a volume of 104.3 m^3 (considering 120 min of reaction and oversized 10% for safety reasons). The maximum temperature allowed was 300ºC (f_T =1.6) and the maximum pressure 100 bar (f_p =1.9). Both temperature and pressure are higher than required (190ºC and 70 bar) for safety reasons. The cost of each of the equipments and total cost are shown in Table A.4.6.

Table A.4.6. Estimate of the cost of equipments required in the PWO process.

Equipment	**Cost (M €)**
Centrifugal pump	0.040
Shell and tube heat exchanger	0.211
Continuous stirred tank reactor	6.150
	Total: 6.401

3.1. Total capital investment

As it was previously indicated, the estimate of the total capital investment was calculated based on the typical percentages for a solid-fluid processing plant with respect to the total cost of the equipments [17]. It is determined as the sum of the fixed-capital investment (I_F), which is the capital needed to supply the necessary manufacturing and plant facilities, and the working capital (I_W), which is the capital needed to operate the plant. In Table A.4.7, it is shown the breakdown of the total capital investment.

Table A.4.7. Breakdown of the total capital investment.

Cost	**Percentage**	**Calculated cost (M €)**
Purchased equipment		6.401
Delivery of the equipment	0.10	0.640
Total Equipment		7.041
Purchased equipment installation	0.39	2.746
Instrumentation and control	0.26	1.831
Piping	0.31	2.183
Electrical systems	0.10	0.704
Buildings	0.29	2.042
Yard improvements	0.12	0.845
Service facilities	0.55	3.873
Total direct costs (I_D)		21.264
Engineering and supervision	0.32	2.253
Construction expenses	0.34	2.394
Legal expenses	0.04	0.282
Contractor’s fee	0.19	1.338
Contingency	0.37	2.605
Total indirect costs (I_I)		8.872
Fixed capital investment (I_F): $I_D + I_I$		30.136
Working capital (I_W)	0.75	5.281
Total capital investment		35.417

3.2. Total production costs

In order to determine total production costs, it was considered fixed production costs, variable production costs, plant costs and general costs. The results are shown in Table A.4.8.

Fixed production costs were calculated taken into account: i) property rates (2% of I_F) and ii) the insurance (1% of I_F). It is assumed that neither rent nor interests/loans will be paid [17].

Variable production costs considered the costs of raw materials, labour, auxiliary services, and other concepts such as maintenance and repairs, operating supplies, laboratory charges and royalties among others. In this sense, it should be taken into account that black liquor was the only raw material, since cooling water and oxygen was considered auxiliary services.

Table A.4.8. Total production costs.

Cost	Percentage	Calculated cost (M €/year)
Property rates	$0.02 \cdot I_F$	0.603
Insurance	$0.01 \cdot I_F$	0.301
Fixed production costs		0.904
Labour and supervision		0.085
Auxiliary services		1.486
Maintenance and repairs	$0.06 \cdot I_F$	1.808
Operating supplies	$0.15 \cdot I_M$	0.271
Laboratory	$0.15 \cdot I_L$	0.011
Royalties		0.074
Plant	$0.6 \cdot (I_M + I_L + I_s)$	1.136
General		0.751
Total		7.430

Regarding labour costs (I_L), it was estimated that 1 worker per shift (considering 3 shifts per day) was needed based on typical labour requirements per team and shift [21]. Besides, it was considered that the salary of the operators was 20000 €/year plus the social security tax (23.6%). Additionally, 15% more will be added in concept of operation supervision (I_s) [17].

It is also necessary to determine the cost of the auxiliary services (cooling water, oxygen, and electricity, among others). In the case, it is estimated that it represents between 10% and 20% of the total productions costs (without depreciation) and the highest possible value was taken as a reference [17].

In terms of maintenance and repair costs (I_M), it is necessary to consider 6% of the fixed capital investment. Besides, operating supplies were also included, the cost being 15% of I_M.

On the other hand, laboratory charges are taken as 15% of labour costs and 1% of the total production costs (without depreciation) are included as royalties.

Considering plant costs, it was estimated that these costs represent 60% of the sum of labour and supervision costs and maintenance and repair costs.

Regarding general costs, it was considered administration costs (20% of the sum of labour and supervision costs and maintenance and repair costs) and distribution and sale costs (5% of the total cost of production without depreciation).

Finally, the total cost of PWO process, which consists of the total capital investment and total production costs, is calculated according to the following Eq. A3 [17]:

$$\text{Total cost} = \frac{(\text{I} \cdot \text{CRF}) + \text{PC}}{\text{Q}} \qquad \text{(A3)}$$

Where: I is the total capital investment, CRF is the capital recovery factor, Q is the average capacity and PC is the total production costs.

The value of the average capacity is 330 000 m^3/year. It was determined considering the basis of calculation (1000 m^3/day) and 330 days of operation.

CRF is calculated by the Eq. A4:

$$CRF = \frac{r\,(1+r)^N}{(1+r)^N - 1} \qquad \text{(A4)}$$

Where: r is the rate of interest in percentage and the N is the useful life in years.

According to [16], it was considered that the value of r and N were 6% and 15 years, respectively. Thus, the value of CRF was 6.

Therefore, the total cost is 667.4 €/m^3.

References

[1] O.Y. Abdelaziz, K. Ravi, M. Nöbel, P. Tunå, C. Turner, C.P. Hulteberg, Membrane filtration of alkali-depolymerised kraft lignin for biological conversion, Bioresour. Technol. Reports. 7 (2019) 100250. doi:10.1016/j.biteb.2019.100250.

[2] A. Bokhary, A. Tikka, M. Leitch, B. Liao, Membrane fouling prevention and control strategies in pulp and paper industry applications: A review, J. Membr. Sci. Res. 4 (2018) 181–197. doi:10.22079/JMSR.2018.83337.1185.

[3] X. Ren, Evaluation of Membrane Filtration for Treatment of Black Liquor in Small-Scale Pulp and Paper Mills in India, Massachusetts Institute of Technology, 2016.

[4] A. Arkell, J. Olsson, O. Wallberg, Process performance in lignin separation from softwood black liquor by membrane filtration, Chem. Eng. Res. Des. 92 (2014) 1792–1800. doi:10.1016/j.cherd.2013.12.018.

[5] O. Wallberg, A.S. Jönsson, R. Wimmerstedt, Ultrafiltration of kraft black liquor with a ceramic membrane, Desalination. 156 (2003) 145–153. doi:10.1016/S0011-9164(03)00337-0.

[6] E. Koivula, M. Kallioinen, T. Sainio, E. Antón, S. Luque, M. Mänttäri, Enhanced membrane filtration of wood hydrolysates for hemicelluloses recovery by pretreatment with polymeric adsorbents, Bioresour. Technol. 143 (2013) 275–281. doi:10.1016/j.biortech.2013.05.129.

[7] Y. Gao, J. Qin, Z. Wang, S.W. Østerhus, Backpulsing technology applied in MF and UF processes for membrane fouling mitigation: A review, J. Memb. Sci. 587 (2019) 117136. doi:10.1016/J.MEMSCI.2019.05.060.

[8] T.A. Saleh, V.K. Gupta, Membrane Fouling and Strategies for Cleaning and Fouling Control, Nanomater. Polym. Membr. (2016) 25–53. doi:10.1016/B978-0-12-804703-3.00002-4.

[9] J. Hermia, Constant Pressure Blocking Filtration Laws - Application Topower-Law Non-Newtonian Fluids., Trans Inst Chem Eng. V 60 (1982) 183–187.

[10] M. Abbasi, R.S. Mohammad, A. Salahi, B. Mirza, Modeling of membrane fouling and flux decline in microfiltration of oily wastewater using ceramic membranes, Chem. Eng. Commun. 199 (2012) 78–93. doi:10.1080/00986445.2011.570391.

[11] J. de Bruijn, R. Bórquez, Analysis of the fouling mechanisms during cross-flow ultrafiltration of apple juice, LWT - Food Sci. Technol. 39 (2006) 861–871. doi:10.1016/j.lwt.2005.06.014.

[12] H. Choi, K. Zhang, D.D. Dionysiou, D.B. Oerther, G.A. Sorial, Influence of cross-flow velocity on membrane performance during filtration of biological suspension, J. Memb. Sci. 248 (2005) 189–199. doi:10.1016/j.memsci.2004.08.027.

[13] S. V. Satyanarayana, P.K. Bhattacharya, S. De, Flux decline during ultrafiltration of kraft black liquor using different flow modules: A comparative study, Sep. Purif. Technol. 20 (2000) 155–

167. doi:10.1016/S1383-5866(00)00086-1.

[14] G. Di Bella, D. Di Trapani, A brief review on the resistance-in-series model in membrane bioreactors (MBRs), Membranes (Basel). 9 (2019) 24. doi:10.3390/membranes9020024.

[15] S.M.K. Sadr, D.P. Saroj, Membrane technologies for municipal wastewater treatment, in: Adv. Membr. Technol. Water Treat. Mater. Process. Appl., 2015. doi:10.1016/B978-1-78242-121-4.00014-9.

[16] E. Chatzisymeon, P. Gikas, D. Mantzavinos, Economic aspects of advanced oxidation processes for olive mill wastewater treatment, in: Prot. Restor. Environ. X, Kerkyra, 2010.

[17] M.S. Peters, K.D. Timmerhaus, R.E. West, Plant Design and Economics for Chemical Engineers, 5th Ed., McGraw-Hill Education, Nueva York, 2003.

[18] CEPCI: Chemical Engineering Plant Cost Index, 2021, Chem. Eng. 132 (2021) 64.

[19] CEPCI: Chemical Engineering Plant Cost Index, 2002, Chem. Eng. 109 (2002) 62.

[20] Netnotion LTDA © 2017, Currency exchange rate from (USD) to Euro (EUR), (n.d.). https://www.currency-calc.com/es/ (accessed November 27, 2021).

[21] G.D. Ulrich, A Guide to Chemical Engineering Process Design and Economics, John Wiley Sons. (1984) 484.

4.2.2. Effect of landfill leachate ageing on ultrafiltration performance and membrane fouling behaviour

Sergio Collado, Daniel Núñez, Paula Oulego, Francisco A. Riera, Mario Díaz*

Department of Chemical and Environmental Engineering, University of Oviedo.

c/ Julián Clavería 8, 33006, Oviedo, Spain

*Corresponding author’s e-mail: mariodiaz@uniovi.es

Phone: +34 985 10 34 39, FAX: +34 985 10 34 40

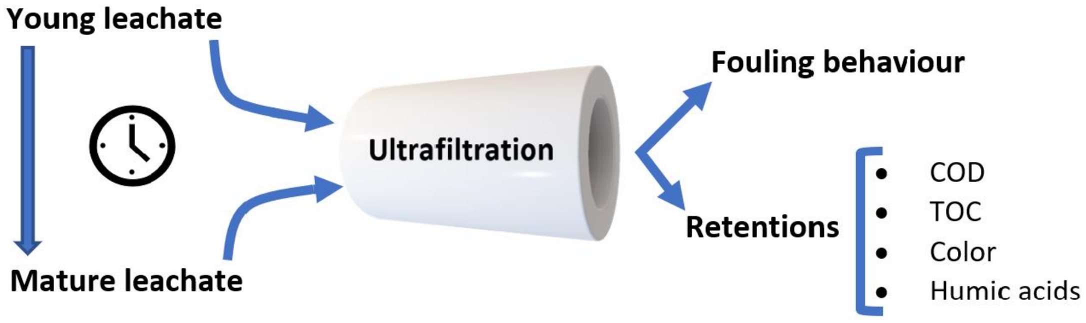

Figura 4.42. Resumen gráfico del artículo *Effect of landfill leachate ageing on ultrafiltration performance and membrane fouling behaviour*.

Artículo publicado en la revista **Journal of Water Process Engineering**

Cuartil: Q1 **Índice de impacto:** 5.485

Referencia: Sergio Collado, Daniel Núñez, Paula Oulego, Francisco A. Riera, Mario Díaz, Effect of landfill leachate ageing on ultrafiltration performance and membrane fouling behaviour, Journal of Water Process Engineering, Volume 36, 2020, 101291.

Abstract

In this study, the effect of ageing on the performance and fouling mechanisms in the ultrafiltration of landfill leachates using titania-zirconia (ZrO_2-TiO_2) tubular membrane was thoroughly studied. Results revealed that the maturation of the leachate has a positive effect on its ultrafiltration, with a twofold higher final permeability compared with the young one. This is the result of the higher organic load, particularly that corresponding to proteins and carbohydrates, of the young leachate.

Resistance-in-series analysis demonstrated that the loss of permeability was mainly due to reversible fouling, caused by cake filtration. Either irrecoverable or irreversible fouling were scarce and not conditioned by the stage of maturation of the leachate. Chemical oxygen demand (COD) rejection for the mature leachate varied with volume concentration ratio (VCR) showing an approximately sigmoidal shape, from an initial value of 18.5% to a final one of 49.6%, with the faster increase at VCR ranging from 1.2 to 1.7, due to the permeation of fatty acids by the ultrafiltration (UF) membrane. On the other hand, COD rejection remained approximately constant at 48% during the ultrafiltration of the young leachate, which can be attributed to the presence of higher molecular weight compounds in its composition.

Keywords: Landfill leachate; Wastewater management; Ageing; Ultrafiltration; Fouling modelling.

1. Introduction

The increasing solid waste landfilling has led to one of the major environmental challenges of today: the efficient management of the leachates generated. These aqueous wastes, which can be defined as the liquid that passes through a landfill and has extracted dissolved and suspended matter from it, are considered a significant threat to surface water, groundwater and soil [1]. Many factors have been reported that influence leachate composition, such as the age of the landfill, the local climate or season, the depth of the waste in the landfill and, mainly, the composition of the waste material [2–4]. This fact makes leachate matrices significantly complex and variable [5], which in turns means that the improvement and/ or development of a generalized treatment method for any leachate to meet the relevant quality standards is not possible [6]. In fact, leachate treatments are based on process schemes which generally comprise some combination of biological, physical and/or chemical treatment [7–10]. Biological treatments are used for removing the biodegradable organic matter content in the leachate; while chemical and physical treatments such as flotation, coagulation-flocculation, precipitation, adsorption or air stripping are employed as pre-treatments in order to improve the efficiency of a subsequent treatment, or when a biological oxidation process is hampered by the presence of bio-refractory materials, like non-biodegradable (humic and fulvic acids) and/or undesirable compounds (heavy metals, AOXs, PCBs…). Besides, these treatments can also be employed as post-treatments after a biological one with the aim of ensuring final polishing level by removing toxic metals and organic compounds [6,10]. Advanced oxidation processes (AOPs), such as ozonation (alone or in combination with UV) and UV/TiO_2 photocatalysis, which are a particular case of chemical treatment, can also be used as post-treatments after biodegradation processes for removing recalcitrant compounds [6]. In addition to the conventional treatments, physical treatments based on membrane technology have emerged as viable alternatives to reach the level of purification needed to fully reduce the negative impact of landfill leachates on the environment. Either as a main step in a landfill leachate treatment chain or as a single treatment step, the use of membrane technologies has shown to be an indispensable means of achieving a high degree of purification of this stream [10]. Among the various membrane technologies, ultrafiltration (UF) is used in separation and purification because of its high efficiency and lower energy consumption, thus reducing treatment costs [11].

UF is effective in eliminating macromolecules and particles; around 50% of organic matter can be separated from the leachate [12,13]. Although a study reported UF as a sufficient treatment to ensure the discharge standards for a leachate [13], this technique is not individually used, but in combination with others. Thus, UF can serve as a pre-treatment prior to reverse osmosis [14–17], nanofiltration [15], evaporation [18] or Fenton oxidation [19]; and as a post-treatment for biologically active carbon [20], adsorption [12,15,21], coagulation [15], lime addition [22], nanofiltration (for the concentrate generated) [23], air stripping and coagulation [24] or Fenton reaction and neutralization [25]. Particularly, this technique can also be effective as a pre-treatment for biological degradation of landfill leachate, since it helps reducing the content in humic acids, which can compromise the efficiency of the biological treatment.

At this point, it should be noted that, to the best of our knowledge, the effect of the landfill leachate age on the membrane performance has not been studied yet. This is surprising because, although there are many factors affecting the composition of such leachates, this varies greatly depending on the age of the landfill and, thus, the degree of solid waste stabilization [26]. In fact, two types of leachates have been defined according to landfill age: young and mature. Young leachates are those which come from landfills less than 1 year old, with chemical oxygen demand (COD) values above 15 g/L and the ratio between the biodegradable matter (as biological oxygen demand (BOD_{5})) and the total organic one (as COD) higher than 0.5. On the other hand, mature leachates are those from facilities which are more than 5 years old (maturation phase) with COD values below 3 g/L and mainly composed of a refractory mixture of humic substances. Their BOD_5 to COD ratio is lower than 0.1 [7,10].

It should be noted that the results of ultrafiltration reported in the bibliography for leachates, either for the individual operation or coupled with other processes, are highly subjected to the age of the specific leachate selected for each experimentation, thus making the comparison between the findings of the different studies difficult.

In view of these considerations, the aim of this work was to study, for the first time ever, the effect of the landfill leachate age on the quality of the effluent treated by UF as a pre-treatment prior to a biological process, as well as modelling the fouling mechanism of the membrane.

2. Experimental

2.1. Landfill leachates

All the leachates used in this study were obtained from the sanitary landfill site La Zoreda and provided by COGERSA (Asturias, Spain). Two different leachates were employed during the experimentation: mature (M) and young (Y). The young leachate was obtained from a new area of the landfill which is in expansion. Regarding the mature leachate, it comes from an area of the landfill where wastes has not been deposited since 2010.

A description of the main physicochemical characteristics of the different leachates can be found in Table 4.38. Higher colour value in young leachate has already been reported [27] and can be explained by higher total organic carbon (TOC) and suspended solid concentrations. Leachates were pre-filtered with a metal mesh filter of 250 µm of pore size and 200 mm of diameter (Cisa, Spain) to remove coarse particles. Samples were stored at 5ºC before being used.

Table 4.38. Main characteristics of the mature and young leachates (average values from 2008 to 2018) and values determined in this study (in brackets).

Parameter	**Type of landfill leachate**	
	Old leachate	**Young leachate**
pH	8.2 ± 0.4 [7.8]	8.8 ± 0.2 [8.7]
COD (mg O_2/L)	4005 ± 592 [3960]	7559 ± 2414 [5548]
TOC (mg/L)	n/a [641]	n/a [1784]
Humic acid (mg/L)	n/a [137]	n/a [90]
BOD_5 (mg O_2/L)	559 ± 280 [372]	2435 ± 974 [3077]
Colour Number	n/a [1.322]	n/a [1.573]
Suspended solids (mg/L)	29 ± 24 [30]	92 ± 65 [100]
NH_4^+ (mg/L)	2200 ± 368 [2323]	2959 ± 427 [3247]
Cl^- (mg/L)	n/a(1)	3329 ± 1182 [3136]
NO_3^- (mg/L)	5 ± 1 [4]	3 ± 2 [2]
NO_2^- (mg/L)	1.0 ± 0.5 [1]	2 ± 1 [2]
Alkalinity (mg $CaCO_3$/L)	212 ± 28 [221]	258 ± 36 [281]
Conductivity (μS/cm)	21089 ± 4557 [23800]	25737 ± 3323 [19990]

(1) n/a= not available

2.2. Experimental setup

A scheme of the experimental set up is shown in Fig. 4.43. All the ultrafiltration experiments were conducted using a locally house made and assembled system. This system consisted of a glass vessel of 3 L, where the corresponding leachate was stored and pumped towards the ultrafiltration module using a Masterflex I/P 7591-55 (Cole-Parmer, USA) peristaltic pump attached to an Easyload Masterflex I/P 77601-10 (Cole-Parmer, USA) pump head. Ultrafiltration cell was composed by a tubular ZrO_2-TiO_2 membrane (600 × 6mm) (TAMI Industries) with an area of 1.14 10^{-2} m^2 and a molecular weight cut-off (MWCO) of 150 kDa. Ceramic membranes are more resistant to mechanical, chemical, thermal or biological stresses than polymeric membranes, and they have been already implemented for wastewater treatment [28]. Also, the use of ZrO_2-TiO_2 in form of particles [29] or membrane additives [30] has been reported to be efficient in reducing the fouling caused by humic acid. As for pore size, membrane MWCO was selected in order to minimize humic acid-caused fouling. In this sense, Yan et al. [31] have reported that, when ultrafiltering humic acids, maximum fluxes can be obtained using membranes within a MWCO range between 100 and 300 kDa. Pressure gauges and valves were placed in the flow line before and after the ultrafiltration module in order to measure and set the value of the transmembrane pressure (TMP). All experiments were carried out at a flow rate of 5.4 L/min and cross flow velocity of 3.2 m/s over the membrane. In order to select the temperature of work, a previous study of ultrafiltration performance at temperatures from 50ºC to 70ºC was performed. Lower fouling rates and higher fluxes were obtained when higher temperatures were used, thus all experiments were carried out at a steady temperature of 70ºC. The permeate flux was determined by weighing of permeate under a TMP of 1.6 bar. Temperature was kept at the desired value using a water bath.

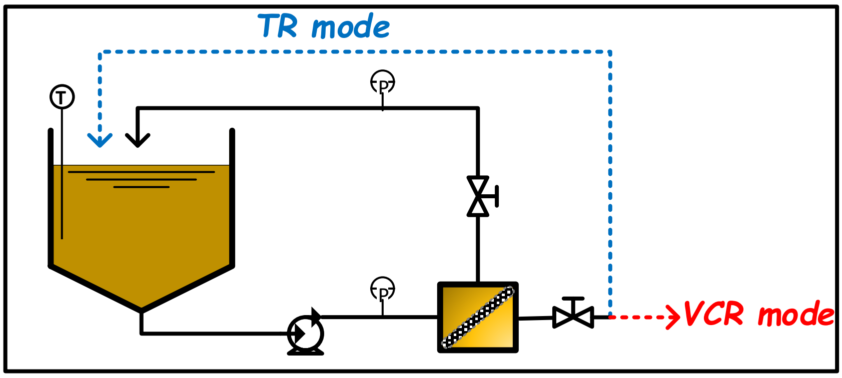

Figure 4.43. Experimental setup scheme.

Two different kinds of experiments were carried out using this experimental setup (see Fig. 4.43): i) Total recycle (TR) mode and ii) volume concentration ratio (VCR) mode. The first one is necessary in order to determine the evolution of membrane fouling with time, while the second one is needed to evaluate the effect of concentration on the permeate flux and fouling resistances.

Regarding TR mode experiment, retentate and permeate were both completely recirculated to the supply tank and permeate flux was periodically measured until achieving a constant value. Afterwards, membrane was washed with distilled water until the permeate flux did not change with time, and then cleaned at 70ºC with 0.5% aqueous solution of basic detergent (Divos 124 VM5 provided by Diversey) until the final flux was higher than 90% of the initial permeate flux [32].

In the case of the VCR mode experiment, retentate was also continuously recirculated to the supply tank, but permeate was discarded. Samples of permeate were periodically withdrawn to measure COD, TOC, colour number (CN) and humic acid retentions, as well as permeate fluxes. Leachate filtration was maintained up to a final VCR of 3. Afterwards, the UF membrane was washed and cleaned in the same way than that used in the TR mode test.

Both TR and VCR mode experiments were performed at least in duplicate, and in all cases the experimental error was below 5%.

2.3. Fouling modelling

In order to define the fouling during the ultrafiltration of both leachates in terms of permeability recovery, the next equation was employed (Eq. 1):

$$J = \frac{TMP}{\mu R_T} = \frac{TMP}{\mu(R_M + R_{rev.} + R_{irrev.} + R_{irrecov})} \tag{1}$$

Where J is the permeate flux (m·s^{-1}), TMP is the transmembrane pressure (kg·m^{-1}·s^{-2}) μ is the dynamic viscosity (kg·m·s^{-1}), R_T is the total fouling resistance, R_M is the intrinsic membrane resistance and $R_{rev.}$, $R_{irrev.}$ and $R_{irrecov.}$ are the reversible, irreversible and irrecoverable fouling resistances, respectively (all resistances in m^{-1}). In a practical way, reversible fouling is removed by physical cleaning, irreversible fouling is eliminated by chemical cleaning and irrecoverable fouling refers to those foulants that cannot be removed by any cleaning step [33]. By measuring the initial tap water flux through the membrane (J_0), and the permeate fluxes achieved at the end of the ultrafiltration (J_S) and after the physical (rinsing with distilled water) (J_{pc}) and chemical (J_{cc}) cleanings, the values of each resistance can be calculated according to the methodology included in the Appendix [34].

In addition to this resistance-in-series model based on permeability recovery, fouling evolution was also modelled by the Hermia's model [35] with the aim of obtaining an in-depth knowledge of the fouling mechanisms involved (Eq. 2).

$$\frac{dJ}{dt} = -K \cdot (J - J_0) \cdot J^{2-n} \tag{2}$$

Where K is a constant, J_0 is the limiting flux (m·s^{-1}), and *n* is a constant with different values for the four simple mechanisms of fouling proposed by Hermia: complete blocking (n=2, K in min^{-1}), standard blocking (n=1.5, K in m^{-1}) intermediate pore blocking (n=1, K in m^{-1}) and cake filtration (n=0, K in min·m^{-2}) [36]. The choice of the best model was based on the sum of squared residuals (SSR), where each residual was equal to the difference between the experimental data and the value predicted by the model.

2.4. Analytical methods

Humic acids were extracted from leachate according to the method proposed by Thurman and Malcolm [37]. Stated briefly, 10 mL of the corresponding sample were acidified with HCl 1 mol/L to pH 1.0, in order to precipitate the humic acids. Then, the sample was filtrated, and the solid fraction was redissolved in a 7 g/L NaOH solution until the initial volume is reached. Absorbance values at 465 nm and 665 nm were measured using a Helios Alpha UV-Vis spectrophotometer (Thermo Fisher Scientific, USA). A calibration curve was constructed by dissolving different amounts of commercial humic acid (Sigma Aldrich) in a 7 g/L NaOH solution. COD was obtained by the dichromate method using a HACH DR/2500 spectrophotometer (Hach Company, USA) [38]. TOC was determined using a TOC analyzer (Shimadzu TOC-V$_{\mathrm{CSH}}$). The CN, which is defined in Eq. 3 [39], was used to monitor changes in the colour of the leachate during the ultrafiltration process. Spectral absorbance coefficients (SAC) are defined as the ratio of the values of the respective absorbance over the cell thickness. Both CN and SAC have units of cm^{-1}. This parameter was measured at 436, 525 and 620 nm using a UV/Vis spectrophotometer (Thermo Scientific, Heλios γ).

$$CN = \frac{SAC_{436}^2 + SAC_{525}^2 + SAC_{620}^2}{SAC_{436} + SAC_{525} + SAC_{620}} \tag{3}$$

Rejection coefficients were defined as follow (Eq. 4):

$$R_i = 1 - \frac{C_{P,i}}{C_{R,i}} \qquad (4)$$

Where $C_{P,i}$ and $C_{R,i}$ the concentration of the analyte *i* in permeate and retentate, respectively.

3. Results and discussion

3.1. Total Recycle mode

Fig. 4.44 shows the evolution of the permeate flux with time during the ultrafiltration of the mature leachate (4.45a) or the young one (4.45b) in a TR mode. The initial water permeability of the membrane was 211.5 L/m^2 h bar. Once the filtration of the leachate started, this permeability decreased rapidly for both assayed leachates, finally reaching constant values of around 37.5 and 17.6 L/m^2 h bar for the mature and the young leachate, respectively, after less than 15 min of filtration. These results correspond to reductions in permeability at the end of the experiment of 82.3 and 91.7%. According to several authors, these drastic flux declines, observed during the first minutes of filtration, may be due to the fast accumulation on the membrane surface of a first layer of fouling, which is thin but very resistant to mass transfer due to its low porosity. After that, the structure of the newly formed layers is less compact, indicating the existence of a porosity gradient through the cake thickness [34,40].

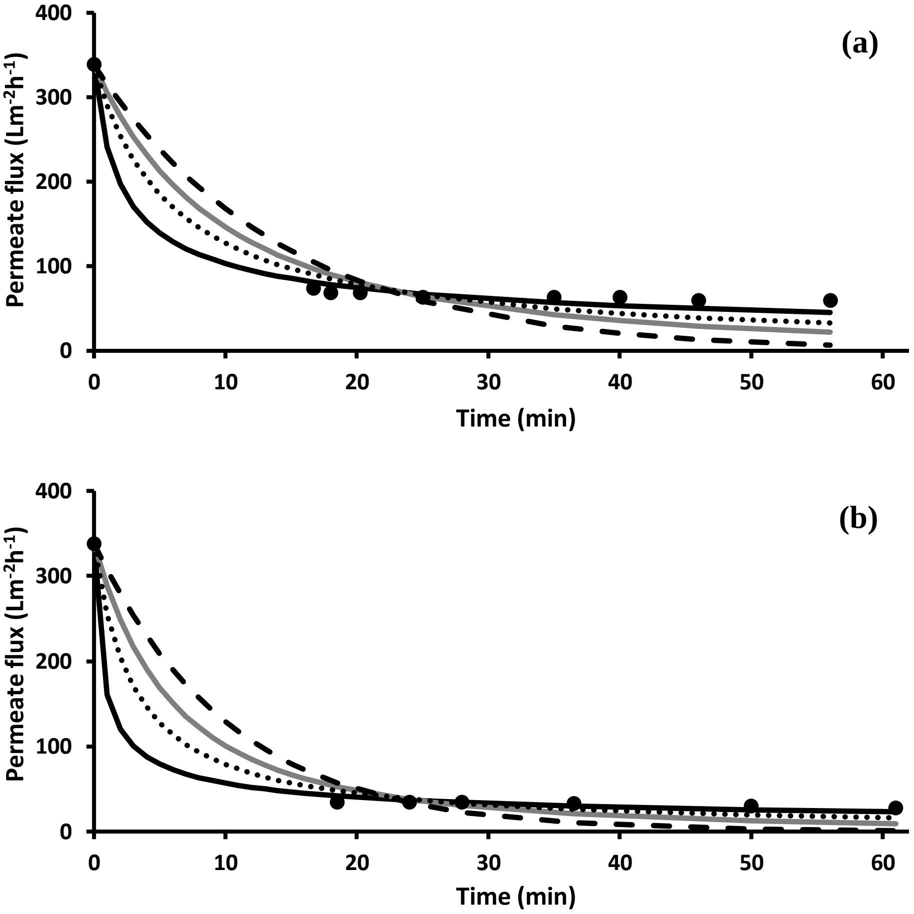

Figure 4.44. Evolution of the permeate flux (●) during the ultrafiltration of the mature (a) or young (b) leachate under TR mode. Cake model (solid black line), standard model (solid grey line), complete model (dashed black line) and intermediate model (dotted line) predictions for each of them. In all cases: 1.6 bar, 70 ºC, flow rate of 5.4 L/min and cross flow velocity of 3.2 m/s.

Therefore, the maturation of the leachate has a positive effect on its ultrafiltration, with a twofold higher final permeability than that obtained with a young leachate. As it was previously explained, the ageing of the leachate involves a reduction in either its COD or BOD_5/COD ratio. This fact, together with the higher concentration of proteins and carbohydrates in the young leachate explain why the old leachate are more easily ultra-filtered than the young one [41,42].

Fig. 4.45 shows the fouling resistances obtained for either the mature or young leachate under TR mode ultrafiltration.

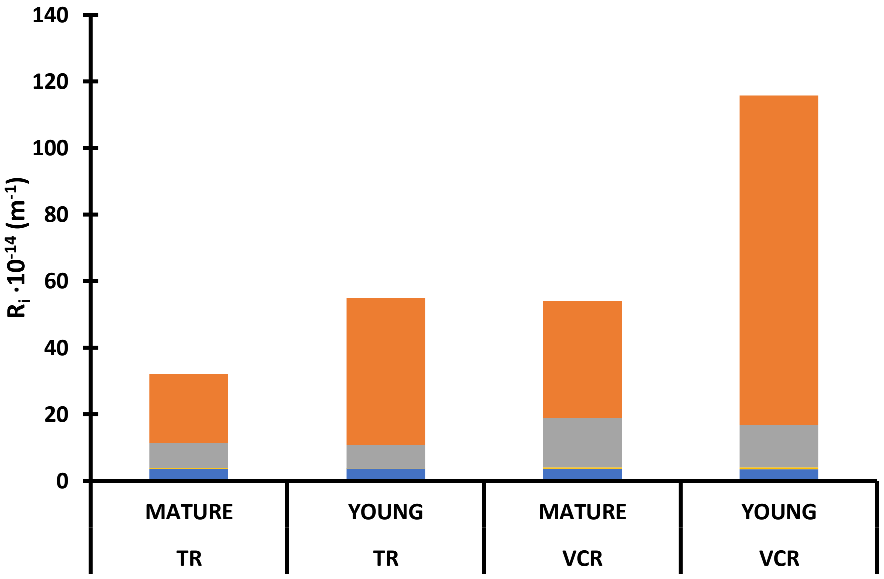

Figure 4.45. Fouling resistances obtained during the ultrafiltration of the mature (a) or young (b) leachate under TR or VCR mode: R_M (🟦), $R_{rev.}$ (🟧), $R_{irrev.}$(■) and $R_{irrecov}$ (🟨). In all cases: 1.6 bar, 70 ºC, flow rate of 5.4 L/min and cross flow velocity of 3.2 m/s.

As expected from the permeability data previously commented, total resistance (R_T) for the young leachate ($4.4 \cdot 10^{15}\ m^{-1}$) is higher than that obtained for the mature one ($2.1 \cdot 10^{15}\ m^{-1}$). Nevertheless, these results also revealed that the flux decline due to irreversible fouling is significantly lower than that caused by the reversible one. Thus, calculating the $^{R_{rev.}}/_{R_{irrev}}$ ratio for both leachates, the values obtained are 2.8 and 6.3 for the mature and young one, respectively. In this regard, it is also interesting to point out that the resistances due to irreversible fouling for both experiments are somewhat similar, indicating that the internal fouling is scarce and not conditioned by the stage of maturation of the leachate. Considering that reversible fouling is widely associated with the cake layer resistance (also known as external fouling), whereas the irreversible one has to do with pore fouling resistance (or internal fouling), results show that the main reason for the permeability decrease during the ultrafiltration of leachates is the external fouling, this being higher for younger leachates. This fact also implies that the initial membrane permeability can be easily recoverable in a high proportion after leachate ultrafiltration by means of membrane relaxation, backflushing or other physical cleaning techniques (standard rising) [43]. In addition, leachate age had a negligible effect on both the irreversible and irrecoverable fouling. Finally, low values of $R_{irrecov.}$ indicated that more than 99.5% of the initial permeability was recovered after cleaning, thus suggesting a long lifespan of the membrane in plant operation, either for mature or young leachates, although a higher number of physical cleaning cycles would be required during the ultrafiltration of the latter. If the filtration sequence (filtration followed by physical cleaning) does not result in complete recovery of membrane fouling status, a chemical cleaning phase is needed, which should be optimized in order to maximize as much as possible the cost-efficiency of the operation.

Fig. 4.44 shows the results of permeate flux and their fittings to the four simple mechanisms of fouling proposed by Hermia. Additionally, Table 4.39 provides the values of the main fitting parameters for each model as well as goodness of fit of the data to the curve.

Table 4.39. Main fouling mechanisms: brief description, fitted parameters and SRR obtained using the experimental data for ultrafiltration of mature and young leachates under TR or VCR modes.

Blocking			**Complete (C)**	**Standard (S)**	**Intermediate (I)**	**Cake (G)**
Figure					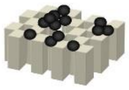	
Description			Particles seal off pore entrances	Particles accumulate inside membrane on the walls of straight cylindrical pores	A portion of the particles seal off pores and the rest accumulate on the top of other deposited particles	Particles accumulate on the membrane surface
Mode	**Leachate***	**n**	**2**	**1.5**	**1**	**0**
TR	**ML**	**K_i**	$(7.0\pm0.6)10^{-2}$	$(2.8\pm0.3)10^{-3}$	$(4.9\pm0.8)10^{-4}$	$(8\pm2)10^{-6}$
		r^2	0.93	0.97	0.98	0.995
		SRR	660	4726	9947	2333
	YL	**K_i**	$(9.6\pm0.9)10^{-2}$	$(4.5\pm0.6)10^{-3}$	$(9.7\pm0.1)10^{-4}$	$(3\pm1)10^{-5}$
		r^2	0.97	0.990	0.995	0.9991
		SRR	2188	850	329	59
VCR	**ML**	**K_i**	$(5.2\pm0.8)10^{-2}$	$(2.1\pm0.4)10^{-3}$	$(3.8\pm0.9)10^{-4}$	$(9\pm3)10^{-6}$
		r^2	0.92	0.95	0.97	0.990
		SRR	9461	6231	3484	1230
	YL	**K_i**	$(1.2\pm0.2)10^{-1}$	$(4.7\pm0.8)10^{-3}$	$(8\pm2)10^{-4}$	$(2.2\pm0.7)10^{-5}$
		r^2	0.94	0.95	0.97	0.995
		SRR	7004	5113	2587	372
Units for K_i:			*1/min*	*1/m*	*1/m*	*min/m^2*

*ML: mature leachate; YL: young leachate

Based on the results obtained, the prevailing fouling model during the ultrafiltration of leachate under TR mode corresponds to cake formation, indicating that the accumulation of leachate particles occurred on the surface of the membrane in a permeable cake of increasing thickness until a limit value is reached. According to this mechanism, the evolution of the permeate fluxes showed in Fig. 4.44 could be explained as follows: the first phase of flux decline observed during the first few seconds or minutes of operation is primarily due to concentration polarization. The second phase of flux decline is slower and is attributed to the formation of a complete surface layer over the initial monolayer. The third phase represents a quasi-steady-state period, wherein the flux decline occurs slowly, and may be due to the consolidation of the fouling layer due to a balance between the deposition of foulants on the cake and their removal due to the shear stress caused by the cross flow [20]. The final achievement of a final cake with an almost constant thickness is consistent with the prevalence of an external fouling observed from the analysis of the resistance-in-series mode. Ma et al. [44] also found that cake filtration was the main fouling mechanism involved during the ultrafiltration of humic acid with and without addition of inorganic salts. Syzdek and Ahlert [14] reported some results during the ultrafiltration of a high-strength industrial landfill leachate which suggested the predominance of cake formation as main fouling mechanism as well. For example, the fouling layer did not block the passage of organic carbon across the membrane, but only created a pressure drop that resulted in a lower flux. The occurrence of this fouling mechanism poses operational implications. When working with a non-foulant stream, a linear relationship between applied TMP and flux is assumed. Nonetheless, if fouling particles present in the stream are larger than the membrane pore size, a fouling cake will eventually deposit on the membrane surface. This phenomenon occurs more drastically when higher pressures are applied, compressing the fouling cake and minimizing membrane flux [45]. It has been reported that, in these cases, Reynolds number happens to be more relevant for flux improving that applied pressure [46], making it possible to minimize the fouling layer by increasing the shear at the membrane surface.

Several authors reported that fouling of the majority of membrane processes applied to leachate treatment was mainly due to the presence of humic substances in the leachate organic fraction [22,47]. If the formation of an external fouling layer, as suggested by previous fouling models, is assumed, then it is also reasonable to suppose that humic acids are mainly retained on the membrane surface. It should be highlighted that interactions between humic acids (as well as other natural organic matter) and the membrane are of hydrophobic nature [48], and thus a high ionic strength of the stream fosters membrane fouling caused by humic acid [31].

As the concentrations of humic acids were quite similar in both leachates because the biodegradability of these compounds is almost null, the lower permeability of the young leachate should be associated with the species which are biologically degraded during its maturation. Considering that the fouling associated with humic substances is approximately the same, the leachates which are degraded during the landfill maturation are responsible for the 75% (calculation based on K_i) of the fouling observed during the ultrafiltration of the leachate in TR mode.

3.2. Volume Concentration Ratio mode

In order to gather information about the influence of solute concentration on the permeability and membrane rejection during the ultrafiltration of either the young or mature leachates, a set of experiments without permeate recirculation to the feed tank were also carried out. It is worth noting here that, whereas the TR mode simulates a continuous filtration, the aim of these experiments, named as VCR mode, is to study the batch filtration and decide the most convenient solute concentration in a continuous filtration.

Figure 4.46 shows the evolution with time of the permeate flux during the VCR mode ultrafiltration of a mature (a) or a young leachate (b). As in the case of TR, the decline in the permeate flux for the young leachate was stronger than that obtained for the mature one. Again, the reduction in the permeability mainly occurred during the first minutes of filtration. Nevertheless, the permeability losses were more noticeable for the VCR mode filtration than for the TR mode operations, as expected due to the gradual increase in the concentration of the feed. So, the final permeate fluxes for VCR mode experiments with mature or young leachates were a 41 and 55% lower than those obtained during the ultrafiltration in TR mode.

These results indicate that the fouling resistance, $(R_T - R_M)$, during the batch ultrafiltration (VCR mode) is approximately twofold higher than that of the continuous one (TR mode) under the same time of filtration (60 min). More specifically, the fouling resistances obtained during TR and VCR mode experiments were $2.8 \cdot 10^{15}$ and $5.0 \cdot 10^{15}$ m^{-1} for the mature leachate and $5.1 \cdot 10^{15}$ and $11.2 \cdot 10^{15}$ m^{-1} for the young one, respectively. Using the resistance-in-series model (see Fig. 4.45), it can be deduced that the main contribution to this resistance is due to reversible fouling, which represented 70% and 88% of the total fouling for the mature and young leachates, respectively. These percentages were pretty similar to those obtained under TR mode. Nevertheless, the irreversible fouling during the batch ultrafiltration increased substantially in comparison to the continuous one, although no significant differences were found between young and mature leachates (Fig. 4.45). Regarding the irrecoverable fouling, its contribution to the total fouling was negligible for both leachates.

Using again the individual fouling models proposed by Hermia [35] (Fig. 4.46 and Table 4.39), the loss of permeability during the batch ultrafiltration of either the mature or young leachate was mainly attributed to the cake formation mechanism, as with the continuous one. The predominance of this fouling model is consistent with the high proportion of reversible fouling [49].

Fig. 4.47 shows the evolution of the rejection coefficients for COD (R_{COD}), TOC (R_{TOC}), colour (R_{CN}) and humic acids (R_{HA}) as well as the permeate flux with the VCR mode during the ultrafiltration of either a mature or young leachate.

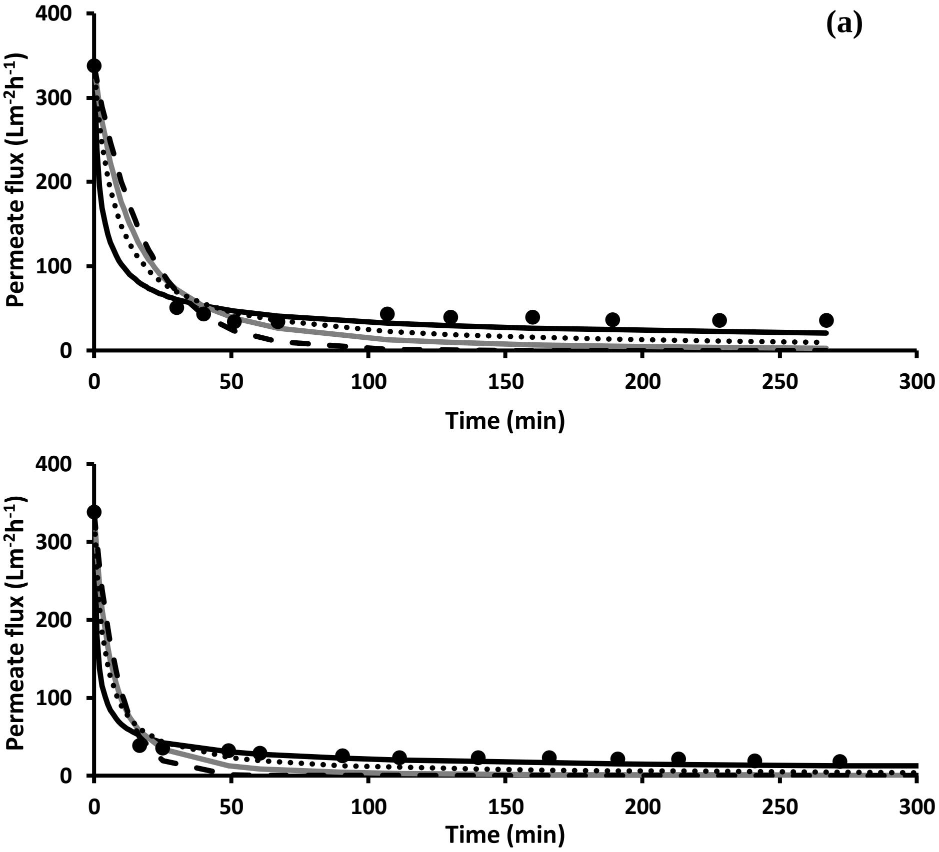

Figure 4.46. Evolution of the permeate flux (●) during the ultrafiltration of the mature (a) or young (b) leachate under VCR mode. Cake model (solid black line), standard model (solid grey line), complete model (dashed black line) and intermediate model (dotted line) predictions for each of them. In all cases: 1.6 bar, 70 ºC, flow rate of 5.4 L/min and cross flow velocity of 3.2 m/s.

Dealing first with permeate fluxes, the evolutions of these with VCR are the expected ones for both leachates, differentiating three periods. Thus, a rapid flux drop was observed initially, which was mainly attributed to concentration polarization, followed by a less marked decrease in the flux due to irreversible fouling and a final period corresponding to a small flux decrease. As can be seen in Fig. 4.46, the short duration of the second period suggests that internal fouling is not significant, as it was deduced from the analysis of resistances. Regarding the latter period, it is usually associated with the foulant deposition on the membrane surface, that is to say, the reversible fouling [50]. During this stage, approximately constant fouling rates of $4.3 \cdot 10^{-3}$ or $7.9 \cdot 10^{-3}$ $m^{-1}h^{-1}$ were observed for the mature or the young leachate, respectively.

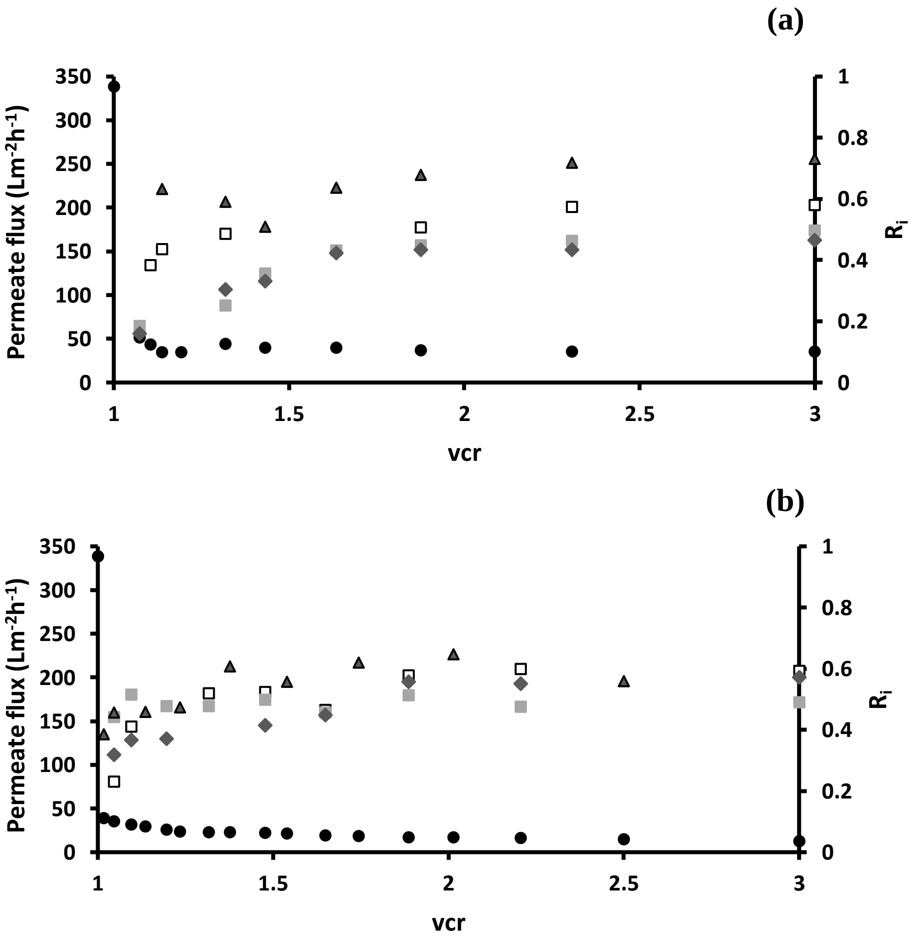

Figure 4.47. Evolution of the rejection coefficients for COD (■), TOC (◆), colour (▲) and humic acids (□) and permeate flux (●) with the VCR mode during the ultrafiltration of either a mature (a) or a young leachate (b). In all cases: 1.6 bar, 70 ºC, flow rate of 5.4 L/min and cross flow velocity of 3.2 m/s.

Regarding the rejection coefficients, their evolutions differed between leachates. For instance, the COD rejection for the mature leachate showed an approximately sigmoidal shape, from an initial value of 18.5% to a final one of 49.6%, with the faster increase at VCR ranging from 1.2 to 1.7. Nevertheless, this parameter seemed to remain approximately constant during the ultrafiltration of the young leachate, although a slight increase was perceived at the beginning of the filtration. Concerning R_{TOC}, it showed similar values to R_{COD} throughout the filtration experiment. Nevertheless, in the case of the young one, the R_{COD} values were slightly higher than that of the R_{TOC} at the beginning of the ultrafiltration. In regard to CN, the rejections were significantly higher for the mature leachate, although a decrease in the R_{CN} for mature leachate during the early stages of the operation could be seen. These differences in the evolution of the COD, TOC and CN rejections for both leachates can be explained on the basis of their composition. A more in-depth and detailed discussion of this statement will be carried out in the next section.

3.3. Fouling mechanism

The previous observations on permeate fluxes and rejection coefficients seem to suggest that there is clear connection between ultrafiltration performance and the changes in the leachate composition due to landfill ageing.

In this regard and before developing this relationship, it is interesting to mention that landfills undergo at least four stages of decomposition during their ageing: an initial aerobic phase, an anaerobic acid phase, an initial methanogenic phase and, finally, a stable methanogenic phase, thus existing a strong relationship between the state of refuse decomposition and its corresponding leachate characteristics [51]. On the basis of size exclusion chromatography results, Aftab and Hur [52] proposed that leachates are composed by five different fractions: biopolymers (>10 kDa), humic substances (approx. 1 kDa), building blocks (300–500 Da), and low molecular neutrals and acids (<350 Da). As the landfill is becoming older, biopolymers are broken up into building blocks and these are decomposed and transformed into simple molecules, such as fatty acids, carbon dioxide and methane, whereas humic substances are hardly modified due to their recalcitrant character [17,53] (see Fig. 4.48). Therefore, a high relative abundance of low molecular weight compounds in the mature leachate but not in the young one is accepted. In this sense, Mohammadzadeh and Clark (2008) reported that leachates generated in an area of old wastes were mainly composed of humic substances and simple fatty acids (mostly acetic and propionic) [53]. Taking into account that COD and TOC measurements include all the organic compounds, the small fatty acids easily passed through the membrane during the first minutes of ultrafiltration of the mature leachate, thus increasing the permeate COD and TOC and reducing the initial R_{COD} and R_{TOC}, as it is observed in Fig. 4.47.

Meanwhile, the proportion of compounds with higher molecular weight in the retentate increased. Once most of the fatty acids had already been removed, the COD and TOC values in the permeate mainly depended on the presence of humic substances on it. Obviously, this causes a progressive increase in the COD and TOC rejection, thereby the rejection coefficients of the compounds tend to approximate to that of the higher molecular size, that is to say, to the humic acids one (R_{HA}), thus explaining the sigmoidal evolution of R_{COD} and R_{TOC} observed in Fig. 4.47. At this point, it should be pointed out that the increase in the rejection of humic acids during the first minutes of filtration was probably due to the rapid development of a fouling layer on the membrane surface, as explained above. This external fouling layer is mainly made up of humic acids and acts as a dynamic membrane, reducing the permeability and increasing R_{HA} [44,54]. The additional barrier would not have influence on the pass of small molecules, such as the fatty acids, so its reject coefficient would not be affected. Once the cake was formed, its compaction and/or the consolidation of irreversible fouling are likely the main reasons why the R_{HA} slightly increased after the external fouling layer was formed (Fig. 4.47) [50,55]. With regard to the high values of R_{CN}, it should be taken into account that mature leachate is mainly composed of humic acids, which are highly coloured, and simple fatty acids, which are colourless. Therefore, permeate results in an almost colourless stream, thus achieving a high colour retention due to humic acid retention.

On the other hand, the composition of a young leachate is more complex. When compared with mature leachates, the lower relative content in small molecules of the young ones can also explain the results depicted in Fig. 4.47. Thus, the small variation in R_{COD} with VCR observed for the young leachate, instead of the sigmoidal tendency of the mature one, can be attributed to the higher abundance of high molecular weight compounds and their cohesive interactions facilitated by the higher ionic strength of the young leachate [56]. Taking into account that the molecular weight cut-off of the membrane is 150 kDa and the predominance of biopolymers (>10 kDa) and humic acids (approx. 1 kDa) in the young leachate, COD and humic acids rejections should be pretty similar to each other, as was experimentally proved (Fig. 4.47) [4,52].

As for R_{CN}, lower values were observed in comparison to that of the mature leachate. This can be explained considering the chemical nature of the young leachate. This stream is highly complex, as opposed to the mature leachate which, as it was previously mentioned, is mainly made up of humic acids and simple fatty acids. Thus, both retentate and permeate will be richer in coloured species, therefore, reducing colour differences between these streams.

Finally, the experimental evidence that total resistance for the young leachate is higher than that of the mature one can be also linked to the leachate composition. Young leachate has a high proportion of biopolymers (>10 kDa), while organic matter in mature leachate consists basically of humic substances. Renou et al. (2009) reported that the major cause of ceramic membrane fouling during the ultrafiltration of landfill leachate was the formation of precipitated humic acid on the surface of the membrane, fostered by the presence of calcium ions [22]. Nevertheless, during the filtration of young leachate, interactions between the deposited humic acid and biopolymers present in the stream are expected, generating a thicker, less permeable fouling cake (Fig. 4.48). In this sense, Jermann et al. (2007) observed that humic acids could act as a bridge between alginate and membrane, resulting in a more stable and less reversible fouling layer [41]. In a similar way, Xiao et al. (2013) also reported the interaction proneness between humic acids, polysaccharides and proteins [42].

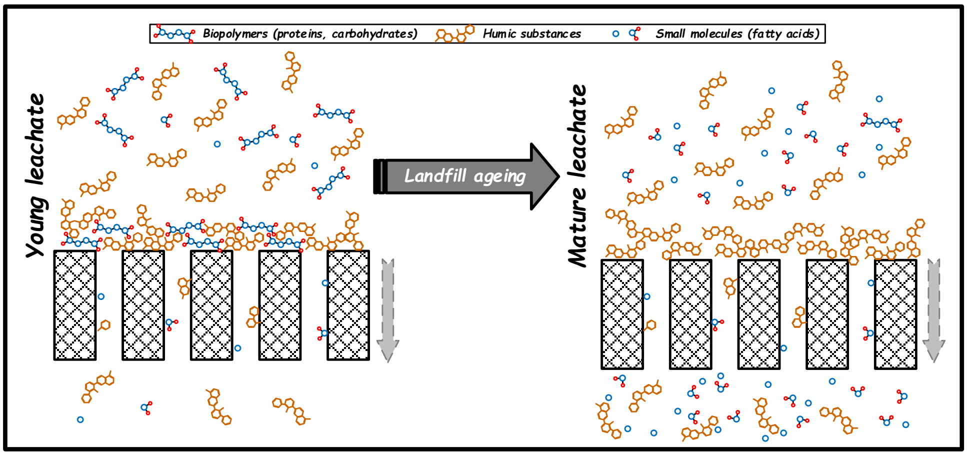

Figure 4.48. Proposed effect of the landfill age on the ultrafiltration of the leachate generated.

4. Conclusions

Results suggest that there is a clear connection between ultrafiltration performance and the changes in the leachate composition due to landfill ageing. Both young and mature leachates cause a very steep permeate flux decline, during the first minutes of filtration, probably due to the fast accumulation on the membrane surface of a first layer of fouling. In a second stage, the flux declines slower, caused by the consolidation of the fouling layer due to a balance between the deposition of foulants on the cake and their removal produced by the shear stress of the cross flow.

The maturation of the leachate has a positive effect on the permeability, with a twofold higher final permeability than that obtained with a young leachate. This finding is likely related to the higher concentration of proteins and carbohydrates in the young leachate. The main reason for the decrease of permeability during the ultrafiltration of leachates is the external fouling, this being higher for younger leachates. Resistance-in-series analysis demonstrated that the loss of permeability was mainly due to reversible fouling. Either irrecoverable or internal fouling were scarce and not determined by the stage of maturation of the leachate. This leads to suggest a long lifespan of the membrane in plant operation, since more than 99.5% of the initial permeability can be recovered after cleaning.

The prevailing fouling model during the ultrafiltration of both leachates is the corresponding to cake formation, either under TR or VCR modes. COD rejection for the mature leachate showed an approximately sigmoidal shape, from an initial value of 18.5% to a final one of 49.6%, with the faster increase for VCR ranging from 1.2 to 1.7. The main reason for this behaviour is due to the fatty acids are not retained by the UF membrane. On the other hand, COD rejection remains approximately constant during the ultrafiltration of the young leachate (48%), which can be attributed to the presence of higher molecular weight compounds in its composition.

Acknowledgements

The authors are grateful for the financial support from the Spanish Ministry of Economy and Competitiveness (MINECO) through Project CTM2015-63864-R and FEDER funds from European Union. Authors also acknowledge the financial support from the Employment, Industry and Tourism Office of Principality of Asturias (Spain) through the project GRUPIN IDI/2018/000127. The author Daniel Núñez thanks the Principality of Asturias for their financial support through the Severo Ochoa scholarship nº BP19-093.

References

[1] D.S. Fernández, M.E. Puchulu, S.M. Georgieff, Identification and assessment of water pollution as a consequence of a leachate plume migration from a municipal landfill site (Tucumán, Argentina), Environ. Geochem. Health. 36 (2014) 489–503. doi:10.1007/s10653-013-9576-1.

[2] C.M. Moody, T.G. Townsend, A comparison of landfill leachates based on waste composition, Waste Manag. 63 (2017) 267–274. doi:10.1016/j.wasman.2016.09.020.

[3] L.M. Chu, K.C. Cheung, M.H. Wong, Variations in the chemical properties of landfill leachate, Environ. Manage. 18 (1994) 105–117. doi:10.1007/BF02393753.

[4] D. Kulikowska, E. Klimiuk, The effect of landfill age on municipal leachate composition, Bioresour. Technol. 99 (2008) 5981–5985. doi:10.1016/j.biortech.2007.10.015.

[5] C.B. Öman, C. Junestedt, Chemical characterization of landfill leachates - 400 parameters and compounds, Waste Manag. 28 (2008) 1876–1891. doi:10.1016/j.wasman.2007.06.018.

[6] J. Wiszniowski, D. Robert, J. Surmacz-Gorska, K. Miksch, J. V. Weber, Landfill leachate treatment methods: A review, Environ. Chem. Lett. 4 (2006) 51–61. doi:10.1007/s10311-005-0016-z.

[7] Y. Peng, Perspectives on technology for landfill leachate treatment, Arab. J. Chem. 10 (2017) S2567–S2574. doi:10.1016/j.arabjc.2013.09.031.

[8] V. Oloibiri, M. Chys, S. De Wandel, K. Demeestere, S.W.H. Van Hulle, Removal of organic matter and ammonium from landfill leachate through different scenarios: Operational cost evaluation in a full-scale case study of a Flemish landfill, J. Environ. Manage. 203 (2017) 774–781. doi:10.1016/j.jenvman.2016.09.055.

[9] R.B. Brennan, E. Clifford, C. Devroedt, L. Morrison, M.G. Healy, Treatment of landfill leachate in municipal wastewater treatment plants and impacts on effluent ammonium concentrations, J. Environ. Manage. 188 (2017) 64–72. doi:10.1016/j.jenvman.2016.11.055.

[10] S. Renou, J.G. Givaudan, S. Poulain, F. Dirassouyan, P. Moulin, Landfill leachate treatment: Review and opportunity, J. Hazard. Mater. 150 (2008) 468–493. doi:10.1016/j.jhazmat.2007.09.077.

[11] X. Shi, G. Tal, N.P. Hankins, V. Gitis, Fouling and cleaning of ultrafiltration membranes: A review, J. Water Process Eng. 1 (2014) 121–138. doi:10.1016/j.jwpe.2014.04.003.

[12] D. Kulikowska, M. Zielińska, K. Konopka, Treatment of stabilized landfill leachate in an integrated adsorption–fine-ultrafiltration system, Int. J. Environ. Sci. Technol. 16 (2019) 423–430. doi:10.1007/s13762-018-1685-z.

[13] K. Tabet, P. Moulin, J.D. Vilomet, A. Amberto, F. Charbit, Purification of landfill leachate with membrane processes: Preliminary studies for an industrial plant, Sep. Sci. Technol. 37 (2002)

1041–1063. doi:10.1081/SS-120002240.

[14] A.C. Syzdek, R.C. Ahlert, Separation of landfill leachate with polymeric ultrafiltration membranes, J. Hazard. Mater. 9 (1984) 209–220. doi:10.1016/0304-3894(84)80018-7.

[15] D. Dolar, K. Košutić, T. Strmecky, Hybrid processes for treatment of landfill leachate: Coagulation/UF/NF-RO and adsorption/UF/NF-RO, Sep. Purif. Technol. 168 (2016) 39–46. doi:10.1016/j.seppur.2016.05.016.

[16] D. Cingolani, A.L. Eusebi, P. Battistoni, Osmosis process for leachate treatment in industrial platform: Economic and performances evaluations to zero liquid discharge, J. Environ. Manage. 203 (2017) 782–790. doi:10.1016/j.jenvman.2016.05.012.

[17] RO & UF membranes: Market opportunities in landfill leachate, Water Wastewater Int. 27 (2012) 46–49.

[18] Y.D. Xu, D.B. Yue, Y. Zhu, Y.F. Nie, Fractionation of dissolved organic matter in mature landfill leachate and its recycling by ultrafiltration and evaporation combined processes, Chemosphere. 64 (2006) 903–911. doi:10.1016/j.chemosphere.2006.01.039.

[19] M.C. Cammarota, L. Yokoyama, J.C. Campos, Ultrafiltration, chemical and biological oxidation as process combination for the treatment of municipal landfill leachate, Desalin. Water Treat. 3 (2009) 50–57. doi:10.5004/dwt.2009.440.

[20] M. Pirbazari, V. Ravindran, B.N. Badriyha, S.H. Kim, Hybrid membrane filtration process for leachate treatment, Water Res. 30 (1996) 2691–2706. doi:10.1016/S0043-1354(96)00183-2.

[21] C.F. Lin, Y.J. Huang, O.J. Hao, Ultrafiltration processes for removing humic substances: Effect of molecular weight fractions and PAC treatment, Water Res. 33 (1999) 1252–1264. doi:10.1016/S0043-1354(98)00322-4.

[22] S. Renou, S. Poulain, J.G. Givaudan, P. Moulin, Amelioration of ultrafiltration process by lime treatment: Case of landfill leachate, Desalination. 249 (2009) 72–82. doi:10.1016/j.desal.2008.09.007.

[23] Y. Xu, C. Chen, X. Li, J. Lin, Y. Liao, Z. Jin, Recovery of humic substances from leachate nanofiltration concentrate by a two-stage process of tight ultrafiltration membrane, J. Clean. Prod. 161 (2017) 84–94. doi:10.1016/j.jclepro.2017.05.095.

[24] K.W. Pi, Z. Li, D.J. Wan, L.X. Gao, Pretreatment of municipal landfill leachate by a combined process, Process Saf. Environ. Prot. 87 (2009) 191–196. doi:10.1016/j.psep.2009.01.002.

[25] O. Primo, A. Rueda, M.J. Rivero, I. Ortiz, An integrated process, fenton reaction - Ultrafiltration, for the treatment of landfill leachate: Pilot plant operation and analysis, Ind. Eng. Chem. Res. 47 (2008) 946–952. doi:10.1021/ie071111a.

[26] P. Oulego, S. Collado, A. Laca, M. Díaz, Impact of leachate composition on the advanced

oxidation treatment, Water Res. 88 (2016) 389–402. doi:10.1016/j.watres.2015.09.048.

[27] B.P. Naveen, P. V. Sivapullaiah, T.G. Sitharami, Effect of aging on the leachate characteristics from municipal solid waste landfill, in: 15th Asian Reg. Conf. Soil Mech. Geotech. Eng. ARC 2015 New Innov. Sustain., 2015: pp. 1940–1945. doi:10.3208/jgssp.IND-06.

[28] S.H. Park, Y.G. Park, J.L. Lim, S. Kim, Evaluation of ceramic membrane applications for water treatment plants with a life cycle cost analysis, Desalin. Water Treat. 54 (2015) 973–979. doi:10.1080/19443994.2014.912162.

[29] S. Khan, J. Kim, A. Sotto, B. Van der Bruggen, Humic acid fouling in a submerged photocatalytic membrane reactor with binary TiO2-ZrO2 particles, J. Ind. Eng. Chem. 21 (2015) 779–786. doi:10.1016/j.jiec.2014.04.012.

[30] J. Guo, S. Khan, S.H. Cho, J. Kim, ZnS nanoparticles as new additive for polyethersulfone membrane in humic acid filtration, J. Ind. Eng. Chem. 79 (2019) 71–78. doi:10.1016/j.jiec.2019.05.015.

[31] W. Yuan, A.L. Zydney, Humic acid fouling during ultrafiltration, Environ. Sci. Technol. 34 (2000) 5043–5050. doi:10.1021/es0012366.

[32] I. Sutzkover-Gutman, D. Hasson, R. Semiat, Humic substances fouling in ultrafiltration processes, Desalination. 261 (2010) 218–231. doi:10.1016/j.desal.2010.05.008.

[33] S.J. Judd, C. Judd, The MBR Book, 2011. doi:10.1016/B978-1-85617-481-7.X5000-4.

[34] I. Rosas, S. Collado, A. Gutiérrez, M. Díaz, Fouling mechanisms of Pseudomonas putida on PES microfiltration membranes, J. Memb. Sci. 465 (2014) 27–33. doi:10.1016/j.memsci.2014.04.002.

[35] J. HERMIA, Constant Pressure Blocking Filtration Laws - Application Topower-Law Non-Newtonian Fluids., Trans Inst Chem Eng. V 60 (1982) 183–187.

[36] M. Abbasi, R.S. Mohammad, A. Salahi, B. Mirza, Modeling of membrane fouling and flux decline in microfiltration of oily wastewater using ceramic membranes, Chem. Eng. Commun. 199 (2012) 78–93. doi:10.1080/00986445.2011.570391.

[37] E.M. Thurman, R.L. Malcolm, Preparative Isolation of Aquatic Humic Substances, Environ. Sci. Technol. 15 (1981) 463–466. doi:10.1021/es00086a012.

[38] L. Vinet, A. Zhedanov, A “missing” family of classical orthogonal polynomials, 2011. doi:10.1088/1751-8113/44/8/085201.

[39] C. Tizaoui, L. Bouselmi, L. Mansouri, A. Ghrabi, Landfill leachate treatment with ozone and ozone/hydrogen peroxide systems, J. Hazard. Mater. 140 (2007) 316–324. doi:10.1016/j.jhazmat.2006.09.023.

[40] V. V. Tarabara, I. Koyuncu, M.R. Wiesner, Effect of hydrodynamics and solution ionic strength on permeate flux in cross-flow filtration: Direct experimental observation of filter cake cross-

sections, J. Memb. Sci. 241 (2004) 65–78. doi:10.1016/j.memsci.2004.04.030.

[41] D. Jermann, W. Pronk, S. Meylan, M. Boller, Interplay of different NOM fouling mechanisms during ultrafiltration for drinking water production, Water Res. 41 (2007) 1713–1722. doi:10.1016/j.watres.2006.12.030.

[42] F. Xiao, P. Xiao, W.J. Zhang, D.S. Wang, Identification of key factors affecting the organic fouling on low-pressure ultrafiltration membranes, J. Memb. Sci. 447 (2013) 144–152. doi:10.1016/j.memsci.2013.07.040.

[43] M. Kraume, D. Wedi, J. Schaller, V. Iversen, A. Drews, Fouling in MBR: What use are lab investigations for full scale operation?, Desalination. 236 (2009) 94–103. doi:10.1016/j.desal.2007.10.055.

[44] B. Ma, Y. Ding, W. Li, C. Hu, M. Yang, H. Liu, J. Qu, Ultrafiltration membrane fouling induced by humic acid with typical inorganic salts, Chemosphere. 197 (2018) 793–802. doi:10.1016/j.chemosphere.2018.01.037.

[45] M. Said, A. Ahmad, A.W. Mohammad, M.T.M. Nor, S.R. Sheikh Abdullah, Blocking mechanism of PES membrane during ultrafiltration of POME, J. Ind. Eng. Chem. 21 (2015) 182–188. doi:10.1016/j.jiec.2014.02.023.

[46] H. Rezaei, F.Z. Ashtiani, A. Fouladitajar, Effects of operating parameters on fouling mechanism and membrane flux in cross-flow microfiltration of whey, Desalination. 274 (2011) 262–271. doi:10.1016/j.desal.2011.02.015.

[47] C.S. Slater, R.C. Ahlert, C.G. Uchrin, Applications of reverse osmosis to complex industrial wastewater treatment, Desalination. 48 (1983) 171–187. doi:10.1016/0011-9164(83)80015-0.

[48] D.H. Kim, H.K. Shon, G. Sharma, J. Cho, Charge effect of natural organic matter for ultrafiltration and nanofiltration membranes, J. Ind. Eng. Chem. 17 (2011) 109–113. doi:10.1016/j.jiec.2010.12.006.

[49] T. Janus, B. Ulanicki, A behavioural membrane fouling model for integrated simulation of membrane bioreactors for wastewater treatment, in: Procedia Eng., 2015: pp. 1328–1337. doi:10.1016/j.proeng.2015.08.964.

[50] A.R. Taherian, M. Mondor, F. Lamarche, Enhancing nutritional values and functional properties of yellow pea protein via membrane processing, Peas Cultiv. Var. Nutr. Uses. (2012) 1–48.

[51] P. Kjeldsen, M.A. Barlaz, A.P. Rooker, A. Baun, A. Ledin, T.H. Christensen, Present and long-term composition of MSW landfill leachate: A review, Crit. Rev. Environ. Sci. Technol. 32 (2002) 297–336. doi:10.1080/10643380290813462.

[52] B. Aftab, J. Hur, Unraveling complex removal behavior of landfill leachate upon the treatments of Fenton oxidation and MIEX ® via two-dimensional correlation size exclusion chromatography (2D-CoSEC), J. Hazard. Mater. 362 (2019) 36–44. doi:10.1016/j.jhazmat.2018.09.017.

[53] H. Mohammadzadeh, I. Clark, Degradation pathways of dissolved carbon in landfill leachate traced with compound-specific 13C analysis of DOC, Isotopes Environ. Health Stud. 44 (2008) 267–294. doi:10.1080/10256010802309814.

[54] M.E. Ersahin, H. Ozgun, R.K. Dereli, I. Ozturk, K. Roest, J.B. van Lier, A review on dynamic membrane filtration: Materials, applications and future perspectives, Bioresour. Technol. 122 (2012) 196–206. doi:10.1016/j.biortech.2012.03.086.

[55] C. de Morais Coutinho, M.C. Chiu, R.C. Basso, A.P.B. Ribeiro, L.A.G. Gonçalves, L.A. Viotto, State of art of the application of membrane technology to vegetable oils: A review, Food Res. Int. 42 (2009) 536–550. doi:10.1016/j.foodres.2009.02.010.

[56] T. Lin, Z.J. Lu, W. Chen, Interaction mechanisms of humic acid combined with calcium ions on membrane fouling at different conditions in an ultrafiltration system, Desalination. 357 (2015) 26–35. doi:10.1016/j.desal.2014.11.007.

[57] M.A. Argüello, S. Álvarez, F.A. Riera, R. Álvarez, Enzymatic cleaning of inorganic ultrafiltration membranes used for whey protein fractionation, J. Memb. Sci. 216 (2003) 121–134. doi:10.1016/S0376-7388(03)00064-4.

Appendix

Determination of R_m, R_{rev}, R_{irrev} and $R_{irrecov}$

Fig. A.4.10 illustrates the evolution of J throughout the experiments. Initial flux (J_o), flux after leachate ultrafiltration and before cleaning (J_s), flux after physical cleaning with water (J_{pc}) and flux after chemical cleaning (J_{cc}) are measured to calculate the resistances model.

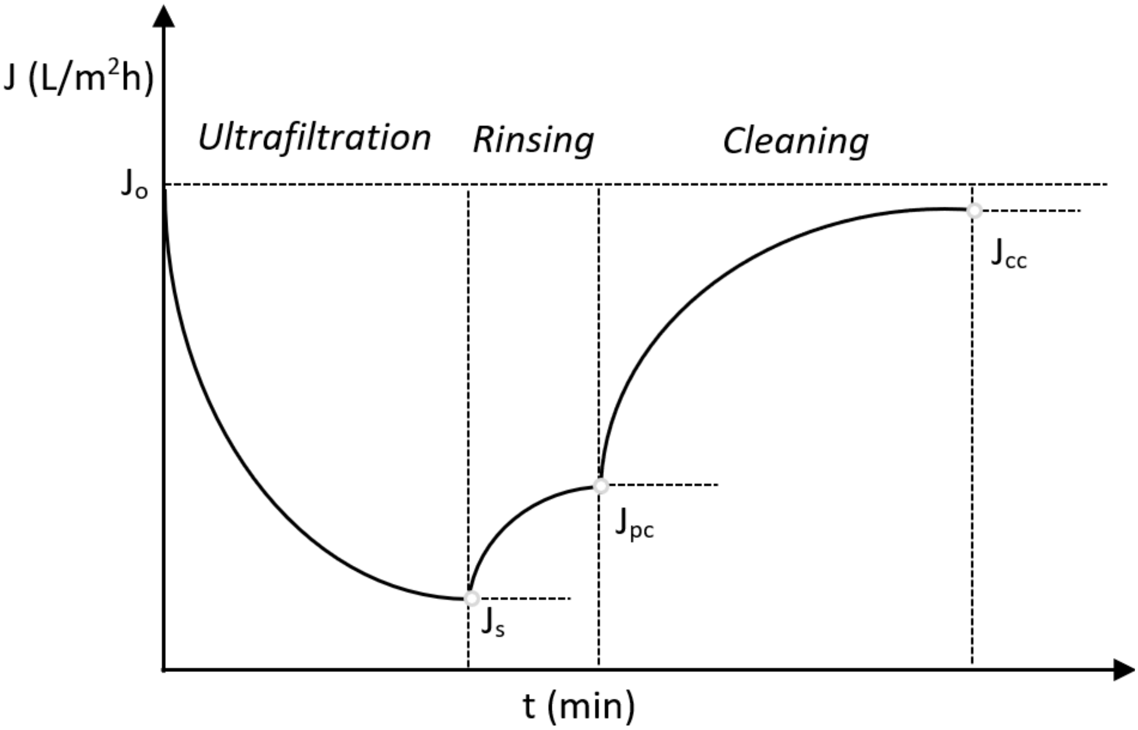

Figure A.4.10. Evolution of flux during ultrafiltration, rinsing and cleaning.

According to Darcy's law (Eq. A1):

$$R = \frac{\Delta P}{\mu J} \tag{A1}$$

Where R is the hydraulic resistance of the membrane, ΔP is the TMP, μ is the viscosity, and J is the permeate flux. Also, according to the resistances-in-series model, total resistance can be expressed as a sum of different resistances (Eq. A2):

$$R_s=R_m+R_{rev}+R_{irrev}+R_{irrecov} \tag{A2}$$

Where R_s is total resistance after operation, R_m is the intrinsecal membrane resistance, R_{rev} is the resistance corresponding to reversible fouling, R_{irrev} is the resistance caused by irreversible fouling, and $R_{irrecov}$ is the resistance referable to irrecoverable fouling.

Through simple operations (eqs. A3-A5), we can obtain R_{rev}, R_{irrev} and $R_{irrecov}$ with the resistances calculated with J_s (R_s), J_o (R_m), J_{pc} (R_{pc}) and J_{cc} (R_{cc}) (Fig. A.4.11) [57].

$$R_{rev}=R_s-R_{pc} \tag{A3}$$

$$R_{irrev}=R_{pc}-R_{cc} \tag{A4}$$

$$R_{irrecov}=R_{cc}-R_m \tag{A5}$$

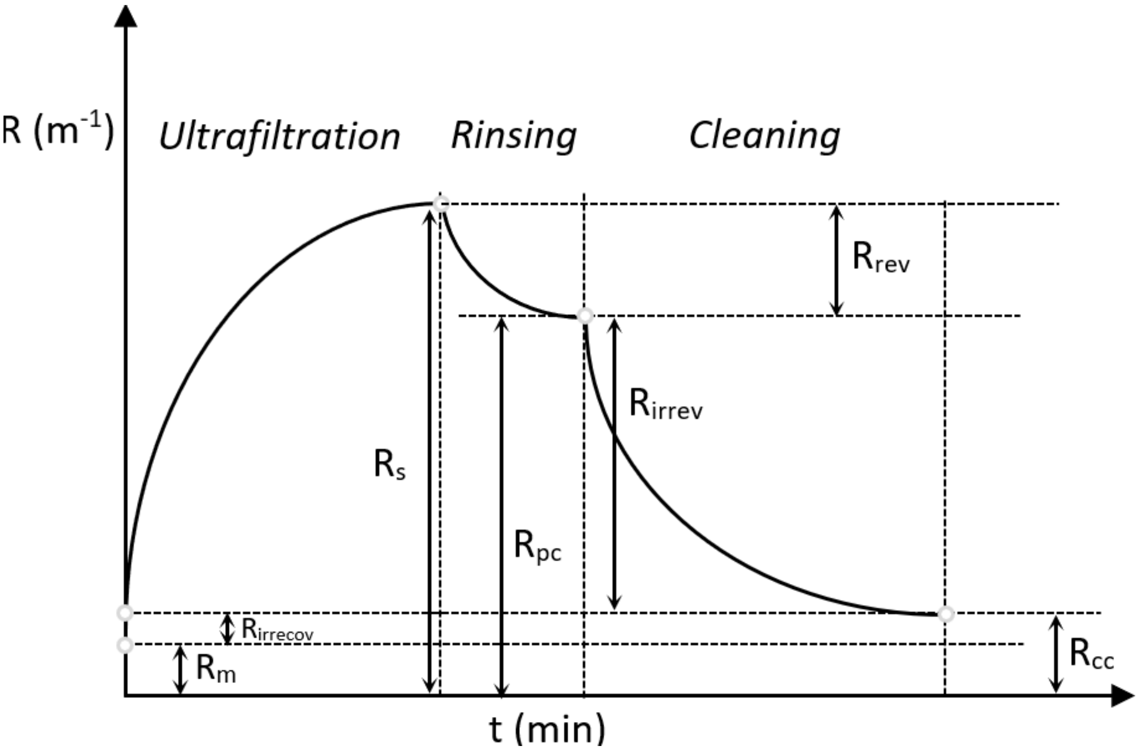

Figure A.4.11. Evolution of resistances during ultrafiltration, rinsing and cleaning. Adapted from [51].

4.2.3. Enhanced treatment of stabilised landfill leachates: wet oxidation and membrane filtration

Daniel Núñez, Paula Oulego, Sergio Collado, Francisco A. Riera, Mario Díaz*

Department of Chemical and Environmental Engineering, University of Oviedo.

c/ Julián Clavería 8, 33006, Oviedo, Spain

*Corresponding author’s e-mail: mariodiaz@uniovi.es

Phone: +34 985 10 34 39, FAX: +34 985 10 34 40

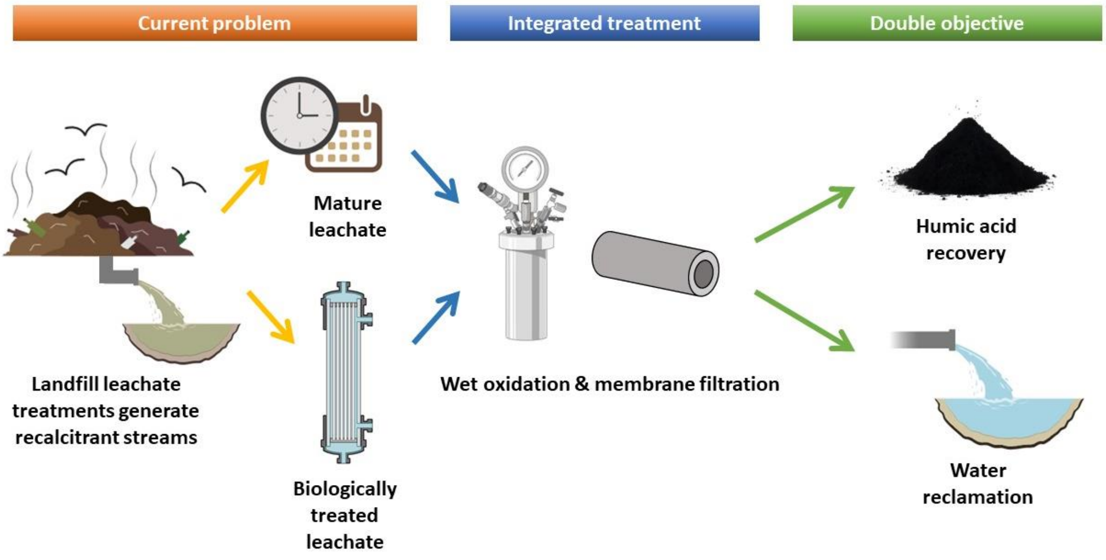

Figura 4.49. Resumen gráfico del artículo *Enhanced treatment of stabilised landfill leachates: wet oxidation and membrane filtration*.

Abstract

Stabilised leachates contain recalcitrant compounds that are difficult to remove by physical-chemical methods. Furthermore, humic acids, a major component of the organic matter present in these leachates, are potentially valuable for industrial and agricultural applications.

Thus, the aim of this study was to investigate the integrated treatment of wet oxidation followed by membrane ultrafiltration of mature (MT) and biologically treated (BT) leachates for the dual purpose of recovering humic acids and obtained reclaimed water, with a particular focus on the impact of wet oxidation and leachate type on membrane fouling mechanisms.

Wet oxidation proved to be an effective treatment for removing recalcitrant compounds with COD removals of 59.2% and 32.6% for MT and BT leachates, respectively. Besides, the oxidation treatment increased 66% the fluxes obtained during the ultrafiltration of BT leachate and enhanced the fouling significantly with a 40% reduction in the total resistance. Flux decay was more severe with MT leachates, both untreated and oxidised, although the fouling produced by these leachates was mainly reversible, with values of reversible resistance of 53% and 72% of the total one, respectively. Cake formation was found to be the main fouling mechanism for the MT leachates, while intermediate pore blocking was the predominant fouling mechanism during the ultrafiltration of BT leachates.

Humic acid rejections up to 73% were obtained filtering untreated MT leachate, the values being around 50% for BT and oxidised MT and BT leachates. The final permeates of the treated leachates met all the criteria for wastewater discharge into public sanitation systems with the exception of boron, conductivity, total phenols, pH (only oxidised leachates) and ammonia (only oxidised MT leachate).

Keywords: Humic acids; Fouling; Hydrothermal treatments; Ultrafiltration; Wastewater management.

1. Introduction

Landfill leachates are wastewaters composed of rainwater that passes through a landfill site and liquids that are generated by the breakdown of the waste within the landfill. These leachates represent an environmental and health risk due to their high concentration of recalcitrant organic matter and toxicity. Besides, considering that the municipal solid waste generation globally exceeds 2 billion tons per year, the suitable management of these leachates clearly supposes a continuing challenge that requires innovative and sustainable solutions [1,2].

Biological treatments are commonly used for the management of these effluents due to their reliability, simplicity and high cost-effectiveness [3]. However, landfill leachates, especially the mature ones, primarily contain non-biodegradable compounds and toxic pollutants, making these effluents more challenging to be treated [4,5]. On the other hand, they are mainly made up of a mixture of humic acids [3,6], which have several agricultural and industrial applications [7–9]. Physical-chemical techniques such as coagulation–flocculation, chemical precipitation, and adsorption among others, can also be used. Nevertheless, none of them are applicable in all scenarios or highly effective for the removal of recalcitrant compounds from stabilised leachate. Furthermore, these techniques have other drawbacks, including high operational costs due to chemical consumption, sensitivity to process pH, and generation of sludge [10–13]. In this regard, the implementation of pressure-driven membrane processes, and particularly, ultrafiltration, for landfill leachate treatment can be an efficient means to recover both humic acid (retentate) and water (permeate). Besides, ultrafiltration is highly effective in retaining various microorganisms, such *as E. coli*, *Enterococci*, anaerobic sulphito-reducer spores, and bacteriophages [14]. However, a major drawback of this technology is membrane fouling, which can limit the efficiency of the process [15,16].

In this context, wet oxidation (WO), as an advanced oxidation process, is gaining importance as an alternative clean technology to these conventional treatments. The oxidation process does not require the use of any toxic chemical reagents, and no harmful compounds, such as SO_2, NO_X

and fly ashes are generated. Additionally, unlike other advanced oxidation processes, such as electrocatalysis [17], photocatalysis [18] and Fenton-like oxidation [19], WO stands out for its dual benefits. It not only facilitates the effective degradation of pollutants but also proves cost-effective and reduces the reaction time, especially when dealing with high concentrations of mature or stabilised leachates [20]. This technique is based on the aqueous oxidation of a waste in liquid phase at high temperatures and pressures in the presence of an oxygen-containing gas (usually air) [21]. One of its main advantages compared to conventional treatments is that it effectively degrades recalcitrant substances without generating a secondary waste stream and with minimal air pollution discharges [22,23]. However, achieving complete mineralization through WO can be highly cost-intensive, as highly oxidized intermediates (mainly short-chain organic acids) tend to be refractory to further total oxidation [24]. For this reason, integration schemes combining wet oxidation with other traditional treatment technologies are commonly employed [21,25,26]. With the aim of the subsequent coupling with another technique, extensive research has been conducted to evaluate the effect of WO on the physical-chemical properties of the leachate, including biodegradability, mineralization, pH, nitrogen removal and toxicity [27–32]. Nevertheless, to the best of our knowledge, studies dealing with how the wet oxidation pre-treatment affects the filterability of the leachate, with the dual purpose of recovery humic acids and obtained reclaimed water, are not available. It should be noted that WO reduces the viscosity of the fluid, modifies the structure and size of the polymeric substances, and precipitates the dissolved metals [33–36]. Moreover, both WO and membrane processes typically require high pressures, allowing for the possibility of designing an integrated process that can operate at the same pressure level. This eliminates the need for a separate decompression step after WO, being only necessary a cooling one. These facts suggest that the coupling of both processes could generate positive synergies. Additionally, knowledge about the effects of WO on the filterability could be helpful not only for the integration of a membrane separation process after the WO, but also for the implementation of the WO as a way of treating the retentate of a previous filtration.

Based on the abovementioned considerations, the aims of the present work were to assess: i) the effect of WO on the filterability of mature and biologically treated leachates on the fouling mechanisms involved in their ultrafiltration, paying special attention to the initial leachate composition, and ii) the recovery of humic acids and reclaimed water from these leachates by ultrafiltration, and the effect of WO on this recovery.

2. Material and methods

2.1. Landfill leachates

The leachates used in this study were obtained from the sanitary landfill site La Zoreda and provided by COGERSA (Asturias, Spain). Two different leachates were employed during the experimentation: mature (MT) and stabilised after biological treatment (BT). The MT leachate comes from an area of the landfill where no waste has been deposited since 2010. Finally, BT leachate refers to a mixture of mature and young leachates (approximately 1:1) after being treated by a nitrification-denitrification process in a membrane bioreactor (MBR).

A description of the physicochemical characteristics of the different leachates is shown in Table 4.40. Gross particles were eliminated with a metal mesh filter of 250 µm of pore size and 200 mm of diameter (Cisa, Spain). Samples were stored at 5 ºC before usage.

Table 4.40. Physicochemical characteristics of the leachates.

	MT leachate	**BT leachate**
pH	7.86	7.62
Colour number	3.07 cm^{-1}	0.63 cm^{-1}
Conductivity	23900 µS/cm	11900 µS/cm
COD	4591 mg O_2/L	1600 mg O_2/L
BOD_5	478 mg O_2/L	19 mg O_2/L
Humic acid concentration	92 mg/L	71 mg/L

2.2. Wet oxidation: apparatus and procedure

Wet oxidation experiments were carried out in a 1-L capacity reactor (Parr T316SS) equipped with two agitators. The reactor was preceded by a 2-L stainless steel water reservoir. The loaded volume in each vessel was about 70% of the total capacity to ensure safe operating conditions. The experiments were performed at 160ºC and 60 bar, with an operating time of 150 min (these conditions were set based on previous experiments [27,29]). Stirrer speed was adjusted to 500 rpm for all oxidations. The operating pressure was provided by bottled compressed oxygen, with the oxygen flow rate regulated at 1800 mL/min using an electronic mass flow controller (Brooks). A back pressure controller located at the end of the gas line was employed to maintain a constant pressure. The oxygen was bubbled through the water reservoir to become saturated with water vapor, and then it was introduced into the reaction vessel. A detailed diagram of the experimental setup can be found in [37].

2.3. Membrane filtration

2.3.1. Experimental setup

Ultrafiltration experiments were performed on a locally-made and assembled system. This system featured a 3 L crystal tank, from which the MT or BT leachate were pumped towards the ultrafiltration module. The pumping was facilitated by a Masterflex I/P 7591-55 (Cole-Parmer) peristaltic pump attached to an Easyload Masterflex I/P 77601-10 (Cole-Parmer) pump head. Ultrafiltration cell consisted of a tubular ZrO_2-TiO_2 membrane (600 × 6mm) (TAMI Industries) with a molecular weight cut-off (MWCO) of 150 kDa. Pressure gauges and valves were positioned in the flow line at the membrane entrance and exit to measure the transmembrane pressure (TMP). The experiments were conducted at temperature of 70 ºC, with flow rate of 4.8-2.4 L/ min and cross flow velocity of 1-0.5 m/s over the membrane. Permeate flux was determined by weighing of permeate under a TMP of 1.6 bar. Temperature was maintained at the target value using a water bath. A scheme of the experimental setup is shown in Fig. 4.50:

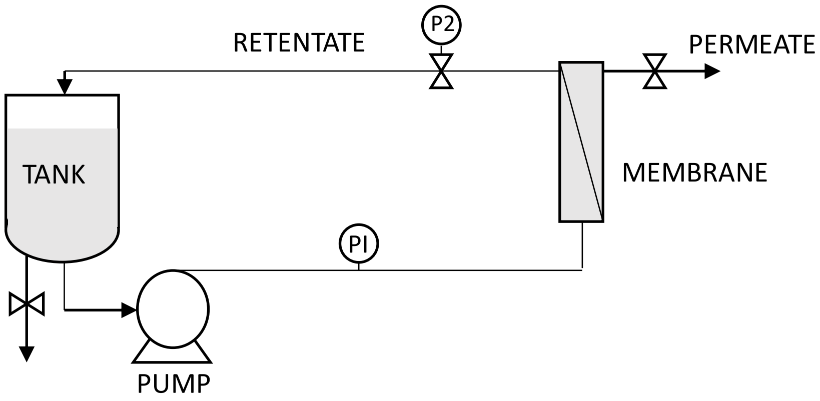

Figure 4.50. Scheme of experimental setup used in the ultrafiltration experiments.

The experiments were conducted in volume concentration ratio (VCR) mode. Leachate retentate was continuously recirculated to the supply tank, while permeate was discarded. Samples were withdrawn at regular intervals to measure the organic matter content in terms of chemical oxygen demand (COD), and humic acid concentration, as along with permeate flux. Retentate was concentrated until a VCR of 3 was reached. After each filtration, the membrane was washed with distilled water until constant flux was achieved. Subsequently, it was cleaned with a 0.5 % basic detergent solution until constant flux was reached. This operation was repeated until final flux was higher than 90% of the initial flux. Flux was also measured during these two steps.

2.3.2. Modelling

Several empirical models were examined to determine which one better fit the fouling results.

The resistance-in-series model analyses the reversibility of the membrane fouling by expressing the total hydraulic resistance of the membrane (R_T, 1/m) as the sum of the resistances caused by reversible fouling (R_{rev}, 1/m), irreversible fouling (R_{irrev}, 1/m), and the resistance generated by the membrane itself (R_m, 1/m) (Eq. 1). Hydraulic resistance can be calculated as shown in Eq. 2:

$$R_T=R_m+R_{rev}+R_{irrev} \tag{1}$$

$$R=\frac{TMP}{\mu J} \tag{2}$$

Where μ is the dynamic viscosity of the leachate at the temperature of operation (kg·m/s), J is the permeate flux (m/s) and TMP is the transmembrane pressure (kg/m·s^2). A detailed description of the calculation of the different resistances can be found in [34].

Hermia's models [38] describe the main fouling mechanism occurring during a filtration. The general equation for the four Hermia models is as follows (Eq. 3):

$$\frac{dJ}{dt} = -K \cdot (J - J_0) \cdot J^{2-n} \tag{3}$$

Where K is a constant, J_0 is the limiting flux (m/s), and n is a constant with different values depending on the fouling mechanism: complete pore blocking (n=2, K in 1/min), standard pore blocking (n=1.5, K in 1/m) intermediate pore blocking (n=1, K in 1/m) and cake formation (n=0, K in min/m^2 [39].

The four Hermia models are described in detail in Table 4.41.

Table 4.41. Description of the Hermia's fouling models.

	Complete pore blocking (CPB)	**Standard pore blocking (SPB)**	**Intermediate pore blocking (IPB)**	**Cake formation (CF)**
Reference	[40]	[41]	[41]	[41]
Figure			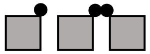	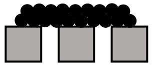
Description	Particles are larger than the pores; leading to blockage of the pores reached by the particles. There is a reduction of active membrane area.	Particles smaller than the pore size enter the pores and become either adsorbed or deposited within the pore. Reduction in pore volume leads to the blinding of pores. There is an increase in membrane resistance due to pore size reduction. Internal pore blocking is independent of feed velocity.	Any particles reaching a pore might seal it over time. Particles might bridge a pore and not block it completely. There is a reduction of active membrane area. The effect is similar to pore blocking but not as severe.	Formation of a cake on the membrane surface by particles that do not enter the pores. The overall resistance comprises the resistance of the membrane and the resistance of the cake.
Equation	$J=J_o\cdot K_b A\cdot t$	$J=Jo\cdot[1+1/2\cdot Ks(A\cdot Jo)^{0,5}\cdot t]-2$	$J=Jo\cdot[1+Ki\cdot(A\cdot Jo)\cdot t]^{-1}$	$J=Jo\cdot[1+2\cdot Kc\cdot(A\cdot Jo)^{2}\cdot t]^{-1/2}$

Fouling was also modelled using Mehta’s model [42], which focuses on the two main phases during a filtration process: in the first phase (domain 1), corresponding to the initial stages of the filtration, a rapid flux decline occurs. In the second phase (domain 2), the rate of the flux decline softens until the flux becomes quasi-stable [43]. The model is expressed as follows (Eq. 4):

$$J = J_0 - J_{\infty 1} \cdot \exp^{-\alpha t} + (J_{\infty 1} - J_{\infty 2}) \cdot \exp^{-\beta t} + J_{\infty 2} \qquad (4)$$

Where $J_{\infty 1}$ is the flux at the end of domain 1 (m·/s); $J_{\infty 2}$ is the flux at the end of domain 2 (i.e., at the end of the experiment) (m/s); and α (1/min) and β (1/min) are two constants determined experimentally that describe the rate of flux decline associated with the membrane fouling and the concentration polarization and gel layer formation, respectively.

Parameters of the Hermia’s and Mehta’s models were adjusted to obtain the best fit by minimizing the sum of residuals (SR), where the residual was equal to the difference between a data point and the model prediction. Relative error distributions of each model were calculated by determining relative error of each point with Eq. 5:

$$e_i = \left(\frac{\left| J_{exp,i} - J_{m,i} \right|}{J_{exp,i}} \right) * 100 \qquad (5)$$

Where e_i is the relative error of point i, $J_{exp,i}$ is J measured in the experiment and $J_{m,i}$ is J predicted by the model.

2.4. Analytical methods

Humic acid was extracted from leachate or permeate samples following the method proposed by Thurman and Malcolm [44]: 10 mL of the corresponding sample were acidified until a pH lower than 1 was reached to precipitate it. The sample was then filtered, and the solid humic acid was redissolved in a 7 g/L NaOH solution. Absorbance at 465 nm and 665 nm in both samples and extracts were measured in a UV/Vis spectrophotometer (Thermo Scientific, Heλios γ), and a calibration curve was constructed by dissolving different amounts of commercial humic acid in a 7 g/L NaOH solution.

Chemical oxygen demand was determined by the dichromate method according to standard methods [45]. pH and conductivity were measured using a pH-meter Basic 20 and a conductivity-meter CM 35 (CRISON, Spain), respectively. Colour number (CN) was determined by measuring the spectral absorption coefficients (SAC) at 436, 525 and 620nm, and according to the following equation:

$$CN = \frac{SAC_{436}^2 + SAC_{525}^2 + SAC_{620}^2}{SAC_{436} + SAC_{525} + SAC_{620}}$$

The biological oxygen demand (BOD_5) was measured by manometry following the Warburg method [46]. The total phenol content was determined by the Folin-Ciocalteu method [47]. The acute toxicity was measured by bioluminescence essays using *Vibrio fischeri*. Finally, the concentration of metals and other elements were determined by an Agilent 7500ce Inductively Coupled Plasma Mass Spectrometer (Agilent Technologies, CA, USA).

3. Results

3.1. Fouling and retention

WO proved to be an effective treatment to oxidise recalcitrant compounds, achieving COD reductions of 59.2% for the MT leachate and 32.6% for the BT leachate (Table 4.42). These results indicated a higher refractory character to oxidation of the BT leachate due to the biological pretreatment, which removed the biodegradable matter present in it. The values of COD removals obtained for the MT leachate were similar to those reported in other works, in which non-catalytic WO [28] or catalytic WO [48] were used. Thus, Zhou et al. achieved COD reductions of approximately 30% when Ce/γ-Al_2O_3 (2 g/L) was used as catalyst at 180ºC and 250 bar for 120 min [20]. Similar removals (27%) were also obtained using catalytic wet peroxide oxidation for 60 min with Al/Fe-pillared montmorillonite as catalyst (20 g/L) [48].

Higher reductions in COD (around 80%), were achieved by combining catalytic WO with promoters, including Na_2SO_3 and H_2O_2, at temperatures and pressures in the range 150-200ºC, 70-250 bar, respectively, for reaction times between 15 and 240 min [28,30].

Additionally, the pH value increased during the WO in both MT and BT leachates. This could be attributed to the release of CO_2 generated due to the oxidation of the organic matter, resulting in a more alkaline environment. Moreover, an alkaline pH can hinder the oxidation process as CO_3^{2-} and HCO_3^- ions remain stable at high pH values, acting as radical scavengers [29].

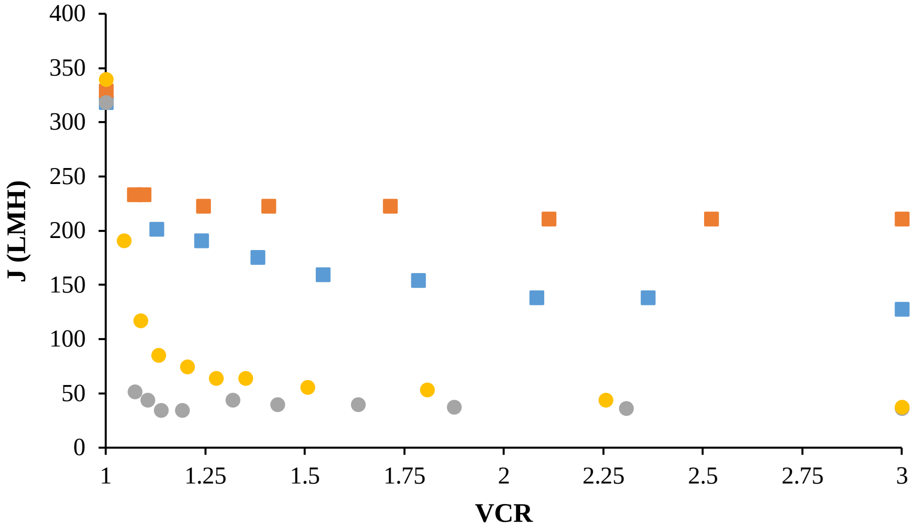

Figure 4.51. Flux evolution for the BT leachate (🟦), oxidised BT leachate (🟧), MT leachate (●) and oxidised MT leachate (●).

The final flux obtained during the filtration of the BT leachate (127 LMH) was 3.5 times higher than that of the MT leachate (35.8 LMH) (Fig. 4.51). This difference can be attributed to the lower organic matter content of the BT leachate resulting from the biological pretreatment. Additionally, after this biological pretreatment, a microfiltration step was applied to remove the activated sludge, which can also favour the subsequent ultrafiltration.

WO treatment significantly increased fluxes obtained during the ultrafiltration of the BT leachate, obtaining a final flux a 66% higher than that obtained with the untreated leachate. As for the MT leachate, during the first stages of the filtration an improvement on the permeability could be observed. Thus, the fluxes obtained with the leachate treated by WO were between 125% and 115% higher than those of the untreated leachate (before reaching a VCR of 1.25). In the case of higher VCR values (in the range 1.75 to 2.25), fluxes slightly enhanced, with values from 43% to 22% higher than in the oxidised leachate. However, the final fluxes (VCR of 3) were almost identical both for the untreated and oxidised MT leachate. This is likely a result of the pores closing more intensely as the ultrafiltration progressed due to increasing concentrations. This finding aligned with that reported by Maartens et al. [49], who also observed this behaviour during the ultrafiltration of natural organic matter with polysulphone membranes at 20ºC and 1.5 bar.

Table 4.42. Physicochemical and rejection values for the MT and BT leachates.

	MT leachate	**Oxidised MT leachate**	**BT leachate**	**Oxidised BT leachate**
pH	7.86	9.93	7.62	9.69
COD (mg O_2/L)	4591	1873	1601	1079
R_{COD}	0.39	0.21	0.42	0.06
Humic acids (mg/L)	210	135	88	69
$R_{Humic\ acids}$	0.73	0.42	0.46	0.45

Higher humic acid content was found in the MT leachate compared to the BT one. This difference may be attributed to the biological treatment (nitrification-denitrification process) in the MBR, which facilitated the removal of humic acid. This finding aligns with the results reported by Ryu et al. [50], who achieved biosorption removals from 5 to 31% when wastewaters containing 50 mg/L of humic acid were treated in MBR systems with sludge concentrations from 200 to 1000 mg/L. The highest humic acid rejections (73%) were obtained when filtering the untreated MT leachate, while the humic acid rejections for the other leachates were below 50%. The humic acid rejection value for the untreated MT leachate was similar to that reported for other authors, who obtained retentions of 74% for natural brown waters (85 mg/L), and 71% for commercial humic acid solution (85 mg/L) after 300 min of ultrafiltration with polysulphone membranes at 20ºC and 1.5 bar [49]. However, our value was lower compared to that reported by Küchler and Miekeley [51], who attained retentions of 80-90% for commercial humic acid solutions, since hydrophilic membranes (Amicon YM2) with lower MWCO (1 kDa) were used. Therefore, these rejections could potentially be improved by selecting a membrane with a different MWCO. In this context, Li et al. [52] determined that membranes with MWCOs of 30-50 kDa were optimal for the recovery of humic acids from primary and secondary sewage sludge. However, the concentration of humic acid in both MT and BT leachates was too low to be used as a fertilizer, requiring an over 100-fold concentrationto meet the required standard of 30 g/L [53]. Apart from this application, humic acids exhibit good surfactant properties [9], making them useful in various industries, such as the manufacturing of dyes in the textile industry [8]. Moreover, the oxidation of humic acids improves their foaming capacity by modifying their molecular size and functional groups [54], potentially increasing the value of humic acids recovered from the oxidised leachates.

As previously indicated, a COD reduction of 59.2% was achieved after the WO treatment of MT leachate. When combined with the subsequent ultrafiltration, this resulted in a total COD reduction of 67.8%, yielding final COD value of 1480 mg O_2/L in the permeate. This is in contrast to the COD value of the permeate in the raw MT leachate, which was approximately 1.9 times higher (2801 mg O_2/L). Regarding the BT leachate, a COD reduction of 32.6% was reached after WO, although the average COD retention of the oxidised BT leachate dropped to 0.6%, compared to the average COD retention of 42% of the unoxidized BT leachate.

3.2. Modelling

3.2.1. Hydraulic resistances

The results obtained with the resistance-in-series model are shown in Fig. 4.52.

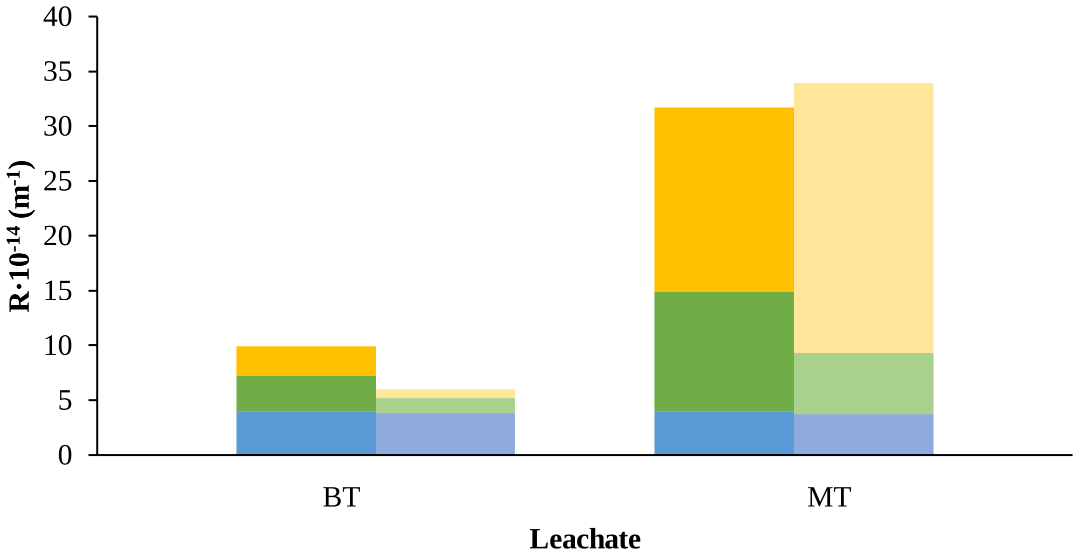

Figure 4.52. Membrane resistances for untreated (🟦) and oxidised (🟦) leachates, irreversible fouling resistance for raw (🟩) and oxidised (🟩) leachates, and reversible fouling resistance for raw (🟧) and oxidised (🟨) leachates.

The WO treatment of the BT leachate resulted in a 40% reduction in the total resistance compared to the untreated leachate. Both reversible and irreversible resistances significant decreases, with the values being 3.3 and 3 times lower, respectively, than those of the untreated leachate (reversible: $2.7 \cdot 10^{14}$ 1/m; irreversible: $3.2 \cdot 10^{14}$ 1/m). Gao et al. [55] also reported a positive effect of pre-treatment with ozonation when ultrafiltering a secondary effluent from a wastewater treatment plant using polyethersulfone membrane. In their study, they achieved a 70% reduction in normalised reversible resistance (R_{rev}/R_m), and a 77% reduction in normalised irreversible resistance (R_{irrev}/R_m). In our case, the reductions in R_{rev}/R_m (69%) and R_{irrev}/R_m (58%) compared to the untreated BT leachates (R_{rev}/R_m=0.68; R_{irrev}/R_m=0.82) were similar to those obtained by Gao et al. In the case of MT leachate, the oxidation treatment did not cause a significative change in the total resistance but did alter its nature. Thus, the resistance of the irreversible fouling decreased importantly, with the value being approximately 2 times lower than that of the untreated leachate ($1.1 \cdot 10^{15}$ 1/m). This fact could be attributed to the change in the size of foulants caused by WO treatment. This finding is in agreement with that reported for other advanced oxidation processes, which led to the breakdown of large molecular weight compounds [55]. In this context, it has been reported that leachates containing lower-size fouling agents tended to produce more reversible fouling in comparison to those with high molecular weight foulants [56]. The shift in fouling characteristics towards a more reversible nature is significant concerning membrane cleaning and lifespan. Reversible fouling can be cleaned by physical methods and does not impact membrane performance and lifespan as much as irreversible fouling does [57].

3.2.2. Flux modelling

The results of the flux modelling are shown in Fig. 4.53 and in Table 4.43. The main fouling mechanism during the filtration of the MT leachates (both untreated and oxidised) was CF, which is characteristic of reversible fouling. Regarding the BT leachates, no Hermia fitted the experimental data properly. Nevertheless, the models with less SR were the pore blocking-based ones (especially IPB), which tend to be more irreversible [58]. These results are in accordance with the resistance-in-series model, as the main resistance during the filtration of MT leachates was produced by reversible fouling, while, in the case of the BT leachates, the fouling was mainly irreversible.

One reason of this difference might be the difference on the fouling nature could be due to the different filtration durations, as BT leachates were filtered for less time (Fig. 4.53). Indeed, the fact that pore blocking occurs in the early stages of the filtration and is replaced by CF mechanism has been reported by several authors [57,59] and it is supported by Mehta’s model [42].

Considering Mehta’s model, it showed the best fitting for both untreated and oxidised leachates. This model analyses the role of membrane fouling (parameter α) and concentration polarization and gel layer formation (parameter β) on the flux decline. Higher α values represent faster initial membrane fouling, while higher β values imply faster stabilisation of the flux by the establishment of the concentration polarization gradient and gel layer formation.

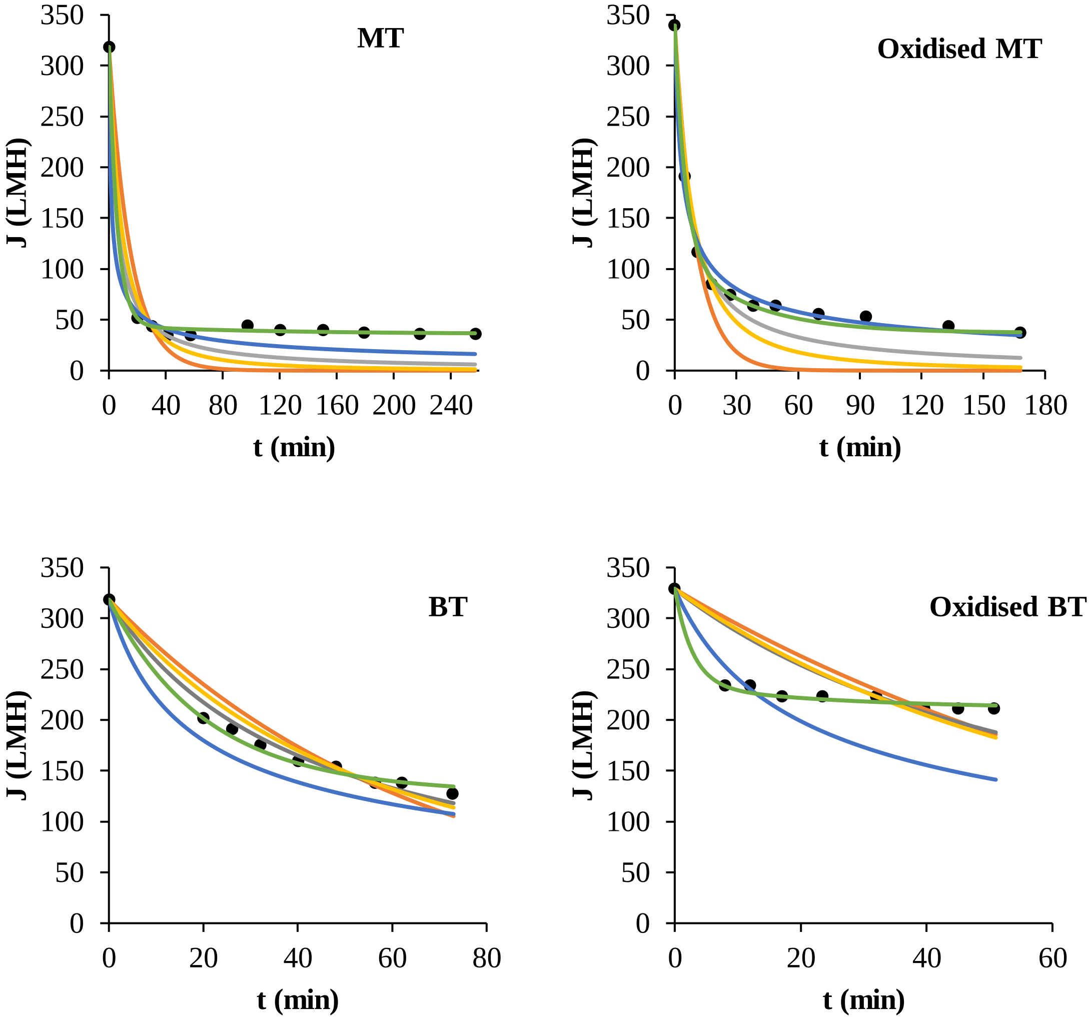

Figure 4.53. Hermia (CPB [—], IPB [—], PPB [—] and CF [—]) and Mehta (—) flux models for the obtained experimental fluxes (●).

WO had different effects on the parameters depending on the leachate. The oxidation of MT leachate caused a faster establishment of the concentration polarization gradient and gel layer formation, while it had the opposite effect for the BT leachate. As for the role of the initial fouling on the flux decline, it remained almost unchanged for MT leachate, while it gained importance after the oxidation of the BT leachate, the α parameter being approximately 9 times higher after WO ($3.49 \cdot 10^{-1}$).

Table 4.43. Fitting parameters for the adjusted models.

		MT	**Oxidised MT**	**BT**	**Oxidised BT**
Hermia's models					
CPB	**K_b (1/min)**	$6.61 \cdot 10^{-2}$	$9.71 \cdot 10^{-2}$	$1.51 \cdot 10^{-2}$	$1.12 \cdot 10^{-2}$
	SR	305.30	398.10	129.97	244.24
SPB	**K_i (1/m)**	$6.34 \cdot 10^{-3}$	$6.03 \cdot 10^{-3}$	$1.03 \cdot 10^{-3}$	$7.40 \cdot 10^{-4}$
	SR	250.95	276.92	90.07	226.42
IPB	**K_p (1/m)**	$6.31 \cdot 10^{-4}$	$4.58 \cdot 10^{-4}$	$7.30 \cdot 10^{-5}$	$4.48 \cdot 10^{-5}$
	SR	194.36	171.42	56.36	208.37
CF	**K_c (min/m^2)**	$7.29 \cdot 10^{-6}$	$2.43 \cdot 10^{-6}$	$5.26 \cdot 10^{-7}$	$4.01 \cdot 10^{-7}$
	SR	122.63	77.93	177.66	310.66
Mehta's model					
$J_{\infty 1}$ **(LMH)**		43.77	116.71	201.60	233.43
α (1/min)		$1.70 \cdot 10^{-1}$	$1.98 \cdot 10^{-1}$	$4.00 \cdot 10^{-2}$	$3.49 \cdot 10^{-1}$
β (1/min)		$8.32 \cdot 10^{-3}$	$2.90 \cdot 10^{-2}$	$6.12 \cdot 10^{-2}$	$3.74 \cdot 10^{-2}$
SR		23.67	42.98	36.42	37.35

3.3. Water reclamation

In addition to humic acid recovery, the possibility of reclaiming water from treated leachate was considered. Maximum allowed values for different parameters for wastewater discharge in secondary treatment plants [60] and final values in the treated permeates are shown in Table 4.44. As only pre-treated (WO and/or biological treatment) leachates met the requirements for discharge into public sanitation systems in terms of COD (<1600 mg O_2/L) [60], raw MT leachate was not taken into consideration in this section.

Table 4.44. Parameters for wastewater discharge into public sanitation systems.

			Values in the final permeate		
		Maximum allowed values	**Oxidised MT leachate**	**BT leachate**	**Oxidised BT leachate**
pH		**6-9**	9.93	7.62	9.69
Colour number		**Undetectable after 1/40 dilution**	0.003	0.005	0.001
Conductivity (µS/cm)		**5000**	12100	12500	11300
BOD_5 (mg/L)		**1000**	280	19	150
COD (mg/L)		**1600**	1480	928	1014
Nitrogen as ammonia (mg/L)		**60**	288	47	48
Metals	*Al (µg/L)*	**15000**	<4.056	54.83	<4.056
	As (µg/L)	**1000**	135.99	128.39	68.61
	Ba (µg/L)	**10000**	39.53	157.90	49.02
	B (µg/L)	**3000**	8499.02	7511.23	6346.27
	Cd (µg/L)	**500**	0.25	0.46	0.14
	Cu (µg/L)	**5000**	116.23	60.11	66.46
	Cr (µg/L)	**5000**	1312.02	242.51	1788.84
	Sn (µg/L)	**5000**	<169.679	0.36	<169.679
	Fe (µg/L)	**10000**	25.91	95.47	6747.29
	Mn (µg/L)	**2000**	4.57	27.93	<197.148
	Hg (µg/L)	**100**	33.13	6.73	28.99
	Ni (µg/L)	**5000**	196.33	151.17	523.54
	Ag (µg/L)	**1000**	5.56	1.18	1.30
	Pb (µg/L)	**1000**	3.75	4.35	0.43
	Se (mg/L)	**0.5**	<7.276	<7.276	<7.276
	Zn (µg/L)	**10000**	62.77	133.60	14.21
Total phenols (mg/L)		**2**	16	16	9
Toxicity (% inhibition)		**-**	57	39	47

After the biological treatment and/or wet oxidation, and the subsequent ultrafiltration, most parameters met the requirements for discharge into public sanitation systems, with only a few parameters exceeding the limits. WO caused the pH of both MT and BT leachates to increase to values slightly higher than the permissible pH range for discharge (6-9), being necessary a neutralization prior to discharge. Conductivity, total phenols and boron also exceeded the maximum permitted levels in all the leachates. Furthermore, ammonia nitrogen was also above the permitted concentration in the MT leachate. Various techniques such as absorption, electrodialysis, ion exchange, flocculation/coagulation or subsequent nanofiltration or reverse osmosis could be employed to meet the required values for these last parameters [61–64].

4. Conclusions

The integrated treatment of wet oxidation followed by membrane ultrafiltration for MT and BT leachates resulted intreated effluents that met the discharge requirements in terms of organic matter (<1600 mg O_2/L). On the other hand, humic acid was efficiently recovered by membrane filtration from untreated MT leachate, achieving rejection up to 73%. However, the modifications caused by the oxidation process could improve the potential valorisation of humic acids. Thus, the analysis of membranes with lower MWCO can be interesting to optimize the recovery of humic acids.

Flux decay was much more severe during the ultrafiltration of the MT leachate, although most of the fouling responsible for this permeation loss was reversible, with a R_{rev} of 53% of the total resistance. Nevertheless, for the BT leachate, the main fouling was irreversible, the value of R_{irrev} being 33% of the total resistance. Wet oxidation had a slight positive effect on MT leachate filtration as a higher mean flux for oxidised leachate was obtained for a VCR of 3 in less time). The effect of oxidation was more noticeable for the BT leachate, achieving a 66% higher flux at VCR of 3 compared to the untreated one. Besides, it also improved fouling significantly, with a reduction of 40% of the total resistance compared to the untreated leachate. The main fouling mechanism was CF (mainly reversible) for both MT leachates, and IPB (irreversible) for BT leachates, which was in accordance with the resistance-in-series model. Mehta model was the model that better fitted the experimental fluxes in all cases.

The requirements for discharge into public sanitation systems were almost met after the integrated treatments, although treatments to lower total phenols, conductivity and boron (and pH and ammonia, depending on the case) should be conducted before the discharge.

References

[1] P. Ghosh, I.S. Thakur, A. Kaushik, Bioassays for toxicological risk assessment of landfill leachate: A review, Ecotoxicol. Environ. Saf. 141 (2017) 259–270. doi:10.1016/j.ecoenv.2017.03.023.

[2] T. Karak, R.M. Bhagat, P. Bhattacharyya, Municipal solid waste generation, composition, and management: The world scenario, Crit. Rev. Environ. Sci. Technol. 42 (2012) 1509–1630. doi:10.1080/10643389.2011.569871.

[3] Y. Peng, Perspectives on technology for landfill leachate treatment, Arab. J. Chem. 10 (2017) S2567–S2574. doi:10.1016/j.arabjc.2013.09.031.

[4] F.A. El-Gohary, G. Kamel, Characterization and biological treatment of pre-treated landfill leachate, Ecol. Eng. 94 (2016) 268–274. doi:10.1016/j.ecoleng.2016.05.074.

[5] F.N. Ahmed, C.Q. Lan, Treatment of landfill leachate using membrane bioreactors: A review, Desalination. 287 (2012) 41–54. doi:10.1016/j.desal.2011.12.012.

[6] S. Renou, J.G. Givaudan, S. Poulain, F. Dirassouyan, P. Moulin, Landfill leachate treatment: Review and opportunity, J. Hazard. Mater. 150 (2008) 468–493. doi:10.1016/j.jhazmat.2007.09.077.

[7] M. Morozesk, M.M. Bonomo, I. da C. Souza, L.D. Rocha, I.D. Duarte, I.O. Martins, L.B. Dobbss, M.T.W.D. Carneiro, M.N. Fernandes, S.T. Matsumoto, Effects of humic acids from landfill leachate on plants: An integrated approach using chemical, biochemical and cytogenetic analysis, Chemosphere. 184 (2017) 309–317. doi:10.1016/j.chemosphere.2017.06.007.

[8] X. Zhu, J. Liu, L. Li, G. Zhen, X. Lu, J. Zhang, H. Liu, Z. Zhou, Z. Wu, X. Zhang, Prospects for humic acids treatment and recovery in wastewater: A review, Chemosphere. 312 (2023) 137193. doi:10.1016/j.chemosphere.2022.137193.

[9] S. Salati, G. Papa, F. Adani, Perspective on the use of humic acids from biomass as natural surfactants for industrial applications, Biotechnol. Adv. 29 (2011) 913–922. doi:10.1016/j.biotechadv.2011.07.012.

[10] T.A. Kurniawan, W.H. Lo, G.Y.S. Chan, Physico-chemical treatments for removal of recalcitrant contaminants from landfill leachate, J. Hazard. Mater. 129 (2006) 80–100. doi:10.1016/j.jhazmat.2005.08.010.

[11] K.Y. Foo, B.H. Hameed, An overview of landfill leachate treatment via activated carbon adsorption process, J. Hazard. Mater. 171 (2009) 54–60. doi:10.1016/j.jhazmat.2009.06.038.

[12] M. Verma, R. Naresh Kumar, Can coagulation–flocculation be an effective pre-treatment option for landfill leachate and municipal wastewater co-treatment?, Perspect. Sci. 8 (2016) 492–494. doi:10.1016/j.pisc.2016.05.005.

[13] S.E.H. Comstock, T.H. Boyer, K.C. Graf, T.G. Townsend, Effect of landfill characteristics on leachate organic matter properties and coagulation treatability, Chemosphere. 81 (2010) 976–983. doi:10.1016/j.chemosphere.2010.07.030.

[14] J. Yang, M. Monnot, T. Eljaddi, L. Ercolei, L. Simonian, P. Moulin, Ultrafiltration as tertiary treatment for municipal wastewater reuse, Sep. Purif. Technol. 272 (2021) 118921. doi:10.1016/j.seppur.2021.118921.

[15] S. Renou, J.G. Givaudan, S. Poulain, F. Dirassouyan, P. Moulin, Landfill leachate treatment: Review and opportunity., J. Hazard. Mater. 150 (2008) 468–493. doi:10.1016/j.jhazmat.2007.09.077.

[16] R. Rautenbach, T. Linn, L. Eilers, Treatment of severely contaminated waste water by a combination of RO, high-pressure RO and NF - Potential and limits of the process, J. Memb. Sci. 174 (2000) 231–241. doi:10.1016/S0376-7388(00)00388-4.

[17] F.C. Moreira, R.A.R. Boaventura, E. Brillas, V.J.P. Vilar, Electrochemical advanced oxidation processes: A review on their application to synthetic and real wastewaters, Appl. Catal. B Environ. 202 (2017) 217–261. doi:10.1016/j.apcatb.2016.08.037.

[18] H. Zeng, S. Liu, B. Chai, D. Cao, Y. Wang, X. Zhao, Enhanced Photoelectrocatalytic Decomplexation of Cu-EDTA and Cu Recovery by Persulfate Activated by UV and Cathodic Reduction, Environ. Sci. Technol. 50 (2016) 6459–6466. doi:10.1021/acs.est.6b00632.

[19] M. Hassan, N. Pous, B. Xie, J. Colprim, M.D. Balaguer, S. Puig, Influence of iron species on integrated microbial fuel cell and electro-Fenton process treating landfill leachate, Chem. Eng. J. 328 (2017) 57–65. doi:10.1016/j.cej.2017.07.025.

[20] Y. Zhou, S. Xu, Y. Zhang, X. Hu, F. Li, X. Chen, H. Cai, J. Wang, L. Shi, X. Chen, Synergistic effect over a remarkable durable and active polymetallic Ru-doped Fe-Co-Ce/γ-Al2O3 nanocatalyst: Interfacial Lewis acid-base pair dependent reaction mechanism for landfill leachate, Chem. Eng. J. 382 (2020) 122938. doi:10.1016/j.cej.2019.122938.

[21] M. Sillanpää, M.C. Ncibi, A. Matilainen, Advanced oxidation processes for the removal of natural organic matter from drinking water sources: A comprehensive review, J. Environ. Manage. 208 (2018) 56–76. doi:10.1016/j.jenvman.2017.12.009.

[22] S.T. Kolaczkowski, P. Plucinski, F.J. Beltran, F.J. Rivas, D.B. McLurgh, Wet air oxidation: A review of process technologies and aspects in reactor design, Chem. Eng. J. 73 (1999) 143–160. doi:10.1016/S1385-8947(99)00022-4.

[23] H. Debellefontaine, J.N. Foussard, Wet air oxidation for the treatment of industrial wastes. Chemical aspects, reactor design and industrial applications in Europe, Waste Manag. 20 (2000) 15–25. doi:10.1016/S0956-053X(99)00306-2.

[24] T. Mandal, S. Maity, D. Dasgupta, S. Datta, Advanced oxidation process and biotreatment: Their roles in combined industrial wastewater treatment, Desalination. 250 (2010) 87–94. doi:10.1016/j.desal.2009.04.012.

[25] S. Collado, A. Laca, M. Diaz, Decision criteria for the selection of wet oxidation and conventional biological treatment, J. Environ. Manage. 102 (2012) 65–70. doi:10.1016/j.jenvman.2012.02.018.

[26] K. V. Padoley, P.D. Tembhekar, T. Saratchandra, A.B. Pandit, R.A. Pandey, S.N. Mudliar, Wet air oxidation as a pretreatment option for selective biodegradability enhancement and biogas generation potential from complex effluent, Bioresour. Technol. 120 (2012) 157–164. doi:10.1016/j.biortech.2012.06.051.

[27] P. Oulego, S. Collado, A. Laca, M. Díaz, Impact of leachate composition on the advanced oxidation treatment, Water Res. 88 (2016) 389–402. doi:10.1016/j.watres.2015.09.048.

[28] A. Garg, A. Mishra, Wet oxidation-an option for enhancing biodegradability of leachate derived from municipal solid waste (msw) landfill, Ind. Eng. Chem. Res. 49 (2010) 5575–5582. doi:10.1021/ie100003q.

[29] P. Oulego, S. Collado, A. Laca, M. Díaz, Tertiary treatment of biologically pre-treated landfill leachates by non-catalytic wet oxidation, Chem. Eng. J. 273 (2015) 647–655. doi:10.1016/j.cej.2015.03.089.

[30] Á. Anglada, A. Urtiaga, I. Ortiz, D. Mantzavinos, E. Diamadopoulos, Treatment of municipal landfill leachate by catalytic wet air oxidation: Assessment of the role of operating parameters by factorial design, Waste Manag. 31 (2011) 1833–1840. doi:10.1016/j.wasman.2011.03.023.

[31] Y. Zhai, L. Zhu, Y. Zhu, C. Peng, T. Wang, X. Liu, C. Li, G. Zeng, Simultaneous total organic carbon and humic acid removals for landfill leachate using subcritical water catalytic oxidation based on response surface methodology, Water. Air. Soil Pollut. 227 (2016). doi:10.1007/s11270-016-2977-x.

[32] Y.L. Zhang, Y.L. Sun, Optimization of Process Conditions on Landfill Leachate Treatment by CWAO Method, Adv. Mater. Res. 849 (2014) 137–141. doi:10.4028/WWW.SCIENTIFIC.NET/AMR.849.137.

[33] O. Suárez-Iglesias, J.L. Urrea, P. Oulego, S. Collado, M. Díaz, Valuable compounds from sewage sludge by thermal hydrolysis and wet oxidation. A review, Sci. Total Environ. 584–585 (2017) 921–934. doi:10.1016/J.SCITOTENV.2017.01.140.

[34] J.L. Urrea, M. García, S. Collado, P. Oulego, M. Díaz, Sludge hydrothermal treatments. Oxidising atmosphere effects on biopolymers and physical properties, J. Environ. Manage. 206 (2018) 284–290. doi:10.1016/j.jenvman.2017.10.043.

[35] J.L. Urrea, S. Collado, P. Oulego, M. Díaz, Formation and Degradation of Soluble Biopolymers during Wet Oxidation of Sludge, ACS Sustain. Chem. Eng. 5 (2017) 3011–3018. doi:10.1021/ACSSUSCHEMENG.6B02664.

[36] J.L. Urrea, S. Collado, P. Oulego, M. Díaz, Effect of wet oxidation on the fingerprints of polymeric substances from an activated sludge, Water Res. 105 (2016) 282–290. doi:10.1016/j.watres.2016.09.004.

[37] L. Pola, S. Collado, P. Oulego, M. Díaz, Production of carboxylic acids from the non-lignin residue of black liquor by hydrothermal treatments, Bioresour. Technol. 284 (2019) 105–114. doi:10.1016/j.biortech.2019.03.066.

[38] J. Hermia, Constant Pressure Blocking Filtration Laws - Application Topower-Law Non-Newtonian Fluids., Trans Inst Chem Eng. V 60 (1982) 183–187.

[39] M. Abbasi, R.S. Mohammad, A. Salahi, B. Mirza, Modeling of membrane fouling and flux decline in microfiltration of oily wastewater using ceramic membranes, Chem. Eng. Commun. 199 (2012) 78–93. doi:10.1080/00986445.2011.570391.

[40] M. Peyravi, M. Jahanshahi, S. Khalili, Fouling of WO3 nanoparticle-incorporated PSf membranes in ultrafiltration of landfill leachate and dairy a combined wastewaters: An investigation using model, Chinese J. Chem. Eng. 25 (2017) 741–751. doi:10.1016/j.cjche.2016.12.001.

[41] Z.F. Cui, H.S. Muralidhara, Membrane Technology, Elsevier, 2010. doi:10.1016/C2009-0-19129-8.

[42] B. Mehta, Processing of model compositional whey solutions with pressure driven membranes, Ohio State University, 1973.

[43] M. Mondor, B. Girard, C. Moresoli, Modeling flux behavior for membrane filtration of apple juice, Food Res. Int. 33 (2000) 539–548. doi:10.1016/S0963-9969(00)00089-2.

[44] E.M. Thurman, R.L. Malcolm, Preparative Isolation of Aquatic Humic Substances, Environ. Sci. Technol. 15 (1981) 463–466. doi:10.1021/es00086a012.

[45] APHA; AWWA and WEF, Standard Methods for the Examination of Water and Wastewater, Am. Public Work. Assoc. (2017) 1469.

[46] D.H. Caldwell, W.F. Langelier, Manometric measurement of the biochemical oxygen demand of sewage, Sewage Work. J. 20 (1948) 202–218.

[47] R.M. Lamuela-Raventós, Folin–Ciocalteu method for the measurement of total phenolic content and antioxidant capacity, Meas. Antioxid. Act. Capacit. Recent Trends Appl. (2017) 107–115. doi:10.1002/9781119135388.CH6.

[48] L.A. Galeano, M.Á. Vicente, A. Gil, Treatment of municipal leachate of landfill by fenton-like heterogeneous catalytic wet peroxide oxidation using an Al/Fe-pillared montmorillonite as active catalyst, Chem. Eng. J. 178 (2011) 146–153. doi:10.1016/j.cej.2011.10.031.

[49] A. Maartens, P. Swart, E.P. Jacobs, Humic membrane foulants in natural brown water: characterization and removal, Desalination. 115 (1998) 215–227. doi:10.1016/S0011-9164(98)00041-1.

[50] J.H. Ryu, J.H. Jung, K.Y. Park, W.J. Song, B.G. Choi, J.H. Kweon, Humic acid removal and microbial community function in membrane bioreactor, J. Hazard. Mater. 417 (2021). doi:10.1016/j.jhazmat.2021.126088.

[51] I.L. Küchler, N. Miekeley, Ultrafiltration of humic compounds through low molecular mass cut-off level membranes, Sci. Total Environ. 154 (1994) 23–28. doi:10.1016/0048-9697(94)90610-6.

[52] H. Li, Y. Li, Y. Jin, S. Zou, C. Li, Recovery of sludge humic acids with alkaline pretreatment and its impact on subsequent anaerobic digestion, J. Chem. Technol. Biotechnol. 89 (2014) 707–713. doi:10.1002/jctb.4173.

[53] H. Li, Y. Li, S. Zou, C. Li, Extracting humic acids from digested sludge by alkaline treatment and ultrafiltration, J. Mater. Cycles Waste Manag. 16 (2014) 93–100. doi:10.1007/s10163-013-0153-6.

[54] Fikret Koc; Ahmet Ergun; Deniz Yilmaz; Serdar Soylemez, Use of oxidized humic acid its salts and derivatives in laundry compositions, WO2015171091A1, 2015.

[55] K. Gao, H. Yang, H. Liu, B. Dong, Alleviating Ultrafiltration Membrane Fouling Caused by Effluent Organic Matter Using Pre-Ozonation: A Perspective of EEM and Molecular Weight Distribution, Membranes (Basel). 13 (2023). doi:10.3390/membranes13040452.

[56] S. Collado, D. Núñez, P. Oulego, F.A. Riera, M. Díaz, Effect of landfill leachate ageing on ultrafiltration performance and membrane fouling behaviour, J. Water Process Eng. 36 (2020). doi:10.1016/j.jwpe.2020.101291.

[57] W. Guo, H.H. Ngo, J. Li, A mini-review on membrane fouling, Bioresour. Technol. 122 (2012) 27–34. doi:10.1016/j.biortech.2012.04.089.

[58] G. Di Bella, D. Di Trapani, A brief review on the resistance-in-series model in membrane bioreactors (MBRs), Membranes (Basel). 9 (2019) 24. doi:10.3390/membranes9020024.

[59] A.R. Costa, M.N. de Pinho, M. Elimelech, Mechanisms of colloidal natural organic matter fouling in ultrafiltration, J. Memb. Sci. 281 (2006) 716–725. doi:10.1016/J.MEMSCI.2006.04.044.

[60] BOE-A-2002-14187, Ley 5/2002, de 3 de junio, sobre vertidos de aguas residuales industriales a los sistemas públicos de saneamiento., n.d.

[61] N. Parsa, G. Khajouei, M. Masigol, H. Hasheminejad, A. Moheb, Application of Electrodialysis Process for Reduction of Electrical Conductivity and COD of Water Contaminated By Composting Leachate, Civ. Eng. J. 4 (2018) 1034. doi:10.28991/cej-0309154.

[62] P. Seruga, M. Krzywonos, J. Pyzanowska, A. Urbanowska, H. Pawlak-Kruczek, Ł. Niedźwiecki, Removal of ammonia from the municipal waste treatment effuents using natural minerals, Molecules. 24 (2019). doi:10.3390/molecules24203633.

[63] L.G.C. Villegas, N. Mashhadi, M. Chen, D. Mukherjee, K.E. Taylor, N. Biswas, A Short Review of Techniques for Phenol Removal from Wastewater, Curr. Pollut. Reports. 2 (2016) 157–167. doi:10.1007/s40726-016-0035-3.

[64] X. Liu, C. Xu, P. Chen, K. Li, Q. Zhou, M. Ye, L. Zhang, Y. Lu, Advances in Technologies for Boron Removal from Water: A Comprehensive Review, Int. J. Environ. Res. Public Health. 19 (2022). doi:10.3390/ijerph191710671.

4.3. Discusión global

Con la disminución de los recursos naturales, el aumento de los flujos de residuos y las preocupaciones ambientales, la necesidad global urgente de prácticas sostenibles de gestión de residuos y recuperación de recursos nunca ha sido tan crítica. A lo largo de los siete artículos presentados en esta tesis se han investigado y propuesto varios métodos para la recuperación de biocompuestos valiosos de diferentes corrientes de residuos, con un fuerte énfasis en los principios de la economía circular. Se ha investigado en lo relativo a la recuperación de proteínas, ácidos húmicos, carbohidratos, ácidos orgánicos de cadena corta, lignina. Las posibles aplicaciones de estos biocompuestos abarcan múltiples campos, tales como producción de biocombustibles e industrias agroalimentaria, farmacéutica, textil o química, entre otras, lo cual subraya la importancia de realizar la transición de los métodos tradicionales de eliminación de residuos a una economía circular, y el potencial de estas actividades para impulsar las economías sostenibles del futuro.

En base al trabajo realizado, cabe destacar que las técnicas de pretratamiento influyen significativamente en la eficiencia de la recuperación de compuestos. En función del tipo de corriente estudiada, la oxidación húmeda, la deslignificación o la filtración con membranas fueron pasos críticos para mejorar la calidad dichas corrientes residuales para su procesamiento posterior y maximizar la extracción de compuestos valiosos.

La aplicación de la filtración por membrana como herramienta de purificación fue un tema central a lo largo de toda la tesis. El tipo de membrana, junto con su tamaño de corte, desempeñan un papel crucial a la hora de optimizar la selectividad y retención de los compuestos deseados. En este sentido, es importante evaluar dónde se quiere obtener el compuesto de interés, atendiendo a las dos corrientes (retenido y permeado) que separa la membrana. A lo largo de esta tesis, se ha buscado tanto recuperar el compuesto de interés en el retenido, concentrándolo (por ejemplo, los ácidos húmicos en el lixiviado); como en el permeado, separando el compuesto de interés de otras moléculas de mayor tamaño (los ácidos orgánicos en el licor negro o en el lodo oxidado); o ambas a través de las etapas de un proceso combinado (fraccionamiento del lodo parcialmente oxidado para separar proteínas de ácidos húmicos y concentrarlos posteriormente). Es importante tener en cuenta que junto con las moléculas de interés se producirá la separación de compuestos no deseados. Por ejemplo, en nuestro caso, los iones metálicos presentes en el lodo oxidado formaron complejos con los ácidos húmicos, no pudiendo separarlos por su tamaño.

Asimismo, el ensuciamiento de la membrana ha sido estudiado con varios modelos a lo largo de los distintos trabajos experimentales. Se observó que, en la gran mayoría de los casos, el ensuciamiento causado por las distintas corrientes estudiadas, tanto en membranas cerámicas como en poliméricas, fue principalmente reversible a través de la formación de una torta de ensuciamiento. Ello resulta positivo de cara al empleo de esta tecnología a nivel industrial, ya que puede eliminarse mediante métodos físicos más sencillos como el *backflushing*, evitando limpiezas químicas y prolongando así el rendimiento y la vida útil de las membranas.

Se realizaron extracciones líquido-líquido para recuperar ácidos orgánicos tanto a partir de varios licores negros (sin pretratar, deslignificado y oxidado) como de lodo secundario oxidado y en todos los casos se observó una fuerte influencia de la matriz en los rendimientos de las extracciones, por lo que el uso de la filtración con membranas como pretratamiento previo a la extracción se justifica de cara a obtener una corriente con la menor cantidad posible de compuestos distintos a los productos de interés.

Tras el trabajo desarrollado en esta tesis, se abren diferentes direcciones por las que se podría seguir para completar la investigación realizada. Algunos de estos aspectos son:

- Caracterizar detalladamente la naturaleza de las biomoléculas recuperadas en los distintos trabajos. Así, a lo largo de la tesis, las proteínas, ácidos húmicos, carbohidratos y lignina se han tratado de forma general. Sin embargo, estos grupos de moléculas presentan mucha variabilidad interna, tanto en cuestión de peso molecular, como funcionalidades y propiedades químicas. Realizando un estudio en detalle de estas características, se puede dar un perfil más preciso de las biomoléculas recuperadas y sus posibles usos (y, por tanto, su valor comercial). En este sentido, la oxidación húmeda produce cambios en las propiedades de las moléculas estudiadas, por lo que también sería conveniente caracterizar los cambios generados por este tratamiento a nivel funcional. A modo de ejemplo, y como se ha referenciado en la discusión del apartado 4.2.3, los ácidos húmicos oxidados aumentan su poder surfactante, aumentando su valor dentro de la industria textil o de cara a su uso como componente de detergentes.

- Explorar las estrategias de recuperación indicadas en el apartado 4.1.4 que no hayan sido aplicadas a los lodos, como las técnicas de adsorción para recuperar proteínas y ácidos orgánicos. En esta línea, sería preciso estudiar más en detalle la recuperación de carbohidratos (por ejemplo, mediante cromatografía de afinidad sobre metales inmovilizados una vez aislada la mezcla proteínas/carbohidratos de los ácidos húmicos, como se propone en la Fig. 4.17) y lípidos (mediante extracción sólido-líquido o líquido-líquido), así como completar el proceso de purificación de proteínas y ácidos húmicos en lodos propuesto en la Fig. 4.17, ya que durante esta tesis solo se ha llegado a su separación parcial. Teniendo todo esto en cuenta, el siguiente paso sería probar experimentalmente la eficacia de los procesos integrados de valorización del lodo secundario de depuradora propuesto en la Fig. 4.35.
- Completar los estudios de filtración con membranas mediante el análisis de otras geometrías (*e.g.*, fibra hueca), materiales y tamaños de corte (rango de ósmosis inversa), junto con otras condiciones de filtración para optimizar los flujos y reducir el ensuciamiento. En este sentido, podrían realizarse estudios sobre flujo crítico, o sobre recubrimientos de membrana específicos para las corrientes estudiadas.
- Siguiendo con los estudios con membranas, resultaría interesante la búsqueda de métodos para separar los iones metálicos de los ácidos húmicos o las proteínas. Alternativamente, se podría estudiar la posibilidad de emplear estas biomoléculas sin necesidad de separar los metales. Para ello, sería necesario realizar estudios de toxicidad a fin de evaluar su uso en alimentación animal o como fertilizante.

- Completar la extracción líquido-líquido de ácidos orgánicos de cadena corta evaluando la eficacia de otros extractantes (por ejemplo, disolventes eutécticos profundos), así como analizando el efecto de otras variables (como el pH) en los rendimientos de las extracciones.
- Ningún sistema de gestión de residuos sostenible puede considerarse completo sin una evaluación profunda de su sostenibilidad y de los aspectos económicos relacionados. Por tanto, sería conveniente realizar una evaluación exhaustiva de la escalabilidad, rentabilidad e impacto ambiental de los procesos propuestos, para poder acercar la investigación aquí presentada a la implementación de soluciones prácticas en el mundo real.
- Extender los métodos integrados de tratamiento y recuperación a otras corrientes residuales de características similares.

Evidentemente, la compleción de todos estos puntos probablemente requeriría más años que los invertidos realizando esta tesis. Pero, citando al alpinista Makoto Fukamachi: «Las montañas no son una meta, sino un camino; y la cima, un escalón. Una vez allí, lo único que queda es seguir avanzando».

Capítulo 5.

CONCLUSIONES

CONCLUSIONES

El análisis del estado del arte en la valorización de los lodos secundarios de depuradora reveló que la investigación relacionada con la recuperación de biomoléculas se ha centrado en la obtención de lípidos, sustancias húmicas y, en menor medida, proteínas. Gracias a la revisión de otros trabajos con corrientes análogas, se han detectado los campos más prometedores en los que se puede ampliar esta investigación, como son la implementación de nuevos agentes de precipitación, la aplicación de membranas en distintos puntos de la operación integrada, el empleo de nuevas metodologías de extracción, el uso de técnicas de adsorción, o el estudio de la recuperación de carbohidratos. Desde esta perspectiva inicial, se concluyó que se considera factible desarrollar un proceso integrado para recuperar lípidos, ácidos húmicos, ácidos grasos de cadena corta y proteínas.

En cuanto al fraccionamiento de los lodos secundarios de depuradora parcialmente oxidados, los mejores resultados fueron obtenidos con membranas de polietersulfona. Las retenciones obtenidas para ácidos húmicos, proteínas y carbohidratos con membranas de polietersulfona de 50, 10 y 3 kDa abren la posibilidad de separar los ácidos húmicos de las proteínas y carbohidratos a través de un tratamiento integrado de membranas.

Durante el proceso de filtración, también se retuvieron gran parte de los iones metálicos pesados presentes en el lodo. La retención de estos metales a través de las membranas de 50 kDa se puede atribuir a la formación de complejos en estado fundamental con los ácidos húmicos, así como a la posible formación de complejos con proteínas o a la precipitación de los metales.

Por otro lado, se consiguió optimizar la producción de ácidos orgánicos de cadena corta a partir de lodos secundarios de depuradora mediante un tratamiento por oxidación húmeda en condiciones moderadas y con largos tiempos de operación.

El empleo de la ultrafiltración con membranas consiguió prepurificar los ácidos orgánicos obtenidos a partir de lodos secundarios de depuradora oxidados. A pesar de las interferencias causadas por la matriz, se consiguió alcanzar un rendimiento de extracción del 34% con una mezcla trioctilamina/tributilfosfato (1:1 v/v) al 10% en octan-1-ol, observándose un incremento del 60% del rendimiento al aumentar la temperatura hasta los 50 ºC.

En cuanto al trabajo con lixiviados, se observó que el envejecimiento del lixiviado tuvo un efecto positivo en su permeabilidad. La oxidación húmeda de los lixiviados estabilizados (maduro y tratado biológicamente) y su posterior filtración con membranas permitió una recuperación de ácidos húmicos y alcanzar los límites permitidos de descarga en la gran mayoría de parámetros requeridos.

Por otro lado, el análisis de las distintas estrategias de valorización del licor negro Kraft para la recuperación de ácidos orgánicos de cadena corta, mostró que los mayores rendimientos se obtuvieron con el proceso integrado que implicaba la deslignificación de licor negro, seguido de un paso de prepurificación con membranas y una extracción líquido-líquido. Al igual que durante la extracción desde lodos secundarios de depuradora, la matriz tuvo un impacto significativo en los rendimientos de extracción, y el aumento de temperatura hasta los 55 ºC tuvo un efecto positivo. En este caso, el extractante más adecuado fue trioctilamina al 30% (v/v) en heptano con el que se consiguieron recuperaciones de hasta el 76%.

Las características del ensuciamiento dependieron tanto del material de la membrana como de la corriente filtrada. Tanto los lodos secundarios de depuradora oxidados como los licores negros provocaron un ensuciamiento principalmente en forma de torta en todas las membranas. En cuanto a los lixiviados de vertedero, el principal ensuciamiento causado por los lixiviados joven y maduro (este último tanto sin pretratar como tras ser oxidado) fue en forma de formación de torta reversible, mientras que el provocado por el lixiviado tratado biológicamente (tanto sin oxidar como oxidado) fue mayormente irreversible, en forma de bloqueo intermedio de poro.

CONCLUSIONS

The analysis of the state-of-the-art in the valorisation of waste activated sludge revealed that research related to the recovery of biomolecules has primarily focused on obtaining lipids, humic substances, and to a lesser extent, proteins. By reviewing other analogous studies, the most promising avenues for expanding this research have been identified. These include the implementation of new precipitation agents, the use of membranes at different stages of the integrated process, the application of novel extraction methodologies, the employment of adsorption techniques, and the exploration of the recovery of carbohydrates. From this initial perspective, it was concluded that developing an integrated process to recover lipids, humic acids, short-chain fatty acids, and proteins is considered feasible.

Concerning the fractionation of partially oxidized waste activated sludge, the best results were obtained with polyethersulfone membranes. The polyethersulfone membranes, with molecular weight cutoffs of 50, 10, and 3 kDa, achieved high retentions for humic acids, proteins, and carbohydrates. This provides the possibility of separating humic acids from proteins and carbohydrates through an integrated membrane treatment.

During the filtration process, a significant portion of the heavy metal ions present in the sludge was also retained. The retention of these metals through the 50 kDa membranes can be attributed to the formation of complexes in the fundamental state with humic acids, as well as to the possible formation of complexes with proteins or the precipitation of metals.

Additionally, the optimization of short-chain organic acid production from waste activated sludge was achieved by subjecting it to wet oxidation treatment under moderate conditions for extended reaction times. The use of membrane ultrafiltration allowed for the preliminary purification of organic acids produced from oxidized waste activated sludge. Despite the interferences caused by the sludge matrix, an extraction efficiency of 34% was achieved with a mixture of trioctylamine/tributylphosphate (1:1 v/v) at 10% in octan-1-ol, and a rise in temperature up to 50 ºC resulted in a 60% increase in yield.

In the case of leachate treatment, it was observed that aging positively impacted the permeability of leachate. Wet oxidation of stabilised leachates (mature and biologically treated) followed by membrane filtration enabled the recovery of humic acids and ensured compliance with discharge limits in terms of the majority of the required values.

Furthermore, the analysis of different valorization strategies for Kraft black liquor for the recovery of short-chain organic acids showed that the highest yields were obtained with an integrated process involving black liquor delignification, followed by a membrane-based pre-purification step and liquid-liquid extraction Similarly to the extraction from waste activated sludge, the matrix had a significant impact on extraction yields, and increasing the temperature up to 55°C had a positive effect. In this case, the most suitable extractant was 30% trioctylamine (v/v) in heptane, which achieved recoveries of up to 76%.

The nature of fouling depended on both the membrane material and the filtered stream. Fouling caused by both oxidized waste activated sludge and black liquors was primarily in the form of cake formation on all membranes. Regarding landfill leachate, primary fouling, observed in both young and mature leachates (both untreated and after oxidation) was in the form of reversible cake formation, whereas the fouling in biologically treated leachate (both untreated and oxidized) was predominantly irreversible, in the form of intermediate pore blocking.

DIFUSIÓN DE LA TESIS DOCTORAL

Publicaciones

El trabajo realizado durante la tesis se ha publicado en los siguientes artículos de investigación:

- Sergio Collado, Daniel Núñez, Paula Oulego, Francisco A. Riera, Mario Díaz, Effect of landfill leachate ageing on ultrafiltration performance and membrane fouling behaviour, Journal of Water Process Engineering, Volume 36, 2020, 101291. Cuartil: Q1. Índice de impacto: 5.485.
- Daniel Núñez, Paula Oulego, Sergio Collado, Francisco A. Riera, Mario Díaz, Recovery of organic acids from pre-treated Kraft black liquor using ultrafiltration and liquid-liquid extraction, Separation and Purification Technology, Volume 284, 2022, 120274. Cuartil: Q1. Índice de impacto: 9.14.
- Daniel Núñez, Paula Oulego, Sergio Collado, Francisco A. Riera, Mario Díaz, Separation and purification techniques for the recovery of added-value biocompounds from waste activated sludge. A review, Resources, Conservation and Recycling, Volume 182, 2022, 106327. Cuartil: Q1. Índice de impacto: 13.22.
- Daniel Núñez, Paula Oulego, Mahdi Nikbakht Fini, Jens Muff, Sergio Collado, Francisco A. Riera, Mario Díaz, Membrane fractioning of pre-treated waste activated sludge for the recovery of valuable biocompounds, Journal of Water Process Engineering, Volume 55, 2023, 104086. Cuartil: Q1. Índice de impacto: 7.53.

Además, los siguientes artículos han sido enviados para su publicación:

- Daniel Núñez, Martina Zabatta, Paula Oulego, Sergio Collado, Francisco A. Riera, Mario Díaz, Production and purification of organic acids from partially oxidised waste activated sludge. Separation and Purification Technology.
- Daniel Núñez, Paula Oulego, Sergio Collado, Francisco A. Riera, Mario Díaz, Enhanced Treatment of Stabilised Landfill Leachates: Wet Oxidation and Membrane Filtration.

Por último, se encuentran pendientes de envío:

- Daniel Núñez, Paula Oulego, Mahdi Nikbakht Fini, Jorge Espina-Casado, Jens Muff, Sergio Collado, Francisco A. Riera, Mario Díaz, Heavy metal removal from hydrothermally treated waste activated sludge by ultrafiltration with polymeric membranes.

Comunicaciones en congresos y seminarios

A continuación, se indican los trabajos derivados de esta tesis doctoral presentados en formato oral o póster en seminarios y congresos:

- Comunicación oral. Lucía Pola Fernández; Daniel Núñez Díaz; Paula Oulego Blanco; Sergio Collado Alonso; José Mario Díaz Fernández. Development of an integrated wet oxidation – ultrafiltration – liquid-liquid extraction process for the production of organic acids from Kraft black liquor. 3rd International Congress of Chemical Engineering (ANQUE-ICCE 3). 19-21/06/2019, Santander (España).
- Comunicación oral. Daniel Núñez Díaz; Paula Oulego Blanco; Sergio Collado Alonso; José Mario Díaz Fernández. Tratamiento con membranas de hidrolizados de lodos. Seminario Técnico: Tratamiento de aguas industriales. 4-5/07/2019, Oviedo (España).
- Comunicación oral. Sergio Collado Alonso; Daniel Núñez Díaz; Paula Oulego Blanco; José Mario Díaz Fernández. Ultrafiltration for recovery of valuable components from hydrolysed sludge. 5th European Conference on Sludge Management (ECSM'2019). 6-8/10/2019, Lieja (Bélgica).
- Comunicación oral. Daniel Núñez Díaz; Lucía Pola Fernández; Paula Oulego Blanco; Sergio Collado Alonso; José Mario Díaz Fernández. Assessment of strategies for revalorization of Kraft black liquor. IWA Young Water Professionals (YWP) Spain 2019. 12-15/11/2019, Madrid (España).
- Comunicación oral. Daniel Núñez Díaz; Paula Oulego Blanco; Sergio Collado Alonso; Francisco Amador Riera Rodríguez, José Mario Díaz Fernández. Closing the economic circle: generation and recovery of added value biocompounds from industrial and urban waste streams. VI International Conference IMFAHE – University of Aveiro (Portugal). 25/052020, Online.
- Póster. Daniel Núñez Díaz; Paula Oulego Blanco; Sergio Collado Alonso; Mahdi Nikbakht Fini; Jens Muff; José Mario Díaz Fernández. Membrane fractioning of hydrothermally solubilized waste activated sludge for the recovery of valuable biocompounds: assessment of membrane material and size. Euromembrane Conference 2021. 28/11-2/12/2021, Copenhague (Dinamarca).
- Póster. Daniel Núñez Díaz; Paula Oulego Blanco; Sergio Collado Alonso; Mahdi Nikbakht Fini; Jorge Espina Casado; Jens Muff; José Mario Díaz Fernández. Heavy metal removal from hydrothermally treated secondary sewage sludge by ultrafiltration with polymeric membranes. Euromembrane Conference 2021. 28/11-2/12/2021, Copenhague (Dinamarca).

- Póster. Martina Zabatta; Daniel Núñez Díaz; Paula Oulego Blanco; Sergio Collado Alonso; Francisco Amador Riera Rodríguez; José Mario Díaz Fernández. Separación y purificación de ácidos orgánicos procedentes de la oxidación de lodos activados. XIV Congreso de la Mesa Española de Tratamiento de Aguas (META 2022). 1-3/06/2022, Sevilla (España).
- Póster. Daniel Núñez Díaz; Paula Oulego Blanco; Sergio Collado Alonso; Francisco Amador Riera Rodríguez; José Mario Díaz Fernández. Lixiviados de vertedero: impacto de la edad en el tratamiento por ultrafiltración. XIV Congreso de la Mesa Española de Tratamiento de Aguas (META 2022). 1-3/06/2022, Sevilla (España).
- Comunicación oral. Daniel Núñez Díaz; Martina Zabatta; Paula Oulego Blanco; Sergio Collado Alonso; Francisco Amador Riera Rodríguez; José Mario Díaz Fernández. Oxidised waste activated sludge as a source of organic acids. IWA Young Water Professionals (YWP) Spain 2022. 16-19/11/2022, Valencia (España).
- Póster. Daniel Núñez Díaz; Paula Oulego Blanco; Mahdi Nikbakht Fini; Jens Muff; Sergio Collado Alonso; José Mario Díaz Fernández. Membrane fouling during fractioning of waste activated sludge. IWA Young Water Professionals (YWP) Spain 2022. 16-19/11/2022, Valencia (España).
- Póster. Daniel Núñez Díaz; Paula Oulego Blanco; Sergio Collado Alonso; Francisco Amador Riera Rodríguez; José Mario Díaz Fernández. Effect of Landfill Leachate Age on Ultrafiltration Performance. I PhD Multidisciplinary Chemical Congress. 19-20/01/2023, Oviedo (España).

Capítulos de libro

A continuación, se indica el trabajo derivado de esta tesis doctoral presentado como capítulo de libro:

- Daniel Núñez Díaz, Paula Oulego Blanco. Efecto del material de membrana en la ultrafiltración de lodos secundarios de depuradora tratados hidrotérmicamente. Avances y contribuciones en I+D+i desde las diferentes ramas de conocimiento. Servicio de Publicaciones de la Universidad de Oviedo. 2021. ISBN: 978-84-18482-31-1.